PBX GENES IN VERTEBRATE LIMB DEVELOPMENT AND THE IMPLICATIONS OF THEIR STUDY TO PRIMATE EVOLUTION

by

TERENCE DANTE CAPELLINI

A dissertation submitted to the Graduate Faculty in Anthropology in partial fulfillment of the requirements for the degree of Doctor of Philosophy, The City University of New York

2007

UMI Number: 3283148

Copyright 2007 by
Capellini, Terence Dante

All rights reserved.

UMI Microform 3283148
Copyright 2007 by ProQuest Information and Learning Company.
All rights reserved. This microform edition is protected against unauthorized copying under Title 17, United States Code.

ProQuest Information and Learning Company
300 North Zeeb Road
P.O. Box 1346
Ann Arbor, MI 48106-1346

© 2007

TERENCE DANTE CAPELLINI

All Rights Reserved

This manuscript has been read and accepted for the Graduate Faculty in Anthropology in satisfaction of the dissertation requirement for the degree of Doctor of Philosophy.

Date	Dr. Michael Steiper Chair of Examining Committee
Date	Dr. Louise Lennihan Executive Officer

Dr. Timothy Bromage

Dr. Benjamin Ortiz

Dr. Licia Selleri
Supervisory Committee

THE CITY UNIVERSITY OF NEW YORK

Abstract

PBX GENES IN VERTEBRATE LIMB DEVELOPMENT AND THE IMPLICATIONS OF THEIR STUDY TO PRIMATE EVOLUTION

By:

Terence Dante Capellini

Advisor:

Dr. Michael Steiper

Primates display considerable differences in their limb proportions and skeletal morphologies. Part of this variation arises from selection acting on embryonic developmental control mechanisms governing limb patterning and morphogenesis. As *Hox* genes are critical regulators of these processes in the limb, it is believed that changes in their embryonic *cis*- and *trans*-regulation underlie many of the morphological differences observed across primates. A major aspect of *Hox* involvement in limb patterning revolves around their ability to target numerous other genes, and part of their DNA binding specificity is achieved through their interaction with cofactors. One such group of cofactors is the *Pre-B Cell Luekemic Factor* (*Pbx*) gene family (*Pbx1-4*). Using compound mutant mice that harbor critical gene deletions for several *Pbx* members, this study examines how the simultaneous loss of multiple *Pbx* genes impacts limb development and skeletal patterning. It is shown that limb and axial morphologies that derive from domains where multiple *Pbx* overlap are more severely affected in compound mutants, than when individual *Pbx* family members are lost in these domains, suggesting a multigenic control of skeletal

patterning by *Pbx*. Importantly, it is demonstrated that *Pbx* controls *Hox* expression in the limb, and therefore regulates limb patterning along the entire proximodistal axis. *Pbx* genes are also shown to regulate *Sonic hedgehog* expression, a gene essential for distal limb and digit development. Interestingly, it is also shown that Pbx functions predominately in the early limb field, as conditional inactivation of *Pbx* in mouse embryos after limb bud establishment results in normal limb patterning. Finally, *Pbx* genes also are shown to lie upstream of most genes involved in girdle patterning and therefore, play critical roles in coordinating development of the entire functional appendage. *Pbx* participation in many genetic networks involved in limb and girdle development reveals that their modulation can provide an evolutionary mechanism to coordinate morphological change in the limb across multiple developmental and functional domains. In this manner, this thesis explores how variation in primate limb proportionalities could have arisen by modulation of a specific *Pbx-Hox-Shh* developmental network during limb development.

Acknowledgements

There are many people I would like to thank for their involvement and support over the course of this thesis project. First, I thank my research advisor and mentor Licia Selleri, for her time and commitment to many aspects of this project including (but not limited to): providing laboratory space to conduct these studies; the initial generation of the single *Pbx* mutant lines, the writing of grants, her knowledge and wisdom of mouse genetics, and overall intellectual support.

Next, I thank my Academic and Thesis Supervisor Mike Steiper for his critical reading of this dissertation, support during the writing stage of this work, and for helping me materialize some of the integrative Evo-Devo concepts on paper.

I thank my initial academic mentor and Thesis Co-Supervisor Timothy Bromage for his intellectual insight and also for the numerous (and highly valued) times we discussed this thesis from its inception. Tim, you have been especially important in helping me think outside the box and pursue this type of integrative research.

I am indebted to Ben Ortiz for inspiring me during his course in developmental biology and more importantly for establishing the initial contact between Licia and me that has allowed all of this research to be accomplished.

I am sincerely grateful for having met, been taught by, and having worked alongside with my colleague and friend Andrea Brendolan. Andrea, you have been exceptionally important throughout the course of this thesis and I deeply appreciate your patience during my initial training and for putting up with me over the course of nearly five years. *E' giunto il momento di andare a camminare sulla neve delle Alpi con le racchette da neve*.

Several of the experiments conducted for Chapter 5 and 6 were performed in collaboration with talented researchers from both Licia Selleri's laboratory as well as from laboratories in the U.S.A. and Italy. I especially thank Giuseppina Di Giacomo for working hard to contribute to figures (5.4-5, 5.11, 5.15-16, 5.22-23, 5.26-27, 6.2, 7.1-2), for her support during the project, and for being an incredibly kind person. I am also highly indebted to Vincenzo Zappavigna (University of Modena-Reggio Emilia, Modena, Italy) and his student Valentina Salsi for performing the biochemical studies highlighted in this chapter (figures 5.21, 5.24-25) and for numerous intellectual discussions regarding the function of Pbx in the limb and girdle. I thank Deepak Srivastava (University of California, San Francisco) for contributing *Hand2* mutant embryos utilized in this work. I thank Naiche Adler (Columbia University) for contributing data to Fig. 6.13 and for providing us with *Tbx4 Cre* mice, originially developed by Tom Jessell (Columbia

University). I thank Mark Lewandoski (NIH) for providing us with the *Msx2 Cre* mouse line used in Chapter 6.

I thank other members of Licia Selleri's laboratory for their assistance and contribution throughout this project: First, Elizabetta Ferretti for the countless embryos she has donated, for her intellectual discussion, and kindness. She has also provided some of the data used to generate figures 7.3-4. Second, Matt Koss for his initial work on the conditional *Pbx1* mutant line, contributing data to Fig. 4.1, and for the numerous times he has listened to me "hypothesize" and "theorize" on the white-erase board in the lab. Go Sabres!!! Third, Athea Vichas for her contribution to figures 7.6, 7.8, 7.15-6 and for just being awesome. Forth, Victoria Wells for her hard work and participation in several of the *Hox* expression studies. Finally, Joseph Giacolone and the late Brunella Bertucci for their assistance with the mouse colonies, and Stefania Asciutti and Maria Milko for their support during the writing stage of the dissertation.

I thank the following researchers at labs at Cornell, Sloan Kettering, and various other institutions, for critical reagents and helpful discussion: Drs. Anderson, Behringer, Boulet, Capecchi, de Crombrugghe, Duboule, Harland, Izpisua-Belmonte, Joyner, Lefebvre, Manley, McMahon, Meijlink, Milenkovic, Niswander, Popperl, Scott, and Tabin for mRNA probes; Drs. Mackem for anti-Hoxd13 antisera, Beachy for *Shh*$^{-/-}$ mice, Hadjantonakis for E8.5 embryos, and Drs. Barna, Di Gregorio, Lacy, Mann, Martin, Niswander, and Tabin for discussions and protocols; Drs. Phil Reno, Burt Rosenman, and Yale Passamaneck for helpful discussions. Maira Biggiogero for her critical reading, overall support, and kindness during the later writing stages of this thesis.

I thank Felix Wolf, the main veterinarian at Weill Medical College of Cornell University as well as his staff in providing excellent and humane treatment of the mice used in these studies.

Importantly, I would like to thank several funding agencies for supporting this research: grants from the National Institutes of Health (HD43997), the March of Dimes and Birth Defects Foundation (6-FY03-071), and the Alice Bohmfalk Charitable Trust to Licia Selleri.

I thank Eric Delson, CUNY, and NYCEP for granting me the Robert Gilleece Fellowship for the initial four years of funding during my preliminary Ph.D. coursework/research. I thank Francisco Ramirez (Hospital for Special Surgery) for an initial stipend during the first year of my Ph.D research period. I highly thank and sincerely respect Carole and Morton Olshan for providing me with a CUNY University Fellowship in their name. I thank CUNY for granting me both the Honors College Instructional Pedagogy Fellowship and the Writing Across the Curriculum Fellowship that has allowed me to pursue dual teaching and research opportunities during the course of this research.

Thank you Russ Hogg and Tara Peburn for your constant intellectual and emotional support. You both have been exceptionally critical to the success of this project in countless ways. I thank Steve Petrus and Jessica Brinkworth for their constant encouragement and enthusiasm, and for helping me cope during the difficult times. I thank Mike and Beth Romano, Brian and Jen Scanlan, and Bryce Mullings for their constant friendship and ability to drag me away from the concrete. I thank Marsha and Dave, for being Marsha and Dave, and for their inspirational speeches at the onset of the writing of this dissertation.

Lastly, and most importantly, I thank my mom Rosanna, my dad Albert, my brother Jeff and his wife Mindy, for being loving individuals and having the incredible patience to see me through this period of my life. I especially thank my mom and dad for being wonderful parents and never inhibiting my curiosity.

Dedication

For Jack and Mia…

…and Giuseppina

Table of Contents

ABSTRACT ..... **IV**

ACKNOWLEDGEMENTS ..... **VI**

TABLE OF CONTENTS ..... **X**

LIST OF FIGURES ..... **XVI**

LIST OF TABLES ..... **XXI**

CHAPTER 1: INTRODUCTION **1**

1.1 INTRODUCTION 1
1.2 EVO-DEVO AND UNDERSTANDING MAMMALIAN AND PRIMATE LIMB DIVERSITY 6
1.3 *CIS* AND *TRANS*-REGULATION, *HOX* GENES, AND THE PRIMATE LIMB 8
1.4 HOX COFACTORS AND *PBX* GENES 11
1.5 THE STUDY 16
1.6 THESIS STRUCTURE 18

CHAPTER 2: DEVELOPMENTAL BASIS FOR LIMB AND GIRDLE EVOLUTION **24**

2.1 INTRODUCTION 24
2.2 EVOLUTIONARY-DEVELOPMENTAL APPROACHES TO THE STUDY OF THE LIMB 25
2.3 MODULARITY, DEVELOPMENTAL GENETICS, AND LIMB EVOLUTION 28
2.4 STUDIES ACROSS VERTEBRATE CLASSES 32
2.5 STUDIES UTILIZING ATYPICAL MAMMALS 40
2.5.1 Studies using chiropterans 40
2.5.2 Studies using cetaceans 48
2.6 STUDIES UTILIZING PRIMATES 54
2.7 CONCLUSIONS AND DIRECTIONS 64

CHAPTER 3: *PBX* AND *HOX* GENES AND THE DEVELOPMENT OF THE LIMB AND GIRDLE **67**

3.1 INTRODUCTION 67
3.2 GENERAL LIMB AND GIRDLE STRUCTURE AND DEVELOPMENT 69
3.2.1. Limb and girdle structure 69
3.2.2 Overview of limb and girdle development 71
3.3 VERTEBRATE LIMB DEVELOPMENT 73
3.3.1 Axial level of limb specification 73
3.3.2 Limb field and bud induction 76
3.3.3 Limb axis (A-P, P-D, and D-V) establishment 80
3.3.3.1 Early events in the establishment of the three limb axes (E8.5-E9.5) 80
3.3.3.2 AER formation and P-D axis establishment (E8.5-E10.5) 86
3.3.3.3 Later A-P axis establishment (E9.5-E11.5) 89
3.3.3.4 *Hox* genes and their roles in axis formation and skeletal patterning 102

3.3.3.5. Maintenance of the developmental axes during bud outgrowth (E9.75-E12) 111
3.3.4. How mesenchymal cells in the limb bud become patterned (E8.5-12) 115
3.3.4.1 Progress zone model 117
3.3.4.2 Early specification model 118
3.3.4.3 Continued outgrowth and patterning of the limb (E12-P0) 121
3.4 GIRDLE DEVELOPMENT 123
3.4.1 Histological and molecular characteristics of the pectoral girdle 124
3.4.1.1 Studies in avian species 124
3.4.1.2 Studies using mouse mutants 127
3.4.2 Histological and molecular characteristics of the pelvic girdle 138
3.5 HOX TRANSCRIPTION FACTORS AND PBX COFACTOR PROTEINS 140
3.5.1 Concerning Hox and their cofactors 140
3.5.2 On Pbx cofactors and homologs, partner cofactors, and their functional relationships with Hox 142
3.5.2.1 Extradenticle (Exd) and Pbx cofactors 142
3.5.2.2 Regarding Pbx and Meis cofactor partners 145
3.5.2.3 Pbx family members and their functionality in embryogenesis 145
3.5.2.4 Pbx proteins function as Hox cofactors in vertebrates 147
3.5.2.5 Pbx has functions outside of their involvement with Hox 149
3.5.2.6 Pbx interacts with partner proteins to confer some of its functions 151
3.5.3 An emerging view of Pbx functionality in the limb 154
FIGURES AND TABLES 155

CHAPTER 4: EXPERIMENTAL METHODS 179

4.1 MOUSE BREEDING 179
4.1.1 Overview 179
4.1.2 Maintenance and generation of *Pbx1;Pbx2* mutant mouse lines 180
4.1.2.1 Breeding strategies and maintenance of *Pbx1* and *Pbx2* knockout lines 180
4.1.2.2 Establishing double heterozygous *Pbx1*$^{+/-}$*; Pbx2*$^{+/-}$ mice 182
4.1.2.3 Generation of compound *Pbx1; Pbx2* mutant (*Pbx1*$^{-/-}$*; Pbx2*$^{+/-}$ and *Pbx1*$^{-/-}$*; Pbx2*$^{-/-}$) embryos 187
4.1.3 Maintenance and breeding of *Shh* mouse lines and curation of *Hand2* embryos 189
4.1.4 Generation and breeding of cre lines, cre reporter lines, and *Pbx1;Pbx2* conditional mutant mouse lines 190
4.1.4.1 Overview 190
4.1.4.2 Assessment of cre activity in transgenic mouse embryos 192
4.1.5 Breeding of additional *Pbx* compound mutant lines 192
4.2 EXPERIMENTAL PROTOCOLS 194
4.2.1 DNA extraction and genotyping 194
4.2.2 Gross morphology 196
4.2.3 Skeletal preparation (bone and cartilage staining) 197
4.2.4 Whole mount *in situ* hybridization 199

4.2.5 *In vitro* transcription....202
4.2.6 Immunohistochemistry....203
4.2.7 Whole mount immunohistochemistry....203
4.2.8 Cell proliferation analysis via BrdU....204
4.2.9 Caspase3 apoptosis assay....204
4.2.10 β-Galactosidase histochemistry....205
4.2.11 Chromatin Immunoprecipitations (ChIP)....205
4.2.12 Electrophoretic mobility shift assay (EMSA)....206
4.2.13 Cell culture and transfection....207
4.2.14 Photo-documentation....208
FIGURES AND TABLES....209

CHAPTER 5: *PBX1* AND *PBX2* ARE REQUIRED FOR DISTAL LIMB PATTERNING VIA THEIR HIERARCHICAL CONTROL OF *HOX* SPATIAL DISTRIBUTION AND *SHH* EXPRESSION....213

5.1 INTRODUCTION....213
5.2 RESULTS....216
5.2.1 Loss of *Pbx1* and *Pbx2* caused not only proximal but also distal fore- and hindlimb defects....216
5.2.2 *Pbx1*, *Pbx2*, and *Pbx3* mesenchymal expression during limb development was dynamic....221
5.2.2.1 Early *Pbx* gene expression in limbs (E8.5-11.0)....222
5.2.2.2 Later limb *Pbx* gene expression (E11-12)....223
5.2.3 In *Pbx1/2 Mut* limbs, early anterior and posterior mesenchymal patterning remained relatively preserved....224
5.2.4 *Pbx1* and *Pbx2* were required for normal *Shh* expression in the limb ZPA....226
5.2.5 *Pbx* and *Hand2* may control *Shh* through parallel pathways; *Shh* and *Pbx* did not form a cross regulatory loop....231
5.2.6 *Hox* gene expression, prior to and after, *Shh* onset was spatially perturbed or absent in *Pbx1/2 Mut* limbs....233
5.2.7 Hox proteins bound *in vivo* to, and activated transcription through, the *Shh* long-range limb enhancer....235
5.2.8 The attenuated expression of *Shh* in *Pbx1/2 Mut* hindlimbs in different genetic backgrounds influenced digit formation and onset of appearance 238
5.2.9 *Pbx1/2 Mut* limb development proceeded in the absence of marked alterations to cellular proliferation and apoptosis....239
5.3 DISCUSSION....240
5.3.1 *Pbx1* and *Pbx2* are required for proximal and distal limb patterning.240
5.3.2 *Pbx* requirement for distal limb patterning is, at least in part, mediated by *Shh* control; posterior digital loss is a consequence of *Shh* absence....243
5.3.3 *Pbx1/2* and *Hand2* may genetically regulate each other; *Pbx1*, *Pbx2*, and *Shh* do not form a genetic regulatory loop....247
5.3.4 *Pbx1* and *Pbx2* hierarchical control of *Hox* spatial distribution mediates *Shh* expression in the limb....248
5.3.5 Proximal mesenchymal interactions of *Pbx1* and *Pbx2* may drive mouse limb outgrowth....255

5.4 SUMMARY OF *PBX/HOX/SHH* INTERACTION IN THE LIMB MESENCHYME AND THE SKELETAL DEFECTS REPORTED *IN PBX1/2 MUT* LIMBS 262
FIGURES 263

CHAPTER 6: DIFFERENTIATING *PBX* ECTODERMAL VERSUS MESENCHYMAL ROLES DURING LIMB DEVELOPMENT 303

6.1 INTRODUCTION 303
6.2 RESULTS 308
6.2.1 The Morphological and molecular phenotypic characterization of global *Pbx1;Pbx2* loss on early limb development 308
6.2.1.1 Ectoderm and AER expression of *Pbx* genes 308
6.2.1.2 Morphological defects in limbs of mutant *Pbx1;Pbx2* double homozygous embryos 309
6.2.1.3 Limb field specification appears slightly altered in *Pbx* compound mutants 310
6.2.1.4 Limb induction was initiated in *Pbx1;Pbx2* mutants 311
6.2.1.5 Early AER gene expression was altered in $Pbx1^{-/-}; Pbx2^{-/-}$ mutants 313
6.2.1.6 Ectodermal markers were severely reduced in *Pbx1/2 Mut* embryos during fore- and hindlimb bud development 313
6.2.1.7 Dorsal-ventral patterning was altered in *Pbx1/2 Mut* embryos 317
6.2.1.8 Genes involved in the formation of the proximal to distal Fgf-RA gradient were disrupted in the absence of *Pbx1* and *Pbx2* 319
6.2.2 The morphological and molecular phenotypic characterization of conditional *Pbx1/Pbx2* loss on limb development (conditional inactivation of *Pbx* in the AER versus limb mesenchyme) 320
6.2.2.1 Overview 320
6.2.2.2 Conditional inactivation of *Pbx1* in the mesenchyme from E9.5 to birth 321
6.2.2.3 Conditional inactivation of *Pbx1* in the ventral ectoderm and AER 324
6.3 DISCUSSION 328
6.3.1 *Pbx* genes exhibit complex expression patterns in vertebrates that underlie intricate roles during embryogenesis 328
6.3.2 *Pbx1/Pbx2* effects on limb bud induction and outgrowth reflect complex hierarchical relationships with the Tbx family of transcription factors 330
6.3.3 *Pbx* are upstream of gene expression in the preAER and AER 332
6.3.4 *Pbx* are upstream of D-V axis determination and AER formation in the limb 335
6.3.5 Late *Pbx1* and *Pbx2* mesenchymal expression is dispensable for limb development 338
6.3.6 The ventral ectodermal and AER expression of *Pbx1* and *Pbx2* are dispensable for normal limb development after E10 341
6.4 SUMMARY 344
FIGURES 346

CHAPTER 7: *PBX* AND THE DEVELOPMENT OF THE PECTORAL AND PELVIC GIRDLE 389

7.1 INTRODUCTION 389
7.2 RESULTS 391
7.2.1 Novel domains of TALE gene expression and protein localization during girdle development 391
7.2.1.1 *Pbx* and *Meis* expression during scapula formation 391
7.2.1.2 *Pbx* and *Meis* expression during posterior axis and pelvic formation 393
7.2.2 Morphological and molecular phenotypes of the scapula in compound *Pbx* mutants 394
7.2.2.1 Morphological defects in compound *Pbx1;Pbx2* mutants 394
7.2.2.2 Compound *Pbx1;Pbx3* mutants and their forelimb and girdle morphological defects 396
7.2.2.3 Compound *Pbx2;Pbx3* and triple heterozygous *Pbx1;Pbx2;Pbx3* mutants and their lack of limb and girdle morphological defects 397
7.2.2.4 The molecular basis of the *Pbx1/2 Mut* scapular defects 398
7.2.2.4.1 Early mesenchymal condensation of scapular blade, head, and neck structures was altered in *Pbx1/2 Mut* embryos 399
7.2.2.4.2 Expression of genes critical for scapular blade formation were altered in *Pbx1/2 Mut* embryos 400
7.2.2.4.3 Expression of genes involved in scapular head, neck, and acromion progenitors were altered in *Pbx1/2 Mut* embryos 403
7.2.3 Morphological and molecular defects in the pelvic girdle of compound *Pbx* Mutants 406
7.2.3.1 Morphological defects in compound *Pbx1;Pbx2* mutants 406
7.2.3.2 Compound *Pbx1;Pbx3* mutants and their hindlimb and girdle morphological defects 407
7.2.3.3 The molecular basis of *Pbx1/2 Mut* pelvic defects 408
7.2.3.3.1 Early mesenchymal condensations of pelvic structures were altered in *Pbx1/2 Mut* embryos 408
7.2.3.3.2 Expression of genes involved in the specification of the ilium, ischium, and pubis formation were altered in *Pbx1/2 Mut* embryos 409
7.3 DISCUSSION 412
7.3.1 *Pbx1* emerges as paramount in the determination of limb and girdle formation 412
7.3.2 *Pbx* are hierarchical upstream factors of scapula development 413
7.3.3 *Pbx* are hierarchical upstream factors of scapular blade morphogenesis 415
7.3.4 Evidence suggests that dermomyotomal function of Pbx underlies their roles in blade morphogenesis 417
7.3.5 *Pbx* lie upstream of scapular neck, head and acromion formation 422
7.3.6 *Pbx* are upstream of pelvic girdle formation 424
7.4 SUMMARY 430
FIGURES 431

CHAPTER 8: CONCLUSIONS AND EVOLUTIONARY IMPLICATIONS 464

8.1 SUMMARY OF THESIS RESEARCH 464
8.2 MODEL OF *PBX* ROLES DURING LIMB AND GIRDLE DEVELOPMENT 469
8.3 *PBX* ROLES IN EVOLUTION 472
8.3.1 Comparative developmental genetics of *Pbx* 473
8.3.1.1 *Pbx* roles in proximal-distal limb patterning in vertebrates and invertebrates 473
8.3.1.2 Conservation of general Pbx function during fin and limb evolution 476
8.3.2 Incorporating *Pbx* into Evo-Devo models on primate limb and girdle evolution 479
8.3.2.1 Limb modularity and *Pbx* 479
8.3.2.2 Girdle modularity and *Pbx* 484
8.3.2.3 Modularity, gene regulation, variation, and *Pbx* 486
8.3.2.4 Mechanisms generating morphological variation via the *Pbx-Hox-Shh* limb developmental network 489
8.3.2.5 Examples in primates 493
8.3.2.5.1 Changes in digit proportionality and specialization 493
8.3.2.5.2 Differences in intralimb proportionality 496
8.3.2.5.3 Forelimb versus hindlimb specializations 499
8.3.2.5.4 Differences in the scapular girdle 502
8.3.2.5.5 Integration of girdle and limb evolution 505
8.3.2.6 The evolutionary forces and generating limb diversity in primates 508
8.4 FUTURE DIRECTIONS 513
FIGURES 516

APPENDIX I.....531

GLOSSARY OF TERMS 532

REFERENCES 539

List of Figures

FIGURE 3.1. THE FORELIMB WITH SCAPULA AND THEIR UNDERLYING EMBRYONIC TISSUE DOMAINS.....155
FIGURE 3.2. THE MOUSE HINDLIMB WITH PELVIS AND THEIR UNDERLYING EMBRYONIC TISSUE DOMAINS.....156
FIGURE 3.3. DEVELOPMENTAL COMPARTMENTS OF THE MOUSE FORE- AND HINDLIMB. 157
FIGURE 3.4. OVERVIEW OF EARLY LIMB DEVELOPMENT IN THE MOUSE (E8.5-E11.5). 158-158
FIGURE 3.5. MAJOR AXES OF THE LIMB AND ITS DEVELOPMENTAL SIGNALING CENTERS. 160
FIGURE 3.6. MOLECULAR INTERACTIONS IN THE E9.0 FORELIMB AND HINDLIMB. 161
FIGURE 3.7. EARLY MOLECULAR INTERACTIONS ALONG THE ANTERIOR-POSTERIOR LIMB BUD AT E9.25 (FL)/E9.75 (HL). 162
FIGURE 3.8. D-V POLARITY IN THE EARLY LIMB BUD AND THE DEVELOPMENT OF THE AER. 163
FIGURE 3.9. UPSTREAM HIERARCHICAL FACTORS REGULATING *SHH* ACTIVATION IN THE PREZPA MESENCHYME AT E9.5-9.75 (FL)/E9.75-E10.25 (HL).....164
FIGURE 3.10. THE SHH SIGNALING PATHWAY.....165
FIGURE 3.11. ANTERIOR TO POSTERIOR GRADIENTS ON SHH, GLI3 AND HOX COMPLEXES DURING LIMB DEVELOPMENT.....166
FIGURE 3.12. *HOX* CLUSTER ORGANIZATION AND EXPRESSION IN THE MOUSE EMBRYO. 167
FIGURE 3.13. *HOX* GENE EXPRESSION IN THE DEVELOPING LIMB.....168
FIGURE 3.14. DOMAINS OF *HOXD* (AND PARTIAL *HOXA*) EXPRESSION AND THE SKELETAL ELEMENTS THEY SPECIFY. 169
FIGURE 3.15. THE REGULATION OF EARLY *HOXD* COLLINEAR AND "REVERSE" *HOXD* COLLINEAR GENE TRANSCRIPTION. 170-170
FIGURE 3.16. THE ZPA-AER MOLECULAR FEEDBACK LOOP. 172
FIGURE 3.17. SKELETAL ELEMENT SPECIFICATION ACCORDING TO THE PROGRESS ZONE MODEL (PZM) AND THE EARLY SPECIFICATION MODEL (ESM).....173
FIGURE 3.18. MOLECULAR AND TISSUE INTERACTIONS DURING SCAPULAR DEVELOPMENT.....174-174
FIGURE 3.19. MOLECULAR AND TISSUE INTERACTIONS GIVING RISE TO THE PELVIS. ..176
FIGURE 3.20. GENETIC, BIOCHEMICAL, AND HOMOLOGY RELATIONSHIPS AMONG PBX AND MEIS GENES/PROTEINS.....177
FIGURE 4.1. CONDITIONAL INACTIVATION OF *PBX1* ALLELE (IN A HOMOZYGOUS STATE) USING A UBIQUITOUSLY-SPECIFICALLY EXPRESSED CRE TRANSGENE UNDER THE *BETA ACTIN* PROMOTER. 209
FIGURE 4.2. PROPORTION OF *PBX* COMPOUND MUTANT EMBRYOS RECOVERED PER GENOTYPE AND GESTATIONAL DAY (E8.5 TO E13.5) FROM SUMMER 2001 TO FALL 2005.....210-210
FIGURE 5.1. GROSS MORPHOLOGY OF *PBX1/2* COMPOUND MUTANT EMBRYOS. .263-263
FIGURE 5.2. LIMB SKELETAL MORPHOLOGY OF *PBX1/2* COMPOUNDS EMBRYOS..265-265

FIGURE 5.3. AMELIORATION OF THE *PBX1*$^{-/-}$;*PBX2*$^{+/-}$ HINDLIMB PHENOTYPE ON INCREASINGLY BLACKSWISS GENETIC BACKGROUNDS. 267
FIGURE 5.4. *PBX1/2/3* EXPRESSION DURING LIMB DEVELOPMENT....268-269
FIGURE 5.5. *PBX1* EXPRESSION IN WILDTYPE (WT) AND *PBX2*$^{-/-}$ (KO) LIMBS. 270
FIGURE 5.6. *PBX2* EXPRESSION IN WILDTYPE (WT) AND *PBX1*$^{-/-}$ (KO) LIMBS. 271
FIGURE 5.7. *PBX3* EXPRESSION IN WILDTYPE (WT) AND *PBX1*$^{-/-}$;*PBX2*$^{+/-}$ (*PBX1/2 MUT*) AND *PBX1*$^{+/-}$;*PBX2*$^{-/-}$ FORELIMBS....272
FIGURE 5.8. MESENCHYMAL GENE EXPRESSION IN *PBX1*$^{-/-}$;*PBX2*$^{+/-}$ (MUT) LIMB. 273-273
FIGURE 5.9. EXPRESSION OF *SHH* IN *PBX1*$^{-/-}$;*PBX2*$^{+/-}$ (MUT) EMBRYOS....275
FIGURE 5.10. EXPRESSION OF *PTC AND GLI1* IN *PBX1*$^{-/-}$;*PBX2*$^{+/-}$ (MUT) LIMBS. 276
FIGURE 5.11. EXPRESSION OF AER MARKERS IN *PBX1*$^{-/-}$;*PBX2*$^{+/-}$ (MUT) LIMBS....277
FIGURE 5.12. EXPRESSION OF PROXIMAL MESENCHYMAL MARKERS IN *PBX1*$^{-/-}$;*PBX2*$^{+/-}$ (MUT) LIMBS. 278
FIGURE 5.13. *GREMLIN* AND *BMP2* EXPRESSION IN *PBX1*$^{-/-}$;*PBX2*$^{+/-}$ (MUT) LIMBS....279
FIGURE 5.14. EXPRESSION OF MESENCHYMAL GENES AFTER *SHH* ONSET IN *PBX1*$^{-/-}$;*PBX2*$^{+/-}$ (MUT) LIMBS....280
FIGURE 5.15. *PBX* AND *HAND2* LIKELY CONTROL *SHH* THROUGH PARALLEL PATHWAYS. 281
FIGURE 5.16. *PBX1/2* EXPRESSION IN *SHH*$^{-/-}$ (KO) LIMBS. 282
FIGURE 5.17. *HOX* EXPRESSION IN EARLY *PBX1*$^{-/-}$;*PBX2*$^{+/-}$ (MUT) HINDLIMBS. 283-283
FIGURE 5.18. *HOX* EXPRESSION IN EARLY *PBX1*$^{-/-}$;*PBX2*$^{+/-}$ (MUT) FORELIMBS....285-285
FIGURE 5.19. *HOX* EXPRESSION IN E11.5 *PBX1*$^{-/-}$;*PBX2*$^{+/-}$ (MUT) HINDLIMBS. 287
FIGURE 5.20. *HOX* EXPRESSION IN E11.5 *PBX1*$^{-/-}$;*PBX2*$^{+/-}$ (MUT) FORELIMBS. 288
FIGURE 5.21. CO-IMMUNOPRECIPITATION ASSAY (CHIP). 289
FIGURE 5.22. *SHH* AND PBX2 CO-LOCALIZATION IN THE HINDLIMB AT E10.25. 290
FIGURE 5.23. *SHH* AND *PBX1* DO NOT CO-LOCALIZE IN THE HINDLIMB AT E10.25 AND E11.0. 291
FIGURE 5.24. ELECTROPHORETIC MOBILITY SHIFT ASSAY (EMSA). 292
FIGURE 5.25. TRANSIENT TRANSFECTION ASSAYS IN P19 CARCINOMA CELLS. 293
FIGURE 5.26. BRDU ANALYSES IN *PBX1*$^{-/-}$; *PBX2*$^{+/-}$ (MUT) LIMBS. 294
FIGURE 5.27. CASPASE3 ANALYSES IN *PBX1*$^{-/-}$; *PBX2*$^{+/-}$ (MUT) LIMBS. 295-295
FIGURE 5.28. AXIAL MALFORMATIONS IN THE *PBX1/2* MUT EMBRYOS AT E13.5..297-297
FIGURE 5.29. *PBX1/2* AND THE CONTROL OF *HOX* EXPRESSION. 299-299
FIGURE 5.30. MODEL OF PBX ACTION UPSTREAM OF HOX AND THE ACTIVATION OF *SHH*. 301-301
FIGURE 6.1. *PBX1* AND *PBX2* EXPRESSION IN THE LIMB ECTODERM AND AER....346
FIGURE 6.2. PBX1 AND PBX2 PROTEINS CO-LOCALIZATION IN THE ECTODERM AND AER. 347-347
FIGURE 6.3. *TBX4/TBX5* EXPRESSION IN *PBX1*$^{-/-}$;*PBX2*$^{-/-}$ AND *PBX1*$^{-/-}$;*PBX2*$^{+/-}$ EMBRYOS. 349-349
FIGURE 6.4. *FGF10* EXPRESSION WAS MARKEDLY REDUCED IN *PBX1*$^{-/-}$;*PBX2*$^{+/-}$ LIMBS. 351-351
FIGURE 6.5. *FGF8* EXPRESSION WAS MARKEDLY REDUCED AND ABSENT IN *PBX1*$^{-/-}$;*PBX2*$^{-/-}$ FORE- AND HINDLIMBS, RESPECTIVELY. 353-353
FIGURE 6.6. *DLX* EXPRESSION WAS HIGHLY ALTERED IN *PBX1*$^{-/-}$;*PBX2*$^{+/-}$ BUDS. ..355-355
FIGURE 6.7. *MSX1* EXPRESSION WAS MARKEDLY ALTERED IN *PBX1*$^{-/-}$;*PBX2*$^{+/-}$ LIMBS..357

FIGURE 6.8. EXPRESSION OF *MSX2* WAS DIFFERENTLY EFFECTED IN THE AER VERSUS MESENCHYME IN *PBX1*$^{-/-}$;*PBX2*$^{+/-}$ LIMBS.....358-358
FIGURE 6.9. *EN1* EXPRESSION WAS INTRICATELY ALTERED *PBX1*$^{-/-}$;*PBX2*$^{+/-}$ EMBRYOS. 360-360
FIGURE 6.10. *WNT7A* EXPRESSION WAS DOWN-REGULATED IN *PBX1*$^{-/-}$;*PBX2*$^{+/-}$ LIMBS. 362
FIGURE 6.11. *LMX1B* EXPRESSION REMAINED PRESERVED IN *PBX1*$^{-/-}$;*PBX2*$^{+/-}$ LIMBS..363
FIGURE 6.12. *CYP26B1* EXPRESSION WAS REDUCED IN *PBX1*$^{-/-}$;*PBX2*$^{+/-}$ LIMBS. .364-364
FIGURE 6.13. TBX4 CRE ACTIVITY DURING HINDLIMB DEVELOPMENT. 366
FIGURE 6.14. EFFICIENCY OF EXCISION OF *PBX1* "FLOXED" ALLELE BY TBX4 CRE DURING HINDLIMB DEVELOPMENT. 367
FIGURE 6.15. GROSS MORPHOLOGY OF E14.5 *PBX1*$^{CL\Delta 3/CL\Delta 3}$; *PBX2*$^{+/-}$; *TBX4*$^{CRE/+}$ AND *PBX1*$^{CL\Delta 3/CL\Delta 3}$; *PBX2*$^{-/-}$; *TBX4*$^{CRE/+}$ MUTANT EMBRYOS WAS NORMAL. 368-368
FIGURE 6.16. SKELETAL MORPHOLOGY OF E14.5 *PBX1*$^{CL\Delta 3/CL\Delta 3}$; *PBX2*$^{-/-}$; *TBX4*$^{CRE/+}$ MUTANT EMBRYOS WAS NORMAL. 370-370
FIGURE 6.17. GROSS MORPHOLOGY OF THE PES OF NEWBORN (P0) *PBX1*$^{CL\Delta 3/-}$; *PBX2*$^{-/-}$; *TBX4*$^{CRE/+}$ MUTANT EMBRYOS WAS NORMAL. 372
FIGURE 6.18. SKELETAL MORPHOLOGY OF THE HINDLIMB AND PES OF NEWBORN (P0) *PBX1*$^{CL\Delta 3/-}$; *PBX2*$^{-/-}$; *TBX4*$^{CRE/+}$ MUTANT EMBRYOS WAS NORMAL. 373
FIGURE 6.19. MSX2 CRE ACTIVITY DURING LIMB DEVELOPMENT. 374-374
FIGURE 6.20. EFFICIENCY OF EXCISION OF *PBX1* "FLOXED" ALLELE BY MSX2 CRE DURING HINDLIMB DEVELOPMENT. 376
FIGURE 6.21. EFFICIENCY OF EXCISION OF *PBX1* "FLOXED" ALLELE BY MSX2 CRE DURING FORELIMB DEVELOPMENT. 377
FIGURE 6.22. GROSS MORPHOLOGY OF E12.75 *PBX1*$^{CL\Delta 3/CL\Delta 3}$; *PBX2*$^{+/-}$; *MSX2*$^{CRE/+}$ AND *PBX1*$^{CL\Delta 3/CL\Delta 3}$; *PBX2*$^{-/-}$; *MSX2*$^{CRE/+}$ MUTANT EMBRYOS WAS NORMAL. 378-378
FIGURE 6.23. GROSS MORPHOLOGY OF E14.5 *PBX1*$^{CL\Delta 3/CL\Delta 3}$; *PBX2*$^{+/-}$; *MSX2*$^{CRE/+}$ AND *PBX1*$^{CL\Delta 3/CL\Delta 3}$; *PBX2*$^{-/-}$; *MSX2*$^{CRE/+}$ MUTANT EMBRYOS WAS NORMAL. 380-380
FIGURE 6.24. SKELETAL MORPHOLOGY OF E14.5 *PBX1*$^{CL\Delta 3/CL\Delta 3}$; *PBX2*$^{-/-}$; *MSX2*$^{CRE/+}$ MUTANT EMBRYOS WAS NORMAL. 382-382
FIGURE 6.25. GROSS MORPHOLOGY OF THE HINDPAWS OF NEWBORN (P0) *PBX1*$^{CL\Delta 3/CL\Delta 3}$; *PBX2*$^{+/-}$; *MSX2*$^{CRE/+}$ AND *PBX1*$^{CL\Delta 3/CL\Delta 3}$; *PBX2*$^{-/-}$; *MSX2*$^{CRE/+}$ MUTANT EMBRYOS WAS NORMAL.....384
FIGURE 6.26. SKELETAL MORPHOLOGY OF THE HINDLIMB AND PES OF NEWBORN (P0) *PBX1*$^{CL\Delta 3/CL\Delta 3}$; *PBX2*$^{-/-}$; *MSX2*$^{CRE/+}$ MUTANT EMBRYOS WAS NORMAL. 385
FIGURE 6.27. SKELETAL MORPHOLOGY OF E14.5 *PBX1*$^{CL\Delta 3/-}$; *PBX2*$^{-/-}$; *MSX2*$^{CRE/+}$ MUTANT EMBRYOS WAS NORMAL. 386
FIGURE 6.28. SCENARIOS OF PBX CONTROL OF EARLY LIMB DEVELOPMENT.....387-387
FIGURE 7.1. *PBX* EXPRESSION IN THE SOMATOPLEURIC MESODERM. 431-431
FIGURE 7.2. PBX AND OTHER TALE PROTEINS CO-LOCALIZED IN THE DERMOMYOTOME DURING SCAPULA DEVELOPMENT.....433-433
FIGURE 7.3. *FGF8* AND *SHH* WERE NORMALLY EXPRESSED IN *PBX1*$^{-/-}$;*PBX3*$^{+/-}$ EMBRYOS DURING LIMB DEVELOPMENT. 435-435
FIGURE 7.4. COMPARATIVE LIMB SKELETAL MORPHOLOGY OF *PBX1*$^{-/-}$;*PBX2*$^{+/-}$ AND *PBX1*$^{-/-}$;*PBX3*$^{+/-}$ EMBRYOS.....437-437

FIGURE 7.5. *SOX9* EXPRESSION WAS MARKEDLY ABSENT AND DISORGANIZED IN THE PRESUMPTIVE SCAPULA DOMAIN OF *PBX1*$^{-/-}$;*PBX2*$^{+/-}$ FORELIMBS. 439
FIGURE 7.6. *EMX2* EXPRESSION WAS REDUCED IN THE PRESUMPTIVE SCAPULAR BLADE DOMAIN OF *PBX1*$^{-/-}$;*PBX2*$^{+/-}$ FORELIMBS.....440
FIGURE 7.7. *TBX15* EXPRESSION WAS MARKEDLY DELAYED AND DISORGANIZED IN *PBX1*$^{-/-}$;*PBX2*$^{+/-}$ FORELIMBS. 441-441
FIGURE 7.8. EXPRESSION OF *ALX4* AND *GLI3* WERE SPATIALLY ALTERED IN THE PRESUMPTIVE SCAPULAR DOMAIN OF *PBX1*$^{-/-}$;*PBX2*$^{+/-}$ FORELIMBS.....443-443
FIGURE 7.9. *CART1* EXPRESSION WAS REDUCED IN THE PRESUMPTIVE SUPERIOR SCAPULAR BLADE DOMAIN OF *PBX1*$^{-/-}$;*PBX2*$^{+/-}$ FORELIMBS.....445-445
FIGURE 7.10. *HOXC6* EXPRESSION WAS SPATIALLY DIFFUSED AND SHIFTED IN *PBX1*$^{-/-}$;*PBX2*$^{+/-}$ EMBRYOS. 447
FIGURE 7.11. *PBX3* EXPRESSION WAS SPATIALLY ALTERED IN *PBX1*$^{-/-}$;*PBX2*$^{+/-}$ FORELIMBS.....448
FIGURE 7.12. *PAX1* EXPRESSION WAS MARKEDLY REDUCED IN *PBX1*$^{-/-}$;*PBX2*$^{+/-}$ FORELIMBS.....449
FIGURE 7.13. EXPRESSION OF THE TENDON PROGENITOR MARKER, *SCX*, WAS DELAYED AND SPATIALLY ALTERED IN *PBX1*$^{-/-}$;*PBX2*$^{+/-}$ FORELIMBS. 450
FIGURE 7.14. *SOX9* EXPRESSION WAS ABSENT FROM THE PRESUMPTIVE PELVIC DOMAIN OF *PBX1*$^{-/-}$;*PBX2*$^{+/-}$ HINDLIMBS. 451
FIGURE 7.15. *EMX2* EXPRESSION WAS REDUCED IN THE PRESUMPTIVE PELVIC GIRDLE DOMAIN OF *PBX1*$^{-/-}$;*PBX2*$^{+/-}$ HINDLIMBS.....452
FIGURE 7.16. EXPRESSION OF *ALX4* AND *GLI3* WERE SLIGHTLY SPATIALLY ALTERED IN THE PRESUMPTIVE PELVIC DOMAIN OF *PBX1*$^{-/-}$;*PBX2*$^{+/-}$ HINDLIMBS. 453
FIGURE 7.17. *TBX15* EXPRESSION WAS SPATIALLY ALTERED IN *PBX1*$^{-/-}$;*PBX2*$^{+/-}$ HINDLIMBS. 454
FIGURE 7.18. EXPRESSION OF THE TENDON PROGENITOR MARKER, *SCX,* WAS POSTERIORIZED IN *PBX1*$^{-/-}$;*PBX2*$^{+/-}$ HINDLIMBS.....455
FIGURE 7.19. *PAX1* EXPRESSION WAS ABSENT FROM THE PRESUMPTIVE PELVIC FIELD AND INTERLIMB FLANK MESODERM OF *PBX1*$^{-/-}$;*PBX2*$^{+/-}$ EMBRYOS. 456-456
FIGURE 7.20. PBX ROLES IN SCAPULAR BLADE DEVELOPMENT (A,B).....458-458
FIGURE 7.21. PBX ROLES IN SCAPULAR NECK/HEAD DEVELOPMENT.....461-461
FIGURE 7.22. PBX ROLES IN PELVIC DEVELOPMENT. 463
FIGURE 8.1. MODEL OF *PBX* ROLES DURING LIMB AND GIRDLE DEVELOPMENT. ...516-516
FIGURE 8.2. COMPARATIVE *PBX* AND *EXD* EXPRESSION AND FUNCTION IN VERTEBRATE AND INVERTEBRATE APPENDAGE DEVELOPMENT. 519-519
FIGURE 8.3. EVOLUTIONARY MODEL OF *HOX-SHH* MODULATION DURING LIMB DEVELOPMENT: HETEROCHRONIC SHIFTS IN EARLY *HOX* COLLINEAR ACTIVATION. 521-521
FIGURE 8.4. EVOLUTIONARY MODEL OF *HOX-SHH* MODULATION DURING LIMB DEVELOPMENT: HETEROCHRONIC RATE SHIFTS IN EARLY COLLINEAR *HOX* EXPRESSION. 523-523
FIGURE 8.5. EVOLUTIONARY MODEL OF *HOX-SHH* MODULATION DURING LIMB DEVELOPMENT: HETEROCHRONIC AND HETEROTOPIC SHIFTS IN EARLY COLLINEAR *HOX* ACTIVATION VIA GENOMIC REPOSITIONING.....525-525

FIGURE 8.6. EVOLUTIONARY MODEL OF *HOX-SHH* MODULATION DURING LIMB COMPARTMENT DEVELOPMENT: HETEROCHRONIC AND HETEROTOPIC SHIFTS IN EARLY COLLINEAR *HOX* ACTIVATION VIA GENOMIC REPOSITIONING. 527-527
FIGURE 8.7. EVOLUTIONARY MODEL OF *HOX-SHH* MODULATION DURING LIMB COMPARTMENT DEVELOPMENT: HETEROCHRONIC AND HETEROTOPIC SHIFTS IN LATE COLLINEAR *HOX* ACTIVATION VIA GENOMIC REPOSITIONING. 529-529

List of Tables

TABLE 3.1. MAJOR STAGES IN THE MOLECULAR CONTROL OF LIMB DEVELOPMENT IN THE MOUSE. 178
TABLE 4.1. EXACT COUNTS OF PBX COMPOUND MUTANT EMBRYOS ACQUIRED PER GENOTYPE PER GESTATIONAL DAY FROM TIMED-MATING (SUMMER 2001-FALL 2005). 212

Chapter 1: Introduction

1.1 Introduction

Primates display considerable variation in their limb proportions and skeletal morphologies. For example, in gibbons, forelimb length greatly exceeds hindlimb length, an adaptation to arboreal brachiation or arm-swinging locomotion. Moreover, while this length increase is recognizable across all of the forelimb's major divisions (the upper arm, forearm, and hand) it is particularly extreme in the latter two compartments (Schultz, 1930; Fleagle, 2001). Interestingly, among gorillas and chimpanzees, which also possess longer forelimbs, length increases are compartmental-specific and only evident in distal regions (i.e., in the forearm and hand), although not to the extreme found in gibbons. In these primates, longer forelimbs appear as adaptations to more terrestrial knuckle-walking locomotion (Schultz, 1930; Reno et al., in press). When coupled with the different life histories of these primates, these findings suggest that skeletal adaptations to distinct locomotor repertoires could result from modulations in similar biological mechanisms (e.g., to growth changes within or across the different skeletal elements of the limb).

With respect to underlying biological mechanism, these morphologies arise ontogenetically and likely reflect previous evolutionary selective events that have shaped limb development in different primates (Chiu and Hamrick, 2002). Specifically, over the course of an organism's ontogeny, selection has favored variations in the regulation of embryonic, fetal, and postnatal developmental processes underlying the formation of their distinct limb morphologies.

Evolutionarily, the modulation of pre- and/or postnatal development has also afforded all primates the phenotypic plasticity necessary to reconcile functional demands with the constraints placed on them by previous anatomical configurations, and accordingly, adapt to different environmental regimes. Over time, as skeletal variations are evolutionarily selected, the developmental pathways underlying them become channeled, and ontogeny and morphology evolve (Raff, 1996; Wagner et al., 2000).

Since primates are under constant selection throughout ontogeny, it is fitting to understand the prenatal developmental mechanisms partially underlying this morphological variation. Accordingly, it is essential to understand how limbs initially form, because not only does this embryonic process reflect adaptation, but it sets the "conditions" that shape future development. In this specific context, "conditions" refer to the molecular and cellular patterning events that lead to the construction of recognizable skeletal elements (Johnson and Tabin, 1997). By focusing on gene function during embryonic limb and girdle formation, developmental genetics research can aid in understanding these molecular conditions and pathways, the link between genotype and phenotype, how developmental processes shape (and are shaped by) morphological evolution, and ultimately, the origins of limb diversity. Moreover, with the emergence of Evolutionary Developmental (Evo-Devo) Biology (Gilbert et al., 1996) it is possible to gauge how developmental mechanisms evolve via comparisons of molecular mechanisms across both distantly and closely related taxa.

Over the past fifty years, several molecular mechanisms underlying vertebrate appendage (e.g., limbs, fins, etc.) development have become elucidated mainly due to research on experimental model systems such as the chick, mouse, and zebrafish (Niswander, 2003). Comparisons of appendage formation across these organisms reveal novel and important properties that are shared by most, if not all, vertebrates studied. To begin with, the appendage, whether it is a limb or fin, can be thought of behaving as a modular system and as is such possesses units or submodules that interact to drive its development and govern its function (Raff, 1996; see Chapter 2). For example, in all studied vertebrates, after forebuds and hindbuds emerge as paired lateral outgrowths of mesoderm (i.e., mesenchyme) capped by ectoderm, they acquire signaling centers (see Chapter 3) that regulate further appendage development. These signaling centers are often regarded to as submodules, which interact to give the appendage anterior-posterior (A-P; e.g., thumb to little finger), proximal-distal (P-D; e.g., shoulder to finger-tip), and dorsal-ventral (D-V; e.g., back of the hand to palm) axis asymmetries (Niswander, 2003; Tickle, 2003).

Another related property is that all vertebrates possess a limited number of conserved factors called *Homeobox* (*Hox)* genes that, via their influence on these signaling centers and the limb's mesenchymal cells, function to pattern the appendage's skeletal elements (Capecchi, 1997). For example, in mammals, *Hox* genes comprise approximately 39 members located in four clusters (HoxA, B, C, and D) on four chromosomes and encode transcription factors that regulate many developmentally critical genes (Krumlauf, 1994; Garcia-Fernandez, 2005).

Shortly after limb bud formation, they function in the formation of the major signaling centers (Zakany et al., 2004; Kmita et al., 2005).

Hox genes also function pene-contemporaneously in the limb to further compartmentalize appendages into several additional proximal to distal developmental submodules (see Chapter 2) that become under relatively discrete genetic control (Raff, 1996; Shubin et al., 1997; Zakany and Duboule, 1999). These submodules include the proximally positioned stylopod (i.e., upper-arm with humerus in forelimb; thigh with femur in hindlimb), an intermediate zeugopod (i.e., forearm with radius and ulna in forelimb; leg with tibia and fibula in hindlimb), and the distally located autopod (i.e., hand or manus with carpals, metacarpals, and phalanges in forelimb; foot or pes with tarsals, metatarsals, and phalanges in hindlimb) (Raff, 1996; Liem et al., 2001). In fact, different *Hox* genes have been demonstrated to pattern these submodules and their elements in compartmental-specific ways (Morgan et al., 1992; Dolle et al., 1993a-b; Small et al., 1993; Condie and Capecchi, 1994; Davis and Capecchi, 1994; Davis et al., 1995; Favier et al., 1995; Davis and Capecchi, 1996; Fromental-Ramain et al., 1996a-b; Mortlock et al., 1996; Goff and Tabin, 1997; Zakany et al., 1997; Wellik and Capecchi, 2003).

From an evolutionary perspective, the idea that several types of developmental submodules exist in the limb (e.g., its signaling centers and P-D compartments), are partially defined by Hox function, and become under relatively autonomous genetic control, suggests that evolution can shape their respective skeletal elements in separately heritable ways. Of course, as all of

these submodules arise during appendage outgrowth and act within the functioning limb, molecular mechanisms can also act ubiquitously across them to influence morphology (Raff, 1996).

Interestingly, despite the similarity that most vertebrates possess in limb development and skeletal patterning, evolutionary modification to Hox function and its effects on the limb's modularity may underlie several of their major morphological transformations. For example, *Hox* gene number and expression patterns differ between tetrapod limbs and fish fins, with such differences coincident with changes in signaling center interaction in tetrapods and their major innovation, the autopod (Sordino et al., 1995; Shubin et al., 1997; Hinchliffe, 2002). Another example includes the forelimb of the mouse and that of the bat, which during embryonic limb or wing development, respectively, possess different patterns of *Hoxd13* gene expression necessary for compartmental-specific growth (Chen et al., 2005; see Chapter 2).

These examples highlight that organisms have departed in some of the embryonic mechanisms utilized to generate appendages: an insight only possible when *Hox* function and expression was compared across these model and non-model organisms. Appropriately, it is becoming more evident that the conservation of genetic mechanisms need not always be the rule (Stopper and Wagner, 2005) and, in this respect, Evo-Devo can offer a way of interpreting evolutionary variation in appendage structure.

1.2 Evo-Devo and Understanding Mammalian and Primate Limb Diversity

The Evo-Devo approach can be extremely powerful when substantial developmental and genetic data are readily available on organisms being studied. This is perhaps why many of the initial Evo-Devo studies were performed using model organisms, such as mouse, chick, salamander, and zebrafish. Studies outlined by Stopper and Wagner (2005) have been able to demonstrate the utility of this comparative approach and provide insight into how morphologically dissimilar organisms have departed in the developmental genetic mechanisms used to construct their appendages (see Chapter 2). Interestingly, there has been a recent incorporation of non-model organisms in these comparisons. In a series of studies focusing on bats (e.g., Sears et al., 2006) and dolphins (e.g., Thewissen et al., 2006) the Evo-Devo approach has shed light on the major developmental and genetic changes that were necessary for these mammals to evolve their respective wing/leg and flipper morphologies.

Recently, it has been argued that Evo-Devo analyses between organisms at lower taxonomic levels (i.e., species, genus, and family) are possible, specifically, if well-defined and tested phylogenies and knowledge on the molecular and/or genetic mechanisms underlying morphological differences are ascertainable (Chiu and Hamrick, 2002; Stopper and Wagner, 2005). Indeed, such fine-grained analyses, while limited, have been successful in identifying genetic and developmental factors governing morphological diversity among several species of three-spined stickleback fish (Peichel et al., 2001; Shapiro et

al., 2004; Colosimo et al., 2005). With respect to understanding primate morphological diversity, Chiu and Hamrick (2002: 94) state:

> "While Evo-Devo research has focused primarily on broad taxonomic comparisons and major transitions such as that from fish fins to tetrapod limbs, its potential for explaining phenotypic differences between closely-related taxa is clearly recognized. In this context, understanding how molecular evolution shapes genetic variation of patterning and growth genes in different primate lineages can be a powerful method for linking genetic and developmental variation to phenotypic (morphological) variation at both the microevolutionary and macroevolutionary scales."

To date, only a handful of studies in Biological Anthropology have utilized this Evo-Devo approach to understand the origins and maintenance of morphological diversity in primates. While several obstacles have hindered progress in this direction (see Chapter 2) not all attempts at integrating developmental genetics into studies on primate evolution have failed. Several studies have explored the relationships between prenatal mechanisms of limb formation and the evolution of primate limbs (Lovejoy et al., 1999; Hamrick, 1999, 2001a, 2001b; 2002; 2003; Lovejoy et al., 2000, 2001; Reno et al., 2000, 2001; in press). Others (e.g., Dorus et al., 2006; Perry et al., 2006) taking a more strict evolutionary genetic approach have identified genes that have undergone relatively rapid evolutionary changes in specific primates, and have attempted to link such changes to phenotypic or morphological outcomes. These initial studies, and those performed on other mammals (see Chapter 2), provide important considerations for understanding primate limb evolution and the origins and maintenance of limb diversity; essentially they support the growing view that

changes in the genetic regulation and function of developmentally critical genes underlie species differences in morphology (Chiu and Hamrick, 2002).

1.3 *Cis* and *trans*-regulation, *Hox* genes, and the primate limb

An important consideration derived from the above work is that the evolution of morphology proceeds via the production and fixation of genetic variations in the *cis*- and *trans*-regulatory elements governing pre- and postnatal embryonic processes. Generally speaking, *cis*-regulatory elements refer to those non-coding DNA sequences (elements) that are contiguous and upstream of the structural-coding regions of genes, and that which control or influence the transcription of a gene located downstream of the element. Multiple *cis*-acting elements are typically found upstream of coding regions and it is believed that their individual or collective activation is important for allowing particular genes to be activated/repressed in specific tissues at exact times during development (Davidson, 2001). *Cis*-acting elements, in this context, confer a "specificity of action, or expression, on the focal protein to a specific cell type, tissue type, and time point in development" (Chiu and Hamrick, 2002: 100). *Trans*-acting elements are those participating in gene regulation at a greater genetic distance; usually these are transcription factors that bind DNA (Davidson, 2001). The arrangement of *cis*- and *trans*-acting elements in different organisms may vary as a result of mutations that accumulate and become fixed within these regions; the result of which can be unique spatial and temporal expression patterns of genes

and therefore functional differences in genes/proteins during development. Such modifications, which have been shown to occur in several cases (e.g., Peichel et al., 2001; Shapiro et al., 2004; Colosimo et al., 2005; Cretekos et al., submitted), can lead to phenotypic variations critical for evolutionary changes in morphology between species.

As mentioned earlier, *Hox* genes encode transcription factors that have been repeatedly shown in multiple model organisms to be critical for the formation of the limb and its skeletal elements. By way of their binding to the DNA of multiple target genes (reviewed in Moens and Selleri, 2006; reviewed in Svingen and Tonnisen, 2006), these transcription factors are thought to pattern the limb's skeletal elements, specifically by providing identity to cells in the early limb bud that eventually become skeletal elements (e.g., by specifying via positional information which embryonic cells form bones of the thigh versus leg). In addition, recently *Hox* genes have been shown to control growth of the limb, and in this context, they may control patterning via their purported control of cell proliferation (Duboule, 1995; Kmita et al., 2005). Indeed, their functional ablation in mice (and their experimental loss in other model organisms) has demonstrated these essential roles in forming different limb compartments along with maintaining growth of the limb bud.

Hox genes and their protein transcription factor products are thus part of the *cis*- and *trans*-regulation of many developmental processes, and it may be that evolutionary changes in these genes underlie appendage variation and morphological evolution within vertebrates, as previously exemplified among

higher level taxonomic comparisons between finned and limbed vertebrates (Sordino et al., 1995; Shubin et al., 1997; Hinchliffe, 2002). As potent regulators of skeletal morphogenesis, it is conceivable then to envision that changes in *Hox* genes underlie some of the primate limb variations mentioned above. Research has been conducted to identify variation in *Hox* structural-coding DNA sequences and protein homology across many different Metazoan taxa (Kappen and Ruddle, 1993; Kappen et al., 1993; Pendleton et al., 1993; Krumlauf, 1994). Interestingly, it has been demonstrated that *Hox* structural coding DNA sequence and protein homology is quite conserved across all mammals, and consequently, it is difficult to explain how primate morphological diversity can result from such strong genetic conservation.

On the other hand, as primates vary in the timing and duration of many pre- and postnatal developmental processes, it is highly probable that their limb diversity is generated at the level of *Hox* gene regulation (i.e., when these genes are activated/inactivated and how their protein products are used by embryonic cells). In other words, that changes in the *cis*- and *trans*-regulation of *Hox*, rather than in *Hox* structural coding regions, underlie evolutionary differences in limb morphologies, because such changes would translate into modifications in Hox function during cell proliferation, differentiation, and the specification of cellular identity. By altering these and other cellular behaviors, modifications in submodule interactions (e.g., between signaling centers or in the limbs three main compartments) could occur in the developing limb, or vice versa. This situation could essentially be possible if organisms harboring genetic variants in

cis- and/or *trans*-regulatory elements arose in specific populations and became fixed overtime. Unfortunately, at this time, little knowledge on the *cis*- and *trans*-regulation of *Hox* is available, and what is known is covered in Chapter 3.

1.4 Hox cofactors and *Pbx* genes

It is becoming increasingly clear that for Hox transcription factors to function efficiently and selectively on target DNA sequences, that they must interact with partner proteins called cofactors (reviewed in Moens and Selleri, 2006). Cofactors increase the DNA binding affinity of Hox proteins to target genes and therefore help *Hox* execute their genetic programs (Mann, 1995; Mann and Chan, 1996; Mann and Affolter, 1998). In this context, cofactors cooperate with Hox in *cis*- and *trans*-regulation of many target genes. In some developmental contexts, cofactors work directly with Hox proteins to autoregulate and crossregulate *Hox* gene expression (Popperl et al., 1995; Maconochie et al., 1997; Jacobs et al., 1999; Ferretti et al., 2000). In this respect, cofactors are part of the *cis*-regulatory system for *Hox* mentioned above.

One important group of Hox cofactors is the Pre-B cell leukemia transcription family (Pbx) of Triple-Acid Loop Extension (TALE) homeodomain proteins (Burglin, 1997; 1998). The first representative of this group to be discovered was that of *Extradenticle* (*Exd*) in *Drosophila* (Peifer and Wieschaus, 1990; Rauskolb et al., 1993; 1995). The vertebrate homolog of *Exd* is *Pre-B cell leukemic factor 1* (*Pbx1*) named according to its discovery as part of a t (1:19) chromosomal translocation leading to human pre-B cell acute lymphoblastic

leukemia (Kamps et al., 1990; Nourse et al., 1990; Rauskolb et al., 1993). Subsequently, three other *Pbx* genes have been discovered in mice (*Pbx2-4*) (Monica et al., 1991; Wagner et al., 2001) and, in general, studied vertebrates possess at least two members of the *Pbx* gene family (reviewed in Moens and Selleri, 2006).

Pbx proteins function broadly during vertebrate embryogenesis and also as more recently demonstrated in postnatal life (Sarno et al., 2005; reviewed in Moens and Selleri, 2006). Like Exd, members of these families have been shown to bind Hox transcription factors and augment their DNA binding affinity. Indeed, the experimental deletion of Pbx protein in specific developmental contexts either partially and/or nearly completely phenocopies the deletion of their Hox partners (reviewed in Moens and Selleri, 2006). While many of the roles of Pbx involve cooperation with Hox, Pbx has also more recently emerged as having Hox-independent functions during embryogenesis. All of these results reiterate the importance of both Pbx and Hox in regulating developmental processes.

The examination of several aspects of *Pbx* gene sequence, number, expression, and protein functionality across studied Metazoan model systems to date has yielded some interesting findings. First, *Pbx1* and its ortholog *Exd* are extremely conserved in their genetic sequence and encode proteins capable of being interchanged in biochemical assays. Second, *Pbx1* (or its orthologs) is found in all studied model systems, while other members of *Pbx* (e.g., *Pbx2-4*) are variably present. Third, these other members (e.g. *Pbx2-4*) display less (but

still significant) sequence homology with *Pbx1/Exd* but among them share strong homology in different organisms and are capable, as proteins, of being interchanged in biochemical assays. Fourth, *Pbx1/Exd* is for the most part expressed in similar tissues or in tissues giving rise to analogous organs in different organisms (reviewed in Moens and Selleri, 2006). Unfortunately, to date little is known about the expression of the other *Pbx* members in model systems (see Chapter 3).

The fact that *Pbx* are evolutionarily conserved across Metazoans indicates that changes in the structural coding regions of these genes may not necessarily account for, or underlie, evolutionary changes in *Pbx* function (and therefore morphogenesis) between biological organisms. However, this situation does depend on at least two aspects of *Pbx/Exd* study: 1) the requirement that more taxa are examined to determine if this degree of conservation persists; and 2) the requirement that *cis* and *trans*-regulatory elements of *Pbx* are explored in depth. With respect to this latter point, if differences in *cis*- and *trans*-regulatory control of *Pbx* are identified between organisms, then they could influence morphology specifically if they underlie changes in the timing and spatial extent of *Pbx* gene expression. Unfortunately, upstream regulatory regions of all vertebrate *Pbx* genes are unknown at present. In this regard (and at this point in time), the study of *Pbx* presents some of the same obstacles as the study of *Hox* regulation and how such underlie evolutionary changes in morphology.

However, given all of the above findings, and specifically, that Pbx and Hox proteins form dynamic complexes to regulate developmental gene

expression, it may be that evolutionary changes in Pbx and Hox function result from organismal differences in: 1) the numbers of individual *Pbx* members present; 2) the expression patterns of those orthologous *Pbx* members present (i.e., expression of *Pbx1* in different organisms); 3) the expression patterns of and between homologous family members (i.e. expression of *Pbx1* versus *Pbx2* in different organisms); and 4) the degree of functional redundancy versus discrete functionality between different *Pbx* family members during embryogenesis.

With respect to these points, what is currently known about *Pbx* gene expression and protein function largely derives from several studies on individual *Pbx* gene loss in different model systems (see Chapter 3). The primary work on understanding individual *Pbx* family member roles during mammalian embryogenesis comes from using single genetic "knockout" mice for individual *Pbx* family members. Briefly, in the "knockout" strategy, critical exonic DNA regions of genes are excised experimentally during homologous recombination, resulting in dysfunctional gene sequences and the complete lack of functional protein production. Licia Selleri, during her tenure at Stanford University, systematically "knocked-out" three of the four *Pbx* genes in mice (*Pbx1*, *Pbx2,* and *Pbx3*) (Selleri et al., 2001; Rhee et al., 2004; Selleri et al., 2004), while other experiments by Hieke Popperl have lead to the production of *Pbx4* "knockouts" (Wagner et al., 2001). To note: in general, *Pbx1* "knockout" mice, for example, are hereafter referred to as *Pbx1* null or *Pbx1*$^{-/-}$ mice, as both alleles for the *Pbx1*

gene have been experimentally deleted using the “knockout” gene targeting strategy.

The results of these “knockout” studies have provided some interesting insights into limb and girdle formation in mammals (discussed at greater length in Chapter 3). Briefly, *Pbx1* null embryos have proximal limb and girdle defects including alterations to the scapular blade and pelvis, fusions of the humerus and femur to their respective girdles, as well as a series of axial and craniofacial malformations. These limb defects correlate well with the loss of *Pbx1* from its known expression in proximal domains and also with those alterations of *Hox* genes believed to specify these same skeletal elements (Selleri et al., 2001). For example, compound mutant *Hoxa9/Hoxd9* (Fromental-Ramain et al., 1996a) and *Hoxa10/Hoxd10* (Wahba et al., 2001) embryos have dysmorphologies in humeral/femoral (i.e., stylopodial) skeletal domains, roughly equivalent to those revealed in *Pbx1* null embryos. Interestingly, despite being expressed in limb tissues, single *Pbx2* (Selleri et al., 2001) and *Pbx3* (Rhee et al., 2004) null mice do not exhibit limb or girdle defects and also survive at least until post-parturition. *Pbx4* mice also lack limb or girdle defects and survive, but *Pbx4* is strongly expressed only in the developing testes of the mouse (Wagner et al., 2001). These latter findings indicate that, alone, mouse Pbx2-4 proteins are not required for normal vertebrate limb and girdle patterning and skeletogenesis. However, this does not exclude the possibility that they cooperate in developing limbs and girdles to govern development and that loss of any one Pbx may be co-opted functionally by another.

1.5 The study

To date, no known published study has focused on whether functional redundancy exists between *Pbx* family members, *in vivo*, and if and how they govern limb and girdle morphogenesis. Given that vertebrates possess multiple *Pbx* genes each of which share strong sequence identity (reviewed in Moens and Selleri, 2006) and additionally encode proteins that can be interchanged in biochemical *in vitro* assays (Chang et al., 1995) it is critical to study this possibility. Furthermore, if evolutionary changes in morphology result from *cis*- and/or *trans*-regulatory changes in *Pbx* and/or *Hox*, then an understanding of *Pbx* genetic interaction during embryogenesis is essential. The study of *Pbx* genetic interaction during limb and girdle development would more clearly identify their important cooperative versus independent roles and reveal their functional complexity in the development of these structures. In addition, if understood via their interaction (or lack thereof) with Hox proteins, then such a study would facilitate a comprehension of how modification of Pbx/Hox function drives limb and girdle evolution specifically in lieu of the modular design of the limb, its submodules, and its functional and developmental interconnection with the girdle.

Therefore, this thesis examines whether selected *Pbx* genes overlap functionally during mouse limb and girdle development and accordingly represents a first study on their differential and/or cooperative roles during any developmental process *in vivo*. By doing so, it serves an initial exploration into

the complex links between *Pbx* gene presence and/or absence (compound genotype) and resulting phenotype, and thus provides a backdrop upon which to interpret evolutionary changes in morphology. In this respect, the concurrent loss of *Pbx1*, *Pbx2,* and *Pbx3* is examined in embryos to identify how they collectively govern limb and girdle morphogenesis. Briefly, in this study single mutant *Pbx* mice (i.e., $Pbx1^{+/-}$, $Pbx2^{+/-}$, or $Pbx3^{+/-}$) are utilized to generate compound *Pbx* mutant embryos (e.g., $Pbx1^{-/-}$;$Pbx2^{+/-}$ or $Pbx1^{-/-}$;$Pbx3^{+/-}$) to study the contributions of different *Pbx* family members to the development of these structures.

The methodological basis for this work comes from the fields of Anatomy, Anthropology, Developmental Biology, Evolutionary Biology, Genetics, and Molecular Biology and as such explores *Pbx* loss from multiple perspectives. On one level, *Pbx* loss during mouse limb development is viewed in terms of gross morphology and anatomy, while on another level, the molecular and genetic events underlying the developmental biology of *Pbx* compound mutants are assayed. Concomitantly, the findings are interpreted via an evolutionary anthropological framework to cast light on how vertebrate (and specifically, primate) appendages evolve.

These levels of analysis, therefore, allow for an operational understanding of the links between genotype and phenotype, a connection that is critical for deciphering how evolutionary changes in morphology are determined by variations in the timing, spatial extent, and functionality of genes during embryogenesis and postnatal life. In so doing, it provides the basis for the future

assessment of whether intra-specific differences in *Pbx* gene dosage, expression, gene number, and *cis*- and *trans*-regulation, are able to generate morphological variations. Furthermore, such a study should also impinge on how Hox functionality is envisioned, given Pbx's roles as Hox cofactors.

Overall, these studies will shape the understanding of how morphological diversity is generated, evolutionarily, especially since the limb's and girdle's skeletal elements develop under *Hox* influence in relatively discrete, genetic controlled autonomous modules that still remain developmentally linked. As there are also Hox-independent Pbx functions, an understanding of them can also shape the perception of how appendage evolution proceeds via changes in Pbx-dependent (non-Hox dependent) developmental systems. Ultimately, understanding Pbx and Hox function during limb and girdle development should provide some insight into how *cis*- and *trans*-regulatory differences in these genes underlie some of the skeletal morphologies that have arisen among different primates (e.g., between gibbons and other apes).

1.6 Thesis structure

This thesis is divided into eight chapters with one appendix. Besides this introduction, each of the remaining chapters examines the ways limbs and girdles form, evolve, and are affected by the loss of developmentally critical genes. Chapter 2 (Developmental Basis for Limb and Girdle Evolution) introduces important evolutionary concepts involved in studying the appendage

from an Evo-Devo perspective and discusses several ways that this approach has influenced the understanding of mammalian and primate limb and girdle evolution. Chapter 3 (*Pbx* and *Hox* genes and the Development of the Limb and Girdle) first provides a review of the histomorphogenesis and molecular control of embryonic limb development by addressing the following questions: 1) How are limbs initiated to form? 2) How are the initial P-D, A-P, and D-V axes of limbs formed? 3) How are these axes maintained during limb bud outgrowth? 4) How do skeletal elements become specified and determined? Next, this chapter also serves as a review on scapular and pelvic girdle development. As *Pbx* genes appear involved in many developmental processes, this backdrop on the limb and girdle is necessary for understanding their functions during the development of these structures. In addition, a review of Hox and Pbx functions to date is provided and serves as an additional level of knowledge upon which to understand limb and girdle development and their evolution. In summary, the first three chapters provide reviews on topics of evolution and development.

Chapter 4 (Experimental Methods) focuses on the experimental protocols utilized during the data collection stage of this thesis research. This chapter provides the backdrop upon which to understand how the assessment of *Pbx* gene function during limb and girdle development was carried out and in addition, how and why particular strains of mice were utilized in these studies.

Chapter 5 (*Pbx1* and *Pbx2* Are Required for Distal Limb Patterning via Their Hierarchical Control of *Hox* Spatial Distribution and *Shh* Expression) presents the first of three data chapters that analyze *Pbx* roles during limb and

girdle development. This chapter highlights how the expression of *Pbx1*, *Pbx2,* and *Pbx3* in limb bud mesenchyme sets the stage for their functional loss in compound *Pbx* mutant mice. By specifically focusing on *Pbx1* and *Pbx2* and compound mutants of these two genes, it is shown how their experimental loss results in extreme limb defects, such as the loss of limbs, and what their roles are during appendage development. Specifically, they are shown as upstream hierarchical regulators of *Hox* gene expression during limb development and by doing so, act to initialize the expression of *Sonic hedgehog* (*Shh*) in the limb. *Shh* is a major factor that drives both the proper formation of limb bud axes and digit element number and identity (Riddle et al., 1993; Chiang et al., 2001). In this manner, *Pbx* are thus shown to be upstream of several important submodules within the developing limb. Also in this chapter, several additional studies are presented that highlight how *Pbx* in different genetic backgrounds (i.e., different strains of mice) may function to generate limb variation and diversity. These data are then reinterpreted in Chapter 8 from an Evo-Devo perspective.

Chapter 6 (Differentiating *Pbx* Ectodermal Versus Mesenchymal Roles During Limb Development) represents the second data chapter geared towards understanding the roles that different *Pbx* genes have during limb development. This chapter begins with novel expression patterns of *Pbx* in the limb ectoderm and then presents data on the complete experimental deletion of *Pbx1* and *Pbx2* from the limb and its consequences for further understanding initial limb bud outgrowth. It next focuses on the alterations of gene expression in the

mesenchyme versus the ectoderm, and its ramifications on understanding their potential functions during limb formation. Accordingly, it presents preliminary findings on the conditional inactivation of *Pbx1* (on a *Pbx2* null background) in the limb ectoderm and mesenchyme and draws some conclusions on the differential roles of *Pbx* family members during limb formation. In brief, the data presented in this chapter indicate that Pbx function is predominantly early during the initial periods of limb outgrowth, where they influence the expression of genes in the mesenchyme and ectoderm. In this respect, *Pbx* represent important genes involved in regulating epithelial (ectodermal)-mesenchymal interactions critical for limb outgrowth. These data are then reinterpreted from an evolutionary perspective in Chapter 8.

Chapter 7 (*Pbx* and the Development of the Pectoral and Pelvic Girdle) focuses on scapular and pelvic girdle formation in compound *Pbx* mutants for all three “girdle” expressed *Pbx* genes (*Pbx1*, *Pbx2*, and *Pbx3*). Accordingly, this chapter begins by demonstrating that *Pbx* overlap in expression in multiple tissues (i.e., proximal anterior limb, somatopleure, ectoderm, and dermomyotome) that are critical for the formation of both girdle structures. Next, it focuses on morphological analyses on the pectoral girdle phenotypes of different compound *Pbx* mutants and thus provides a basic understanding of how *Pbx* cooperate during scapula formation, i.e., *Pbx1* synergizes with *Pbx2* and/or *Pbx3* to govern scapula patterning and morphogenesis. Coupled with this morphological analysis is a molecular characterization of the compound *Pbx1;Pbx2* mutant girdle phenotype. Studies in this section demonstrate that

specific genetic pathways are affected by the loss of *Pbx*, and that in general, *Pbx* appear to reside upstream of most known developmental pathways regulating scapula patterning and morphogenesis. Finally, in subsequent sections of this chapter, a similar analysis and conclusion was reached for the pelvic girdle. These data are then reinterpreted in Chapter 8 from an Evo-Devo perspective.

Chapter 8 (Conclusions and Evolutionary Implications) re-examines the findings from the previous three chapters in an evolutionary context. It discusses the implications of the novel findings of *Pbx* cooperative involvement in limb and girdle development to the understanding of Hox function, modularity, and the evolution of vertebrate, specifically mammalian and primate appendage. In this context, it readdresses some of topics introduced in Chapters 2 and 3 but more specifically using the knowledge gained on the studies conducted in this thesis. With specific importance to understanding primates and the evolution of their limb and girdle diversity, it discusses several ways of how knowledge on *Pbx* functionality impinges on how morphological diversity is generated in more fine-grained or lower taxonomic levels. Coupled to this discussion, are points of interest regarding the functional and developmental autonomy versus integration of the vertebrate, specifically primate, limb and girdle. Therefore, it also reemphasizes how concepts of evolutionary biology are impacted by knowledge from developmental biology and model systems. Included at the end of the chapter is a brief comment on future directions.

Appendix I provides a list of the probes used in this study and those researchers who have kindly provided them.

Chapter 2: Developmental Basis for Limb and Girdle Evolution

2.1 Introduction

The skeletal morphology of an adult organism depends upon the interplay between pre- and postnatal developmental processes as well as the functional demands placed on the organism throughout its ontogeny. Much focus in Biological Anthropology has historically been on either postnatal developmental mechanisms governing primate skeletal morphology or functional aspects of the primate skeleton (Fleagle, 2001). On the other hand, little research has been conducted on how prenatal developmental mechanisms influence postnatal skeletal morphology and its evolution in primates. Those studies that have been conducted and which are discussed in this chapter are the focus of the modern field of Evolutionary Developmental (Evo-Devo) Biology (see Gilbert et al., 1996).

The principle goal of Evo-Devo, as summarized by von Dassow and Munro (1999), is to understand how morphological diversity results from evolutionary adaptive diversification in developmental mechanisms. Accordingly, the genetic, molecular, cellular, and histological architecture of developmental systems can be analyzed to identify whether specific properties of the system confer evolvability to a particular morphology, particularly since morphologies result from complex interactions that occur among these levels during development. With respect to understanding the evolution of mammalian, specifically primate limbs, Hamrick (2001a: 361) refines this focus as the identification of “the genetic interactions during pattern formation that confer

evolvability of morphogenetic fields such as the limb." In this case, understanding how pattern formation ensues should provide insight into how this complex process permits or constrains the evolution of primate limbs.

The focus of the research presented in this dissertation is on the function of *Pbx* genes during appendage development and more specifically on how their function impinges on the understanding of pattern formation in the limb and girdle. As Pbx proteins are often regarded as Hox-cofactors, and Hox are crucial for patterning the limb (and girdle), deciphering Pbx function will improve our understanding of those genetic interactions that occur during pattern formation. Additionally, these data, if evaluated from an evolutionary perspective, will also elucidate how evolvability is conferred to developing appendages and their segments.

In the context of this aim, this chapter introduces several key Evo-Devo principles and discusses the importance of utilizing data from the Evo-Devo perspective. Since most of the studies to date have not been on primates, those focusing specifically on mammals, and when possible on primates, are discussed below. These studies will not only illustrate this novel perspective, but also will provide an evolutionary framework for the developmental studies presented in this dissertation.

2.2 Evolutionary-developmental approaches to the study of the limb

Mammals exhibit tremendous variation in their appendage morphologies; comparing for example a bat wing, a dolphin flipper, and a horse forelimb (Liem

et al., 2001). Much of this diversification is readily identifiable across the three main developmental axes of the appendage. For example, the bat wing, consisting mainly of the posterior four digital elements, has been expanded anterior-posteriorly to aid in flight, while the distal limb of a horse has been reduced in this dimension and consists of one truly functional weight-bearing digital ray. Additionally, the bat wing has been expanded along the P-D axis through increases in the lengths of each of the metacarpal and phalangeal elements, whereas in dolphins, P-D length increases result from the addition of phalangeal elements typically to the central two digits of the flipper (Vaughan et al., 2000).

During embryogenesis, each axis lies under the molecular control of several signaling centers (see below), which via their effects on these axes, function to pattern the skeletal elements of the limb. The current dogma in developmental biology is that these signaling centers accomplish this patterning through the assignment of positional information (PI) to cells (Wolpert, 1969), which come about via long- and short-range signaling molecules coming directly from or being influenced by these centers (reviewed in Tabata and Takei, 2004). Cells that are exposed to or assigned PI along these three cardinal axes, then execute or interpret this information through differentiation into specific cell types at exact times and spatial locations. Throughout mammalian evolution these signaling centers and their roles in axis specification have been modified, resulting in alterations to PI and thus patterning changes to skeletal elements

(Lovejoy et al., 1999) within the limb's three major compartments: the stylopod, zeugopod and autopod (see Chapters 1 and 3).

Studies on the molecular basis of each of these limb compartments have led to the idea that part of the patterning of skeletal elements is specific to each and is accomplished by "patterning genes" such as *Hox* genes (See Chapter 3). For example, mutations in specific *Hox* genes result in compartmental-specific skeletal alterations (e.g., Capecchi, 1997), likely via altering target genes specific within these domains (Davis and Capecchi, 1996; Salsi and Zappavigna, 2006). At the same time, *Hox* gene expression and function has been shown to be critical for the formation of P-D and A-P limb's primary axes (Zakany et al., 2004; Kmita et al., 2005) and thus skeletal abnormalities occurring from Hox loss of function may result from alterations in PI, either directly or indirectly. Overall, given that these compartments (and their respective elements) arise under the influence of both early signaling centers and later compartmental-specific genetic networks, pattern formation is a dynamic process and resultant morphology should be considered as a read-out of both processes (Lovejoy et al., 1999).

Indeed, intense interest in the field of limb development has recently been on understanding the interrelationships between axis specification, PI, and skeletal element patterning within and between compartments. For example, a recent review by McGlinn and Tabin (2006) discusses some of these interrelationships, specifically for the formation of the digits of the autopod. In light of the current studies on limb development as well as the dynamic nature of

skeletal element specification, a growing perspective in the Evo-Devo community is that the limb and its components behave as a modular system (Raff, 1996).

2.3 Modularity, developmental genetics, and limb evolution

Modularity refers to the idea that organisms and their morphologies can be compartmentalized into basic building blocks (i.e., modules or modular units) that in the context of development are distinctive in their: genetic and autonomous specification; hierarchical organization; interactions with other modules; spatial location; time of occurrence; and capability to dynamically change (Raff 1996). Von Dassow and Monroe (1999: 313) define a developmental module as "a collection of elements whose intrinsic behaviors and functional interactions yield a mechanistic explanation of an identifiable developmental process or transformation." In both definitions, it is readily apparent that the concept of modularity (and thus the division of an organism or its morphology into developmental modules) is a heuristic device, geared towards identifying how evolvability is conferred to developmental systems. The limb bud can be thought of as a modular system specifically with respect to each of the properties identified above.

The first property of a module is that it is a unit of developmental action that is considered genetically autonomous (Raff, 1996; Schlosser and Wagner, 2004). Limb buds can be argued to possess this property as they contain the intrinsic molecular information necessary to regulate their own development. For example, once the bud is induced, its subsequent development is relatively self-

contained with the specification of its skeletal elements dependent on intrinsic genetic patterning information. The degree of self-containment is supported by the findings that if the proper signal is provided to the flank of an embryo, a limb will be induced to form with all skeletal elements (reviewed in Niswander, 2003).

Developmental modules also possess the property subcompart-mentalization or submodularity, whereby the functional components of the module are hierarchically arranged into submodules that interact (Raff, 1996). The limb's submodules can be operationally defined, albeit not easily. For example, each of the limb's three main compartments, the stylopod, zeugopod, and autopod, can be thought of as submodules, if they possess a genetic specification that is relatively autonomous and also a functionality that contributes to the overall operation of the limb (see Chapter 3 for a more detailed discussion). Similarly, the unique patterns of *Hox* gene expression and target specification during limb development can also be thought of as submodules. In this respect, Reno et al. (1999; in press) has defined several submodules for the primate zeugopod and autopod, as the development of skeletal elements in these domains appears to relate to specific *Hox* gene expression patterns and activity (see below).

Traditionally, those signaling centers that drive limb formation and that which have both direct and indirect effects on the specification of limb's skeletal elements are thought of as submodules. These signaling centers include the zone of polarizing activity (or ZPA) in the posterior of the limb bud, the apical ectodermal ridge (AER) along the distal limb tip, the dorsal ectoderm (DE) and

also the progress zone (PZ) or cellular zone subapical to the AER. Each of these centers and their importance to limb bud development are shown in Figure 3.5. For now, these submodules have been shown to interact during limb development (reviewed in Niswander, 2003) and thus are part of several autonomous molecular and genetic loops that comprise the limb developmental module. In addition, they are hierarchically arranged in a manner that reflects their spatio-temporal action on limb development.

The idea that the limb's signaling centers spatially and temporally act during development indicates another property of a module. As modules (and their submodules) operate during development they exist transiently at a particular time and space during ontogeny, although their influence on morphology is long lasting. While some modules may exist diachronically (e.g., consider a cell type such as an adult stem cell), most exist briefly and in specific anatomical regions to execute their genetic effect. It is not to say that modules cannot be ubiquitous in location (i.e., exist in multiple places), but many developmental modules are spatially determined and have a physical reality. For example, the limb and its signaling centers display this property. The ZPA and AER submodules are transient structures that are required to persist in specific anatomical regions and only during limb morphogenesis. Even the limb bud proper is a transient structure with submodules that have specifically evolved to drive the morphogenesis of the bud itself. In this manner such regulative development allows for the bud to progress and eventually lead to the specification of the limbs major skeletal elements. It is interesting to consider

that many of the mechanisms responsible for maintenance of limb bud outgrowth and axes determination proper may have evolved initially for this purpose in early chordates and that subsequently these mechanisms were co-opted for the patterning of skeletal elements in vertebrates.

Another property of modularity is that of the interconnectivity among its submodules as well as among modules themselves. The limb's submodules are highly integrated and critical to limb bud outgrowth and skeletal patterning. For example, as discussed in detail in Chapter 3, the maintenance of the AER during limb bud formation requires signals from at least two submodules, the ZPA and DE. With respect to the interaction between modules, genetic actions from one module may trigger changes in developmental gene expression patterns in another. In this way, even developmental modules are nested for functional integration. For example, the fact that limb buds are induced to form off the body wall reflects the degree of integration between the early limb bud and body wall modules.

Developmental modules also possess the capacity for developmental plasticity or flexibility. This flexibility affords the module the ability to change during development, and via changes in their underlying genetic networks, over the course of evolution. The ability of a module to change developmentally or to evolve (its evolvability) is directly contingent of the genetic structure of its submodules and their interaction. As changes in the genetic structure of organisms underlie their evolution it becomes apparent that one can view the evolution of morphology as the evolution of modular systems.

Given that the limb can be thought of as modular system it is important to consider how its modularity facilitates or constrains the evolution of the limb and its components. In this context, understanding the evolution of the limb skeleton is critically tied to deciphering the manner in which the limb's submodules have integrated and changed in their interaction over the course of vertebrate history (i.e., one major task of Evo-Devo). Different vertebrates have undoubtedly experienced alterations in the interactions between submodules as well as changes within the submodules, themselves. These changes are critically tied to *cis*- and *trans*-regulatory changes in gene expression and protein function. Several examples are provided below that highlight how evolutionary changes in gene regulation alter modular and submodular interaction of the limb and therefore drive (and reflect) adaptive specializations in morphology.

2.4 Studies across vertebrate classes

In a recent comprehensive comparative analysis, Stopper and Wagner (2005) reviewed numerous studies on limb developmental biology for several model and non-model organisms spanning different classes of vertebrates (e.g., anurans, urodeles, reptiles, and mammals). Their comparisons, while performed at the level of the vertebrate class and not at lower taxonomic levels (i.e., family, genus or species), shed light on some novel aspects of limb evolution and developmental biology in different vertebrates and highlight (as well as introduce) several important Evo-Devo concepts.

In the following chapter, a background on limb development is provided that focuses on the mechanisms governing limb outgrowth, the onset of axes formation in the limb, the maintenance of these limb axes, and also the specification of skeletal elements. Stopper and Wagner (2005) demonstrate that vertebrates display some substantial variations in the molecular control of these events during limb development. Of particular importance is that their comparisons have revealed differences in the molecular control of the P-D, D-V, and A-P axes (and their underlying signaling centers) responsible for patterning the limb skeleton. Accordingly, it is changes in these axes that underlie alterations in the modular organization of the limb.

Interestingly, many of these variations occur prior to, or during, the period of limb development typically referred to as the "phylotypic" stage. This stage is often characterized by the initiation and early development of the limb bud prior to chondrogenesis (Raff, 1996). A current view is that evolutionary changes in the limb across many vertebrates have their basis in *cis*- and *trans*-regulatory changes occurring in stages after this phylotypic stage, that is during chondrogenesis (Reno et al., in press). However, Reno et al. (in press) as well as other studies by this group (Lovejoy et al., 1999; 2003) also argue that the assignment of PI, via the action of patterning genes during the "phylotypic" stage, is critical in the process of morphological development and that changes in PI can drive evolutionary changes in the skeleton. As will be explored in Chapter 3 and the remainder of this thesis, the assignment of PI is critically tied to the development of the limb's axes and therefore the interaction of its submodules.

Stopper and Wagner (2005) have demonstrated specific differences between several classes of vertebrates with respect to the stage of limb initiation. For example, an important limb-initiating factor, the *T-Box related* (*Tbx*) gene *Tbx3* shown in chicks to influence to location of limb bud formation (Rallis et al., 2005), has no affect on the axial level where limbs form when removed experimentally from mice (Davenport et al., 2003). Therefore, between birds (reptiles) and mammals, molecules controlling axial level appear to have been modified.

With respect to limb identity (i.e., whether a limb field becomes specified to form a forelimb with identifiable forelimb elements or a hindlimb with identifiable hindlimb elements), functional divergence is present for two genes controlling identity between anurans, urodeles, reptiles, and mammals. For example, in the chick, forelimb and hindlimb identity is partially determined by the expression of *Tbx5* and *Tbx4*, respectively (Logan et al., 1998; Rodriguez-Esteban et al., 1999; Takeuchi et al., 1999), while in the mouse, this specific *Tbx* expression is critical only for the initiation of limb outgrowth and not identity (Minguillon et al., 2005). In this manner, distantly related taxa have acquired different ways to achieve limb identity and to initialize outgrowth despite having limbs that share fundamental similarities in their organization (i.e., both possess all three axes, the same three signaling centers, and possess homologous skeletal elements in each P-D compartment).

In terms of P-D axis specification, several molecules responsible for its development and outgrowth have functionally diverged. For example, *Fibroblast*

growth factor gene *Fgf8* a major P-D outgrowth gene expressed in the AER of chick (Mahmood et el., 1995; Vogel et al., 1996) and mouse (Crossley and Martin, 1995; Xu et al., 1998) is only minimally expressed in AER tissues of anurans (Christen and Slack, 1997) and urodeles (Han et al., 2001). Furthermore, in urodeles, expression has been heterotopically shifted to the underlying mesenchyme and concurrently fades in the distal epidermis above the digits. Finally, even the AER is not necessarily formed in urodeles (Sturdee and Connock, 1975; Tank et al., 1977), some anurans (Richardson et al., 1998), and some reptiles (i.e., studied snakes; Cohn and Tickle, 1999) while in most reptiles (Raynaud and Pieau, 1985) and all studied mammals (Sedmera et al., 1997a-b) limb AER is critical for P-D outgrowth.

The genes regulating D-V axes formation and identity have become functionally divergent between several of the studied taxa. The *Wingless related* gene *Wnt7a* (or its homolog) is required in both chicks (Dealy et al., 1993; Rodriguez-Esteban et al., 1997) and mice (Parr et al., 1993; Kimmel et al., 2000) to govern dorsal identity of the forming limb. Specifically, in these model organisms *Wnt7a* is present only in the dorsal ectoderm where it functions to drive the expression of dorsalizing mesenchymal genes such as the *LIM homeobox transcription factor Lmx1b* (Chen and Johnson, 2002). In anurans, *Wnt7a* is present throughout both the ectoderm (both dorsal and ventral) and mesenchyme and does not function directly in dorsal identity (Christen and Slack, 1998).

Likewise, genes expressed in the A-P axis appear to have functionally diverged in different taxa. As a posteriorly expressed gene in the limb bud, *Sonic hedgehog* (*Shh*) is linked in mammals (Chang et al., 1994) and chicks (Riddle et al., 1993) to the ZPA and the specification of posterior digit identity and number (reviewed in Tabin, 2006). In several anurans (Endo et al., 1997; Hanken et al., 2001) and urodeles (Imokawa and Yoshizato, 1997; Torok et al., 1999), as in mammals and reptiles, this gene is present, although in the first two taxa there are some changes in the proximal extent of its expression. What is also important is that in some anurans (Endo et al., 1997), polarizing activity (see Chapter 3) and *Shh* expression are not completely correlated as they have been shown in mice and chick suggesting that tissue competence and its ability to generate pattern may rely on additional factors or redundant factors operating with (or without) *Shh*.

With respect to pattern formation, digit number and identity is partially determined by *Hox* gene expression during autopodial formation. *Hoxa13* expression coincides with the distal phalangeal extension of the digits in anurans (Lombardo and Slack, 2001) while in chick, for example, the expression of *HoxA* genes have not yet been reported for this period. Functional studies on mice indicate that *Hoxa13* null mice have digital defects although the expression of this gene normally occurs in the interdigital and peridigital tissue fields (Knosp et al., 2004; Reno et al., in press). These data suggest that *HoxA* genes have been utilized differently by evolutionary distinctive taxa to drive digit formation (Stopper and Wagner, 2005).

These analyses performed by Stopper and Wagner (2005) shed light on the great diversity in developmental mechanisms underlying limb outgrowth and skeletal patterning of the appendage's three compartments. Such understanding of diversity is critical for many reasons. For example, Stopper and Wagner (2005: 3) state that: "data on extant developmental mechanisms from multiple taxa can be used to reconstruct ancestral mechanisms of limb development for all tetrapods, or any clade within tetrapods, and thus help reveal the changes in developmental mechanisms associated with the origin of the limb and evolutionary transitions in limbs within tetrapods." They also indicate that developmental mechanisms themselves can be taken as characters in phylogenetic analyses and can used to understand the ontogenetic processes that have been the basis of evolutionary transformations in morphology.

With respect to this last point, based on their studies, these authors develop a two-part classification for the typology of morphology characters. There are those formed by core mechanisms and those formed by ancillary mechanisms. Core mechanisms consist of those developmental processes that are essential for morphological character identity, while ancillary mechanisms are those that are unessential to the process of character development but can change overtime due to natural selection with little or no phenotypic outcome. Accordingly, they argue it is possible that specific developmental processes are "unmodifiable" and in this way constrained by their essential roles during limb development.

Selection for the genetic networks that underlie character formation can also be thought of in terms of modularity and their "mechanisms." Core mechanisms may consist of the refined genetic and molecular interactions that occur between developmental submodules of the limb; and insofar that the limb and its specific morphology are under positive selection, specific-interactions between these submodules ensure the presence and perpetuation of these core mechanisms. It may well be that heterochronic shifts in evolutionary morphology result from altering the timing of these interactions within submodules and thus the effectiveness or "integrated-ness" of core mechanisms, rather than resulting in the complete loss or abrogation of the core mechanisms themselves. Heterotopic shifts in morphology, may reflect the co-option of new submodules and the genetic and molecular mechanisms typically not utilized by these tissues (i.e., ancillary mechanisms). The result of both of these circumstances is that core mechanisms may not be lost between taxa but only restructured temporally and spatially during ontogeny. On the other hand, if a particular morphology is selected against or an alterative pathway is under positive selection (e.g., by way of changes in ancillary mechanisms that have evolved over time), then core mechanisms may be lost – specifically if the morphological change is drastic enough and requires the loss of interacting submodules for its development.

In the context of limb modularity and also of genetic networks, morphology can thus be viewed as the product of interacting genetic and molecular submodules that represent the core developmental mechanisms required for the generation of specific morphology. At the same time, evolution of morphology

reflects both the ways in which core mechanisms are structured *vis a vis* the way modules interact and how genetic and molecular networks become defined. Loss of a particular network's pathway may be co-opted by other processes, especially if those networks are ancillary or possess considerable redundancy resulting in the maintenance of morphological identity. However, if such identity is selected against, pathways may be lost and core mechanisms altered/lost forever.

For example, during snake embryogenesis rudimentary hindlimb buds are initiated but then regress due to changes in the alteration of the ZPA and the AER (Cohn and Tickle, 1999). In this case, initial core mechanisms of limb bud induction were unaltered but those later acting core mechanisms, conserved across most tetrapods (e.g., those governing the induction of *Shh* as well as the interaction of *Shh* and *Fgf* pathways), appear to have been lost presumably due to intense selection for "limblessness" and axial locomotion in snakes. From the context of modularity, the developmental submodules of the AER and ZPA have had their interactions altered, leading to regression of the AER and the loss of ZPA signaling. In this manner, those networks responsible for the maintenance of the *Fgf-Shh* feedback loop (see Chapter 3) have not been maintained as limbs have been selected against over the course of snake evolution. Of course, it is difficult to establish whether the "limblessness" in snakes was due primarily to an abrogation of the *Shh-Fgf* network or that this loss of interaction evolved secondarily overtime after limbless states had already evolved due to alterations to other networks.

2.5 Studies utilizing atypical mammalian models

Novel insights on limb evolution in mammals have recently been obtained due to the study of atypical model organism embryogenesis. Studies on bats and dolphins have provided important findings on several of the major developmental changes that have occurred in these organisms to generate their unique limb morphologies. As both mammals possess limb skeletons that are highly derived compared to the more typical mammalian pattern, the study of limb development in these organisms have provided critical insight into how limbs change via alterations in their developmental submodules and how they diverge via genetic alterations in *cis*- and *trans*-regulatory networks.

2.5.1 Studies using chiropterans

Studies by Chen et al. (2005), Sears et al. (2006), and Cretekos et al. (2005; submitted) have compared limb development in the bat (*Carollia perspicillata*) and mouse (*Mus musculus*) developmental systems. When their studies are coupled with those from paleontology, each supports the argument that the bat forelimb evolved relatively rapidly (from a more mouse-like morphological pattern) possibly due to changes in only a few critical genes. Sears et al. (2006) focused on how the elongated posterior digits characteristic of bat wings may have evolved due to modifications in the function of specific genes expressed in their digital perichondrium and subjacent growth plates. Specifically, the expression of the gene encoding bone morphogenetic protein 2

(Bmp2) in the digital perichondrium was observed to be up-regulated in bats versus mice. In addition, they demonstrated that Bmp proteins are capable of inducing proliferation and element elongation of bone cells in culture. In this context, the up-regulation of forelimb digital *Bmp2* expression may be one mechanism leading to development of elongated digits, as this modification was not found either in mice forelimbs or hindlimbs or in bat hindlimbs which lack the digital elongation observed in wing digits. Sears et al. (2006) further suggest that it was not changes in the structural coding regions of this *Bmp2* gene that led to their up-regulation, but *cis*-regulatory modifications that led to increased perichondrial expression in limbs and the rapid evolution of bat forelimb morphologies. They base this assertion on their finding that only *Bmp2* was up-regulated in the bat wing perichondrium, whereas *Bmp4* and *Bmp7* remained unchanged in these domains.

In a separate study, Chen et al. (2005) compared *Hoxd13* expression in the developing wing versus hindlimb bud of bats and in the respective mouse limb buds. Typically, the expression of *Hoxd13* in mammalian species is dynamic during limb morphogenesis and as this gene encodes an important transcription factor, it is believed to target numerous genes involved in skeletal development (Salsi and Zappavigna, 2005). In mice, *Hoxd13*-null embryos lack well formed autopodial digits implicating this gene in digit specification and maturation (Favier and Dolle, 1997; Zakany and Duboule, 1999). Despite the strong gene sequence and protein similarity of Hoxd13 between bats and mice (approximately 95%), Chen et al. (2005) observed a specific up-regulation and

posterior expansion of *Hoxd13* in the bat wing autopodium; a heterotopic shift neither identified in mice limbs nor in bat hindlimbs. The specific alteration in bat forelimbs indicates that shifts (i.e., heterochronic and heterotopic) in *HoxD* gene expression underlie the formation of the limb and the locations and sizes of the mesenchymal condensations giving rise to elongated bat forelimb elements.

Chen et al. (2005) observations on the posterior expansion of *Hoxd13* in bats, specifically in proximal autopodial and distal-posterior zeugopodial domains, have additional importance to understanding the evolution of bat wings. Herault et al. (1997) and Peichel et al. (1997) have demonstrated that when distally expressed *HoxD* genes (e.g., *Hoxd13*) are mis-expressed proximally in the limb bud, they inhibit the function of those *HoxD* genes (e.g., *Hoxd10-12*) endogenously expressed in the proximal limb bud and lead to marked skeletal alterations in the domains of ectopic expression (posterior prevalence, see Chapter 3). Accordingly, the more proximal and posterior expansion of the *Hoxd13* field in bat wing buds makes it possible that the typical expression of *HoxD* genes in the distal zeugopodial domain may be repressed. If these endogenous *HoxD* genes are thought as positive regulators of radius and ulna formation in the limb (Boulet and Capecchi, 2002), then their repression may coincide with the loss or reduction in either of these zeugopodial elements. For example, mice lacking *Hoxa11/Hoxd11* (Davis et al., 1995; Boulet and Capecchi, 2004) have reduced skeletal elements in their zeugopodial regions. However, in the mouse case, loss of these genes is global and absent from the entire zeugopodial domain. Interestingly, bat forelimbs are not just characterized by the

proximal to distal expansion of the anterior radius and posterior digits of the autopod but also the severe distal reduction of the posteriorly positioned ulna. Therefore, it is possible that selection for digit elongation, *vis a vis* a posterior and proximal expansion of *Hoxd13,* has lead to the secondary repression of posterior genes normally specifying the ulna, and therefore, ulna reduction. This reduction would be specific to the ulna, as this bone forms from posterior mesenchymal condensations (Harfe et al., 2004). Therefore, reduction of the ulna may not have occurred as a result of negative selection but as a pleiotropic consequence of the positive selection for the elongation of the handplate (the main elements of the wing).

The ramification that this insight has for phylogenetic analyses is not trivial. If, as is often the case, limb morphology is subdivided or "atomized" into characters for evolutionary analyses (often with the assumption that each character results via particulate inheritance, Lovejoy et al., 1999), then the use of distal ulna reduction as a character with that of radius elongation will weigh more heavily on phylogenetic trees than those that do not fail to consider the developmental integration of traits. This type of scenario demonstrates that the atomization of traits for phylogenetic or functional analyses may be inappropriate as initially suggested by Gould and Lewontin (1979) in their critique of the "Adaptationist Paradigm" and expanded upon by Lovejoy et al. (1999). In this context, considering the total morphological pattern of an organism and its developmental and functional integration more accurately reflects the manner in which morphology is actually generated and how selection operates on the

functional phenotype (Lovejoy et al., 1999). Other anatomical traits that are associated or developmentally integrated may change only as result of selection in favor of related morphologies. And the use of these traits may confound phylogenetic or even cladistic analyses.

In regard to issues of limb modularity, these studies highlight the role that heterotopic shifts in gene expression may have in generating limb diversity. In this particular example, changes in *Hoxd13* expression in bats appears to have a strong influence of skeletal morphology across more than one limb compartment (i.e., in both the zeugopodial and autopodial regions), while the corresponding gene expression (and abrogation) in mouse is more limited in its known genetic effects (i.e., to the autopod). This change in modular gene expression can be regarded as such only if either each compartment constitutes a limb submodule or the perichondrial submodules of the limb are more accurately defined as targets of Hox activity, as was recently demonstrated for primates by Reno et al. (in press; see below). Regardless of the mechanism of this difference, the idea that the effects of specific gene expression patterns may vary in different organisms and across compartments suggests that alterations in modular systems are significant sources of variation for evolution.

With respect to underlying biological mechanism, one potential mechanism to develop longer wings (i.e. across both distal limb compartments of the zeugopod and autopod) would simply be by modifying upstream *cis*-regulatory regions rather than altering independently either the regulation of compartmental-specific promoters or post-translational mechanisms

(modifications) in specific limb domains. In this manner of thinking, the most parsimonious alteration could be conceived as reflecting a single change in *cis*-regulation of *Hoxd13* rather than correlated changes in downstream networks. The same scenario could be envisioned for that of *Bmp2* as suggested by Sears et al. (2006). Future work on bats and mice addressing whether *cis*-regulatory divergence in *Hoxd13*, *Bmp2*, or any other known gene, underlie species-specific morphologies will be important.

In an example of such a "futuristic" study, Cretekos et al. (submitted) have recently performed elaborate enhancer replacement gene targeting techniques to explore the likelihood that specific bat non-coding *cis*-regulatory regions are indeed capable of positively influencing bone growth in mouse forelimbs. They examined mouse and bat upstream regulatory and structural coding sequences of the *paired-related homeobox 1* (*Prx1*) gene, whose protein product, when specifically present in the perichondrium of long bones, drives P-D outgrowth of zeugopodial and autopodial elements. For example, mouse $Prx1^{-/-}$ embryos display shorter zeugopodial and autopodial elements, whereas compound *Prx1;Prx2* (*Prx2* is a related family member also expressed in the limb) mutants have more drastically shortened elements in these two domains (ten Berge et al., 1998). Examination of the structural coding regions of *Prx1* displayed nearly 99% sequence identity between mouse and bat along with similar homology on the protein level. On the other hand, these researchers found that two specific enhancer elements upstream of the structural coding regions of the genes, both displayed approximately 65% identity between mouse and bat, suggesting

evolutionary divergence in *cis*-regulatory regions may be responsible for the long bone length differences between these two taxa.

Cretekos et al. (submitted) next utilized a replacement gene targeting strategy and created a mouse where the *Prx1* gene was under the control of the bat enhancer. Unfortunately, at this time, gene targeting in bat embryos is not possible and therefore the reciprocal experiment could not be performed. To complement the development of this construction, they also demonstrated using transgenic mice that both enhancers are capable of driving normal expression of *Prx1* in limbs of mice and that they indeed behave as *bona fide* regulatory elements. This replacement strategy led to mice with statistically significant length increases (when compared to wildtype mice) in all elements of the forelimb but not in the hindlimb indicating that *cis*-regulatory divergence at the bat/mouse *Prx1* enhancer is capable of driving morphological differences between these taxa and within the bat itself.

Cretekos et al. (submitted) also generated a mouse whereby the enhancer sequence was deleted altogether and where the mouse *Prx1* gene was being driven by this “deleted” element. They discovered that despite the loss of this specific *cis*-regulatory element, limbs formed normally with no length increases (compared to wildtype mice). Cretekos et al. (submitted) thus surmised that other enhancer elements are embedded in this upstream sequence and perhaps capable of buffering against the effects of the loss of the single enhancer element. They also suggested that the presence of multiple enhancer elements (and multiple *Prx* genes) might be driving the substantial increase in lengths

observed more in bat wings then in mouse forelimbs harboring the bat enhancer. In other words, that in natural settings, enhancer and gene redundancy has been important in the development of bat wing morphology particularly when compared to mice.

An additional aspect of this work that is critical for understanding how *cis*-regulatory elements underlie variation in morphology is the finding that limb element lengths across all compartments were affected using the bat enhancer element as compared to when the mouse enhancer was utilized. When taken in the context of previous findings by ten Berge et al. (1998) that *Prx1* (and *Prx2*) only drive zeugopodial and autopodial length changes in mice, these novel findings indicate that heterotopic shifts in gene expression may be capable as an outcome of enhancer divergence between taxa, or arguably, perhaps as the result of the accumulation of mutations in redundant enhancers and their subsequent cooption to driving expression of *Prx* in new limb territories. Such heterotopic shifts in expression may involve different developmental submodules (between mice and bats) specifically, if each limb compartment (i.e., stylopod, zeugopod, and autopod) or perichondrial domain constitutes a true developmental submodule. As mentioned, heterotopic shifts in *Hoxd13* expression were also revealed by the work of Chen et al. (2005) although its underlying biological mechanism is not known. Overall, Cretekos et al.'s (submitted) findings represent the first test of the effects of enhancer or *cis*-regulatory divergence between mammalian taxa on morphology and in this regard are critical for understanding how variation in limb evolution in mammals

is generated. In addition, studies such as these will not only help understand the basis of evolutionary change in the skeleton (or any structures) in specific vertebrates but should shed light on the genetic and developmental interconnections between control regions and structural regions of genes and how they shape basic biology.

Another critical component of these chiropteran studies is that they demonstrate that suites of developmental genes associated with anatomical trait variation and specialization are important places to examine for understanding evolutionary diversification between taxa. In the case of bats, suites of perichondrial-expressed genes (i.e., *Bmp2*, *Hoxd13*, and *Prx1*) have now been implicated as the major factors governing limb specialization. Given that all of these genes work within the developmental module of the limb and within perichondrial submodules, selection may have acted rapidly to modify modular growth of the limb. In this manner of thought, it is possible then to conceive that the evolution of the bat wing reflects modular evolution more clearly. However, as is the case of “limblessness” in snakes, it remains to be determined if genetic changes in these regulatory elements and tissue domains constitute the initial step in the evolution of the wing morphology or represent secondary modifications.

2.5.2 Studies using cetaceans

Studies performed on cetaceans, such as dolphins and whales, have revealed how morphological specializations in fore- and hindlimbs can be

generated by genetic and molecular alterations affecting limb modularity. Cetaceans display unique forelimbs that have been modified into flippers consisting of relatively reduced stylopodial and zeugopodial elements and greatly elongated autopodial elements. In addition, the morphology of both the two proximal-most limb compartments allow for only very limited movement. Concomitantly, all elements of their hindlimbs (including the hindlimb itself) have been significantly reduced, if not lost (Vaughan et al. 2000). This unique pattern of limb-specific morphological specialization has evolved as adaptations to an aquatic environment from a land dwelling mammalian artiodactyl ancestor (O'Leary, 2001). Accordingly, they (e.g., dolphins) have adopted a locomotive strategy consisting of vertical undulation characterized by the need for stabilization and steering (i.e., via forelimb use) and a reduction in posterior drag (i.e., via hindlimb loss). What is becoming clear through developmental studies particularly in dolphins (whose embryos are more readily available than larger whales) is that the mechanisms generating fore- versus hindlimbs have diverged in these organisms.

The evolutionary development of the unique cetacean flipper morphology involved substantial changes to both the duration and spatial extent of submodule interaction in the limb. Cetacean flippers exhibit hyperphalangy, with more phalanges per digit than other mammals. For example, dolphins of the genus *Stenella* possess 9 phalanges on digit 2 and 7 on digit 3 (with 1 on digit 1, 4 on digit 4, and 1 on digit 5), while some whales of the genus *Globicephala*, have up to 14 phalanges on digit 2 (Howell, 1970). It is also known that in most

whales phalangeal number is reduced in adults as compared to fetal periods. This latter change is attributed to a “regression of the most distal phalanges as a consequence of the forces acting on the leading edge of the flippers (Klima, 1992)” (Bejder and Hall, 2002: 450). Overall, the pattern of hyperphalangy in cetaceans is believed to reflect the forelimbs involvement in stabilization and steering rather than in propulsion.

Histomorphological studies on embryonic forelimbs of spotted dolphin (*Stenella attenuata*) demonstrate that the AER over digits 2 and 3, those two rays that possess the most phalanges (6 and 6, respectively), is thickened and persists longer than the AER over digits 1, 4, and 5 (with 2, 4, and 2 digits each, respectively) (Richardson and Oelschlager, 2002). In fact, these researchers identified two phases of AER thickening over these digits, as opposed to just one phase for the other three digits of the flipper. Furthermore, these authors have discovered that phalangeal formation is additive and that over time each new phalange gets added distally to the limb. In light of this finding, they suggest that heterochronic changes in gene expression may be underlying species-specific differences in hyperphalangy in cetaceans. Indeed, it may well be that *cis*- and *trans*-regulatory modifications occurring throughout AER formation and maintenance in cetaceans has lead to longer submodule interactions between the AER and the underlying limb mesenchyme in specific digital domains.

Hindlimbs in modern cetaceans have been drastically reduced, a change that appears coincident with the switch to the use of flukes, or outgrowths of skin, along the rear of the animal that aid in vertical axial undulation and reduce drag

forces typically caused by protruding hindlimbs. According to Lande (1978) hindlimb reduction in whales occurred over 10-20 million years and was therefore a gradual process. Studies on dolphin embryos demonstrate that even though hindlimbs become vestigial, hindlimb buds initially develop relatively normally, although they are reduced in size compared to forelimb buds. While both fore- and hindlimbs possess AER tissues, it is only in the forelimb that limb development continues via the perpetuation of important AER-mesenchymal interactions. The AER in dolphin hindlimbs appears slightly underdeveloped but allows for the progression of bud development and the formation of mesenchymal condensation formation (Sedmera et al., 1997a-b). Subsequently, some molecular cues are lost from the AER or the ZPA mesenchyme that lead to the regression of the limb and the loss of distal condensation formation, a view initially advocated by Bejder and Hall (2002).

Thewissen et al. (2006) examined spotted dolphin (*Stenella attenuata*) development and found that disruptions to the limb's submodule interactions indeed underlie the regression of their hindlimb buds. Normally, as observed in various vertebrate models (e.g., in chick, mice, and others), *Shh* is initiated in the ZPA submodule and its expression functions to establish a positive feedback loop between the AER submodule (and *Fgfs* expressed in this tissue) and the ZPA, itself (reviewed in Niswander, 2003). In dolphins, Thewissen et al. (2006) first corroborated Sedmera et al. (1997a,b) findings that hindlimb AER formation ensues, and second that it possesses some function, by examining the expression of *Fgf8*, a gene critically involved in AER formation/function. They

found that in early dolphin embryos *Fgf8* was expressed in patterns similar to those observed in mouse and chick, however, that later, after initiation, the expression of this gene was markedly reduced. They next found that *Shh* expression in the ZPA region was never initiated in the dolphin hindlimb, while it was initiated and maintained correctly during forelimb growth and development. In line with these studies, they also demonstrate that the gene *heart and neural crest derivatives expressed 2 (Hand2)*, an upstream activator of *Shh*, was not initiated, suggesting that the mesenchymal patterning leading to ZPA establishment does not commence properly in dolphin hindlimb buds. Therefore, at or during initial hindbud formation, several of the genes specific to the functional ZPA submodule of the limb became down-regulated leading eventually to premature abrogation of the AER-ZPA submodule interaction and the cessation of hindbud outgrowth.

Interestingly, this pattern is also similar (though not identical) to what happens in snake embryos with hindlimbs that initialize formation but then experience a marked abrogation. Evolutionarily, “limblessness” in snakes was not always the rule indicating that overtime, pathways involved in hindlimb formation became selected against and other locomotor repertoires became favored (Cohn and Tickle 1999). Similar to snake evolution, it remains unclear as to whether hindlimb reduction in cetaceans was caused by the initial loss of *Hand2* and *Shh*, or whether other regulatory changes led to hindlimb abrogation and eventually to the loss of interaction between these two critical developmental submodules of the limb (Thewissen et al., 2006).

Recent evidence suggests that in snakes and cetaceans, hindlimb reduction/loss results from changes in main body axis specification that may have altered to timing of limb induction as well as the expression of *Hand2* and *Shh* in the limb. In this manner of thinking, loss of signaling between the ZPA and AER is a secondary consequence to alterations in the expression of genes involved in the establishment of body axis and the specification and formation of pre-limb mesoderm. For example, according to Thewissen et al. (2006) and several others (Cohn and Tickle, 1996; Cohn et al., 1997; Cohn and Tickle, 1999) alterations in molecular activity along the rostral-caudal embryonic axis may have modified patterns of *Hox* expression in both the paraxial mesoderm and the lateral plate mesoderm (see Chapter 3). Such alterations in *Hox* are believed to affect the patterning of the lateral plate mesoderm, the timing of limb bud induction, and the axial level where limbs form (Charite et al., 1994; Cohn et al., 1997). In addition, the lateral plate mesoderm is a critical tissue that gives rise to the ZPA and provides important signals to the AER necessary for limb bud outgrowth (reviewed in Niswander, 2003). Therefore, complex changes in the cetacean body axis, as tied to patterns of locomotor changes in these organisms, may have been the primary factor eventually leading to their hindlimb reduction. A similar idea has been put forth for snakes that like dolphins possess both elongations in the axial skeleton, and reductions in hindlimbs. Cohn and Tickle (1999) have already linked forelimb loss in snakes to the expansion of their thoracic vertebral region via changes in *Hox* expression. At this point it remains unclear as to whether cetacean hindlimb loss initially resulted from changes in

the body axis specification associated with more vertical undulating movement, changes in the necessity for a reduction in drag (as would be produced by the presence of hindlimbs) or systematic changes due to both of these factors.

2.6 Studies utilizing primates

To date, little research has been conducted that examines primate morphological variation from an Evo-Devo perspective. This stems from the fact that several obstacles prevent primate embryos from being readily available for these analyses: First, there is an ethical dilemma in using primates in developmental work due to both their close relationship to humans as well as their highly endangered status. Second, they present biological obstacles such as their relatively slower gestational time-periods (and overall longer life histories) compared to the typical mammalian model, the mouse. Third, experimentally, there is the difficulty in standardizing time-mating procedures necessary to get a control of embryonic developmental progression, as well as the difficulty in acquiring complete staged embryonic series to conduct developmental biology work. Fourth, there are economic barriers in that the cost involved in primate husbandry and breeding is exceptionally higher then those for typical model organisms. Finally, there is also the general dearth of direct data from comparative primate developmental biology, which, unfortunately, feeds back on to these obstacles.

Despite these obstacles some attempts have been made to understand the evolution of primate morphology from a developmental perspective.

Research by Hamrick (2001b) compared digit proportionality and developmental data of mouse lemurs (*Microcebus murinus*) and other primates to those of other mammals (e.g., Virginia opossum (*Didelphis virginiana*), etc.) and fossil primates (e.g., *Notharctus*, *Adapis*, etc.) to determine if the derived primate hand proportionality (i.e., relatively short metacarpals and long phalanges) results from alterations in the early patterning of the digital rays (i.e., during the pattern formation stages of digit morphogenesis). His study indicates that digital ray proportions of primates are generated during early joint formation stages of development, and that developmental and morphometric differences between primates (extant and extinct) and other mammals supports the idea that the earliest primates possessed hands that were already capable of grasping.

In related studies, Hamrick (1999; 2001a) focused on how evolutionary variation in mammalian digit integumentary structures, such as nails, hooves, and claws, arises via changes in genetic regulation of epithelial and mesenchymal interactions during distal digit morphogenesis. As most primates possess nails (with few exceptions having claw-like structures on several, if not all, digits), they share several critical developmental stages of distal appendage development with extant “clawed” and “hoofed” mammalian ancestors. Accordingly, he argues that the development of nails may be due to regulatory changes in the control of *Bmp4* or *Msh homeobox1/2* (*Msx1/Msx2*) expression in the mesenchyme and epithelium, respectively, during late stages of digit morphogenesis, which drive variation in these types of structures (Hamrick 2001a). Furthermore, as the expression of these genes (including several

others) not only governs integumentary formation but also plays critical roles in distal-most phalangeal skeletogenesis, the patterning information provided by these genes may be developmentally linked and not easily uncoupled during evolution. In other words, regulatory changes during distal digit morphogenesis may have downstream consequences on epithelial-mesenchymal interactions and therefore, integumentary phenotypic variation.

Hamrick (2001a) also suggests that the presence of such tightly controlled regulatory interactions in the distal limb may have afforded this domain the potential to evolve more readily than that of the proximal limb, which appears to be marginally affected by such genes operating late in limb development. This idea of proximal versus distal limb evolvability, was initially established by Hinchcliff (1989, 1991) in his proximal stabilization theory. Accordingly, he argued that the evolutionary alteration of the proximal stylopod and girdle is constrained and relatively conserved across vertebrate forms while more distal structures of the zeugopod and autopod have become more divergent.

This theory has had some support from developmental-based studies. For example, most of the known genetic pathways involved in proximal limb development are also those operative during early limb bud formation and morphogenesis. Indeed, very few mice have been identified harboring mutations that affect proximal structures alone and without an affect on overall limb bud development. On the other hand, most genes shown to influence later submodule interaction (such as between the ZPA and AER) affect distal

autopodial outgrowth and digital patterning but not typically at the expense of more proximal limb element specification and morphogenesis.

In a series of recent papers (Reno et al., 2000; Lovejoy et al., 2001; Reno et al., 2001; Reno et al., in press) Reno and colleagues examined whether a developmental perspective can be used to explain distal limb variation present among higher primates, such as apes. Such variation includes, for example, the presence of relatively long posterior digital rays in more suspensory apes such as gibbons, siamangs, and orangutans, but not in humans and gorillas, each of which display digital rays more similar to more ancestral catarrhine-like primates (consisting of a more generalized hand with shorter metacarpal and phalangeal regions).

Following some preliminary findings presented in Reno et al. (2000), Lovejoy et al. (2001) examined intraspecific variation in the extant adult hominoid (chimpanzee, gorilla, orangutan, gibbon, and human) limb and found that the lengths of the posterior four digits and distal radius are strongly correlated with each other but not to the proximal radius. They suggested that such a finding indicates the presence of a developmental module that includes the growth plates of the distal radius, ulna, and posterior digital rays. Indeed, they found a developmental module defined by *Hoxd11*, which was the only *Hox* to be both expressed in the vicinity of the growth plates during distal limb chondrogenesis and which displayed a skeletal phenotype in mutant mice. Therefore, they argued that systematic downstream genetic modifications within *Hoxd11* territories, such

as in changes of *Hoxd11* expression or in the responses of downstream genes to Hoxd11 function, could underlie distal limb primate morphological variation. In addition, given the assertion that HoxD proteins compete for regulation of target genes (Davis and Capecchi, 1996), such as growth promoting factors, the action of multiple Hox proteins could underlie the observed phenotypic variation across the distal limb and its developmental module.

For example, the unique morphological changes seen in gibbons (e.g., in the exceptional growth of their distal radius and four posterior digits) may correspond to an up-regulation of *Hoxd11* during zeugopodial morphogenesis and a subsequent up-regulation of both *Hoxd13* and *Hoxa13* (which are expressed in the vicinity of the autopod but not the zeugopod) during autopodial morphogenesis. These regulatory changes would theoretically allow for digital growth as well as the suppression of *Hoxd11* distally (by way of out-competition by Hox13 proteins), which, if remained active, could lead to digits that are disproportionately long and potentially dysfunctional. The consequences of an up-regulation of these particular genes may also have lead to an increase in thumb length, a trait that gibbons are unique in among suspensory primates.

Reno et al. (2001) investigated the underlying *Hox* expression patterns in mice and whether the adult intraspecific variation identified in Lovejoy et al. (2001) was also present in an ontogenetic series of human, chimpanzee, and gorilla specimens. In this work, they have found further support for Lovejoy et al. (2001) on digital and radial skeletal element morphology and proportionality and more clearly defined their concepts of *Hox*-based modules in the limb.

Reno et al. (in press) have built upon the methodological and theoretical perspectives of these previous works and more thoroughly explored the relationships between changes in *HoxD* targets and the intraspecific variation found across primate distal limbs. They have first identified unique patterns of *Hox* expression within the chondrogenic phases of skeletal element growth, specifically focusing on the mouse perichondrium. It is during this period of time and in these locations that Hox proteins may be directly functioning on growth promoting genes in the growth plates of limb bones. They next performed morphometric analyses on extant primate forelimb skeletons, specifically, New World monkeys, Old World monkeys, and apes.

Indeed, they have identified several developmental submodules of Hox function in the limb based on both unique patterns of morphometric covariation in distal limb domains and perichondrial *Hox* expression. These submodules include: (1) the posterior digital submodule defined by the combinatorial expression of *Hoxa13* and *Hoxd10-13* and evinced by strong morphometric correlations among length measurements of the posterior metacarpals of digits 2-5 in all taxa studied; (2) a distal first digit submodule defined by the unique anterior expression of *Hoxa13* and *Hoxd13* and indicated by a lack of statistical correlation between length measurements of the proximal first digital phalanx and the posterior digital elements in catarrhines; (3) a submodule consisting of the distal zeugopod as indicated by the independent growth of this region in particular primates (*P. frontata* and *E. patas*) from that of the more posterior digits; and (4) an inter-connected zeugopod-autopod submodule consisting of the

distal radius (and ulna) and the four posterior digits, and defined by the pattern of expression of *Hoxd11*. This particular module is borne out of the additional findings that in all three anthropoid groups studied, the lengths of the posterior (digit 2-5) metacarpals significantly correlate with that of the distal radius, in a manner independent from changes in both the proximal radius and that of digit one. Reno et al. (in press) also indicate that as many primates display single digital length increases (e.g., *Daubentonia*), which represent specialized adaptations, such modifications perhaps occur to even later, downstream, unknown distal autopodial modules, whose sphere of influence is outside that of global Hox domains. These modules could correspond to those domains involving distal integumentary formation as outlined by Hamrick (2001a).

Reno et al. (in press) further explored the potential of using modular data to address the issue of potential evolvability in different primate lineages. Given the relative independence of several of the proposed developmental submodules, they suggest that often simple up- or down-regulations of specific *Hox* genes or their targets in these domains, could help explain some of the variability seen in primate skeletal proportions. For example, they argue that the unique distal limb morphologies of both *Ateles* and *Colobus*, (i.e., possessing elongated posterior digits, greatly reduced (if not residual) anterior “thumb” digits, and concomitantly lack the distal zeugopod length increases seen in other primates, such as suspensory apes), can be envisioned by different scenarios of *Hox* alteration (Reno et al., in press). One possibility is that an up-regulation of *Hoxd11* distally allows for more growth of posterior digits. Another is that given

the posterior digit specific expression of *Hoxd12*, a simple up-regulation of this gene may have been sufficient. However, in both instances, thumb reduction may not be explained. Instead, they also suggest that perhaps modification to the control of *Hox13* genes (i.e., *Hoxd13* and *Hoxa13*) may be sufficient. For instance, the reduction of Hox13 proteins in territories where other Hox (i.e., Hoxd10-12) are endogenously present would allow these Hox proteins to compete for targets more efficiently and improve growth, as experimental evidence in chicks suggests. Also, a decrease in Hox13 paralog level would explain the observed reduction in digit one, specifically since experimental evidence indicates that digit one loss is accompanied with heterozygous loss of *Hoxa13* in mice.

With respect to their example on gibbon skeletal proportionality (discussed in Lovejoy et al., 2001 and expanded in Reno et al., in press), it is interesting that these primates are also characterized by overall increased forelimb lengths compared to other taxa, which according to the perspective outlined by Reno et al. (in press) could be explained as having resulted from up-regulations in multiple *HoxD* genes. In this manner, alterations to the control of the entire *HoxD* cluster may underscore several of the changes that gibbons have undergone, while in other primate lineages, changes to localized *Hox* genes (via modifications to their individual promoters) or targets (within submodules) may help explain their evolutionary changes. This topic is re-evaluated in Chapter 8, using the insight provided by the studies conducted in this thesis.

These data by Reno et al. (in press) suggest that the primate limb can be analyzed via postnatal ontogenetic series, specifically if patterns of mouse *Hox* expression are in accordance with those seen in primates. However, such data on primates is indeed lacking and future work may need to elucidate how *Hox* gene expression occurs in primates. Transgenic mouse lines, mis-expression studies, and bioinformatics should help provide clarification in this respect. These authors also understand the need for more direct data regarding the actual targets of Hox proteins during these late phases which, if found, would provide for mechanistic links between Hox and their growth effects. Reno et al. (in press) further indicate that it is necessary to examine *cis*- and *trans*-regulatory elements governing *Hox* gene expression as well as those of their target genes.

Recent work has taken a more comparative genetic approach at identifying whether primates possess significant variation in developmentally critical genes and how such genetic differences could translate to morphological variation. Perry et al. (2006) examined, across 27 primate species, the coding and non-coding regions of two genes, *Msx1* and *Paired-box 9* (*Pax9)*, known to be involved in embryonic and postnatal development. As both of these genes have been shown in mice to govern craniofacial, dental, organ, and limb development (Maas et al., 1996; Peters et al., 1998) and primates display considerable variation in craniofacial, craniodental, and limb morphology, these genes appeared as good candidates for comparative genetic study. They identified four non-coding sequences in these two genes that are conserved with

other mammals. Of those found for *Msx1*, one sequence (i.e., *CNS1* or *Conserved Noncoding Sequence 1*) appears in an upstream region of *Msx1* and could be involved in this gene's regulation. Those sequences found for *Pax9* (i.e., *CNS1* and *CNS2*) were found in this gene's first intron and have not yet been assessed for functional significance (the authors indicate that often CNS that are found in first introns have a role in transcriptional regulation). Interestingly, the primates analyzed for *Pax9 CNS2* display marked divergence to that of mice, but not to dogs, suggesting that mice have evolved differently. However, the overall conservation indicates that developmentally the control of these genes (*sensu stricto*) has been under intense stabilizing selection.

Among coding regions, these authors also found, in general, that amino acid sequences have been under intense selection or functional constraint. However, they did discover that *Tarsius syrichta* possessed a unique pattern of amino acid divergence in *Msx1* exon 1 that was significant when compared to all other primate taxa analyzed. Interestingly, members of the genus *Tarsius* possess unique craniodental specializations, such as the absence of deciduous incisors and reduced lower numbers of permanent incisors. In mice, *Msx1* is expressed in the early dental anlagen and in $Msx1^{-/-}$ mice the dentition does not form (Lallemand et al., 2005). It is possible that the modification to the amino-acid sequence of Msx1 alters its function in such a way that it underlies the dental loss observed in *Tarsius*. Future work using transgenic mice may help elucidate this scenario. In addition, as *Msx1* and its related family member *Msx2* are critically involved in limb morphogenesis (Lallemand et al., 2005), it will be

interesting to determine if similar patterns of nucleotide divergence exist for *Msx2* and whether transgenic mice harboring *Tarsius* Msx1 structural elements display limb alterations.

Recent work by Dorus et al. (2006) indicates that *Shh,* a gene whose protein product is critically involved in limb, craniofacial, neurological (i.e., brain), and other organogenetic processes, has evolved in an accelerated fashion in primates when compared to other mammals. Furthermore, the strong and statistically significant acceleration in nucleotide divergence is highest in the ape lineage leading to humans. The specific nucleotide divergence is found in a coding region for a domain critical for post-translational modification and Shh function (reviewed in McGlinn and Tabin, 2006). These changes suggest that the post-translational modification of Shh has markedly evolved and indeed may underlie the major limb and brain specializations seen in the evolution of human lineages. The next step in these two on-going comparative genetic studies (Perry et al., 2006 and Dorus et al., 2006) will be identify whether the identified divergence translates to functional differences as assessed using transgenic mouse models or cell culture readouts.

2.7 Conclusions and directions

The studies described above provide a glimpse of the power that the Evo-Devo perspective has in elucidating various aspects of mammalian, specifically primate, evolution. To date, however, studies of an Evo-Devo nature as applied to primates are in general lagging behind those performed on other model

mammals and vertebrates. Critical to their success will continue to be first hand knowledge on gene function in different model organisms, as such data provides a “place” to start scanning the genomes of primates possessing disparate morphologies. The examples discussed above by Chen et al. (2005), Sears et al. (2006), and Cretekos et al. (submitted) comparing bats and mice as well as those by Dorus et al. (2006), Perry et al. (2006), and Reno et al. (in press) are testament to the need for such foundational work. Concomitantly, without knowledge on basic gene function and complexity in genetic interactions during development, studies on how genetic nucleotide divergence among primates underlies real species differences in morphology will be merely speculative. In other words, examination of basic and complex gene function in model organisms allows for the requisite knowledge upon which to bridge comparative studies of molecular and morphological specializations in extinct and extant taxa.

The studies carried out in this dissertation examine the complex interplay between gene family members during limb development. By studying the genetic interactions of different *Pbx* family members *in vivo* as well as their interaction with major patterning molecules (e.g., *Hox, Shh*) some of the mechanisms underlying pattern formation of the limb are elucidated. Knowledge on this genetic interaction can then be applied in comparative studies of morphological and molecular nature that examine skeletal variation and nucleotide divergence in regulatory regions for some of the molecules critical to early limb patterning.

The next several chapters focus on the molecular control of limb development and *Pbx* (Chapter 3), the methods used to study gene interaction

during embryonic development (Chapter 4), and the genetic interactions of *Pbx* family members during limb (Chapters 5 and 6) and girdle (Chapter 7) formation. Only after these chapters will it be possible to re-address how the novel experimental data on *Pbx* genetic interaction (and interaction with other critical factors in limb and girdle development) produced in this work, impacts the understanding of the evolution of mammalian and primate skeletal morphologies (Chapter 8). The perspective introduced in this chapter will be important to this interpretation.

Chapter 3: *Pbx* and *Hox* genes and the Development of the Limb and Girdle

3.1 Introduction

The vertebrate limb has long been a subject of study among embryologists and developmental biologists. Research in the early Twentieth Century on limb development was conducted on mammalian species such as the rabbit and non-mammalian species such as chicks, frogs, and salamanders, because each was amenable to experimental manipulation, easily available, and relatively inexpensive to acquire and breed (Harrison, 1918; Zwilling, 1955). These studies were both descriptive and mechanistic. For example, several focused on the tissues that give rise to the limb, as well as on the duration of limb development in select organisms. Other studies of a more mechanistic nature examined tissue interactions between the limb and the embryonic flank in order to understand its derivation (Harrison, 1918). Later studies involved non-directed genetic strategies using animals harboring natural mutations (i.e., specifically in chick) and/or tissue manipulations (Zwilling, 1955). From all of these studies, a plethora of data was derived which provided an empirical backdrop upon which to interpret more recent findings.

Over the past twenty years, the molecular mechanisms governing limb development have been explored due to advances in mouse developmental genetics and experimental techniques on chick embryos. Studies exploring the phenotypic consequences of both natural and induced (i.e., via gene targeting strategies) mutations in these model organisms have revealed important insights

into the following questions: (1) When, where, and how are limbs specified to form? (2) How are limbs induced to form? (3) How are the main axes of the limb established and maintained during bud outgrowth? (4) How do skeletal elements of the limb become patterned (i.e., initially specified and later determined)?

From a functional point of view, limbs are often grouped with that of their adjoining girdles (e.g., the scapula and pelvis). For the most part, past studies using chick/quail chimeras and mouse developmental genetics have indicated that girdles form in relative isolation from limbs. For example, most of the genes involved in limb development (as described in section 3.2) have little if any influence on girdle formation. However, recent studies indicate that there are molecular and histological domains shared early during their development. Nevertheless, to date, there is still little known regarding how the scapula and pelvis are formed during prenatal development and how their formation relates to that of the limb.

Since this thesis focuses on *Pbx* gene function in the mouse system, this chapter highlights mainly those findings from this model organism (note: detailed historical reviews on the use of the mouse as a developmental system is provided in Silver, 1995 and Nagy et al., 2003.) At times, however, findings from chick and other organisms are addressed, particularly if they provide historical and empirical insight into the developmental understanding of the limb and girdle.

Besides the introduction, this chapter is organized into four additional sections. Section 3.2 provides a basic overview on limb and girdle organization as well as a brief summary on how they form (General Limb and Girdle Structure

and Development). In doing so, it outlines the major tissues involved in their formation as well as the stages of their development in the mouse. Section 3.3 reviews in detail the molecular and histological basis of limb development specifically focusing on the four main questions asked above (Vertebrate Limb Development). In addition, this section covers *Hox* gene organization and function in the limb. Section 3.4 focuses on the prenatal mechanisms that regulate pectoral (i.e., scapula) and pelvic girdle formation (Girdle Development). As less is known in mouse regarding the formation of these structures, data from the chick system are addressed to understand the tissues and molecules involved in girdle patterning and morphogenesis. Finally, Section 3.5 provides a look at both Hox transcription factors and Pbx cofactors in terms of their structure and function (i.e., embryonic) within vertebrates (Hox Transcription Factors and Pbx Cofactors).

3.2 General limb and girdle structure and development

3.2.1. Limb and girdle structure

In general, vertebrate appendages can be divided into fins (e.g., in aquatic organisms) and limbs (e.g. in terrestrial organisms). In both forms, two ventral-lateral facing sets often exist, one situated rostrally and the other more caudally along the body axis. Many finned vertebrates (e.g., chondrichthyans) possess additional midline fins (i.e., anal, dorsal, caudal, etc.). In fact, recent evidence suggests that the developmental basis for paired fins arose via the same mechanisms that governed these mid-line fins (Freitas et al., 2006). The axial

positions of these paired appendages depend partially on patterns of *Hox* gene expression during embryogenesis (see section 3.3).

In terrestrial vertebrates (or those organisms which are either semi-terrestrial or secondarily aquatic) limbs are referred to as forelimbs and hindlimbs and are used in a variety of contexts, including, for example, locomotion, positional behavior, and stabilization (Liem et al., 2001). Each appendage is connected to the main body axis via a series of osseous and muscular connections with a girdle. Rostrally, the forelimb is connected to the scapula, the main endochondral element of the pectoral girdle, and osseous cranial articulations have not evolved as they have in many fish species (Fig. 3.1A). The scapula in turn is connected to the main body axis via the clavicle, and a series of strong muscular attachments.

Of the two pectoral skeletal elements, the scapula is larger and possesses several important anatomical features (Fig. 3.1B). Most evident is it's dorsal-lateral facing blade that is separated by an osseous spine into unequal-sized superior and inferior components (supraspinatous and infraspinatous fossae, respectively). This spine runs medial-lateral across the blade and terminates distally at the acromion process that articulates with the clavicle. The lateral-most aspect of the blade connects to the neck and head of the scapula, the latter which includes the glenoid fossa, a distal-lateral facing surface for articulation with the humeral head. Finally, just superior to this fossa is an additional element, the coracoid process.

In the caudal embryo, the hindlimb is connected to the main body axis via the pelvis (Fig. 3.2). The mouse pelvic girdle consists of two paired bones, the innominate or pelvic bones that abut ventrally at the symphysis and articulate dorsally with the axial skeleton at the sacroiliac joint (via articulation with sacral vertebrae). Each pelvic bone consists of three major skeletal elements (Fig. 3.2): (1) a superior or rostral facing ilium; (2) a ventral facing pubis (which articulates ventrally with the pubic of the contralateral pelvis bone); and (3) a dorsal-posterior facing ischium. These three elements fuse to form the laterally oriented acetabulum or hip socket, upon which inserts the proximal femoral head.

The vertebrate fore- and hindlimb proper consists of three main compartments (Fig. 3.3): (1) the proximal stylopodium (Gr., *stylos* = pillar + *podion* = small foot) that consists of the brachium (represented by the humerus) in the forelimb and the thigh (represented by the femur) in the hindlimb; (2) the middle zeugopodium (Gr., *zeugma* = a yolking or joining together) that consists of the antebrachium (represented by an anterior radius and posterior ulna) in the forelimb and the crus (represented by an anterior tibia and posterior fibula) in the hindlimb; and (3) the distal autopodium (Gr., *autos* = self) that consists of the manus (represented by the carpals, metacarpals, and phalanges) in the forelimb and the pes (represented by the tarsals, metatarsals, and phalanges) in the hindlimb (Liem et al., 2001).

3.2.2 Overview of limb and girdle development

The mouse model system has been extensively used to understand the molecular mechanisms regulating limb development. This is particularly the case because it is readily amenable to genetic manipulation (e.g., mutants can be generated via targeted mutagenesis), easy to breed (e.g., timed-mating can be easily established), has a short gestational period (e.g., 18-21 days), and is relatively inexpensive to breed compared to larger mammals (e.g., primates, sheep, pigs, or dogs). While important for limb development, at this point in time there are considerably fewer studies demonstrating the contribution of the mouse system to understanding girdle formation. Accordingly, much of what is known regarding the tissues involved in girdle formation comes from the chick. An outline of the major stages of chick formation is provided in Hamburger and Hamilton (1951) and is not discussed in detail.

The major stages of mouse limb development and the sections that discuss these stages in detail are outlined in Table 3.1. Less is known as to the exact timing of girdle development and therefore, discussion of this topic is saved to the section on girdle development. Critical to understanding the progression of limb development is also a brief mention of several of the major tissues involved in their genesis. Accordingly, in the mouse, from approximately 7.5 to 9.5 days gestation (hereafter, E7.5-9.5), the non-cranial mesoderm of the developing embryo is arranged axially into several adjacent layers (Fig. 3.4A): (1) the chordamesoderm (CM), which gives rise to the notochord; (2) the paraxial mesoderm (PM) which gives rise to somites; (3) the intermediate mesoderm (IM) which aids in the formation of the urogenital system; and (4) the lateral plate

mesoderm (LPM) which forms the heart, blood vessels, blood cells, tissues lining body cavities and of the body wall, and will undergo specific outgrowths to form limbs (Gilbert, 2006). These tissues will undergo several interactions leading to the formation of fore- and hindlimbs at specific axial locations in the body (Fig. 3.4B-D), the development of several signaling centers driving limb bud formation (Fig. 3.5), and ultimately to the patterning and formation of skeletal elements of the limb (Fig. 3.3).

3.3 Vertebrate limb development

3.3.1 Axial level of limb specification

One of the first events involved in limb formation is the specification of the axial levels where limbs form. It was demonstrated long ago by the work of Harrison (1921), Swett (1937), and Slack (1976) using surgical manipulations of either chick and salamander embryos that limb bud position was determined well before bud induction and outgrowth. For example, transplantation of early pre-limb region mesoderm to different (non-limb forming) somite levels resulted in ectopic limb formation (Harrison, 1921). Stephens et al. (1993a-b) corroborated these findings in the chick, when they grafted early (stage 12; e.g. prior to limb bud formation) rostral embryonic flank tissues to caudal somite levels in older embryos (Stage 16-18; e.g., when limbs form) and found that they were capable of inducing ectopic forelimb structures. Therefore, the specification of limb compartments in the LPM along the axis occurs early in development (i.e., well before limbs emerge). In addition, these pre-limb fields appear to have the (molecular) capability of inducing limb formation. In the mouse it is unknown as

to when, at the earliest, the LPM (or PM) is capable to induce limbs and/or possesses the conditions to promote fore- and hindlimb development (Capdevila and Belmonte, 2001).

An important component of the PM and LPM mesoderm's ability to specify limb bud position is the proper expression of *Hox* genes along the rostral to caudal embryonic axis across these tissue layers (Cohn et al., 1997) (note: an excellent review of the axial expression and function of *Hox* genes is provided by Pearson et al., 2005). Many mutant mice homozygous for single *Hox* genes display axial homeotic transformations, where one vertebral segment is transformed into another adjacent segment (e.g., Ramirez-Solis et al., 1993; Condie and Capecchi, 1993; Horan et al., 1994). In addition, as multiple *Hox* genes overlap in their axial expression domains, these transformations are exacerbated in compound *Hox* mutants (e.g., Condie and Capecchi, 1994; Kostic and Capecchi, 1994; Horan et al., 1995; Favier et al., 1996; Fromental-Ramain et al., 1996a; Chen et al., 1997; de la Cruz et al., 1999; van den Akker et al., 2001; Wellik and Capecchi, 2003). Evidence for *Hox* role in limb bud specification comes from *Hox* mouse mutants that display potential alterations in limb bud location. For example, Rancourt et al. (1995) demonstrated that, in addition to having thoracic vertebral defects, the axial level of scapula formation is shifted in *Hoxb5*$^{-/-}$ mice suggesting that forelimb level may also have been altered. In addition, these defects were exacerbated in compound *Hoxb5;Hoxb6* mutants (Rancourt et al., 1995). Furthermore, comparative studies of mice and other model organisms demonstrate that all of their forelimbs form at the anterior

extent of *Hoxc6* expression in the developing axis (Oliver et al., 1988a-b; Molven et al., 1990; Burke et al., 1995). However, the extent of Hoxc6 functionality in this regard is unclear because while *Hoxc6*$^{-/-}$ mouse embryos possess axial vertebral alterations, limbs form at normal somite levels. This finding may indicate that there exists a high degree of functional redundancy among *Hox* genes in specifying limb location.

Work in the chick has also supported the role for *Hox* in specifying limb bud position. For example, Cohn et al. (1997) demonstrated by experimentally altering the expression boundaries of several *Hox* genes (i.e., *Hoxb9*, *Hoxc9*, and *Hoxd9*) that ectopic limbs formed at different axial levels. However, in these experiments, shifts in the normal axial level where limbs form were not observed. Compiling data from both mouse and chick systems has led these researchers to suggest that limb position is specified early in axial formation according to a tightly regulated code of overlapping *Hox* expression which specifies mesodermal cells following a ratchet-like mechanism (Cohn et al., 1997).

It may well be that axial *Hox* gene expression in the PM and LPM promotes interactions between these tissues or may also specify fields of tissue competence that permit limb formation. For example, Hayashi and Ozawa (1995) demonstrated that the LPM in the vicinity of the chick limb field induces myoblasts (i.e., muscle progenitors) from the PM-derived somites to enter the forelimb proper. While these events occur after limb induction, it may that earlier *Hox* specification of A-P somite boundaries is critical in this regard.

3.3.2 Limb field and bud induction

After limb bud position is specified, limb bud formation commences and involves tissue interactions primarily between the PM, IM, and LPM (i.e., during a stage called limb field induction) and secondarily between the LPM and the overlying ectoderm (i.e., during a stage called limb bud induction). During limb field induction, a series of molecular interactions occur within the main mesodermal layers that eventually trigger marked novel gene expression patterns in the LPM. As mentioned, one component of this process involves the induction of *Hox* expression in the LPM that is believed to help provide competency and patterning information for limb field induction.

Another class of genes, encoding Fibroblast Growth Factor (Fgf) proteins, is strongly implicated in limb field induction. Fgfs constitute a large family of polypeptide growth factors that, by way of their binding to Fibroblast Growth Factor receptors (FgfRs) and the activation of signal transduction processes, serve as signaling molecules for many developmental processes (Thisse and Thisse, 2005). In mammals, there are twenty-two Fgfs and four FgfRs, although there are several splice variants for the receptor proteins. Throughout mouse limb development at least seven Fgfs (i.e., Fgf2, 4, 7, 8, 9, 10, and 17) and two FgfRs (i.e., FgfR1 and R2) are expressed where they play diverse roles.

With respect to limb field induction, Fgf8 is one candidate that may signal from the IM (specifically from the nephrogenic mesenchyme) to the LPM (Crossley et al., 1996; Vogel et al., 1996; Martin, 1998). However, functional loss of the nephrogenic mesenchyme in the mouse or blocking the posterior migration

of this tissue's cells in chick results in normal limb formation, suggesting that the IM may not be essential for limb field induction (Fernandez-Teran et al., 1996; 1997; Bouchard et al., 2002). In addition, in mice, conditional inactivation of *Fgf8* during initial mesoderm formation (i.e., during the primitive streak stage) leads to limb formation. Therefore, if *Fgf8* is involved in IM to LPM signaling it may act redundantly with other Fgfs and its loss in these experiments may have been co-opted. At this point in time, if the IM is considered important for limb field induction, its critical signaling molecules remain unknown.

Fgf signaling, however, does have important early roles within the LPM for limb field induction. It has been demonstrated that, once activated, the LPM expresses Fgfs which may lead to *Hox* gene expression. For example, in the experiments mentioned above by Cohn et al. (1997), Fgf-soaked beads were utilized to alter endogenous Fgf levels and the axial level of *Hox9* gene expression, and such alterations led to the formation of ectopic limbs. While the status of Fgf remains unclear in terms of IM to LPM signaling, its specific affect on *Hox* gene expression in the LPM demonstrates its importance sometime during early limb field induction.

With respect to limb bud induction, Fgfs have several roles. Once activated in the LPM, *Hox* gene expression is believed to up-regulate *Fgf8*, which has been demonstrated to cause adjacent LPM cells to synthesize another Fgf, Fgf10 in the limb bud mesenchyme. Importantly, Fgf10 has been shown to be critical in this tissue for the formation of limbs, specifically as *Fgf10*$^{-/-}$ embryos lack limbs altogether (Min et al., 1998; Ohuchi et al., 1997; Sekine et al., 1999).

Recently, several T-box transcription factors (Tbx) have been shown to be crucial for early limb field and bud induction. Specifically, the genes *Tbx5* and *Tbx4* are expressed in the respective forelimb and hindlimb mesenchyme and *Tbx5*$^{-/-}$ and conditional *Tbx4*$^{-/-}$ embryos fail to form these respective limb types (Agarwal et al., 2003; Adler, unpublished). With respect to Tbx5, biochemical and molecular data provide strong evidence that its early expression in the LPM serves to directly activate the promoter of *Fgf10* (Fig. 3.6). Furthermore, recent work in chick has demonstrated that PM signaling leads to the early activation of Tbx5 supporting this early upstream role (Saito et al., 2006). In addition to its effects on Fgf signaling, *Tbx5* loss impinges on the activity of Wingless (Wnt) signaling (Agarwal et al., 2003), which has additionally been implicated in limb bud induction along with its known roles in dorso-ventral patterning (see below). Therefore, *Tbx5* appears essential for forelimb outgrowth as it is upstream of two molecular pathways critical for limb bud induction. Finally, these studies have been supported by chick experiments, which demonstrate that upon mis-expression of *Tbx5* in the flank at the forelimb level the formation of an entire limb or limb-like structure can be induced (Ng et al., 2002).

The role of *Tbx4* in hindlimb development is less clear (Fig. 3.6). While *Tbx4*$^{-/-}$ mutants initially form hindlimbs, they regress shortly after the bud stage. This may result from the finding that in the mouse Tbx4 may only partially activate *Fgf10* and require additional partners/factors for sustaining activation of this gene (Minguillon et al., 2005). One such partner may be *Sall4*, whose co-expression with *Tbx4* in the limb mesenchyme induces and maintains *Fgf10*

activation. Interestingly, *Sall4*$^{-/-}$ mutants also possess severe hindlimb defects (Koshiba-Takeuchi et al., 2006). Therefore, it is likely that both *Tbx4* and *Sall4* either genetically interact directly or in parallel to govern hindlimb bud outgrowth.

With respect to limb type specification, there exist discrepancies between data from the chick and that of the mouse. In the mouse, *Tbx5* plays a critical role in limb outgrowth but not in the determination of limb field patterning and identity, a situation that is unlike that found for the chick, where *Tbx5* appears upstream of genes responsible for determining "forelimbness." A similar situation holds for Tbx4 where it also appears partially upstream of limb bud induction but not identity. For example, when mis-expressed in the mouse forelimb field, this "hindlimb-specific" gene induces the formation of a perfectly normal forelimb (Minguillon et al., 2005). At this point in time, the only gene known in mice to specify limb field identity appears to be that of *Pitx1* which has been shown to be genetically upstream of most markers involved in hindlimb identity (Marcil et al., 2003; Minguillon et al., 2005). Furthermore, ectopic mis-expression of *Pitx1* in the forelimb field leads to the partial transformation of a forelimb into a hindlimb (Minguillon et al., 2005).

Once the LPM receives signals (via Tbx, Wnt, or other factors) and *Fgf10* expression is underway, a series of reciprocal interactions with the ectoderm occurs which promotes cellular outbudding of the mesenchyme (Fig. 3.6). In mice, Fgf10 signals through Wnt3a to trigger *Fgf8* expression in the ectoderm (Barrow et al., 2003). Once expressed, Fgf8 then triggers through Fgfr2 in the underlying mesenchyme *Fgf10* expression that promotes cellular growth and

proliferation (Xu et al., 1998; Lizarraga et al., 1999). At this stage, proliferation occurs although at a rate that is not substantially different from that seen throughout the developing embryo. This reciprocity between the ectoderm and mesenchyme propagates limb bud outgrowth even as the ectoderm matures.

Interestingly, tissue transplantations in chick by Saunders (e.g., Saunders et al., 1958; Bell et al., 1959; 1962) foreshadowed the critical molecular role of the ectoderm during initial limb bud outgrowth. By removing the overlying ectoderm of early flank and limb buds, Saunders was able to terminate limb bud development, in manner according to timing of ectodermal removal. More recently, if beads soaked in Fgf8 or Fgf10 protein are placed in the developing flank, ectopic limbs form, whereas if they are placed after ectodermal removal, limb outgrowth/initiation is rescued and normally proceeds (reviewed in Niswander, 2003). Therefore, all of these studies provide strong evidence for the roles of both the mesenchyme and the ectoderm in governing limb outgrowth.

3.3.3 Limb axis (A-P, P-D, and D-V) establishment

3.3.3.1 Early events in the establishment of the three limb axes (E8.5-E9.5)

At the onset of limb outgrowth, the bud possesses a partial molecular asymmetry along all three axes due to the expression of genes in the flank (Fig. 3.7). This expression allows for a prepatterning to occur, which is particularly evident along the A-P axis. For example, *Hand2* is initially expressed along the flank prior to limb bud outgrowth, although at the onset of budding it loses its anterior expression domain and becomes posteriorized (te Welscher et al.,

2002). In contrast, at bud onset, Aristaless family genes such as *Alx3*, *Alx4*, and *Cart1*, and the zinc finger protein gene *Gli3* become anteriorly expressed (Beverdam and Meijlink, 2001). In addition, several additional T-box genes (i.e., *Tbx2* and *Tbx3*) become both anteriorly and posteriorly expressed (Gibson-Brown et al., 1996; 1998; Rallis et al., 2005; King et al., 2006).

With respect to *Gli3*, *Alx4*, and *Hand2*, te Welscher et al. (2002) demonstrated that a mutual antagonism exists between their proteins in the early limb bud (Fig. 3.7). Specifically, it was shown that Gli3 restricts Hand2 expression to the posterior limb domain. This is important since *Hand2* has been shown to be genetically upstream of *Shh*, a gene essential for ZPA and skeletal element determination (Charite et al., 2000). Concurrent with this restriction, Hand2 has been shown to prevent the expansion of Alx4 and Gli3 into posterior limb domains (te Welscher et al., 2002). In the anterior mesenchyme, Gli3 further appears to function upstream of Alx4 activation (te Welscher et al., 2002). In addition, fate mapping studies in amphibian and chick systems have demonstrated that forelimb stylopod and girdle progenitors arise from the anterior compartment of the limb field (Koussoulakos, 2004) while experimental mouse genetics demonstrate that compound mutants for *Alx4*, *Gli3*, and other anteriorly expressed genes (i.e., *Cart* 1) result in scapula alterations (Kuijper et al., 2005). Therefore, the mutual antagonism that exists predominately between Hand2 and Gli3 establishes unique posterior and anterior zones that are critical for later limb and girdle development.

Tbx2 and *Tbx3* roles during this initial A-P asymmetry stage are unclear in the mouse, although, their experimental deletion appears to alter later digital patterning (Davenport et al., 2003). Conversely, in the chick, *Tbx2* and *Tbx3* are thought to delineate the anterior and posterior mesenchyme that propagates into the limb and in some chick mutants, altered *Tbx2* and *Tbx3* expression reflects these tissue outgrowth alterations (Rallis et al., 2005). In this manner, both *Tbx2* and *Tbx3* may act as cues to delineate the A-P extent of the limb field (i.e., the rostral-caudal expanse of tissue, across a specified number of somites, that will undergo induction and form the limb).

Early P-D axis establishment is under the continued control of those genes present in both the mesenchyme and ectoderm during initial limb bud outgrowth (i.e., *Fgf8*, *Fgf10*, etc.). In addition, several other molecular factors are critical to P-D axis establishment. At the onset of limb induction, Meinox family genes, *Meis1* and *Meis2*, are first expressed in the LPM but then become restricted to the proximal bud mesenchyme, where their initial function remains uncertain. In the chick, mis-expression of *Meis1* and/or *Meis2* in the distal limb bud causes proximalization of the limb (i.e., distal structures take on a more proximal identity), thereby evincing their roles in early P-D establishment and skeletal patterning (Mercader et al., 1999). However, in the mouse, mutants for each of these two genes lack limb defects, perhaps suggesting a multifaceted (i.e., redundant) control of proximal limb identity (Hisa et al., 2004; unpublished data). Recent work on *Pbx1* (a cofactor which often dimerizes with Meis proteins, see Section 3.5) also demonstrates its role as a proximal mesenchyme marker

specifically as mice deficient for this gene have proximal defects in the limb and girdle (Selleri et al., 2001).

Once limb bud induction commences, Fibroblast growth factor signaling from the ectoderm (and future AER) to the limb mesenchyme establishes a gradient of Fgf signaling which is highest in the distal limb bud. This gradient is initially established via Fgf8 and Fgf10 signaling loop to/from the ectoderm and mesenchyme, respectively and continues during limb outgrowth (Niswander and Martin, 1993a-b; Olwin et al., 1994; Niswander et al., 1993; 1994a-b). The functions of this distal signaling are to promote cell survival, proliferation, and distalization of the limb.

It is additionally understood that soon after limb initiation (E9.5/E10.0), retinoic acid (RA) acts in the mesenchyme as an essential modulator of P-D outgrowth (Mercader et al., 2000); and several RA related genes are expressed in the limb where they appear to modulate it's signaling. In the proximal limb mesenchyme, retinaldehyde dehydrogenase 2 (RaldH2) acts to convert retinol into functional or active RA (Niederreither et al., 1999; Hsu et al., 2000). RA in this proximal domain early in bud outgrowth is probably aiding in growth promotion, specifically evinced by the findings that *RaldH2*$^{-/-}$ embryos fail to form limbs and that administration of RA to these embryos rescues, in a dose dependent manner, limb bud formation (Mic et al., 2004). In the distal limb, the cytochrome P450 enzyme, Cyp26b1, has been shown to inactivate RA in this domain (Abu-Abed et al., 2002; Yashiro et al., 2004). The normal degradation of RA in distal domains may allow cells to be differentially affected by other

signaling molecules (e.g., Fgfs) and remain in an active state. Indeed, in *Cyp26b1*$^{-/-}$ mouse embryos, limbs are truncated, have extended proximal identities, as well as the loss of distal identities (Yashiro et al., 2004). Therefore, there appears to be a unique P-D gradient of RA in the limb, highest proximally and lowest distally, that allows limb bud outgrowth and skeletal element specification to occur in a highly coordinated fashion (Mercader et al., 2000). Finally, other RA-related genes, such as the retinoic acid receptor genes (i.e., *RAR*α, *RAR*β, *RAR*γ, *RXR*α, *RXR*β, and *RXR*γ) are expressed throughout limb bud development, suggesting that cells within this RA gradient may have the capabilities to differentially respond to different RA levels (Dolle et al., 1990). Indeed, compound mutant mice for these genes display severe limb skeletal defects (Lohnes et al., 1994). Overall, with respect to initial P-D axis determination, limb outgrowth could thus be construed as the cellular readout (via the control of cell proliferation and programmed death) of opposing RA and Fgf gradients (Mercader et al., 2000).

The formation of the early P-D axis is also critically connected to D-V axis development (Niswander, 2003). After initial limb bud formation the mechanisms that regulate D-V axis formation and skeletal patterning are under the control of the ectoderm. The role of the ectoderm is highlighted by chick experiments where 180-degree rotation of this tissue with respect to the underlying mesenchyme results a similar inversion in the patterning of the mesenchyme

(MacCabe et al., 1974; Pautou, 1973; Geduspan and MacCabe, 1986; 1987; 1989).

From a molecular/genetic perspective, only recently have several of the major ectodermal regulators of D-V axis formation and patterning been identified (Fig. 3.8). Two critical genetic regulators are *Engrailed1* (*En1*), expressed in the ventral ectoderm, and *Wnt7a*, expressed in the dorsal ectoderm. Genetic studies in *En1*$^{-/-}$ and *Wnt7a*$^{-/-}$ mice demonstrate D-V patterning defects and the absence of normal ectoderm AER initiation (Parr and McMahon, 1995; Loomis et al., 1996; Cygan et al., 1997; Loomis et al., 1998). Specifically, *En1*$^{-/-}$ mice have ventro-proximally broadened AER, partial dorsal transformations of the ventral forelimb paw, and digital fusions (Wurst et al., 1994; Loomis et al., 1996; Cygan et al., 1997). *Wnt7a*$^{-/-}$ mutant mice possess ventral structures such as footpads on the dorsal surfaces of their paws; and display the loss of posterior digits indicating an additional role of *Wnt7a* in digital patterning along the A-P axis (Parr and McMahon, 1995).

As both genes are expressed in the ectoderm, they have been shown to interact, particularly at the D-V interface (Fig. 3.8). En1 has been shown to inhibit Wnt7a signaling ventrally, and restrict it to the dorsal ectoderm where it serves to influence the underlying mesenchyme to express the transcription factor *Lmx1b* (Loomis et al., 1996; Logan et al., 1997). *Lmx1b* has also been shown to be critical for dorsal mesenchymal patterning (Riddle et al., 1995; Vogel et al., 1995; Chen et al., 1998b). Interestingly, *Lmx1b* expression prior to *Wnt7a* is present throughout the limb's ventral and dorsal mesenchyme but then

becomes restricted to the dorsal mesenchyme via the interaction of En1 and Wnt7a. Studies on the genetic interactions of these two genes indicate that D-V patterning is intimately linked to P-D axis and AER formation (see below).

3.3.3.2 AER formation and P-D axis establishment (E8.5-E10.5)

During early limb bud induction, the ectoderm overlying the limb mesenchyme consists of a single flattened cuboidal epithelium. Shortly after induction, a subpopulation of this ectoderm migrates to the limb's distal surface where it transforms into the tightly packed pseudostratified columnar epithelium of the AER (Fig. 3.5) (Niswander, 2003). In this manner, AER formation involves three stages: (1) induction of specific ventral ectodermal cell populations; (2) migration of these cells along a ventral border to the distal D-V interface of the bud; and (3) compaction of these cells into a pseudostratified epithelium (Niswander, 2003).

When limb bud outgrowth commences, Fgf10 signaling in the distal mesenchyme induces *Fgf8*, which also leads to changes to the ectoderm. In mice, this initial ectodermal cell population is ventrally positioned in the limb and fate-mapping studies suggest a ventral origin for the AER (Kimmel et al., 2000). On the other hand, in the chick, *Fgf8* expressing and non-expressing ectodermal cells are situated both dorsally and ventrally and AER precursors arise from both of these populations (Altabef et al., 1997). In the mouse, once the ridge precursors are specified, they express other genes such as *En1*, *Dlx*, and *Msx2*

and migrate distally to become concentrated at the limb bud apex where they eventually form the AER.

Critical to the distal localization of cells are a series of genetic interactions between the dorsal and ventral ectodermal borders of the limb bud. While ventral expression of *En1* is essential for ventral fate, it also is critical in the AER compaction. Specifically, in addition to their ventral defects, *En1*$^{-/-}$ mice have limbs with AER cells that fail to form a strong tight epithelial layer at the distal tip (Loomis et al., 1998). Likewise, in limbs where *En1* has been mis-expressed, compaction is altered quite drastically and AER are flattened and extend more ventrally than normal (Kimmel et al., 2000). On the other hand, *Wnt7a* expression in the dorsal ectoderm delineates the dorsal boarder of the AER forming cells, and in this way helps to restrict its formation ventrally (Adamska et al., 2003). *Wnt7a*$^{-/-}$ embryos have duplications of the AER and are appropriately called “double ridge” mutants.

Actual compaction of pre-AER cells into pseudostratified epithelium requires that the initial D-V boundaries are refined at the distal tip. As shown in Figure 3.8, initially (at 28 to 29 somites) prior to AER formation, *Wnt7a* expression is present in the majority of the ectoderm, while, a small ventral ectodermal population expresses *Fgf8, En1, Dlx2*, *Msx2*, among other genes. At this time, in the mesenchyme, *Lmx1b* transcripts occupy the entire limb bud domain. As ventral pre-AER cells commence to their more distal tip (from 28 to 33 somites), *En1* expression becomes solely expressed and appears to inhibit the expression of *Lmx1b* in the subjacent ventral mesenchyme via a repression

of Wnt7a ventrally. Over the course of development (from 28 to 36 somites), the dorso-ventral mesenchymal and ectodermal interfaces become more refined and distinct, and the pseudostratified epithelium forms (Bell et al., 1998).

En1 and Wnt7a function during D-V and AER formation is also contingent on the proper activation and signaling of Bone Morphogenetic Proteins (Bmps) and an additional member of the Wnt ligand family. Conditional targeting of the type I Bmp receptor (*BmpRIA*) gene in mice and molecular gain and loss of function studies in the chick demonstrate that Bmp signaling is necessary and sufficient to regulate D-V patterning (Ahn et al., 2001; Pizette et al., 2001). Bmp signaling within the ventral ectoderm positively controls *En1* expression (Ahn et al., 2001). Thus, Bmp is upstream of *En1* in D-V patterning. At the same time, Bmp signaling also lies upstream of AER formation, although in this manner it works partially through different factors such as members of the Msx family (Pizette et al., 2001). These studies indicate that D-V patterning and AER induction are coordinately regulated by Bmp, and suggest that En1 and Msx function independently of one another yet downstream of Bmp to differentially mediate these two aspects of limb development. In fact, mice where *BmpR1A* is conditionally inactivated have complete abrogation of hindlimbs evincing its hierarchical upstream role (Hill et al., 2006).

Throughout AER formation, numerous genes become expressed in the relatively unorganized ectoderm and remain active in the mature pseudostratified epithelium. These genes include (but are not limited to): *Bmp2*, *Bmp4*, *Bmp7(?)*, *CD44*, *Cv43*, *Dlx1*, *Dlx2*, *Dlx5*, *Dlx6*, *FgF2*, *Fgf4*, *Fgf8*, *Fgf9*, *Fgf17*, *Msx1*, and

Msx2. Many of these genes (e.g., *Dlx*, *Msx*) code for transcription factors, indicating that mature AER gene expression is not only quite complex and dynamic but subjected to tight temporal and spatial regulation. Several of these genes also code for signaling molecules, the most important (thus far studied) are the Fgfs that have known short and long distance effects to the developing bud. Based on genetic ablation studies in mice, another critical aspect of AER gene function is the tremendous degree of genetic redundancy among factors. Typically, mutant mice for any one single AER-expressed gene lack observable phenotypic defects or display only slight alterations in limb development. However, double mutant mice for many members of each gene family (e.g., *Fgf*, *Dlx*, *Msx*, *Bmp*, etc) typically show drastic alterations in limb bud outgrowth (e.g., Robledo et al., 2002; Sun et al., 2002; Lallemand et al., 2005).

3.3.3.3 Later A-P axis establishment (E9.5-E11.5)

That the early E9.5 fore- and E10.0 hindlimb bud, respectively, possess A-P polarity, has been known since the work of Saunders and Gasseling (1968). These authors identified that the most posterior region of the limb bud acquires the potential to determine posterior skeletal fate. Using transplantation experiments in the chick, they demonstrated that when an early limb bud's posterior tissue was placed in the same chick on its contralateral limb's anterior surface, mirror image duplications formed for most zeugopodial and autopodial elements. When older posterior tissue explants were placed in the same manner, it still caused duplications, but to a lesser extent (i.e., only more distal autopodial

elements were anteriorly duplicated). These results indicated that the posterior tissue had a polarizing effect on the limb and was able to act as an organizing center guiding proper morphogenesis. As a result, this region was called the zone of polarizing activity (ZPA) (Saunders and Gasseling, 1968) (Fig. 3.5).

The discovery of the ZPA, led to the idea that early A-P patterning is essential for the formation of proper morphological pattern. These experiments also lead to the conclusion that the ZPA emits some sort of morphogen or molecule capable of signaling across the limb bud's A-P domain, whose diffusion establishes a spatial gradient with its high point in the posterior limb bud mesenchyme. In this system, cell fates are specified according to distinct threshold values depending on their distance from the ZPA (Wolpert, 1969).

These insights led to the search for the molecular basis of ZPA function and eventually to the discovery of *Shh*, a gene whose expression in the posterior limb (Echelard et al., 1993; Krauss et al., 1993; Riddle et al., 1993) nicely correlates with those tissues possessing ZPA activity. *Shh* encodes a secreted protein related to the Drosophila protein, Hedgehog. Several experiments were performed that directly link Shh to this polarizing potential. These experiments involved either the placement of Shh-soaked beads or chick fibroblasts virally transfected with the *Shh* gene into regions of limbs that corresponded to the areas where ZPA grafts were placed in earlier studies (Echelard et al., 1993; Krauss et al., 1993; Riddle et al., 1993; Lopez-Martinez et al., 1995). In these experiments, mirror image duplications also formed in ectopic anterior locations unequivocally pointing to Shh as the active polarizing agent in the ZPA.

Recent research has focused on two related issues regarding ZPA formation, specifically, how it forms molecularly and how its maintenance leads to the formation of morphologically distinct digits in the autopod. In the search for how *Shh* expression is initiated and therefore how the main A-P axis becomes established via ZPA formation, studies examined early prepatterning stages and the expression of genes turned on prior to *Shh* expression. The early A-P axis expression/distribution of *Alx4, Gli3, Hand2*, *Hox*, and RA suggested that they lie critically upstream and determine the spatio-temporal onset of *Shh* expression in the posterior limb bud (Charite et al., 2000; te Welscher et al., 2002) (Fig. 3.9).

Research in the 1990's demonstrated that RA is indeed capable of inducing *Shh* expression when misapplied in the limb (Helms et al., 1994). For example, when anteriorly placed in the chick limb bud, RA-soaked beads caused ectopic expression of *Shh* and mirror image duplications. Furthermore, this polarizing potential of RA was time and dose dependent: the earlier the ectopic implantation of RA-soaked beads, the more complete the anterior duplication of the entire limb skeleton (Niswander, 2003). While RA is still considered an important limb factor, it has been difficult to demonstrate its *in vivo* upstream and direct role on *Shh* initiation because: (1) RA activity is not isolated to the ZPA (but resides broadly in the limb mesenchyme; and (2) RA levels in the limb do not reach levels of those of soaked beads (McGlinn and Tabin, 2006; Tickle, 2006).

The relationship between RA and *Shh* initiation has become better understood due to work on individual *Hox* genes in the limb, which have also been shown to lie upstream of *Shh* (Zakany et al., 2004) (Fig. 3.9). Interestingly,

upon ectopic RA application in the chick wing bud, several *Hox* genes were found to be up-regulated. In particular, *Hoxb8* expression was up-regulated in the anterior forelimb field prior to ectopic *Shh* activation (Lu et al., 1997). Normally it is posteriorly expressed in the forelimb bud in a manner that significantly overlaps with the future ZPA. When taken in this context, *Hoxb8* in the forelimb appeared as an excellent candidate activator of *Shh* in the ZPA. Indeed, Charite et al. (1994) demonstrated that when Hoxb8 protein is ectopically expressed throughout the forelimb bud, both the anterior and posterior mesoderm express *Shh*, creating two ZPAs and mirror image forelimb duplications. Therefore, *Hoxb8* may be a potential activator of *Shh* as well as a mediator of RA's effects on *Shh* in the ZPA. However, two important points must be considered: (1) while forelimb *Shh* expression may indeed be contingent on *Hoxb8*, hindlimb ZPA formation occurs independently of *Hoxb8*, as it is not expressed in the hindlimb; and (2) studies on mice lacking *Hoxb8* or all three *Hox8* paralogs, lack limb defects and possess normal *Shh* expression (van den Akker et al., 2001) thereby indicating that *Hoxb8* in mice is either not essential for *Shh* activation, or that it must work with numerous other *Hox* genes in this process.

With respect to the first point (1), recent work on micro-RNA has provided some important insights. Hornstein et al. (2005) have demonstrated that the hindlimb-specific expression of *miR-196* leads to the degradation of Hoxb8 in this domain. Furthermore, when applied ectopically in the forelimb, *miR-196* prevents the induction of *Hoxb8* by RA and attenuates but not terminates *Shh*

expression. In addition, conditional inactivation in the hindlimb of *Dicer*, a gene which encodes a key enzyme involved in *miR-196* functionality, results in the ability of *Hoxb8* to be induced by RA indicating that evolutionary divergence in miRNAs, RA, and *Hox* genes has established a system that prevents specific *Hox* genes from being expressed in hindlimb domains. In this manner, the expression of other *Hox* paralogous genes, such as *Hox9* paralogs, may be important for *Shh* initiation in the hindlimb (Robert and Lallemand, 2006).

With respect to the second point (2), more recent work suggests that early *Hox* gene collinearity in the limb is essential for the posterior activation of *Shh* (Zakany et al., 2004; Tarchini and Duboule, 2006). The activation of *HoxA*, *HoxB*, *HoxC*, and *HoxD* gene transcription results in the presence of an overlapping and nested *Hox* expression pattern along the posterior limb (see below). Of these gene clusters, *HoxA* and *HoxD* appear most important, although the contribution of the other clusters should not be disregarded.

Research on ectopic *HoxD* mis-expression supports their upstream role in *Shh* activation. For example, *Hoxd12* mis-expression has led to *Shh* up-regulation further supporting the roles of multiple Hox proteins in this regard (Knezevic et al., 1997). However, similar to the loss of *Hoxb8* paralogs, loss of *Hoxd12* does not result in *Shh* absence. These data suggest either that *Hox* can operate redundantly in their activation of *Shh* transcription and/or that the precise spatio-temporal execution of *Hox* gene expression is a necessary prerequisite for *Shh* activation.

Studies utilizing limb-specific deletions of partial *Hox* clusters strongly support the role of multiple Hox proteins acting directly upstream of *Shh*. Duboule and colleagues have altered the chromosomal position and collinear activation of *Hox* genes during limb development by using the TAMERE gene targeting strategy (see Herault et al., 1998b; 2002). In these studies, repositioning *Hoxa9-13* and *Hoxd9-13* to more 3' positions on the chromosome led to *Shh* absence in mutant limbs (Zakany et al., 2004). Indeed, their earlier work also demonstrated that the loss of *Hoxd9-13* results in severe patterning alterations in the limb, albeit in these studies, the onset and duration of *Shh* expression was not thoroughly investigated (Zakany et al., 1997). Most recently, functional and conditional inactivation of the entire *HoxA* and *HoxD* clusters from the limb mesenchyme, led not only to complete *Shh* absence but also to truncations of the limb, proximal to the mid-zeugopodial region (Kmita et al., 2005). These data suggest that *Hox* collinear activation is required for mesenchyme cell patterning, including the initiation of *Shh* expression in posterior limb cells. Nevertheless, it is uncertain as of yet whether Hox proteins directly activate *Shh* transcription or that *Hox* gene expression is necessary to trigger an intermediate molecule that then directly acts on *Shh*.

Other transcription factors have also been shown to lie upstream of *Shh* during development (Fig. 3.9). *Hand2* is expressed in the limb's posterior mesoderm immediately prior to *Shh* expression and *Hand2*$^{-/-}$ embryos never express *Shh* (Charite et al., 2000). In addition, ectopic *Hand2* expression in the anterior region of the mouse limb leads to a second ZPA and duplications of the

digits (Charite et al., 2000). Therefore, it appears that *Hand2* is critical for *Shh* activation, although whether Hand2 proteins directly regulate *Shh* expression, or do so by first inducing *Hox* gene expression, remains unknown (Yelon et al., 2000). Interestingly, *Hand2* also appears downstream of *Shh* suggesting that a regulatory loop may exist between these two genes (Zakany et al., 2004).

Recently, *Tbx3* has also been shown to be upstream of *Shh* (Davenport et al., 2003) (Fig. 3.9). *Tbx3* is expressed in distinct anterior and posterior domains of the limb and *Tbx3*$^{-/-}$ mouse embryos display a low penetrance of *Shh* absence (less than 15% of cases), suggesting that its effects on *Shh* may be indirect and sensitive to other developmental fluctuations occurring in these mutants. For example, in the chick *Tbx3* mis-expression alters the size of the forelimb field, alters the expression of *Hand2*, *Gli3*, as well as *Shh* which indicates that *Tbx3* may be acting earlier to control initial limb A-P axis asymmetry (Rallis et al., 2005). *Tbx2*, is also expressed in the vicinity of the ZPA, although mouse mutants for this gene display no evidence of *Shh* disruption (Harrelson et al., 2004). Instead, mis-expression studies in the chick suggest that Tbx2 regulates the anterior extent of the Shh protein domain and not initiation (Suzuki et al., 2004). Overall, the findings that two early limb field markers (*Tbx3* and *Hand2*) lie upstream of *Shh* support the hypothesis that intrinsic patterning cues may already be established at bud onset and have partitioned the limb into relatively naïve, yet competent, developmental domains.

Finally, the initiation of *Shh* expression has also been examined from the perspective of its *cis*-regulation. Specific mutant mice, such as *Hemimelic Extra-*

toes, *Sasquatch*, and *M100081*, harbor mutations in domains that are in *cis* approximately 1 mega-base (mb) and 3' of the *Shh* coding sequence (Lettice et al., 2002; 2003; Sagai et al., 2004). These mutants display anterior digit duplications in a similar to fashion to mice where *Shh* is mis-expressed in the anterior limb field. These mutations have been mapped to a 500 base-pair (bp) element that is extremely conserved among vertebrates; and a 450 bp fragment of this element has been shown to drive normal expression of *Shh* in transgenic mice (Lettice et al., 2003). Furthermore, deletion of this element, deemed as a long-range limb-specific *Shh* enhancer, results in *Shh* absence in the limb (Sagai et al., 2005). Interestingly, additional work on the enhancer element using *Hemimelic Extra-toes* mutant mice, indicates that it may contain sequences that restrict its ability to drive expression only in the posterior mesenchyme (Maas and Fallon, 2005).

While the mechanisms that govern *Shh* activation remain unclear more is known about Shh function during limb development. Historically, most of this function has been explored indirectly through investigations on the ZPA. These ZPA explant and extrication experiments, as well as experiments utilizing Shh-soaked beads, proved limited and did not efficiently demonstrate the true role(s) of Shh in the limb. More recent studies on mice where the *Shh* locus has been altered in several ways, more clearly depicts its functions.

Chiang et al. (1996) demonstrated by generating $Shh^{-/-}$ embryos that *Shh* is required for distal limb development as these mutants display severe zeugopodial and autopodial defects. Specifically, in the forelimb, skeletal

elements of digits 2-5 and the distal ulna are absent, whereas the humerus, radius, and digit one appear unaffected. In their hindlimbs, distal elements are more severely affected with the condensations for the tibia, fibula, and all four posterior digital rays, absent. One possible mechanistic explanation for the loss of most zeugopodial and autopodial condensations is the presence of marked and extensive abnormal cell death in the distal domain of *Shh*$^{-/-}$ limb buds (Chiang et al., 2001). This apoptosis suggests that Shh protein may influence skeletal condensation number and morphology by controlling cell survival.

The finding that *Shh* mutants lack posterior digits suggests that it is important in regulating both skeletal identity and digit number. In this respect, the Shh signaling pathway has appeared critical since when many of the pathway's genes are experimentally deleted these aspects of digit morphogenesis became apparent. Normally, in Shh protein absence at the cell membrane, its receptor Patched represses Smoothened, and the Gli3 transcription factor is proteolytically cleaved and acts as a transcriptional repressor (Fig. 3.10A). However, when Shh is present, its binding to Patched relieves Smoothened repression, and inhibits Gli3 proteolytic cleavage, thereby generating transcriptional activator forms (Fig. 3.10B) (Niswander, 2003).

The concentration of Shh is thus believed to regulate target gene expression by controlling the ratio of Gli3 repressor and activator forms (Wang, 2000) (Fig. 3.11). This interactive control is demonstrated by the relative distribution of these proteins across the limb bud with higher levels of Gli3 activator posteriorly and more elevated levels of repressor anteriorly. These

differential gradients are also reflected by the presence of additional Gli proteins (Gli1 and Gli2) that are downstream of Shh and Gli3 proteins and have limited, but important roles in the signal transduction pathway.

Studies on the signal transduction pathway have shed light on the observed phenotypes of *Shh*$^{-/-}$ embryonic limbs (Chiang et al., 1996). Specifically, the ectopic apoptosis observed in *Shh*$^{-/-}$ limbs may have resulted from the abnormally high levels of Gli3 repressor produced in the absence of Shh and present ubiquitously across the A-P axis. In fact, removing one functional copy of *Gli3* from an already *Shh* deficient background (i.e., *Shh*$^{-/-}$*;Gli3*$^{+/-}$) results in a marked decrease in ectopic apoptosis and an amelioration of the *Shh* null phenotype. For example, in *Shh*$^{-/-}$*;Gli3*$^{+/-}$ embryos, both zeugopod, and autopod skeletal elements develop, presumably because sufficient chondrocyte progenitors escape cell death and become available to form condensations. *Shh*$^{-/-}$*;Gli3*$^{+/-}$ embryos do have fewer digits (3–4) than wildtype pattern (te Welscher et al., 2002), and the digits which form all resemble digit 1 as determined by phalangeal number. Interestingly, further removing both functional copies of *Gli3* (i.e., *Shh*$^{-/-}$*;Gli3*$^{-/-}$) eliminates ectopic apoptosis altogether, and restores the Gli3 phenotype (i.e., limbs with 6-11 digits); however, each digit is morphologically indistinguishable, and difficult to categorize (te Welscher et al., 2002).

While the Gli3 repressor/activator ratio and Gli3/Shh ratio are essential for limb development, little information is available as to the direct function of Shh (if any exists) outside any effect mediated through Gli3. That information which is available suggests that the presence of Shh protein along a spatial

morphogenetic gradient in the limb is necessary to initiate threshold responses for cells across the limbs A-P axis (i.e., it provides positional information to the limb by behaving as a morphogen) (McGlinn and Tabin, 2006). In this fashion, the differential distribution of Shh has been argued to specify digit 2-5 identities.

To understand this process of digit specification further, Harfe et al. (2004) generated a mutant mouse where all *Shh*-expressing cells and their descendants were marked and detectable for visualization. Through the use of the Cre-Lox system, the *Shh* promoter, and a reporter construct containing ROSA, they were able to induce permanent Beta-galactosidase (Beta-Gal) and/or green fluorescent protein (GFP) expression in cells that once expressed *Shh*. They could therefore trace from the onset of *Shh* expression, or at specific time points during mouse limb bud development, cells that at one point were fated in the ZPA. Detection of Beta-Gal at time points before or directly after *Shh* onset required the additional use of an inducible system using Tamoxifen induced cre-recombinase, coupled with a ROSA reporter line (see Harfe et al., 2004).

The first result of these cell lineage (fate-mapping) studies was that ZPA cells, once they expressed *Shh*, were not eliminated by apoptosis. Rather, they gave direct rise to descendants that either remained posteriorly as ZPA cells (and maintained *Shh* expression) or lost direct *Shh* activation, and expanded/ migrated distal-anteriorly to populate the zeugopodial and autopodial regions. Specifically, the direct descendants of *Shh* gave rise to the limb's most posterior digits (5 and 4), the posterior part of digit 3, as well as the distal ulna/fibula. (recall, that the global $Shh^{-/-}$ mouse lacks these structures plus digit 2).

Therefore, these fate-mapping studies provide strong evidence that: (1) digit 2 is not made up of cells that once expressed *Shh*; (2) morphogenesis of digit 2 may be more clearly linked to the morphogenetic aspect of Shh signaling (i.e., that Shh acts as a diffusible morphogen); and (3) digit one remains outside the direct influence of *Shh* expression/protein distribution.

Harfe et al. (2004) also sought to understand how identities for digits 3 to 5 become specified. Using their Tamoxifen induced Cre-reporter construct they irreversibly marked cells at time points after *Shh* initiation. They found that overtime, the fates of "once *Shh*-expressing" cells became posteriorly restricted such that the longer the time that they expressed *Shh* the more posterior they became in identity. In this manner, cells that either are formed prior to *Shh* expression give rise predominately to all three posterior digits, whereas those that continually express *Shh* for the duration of limb outgrowth remain strictly posteriorly. Therefore, digit 3 appears to be most sensitive to Shh activity, as its formation requires only temporary *Shh* activation (i.e., not sustained *Shh* expression over the course of ZPA formation).

These results support the notion that ZPA cells somehow acquire a memory of the Shh signal (see Zeller, 2004). Such data are in agreement with earlier studies on ZPA and Shh bead explants, which found that the later such explants are made, the more rudimentary the anterior duplication and the more indistinguishable the forming digits become (reviewed in McGlinn and Tabin, 2006 and Tickle, 2006). What remains unclear from these studies is how the identity of digit 2 becomes specified particularly in light of the increasing evidence

against Shh as acting strictly in a morphogenetic manner. It is possible that *Shh* expression in the ZPA triggers instructive behaviors that allow cells to not only migrate and populate the posterior zeugopod and autopod but also to trigger downstream genes that may then act as the morphogens necessary to determine digit morphogenesis. In this manner, as shown by Harfe et al. (2004), not all cells that become digits 3-5 (and the distal ulna and fibula) are *Shh* expressing cells or descendants thereof. Indeed, there does appear to be mixing of cells through repopulation, which possibly indicates that "once *Shh* expressing" cells have the property to instruct nearby non-expressing cells to form the mesenchymal condensations of the digits.

In a complementary study, Ahn and Joyner (2004) labeled mouse limb bud cells responding to Shh signaling by analyzing *Gli1* transcriptional activation. *Gli1* is a transcriptional target of Shh signaling as discussed by Wang et al. (2000). In their assay, Ahn and Joyner (2004) engineered *Gli1* to allow for permanent activation of an inducible Beta-Gal lineage marker at specific time points in cells responding to Shh. Accordingly, cells responding to Shh would trigger *Gli1* and the downstream expression of Beta-Gal. Their findings establish that the mesenchymal cells giving rise to digits 2 to 5 and the distal ulna arise via Shh signaling. Accordingly, these cells were not only detectable by Beta-Gal staining but also possessed *Gli1* promoter activity and expression.

Overall, the current state of knowledge is that the posterior autopod and posterior zeugopod of the vertebrate limb bud is patterned predominately by a kinetic memory in cells. In this manner, cells throughout the limb are exposed to

varying strengths and differing durations of Shh and this has repercussions on Gli3 repressor activity and ultimately element identity. While this viewpoint explains well the formation of identifiable digits whether this mechanism is working to codify ulnar identity is more problematic and currently unclear.

3.3.3.4 *Hox* genes and their roles in axis formation and skeletal patterning

Before moving on to how axis maintenance is regulated and ultimately how skeletal elements become patterned it is important to review what is known about *Hox* genes, due to their involvement in these aspects of limb development. Indeed, *Hox* genes are important patterning genes for many tissues in the developing embryo (Hunt and Krumlauf, 1992). In mammalian vertebrates, as in all studied tetrapods, *Hox* genes are organized into 4 clusters (*HoxA*, *HoxB*, *HoxC* and *HoxD*) comprising 39 genes in total (Fig. 3.12) (Carroll et al., 2005). In many marine vertebrates, such as the actinopterygians, several of the clusters have been duplicated resulting in a minimum of seven clusters (van der Hoeven et al., 1996). In invertebrates, such as *Drosophila*, *Hox* genes are organized in one cluster (*HomC*) and this single cluster organization is argued to be derived from a more simplistic single cluster organization shared between basal invertebrates and vertebrates (Gilbert, 2006). A review of *Hox* gene evolution is provided by Garcia-Fernandez (2005).

Phylogenetic studies on inter-*Hox* cluster organization indicate that 3' members of the same number (i.e., *Hoxa1* and *Hoxd1*) are very similar in sequence to one another, and are evolutionary related (Krumlauf, 1994; Garcia-

Fernandez, 2005). They are therefore considered to be of the same paralogous group. Not all clusters, as shown in Figure 3.12, contain paralogs, thus reflecting the unique evolutionary history of each cluster (Carroll et al., 2005).

In both invertebrates and vertebrates, *Hox* genes are organized on the chromosome(s) in the physical order in which they are temporally and spatially expressed during development. For example, in the developing mammalian embryo, 3' *Hox* are expressed first and predominately rostrally (i.e., they possess the most rostral expanded domains) along the head to tail axis, while *Hox* located 5' in the cluster become expressed later and more caudally (Fig. 3.12). This principle is known as temporal and spatial collinearity. Interestingly, *Hox* genes on different chromosomes are also roughly expressed at similar axial levels and at roughly similar times. For example, early 3' *Hoxa1* and *Hoxd1* are expressed approximately at the same time and rostral in the developing embryo.

Members of all four *Hox* gene clusters are expressed throughout limb development. *HoxA* cluster genes are predominately expressed along a proximal to distal gradient during limb development (Fig. 3.13A). At the onset of limb bud formation (E9.0-E10.0 FL, E9.75-10.25 HL), *Hoxa9* is expressed throughout the bud mesenchyme. Shortly after, *Hoxa10* is expressed in a domain that significantly overlaps with *Hoxa9*. These two genes continue to be expressed proximally as the limb bud develops and the autopod forms. Directly before and/or at *Shh* onset, distal *Hoxa11* and *Hoxa13* become expressed along the limb bud and as the bud matures, transcripts of *Hoxa11* remain expressed mid-way in the limb, while those of *Hoxa13* remain distal and throughout the autopod.

HoxB cluster genes are mainly expressed in the forelimb, and as mentioned, the expression of *Hoxb8* has been shown precede and spatially overlap with *Shh* (Charite et al., 1994) (Fig. 3.13B). However, *HoxB* genes are typically expressed in stable but low transcript numbers and their loss appears to have little affect on limb formation (e.g., van der Ackker et al., 2001). Unlike the *HoxB* genes, *HoxC* genes are expressed mainly in the hindlimb bud, although some 3' *HoxC* (i.e. *Hoxc6*) are expressed and important to forelimb girdle development (see Section 3.4) (Fig. 3.13C). Transcripts for 5' *HoxC* (i.e., *HoxC9-13*) are found throughout the proximal to distal hindlimb where they overlap significantly with each other and with those of *HoxA* and *HoxD* (Nelson et al., 1996). Interestingly, loss of any single *HoxC* gene and/or of the entire *HoxC* cluster does not affect hindlimb development (Suemori and Noguchi, 2000).

HoxD genes are the most dynamically expressed of the clusters in limb development and because of this, they are thought to have more fundamental roles (Fig. 3.13D). *HoxD* expression has been previously argued to occur in three distinct phases (Duboule, 1994a-b; Nelson et al., 1996), although recent evidence suggests that this tri-phase expression is more an artifact of limb bud outgrowth and the organization of the *HoxD* cluster (Tarchini and Duboule, 2006). Nevertheless, the traditional tri-phasic expression is discussed below as it provides a dynamic view of *Hox* expression and regulation during limb outgrowth.

The earliest *HoxD* expression in the limb (i.e., Phase I) occurs from E8.5-E9.5 (FL) and E9.5-10.25 (HL) as *Hoxd1-9* are present throughout the entire limb bud, and *Hoxd10* is present in a slight posteriorly restricted domain (Tarchini and

Duboule, 2006). Phase II *HoxD* expression spans from E9.5-E11.0 (FL) or E10.25-E11 (HL) and is now believed to be a temporal and spatial expansion of Phase I into distal domains of the limb. Thus, 3' *HoxD* continue to be expressed ubiquitously across the A-P axis, while more 5' *Hox* (i.e., *Hoxd10-13*) continue the pattern of tiered posterior restriction seen first for *Hoxd10*. This "nested" pattern ultimately results in *Hoxd13* as being the most posteriorly restricted and temporally delayed *HoxD* gene. Interestingly, this schema is a derivation of the spatial and temporal *HoxD* collinearity found along the embryonic axis whereby 3' *HoxD* have the earliest and most expanded rostral domains, while 5' *HoxD* have later and most caudal restricted domains (Tarchini and Duboule, 2006).

Phase III expression begins during the onset of autopod formation in both limb types (E11-12.5 FL; E11-E12.5 HL) and is a pattern uniquely found in the limb (Zakany et al., 1997; Cobb and Duboule, 2005). This pattern is characterized by a reversal in the timing and spatial gradient of early 5' *HoxD* expression, whereby the most 5' member, *Hoxd13*, is expressed earliest and in the largest anterior to posterior gradient (highest anteriorly) while the most 3' member, *Hoxd10*, is expressed latest and in the most posteriorly restricted domain. This phase is also called the "reverse" collinearity phase of HoxD expression, specifically because the spatio-temporal sequence of expression is opposite to the normal *HoxD* arrangement on the chromosome.

There exists an additional period of *Hox* gene expression that occurs later in limb development (after E11.5-12 in the forelimb and hindlimb) during the time when skeletal elements initiate and progress through endochondral ossification.

During this time, *HoxD* paralogs are present in the developing limb perichondrium and perhaps growth plate, where they are suggested to play diverse roles involved in the maturation of chondrocytes (Boulet and Capecchi, 2004; Reno et al., in press). Additionally, they also influence the pattern of myogenesis and neurogenesis in the developing prenatal (and postnatal) limb (e.g., Yamamoto et al., 1998; Yamamoto and Kuroiwa, 2003).

The basis for the Phase concept of *Hox* expression likely derives from at least two pervasive concepts in limb developmental biology. The first concept is that different *Hox* paralogs specify compartmentally distinct skeletal elements in the limb (Fig. 3.14), a concept borne out of numerous studies utilizing specific *Hox* knockout mice (Capecchi, 1997). The second concept is the progress zone (PZ) model of limb development, which argues that proximal elements become specified earlier in limb formation, while distal elements are specified later (see section below). Historically, these two concepts have been coupled, presumably because the PZ model pre-dated findings on *Hox* and was used to interpret findings on *Hox* expression and function during limb formation.

For example, as Phase I is predominately defined by *Hoxd9-10* (and *Hoxa9-10*) expression and knockouts for these genes result in proximal skeletal alterations (Fromental-Ramain et al., 1996a; Wahba et al., 2001), this phase has been associated with humerus and femur specification. This association is in accordance with the PZ model that argues that proximal limb elements are specified first. Likewise, as Phase II was demarcated by *Hoxd11-12* (and *Hoxa11*) expression and knockouts for these genes result in alterations in

zeugopodial elements, Phase II was correlated with radius/tibia and ulna/fibula specification (Boulet and Capecchi, 2004). Finally, as Phase III was demarcated by the "reverse" collinear expression of *Hoxd13* (and *Hoxa13*) across the autopod, and knockouts for these genes result in loss of distal skeletal structures, this phase has been correlated to digital development (Fromental-Ramain et al., 1996b; Mortlock et al., 1996; Post and Innis, 1999). With respect to this latter phase, it appears that autopod formation is directly contingent upon the 13 *HoxA* and *HoxD* paralogs; e.g., while single *Hoxa13*$^{-/-}$ or *Hoxd13*$^{-/-}$ embryos possess minor autopodial defects (Dolle et al., 1993a), the progressive loss of all four *Hoxa13* and *Hoxd13* alleles (i.e., *Hoxd13*$^{-/-}$*;Hoxa13*$^{-/-}$) results in marked absences and alterations in all digital rays (Fromental-Ramain et al., 1996b).

Recent studies on Hox function more clearly indicate that their synergistic and compound involvement is critical for patterning most skeletal elements of the limb. In these studies, partial to entire *Hox* clusters were deleted during limb formation using conditional gene targeting strategies. For example, loss of all *HoxA* and *HoxD* cluster genes completely abrogates bud formation and arrests limb skeletal element development distal to the stylopod (Kmita et al., 2005). Thus, Hox can be argued to play roles in the following: (1) the maintenance of the limb bud proper via their control on tri-axis formation; and (2) the maintenance of limb bud outgrowth via their purported upstream effects on cellular proliferation and growth (Duboule, 1995; Kmita et al., 2005).

While much is known about *Hox* expression and function during limb patterning and growth, less is known about the genetic regulation of early

collinear and late “reverse” collinear expression. Recent studies on *HoxD* gene regulation has shed light on how individual *Hox* genes in this cluster may be spatio-temporally controlled. Zakany et al. (2004) found that by both inverting and deleting large genomic sequence fragments of the mouse *HoxD* cluster that early collinear expression of *Hoxd11*, *Hoxd12*, and *Hoxd13* in limb buds was altered and that this alteration led to a loss of limb A/P axis asymmetry. This and other previous findings (Spitz et al. 2001; Kmita et al., 2000a-b; 2002; 2003) led these researchers (Zakany et al., 2004) to propose the existence of an early limb control region (ELCR) located 3’ to *Hoxd1* on the *HoxD* cluster (Fig. 3.15). Tarchini and Duboule (2006) have explored the functionality of this proposed ELCR and found that it controls the collinear regulation of *HoxD* genes in a 3’ to 5’ order. Specifically, 3’ *Hox* genes (e.g., *Hoxd1*) are expressed earliest in the bud and have the most anterior expanded domain, while 5’ genes (e.g., *Hoxd13*) are expressed later and only posteriorly. They have posited that the distance of individual *Hox* gene promoters to this ELCR determines their spatio-temporal expression in a manner that is independent of individual promoter specificity. In addition, they argue for an additional domain 5’ of *Hoxd13* which serves to antagonize the early spatial and temporal expression of 3’ genes.

Where the ECLR exactly is located 3’ of the cluster and which factors drive its expression will be major future questions. As shown for early 3’ *HoxD* (i.e., *Hoxd1*, etc) promoter regulation, cross- and/or auto-regulation may be critical to the establishment of this collinear activation. In addition, chromatin remodeling will certainly also play critical roles in the regulation of the

progression of 3' to 5' *Hox* expression (Bickmore et al., 2004; Cao et al., 2005; Wysocka et al., 2006). Interestingly, analyses on the mutant chick "limbless" indicate that early *HoxD* gene collinearity can normally occur in the absence of both ZPA and AER signals (Grieshammer et al., 1996; Noramly et al., 1996; Ros et al., 1996). Thus, initial *Hox* expression (i.e., Phase I/II) appears to not be under the direct control of the ectoderm and early A-P establishment. However, other potential regulatory inputs involved in the early limb bud (i.e., *Hoxb8*) may be upstream of 3' and 5' *HoxD* expression. For example, both RA and *Hoxb8* mis-expression induces a very broad domain of ectopic expression of 5' *HoxD* genes (at E10.5) (Charite et al., 1994), suggesting that both RA and 3' *Hox* may be involved in later *Hox* activation, perhaps via ELCR regulation. It may well be that ELCR activation cascades through auto-regulation and activation by other factors to perpetuate the posterior expression of more 3' and 5' *Hox* members. Finally, studies in this thesis also support the possibility that early collinearity has a tight regulation that may involve *Pbx* (see Chapter 5).

Much more is known regarding the regulatory control and organization of "reverse" *Hox* collinearity in the autopod (Fig. 3.15). Zakany et al. (2004) argue that, once activated posteriorly in the limb, *Shh* protein appears to subsequently control *HoxD* gene transcription in presumptive digits. *Shh* is believed to either operate directly or indirectly on a known enhancer region located 5' to the *HoxD* cluster called the global control region (GCR). The GCR appears to regulate multiple genes that reside in *cis* with the *HoxD* cluster, and within this element

lies the digital enhancer, a regulatory sequence, which drives expression of *cis*-acting genes such as *Evx*, *Lnp,* and several *HoxD* cluster genes (Zuniga, 2005).

Similar to the ELCR, the distance that individual *Hox* gene promoters are to the GCR appears to regulate their timing and spatial expression (Herault et al., 1998a; Kmita et al., 2003). Accordingly, *Hoxd13*, which lies nearest to the GCR, is expressed first and in the broadest anterior to posterior gradient in the developing autopod, while *Hoxd10,* which lies further away, is expressed last and mostly posterior. However, unlike that seen for early collinearity, the transcriptional efficiency of individual *Hox* gene promoters depends on their distance to the GCR, such that those located closest (i.e. 5' *Hoxd13*) have greater transcriptional efficiency when compared to those furthest away (i.e., *Hoxd10*), that are activated less efficiently and transiently. Therefore, there exists what Kmita et al. (2002) argue to be "transcriptional leakiness" among *Hox* promoters.

The mechanisms that regulate "reverse" collinearity remain elusive but the concept of "transcriptional leakiness" may prove important to understanding its control. In this manner, if Shh leads "directly" to the activation of the digital enhancer, then the conformational changes that enhancer element must undergo may be critical to the development of this leakiness. Alternatively, perhaps Shh triggers a transcription factor that leads to the direct activation of *Hox* promoters individually and that their specific sequence organization may be critical.

On a different level, it has been argued that Shh operates through Gli3 in regulating *HoxD* "reverse" collinearity. Studies on the direct interaction of 5'

HoxD and Gli3 proteins (Chen et al., 2004) indicate that their ratio across the limb regulates digit pattern and identity and that Gli3 acts as a strong transcriptional repressor of 3' *HoxD* gene expression. In this context, the leakiness of transcriptional efficiency (specifically for 3' members) may relate to the extent of Gli3 repression on individual *Hox* promoters and/or the effects of conformational changes of the digital enhancer on individual *Hox* expression (Tarchini and Duboule, 2006) (Fig. 3.11).

Either way, if Shh does "directly" or indirectly activate the digital enhancer in the GCR then it would act as a relay between early *Hox* collinearity and later "reverse" collinearity. In this case (Fig. 3.15), a genetic network would exist between early Hox activation of *Shh* and later Shh activation of *Hox*, thus connecting together the formation of the A-P and P-D limb developmental axes. In this manner, it can be suggested that the roles for early *Hox* would be important to specification of elements, and also the maintenance of a system which results in the progressive determination of skeletal element identity and morphology, initially established prior to or at the onset of this genetic network.

3.3.3.5. Maintenance of the developmental axes during bud outgrowth (E9.75-E12)

Using chick embryos, Saunders, Summerbell, and others demonstrated that the AER is necessary for P-D outgrowth as its removal at any stage of development resulted in limb growth arrest (Saunders, 1948; Summerbell, 1974). Detailed grafting experiments in which the AER was transplanted to different

locations along the bud and flank, also demonstrated that the AER had the potential to drive limb mesenchymal growth. For example, placing wing bud AER over the posterior or caudal mesenchyme led to the formation of a leg. Conversely, placing hindlimb AER over presumptive wing territories produced wing structures. Finally, interchange of early or late AER onto any stage limb mesenchyme appeared to facilitate outgrowth similarly, thus indicating that the AER, once established, provides growth inducing signals and that for a specified time, such signals do not significantly change in quality during development (Carlson, 1975, Maden, 1984, Koussoulakos et al., 1990). Overall, these results suggest that the AER controls limb growth rather than provides cells with "identity," as such is deemed to be a characteristic of the mesenchyme (Niswander, 2003).

Interestingly, when the AER was grafted over non-limb mesoderm it regressed, and limbs failed to form. In this manner, the limb mesenchyme possesses a property essential to limb outgrowth perhaps afforded by *Shh* (ZPA) and the complex *Hox* molecular environment during limb outgrowth (Niswander, 2003). Accordingly, it is now known that an interaction occurs between the AER and ZPA that ensures the formation of each signaling center and the limb.

Indeed, once the AER is established, several molecules (i.e., Fgfs) signal to the underlying mesenchyme and trigger the genes necessary for AER progression and maintenance. Specifically, it was demonstrated that Fgf2 or Fgf4 soaked beads could rescue limb outgrowth once the AER was stripped from the developing mesenchyme (Niswander et al., 1993; Fallon et al., 1994). Now

it is known that *Fgf2*, *Fgf4*, *Fgf8*, *Fgf9*, and *Fgf17* are expressed in the AER and help maintain limb outgrowth (Martin, 1998). Most recent work demonstrates that while both *Fgf4* and *Fgf8* together are important for limb outgrowth, removal of *Fgf4* with any other *Fgf* (other than *Fgf8*) results in limb outgrowth (Martin, 2001). This and other data demonstrate that *Fgf8* is essential in the AER for limb bud outgrowth (Sun et al., 2002).

Indeed, Fgf8 is the earliest and most widely expressed of the Fgfs in the AER and in this manner, perhaps the most essential (Lewandoski et al., 2000). Nevertheless, that both *Fgf4* and *Fgf8* have unique spatio-temporal expression patterns helps explain why, if they are collectively deleted, they more drastically alter limb development then if ablated either individually or with other *Fgfs* (Sun et al., 2002). In fact, genetic evidence for their critical roles in limb outgrowth followed the work of Sun et al. (2002) and Boulet et al. (2004) who used a Cre-Lox system to conditionally inactivate both genes from the AER during mouse limb development. Prior to this approach it was not possible to distinguish the different roles of Fgf4 and Fgf8 during limb development, as single homozygous *Fgf4* or *Fgf8* mice die *in utero* before limb development (Feldman et al., 1995; Sun et al., 1999). However, when *Fgf4* and *Fgf8* were both conditionally inactivated in the ectoderm prior to AER formation, using Cre recombinase under the *Msx2* promoter (expressed in the AER), limbs did not form.

Another important finding derived from the conditional *Fgf4/Fgf8* double-knockout mice is that *Shh* expression is not induced further substantiating earlier experimental work demonstrating that the AER and ZPA interact during limb

development (Niswander et al., 1994a; Sun et al., 2002). In fact, this AER-ZPA interaction is contingent on a network of genes that form a feedback loop between these two signaling centers (Niswander et al., 1994a) (Fig. 3.16). In the first part of the loop (i.e., signaling from the ZPA to the AER) it is known that Shh signaling leads, through a cascade of gene and protein expression, to *Fgf4* expression in the posterior AER (reviewed in Niswander, 2003). Accordingly, Shh signals first through the formin protein (first identified in mice that harbor the natural mutation for the formin protein called *limb deformity*) in the mesenchyme to maintain the downstream expression of *Gremlin*, a Bmp antagonist. Through Gremlin inhibition of Bmp signaling, *Fgf4* expression in the AER ensues, as Bmps are inhibited from their inhibition of Fgf4 (Zuniga et al., 1999). Accordingly, *Shh* positively regulates *Fgf4*. In the second part of the loop (i.e., signaling from the AER to ZPA) Fgf8 and subsequently Fgf4 (along with other AER Fgfs) signal to the underlying posterior mesenchyme via Fgfr2 to activate *Shh* expression. Unfortunately, much less is known about this aspect of the feedback loop. The tightness of the entire loop is demonstrated by the finding that eliminating the expression of *Fgf*, *Shh* (Laufer et al., 1994; Niswander et al., 1994a), or any of those genes involved abrogates the loop and terminates limb bud formation.

Shortly after autopod formation, this feedback loop breaks down presumably due to changes in both AER and ZPA signaling (Niswander, 2003). Accordingly, it is only after digit anlagen formation that *Fgf4* but not *Fgf8* expression begins to disappear (Niswander and Martin, 1992; Duprez et al., 1996), a reduction that correlates well with the down-regulation of *Shh*

expression in the ZPA. At this time, *Fgf8* expression remains directly in the AER overlying the digits and becomes lost from the ectoderm covering the interdigital spaces. In this way, *Fgf8* expression regulates phalangeal formation in each digital ray. Indeed, when beads of Fgf protein are applied to the distal limb well after when *Fgf8* expression normally disappears, additional phalanges develop on the digits subjacent to this ectopic source (Sanz-Ezquerro and Tickle, 2003).

The DE also plays important roles in the maintenance of the P-D, A-P, and D-V axes (Niswander, 2003) (Fig. 3.8). As Wnt7a is expressed in the DE it is important for maintaining *Lmx1b* expression in the underlying dorsal mesenchyme and the D-V patterning of the skeletal elements that form from this tissue (Chen and Johnson, 2002). Additionally the DE has an important role in maintaining the A-P axis, as it has been demonstrated that DE removal after *Shh* initiation, results in *Shh* reduction (Adamska et al., 2003). Furthermore, if *Wnt7a* is deleted, via gene targeting, a similar *Shh* loss occurs (Parr and McMahon, 1995). This interplay is also quite complex, as the DE and AER must both be operative for normal limb development.

3.3.4. How mesenchymal cells in the limb bud become patterned (E8.5-12)

The complex and dynamic patterns of *Hox* gene expression throughout early limb development and the loss of specific skeletal structures in *Hox* null mutants indicate that these transcription factors function in skeletal patterning and morphogenesis. In fact, it has been argued that Hox proteins target many

downstream genes to execute their patterning and growth promoting ability (Davis and Capecchi, 1996). Some of these target genes may include those important for axis establishment (e.g., *Shh*). An interesting aspect of this latter relationship is that often *Hox* gene expression is greatly perturbed in mutants that are upstream of the major signaling centers in the limb and control axis formation. For example, in the *Shh*$^{-/-}$ mutant, 5' *HoxD* gene expression during autopod formation is severely reduced and present only for *Hoxd13* (Chiang et al., 1996). Similarly, *Hox* gene expression is drastically reduced in conditional *Fgf4*$^{-/-}$;*Fgf8*$^{-/-}$ mutants indicating that for both of these A-P and P-D determinants, *Hox* also lie downstream of axes formation (Sun et al., 2002). The resulting picture is that *Hox*-based patterning of the limb's skeletal elements is a highly coordinated process that requires the assignment of patterning information and its execution via the proper functioning of the limb's signaling centers.

Until recently, the assignment of this positional information (PI) was believed to be the product of molecular and morphogenetic gradients (e.g., Shh, Hox, etc.) established specifically after the major axes formed. However, the experiments by Moon et al. (2000), Sun et al. (2002), and Boulet et al. (2004) challenge this long held view that axis formation is coordinated in a manner that leads to the assignment of PI and the progressive specification of limb elements; a process posited to occur under the Progress Zone (PZ) Model (Wolpert, 1969). Conversely, their data support an alterative model, called the Early Specification (ES) Model, where skeletal element specification occurs earlier during the initial

stages of bud formation (Dudley et al., 2002). These models and the experimental evidence for each are discussed below.

3.3.4.1 Progress zone model

This model was originally borne out of studies conducted by Saunders, Summerbell, Wolpert, and others on how ectoderm (AER) extrication affects skeletal element formation in the chick. Accordingly, these researchers discovered that the timing of AER extrication greatly affected the formation of limb compartments but in a proximal to distal sequence. For example, in the chick wing, removal of the AER shortly after its formation typically resulted in the presence of only the most proximal stylopod element (i.e., the humerus). On the other hand, removal of the wing AER during hand-plate formation resulted in the presence of most skeletal elements with the exception of the digits. Therefore, under this model, it was argued that the limb's skeletal elements become progressively specified via the sequential distalization of mesenchymal cells to form and condense into compartmentally specific skeletal elements (Fig. 3.17).

According to this model (reviewed in Niswander, 2003), Fgfs from the AER diffuse proximally into the PZ, a 300 um mesenchyme domain subapical to the AER. Based on the known roles of Fgfs as growth promoters, cells in the PZ are maintained in an undifferentiated, actively proliferating state. The time cells spend in the PZ determines their identity, such that the first dividing cells acquire proximal characteristics, while later dividing cells acquire more distal characteristics. When cells exit the PZ, they do so proximally, and differentiate

according to this “identity” and in response to intrinsic PI cues (i.e., transcription factors, signaling molecules, and diffusible morphogens) in the surrounding mesenchyme. In this manner of sequence, stylopodial elements are first specified and then mature, followed by zeugopodial and autopodial elements. After this progressive specification is complete the AER and PZ disappear.

3.3.4.2 Early specification model

In contradistinction to the PZ Model, Dudley et al. (2002) put forth the ES Model (Fig. 3.17), whereby cell fate specification and the attainment of “identity” for the limb’s different compartments occur early during the onset of bud out-growth. If true, specification would occur prior to Fgf influence and the PZ would only be involved in mesenchymal cell maturation, not in their initial specification.

To develop this model, Dudley et al. (2002) reinterpreted previous findings and performed several critical experiments. First, they recapitulated Rowe et al. (1982) findings that upon AER removal, directly subjacent distal limb mesenchyme undergoes temporary and extensive cell death. Moreover, that AER removal in chick at specific limb forming stages (i.e., stages 18-22) always resulted in a relatively constant 200 μm zone of cell death, except after stage 24, when its removal did not significantly affect cell survival. These rediscoveries were next combined with chick experiments where Dudley et al. (2002) color-labeled mesenchymal cell compartments during early bud formation and subsequently removed AER at different stages. These studies revealed some novel insights to limb development.

First, they found that cells that contribute to all P-D segments exist in stratified domains early in bud formation. Specifically, utilizing different colored lipophilic dyes to label the surface membranes of mesenchymal cells at different time periods, they could track the movement, expansion, and differentiation of these cells over time. For example, by labeling at stage 19 (i.e., during early bud formation), they found that cells that were fated to the stylopod were positioned 200–300 μm from the AER, while those fated for zeugopod and autopod precursors were positioned 100–200 μm and within 100 μm of the AER, respectively. Therefore, they found a cellular stratigraphy that eventually formed the three main limb compartments, and that which was established very early in bud formation. Also, they found by labeling later in time that fate maps changed because of morphogenetic movements and growth.

Their next experiments explored the consequences of AER removal and cell death on the formation of these stratified domains. Specifically, they found that those limb elements which formed after AER extrication reflected the population of all three compartmental progenitors that were positioned outside the zone of cell death. In this manner, only those cells that survived the process were able to differentiate according to their prepatterned or initial specified proximal to distal fate. They found that the cellular progenitor population which resided in the zone of cell death changed over time, even though this domain was present always after AER extrication and was of the same dimensions. Therefore, they argued the following: early in limb formation, essentially all P-D progenitors resided in the future region of cell loss, thus, extrication of the AER

resulted in the death of all of these cells and therefore the near complete absence of all limb elements. Later, the very configuration of the cellular stratigraphy allowed more proximally fated cells to reside outside of the zone and escape cell death after AER extrication. Thus, only more proximal elements remain and distal truncations occurred.

Several problems persist with Dudley et al. (2002) studies and thus this model's validity remains under question. First, because earlier fate-mapping strategies were inaccurate (i.e., specifically for fate-mapping later in time and for older limbs) and, second, because AER extrication late in development only results in minimal cell death and reduced proliferation, it still remains to be tested whether the purported zone of cell death correlates closely with the observed truncations at different stages. Another issue with the ES Model relates to the timing of P-D compartmental specification. While in the PZ Model compartmental specification depends on the amount of time cells remain in the PZ and under the influence of Fgfs, according to the ES Model all compartment progenitors are specified early in the limb bud, perhaps during induction and before the influence of the AER. However, with respect to the ES Model, Dudley et al. (2002) evidence indicates only that the fate of the cells, not their state of specification is determined. In this manner, it remains unknown as to the specification status of the cellular compartments labeled and therefore, if cells in these compartments are flexible enough to adopt different fates. In addition, there is a lack of data as to when this initial cell specification occurs, and whether the cellular stratigraphy is an intrinsic property of the early limb field or the product of sequential

specification by extrinsic mesenchymal and ectodermal signals during initial limb field and bud induction.

While these problems still persist, the discovery of some uniquely proximal limb markers, such as the *Paired leucine zinc finger* (*Plzf*) (and its interaction with *Gli3*) (Barna et al., 2005) as well as recent work on Fgf function provides strong evidence for the ES Model. For example, Barna et al. (2005) identified a genetic interaction between *Plzf* and *Gli3* that leads to the patterning of the proximal but not distal elements; specifically compound homozygous mutant *Plzf*;*Gli3* mice possess characteristic loss and reductions in the stylopod providing evidence that distinct factors affect specific compartments in limb development.

Additional support for the ES Model comes from experiments on Fgf function in the limb. Specifically, when *Fgf8* is conditionally inactivated early during initial limb bud outgrowth, only the stylopod is lost or severely reduced, while the zeugopod and autopod remain relatively unscathed (i.e., only anterior digits 1 and 2 are reduced) (Moon and Capecchi, 2000). The relative lack of distal phenotype is believed to result from the action of other Fgfs in the limb AER (which are activated after Fgf8) and their ability to rescue AER formation and function. This proximal loss alone is incompatible with the PZ Model (see Niswander, 2003).

3.3.4.3 Continued outgrowth and patterning of the limb (E12-P0)

Regardless of the model followed, the continued growth and development of the limb involves the execution of this PI into readily identifiable skeletal

elements, a process also controlled and coordinated by various signaling centers during early limb development. It is important to consider that while PI is assigned early in the limb, patterning at this stage is not definitive or final. In fact, later events are additionally important to pattern skeletal structures.

Recently, experiments on the molecular control of digit patterning and formation indicate that while Shh, Gli3, and Hox are important for determining initial digit identity and number, later events during digital plate or autopod maturation are also critical. Studies on digital patterning, specifically after initial hand- and footplate formation, have demonstrated that subsequent fine tuning of digit formation is under the control of several major signaling centers in the autopod: the digital mesenchymal condensations, the overlying ectodermal remnants of the AER, and the interdigital mesenchyme (see Robert and Lallemand, 2006). Interactions between Bmps (and their antagonists), Fgfs, Hox, and several other proteins across these regions appear crucial for the formation of digits and also the locations where interdigital regions form. Reviews on this later stage of digital autopodial patterning and formation is provided by McGlinn and Tabin (2006), Robert and Lallemand (2006), and Tickle (2006).

The actual transformation of different skeletal elements from the initial PI assigned to mesenchymal cells is less understood from the molecular perspective. It is known that mesenchymal cells in specific locations in the limb must condense, however, the signals necessary to not only induce this process but to spatially coordinate it remain unclear. Once mesenchymal condensations form they are identifiable via their cellular expression of the *SRY-box* gene, *Sox9*,

a major marker of mesenchymal cells. The patterns of *Sox9* expression have aided in determining the locations of condensation formation in the stylopodial, zeugopodial, and autopodial regions of both limbs (Karsenty and Wagner, 2002).

After mesenchymal condensations form, they begin to exhibit localized cellular differentiation and thus undergo chondrogenesis. During this process, mesenchymal cells differentiate into chondrocytes, begin secreting chondrocyte extracellular matrix proteins and minerals and eventually form rudimentary skeletal element templates. These templates will then begin the process of bone formation via endochondral ossification. Reviews of these processes are provided in Karsenty and Wagner (2002), Nakashima and de Crombrugghe (2003), and Goldring et al. (2006). Furthermore, at this stage, joints begin to form between specific elements as indicated by the expression of *Gdf5* (Merino et al., 1999; Storm and Kingsley, 1999) while muscles, tendons and ligaments arise according to several processes (reviewed in Gilbert, 2006).

3.4 Girdle development

Unlike the limb, currently, there have been only a limited number of studies examining scapular and pelvic formation and as a result, little is known regarding the tissues and genes involved in their patterning and morphogenesis. With respect to the pectoral girdle, most studies have concentrated on the development of the scapula rather than on the clavicle and therefore the remaining text is devoted to the former. In addition, much less is known about pelvic development, as relatively more mouse and chick mutants have been

identified with pectoral defects. Therefore, the last part of this section briefly discusses those findings for the pelvic girdle.

The typical experiments that have been performed to study girdle formation consist of tissue grafting and swapping in avian species and gene deletion in mice. The former have been responsible for identifying tissues and cell populations that give rise to girdle elements, and have provided insight into the nature of tissue interactions underlying girdle formation, while the latter have been critical in identifying several genetic regulators of girdle formation.

3.4.1 Histological and molecular characteristics of the pectoral girdle

3.4.1.1 Studies in avian species

Chick/quail grafting experiments have provided key insights into the tissues giving rise to the scapula. Huang et al. (2000) have demonstrated that the avian scapula is made up of at least two different progenitor populations; cells from the somatopleuric region of the LPM, and cells from the dorsal-posterior dermomyotomal region of the somite. The somatopleuric contribution gives rise to the glenoid fossa, coracoid tubercle, and acromion, structures of the scapula neck, head, and spine (Ehehalt et al., 2004) (Fig. 3.1B). The dermomyotomal contribution gives rise to the scapula blade and proximal spine; albeit in manner that is highly complex and involves the coordination of cues from the somites, it's overlying ectoderm, and the somatopleure (Fig. 3.1B).

The complexity in the dermomyotomal origin of the scapula blade is underscored by the complex organization of the dermomyotome itself and how it

differentiates during somite formation and maturation. Somites, the derivatives of the PM, form and are cranially to caudally patterned along the embryonic axis under the influence of nested *Hox* gene expression (Garcia-Fernandez, 2005). Specifically, partially overlapping domains *Hox* expression possibly prepattern cells of the somites to give rise to scapula tissues (Huang et al., 2006) (Fig. 3.18A). Accordingly, during and/or shortly after this Hox influence, the dermomyotome forms as a dorsal subdivision of the somite, (Gilbert, 2006) (Fig. 3.18B). It later subdivides into two domains, the epaxial domain situated dorsal-medially and the hypaxial domain, located ventral-laterally (Burke and Nowicki, 2003; Cheng et al., 2004).

Recently, the molecular regulation of these dermomyotomal domains has been shown to differ. In the epaxial domain, regulatory signals arise from medial structures such as the notochord and neural tube, whereas the hypaxial region receives signals from the adjacent somatopleuric mesoderm (Rong et al., 1992; Chiang et al., 1996; Teillet et al., 1998; Huang et al., 2000; Ehehalt et al., 2004). Teillet et al. (1998) have specifically demonstrated that ablation of axial tissues (and their signals) results in normally patterned scapula blades, further indicating that hypaxial dermomyotomal specification occurs from lateral signals.

Huang et al. (2000) have shown that only specific hypaxial dermomyotomal cells of the brachio-thoracic region give rise to different superior/inferior domains of the scapula blade and spine. In the chick, somites 17-24 give rise to different parts of the scapular blade, cranial to caudal, but do not mix from one level to the next (Ehehalt et al., 2004). In addition,

dermomyotomal cells from the cervical region are incapable of forming scapular elements, indicating that it is an intrinsic ability of brachio-thoracic dermomyotome to form the scapula blade (Ehehalt et al., 2004) (Fig. 3.18A).

Once hypaxial dermomyotomal cells have been specified as scapular progenitors, signaling from the ectoderm is critical for their maturation, migration, and differentiation into prechondrogenic mesenchyme and cartilage (Fig. 3.18B). Wang et al. (2005) has argued based on the work of Moeller et al. (2003), Rodriguez-Niedenfuhr et al. (2003), and Ehehalt et al. (2004) that Wnt signaling from the ectoderm overlying the hypaxial dermomyotome is critical for keeping cells in an undifferentiated epithelial state and that the cessation of such signals, which occurs normally in a cranial to caudal sequence during somitogenesis, leads to their differentiation into mesenchyme; an initial step into forming scapula cartilages. Interestingly, while Huang et al. (2000) demonstrated that only brachio-thoracic dermomyotome are capable of forming scapula blade condensations, Ehehalt et al. (2004) demonstrated that the ectoderm overlying the cervical region is capable of inducing ectopic brachio-thoracic dermomyotome to form scapular mesenchymal and cartilage condensations. This finding suggests that signaling in the ectoderm (e.g., possibly by Wnts) is responsible for inducing differentiation, specifically since cervical ectoderm may have been more mature and lost specific signaling capable of maintaining somites in an undifferentiated epithelial state.

During and/or shortly after the transition to dermomyotomal mesenchyme additional signaling from the somatopleure appears critical for scapula blade

morphogenesis (Fig. 3.18B). Bmp signaling from the somatopleuric mesoderm appears to facilitate the expression of early scapula progenitor marking genes, such as *Pax1* (Wang et al., 2005). For example, blocking somatopleuric to dermomyotomal signaling and/or inhibiting Bmp signaling to the dermomyotome using Bmp antagonists in chick results in both the down-regulation of *Pax1* and the absence of the scapula blade. In this manner, the coordination of both ectodermal and somatopleuric signaling leads to dermomyotomal differentiation and the formation of scapular cartilages.

Overall, with respect to the dermomyotomal origin of the scapular blade Wang et al. (2005:17) put forth a three stage model, where by: (1) *Hox* expression patterns provide positional information and specify the axial level somites giving rise to scapula forming dermomyotome (Fig. 3.18A); (2) once specified, the dermomyotome becomes compartmentalized and its hypaxial cells form and begin differentiation into mesenchyme (at which point they emigrate laterally to the subectoderm) (Fig. 3.18A); and (3) differentiated mesenchyme via the influence of ectodermal and somatopleuric signals “realize their intrinsic scapula-forming program” and become scapular blade cartilages (Fig. 3.18B).

3.4.1.2 Studies using mouse mutants

Genetic ablation studies in mice have elucidated several of the molecular factors responsible for regulating some of the tissue interactions discussed above. These studies have been useful also in understanding patterning of, and signaling from, the somatopleure specifically since most genes that have been

inactivated are expressed in this domain and the LPM. Interestingly, given their LPM expression, several of these genes also have roles in limb development. It is of equal import that very few genes that pattern the scapula progenitors in the dermomyotome or which encode signaling molecules responsible for progenitor cell migration have been identified.

With respect to either dermomyotomal or somatopleuric patterning of the scapular blade, several genes have been shown to play critical roles. *Tbx5* is expressed in the early limb mesenchyme and nascent limb bud in the "scapula" forming domain. In fact, *Tbx5*$^{-/-}$ mouse embryos lack forelimbs and scapulae, indicating that Tbx5 may function when somatopleuric mesoderm triggers partial differentiation of dermomyotome (Fig. 3.18B). However, it is also possible that Tbx5 plays a role in scapula progenitor maturation once they have migrated to their more lateral domains.

As discussed (Section 3.3), a downstream target of Tbx5 is *Fgf10* in the LPM (Ng et al., 2002; Agarwal et al., 2003). Importantly, besides limb agenesis, *Fgf10*$^{-/-}$ embryos lack the posterior one-third of the scapula (Min et al., 1998; Sekine et al., 1999), suggesting that Tbx5 role in *Fgf10* activation has farther-reaching effects than just regulating limb bud outgrowth (Fig. 3.18B). However, it is unclear whether the *Fgf10* loss from the LPM is directly (i.e., in a cell autonomous manner in the mesenchyme) or indirectly (i.e., in a cell non-autonomous manner through its signaling to the ectoderm) responsible for scapula blade defects in both *Fgf10* and *Tbx5* homozygous mutants. With respect to its direct influence, if Fgf10 function is disrupted early perhaps during

somatopleuric signaling, blade progenitors may not be induced to properly differentiate. With respect to its indirect influence, if abrogation of Fgf10 function occurs early enough it may have a more global affect on ectodermal signaling over both the LPM and somites, with the latter having more apparent ramifications on scapula blade progenitor cell differentiation.

Several *Hox* genes also have also been implicated in scapula (and blade) patterning as suggested above. For example, *Hoxa5*$^{-/-}$ mutant embryos display, approximately sixty-percent of the time, a residual and/or missing acromion process but lack any defects in the scapular blade and limb (Aubin et al., 1997) (Fig. 3.18C). However, it is known that paralogous Hox proteins may act redundantly during development, and in this regard, while *Hoxa5*$^{-/-}$ and *Hoxc5*$^{-/-}$ mutants possess normally positioned scapula, *Hoxb5*$^{-/-}$ mutants display a rostral shift in the axial location of scapular formation (Rancourt et al., 1995) and that this shift is more severe in compound mutants. Therefore, it is only after multiple *Hox* paralogs are removed that scapula blade defects become evident, indicating that *Hox* may pattern the dermomyotome or operate within the LPM redundantly.

Hoxc6 is also strongly expressed in the somatopleure/LPM and anterior limb field, yet in mice *Hoxc6* deletion does not result in scapula defects, possibly due to redundancy. However, alterations in its expression have been shown to cause shoulder malformations in chicks (Oliver et al., 1990). In addition, RA application to chick proximal limbs result in duplications of the distal scapula blade, neck, and head region (Oliver et al., 1990) with an expansion of the *Hoxc6* domain (Fig. 3.18C). This finding suggests that, as in the limb, RA is a critical

upstream regulator of *Hoxc6*-based patterning of the scapula. Supporting evidence also comes from compound RARα;RARγ mutants which have scapular agenesis (Lohnes et al., 1994), implicating that Hox and RA interactions are essential. Given the known effects of RA on axial *Hox* expression (see Gilbert, 2006), it may be that cranial-to-caudal RA signaling and its effects on *Hox*-based somitic, somatopleuric, and lateral plate mesodermal patterning lies upstream of girdle formation.

Pbx1 has been shown to dually regulate the development of the proximal limb and the scapula (Selleri et al., 2001) (Fig. 3.18C). For example, in the forelimb region of *Pbx1*$^{-/-}$ mouse mutants, the humeral head remains fused to the scapula head and the glenoid cavity is obliterated. In addition, the deltoid tuberosity remains fused to the dysmorphic humeral shaft but just distal-lateral to fused gleno-humeral joint. This indicates that Pbx1 function in the somatopleure/LPM may occur within both medial and lateral compartments, and thus affects scapular neck/head and proximal limb formation (Fig. 3.18C). *Pbx1*$^{-/-}$ embryos also possess scapular blade defects such that the superior-to-inferior dimensions are reduced and the blade appears thinner with a reduced dorsal spine and acromion process (Selleri et al., 2001). This latter data suggests that *Pbx1* expression in the somites and/or perhaps in their derivatives or in the somatopleure markedly drive blade formation (see Chapter 7).

Research on *Emx2* (the vertebrate homolog of *Drosophila empty spiracles*) in the chick and mouse has aided in understanding its role in girdle formation. In the chick, *Emx2* expression has been shown to precede expression

of *Sox9*, a critical factor required for mesenchymal cell condensation in both somite and limb derivatives (Bi et al., 2001). *Emx2* is expressed in various somatopleuric and limb tissues as well as in the prechondrogenic condensed mesenchyme of the scapula (Pellegrini et al. 2001). Interestingly, *Emx2*$^{-/-}$ mice possess skeletal elements of the scapula head but lack completely cartilages of the blade. This finding suggests that blade loss in homozygous mutants may not result from the failure to form scapular blade progenitors (Prols et al., 2004) but from defects in cell migration and/or signaling or chondrogenesis (Fig. 3.18B). In this manner, and in agreement with that found in chick, *Emx2* may be providing a mechanism of positional information for cells that are already fated in the dermomyotome to contribute to the scapula blade.

Recently, it has been demonstrated that the conditional inactivation from the LPM of *Beta-catenin* in mice, a critical factor involved in the Wnt signaling pathway, leads to *Emx2* down-regulation and a concomitant loss and/or reduction of only the scapular blade (Fig. 3.18B). Furthermore, a subsequent distal shift in *Hoxc6* expression and a marked down-regulation of *Pax1* (see below) is observed in these specific *Beta-catenin* mutants, indicating that all three genes are additionally downstream of the Wnt signaling (Hill et al., 2006). While *Beta-catenin* is expressed in both limb (and limb field) ectoderm and mesoderm, the inactivation of *Beta-catenin* was mesodermal (i.e. via the expression of the *Prx1 Cre* in the mesoderm) and therefore the loss of these genes appears to be the result of a mesenchyme signaling alteration. However, the finding that ectoderm removal leads to scapula blade agenesis makes

understanding the effects of this specific deletion difficult since mesenchymal and ectodermal interactions are critical to the formation of the scapula and limb (Ehehalt et al., 2004). In this manner, the loss of *Wnt* signaling from the mesenchyme may either act directly to down-regulate these genes (i.e., *Emx2* may be a direct target of Wnt signaling in the mesenchyme, Hill et al., 2006) and/or act indirectly through its effects on ectodermal signaling to alter the expression of these genes.

Until this point, many of the genes discussed have likely roles in the dermomyotome and/or proximally in the somatopleure/LPM to govern early blade formation. Several other genes, and complex interactions among them, have been demonstrated to influence scapula blade patterning and many of these are expressed after the bud forms, specifically in the anterior limb field. These genes include *Gli3*, *Alx3*, *Alx4*, *Cart1*, and *Tbx15*. In most cases, the experimental deletion of any one of these genes results only in minor scapula blade malformations. However, in all cases thus far studied, their compound loss in mutant mice demonstrates that various genetic interactions are required for scapula morphogenesis (Fig. 3.18B).

Scapula defects in *Gli3* null mutants consist of a reduction in the superior and inferior aspects of the blade, giving it an indented appearance (Hui and Joyner, 1993). These scapula defects become exacerbated and the scapula exhibit additional phenotypes (i.e., the presence of an infraspinatus foramen) when *Gli3* homozygosity is coupled with heterozygosity for a null mutation in *Tbx15* (see below), indicating that both of these genes synergize during scapula

formation (Kuijper et al., 2005). *Alx3* and *Alx4* also genetically interact during scapular blade patterning as both genes are expressed in the anterior proximal limb field (Fig. 3.18B); specifically, while single *Alx3*$^{-/-}$ and *Alx4*$^{-/-}$ embryos possess relatively normal scapula, compound mutant *Alx3*$^{-/-}$; *Alx4*$^{-/-}$ embryos display shortening of the scapular blade. This genetic interaction during pectoral girdle formation is complicated by the presence of additional Aristaless family genes (e.g., *Cart1*) whose expression overlaps with *Alx3* and *Alx4*. For example, while *Cart1*$^{-/-}$ mutant scapula have a shortened superior border, this defect is exacerbated in *Alx3*$^{-/-}$;*Cart1*$^{-/-}$ and *Alx4*$^{-/-}$;*Cart1*$^{-/-}$ double mutants.

Kuijper et al. (2005) present evidence on the complex interactions of *Alx3*, *Alx4*, *Cart1*, *Gli3*, and *Tbx15* during scapula patterning, through their discovery of the following: (1) that *Tbx15* and *Gli3* genetically interact to form the central scapular blade; 2) that *Tbx15;Gli3* double mutants provide evidence that *Gli3* and its interaction with several genes is essential for inferior blade formation, while *Tbx15*;*Alx4 (Alx3)*;*Cart1* triple mutants demonstrate that *Alx4 (or Alx3)* and *Cart1* interaction is necessary for superior blade formation (Fig. 3.18B).

With respect to scapular blade formation, *Tbx15* is expressed within the proximal limb bud and *Tbx15*$^{-/-}$ mutant embryos possess a scapular foramen or hole in the middle of the blade (Kuijper et al., 2005). This phenotype is similar to that found in the mutant for the Polycomb homolog *M33* (Core et al., 1997) and in mice homozygous for *Extratoes* (*Xt*), an mutant allele of *Gli3* (Johnson, 1967; Hui and Joyner, 1993). The similarity of phenotypes between the *Xt* and *Tbx15* null mutants led Kuijper et al. (2005) to examine scapula formation in compound

Gli3;Tbx15 mutant mice. Indeed, they discovered that the foramen is more drastic and reflects a synergistic function of both genes (i.e., in *Gli3*$^{+/-}$*;Tbx15*$^{-/-}$ the foramen is enlarged, while in *Gli3*$^{-/-}$*;Tbx15*$^{+/-}$ it is shifted posteriorly). Furthermore in *Gli3*$^{-/-}$*;Tbx15*$^{-/-}$ mutant mice, only the superior scapular blade remains and takes the appearance of a single longitudinal skeletal element. This demonstrates that *Gli3* and *Tbx15* genetically interact to form the central blade and additionally that *Gli3* specifically influences inferior (posterior) blade formation. Interestingly, embryos concurrently lacking *RAR*α and *RAR*γ (i.e., *RAR*$\alpha^{-/-}$*; RAR*$\gamma^{-/-}$) display a range of phenotypic presentations including the loss of the inferior scapula border, a superior reduction in the blade, and also a slight foramen (Lohnes et al., 1994).

Genetic interactions between *Tbx15*, *Alx4* (*Alx3*), and *Cart1* were also examined to see their effects on scapula blade formation. Double and triple mutants (i.e., *Alx4*$^{-/-}$*;Tbx15*$^{-/-}$, *Cart1*$^{-/-}$*;Tbx15*$^{-/-}$, *Alx4*$^{-/-}$*; Cart1*$^{-/-}$*;Tbx15*$^{+/-}$, and *Alx4*$^{-/-}$*; Cart1*$^{-/-}$*;Tbx15*$^{-/-}$) demonstrate that *Alx4* (*Alx3*) and *Cart1* are essential for superior (anterior) blade formation. Indeed, in a manner similar to the compound loss of *Gli3* on inferior blade formation, *Alx4*$^{-/-}$*;Cart1*$^{-/-}$*;Tbx15*$^{-/-}$ mutants present as a single longitudinal skeletal element but in the inferior part of the scapula.

Kuijper et al. (2005) also demonstrated that *Emx2* effects on blade formation must be occurring independently or in parallel with those of *Gli3, Alx3*, *Alx4*, *Cart1*, and *Tbx15* as the expression of *Emx2* in single and compound mutants for these genes remained relatively unaltered. This suggests that

several different pathways impinge on blade development, although at this stage it is unclear as to the spatio-temporal order of their influence.

At this point, most discussion has centered on scapula blade formation, although in most of the mutants discussed above alterations are also evident in the scapula head, spine, and acromion suggesting that many of these genes interact in the LPM and between it and the descendants of the somites. For instance, Kuijper et al. (2005) also identified that markers of the LPM were altered in several *Gli3; Alx4*;*Cart1*;*Tbx15* compound mutants. For example, *Pax1*, a marker of spine and acromion formation, was spatially altered in *Alx4;Cart1* mutants in a dose dependent manner and was also reduced in both single *Tbx15* and *Gli3* null mutants and in compound mutants for these genes.

Pax1 has been shown to aid in the specification of cells of the anterior limb bud, and these progenitors have been fated to shoulder regions of the developing avian skeleton (Saunders, 1948; Bowen et al., 1989; Vargesson et al., 1997). Expression studies in mice have corroborated these results (Timmons et al., 1994). Moreover, several mouse mutants that have alterations in, or abrogations of, the *Pax1* locus possess scapular defects (Balling, 1994; Timmons et al., 1994; Dietrich and Gruss, 1995; Wilm et al., 1998; Adham et al., 2005). For example, both natural *Pax1* allelic variants (e.g., *undulated* (*un*) mice, Timmons et al., 1994) and targeted *Pax1* null mutants (Wilm et al., 1998) exhibit specific spine defects. Specifically, in *Pax1*$^{-/-}$ embryos there is the fully penetrant absence of the distal spine and acromion (Wilm et al., 1998) (Fig. 3.18C).

Hoxa5$^{-/-}$ embryos, as mentioned, also possess defects in the acromion (Aubin et al., 1998) as well as several additional axial defects that roughly phenocopy those found in *Pax1* null mutants. These findings led Aubin et al. (2002) to investigate the interaction of both genes during formation of the scapular head and spine. Aubin et al. (2002) discovered that compound *Hoxa5;Pax1* (*un/un*) mutants display more severe spine and acromion defects than those seen in either single mutant. They additionally demonstrated that while *Pax1* is a key regulator in the determination of prechondrogenic mesenchymal formation of the scapula, *Hoxa5* is necessary for the correct specification of cell lineages during chondrogenesis in a manner that also relies on the presence of *Sox9*. They argue that *Hoxa5* may provide essential regional cues for acromion formation by ensuring that *Pax1* is initiated properly.

In addition to the loss of the blade, *Emx2*$^{-/-}$ embryos also lack the spine and the proximal part of the acromion process, suggesting that this transcription factor lies upstream or genetically interacts with other critical regulators of scapular formation. One such regulatory interaction may involve *Pax1* (Timmons et al., 1994). Both *Pax1* and *Emx2* are expressed in the anterior and proximal limb field; and interestingly, *Pax1* expression in *Emx2*$^{-/-}$ embryos is extended anterior-dorsally suggesting that they genetically interact in the LPM to pattern the spine (Pellegrini et al., 2001). Importantly, these data also demonstrate that the LPM giving rise to the scapular head, neck, and spine remains present (Pellegrini et al., 2001) in *Emx2*$^{-/-}$ embryos, since *Pax1* marks this domain, although not exclusively. Therefore, Emx2 may function in patterning the spine

and acromion in a similar manner to how it behaves in blade formation, where it appears to influence how progenitor cells mature into skeletal tissues. Finally, *Emx2* may also interact with *Hoxc6* to pattern the scapula head although how this occurs remains unclear (Pellegrini et al., 2001).

To date, the picture that emerges of the genetic regulation of scapula formation, can be summarized as follows: several critical factors such as *Tbx15* and *Gli3* pattern the inferior blade while *Tbx15*, *Alx3*, *Alx4*, and *Cart1* pattern the superior blade. In addition, parallel pathways for blade patterning exist and also involve the *Emx2* and *Pbx1* (and possibly *Pbx2* and *Pbx3*). The action of all of these genes appears to occur in the LPM and scapula mesenchyme; and after the initial specification of scapula blade progenitors in the somites; although for the latter genes, the possibility still holds that they play an earlier role. The interaction of the ectoderm and mesoderm, specifically via Wnt and Fgf signaling, appears critical throughout both of these early and late stages of scapula formation. In terms of the patterning of the LPM and that of the scapular head and spine, several genes including *Pax1*, *Hoxa5*, *Hoxc6*, and *Pbx1* appear important in this regard. The interactions between these genes (and those unknown) help partition the LPM into potentially girdle and non-girdle or limb domains that aid in the fine-tuning of specification in these structures. The presence of additional genes known to critically affect both limb and girdle domains, such as *Tbx5*, *Pbx1,* and *Fgf10* is testament into the need to subdivide these domains and pattern them correctly. In this regard, the action of RA, Fgfs, and Wnts may also play a role.

Finally, on a different note, Matsuoka et al. (2005) have recently demonstrated that post-otic neural crest cells (i.e., migrating cell populations arising from the ectoderm of the dorsal-most aspect of the neural tube) contribute to scapular endochondral and perichondrial tissues as well as to the connective tissues of the muscles inserting into this element. They also demonstrate that they contribute to the clavicle, a dermal-derived skeletal element. By utilizing a *Sox10-cre* construct crossed to *Rosa GFP* (green fluorescent protein) reporter system they traced neural crest cells and demonstrated that they contribute specifically to the entire superior border, the scapula spine including the acromion, as well as the coracoid process. By forming endochondral and perichondrial tissues of these structures they provide (and help anchor) major attachment regions for the branchial muscles (e.g., the trapezius). Interestingly, they demonstrate that these crest cells form these attachment points regardless of their ossification mode (i.e., endochondrally or dermally). Overall, these data reveal once again the critical role that signaling has during scapula morphogenesis and patterning, specifically as it influences the coordinated migration of multiple, diverse cell populations (i.e., mesenchyme of dermomyotomal, somatopleuric and neural crest origin).

3.4.2 Histological and molecular characteristics of the pelvic girdle

Despite their roles in scapular formation, most of the above genes have only minor (and/or poorly known) roles in pelvic patterning and morphogenesis. For example,*Tbx15* and its interactions with *Gli3* do not influence the formation of

the pelvic girdle as both single *Tbx15*$^{-/-}$ and *Gli3*$^{-/-}$ mutants and double *Tbx15;Gli3* compound mutants (i.e., *Gli3*$^{+/-}$*;Tbx15*$^{-/-}$, *Gli3*$^{-/-}$*;Tbx15*$^{+/-}$, *Gli3*$^{-/-}$*;Tbx15*$^{-/-}$) lack pelvic defects (Kuijper et al., 2005). On the other hand, the interactions identified between *Alx4*(*Alx3*)*;Cart1* for the scapula were also identified for the pelvis; specifically, compound *Alx4;Cart1* mutants exhibit the loss of the anterior pubic ramus (also evident in *Alx3;Alx4* double null mice; Kuijper et al., 2005). Furthermore, and unlike that of the pectoral girdle, these defects were not exacerbated with the concomitant loss of *Tbx15*. Interestingly, null mutations in *Prx1* and *Prx2* (ten Berge et al., 1998), other Aristaless family genes, result in the loss of the pubis. These findings suggest that complex interactions have evolved among Aristaless genes during both pelvic and pectoral girdle development.

Other genes operating upstream in the somatopleure also affect pelvic formation. For example, ilium loss is also observed in *Pitx1*$^{-/-}$ embryos (Lanctot et al., 1999) indicating that this gene plays a role not only in limb but pelvic field formation. Furthermore, in conditional *Tbx4*$^{-/-}$ embryos (*Tbx4* is downstream of *Pitx1*) the ilium is reduced and dysmorphic (Adler, Papaioannou, unpublished results) (Fig. 3.19). *Emx2*$^{-/-}$ and *Pbx1*$^{-/-}$ embryos also possess a specific reduction in the ilium and a loss of an articulation between it and the remaining caudal pelvic bones (Pellegrini et al., 2001; Selleri et al., 2001; Chapter 7). Recent unpublished observations on compound mutants further demonstrate that at least two of these genes genetically interact, as compound *Pbx1*$^{-/-}$*;Emx2*$^{+/-}$ completely lack the ilium and also the articulation between the inferior pubic ramus and the ischium, whereas *Pbx1*$^{-/-}$*;Emx2*$^{-/-}$ additionally lose the pubis altogether

(Zappavigna, Capellini, and Selleri, unpublished data). As all of these genes are expressed in the LPM and somatopleure, they may impact on the expression of *Fgf10*, a critical factor during pelvic morphogenesis, as demonstrated by the near total lack of pelvic structures in *Fgf10*$^{-/-}$ mice (Sekine et al., 1999).

Overall, the molecular and histological understanding of pelvic skeletal element formation is less clear as both the initial tissues and many of the molecules involved in its formation have remained elusive. To date, it appears that *Pitx1* is one upstream factor that critically influences the formation of the pelvic field, although its role with other genes, such as *Alx3*, *Alx4*, *Cart1*, *Pbx1*, *Emx2*, *Fgf10*, and *Tbx4*, remain critical for the formation of the individual pelvic skeletal elements (Fig. 3.19).

3.5 Hox transcription factors and Pbx cofactor Proteins

3.5.1 Concerning Hox and their cofactors

A review of the many stages of limb and girdle development, as presented above, point to the role of *Hox* genes as critical upstream factors of many of these processes. How exactly Hox operate in these different contexts to pattern skeletal morphology is complex and most likely reflects their abilities to target many genes. Part of this targeting process likely involves the use of cofactors, which improve the DNA binding specificity of Hox proteins. Below, a discussion ensues on how *Hox* genes appear to aid in patterning, with a specific interest on Pbx proteins and their known functions during embryogenesis.

As mentioned, *Hox* genes encode homeodomain-containing DNA binding proteins (transcription factors) that are expressed in various tissues of the developing embryo and adult animal (Krumlauf, 1994; Lumsden and Krumlauf, 1996). While the exact mechanisms underlying how *Hox* genes pattern tissues remain elusive, their main function as transcription factors and DNA binding proteins is critical for such patterning to take place. It has been argued based on both their overall ubiquitous expression pattern (i.e., as a group they are expressed in many diverse tissues) as well as their individual precise spatio-temporal expression patterns (i.e., individual *Hox* genes are expressed in overlapping and discrete domains in embryonic tissues) that they must regulate many genetic networks and target numerous genes (Carroll et al., 2005). As transcription factors, Hox proteins have potentially many target DNA sequences, and their role as DNA-binding proteins allows them to bind to such sequences.

Although purified Hox proteins have been shown to bind DNA, albeit weakly *in vitro*, the high degree of conservation among their homeodomains results in poor sequence specificity (Hoey and Levine, 1988). This situation raises the problem of how their *in vivo* specificity is achieved, specifically on multiple, perhaps diverse, target DNA sequences. Currently, it has became well established that Hox DNA binding specificity is achieved through interactions with other DNA binding proteins, which act as cofactors (Mann, 1995; Mann and Chan, 1996; Mann and Affolter, 1998).

Hox cofactor proteins were originally identified as the products of genes that were disrupted in body patterning mutants in *Drosophila*. In this manner,

mutations in these genes roughly phenocopied mis-patterning or homeotic phenotypes brought about via altered *Hox* control (see Moens and Selleri, 2006). Interestingly, over the past few years research on several Hox cofactor homologs demonstrate their importance in vertebrate morphogenesis. In some vertebrate organ systems, these cofactors aid in Hox DNA binding ability, a characteristic shared with their known functions in invertebrates. At the same time, however, some cofactor proteins have additional or divergent functions that are Hox-independent.

3.5.2 On Pbx cofactors and homologs, partner cofactors, and their functional relationships with Hox

3.5.2.1 Extradenticle (Exd) and Pbx cofactors

The first Hox cofactor identified was *Drosophila* Exd, the ortholog of the vertebrate Pbx proteins. Mutations in *Exd* result in homeotic transformations in specific fly body segments where they are normally expressed. Interestingly, in these mutants, *Hox* gene expression is not altered (Peifer and Wieschaus, 1990; Rauskolb et al., 1993; 1995), which indicates that Exd functions in parallel to Hox to alter the morphological consequences of their activities.

The first vertebrate homolog of *Exd* to be discovered was that of *Pbx1*. *Pbx1* was independently identified due to its mutation by t (1:19) chromosomal translocations leading to human pre-B cell acute lymphoblastic leukemia (Kamps et al., 1990; Nourse et al., 1990; Rauskolb et al., 1993). The genetic similarities, specifically in terms of sequence homologies, between *Exd* and *Pbx* genes are

quite high (Fig. 3.20). This genetic homology also translates into a high degree of protein homology, specifically with respect to key functional DNA and Hox binding regions. In terms of biochemical structure, Exd and Pbx comprise the PBC subclass of the triple acid loop extension (TALE) homeodomain proteins, referring to the conserved PBC motif N-terminal to the TALE homeodomain (Burglin, 1997; 1998).

In vitro, Pbx or Exd proteins both cooperate with a broad subset of Hox proteins to bind a paired recognition element on DNA with high specificity (Chan et al., 1994; 1996; Chang et al., 1995). Based on a limited number of such recognition elements, early work suggested that the sequence specificity of a given Hox protein in the presence of Pbx/Exd was defined (Chan et al., 1997; Ryoo et al., 1999). However, recent evidence has indicated that the sequence requirements for DNA binding by Hox complexes are difficult to predict (Ebner et al., 2005).

The primary interaction between Pbx/Exd and Hox is through the three amino acid loop in the Pbx homeodomain, which binds a tryptophan-containing hexapeptide motif (N-Y/F-P/D-W-M-K/R) N-terminal to the homeodomain. This binding is observed between Pbx and 3' Hox proteins of the paralogous groups 1-9 as well as the 5' paralog 10 group. All other Hox proteins belonging to 5' distal groups (11-13) do not bind with Pbx in the manner described (Chang et al., 1995; Knoepfler and Kamps, 1995; Neuteboom et al., 1995; Passner et al., 1999; Phelan et al., 1995; Piper et al., 1999). While the observed binding of Pbx and Hox can be initiated *in vitro* and has been demonstrated *in vivo* at the

aforementioned domains, recent work on Hox/Exd binding suggest that other regions, outside of the hexapeptide motif are important and can bind such proteins together (see Galant et al., 2002; Merabet et al., 2003).

The *in vivo* effects of cofactor binding on Hox function are still controversial. In a manner that appears to be based on the target DNA sequence and the Hox protein itself, complexes of Hox:Exd or Hox:Pbx have been shown to act as transcriptional activators or as transcriptional repressors. Interestingly, what comes from these studies is that "activation" versus "repression" abilities may be determined by the presence of other cofactors into the transcriptional machinery. Of course, such recruitment of other cofactors is also tied to the specific target's regulatory DNA sequence, on their nuclear presence in and around such a complex, and also on extracellular signals (Saleh et al., 2000; Kobayashi et al., 2003; Gebelein et al., 2004). Alternatively, some research suggests that if the Hox hexapeptide is mutated, that the activity of a transcriptional complex can go from repression to activation, leading to the expression of target genes. In this context, the actual cofactor binding may lead to conformational changes in the complex binding to the target sequence thereby evincing the roles of cofactor/Hox relationship in gene expression (Galant et al., 2002; Merabet et al., 2003). In other words, such binding may determine the way in which Hox proteins regulate their targets (Peifer and Wieschaus, 1990; Pinsonneault et al., 1997).

3.5.2.2 Regarding Pbx and Meis cofactor partners

Another Hox cofactor group known to interact with Pbx are those of the Meis class of TALE homeodomain proteins (Burglin, 2005) (Fig. 3.20). Meis have been shown to regulate Hox activity both as components of the DNA-bound Hox complex and by regulating Pbx/Exd activity in the absence of DNA (Moskow et al., 1995; Chang et al., 1997a-b; Chen et al., 1997; Knoepfler et al., 1997; Berthelsen et al., 1998a-c). As the invertebrate Exd is the vertebrate Pbx ortholog, Homothorax (Hth) is the invertebrate ortholog of both vertebrate Meis and Prep proteins. Meis/Prep proteins interact directly with Pbx/Exd and participate in the DNA-bound Hox complex, recognizing a split sequence on the regulatory regions of target genes (Mann and Affolter, 1998; Jacobs et al., 1999; Ryoo et al., 1999; Ferretti et al., 2000; Ebner et al., 2005). Meis/Prep proteins also promote the nuclear localization (Rieckhof et al., 1997; Abu-Shaar et al., 1999; Berthelsen et al., 1999; Mercader et al., 1999; Jaw et al., 2000) and stability (Jaw et al., 2000; Waskiewicz et al., 2001; Longobardi and Blasi, 2003) of Pbx proteins. Finally, Meis/Prep proteins have been observed to interact directly with a subset of Hox proteins in a manner that only descriptively and not functionally (as of yet) is independent of the Hox hexapeptide (Shen et al., 1997; Williams et al., 2005).

3.5.2.3 Pbx family members and their functionality in embryogenesis

Vertebrates possess multiple Pbx family members (Fig. 3.20). In addition to *Pbx1*, *Pbx2* and *Pbx3* were then discovered based on their homology to *Pbx1*,

but have yet to be implicated in disease (Monica et al., 1991). *pbx4* was identified in a forward genetic screen in the zebrafish as a mutant in which Hox-dependent patterning events were disrupted (Popperl et al., 2000; Waskiewicz et al., 2002). Subsequently, mammalian *Pbx4* gene was then discovered but is expressed exclusively in the testis (Wagner et al., 2001) and is not orthologous to zebrafish *pbx4*. Currently, *pbx4* in zebrafish is orthologous to the mammalian *Pbx1*. On the protein level, various isoforms exist for these Pbx family members. For example, mammalian Pbx1 and Pbx3 have two alternative splice variants (Pbx1a-1b, Pbx3a-3b) with different C-terminal regions.

Experiments in zebrafish indicate that the functional differences between *pbx* genes are likely to be due to expression differences rather than in their biochemical activities (Popperl et al., 2000). Accordingly, ectopic expression of any zebrafish *pbx* gene can completely rescue the embryonic phenotype of a *pbx4* mutant (*Lazarus*). Interestingly, even the use of *Drosophila Exd* can rescue this same mutant phenotype, a scenario that highlights the high degree of functional conservation across this protein family.

Consistent with this observation, is that the *in vitro* DNA binding properties of different Pbx proteins appear very similar: mammalian Pbx1, Pbx2, and Pbx3 exhibit identical DNA cooperative binding with a subset of Hox proteins *in vitro* (Chang et al., 1995). If the current line of experimentation between *Drosophila* and Zebrafish is telling then such data allows for a prediction regarding *Pbx* gene function in vertebrates. Specifically, one could predict that where the expression of Pbx family members overlap, their functions may be partially redundant. As is

shown in Chapters 5-7, different *Pbx* genes are expressed in both overlapping as well as temporally and spatially distinct patterns during limb development.

3.5.2.4 Pbx proteins function as Hox cofactors in vertebrates

Several lines of evidence demonstrate that Pbx proteins function as Hox cofactors in vertebrates as Exd functions in *Drosophila*. First, it has been shown that *Hox* regulatory elements include Pbx binding sites (Popperl et al., 1995; Maconochie et al., 1997; Ferretti et al., 2000; Manzanares et al., 2001; Samad et al., 2004). For example, conserved paired *Hox/Pbx* regulatory elements are present in the promoters of mammalian *Hox* genes themselves. In addition, it has been shown that these elements are critical for regulation. For example, it is known that 3' *Hox* gene expression in the vertebrate hindbrain is highly auto- and cross-regulated (reviewed in Nonchev et al., 1997). In these domains, *Hoxa1* is required for the normal onset of *Hoxb1* expression, and *Hoxb1* is required for its own maintenance (Popperl et al., 1995; Studer et al., 1998). In these two examples, the Hox recognition element consists of a paired Hox/Pbx binding site (often with a nearby Meis/Prep site), and mutating either the Hox- or the Pbx-binding element prevents reporter expression in transgenic mice (Popperl et al., 1995; Maconochie et al., 1997; Ferretti et al., 2000; Manzanares et al., 2001; Samad et al., 2004).

Second, *Pbx* mutants in both fish and mice either partially or completely recapitulate *Hox* loss-of-function phenotypes (see Studer et al., 1996; McClintock et al., 2002; Cooper et al., 2003; Arenkiel et al., 2004). Third, it has been shown

experimentally that *Pbx* and *Hox* genes interact genetically. For example, *Pbx1* and *Hoxa2* genetically interact to pattern branchial arch 2-derived craniofacial structures in the mouse (Depew, Ferretti, Rijli, and Selleri, unpublished results). Other examples are described in Waskiewicz et al. (2002), Cooper et al. (2003), and Brendolan et al. (2005). Fourth, Pbx is required for Hox activity both *in vitro* and *in vivo* (see Krosl et al., 1998; Thorsteinsdottir et al., 1999; Popperl et al., 2000; Cooper et al., 2003).

Fifth, Hox and Pbx may jointly and synergistically promote cell proliferation (Borrow et al., 1996; Nakamura et al., 1996b; Shen et al., 1996; Sauvageau et al., 1997; Thorsteinsdottir et al., 1997a-b; Krosl et al., 1998; Schnabel et al., 2000; Knoepfler et al., 2001; Yaron et al., 2001; LaRonde-LeBlanc and Wolberger, 2003), as from their original discoveries, both *Hox* and *Pbx* genes have been implicated as proto-oncogenes in human leukemia (see Kamps et al., 1990; Nourse et al., 1990). This role of Hox and Pbx in leukemic cells may reflect a co-operative role for Hox:Pbx complexes in promoting cell proliferation during normal development. A role of Hox proteins in the regulation of progenitor cell proliferation has been suggested based on studies of *Hox* null mice (Duboule, 1995; Hombria and Lovegrove, 2003). *Hox* over-expression in the chick limb bud demonstrates that *Hoxd11* and *Hoxd13* pattern the limb skeleton by regulating cell division rates in the chondrocyte proliferative zone (Goff and Tabin, 1997). Furthermore, *Hoxc8* over-expression causes cartilage defects such as accumulation of proliferating chondrocytes and reduced maturation (Yueh et al., 1998). Most recently, Kmita et al. (2005) and Tarchini and Duboule (2006) have

suggested that the primary role of *Hox* in the limb is to ensure proper growth through proliferation control. Similarly, analyses of *Pbx1* mutant mice reveal a function for Pbx1 as a promoter of progenitor cell proliferation, since virtually every organ system is affected by the mutation is hypoplastic and/or aplastic and is characterized by a reduction in proliferating cells (DiMartino et al., 2001; Selleri et al., 2001; Kim et al., 2002; Manley et al., 2004; Brendolan et al., 2005).

Sixth, *in vivo* work supports the biochemical findings that some Hox functions require the Hox hexapeptide motif (Carpenter et al., 1993; Mark et al., 1993). Seventh, recent work on Meis/Prep proteins as Hox cofactors indicates that they are required for the normal functioning of Hox-Pbx complexes. Hox/Pbx binding sites upstream of Hox target genes are often associated with essential Meis/Prep sites, and Meis/Prep proteins bind these targets cooperatively with Hox and Pbx *in vitro* (Chang et al., 1997a-b; Berthelsen et al., 1998a-c; Ebner et al., 2005). In the mouse, *Meis1* and *Prep1* mutants are embryonic lethal and exhibit a variety of abnormalities including hematopoeitic and angiogenic defects and severe organ hypoplasia (Hisa et al., 2004; Azcoitia et al., 2005). The ontogeny of these defects and their similarity to *Hox* or *Pbx* phenotypes has been investigated in *Prep1* mutants (Ferretti et al., submitted for publication).

3.5.2.5 Pbx has functions outside of their involvement with Hox

Some aspects of *Pbx* phenotypes suggest that Pbx and Meis/Prep may act more broadly, to modulate the activity of non-Hox homeodomain proteins or even non-homeodomain proteins. In addition, there are domains of *Pbx* (and

Meis) expression in the mouse and zebrafish that do not overlap with *Hox* expression and yet *Pbx* mutants (both single and compound) possess abnormal phenotypes in these domains. Regarding the non-Hox function of Pbx during embryogenesis, there exists a precedent for such findings in invertebrate systems as much of the work on Pbx homologs has been carried out more extensively and more easily in these systems. These functions are reviewed quite extensively in Moens and Selleri (2006).

Work done in mice also indicates that Pbx participates in the regulation of several developmental processes, in a manner that is Hox-independent. Much of this work is also reviewed in Moens and Selleri (2006). However, one example is that Pbx proteins function as partners for "orphan" Hox proteins. "Orphan" or "metaHox" genes are thought to be ancient duplicates of clustered *Hox* genes (Brooke et al., 1998). For example, in *Pbx1*$^{-/-}$ embryos, spleen are absent, a defect that directly phenocopies the spleen agenesis of *Hox11* null mice (Roberts et al., 1994; Dear et al., 1995; Brendolan, 2005). *Hox11* encodes a non-clustered orphan Hox protein that binds DNA with Pbx1 through a conserved hexapepetide motif (Dear et al., 1993; Allen et al., 2000). Furthermore, *Pbx1* and *Hox11* genetically interact in spleen formation, since *Pbx1*$^{+/-}$*;Hox11*$^{+/-}$ mice develop hypoplastic and malformed spleens, whereas single heterozygotes exhibit normal spleen development (Brendolan et al., 2005).

Pbx proteins have also more recently been shown to function as partners for non-homeodomain transcription factor proteins. For example, Knoepfler et al. (1999) showed that Pbx bound DNA co-operatively with the myogenic bHLH

proteins MyoD, myf5 and others. As for Pbx-Hox interactions, these Pbx-bHLH interactions occurred via a conserved tryptophan motif N-terminal to the bHLH DNA binding domain. Although a requirement for Pbx in muscle development has yet to be demonstrated, a recent study elegantly demonstrated the mechanism of Pbx-MyoD interaction during myogenic differentiation *in vitro* (Berkes et al., 2004). During muscle differentiation, MyoD activates expression of *myogenin* and a number of other targets. Berkes et al. (2004) showed that chromatin remodeling and activation of a subset of these targets involves the binding of a Pbx-Meis-MyoD complex to a divergent E-box element in their promoters. Since Pbx-Meis can bind this element in undifferentiated cells in the absence of MyoD, Berkes et al. (2004) postulate that Pbx-Meis acts as a molecular “beacon” or “mark” for the subsequent recruitment of MyoD and activation of the myogenic program. Whether this is a general model that also applies to the better known role of Pbx and Meis as co-factors for Hox proteins remains to be determined.

3.5.2.6 Pbx interacts with partner proteins to confer some of its functions

Often, Pbx interacts with partner proteins to confer some functionality either with or without Hox. It is interesting that Prep and Meis share structural and expression domain similarities with Pbx and *in vitro* and *in vivo* form heterodimers. Pbx-Meinox heterodimers also show the same *in vitro* binding specificities; i.e., they bind to TGACAG or TGATTGACAG sequences, sites not recognized by Pbx-Hox dimers. In addition, they can interact with the Pbx-Hox target site (TGATNNATNN) (Chang et al., 1997a-b; Knoepfler et al., 1997;

Berthelsen et al., 1998a-c; Jacobs et al., 1999: Ferretti et al., 2000). Moreover, unlike Pbx-Hox complexes, the Pbx-Meinox dimers do not show direct transcriptional activation properties (Berthelsen et al., 1998a-c; Goudet et al., 1999) leaving unclear the function of these heterodimers.

The formation of heterodimers between Pbx and Meis (or their homologs Exd and Hth) often is the consequence of their regulatory interaction development. In fact, Exd/Pbx activity is regulated post-transcriptionally by a nuclear translocation regulatory mechanism involving Meis/Hth. *In Drosophila*, Exd is essential to establish the proximal-distal axis in the developing limb-bud and is required for patterning of the proximal region of the fly leg, where it is subjected to nuclear-cytoplasmic regulation. Typically, Exd is expressed uniformly in leg imaginal disc (i.e., Exd is present in the domains of the proximal and distal fly leg). However, in the proximal part of the developing leg, Exd is localized in the nucleus via its interaction with Hth and its activity prevents the cells from responding to proteins such as decapentaplegic (Dpp) and Wingless (Wg). On the contrary, in the distal region of the leg, where Exd is cytoplasmic, it is in an inactive form, and this, in turn, allows the activation of Dpp and Wg signaling proteins, which are, in turn, activated by Hh (Hedgehog) (Gonzalez-Crespo et al., 1998). As mentioned, the positive regulator of Exd nuclear translocation is the Meinox protein Hth. In the absence of Hth, Exd remains in the cytoplasm and it is not functional. In the presence of Hth, Exd translocates to the nucleus, a process that requires direct interaction between Exd and Hth (Rieckhof et al., 1997; Kurant et al., 1998; Pai et al., 1998). Thus, both Hth and

Exd are required for proximal, but not distal, leg development. Ectopic expression of Hth distally induces nuclear localization of Exd, blocking the distal development and resulting in truncated appendices (Morata, 2001).

The correlation between P-D limb patterning and subcellular localization is evolutionarily conserved (Gonzalez-Crespo et al., 1998; Capdevilla et al., 1999; Mercader et al., 1999). For example, Meis1 and Prep1 can also substitute for Hth to induce the nuclear localization of Exd in salivary gland and antennal and leg imaginal discs (Rieckhof et al., 1997; Berthelsen et al., 1999; Jaw et al., 2000). Mis-expression of Meis1/2 in distal chick limbs produce proximalization of distal structures (Capdevilla et al., 1999; Mercader et al., 1999). Ectopic expression of human Prep1 in *Drosophila* imaginal discs weakly affects eye formation but affects leg and antennal development (Jaw et al., 2000).

Likewise, in the developing mouse limb bud, Pbx1 is cytoplasmic in the distal part and it is nuclear only in the proximal part, due to the presence of the Hth orthologs Meis1 and Meis2 proximally (Gonzalez-Crespo et al., 1998, Mercader et al., 1999; Kilstrup-Nielsen et al., 2003). Both Exd and Pbx proteins contain a nuclear localization signal (NLS), as well as a nuclear export signal (NES). The NES signal is mapped in the PBC domain, which is also involved in Meinox protein interaction. Since Meinox does not carry an already defined (NLS), a model has been proposed in which the heterodimerization of Exd-Pbx with Hth-Meinox induces nuclear translocation of Meinox-Pbx dimers, which is then kept in the nucleus through the blocking of the NES (Bethelsen et al., 1999).

3.5.3 An emerging view of Pbx functionality in the limb

The current understanding of Pbx function in the vertebrate limb is quite complex. In vertebrates, the proximal expression of *Pbx1* corresponds well with Exd presence in the fly proximal imaginal disc. In both flies and mice, such proximal protein nuclear localization requires their partner proteins. In vertebrates, additional complexity is generated because four *Pbx* genes are present, *Pbx1*, *Pbx2*, *Pbx3*, and *Pbx4* with at least five additional Meinox genes, *Meis1*, *Meis2*, *Meis3*, and *Prep* (i.e., *Prep1* and *Prep2*). With respect to the Meinox class, *Meis1* and *Meis2* appear to be expressed only proximally in the limb, a situation that mirrors its homolog's (Hth) expression in the fly. *Prep,* on the other hand, appears to be expressed more distally in vertebrate limb buds, a divergent property of these proteins from their fly homologs. Vertebrate Pbx proteins also possess divergent localization patterns. For example, while *Pbx2* and *Pbx3* are expressed in overlapping expression domains with *Pbx1* proximally in the limb, *Pbx2* (and partly *Pbx3*) is also expressed distally and in the nucleus. In this manner, *Pbx* occupies novel domains and indicates additional levels of complexity from flies. This thesis addresses some of this complexity by focusing on the functionality of *Pbx* genes during limb development.

Figures and Tables

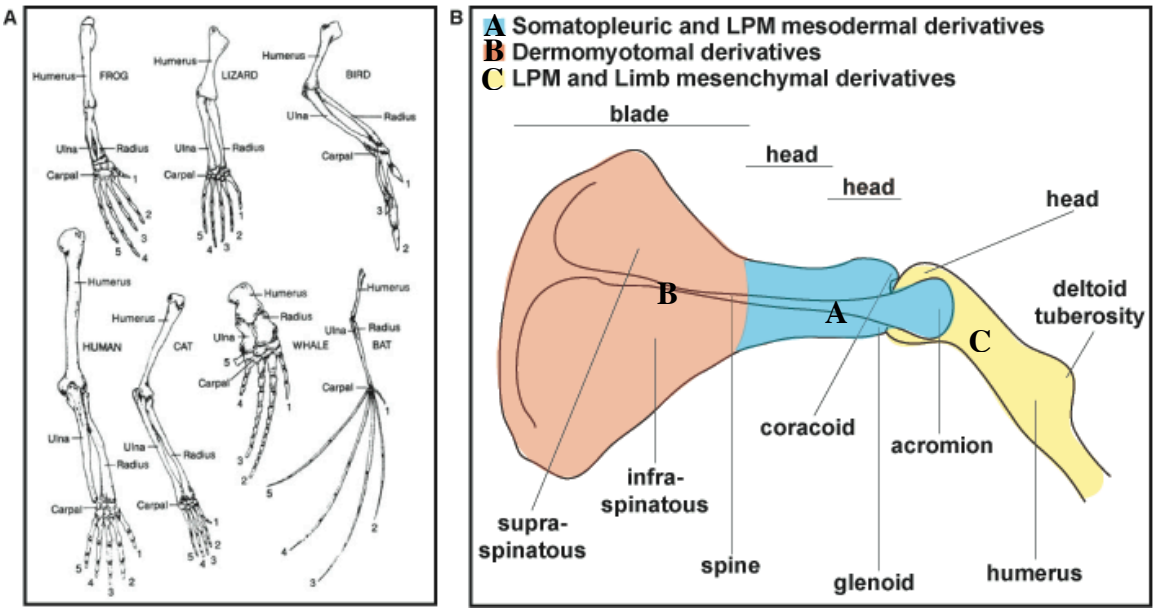

Figure 3.1. The forelimb with scapula and their underlying embryonic tissue domains.

(A) Comparative forelimb skeletal morphology from several vertebrate species. Adapted from Carroll et al. (2005). (B) Skeletal structures of the scapula and proximal humerus along with a depiction of the embryonic tissues that give rise to each structure (compare letters in each domain). See text. In (A) Proximal (top); anterior (right); In (B) Proximal (left); superior (top); LPM, Lateral Plate Mesoderm.

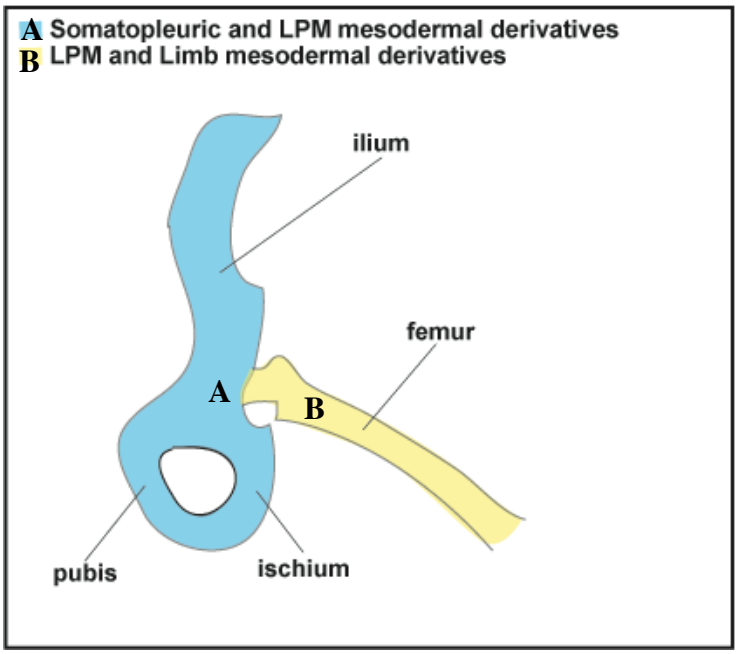

Figure 3.2. The mouse hindlimb with pelvis and their underlying embryonic tissue domains.

Skeletal structures of the pelvis and proximal femur of the mouse hindlimb along with a depiction of the embryonic tissues that give rise to each structure (compare letters in each domain). See text. Proximal (left); superior/rostral (top); LPM, Lateral Plate Mesoderm.

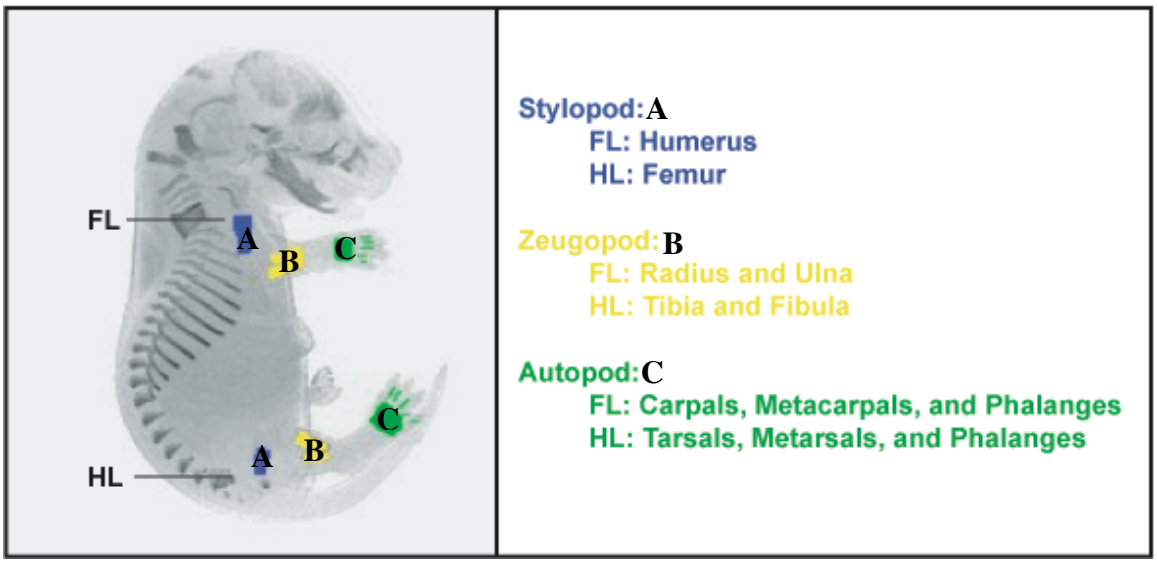

Figure 3.3. Developmental compartments of the mouse fore- and hindlimb.

See text for details and match letters for each domain. Adapted from Martin (1990). Proximal (left); anterior (top); FL, Forelimb; HL, Hindlimb.

Figure 3.4. Overview of early limb development in the mouse (E8.5-E11.5).

(A) At E8.5, a transverse line drawing depicts the arrangement of the axial mesoderm into several tissue domains (see text). Adapted from Gilbert (2006). (B) At E9, the embryo has rudimentary forelimbs and hindlimb fields (left). A cross section (line, left) at the mid-forelimb (right) demonstrates a loosely organized mesenchyme (lowercase a) covered by a distal ectodermal cap (lowercase b) corresponding to the preAER. (C) At E11, both limb types are more developed (left) with the hindlimb normally delayed compared to the forelimb. A closer view (right) of the distal forelimb reveals a distal aggregation of ectodermal cells called the AER (lowercase b and arrows). (D) At E11, a cross section (left) through the mid-forelimb reveals a loosely organized mesenchyme with a distal pseudo-stratified epithelial AER (inset right). Adapted from Martin (1990). In (A) Dorsal (top); lateral (far left and far right); In (B, right) Proximal (right); dorsal (top); In (C, right) Distal (out of page); anterior (top-right); In (D; right) Proximal (left); dorsal (bottom); A, Anterior; D, Dorsal; FL, Forelimb; HL, Hindlimb; P, Proximal.

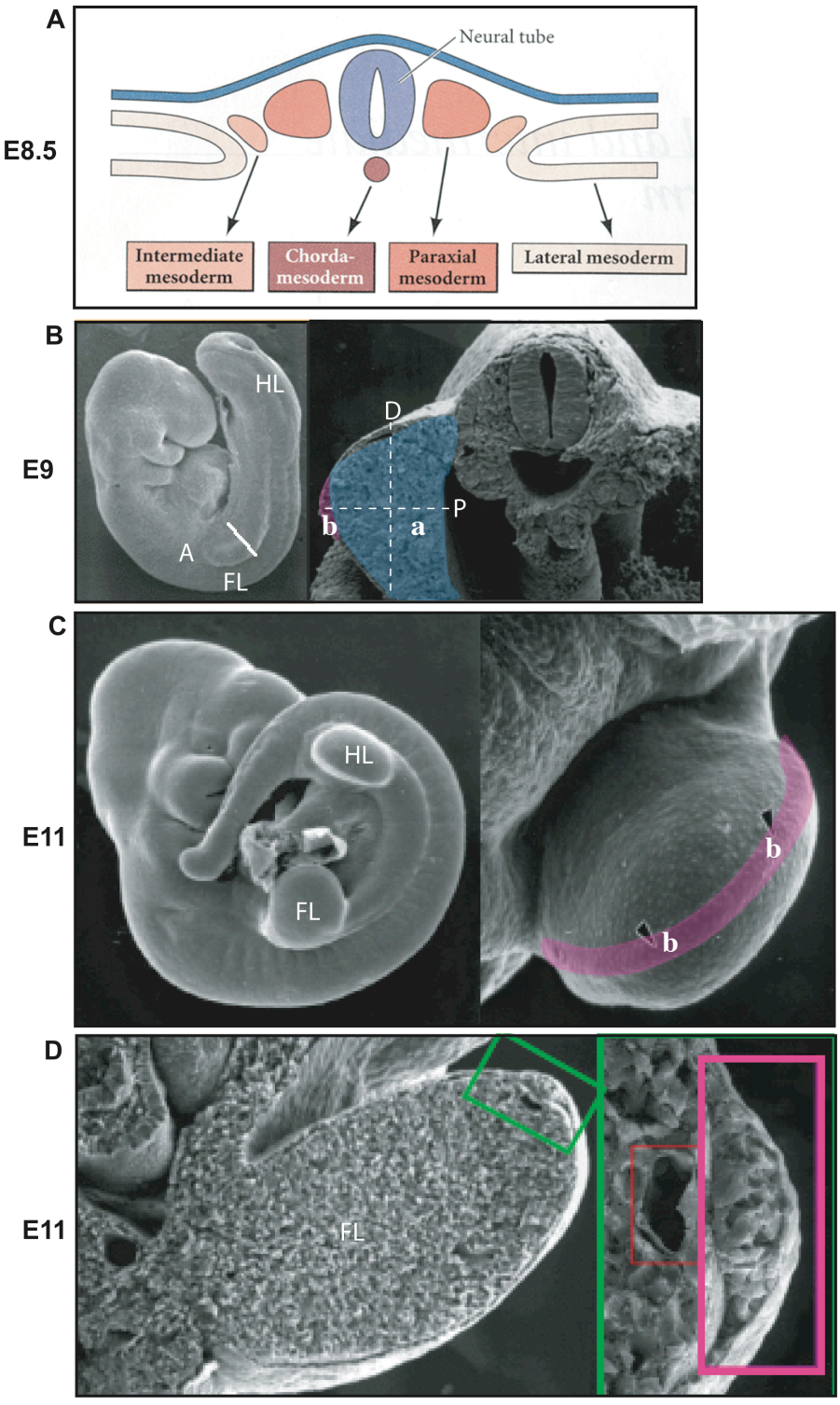
A
E8.5
Neural tube
Intermediate mesoderm
Chorda-mesoderm
Paraxial mesoderm
Lateral mesoderm
B
E9
HL
A
FL
D
P
b
a
C
E11
HL
FL
b
b
D
E11
FL

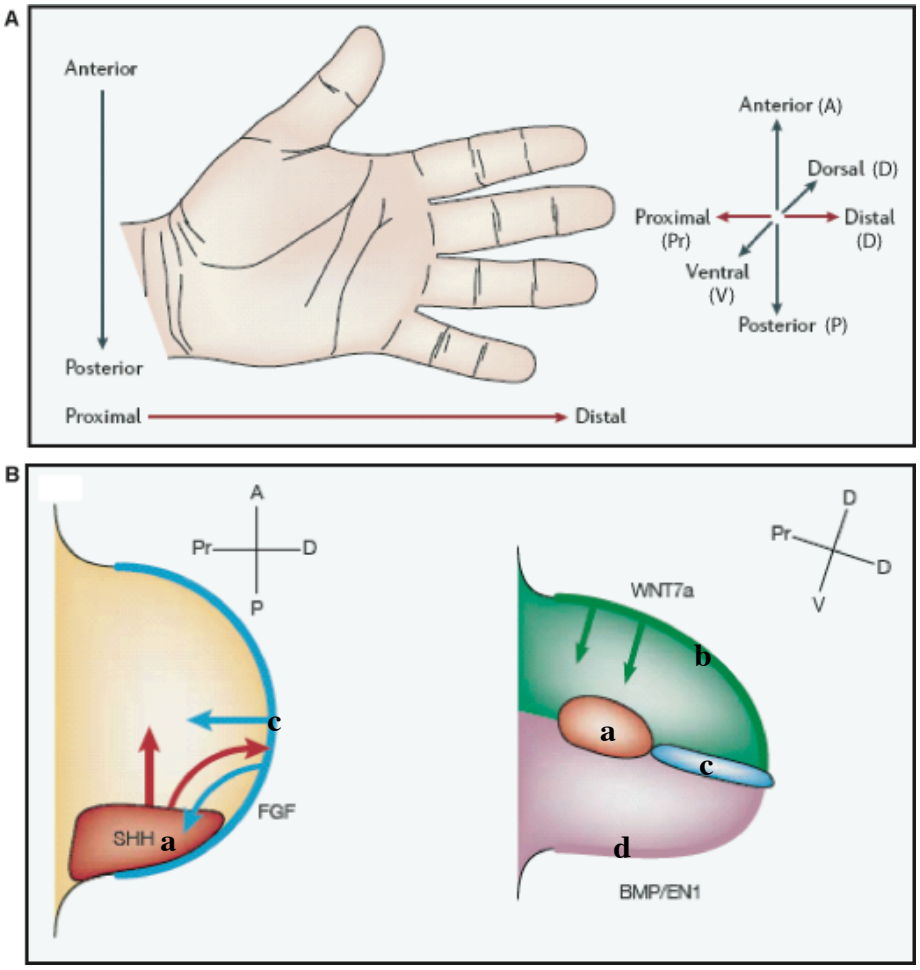

Figure 3.5. Major axes of the limb and its developmental signaling centers.

(A) Developmental axes of the autopod (and limb). Adapted from Tickle (2006). (B) Major signaling centers in the limb. On left, the AER (c) runs anteriorly to posteriorly along the distal limb and expresses *Fgfs*. Also, in the underlying posterior mesenchyme, the ZPA (a) is present and expresses *Shh*. On right, a transverse section (at a level just anterior to the Shh domain on left) reveals the dorsal ectoderm (b) expressing *Wnt7a* and a ventral ectoderm (d) expressing *Bmp* and *En1*. See text. Adapted from Niswander (2003).

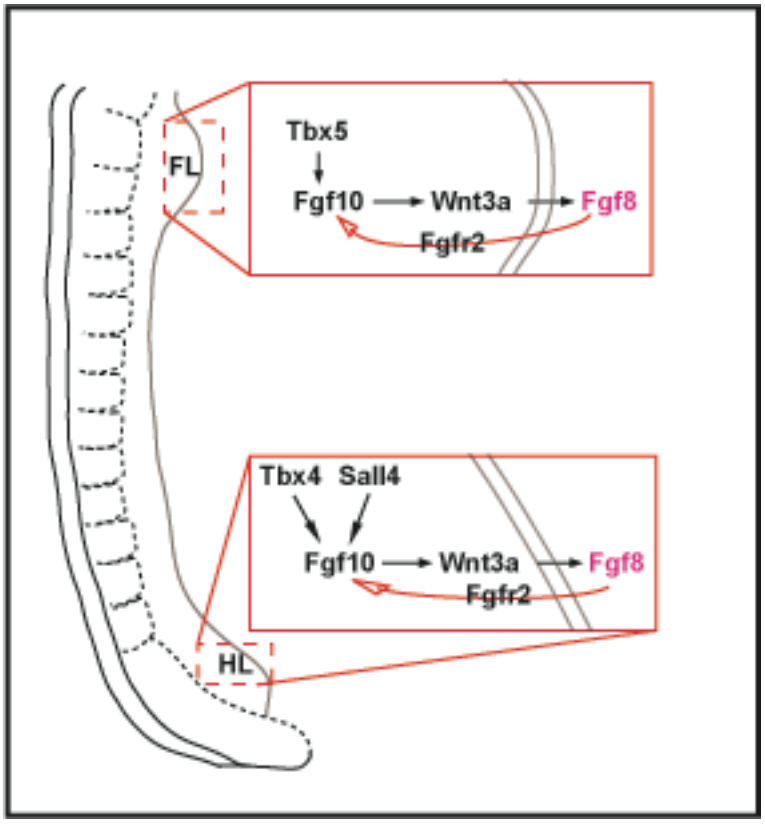

Figure 3.6. Molecular interactions in the E9.0 forelimb and hindlimb.

See text for details. In both limb domains, *Fgf8* ectodermal expression is highlighted on the right and its signaling through Fgfr2 to the mesenchyme is indicated by the long curved arrow. Proximal (left); anterior (top); FL, Forelimb; HL, Hindlimb.

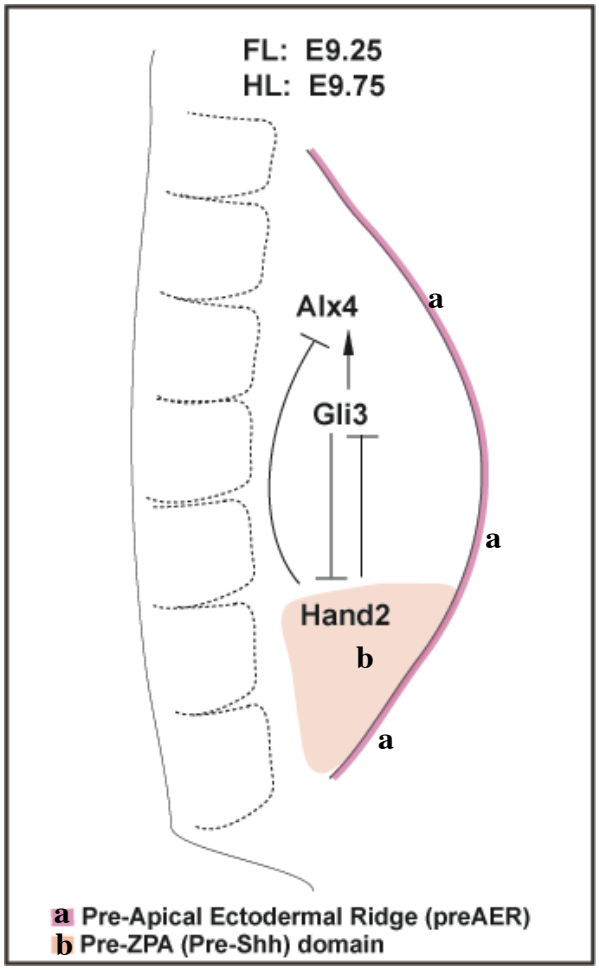

Figure 3.7. Early molecular interactions along the anterior-posterior limb bud at E9.25 (FL)/E9.75 (HL).

See text for details. Arrow indicates activating role while T-lines indicate inhibitory/repressive roles. Proximal (left); anterior (top).

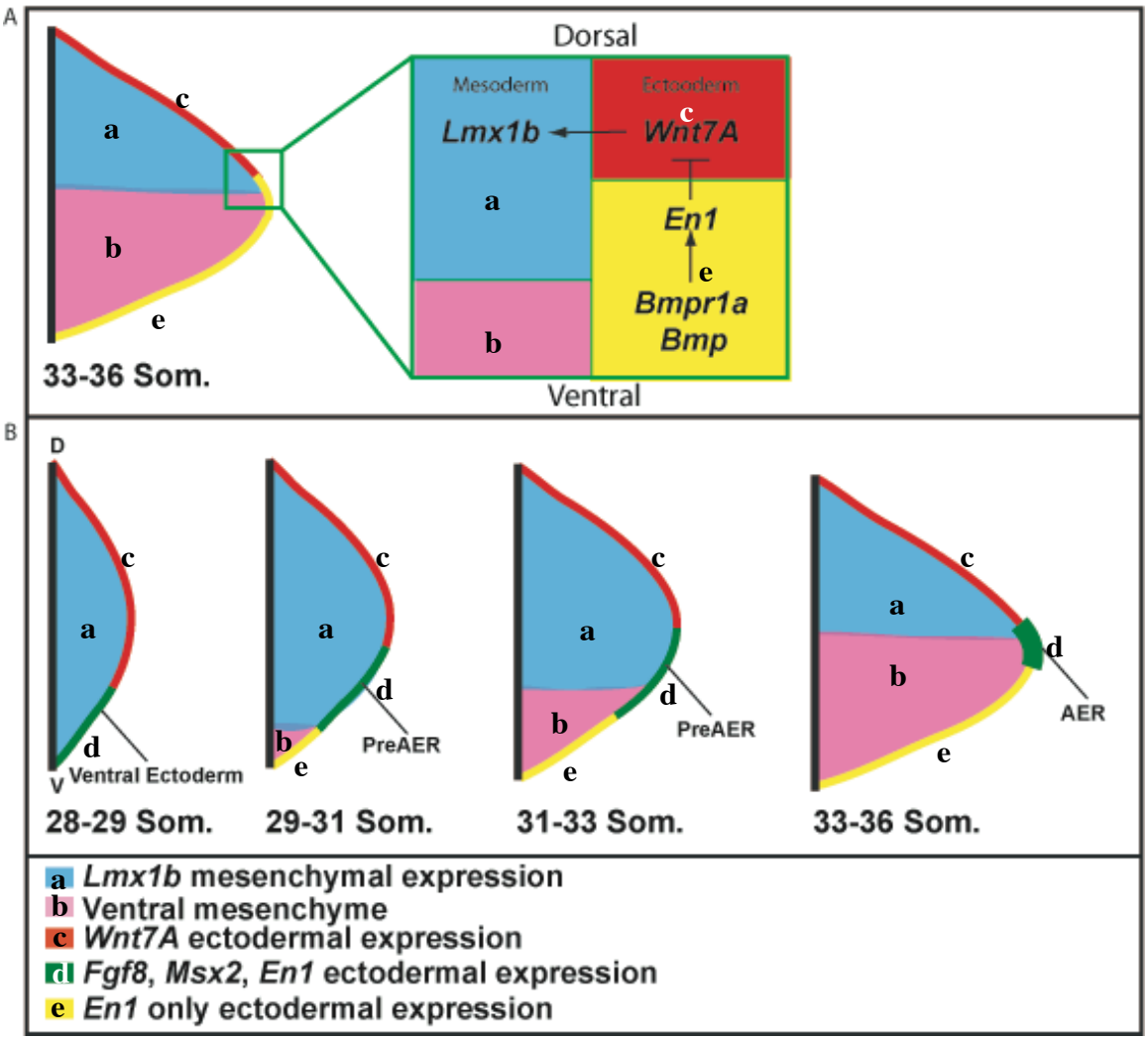

Figure 3.8. D-V polarity in the early limb bud and the development of the AER.

(A) A depiction of an E10-10.5 (33-36 Som.) limb bud with the molecular interactions that determine dorsal versus ventral mesenchymal and ectodermal fate. (B) A developmental progression through the mesenchymal and ectodermal events leading to D-V axis determination and AER formation. The thickness of the green line in the distal limb, illustrates the transformation of columnar to pseudostratified epithelium characteristic of AER formation. See text. Redrawn and modified from Bell et al. (1998). Proximal (left); anterior (top); FL, Forelimb; HL, Hindlimb; Som., Somites.

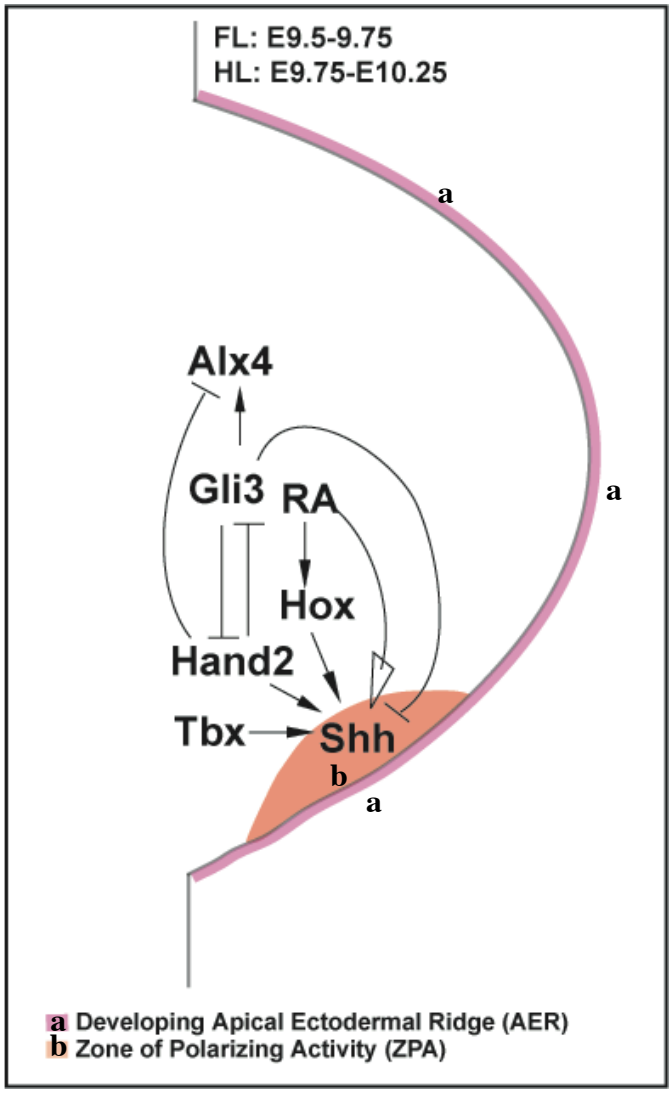

Figure 3.9. Upstream hierarchical factors regulating *Shh* activation in the preZPA mesenchyme at E9.5-9.75 (FL)/E9.75-E10.25 (HL).

See text for details. Black arrows indicate direct activating roles, open white arrowheads indicate potential indirect roles, and T-lines indicate inhibitory/ repressive roles. Proximal (left); anterior (top).

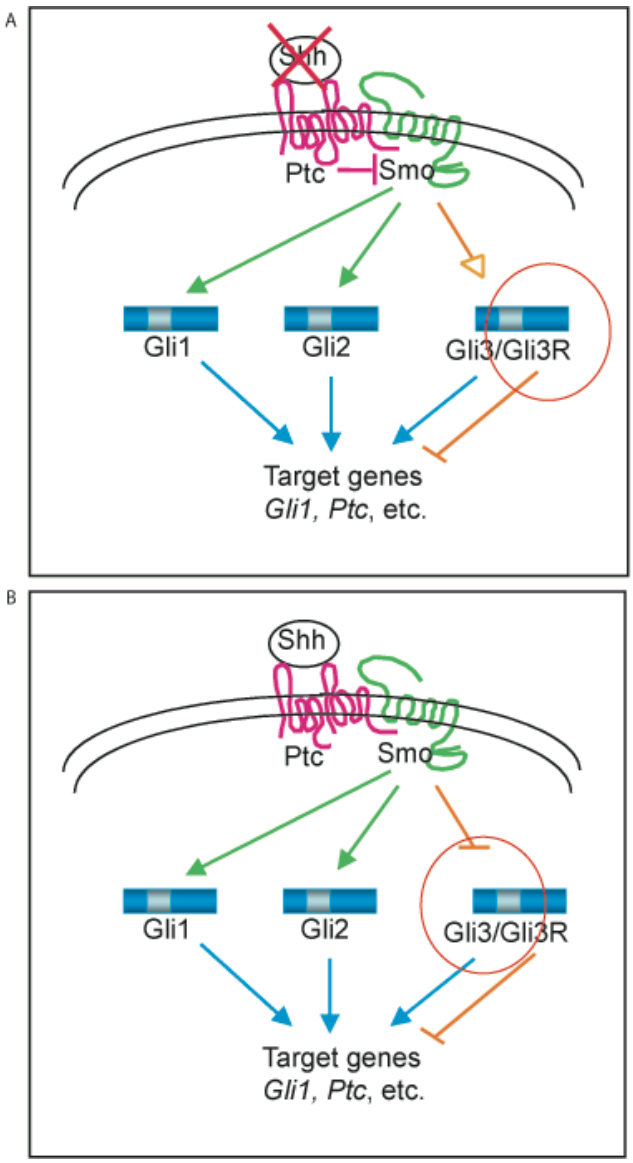

Figure 3.10. The Shh signaling pathway.

(A) Signal transduction in the absence of Shh (X over Shh), leads to production of Gli3R (ellipse) and its repressive effects on target genes (T-line from Gli3R). (B) Signal transduction in the presence of Shh, leads to production of Gli3 activator forms (circle) and the activation of target genes (arrow from Gli3). See text. Adapted from Niswander, 2003).

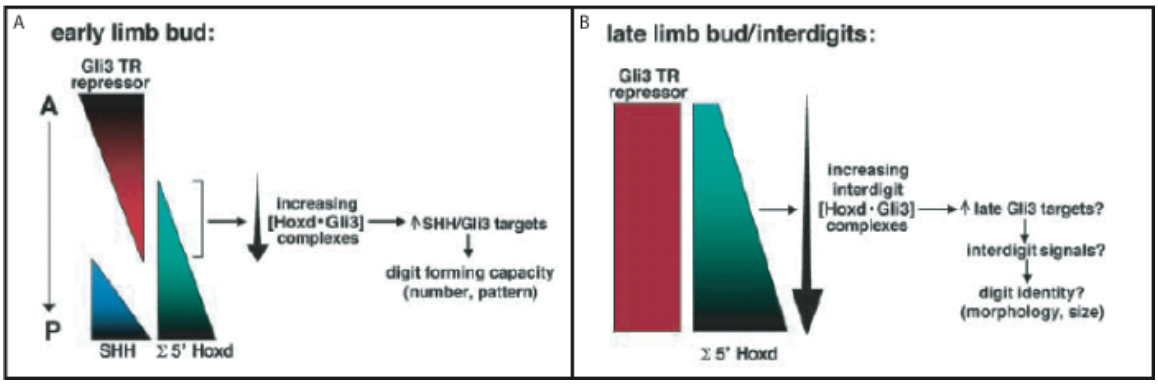

Figure 3.11. Anterior to posterior gradients on Shh, Gli3 and Hox complexes during limb development.

(A) Gli3, Hox, and Shh complex gradients and their effects on target genes and digit formation in the early presence of Shh activation. Different gradients indicate gradients for each protein or protein complex. (B) Gli3 and Hox complex gradients in the absence of Shh during late digital patterning. Different gradients indicate gradients for each protein or protein complex. See text for details. Copied from Chen et al. (2004).

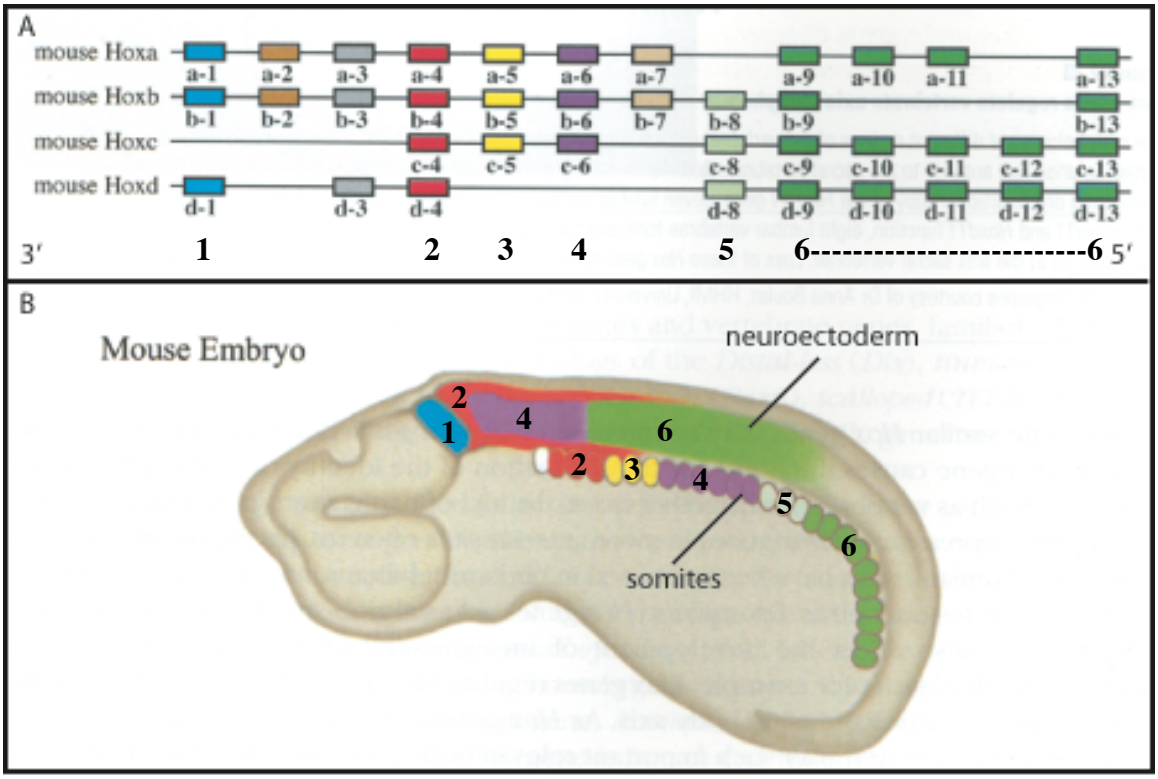

Figure 3.12. *Hox* cluster organization and expression in the mouse embryo.

(A) Organization of the four *Hox* clusters (A-D) in the mouse. Boxes with paralog numbers represent individual *Hox* genes organized from 3' (left) to 5' (right) on each cluster. Paralogous 3' *Hox* are indicated by the same numbered suffixed box (e.g., a-1, b-1, d-1). (B) *Hox* expression in the mouse embryo along the dorsal neuroectoderm, mesoderm, and somites. Each number reflects the specific paralogous group listed in (A). See text for details. Copied from Carroll et al. (2005).

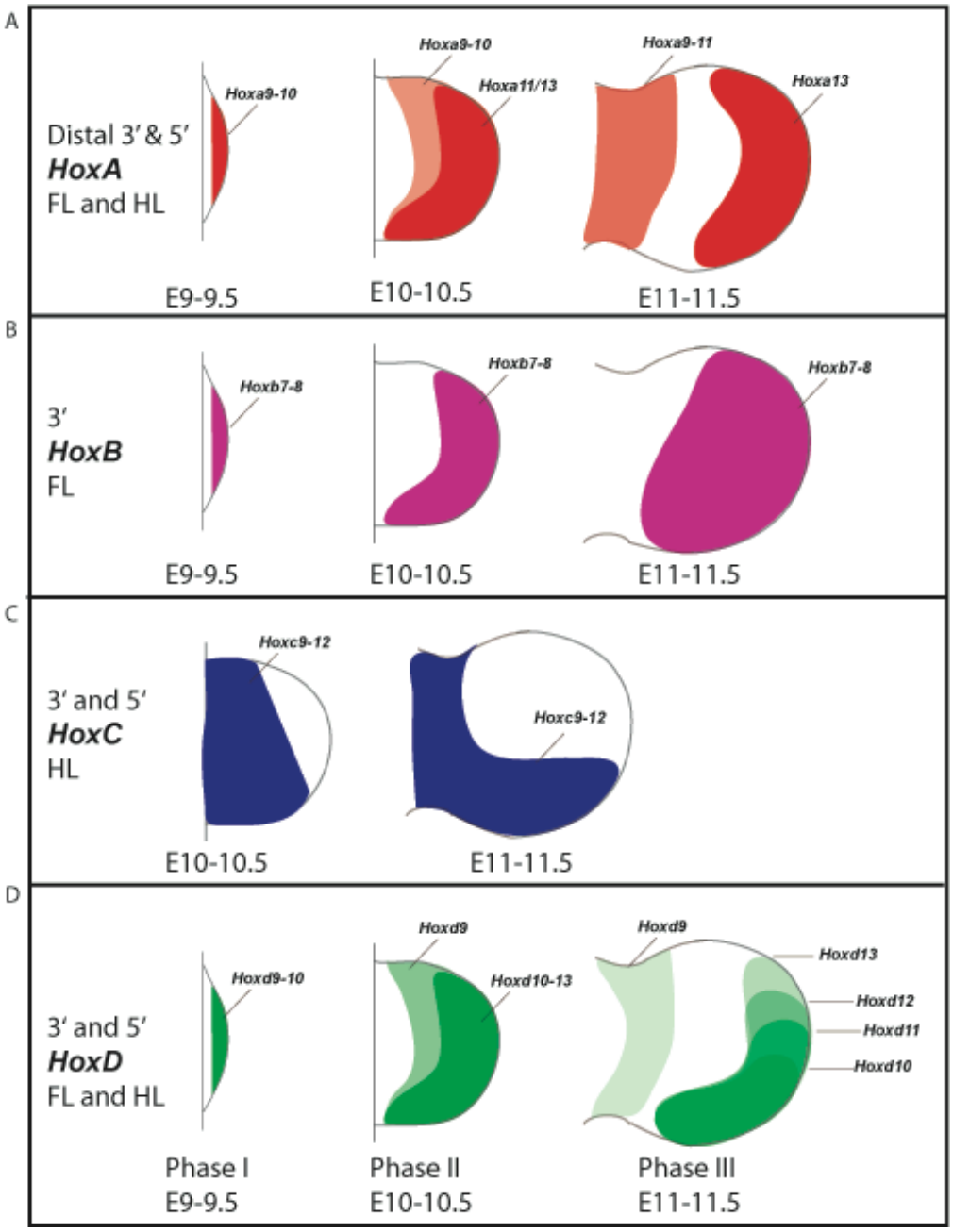

Figure 3.13. *Hox* gene expression in the developing limb.

(A) Distal 3' and 5' *HoxA* gene expression in both limb types. (B) Select 3' *HoxB* gene expression in the forelimb. (C) Distal 3' and 5' *HoxC* gene expression in the hindlimb. (D) Distal 3' and 5' *HoxD* gene expression in both limb types. In all cases, different shades indicate gradient expression and/or temporal loss. See text. Proximal (left); anterior (top). FL, Forelimb; HL, Hindlimb.

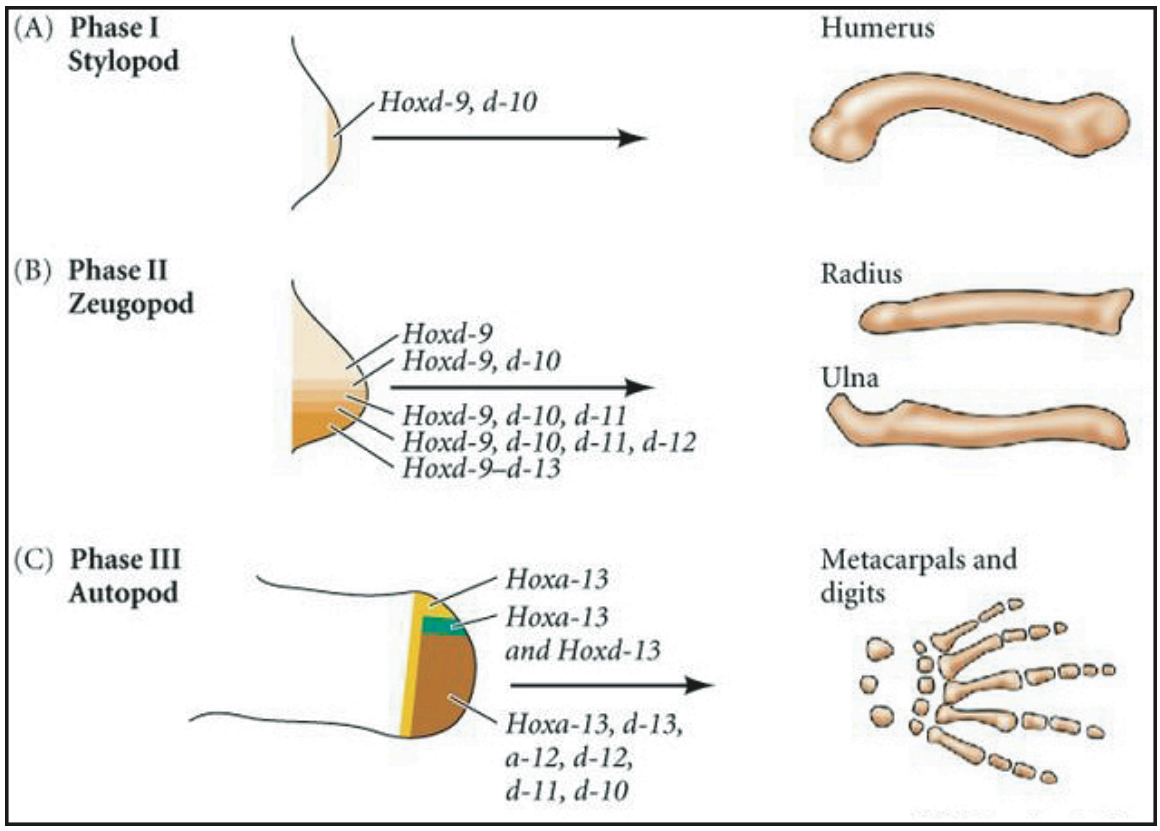

Figure 3.14. Domains of *HoxD* (and partial *HoxA*) expression and the skeletal elements they specify.

(A) Early distal Phase I expression of 3' and 5' *HoxD* (left) specifies the humerus (right). (B) Phase II expression of 3' and 5' *HoxD* (left) specifies the anterior radius and the posterior ulna (right). (C) Phase III expression of 5' *HoxA* and *HoxD* (left) specifies the elements of metacarpals and digits (right). The same relative patterns exist for the hindlimb (data not shown). Different shades of gray indicate different anterior-posterior expression levels for individual *Hox*. See text for details. Adapted from Gilbert (2006). Proximal (left); anterior (top).

Figure 3.15. The regulation of early *HoxD* collinear and "reverse" *HoxD* collinear gene transcription.

In both diagrams, the *HoxD* cluster is arranged from 3' to 5' with control regions (ELCR and GCR) located at either end. Individual *HoxD* genes (boxes with white lettering) with an intronic region (box with "i") between d4 and d8 initialize transcription in the direction of the ELCR. (A) Early *Hox* collinear activation proceeds 3' (i.e., *Hoxd1*) to 5' (i.e. *Hoxd13*) (depicted by the largest arrow), such that 3' *Hox* are typically activated first (as they are closest to the ELCR; upper curved short arrow indicates activation) and are expressed throughout the limb bud (E9 limb bud, right). In addition, individual Hox may autoregulate and cross-regulate each other's expression (dashed curved arrow). 5' *Hox* are activated later (as they are furthest from the ELCR) and are restricted to the posterior limb domains (E10 limb bud, far right) with Shh ("*"). Finally, the increasingly posterior restriction of 5' *Hox* during early collinearity results from their inhibition (T line) by an antagonistic domain (circle) located 5' of *Hoxd13*. (B) Diagram depicts the regulation of late *Hox* "reverse" collinear transcription during autopod development. In this model, a 5' global control region (GCR) activates 5' *Hox* (*Hoxd13*-*Hoxd10*) with decreasing transcriptional efficiency (i.e., the shorter and thicker the curved arrow the greater the efficiency) and no longer is influenced by either the 5' antagonistic domain (circle) or ELCR (rectangle). This mechanism leads to the "reverse" 5' *HoxD* expression pattern (E11.5 limb bud, right). (A) Proximal (left); anterior (top).

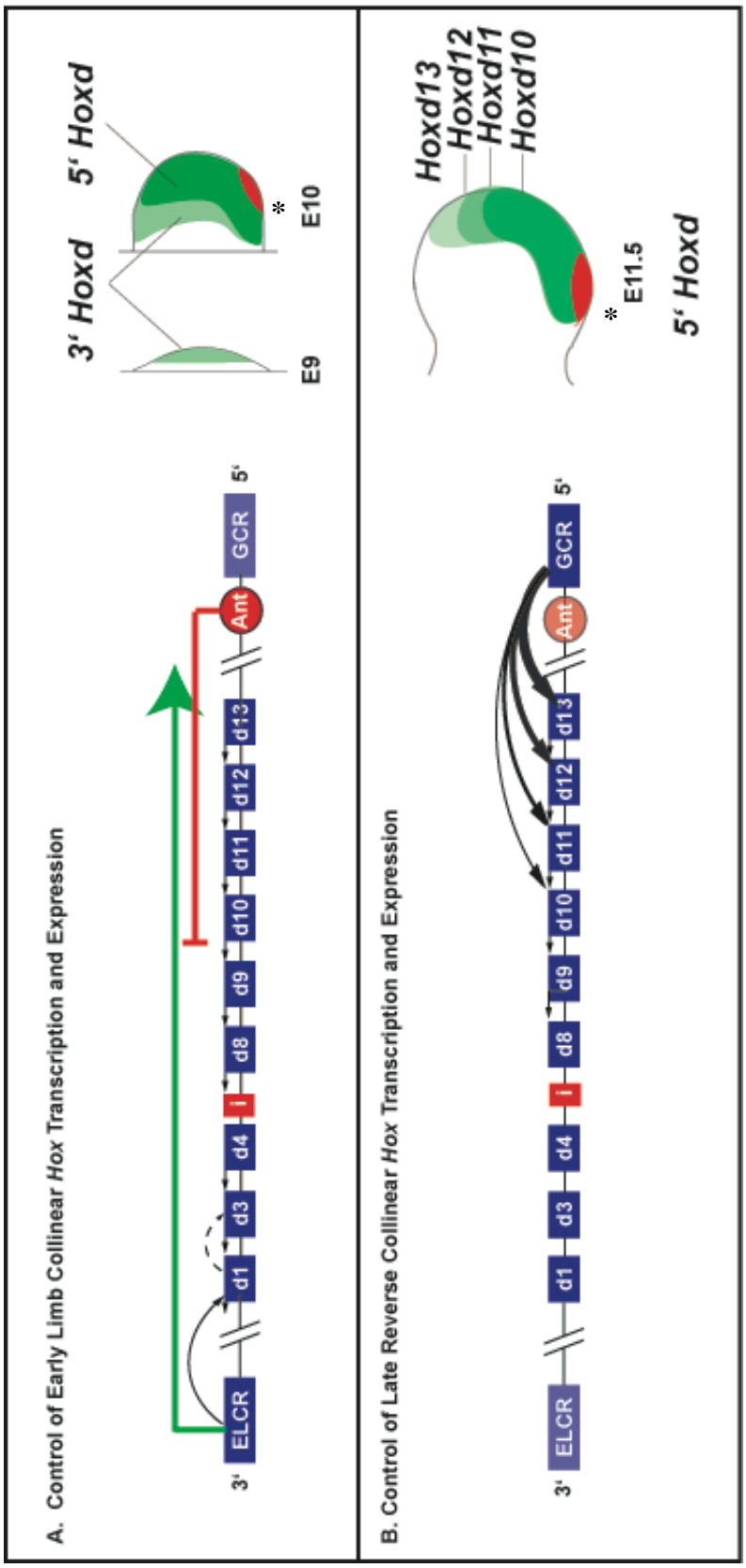
A. Control of Early Limb Collinear Hox Transcription and Expression
3' Hoxd
5' Hoxd
E9
E10
3'
ELCR
d1
d3
d4
i
d8
d9
d10
d11
d12
d13
Ant
GCR
5'
B. Control of Late Reverse Collinear Hox Transcription and Expression
Hoxd13
Hoxd12
Hoxd11
Hoxd10
E11.5
5' Hoxd

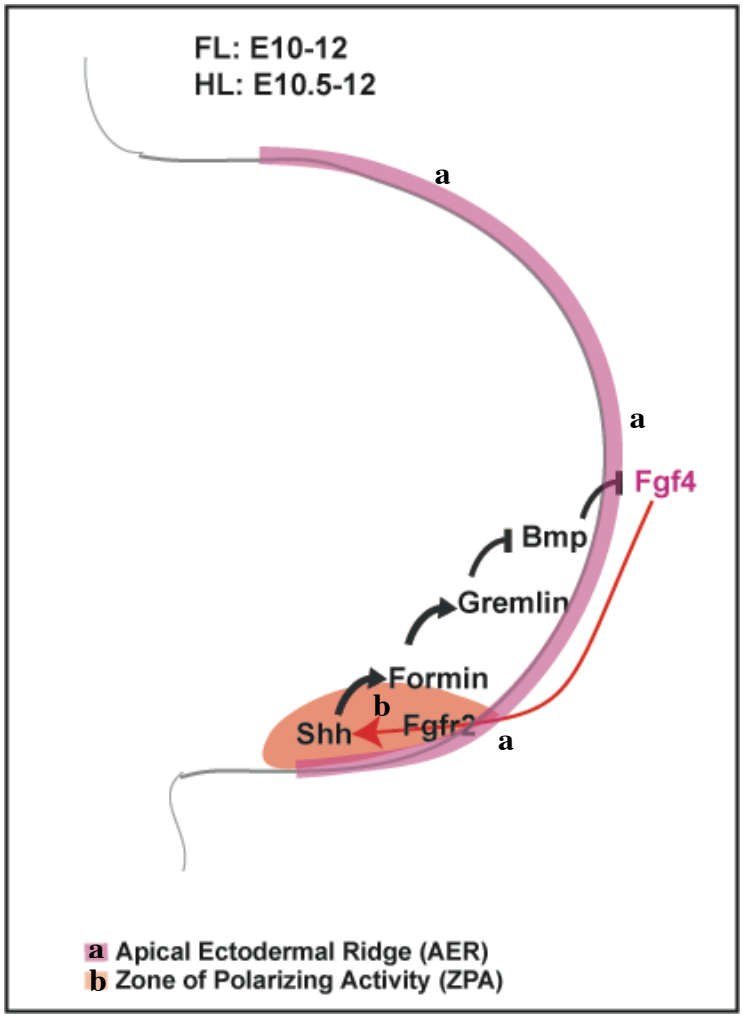

Figure 3.16. The ZPA-AER molecular feedback loop.

See text for details. Arrows indicate direct activating roles, long arrow indicates Fgf signaling from the AER (a) via Fgfr2 to the ZPA (b), and T-lines indicate inhibitory/repressive roles. Proximal (left); anterior (top).

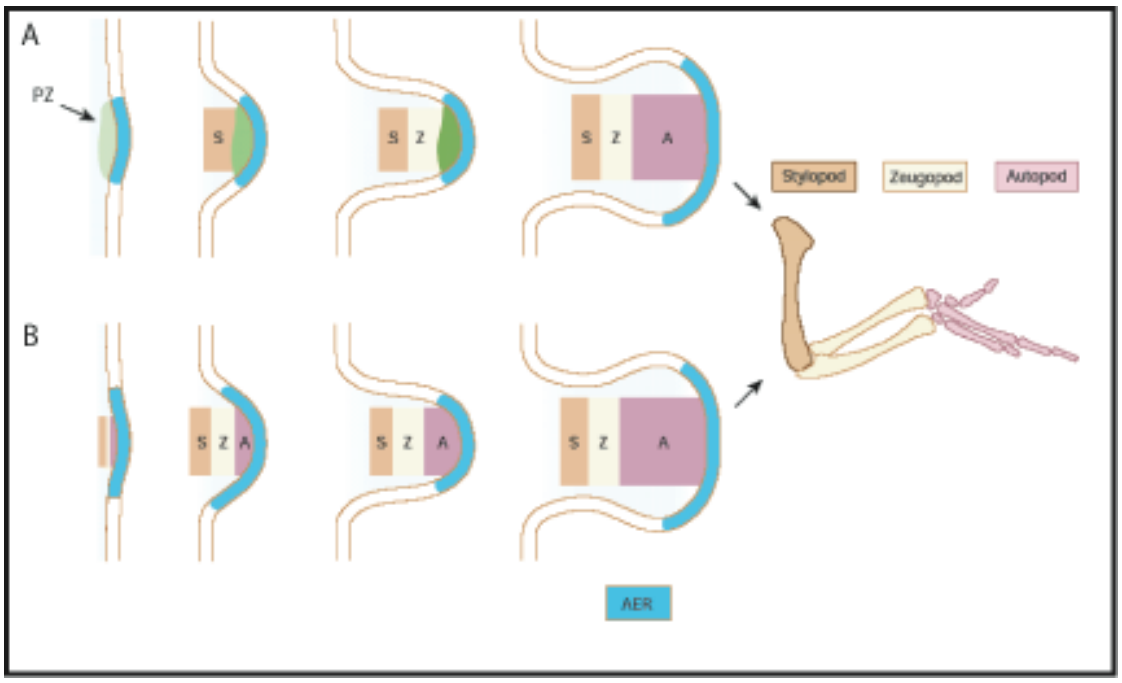

Figure 3.17. Skeletal element specification according to the Progress Zone Model (PZM) and the Early Specification Model (ESM).

(A) Diagram illustrates the progressive specification of skeletal elements (right) according to the PZM (left). (B) Diagram illustrates the early specification of skeletal elements (right) according to the ESM. Letters in each box (e.g., "A") indicate structure the cells will eventual give rise to (e.g., "Autopod"). See text for details. Adapted from Mariani et al. (2003). Proximal (left); anterior (top).

Figure 3.18. Molecular and tissue interactions during scapular development.

(A) Early (E9-10) specification by axial *Hox* expression of a specialized compartment (a) of the dermomyotome (b) to be fated to the scapular blade (e.g., E13.5, right). Line for *Hoxc6* expression denotes the level where the forelimb develops. (B) Diagram of a transverse section at the anterior forelimb (AL) level demonstrating the major tissues involved in forming the scapular blade. Left box illustrates molecular signaling from the body ectoderm (BE) to the dermomyotome (D). Middle box illustrates the molecular interactions between the somatopleure (So) and the dermomyotome (D). Right box illustrates the molecular interactions between the somatopleure (So) and anterior limb (AL); along with a depiction of those genes (specifiedby lettered domains) that specify the unique scapular blade domains seen below at E13.5. See text for details. (C) Diagram of an E13.5 scapula demonstrating that from E9-12, specific genes function to give rise to the structures of the scapular neck, head, and acromion process (a). In all cases, arrows indicate activating roles, while questions marks (?) depict unclear relationships. Proximal (left); AL, anterior limb; BE, Body Ectoderm; Cond., Condensation; D, Dermomyotome; Diff., Differentiation; DL, Distal Limb; LE, Limb Ectoderm; Mig., Migration; Nc, Notochord; Pat., Patterning; Sc, Scleratome; So, Somatopleure.

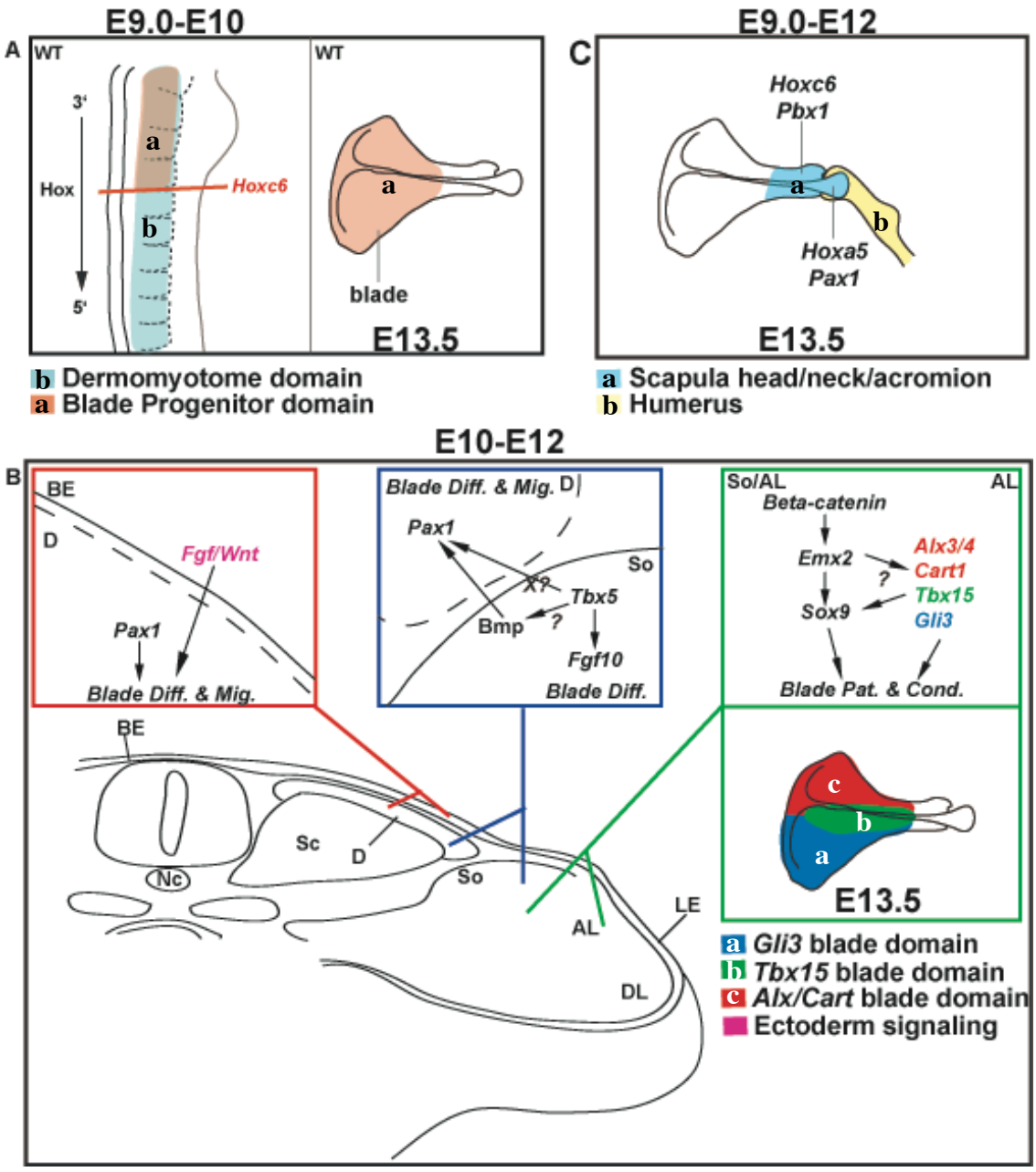
E9.0-E10
A
WT
WT
3'
Hox
5'
a
b
Hoxc6
a
blade
E13.5
b Dermomyotome domain
a Blade Progenitor domain
E9.0-E12
C
Hoxc6
Pbx1
a
b
Hoxa5
Pax1
E13.5
a Scapula head/neck/acromion
b Humerus
E10-E12
B
BE
D
Fgf/Wnt
Pax1
Blade Diff. & Mig.
Blade Diff. & Mig. D
Pax1
So
X?
Tbx5
Bmp
?
Fgf10
Blade Diff.
So/AL
AL
Beta-catenin
Emx2
Alx3/4
Cart1
?
Tbx15
Sox9
Gli3
Blade Pat. & Cond.
BE
Sc
D
Nc
So
AL
LE
DL
c
b
a
E13.5
a Gli3 blade domain
b Tbx15 blade domain
c Alx/Cart blade domain
Ectoderm signaling

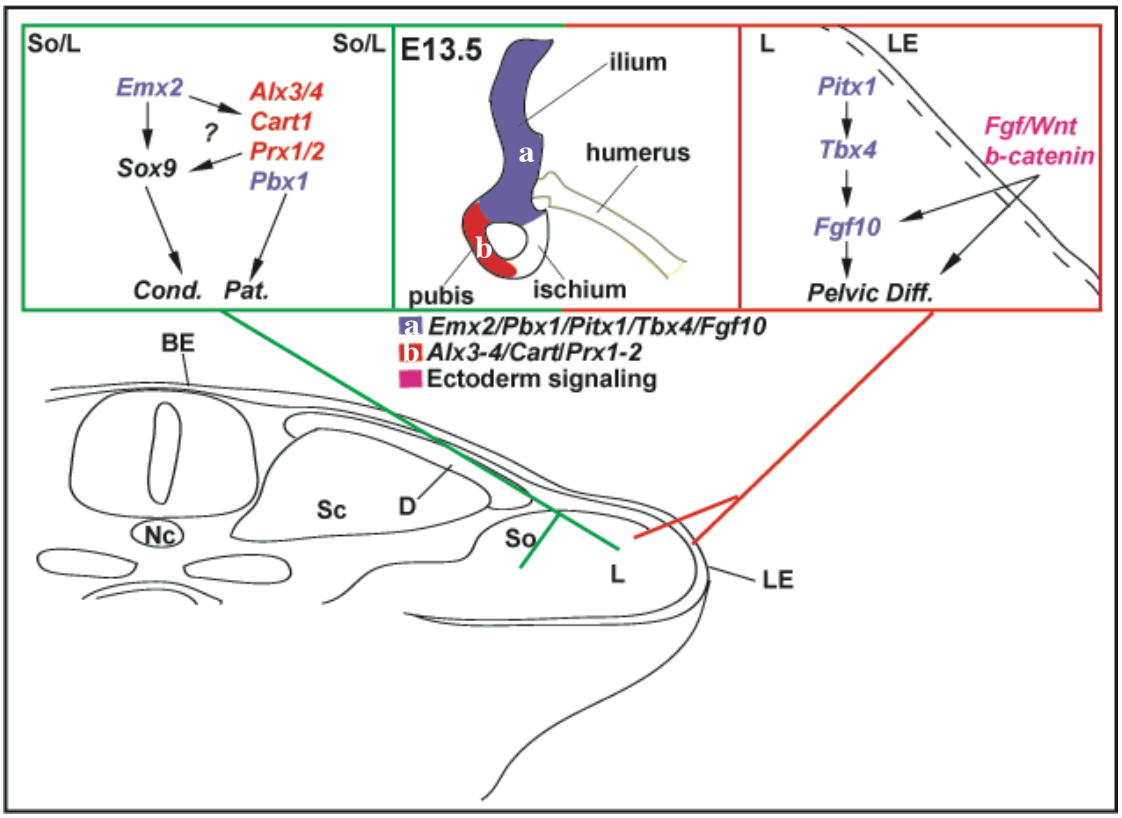

Figure 3.19. Molecular and tissue interactions giving rise to the pelvis.

A diagram of a transverse section at the hindlimb (L) level demonstrating the major tissues involved in pelvic formation. Left box illustrates the molecular interactions between the somatopleure (So) and limb (L); along with a depiction of those genes that specify the unique pelvic elements seen to the right at E13.5. Right box illustrates the molecular interactions between signaling from the limb ectoderm (LE) to the limb (L), along with those limb genes that specify the unique pelvic elements seen to the left at E13.5. See text. Proximal (left). BE, Body Ectoderm; Cond., condensation; D, Dermomyotome; Diff., Differentiation; L, Limb; LE, Limb Ectoderm; Nc, Notochord; Pat., Patterning; Sc, Scleratome; So, Somatopleure.

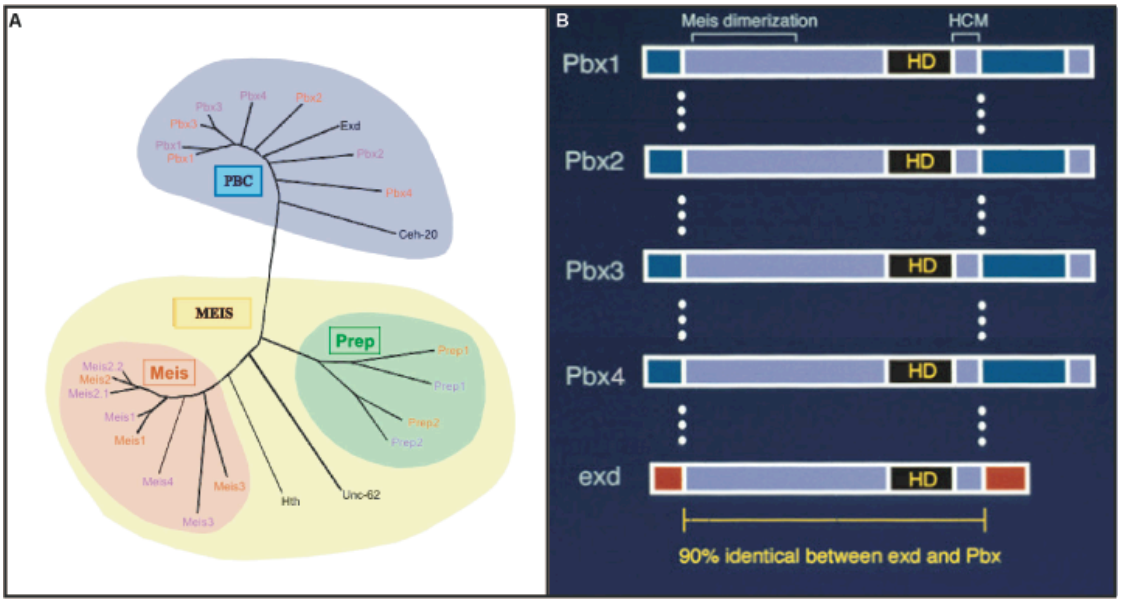

Figure 3.20. Genetic, biochemical, and homology relationships among Pbx and Meis genes/proteins.

(A) Homology relationships between Pbx (PBC) and Meis/Prep homeoproteins, (adapted from Moens and Selleri, 2006). (B) Homology between vertebrate Pbx family members and their invertebrate ortholog, Exd. In accordance with the 90% sequence identity between Exd and Pbx, all share stronger identity in their meis dimerization domains, homeodomains, and HCM domains. See text for details.

Limb Event/Process	Gest. Day (E)	Tissues/Centers	Section	Figures
Organization of major pre-limb tissues	E7.5-8.5	PM, IM, LPM	3.2.2	3.4A
Axial specification of FL and HL fields	Prior to E9	PM, IM. LPM	3.3.1	3.4B
*Limb field and bud induction	E8-E9.5	PM, IM, LPM	3.3.2	3.4B, 3.6
Limb field induction	E8-E9	PM, IM. LPM	3.3.2	3.6
Limb bud induction	E8.5-9.5	LPM and ectoderm	3.3.2	3.6
*Limb axis establishment	E8.5-11.5	Limb mesoderm and ectoderm	3.3.3	3.4B-D
Early A-P. P-D, & D-V establishment	E8.5-9.5	Limb mesoderm and ectoderm	3.3.3.1	3.6-7
Early AER formation and P-D establishment	E8.5-10.5	Limb mesoderm and ectoderm	3.3.3.2	3.8
Later A-P axis establishment	E9.5-11.5	Limb mesoderm and ectoderm	3.3.3.3	3.9, 3.16
Role of Hox in axis establishment/patterning	E9.5-11.5	Limb mesoderm	3.3.3.4	3.12-15
Maintenance of limb bud axes	E9.75-12	Limb mesoderm and ectoderm	3.3.3.5	3.16
*Mesenchymal specification/skeletal patterning	E8.5-12	Various tissues	3.3.4	3.14, 3.17
Progress zone model	E9-12	Limb mesoderm and ectoderm	3.3.4.1	3.17
Early specification model	E8.5-9.5	Limb mesoderm and ectoderm	3.3.4.2	3.17
Continued skeletal patterning	E11.5+	Various tissues	3.3.4.3	5.2
Mesenchymal condensation	E11.5-12.5	Limb mesenchyme	3.3.4.3	5.2
Chondrogenesis	E12+	Limb mesenchyme and cartilage	3.3.4.3	5.2
Osteogenesis	E13.5/14+	Early cartilage and bone	3.3.4.3	5.2

* hindlimb development is delayed by approximately 0.5 days when compared to forelimbs.
Abbreviations: A-P, anterior-posterior; AER, apical ectodermal ridge; D-V, dorsal-ventral; FL, forelimb; HL, hindlimb; IM, intermediate mesoderm; LPM, lateral plate mesoderm; P-D, proximal-distal; PM, paraxial mesoderm.

Table 3.1. Major stages in the molecular control of limb development in the mouse.

Chapter 4: Experimental Methods

4.1 Mouse breeding

4.1.1 Overview

Throughout the course of this dissertation research, multiple strains of mice were utilized harboring null mutations for genes critically involved in limb and girdle development. Mice lacking such non-functional alleles are hereafter referred to as knockout or gene-deficient mice. Initially, mice possessing a single null allele for *Pbx1* (Selleri et al., 2001) or *Pbx2* (Selleri et al., 2004) (i.e., heterozygote $Pbx1^{+/-}$ or $Pbx2^{+/-}$) were intercrossed in order to generate most of the compound mutant knockout lines utilized in this study (see Section 4.1.2). These particular mice were used to examine limb and girdle development and the results of their study are presented in Chapters 5-7. Several additional mouse lines were utilized as well. For studies in Chapter 5, $Shh^{+/-}$ mice were acquired from Dr. Phil Beachy (Chiang et al., 1996; 2001) and were used to identify genetic regulatory interactions between *Shh*, *Pbx1* and *Pbx2*. Similarly, *Hand2* knockout embryos (Charite et al., 2000) were kindly provided by Dr. Deepak Strivastava to explore genetic interactions between *Hand2*, *Pbx1* and *Pbx2* (see Section 4.1.3). For studies in Chapter 6, $Tbx4^{cre}$, $Msx2^{cre}$, and *R26R* mouse lines were employed along with a line harboring a conditionally inactivated allele for *Pbx1* (i.e., $Pbx1^{cl/cl}$) to examine the tissue-specific deletion of *Pbx* during limb development (see Section 4.1.4). For studies in Chapter 7, additional compound *Pbx* mice were generated, such as *Pbx1;Pbx3*, *Pbx2;Pbx3,* and *Pbx1;Pbx2;Pbx3* mutants. The generation of these latter lines will not be

discussed in detail as most embryos were donated to studies in this thesis by Dr. Elisabetta Ferretti and Dr. Licia Selleri (see Section 4.1.5). All mouse colonies were housed in climate-controlled rooms at the Cornell University Medical Center Animal Facility, and all mouse work was performed following IACUC approved protocols.

4.1.2 Maintenance and generation of *Pbx1;Pbx2* mutant mouse lines

4.1.2.1 Breeding strategies and maintenance of *Pbx1* and *Pbx2* knockout lines

Initially, several mouse lines harboring null mutations for *Pbx* family member genes were utilized to generate compound mutant *Pbx1;Pbx2* mice and embryos. Initially, heterozygous *Pbx1*$^{+/-}$ and *Pbx2*$^{+/-}$ mice were originally generated by Dr. Licia Selleri at Stanford University, but had to be re-derived upon their entry into the Cornell University Medical Center Animal Facility. Accordingly, for re-derivation, sperm from adult *Pbx1*$^{+/-}$ and *Pbx2*$^{+/-}$ males were used to impregnate ova from super-ovulated wildtype females via *in vitro* fertilization. This procedure produced a percentage of *Pbx1*$^{+/-}$ or *Pbx2*$^{+/-}$ offspring. *Pbx1*$^{+/-}$ mice comprised two different lines, *Pbx1 (38)* and *Pbx1 (176),* each named according to the male sperm donor. *Pbx2*$^{+/-}$ mice also were re-derived from two sperm cell lines, *Pbx2 (68)* and *Pbx2 (GS45)*. All lines were initially re-derived onto a common genetic background strain called C57BL/6 and then were subsequently backcrossed on C57BL/6 for at least eight generations.

These new *Pbx* mouse lines were next tested to determine if, in their homozygous state, they exactly recapitulated the previously reported phenotypes for the complete loss of *Pbx1* (i.e. *Pbx1*$^{-/-}$) or *Pbx2* (i.e. *Pbx2*$^{-/-}$) from mouse tissues (Selleri et al., 2001; Selleri et al., 2004). Indeed, no observable variation was identified between the previously published and newly derived strains (as published in Brendolan et al., 2005). Therefore, all re-derived lines were used to generate compound mutant mice, so long as intercrossing of different *Pbx1* (or *Pbx2*) lines (e.g., *Pbx1* [38] vs. *Pbx1* [176]) was not carried out. This strategy was employed: (1) to maintain the purity of the individual lines; (2) to prevent the possibility of abnormal phenotypic variation from arising as a result of the genetic interaction of slightly different allelic variations in each strain and; (3) to be reassured that if a subtle phenotype occurred, after multiple backcrosses on C57BL/6, that it was the product of such purification and not of the genetic interaction between two different accumulative variants.

The generation and expansion of *Pbx1*$^{+/-}$ mice was performed by breeding adult *Pbx1*$^{+/-}$ male and C57BL/6 wildtype female mice (unless otherwise noted, all breeding male and female mice were, at minimum, 8 weeks old). This mating strategy provided the best means to acquire *Pbx1*$^{+/-}$ offspring, although, it yielded lower numbers than expected by Mendelian ratios. These findings, as reported in Brendolan et al. (2005), suggest that *Pbx1*$^{+/-}$ confers some form of deleterious characteristic to its carriers, the nature of which remains unknown. Observations on newborn *Pbx1*$^{+/-}$ pups indicated that they were approximately 10% smaller in body size for the first month suggestive of a systemic defect in development.

However, after weaning at 21 days post-parturition these pups achieved relatively normal body sizes as compared to wildtype littermates.

The generation of *Pbx2*$^{+/-}$ and *Pbx2*$^{-/-}$ offspring was more simple given the fact that even on a very permissive C57BL/6 background, both mutant genotypes were born according to the numbers expected by Mendelian ratios and survived to old age with no known abnormal phenotype (Selleri et al., 2004). Accordingly, all *Pbx2* mice were maintained in the completely null form (*Pbx2*$^{-/-}$) and matings of such to each other or to *Pbx1* were performed to maintain the *Pbx2* colony and to produce compound mutant progeny, respectively.

4.1.2.2 Establishing double heterozygous *Pbx1*$^{+/-}$*; Pbx2*$^{+/-}$ mice

In order to generate compound *Pbx1;Pbx2* mutant embryos that possessed abnormal limb phenotypes (i.e. *Pbx1*$^{-/-}$*; Pbx2*$^{+/-}$ or *Pbx1*$^{-/-}$*; Pbx2*$^{-/-}$ embryos), adult *Pbx1*$^{+/-}$*; Pbx2*$^{+/-}$ mice had to be first generated and eventually intercrossed. Several approaches were used to generate these *Pbx1*$^{+/-}$*; Pbx2*$^{+/-}$ mice, each of which had their advantages and disadvantages. These breeding schemes, as outlined below, were based on the limited knowledge of the *in utero* interaction of different *Pbx* genotypes (Note: unless otherwise noted, all *Pbx1* or *Pbx2* heterozygotes and homozygotes are of the genetic background C57BL/6). These crosses were as follows:

(1) Intercrossing *Pbx1*$^{+/-}$ males with *Pbx2*$^{+/-}$ females;

(2) Intercrossing *Pbx1*$^{+/-}$ males with *Pbx2*$^{-/-}$ females;

(3) Intercrossing *Pbx1*$^{+/-}$ females with *Pbx2*$^{+/-}$ males;

(4) Intercrossing *Pbx1*$^{+/-}$ females with *Pbx2*$^{-/-}$ males;

(5) Intercrossing *Pbx1*$^{+/-}$; *Pbx2*$^{+/-}$ males with C57BL/6 wildtype females;

(6) Intercrossing *Pbx1*$^{+/-}$; *Pbx2*$^{+/-}$ males with Blackswiss wildtype females; and

(7) Intercrossing Blackswiss *Pbx1*$^{+/-}$; *Pbx2*$^{+/-}$ males with C57BL/6 wildtype females.

The initial breeding strategies as outlined in (#1) and (#2) were extremely inefficient as the numbers of *Pbx1*$^{+/-}$; *Pbx2*$^{+/-}$ born from these matings were extremely lower than the numbers expected. In addition, the body sizes of those *Pbx1*$^{+/-}$; *Pbx2*$^{+/-}$ mice that were born and survived life's first three weeks, were noticeably (and approximately) 30-50% smaller than wildtype littermates. These preliminary findings suggested that some form of *in utero* and/or neonatal genetic interaction occurs between *Pbx1* and *Pbx2* affecting the survivorship of *Pbx1*$^{+/-}$; *Pbx2*$^{+/-}$ mice. Indeed, Sarno et al. (2005) demonstrate that *Pbx, Meis,* and *Hox* genes are expressed in the adult human and mouse female endometrium, suggesting that there exists a biological basis for the observed incompatibility between *Pbx1* and *Pbx2*.

Intercross strategies (#3) and (#4) were not employed given that *Pbx1*$^{+/-}$ females were always used in the generation of the compound mutant embryos that display severe limb abnormalities. When utilized however, a similar low yield of *Pbx1*$^{+/-}$; *Pbx2*$^{+/-}$ mice and reduced littersizes were observed, further suggesting that a genetic interaction occurred between *Pbx1* and *Pbx2 in utero*.

The observed difficulty in generating *Pbx1*$^{+/-}$*; Pbx2*$^{+/-}$ mice, led to a drastic change in breeding strategy. At first, breeding scheme (#5) appeared theoretically promising, although an important observation made it clear that mating C57BL/6 wildtype females with *Pbx1*$^{+/-}$*; Pbx2*$^{+/-}$ males would be problematic. Dr. Andrea Brendolan (personal communication) observed that the discrepancy between the numbers of expected and observed *Pbx1*$^{+/-}$ mice born from crosses of single *Pbx1*$^{+/-}$ males to C57BL/6 wildtype females grew as *Pbx1* mice were further backcrossed onto the C57BL/6 background. Having already observed considerably low numbers of *Pbx1*$^{+/-}$*; Pbx2*$^{+/-}$ mice following mating scheme (#5) and taking into account this information, lead to the realization that utilizing wildtype C57BL/6 females to generate *Pbx1*$^{+/-}$*; Pbx2*$^{+/-}$ mice (according to scheme #5), could lead to major difficulties in the future in acquiring sizable numbers of *Pbx1*$^{+/-}$*; Pbx2*$^{+/-}$ offspring required in this study. Therefore, upon discussion with Drs. Licia Selleri and Bridget Hogan (of Duke University) the suggestion to cross *Pbx1*$^{+/-}$*; Pbx2*$^{+/-}$ mice to an outbred line, Blackswiss (who typically are less permissive and give birth to larger littersizes), was investigated.

This novel strategy (outlined in schemes #6 and #7) certainly resulted in larger littersizes and also in higher survivorship of both *Pbx1*$^{+/-}$ and *Pbx1*$^{+/-}$*; Pbx2*$^{+/-}$ mice. However, a concern that arose upon this observed increase in fertility was whether it was accompanied by a corresponding amelioration in mutant embryo phenotype (i.e. in *Pbx1*$^{-/-}$*; Pbx2*$^{+/-}$ and *Pbx1*$^{-/-}$*; Pbx2*$^{-/-}$). To assess this possibility, *Pbx1*$^{-/-}$*; Pbx2*$^{+/-}$ mutant embryos were acquired from both pure C57BL/6 crosses and these Blackswiss/ C57BL/6 intercrosses, and two assays

were performed, one examining skeletal morphology (at E13.5) and the other focusing on gene expression patterns (E10.5).

To acquire mutant embryos for these assays, timed matings (see below) were established between *Pbx1*$^{+/-}$*; Pbx2*$^{+/-}$ (C57BL/6) males and either *Pbx1*$^{+/-}$*; Pbx2*$^{+/-}$ (C57BL/6) females or *Pbx1*$^{+/-}$*; Pbx2*$^{+/-}$ (50:50, Blackswiss:C57BL/6) females. In addition, to further increase the percentage of Blackswiss contribution in embryos, *Pbx1*$^{+/-}$*; Pbx2*$^{+/-}$ (50:50, Blackswiss:C57BL/6) males were mated to *Pbx1*$^{+/-}$*; Pbx2*$^{+/-}$ (50:50, Blackswiss:C57BL/6) females. All mutant offspring possessed varying contribution of Blackswiss background. Embryos were then harvested according to standard protocols (see below) at E10.5 and E13.5, time points critical for the aforementioned assays.

Analysis of embryos with a maximum of 50% Blackswiss background contribution indicated that the phenotype of the forelimb skeleton remained the same (N=6, 50:50 blackswiss/C57BL/6; N=4 C57BL/6)(data not shown) and was therefore not ameliorated (see Chapter 5 for a discussion of these findings). However, while the forelimb morphology appeared relatively unchanged between background contributions, hindlimb morphology, particularly within autopodial/zeugopodial regions, appeared ameliorated in these same percentage Blackswiss *Pbx1*$^{-/-}$*; Pbx2*$^{+/-}$ mutant embryos (Fig. 5.3). Specifically, approximately 3 of 6 embryos displayed an improvement in digit number, as the anlagen of an additional cartilaginous ray was present (i.e., at least two hindlimb autopod digits were present instead of one digit observed in mutants on a pure C57BL/6 background). Furthermore, as the proportion of Blackswiss increased (i.e., by

mating *Pbx1*$^{+/-}$; *Pbx2*$^{+/-}$ (50:50, Blackswiss: C57BL/6) males to *Pbx1*$^{+/-}$; *Pbx2*$^{+/-}$ (50:50, Blackswiss:C57BL/6) females, an additional digit often appeared, making three digital anlagen present. While it is uncertain how such a phenotype corresponded directly to the contribution of Blackswiss background, it follows well with changes in expression data as outlined below.

A similar analysis was carried out using *in situ* hybridization (described below) on E10.5 *Pbx1*$^{-/-}$; *Pbx2*$^{+/-}$ embryos with different percentage background contributions. As will be demonstrated in Chapter 5, one critical factor that figures prominently in mediating the hindlimb skeletal dysmorphology of *Pbx1*$^{-/-}$; *Pbx2*$^{+/-}$ embryos (at E13.5), is the absence of *Shh* mRNA expression during periods of early limb development (at E9.75-E12.5). On a pure C57BL/6 background, *Shh* expression was never observed along the posterior polarizing region of *Pbx1*$^{-/-}$; *Pbx2*$^{+/-}$ embryos at all gestational days studied (N=15, at all days E9.75-12.0)(Fig. 5.9). Analyses of *Pbx1*$^{-/-}$; *Pbx2*$^{+/-}$ embryos acquired from matings of *Pbx1*$^{+/-}$; *Pbx2*$^{+/-}$ (C57BL/6) males with *Pbx1*$^{+/-}$; *Pbx2*$^{+/-}$ (50:50, C57BL/6: Blackswiss) females, revealed that *Shh* expression was present, albeit extremely reduced, at E10.0 (N=5, 2 of 5 embryos with reduced expression, at all days; data not shown).

The findings by *in situ* hybridization and skeletal preparation on *Pbx1*$^{-/-}$; *Pbx2*$^{+/-}$ mutant embryos possessing increased percentages of Blackswiss genetic background are not mutually exclusive but may indeed be interrelated (see Chapter 5). Accordingly, the presence of extra hindlimb digits in the *Pbx1*$^{-/-}$; *Pbx2*$^{+/-}$ (50% Blackswiss) mutant embryo, specifically when compared to that

found on a C57BL/6 background, is in agreement with the similar findings of increased *Shh* expression observed in *Pbx1*$^{-/-}$*; Pbx2*$^{+/-}$ (50% Blackswiss) mutants. Therefore, the improvement in *Shh* signaling (at E10.5) that occurs on Blackswiss may be underlying the amelioration in digit number seen in these same Blackswiss embryos at later days (at E13.5). Overall, these data suggest that utilizing Blackswiss outbred strain to improve mating yield could occur so long as the percentages of such background is minimized and held constant.

The above analyses lead to the use of mating strategies that both maximized the yield of *Pbx1*$^{+/-}$*; Pbx2*$^{+/-}$ offspring (for mating adults) and minimized the effects that the Blackswiss background had on the *Pbx1*$^{-/-}$*; Pbx2*$^{+/-}$ mutant phenotype. Therefore, mating strategies (#6 and #7) were utilized, with the caveat that *Pbx1*$^{+/-}$ or *Pbx1*$^{+/-}$*; Pbx2*$^{+/-}$ (50:50, Blackswiss:C57BL/6) females were mated to pure C57BL/6 *Pbx1*$^{+/-}$*; Pbx2*$^{+/-}$ males (#6) for the generation of *Pbx1*$^{-/-}$*; Pbx2*$^{+/-}$ mutant embryos (or the reciprocal strategy, #7).

4.1.2.3 Generation of compound *Pbx1; Pbx2* mutant (*Pbx1*$^{-/-}$*; Pbx2*$^{+/-}$ and *Pbx1*$^{-/-}$*; Pbx2*$^{-/-}$) embryos

In order to acquire mutant embryos at different, yet specific, days of gestation, timed intercross matings between adult *Pbx1*$^{+/-}$*; Pbx2*$^{+/-}$ males and *Pbx1*$^{+/-}$*; Pbx2*$^{+/-}$ females were established. Accordingly, in the evening, male and female *Pbx1*$^{+/-}$*; Pbx2*$^{+/-}$ mating pairs were isolated, and expected to copulate overnight. After successful copulations, mucous plugs formed within the vaginal canal and, appropriately, the next morning females were designated as “plugged”

at gestational day E0.5 (for standardization, it is assumed that 12 hours or 0.5 days passed since copulation and initiation of plug development).

Next, females were then sacrificed on the gestational day needed (i.e. E8.5-E13.5 for these studies). First, pregnant females were anesthetized and then cervically dislocated, a technique that rapidly excised the cervical spinal cord from the base of the brain. Females were then placed in anatomical orientation and sagittal or parasagittal incisions were made from the perineum to the superior thoracic region. The entire uterine pouch with its respective contents (i.e., embryos and maternal tissue) were then excised from the female and placed in Phosphate Buffered Saline (PBS) on ice. Embryos and their surrounding uterine tissues were finally dissected in PBS.

After the uterine and placental tissues were removed, two tissues still surrounded the embryo, an external yolk sac derived from both maternal and fetal cells, and an internal tissue, the allantois, derived solely from the fetal cell progenitors. For all embryos, the yolk sac was removed and the fetal and maternal components were separated. The fetal portion was then utilized for genotyping (as discussed below). However, for earlier embryos, genotyping via yolk sac DNA proved very difficult, and so embryos at E8.5-E9.0, were first cleared of all tissues including the allantois and directly utilized in planned experiments. After experimentation and imaging, these embryos were then processed for genotyping using embryonic DNA. For all gestational days allantois tissue was discarded as the failure to remove it could prevent mRNA probe penetration during *in situ* hybridization and/or mask embryonic gene

expression with its own patterns. Finally, for all gestational days, once the embryo was dissected it was then treated accordingly for the protocols and methods described in the next section.

Of note, all embryos utilized in the protocols described below were somite-matched using standard somite-counting procedures (Capellini et al., 2006). These techniques allowed for the precise control of developmental age, independent of limb size, and thus more accurately allowed for the comparison of morphology and gene expression patterns across genotypes. Accordingly, often embryos were pooled across litters to match for somite number, although at times, littermate embryos were also added to demonstrate any apparent developmental delay or similar perturbation.

4.1.3 Maintenance and breeding of *Shh* mouse lines and curation of *Hand2* embryos

Studies in Chapter 5 employed the use of additional mouse lines in order to examine genetic interactions and hierarchical relationships between Pbx and known regulators of limb bud outgrowth. (1) Mice harboring one null allele for *Shh* were acquired from Dr. Phil Beachy (Chiang et al., 1996; 2001) and back-crossed to C57BL/6 to generate adequate numbers and appropriate background states for the study. Next, timed matings were established, as described above, between male and female $Shh^{+/-}$ mice to acquire homozygous mutants that display severe limb defects. These embryos were then used to identify genetic regulatory interactions between *Shh*, *Pbx1* and *Pbx2*, i.e., *Pbx* gene expression was assessed in these mutants to see if it was absent, down-regulated, up-

regulated, or remained normal. (2) *Hand2* knockout embryos (Charite et al., 2000) were kindly provided by Dr. Deepak Strivastava to explore genetic interactions between *Hand2*, *Pbx1*, and *Pbx2*.

4.1.4 Generation and breeding of cre lines, cre reporter lines, and *Pbx1;Pbx2* conditional mutant mouse lines

4.1.4.1 Overview

In Chapter 6, a different strategy was employed to explore the consequences of *Pbx* gene loss on the development of the limb and girdle. Accordingly, the use of a conditional or "floxed" *Pbx1* allele was engineered so as to allow its specific deletion from tissues that harbor the enzyme, called Cre recombinase. In this manner, *Pbx1* could be removed from critical and specific tissue domains and at exact times to determine how its loss impinges on patterning and morphogenesis of the limb. The construction of this *Pbx1* conditional allele is described in (Ferretti, Selleri, in preparation).

To inactivate the "floxed" or conditional allele (*Pbx1* exon 3) in a "conditional" manner in mice, this line could be crossed to mice that express any selected recombinase (i.e., $Tbx4^{cre}$, $Msx2^{cre}$, $Beta\ Actin^{cre}$). This first test cross of this Cre-Lox system was established in order to determine whether germline deletion of this conditional *Pbx1* allele (in a homozygous state) recapitulated that seen in the global deletion of *Pbx1*. To accomplish this task, it was first considered that utilizing mice harboring the ubiquitously-specifically expressed *Cre* transgene under the Beta Actin promoter ($BetaActin^{cre/+}$) and heterozygous

for the global null allele (i.e., *Pbx1*$^{+/-}$) would be appropriate. It was thought that breeding this line to *Pbx1*$^{cl/cl}$ mice, would yield 25% *Pbx1*$^{cl/-}$; *BetaActin*$^{cre/+}$ offspring. However, since single global *Pbx1* heterozygous mice have an abnormal phenotype i.e., they are smaller in body-size, there was a concern that the additional loss of Pbx1 protein via this approach would result in lethality; and so this basic breeding scheme was not possible. Instead, *BetaActin*$^{cre/+}$ mice were mated directly to mice homozygous for the *Pbx1* "floxed" allele (*Pbx1*$^{cl/cl}$) and of the generated progeny, 25% were *Pbx1*$^{cl/+}$*;BetaActin*$^{cre/+}$. Next, by interbreeding this offspring, 12.5% of the progeny were *Pbx1*$^{cl/cl}$;*BetaActin*$^{cre/+}$. Thus, under the assumption that the *Pbx1* "floxed" locus and the *Cre* transgene were not linked, mice that harbored this *Cre* transgene and were homozygous for the *Pbx1* "floxed" allele were able to be produced after two generations (12.5%). In Beta Actin Cre-expressing cells (i.e., all cells of the embryo, since this Cre is present everywhere) where *Pbx1* was also expressed, these mice possessed a homozygous deletion of *Pbx1* (i.e., hereafter referred to as *Pbx1*$^{cl\Delta 3/cl\Delta 3}$; *BetaActin*$^{cre/+}$) and therefore functional Pbx1 protein was absent in the germline and throughout development. Importantly, the phenotype of these specific mice recapitulated that observed in single global *Pbx1* null mice (Fig. 4.1).

During the studies reported in Chapter 6, this strategy of conditional deletion was carried out using other *Cre* transgenic lines, where *Cre* was expressed in specific tissues, such as the limb mesenchyme versus the ectoderm.

4.1.4.2 Assessment of cre activity in transgenic mouse embryos

To assess the spatial activity of recombinase in tissues that express Cre under the promoter of selected genes (e.g., *BetaActin*^{cre}, *Tbx4*^{cre}, *Msx2*^{cre}), each specific line was crossed to the Cre reporter line R26R (Soriano, 1999). This Cre reporter system has a particular allelic organization whereby loxP sites flank a DNA segment that prevents expression of a lacZ gene. Therefore, when mice that are heterozygous or homozygous for this flanked allele, are crossed with mice that harbor a Cre under the promoter of a tissue-specific gene, the loxP sites and the intervening stop region are excised and LacZ is expressed in cells/tissues in all embryos harboring this recombination. When stained for LacZ detection, the result is a readout of Cre activity in specific tissues. However, while this strategy is critical for identifying cells that have undergone this recombination, since LacZ activity is constitutive and continues to be expressed after the event, staining for LacZ will also reveal all cells that have a one time point expressed Cre; and therefore, even those that may have already repressed and/or silenced the gene controlling Cre expression. As a result of this problem, it is important to assess the spatio-temporal extent of Cre activity (via LacZ staining, see below) to that of the expression of the gene which controls its activity (via *in situ* hybridization, see below).

4.1.5 Breeding of additional *Pbx* compound mutant lines

Studies performed in Chapter 7 employed the use of additional compound *Pbx* mutant lines to examine genetic interactions among *Pbx* family members

during pectoral and pelvic girdle development. In this regard, generation of both double compound *Pbx1;Pbx3* and *Pbx2;Pbx3* mutant as well as triple compound *Pbx1;Pbx2;Pbx3* mutant embryos ensued and was conducted by Dr. Elisabetta Ferretti for her studies on craniofacial morphogenesis in *Pbx* mutant embryos. Importantly, as her focus was largely on the craniofacial skeleton, all limbs and girdle structures could be donated to the studies performed for this thesis. Briefly, to acquire these compound mutants, intercrosses of *Pbx1* to *Pbx3*, *Pbx2* to *Pbx3*, as well as *Pbx1*;*Pbx2* to *Pbx3* mice were performed similar to that described above (Section 4.1.2). Because of the perinatal and *in utero* lethality of several of these *Pbx* compound mutants, special breeding modifications had to be made in order to acquire double and triple heterozygous adults for *Pbx1;Pbx3*, *Pbx2;Pbx3*, and *Pbx1;Pbx2;Pbx3*. For example, to acquire $Pbx1^{+/-}; Pbx3^{+/-}$ adults and to circumvent their perinatal lethality on a pure C57BL/6 background, the double heterozygous genotype had to be placed on a mixed C57BL/6/Blackswiss background. After, intercrossing $Pbx1^{+/-}; Pbx3^{+/-}$ males with genotypically equivalent females could be performed to acquire an array of progeny of differing genotypes and phenotypes which could be used in the studies outlined in Chapter 7. Similar mating schemes were employed for double *Pbx2;Pbx3* mutants. The generation of $Pbx1^{+/-};Pbx2^{+/-}; Pbx3^{+/-}$ embryos was also carried out following the same mating schemes adopted above, however, since, these triple heterozygote embryos died *in utero*, analyses of more complex genotypes could not be carried out. Therefore, only these triple heterozygous mutants were examined for limb and girdle defects.

4.2 Experimental protocols

Numerous experimental protocols were employed to ascertain how *Pbx* govern limb and girdle patterning and morphogenesis. These protocols are outlined below. With respect to sample sizes, for all procedures involving the use of mutant mouse embryos (e.g., *in situ* hybridization, skeletal preparation, etc.), at least three embryos per genotype per gestational day were utilized. All possible controls were utilized in these experiments to ascertain the specific molecular and morphological phenotypes in specific *Pbx* compound mutant genotypes.

4.2.1 DNA extraction and genotyping

All single and compound mutant mice, both adult and embryonic, were genotyped using the following procedures for DNA extraction and Polymerase Chain Reaction (PCR). DNA was extracted from two different tissues: tail samples from adult mice and yolk sacs from embryos. In addition, DNA extraction was performed directly on E8.5-E9.5 embryos if their yolk sacs provided little clean DNA for genotyping by conventional methods. Tail samples were acquired by the following protocol: Twenty-one day-old mice were anesthetized using an Isofluorine Unit, fitted with a numbered ear-tag, and 0.5 cm of their distal tail was excised using sterile razor blades and placed in eppendorf tubes. Yolk sac samples were recovered from the fetal portion of the yolk sac and also placed in eppendorf tubes.

Both tail and yolk sac samples were placed in Lysis solution consisting of 0.5% SDS, 0.1 M NaCl, 50 mM Tris (pH 8), 2.5 mM EDTA, and 100 µg/ml Proteinase K at 55°C overnight. The next day 8 M Potassium Acetate and 0.5 ml of Chloroform were added to each tube and placed in –20°C freezer for at minimum 15 min for precipitation. Following a 5 min microfugal spin at 9,000 RPM, the aqueous supernatant phase was recovered and transferred to a clean tube. Pure microbiology grade 100% Ethanol (ETOH) was next added and tubes were spun for approximately 10 min at 14,000 RPM. Once finished, the ETOH was removed leaving a DNA pellet, then replaced with 70% ETOH and spun once more for 10 min at 14,000 RPM. Next, the samples were decanted and air-dried for about 15-30 min to remove traces of residual ETOH. Finally, tail sample DNA was resuspended at 37°C in 100 µl of ddH_20 and yolk sac DNA resuspended in 25 µl of ddH_20.

Genotyping was performed on these samples using standard PCR protocols as described in Selleri et al. (2001; 2004). Embryos and mice from complex crosses were genotyped typically for the global *Pbx* allele (i.e., *Pbx1, Pbx2,* and/or *Pbx3*), the conditional *Pbx1* allele (i.e., $Pbx1^{cl}$), and/or for the specific Cre line utilized (i.e., $Tbx4^{cre}$ or $Msx2^{cre}$). *Shh* genotyping was performed as described in Chiang et al. (1996; 2001) and *Hand2* embryos were genotyped by laboratory members of Deepak Strivastava laboratory. *Pbx* global primers were specifically designed to amplify both wildtype and mutant sequences for *Pbx1*, *Pbx2*, and *Pbx3*, and are described in Selleri et al. (2001), Selleri et al. (2004), and Rhee et al. (2004). Primers used to amplify *Shh* mutant sequences

were acquired from Chiang et al. (1996, 2001). Primers used to amplify *Tbx4*^{cre}, *Msx2*^{cre}, and *R26R* were acquired Adler et al. (in press), Lewandoski et al. (2000), and www.jax.org, respectively.

Specific primer oligonucleotides used to amplify *Pbx1* conditional sequences were:

Pbx (For2) 5' ATC AGT GCC ATT TCT CCA GCC 3'

Pbx (Rev2) 5' TGG GTA TCC ATT CCA AAG GTG G 3'

Pbx (Neo2) 5' TTC CTC GTG CTT TAC GGT ATC G 3'

And PCR amplification and gel electrophoresis, band sizes of 200 bp for wildtype (wt) fragments and 240 bp for *Pbx1* fragment were obtained.

4.2.2 Gross morphology

Studies presented in Chapters 5-7 employed several methods to examine the soft tissue of embryos of different genotypes. In the majority of cases, specifically in Chapters 5 and 7, embryos were examined at gestational days E9.5 to E13.5 for defects in gross morphology. Studies in Chapter 6 additionally focused on E14.5 embryos and newborn (P=0 or P0) mice. Accordingly, embryos were typically left in PBS for inspection and imaged using a dissection scope and digital imaging camera. Often, embryos were first placed in 95% ETOH and then photographed, particularly if there was a concern that tissue fixation was required to preserve them for future experimentation. In all of these analyses, approximately 2-3 embryos were examined per mutant and wildtype genotype.

4.2.3 Skeletal preparation (bone and cartilage staining)

Studies performed in Chapters 5-7 relied on the examination of skeletal morphology to assess *Pbx* gene function during development. In order to examine hard tissue morphology, approximately three embryos each at E12.5, E13.5, and E14.5 and newborn pups at P0 were treated using a protocol adapted from McLeod (1980) on Alcian Blue and Alizarin Red staining. Initially, harvested embryos and newborn mice were immediately placed in 95% ETOH/ddH_2O for 2 hours at room temperature (RT). Newborn pups were skinned, eviscerated and the majority of remaining soft tissue (i.e., muscles, organs, fat, etc.) was removed. This approach was necessarily to ensure that staining reagents penetrated the tissue and dyed the skeletal elements properly. E13.5 and E14.5 embryos were carefully eviscerated to remove the liver and lower gastrointestinal organs, but without damaging the ribs or vertebral processes. These embryos also had most skin and some adipose tissue removed in and around their torso and behind their pectoral girdles. The limb dermis was slightly perforated to allow penetration of staining materials. E12.5 embryos were spared from all of these processes due to their delicate nature. After, all specimens, regardless of gestational day, were placed in fresh 95% ETOH/ddH_2O for at least 5 days to dehydrate tissues and then soaked in 100% Acetone for 2 days in order to remove lipids present in all tissues. Specimens were then subjected to a staining solution at RT, in the dark, for 3 days. The staining solution consisted of the following chemicals: 0.3% Alcian Blue/70% ETOH; 0.1% Alizarin Red S/95%

ETOH; Glacial Acetic Acid in 70% ETOH. Alcian Blue is a copper phthalocyanin basic dye that is water-soluble and is colored blue due to its copper content. This dye is known to form salt linkages with the acid groups of acidic mucopolysaccharides, and thus stains the glycoproteins present in the extracellular matrix of cartilage. Alizarin Red is typically derived from the plant species *Rubia tinctorum* and is believed to bind to the Ca^{+} ions present in the extracellular matrix of ossifying bone. In this manner, both Alcian Blue and Alizarin Red serve well to stain many of the main skeletal tissues present in the early embryo/mouse undergoing chondrogenesis and ossification. After staining, specimens were washed in distilled water to remove residual tissue and remaining staining solution and then placed in 1% Potassium Hydroxide (KOH) for approximately 8-12 hours. KOH cleared the embryonic/newborn soft tissues of their staining and "macerated" the remaining tissues. In order to prevent excessive damage to these specimens (as they became extremely delicate during this process), they were then placed in graded series of Glycerol and KOH, with the following concentrations, 20%→ 50%→ 80% Glycerol/1% KOH for 2-7 days. Glycerol not only inactivated the KOH but also both strengthened the skeletal tissues through hardening and further cleared specimens of non-specific staining residues. Finally, specimens were stored in 100% Glycerol until they were dissected further and then imaged using a digital camera and dissecting microscope setup. Specimens were then stored long term at 4°C in 100% Glycerol.

4.2.4 Whole mount *in situ* hybridization

Studies performed in Chapters 5-7 utilized whole mount and slide *in situ* hybridization to determine whether the expression of genes functionally critical during limb and girdle development was altered in embryos lacking Pbx function. Below a description of the specific whole mount protocol follows. For section *in situ* hybridization, see Brendolan et al. (2005).

For each mRNA probe approximately 3 embryos per mutant genotype per gestational time point were analyzed by whole mount *in situ* hybridization. Embryos utilized for this procedure were fixed overnight in 4% PFA/PBS (pH 7.4) at 4°C. The next day, embryos were rinsed in PBS with 0.1% Tween (hereafter, PBT) 2 times for 10 min each at 4°C and then placed through an increasing Methanol/PBT series 25% → 50% → 75% → 100% for dehydration. The timing of each wash varied and was based on embryonic day and genotype (i.e., 5-7 min for E9.5, 10 min for E10.5, 15 min for E11.5 and 20-25 min for E12.5; double mutant embryos at gestational day E9.5 or E10.5 were typically treated as E9.5 wildtype for all washes and treatments in this *in situ* hybridization protocol). The added advantage of dehydrating by Methanol, rather than ETOH, was that the former has a permeabilizing affect on cell membranes, which aided in the penetration of the mRNA probe utilized during *in situ* hybridization. After dehydration, embryos were stored in pure Methanol in 2 ml screw-capped microtubes at –20°C.

When embryos were required for *in situ* hybridization, they were removed from storage and rehydrated using a reverse Methanol/PBT series (75% → 50%

→ 25% Methanol/PBT for 10 min each at RT and then 2 times for 10 min at RT in PBT. Next, embryos were bleached using 6% Hydrogen Peroxide (H_2O_2)/PBT for at least 1 hour at RT with gentle rocking. This treatment not only removed endogenous peroxidase that interferes with antibody activity but also clarified embryos to aid in the observation of gene expression. Residual H_2O_2 was then removed by washing 3 times in PBT at RT (timing varied based on gestational day, see above). Embryos were then treated with Proteinase K/PBT (10 µg/ml) to disaggregate protein interactions surrounding transcribed mRNA. These treatments were also done at RT and embryos were not rocked during this process. Proteinase K/PBT treatment was then neutralized using Glycine/PBT (5 mg/ml), 2 times for 5 min each (not variable) and then the residual Glycine was removed using 3 PBT washes at RT for 7 min each. Re-fixation of the embryos, with their protein-protein interactions "relaxed" was carried out using 4% PFA/ 0.2% Glutaraldehyde/PBT (pH 7.4) for 20 min at RT with shaking. Next, embryos were washed in PBT to remove fixative and to prepare them for prehybridization.

The prehybridization step utilized a mixture of several reagents that allowed for the proper opening of the mRNA template for hybridization to the mRNA probe. Accordingly, embryos were placed in a solution containing 50% Formamide, 5X SSC, 50 µg/ml Yeast tRNA, 1% SDS, 50 µg/ml Heparin, and 0.1% CHAPS for 2 hours at 70°C. After prehybridization, a hybridization mix consisting of prehybridization mix plus a mRNA sense or antisense Digoxigenin- or Fluorescein-labeled probe at a final concentration of 1 µg/ml, was used at 70°C overnight.

The next day, embryos were washed through a series of SSC solutions (5X SSC and 2X SSC, 3 times each for 30 min, and 0.2X SSC and 0.1X SSC, 1 time each for 30 min) at 70°C in order to remove nonhybridized mRNA probe. After three brief 5 min rinses in Tris Buffered Saline/0.1% Tween (TBST), embryos had the Digoxigenin (and/or Fluorescein) and non-specific protein binding sites blocked utilizing 10% Sheep Serum in TBST for 3 hours at RT. After which, embryos were then incubated overnight at 4°C in fresh blocking reagent/sheep serum and primary antibody mix with AP-conjugated anti-Digoxigenin or AP-conjugated anti-Fluorescein antibody (Roche) at 1:5000 dilution.

The next day, residual antibody and sera were removed from the embryos using 3, 5 min washes in TBST and then, at least 5, 1 hour washes in TBST at RT or 4°C (if left overnight). After washing, embryos were then incubated in NTMT solution (pH 9.5) in order to equilibrate the tissue to the pH where an active Alkaline Phosphatase reaction takes place. In order to detect the AP-conjugated antibody-labeled hybridized probe complex, via the Alkaline Phosphatase reaction at pH 9.5, a colorimetric substrate of NBT/BCIP or BCIP in NTMT buffer (Roche) was used. This detection took typically from 1 hour (for most mRNA probes utilized) to overnight for color to fully develop. Positive hybridization was visualized by purple (NBT/BCIP), turquoise (BCIP), or red (NBT) signal.

For two-color *in situ* hybridization, after the detection of the first probe (preferentially the fluoresceinated one) the embryos were once again fixed in 4%

PFA (pH 7.4) and the antibody was inactivated by washing twice for 20 min in 100 mM Glycine-HCl (pH 2.2). Then blocking, antibody incubation and color development steps were repeated as described above.

The NBT/BCIP staining was then stopped by washing embryos 2 times in PBT for 10 min and then storing in 4% PFA/PBT (pH 7.4) to preserve staining. Embryos were then imaged in PBT using dissection microscope and digital camera. Long-term storage of treated embryos consisted of re-fixation in PFA/PBT and storage at 4°C in opaque 2 ml screw-cap containers to prevent light based degradation of the signal.

4.2.5 *In vitro* transcription

The technique of *in situ* hybridization requires the use of a chemical- or radioactive-labeled mRNA probe for hybridization to the gene under study. Single stranded sense and antisense mRNA probes were generated by the process of *in vitro* transcription for all clones utilized throughout this study. Such clones are listed in Appendix A. Accordingly, T3, T7 or Sp6 RNA Polymerase (Roche), Digoxigenin- or Fluorescein-RNA Labeling Mixture (Roche), RNase Inhibitor (Roche), linearized DNA clone, and Diethylpyrocarbonate-treated (DEPC) ddH_20 (Sigma), were placed in a 1.5 ml eppendorf for two hours at 37°C. After which, the constructed Digoxigenin- or Fluorescein-Labeled mRNA probe was then precipitated, purified, resuspended in DEPC ddH_2O, and stored at –80°C to prevent RNA degradation.

4.2.6 Immunohistochemistry

Studies in Chapters 6-7 examined Pbx protein localization during limb development. Embryos were processed and embedded for *in situ* hybridization on section (see Brendolan et al., 2005) and were then cryo-sectioned into 10 µm-thick serial specimens. Next, sections containing the limb were post-fixed in ice-cold Acetone for 10 min and endogenous peroxidase was quenched by 0.5% H_2O_2. Antigen retrieval was performed by boiling slides for 15 min in a microwave oven in 0.01 M Citric Acid (pH 6). Sections were then incubated in 10% Sheep Serum in PBT at RT for 1 h to block non-specific binding sites, and finally incubated in primary antibody (Biogenesis) diluted 1:200 in PBS/0.1% TritonX-100 at 4°C overnight. The sections were then incubated with Biotin-SP-conjugated Goat anti-Rabbit IgG secondary antibody (Jackson Immuno Research) diluted 1:500 in PBS at RT for 30 min and finally the signal was detected with the ABC staining kit (Vector Laboratories) using 3,3 diaminobenzidine (Sigma) as a substrate.

4.2.7 Whole mount immunohistochemistry

Studies presented in Chapter 5 required that the specific protein CD44 be examined for its localization in both mutant and wildtype embryonic apical ectodermal ridge (AER) tissues. Accordingly, embryos were dissected at E10.5, fixed with 4% PFA/PBS (pH 7.4) overnight and processed for immunohistochemistry to detect the localization of CD44 in the AER. Embryos were permeabilized in 0.1% TritonX-100/PBS, blocked in 3% BSA/0.1% TritonX-

100/PBS and then incubated in anti-CD44 (antibody IM7 rat monoclonal from Pharmingen) overnight at 4°C. The embryos were then washed in 0.1% TritonX-100/PBS and incubated with an anti-rat Alexa 568 (Molecular Probes-Invitrogen) overnight. After rinsing, the embryos were visualized with an inverted fluorescence microscope.

4.2.8 Cell proliferation analysis via BrdU

Studies throughout this thesis required that the observed defects in limb development be coupled with mechanistic changes in cell behavior, such as in proliferation and in programmed death (i.e., apoptosis). With respect to analyses of proliferation, pregnant *Pbx1*$^{+/-}$;*Pbx2*$^{+/-}$ female mice, carrying possible mutant embryos at E9.5, E10.5, E11.5, and E12.5 were injected intraperitoneal with 5-Bromo-2-deoxy-Uridine (BrdU) (50 µg/g of body weight) and BrdU incorporation was assayed as previously described (Selleri et al., 2001). The number of BrdU-positive cells (dark brown nuclei) within the developing limb were counted across all sagittal and/or transverse sections (total of 10 mm thickness) for each genotype. Quantitative analysis of BrdU Immunoperoxidase-stained sections was done on a Nikon microscope equipped with a video camera and biostatistical software.

4.2.9 Caspase3 apoptosis assay

Caspase3 antibody staining was used to distinguish apoptotic cells from non-apoptotic cells in mutant versus wildtype embryos. Initially, paraffin

embedded embryos were sectioned to 10 µm using a Leica microtome and treated as described above for immunohistochemistry. After blocking, the Rabbit anti-Caspase3 (R&D Systems, Cat# AF-835) primary antibody (Biogenesis) was diluted 1:2000 in PBS/0.1% TritonX-100 at 4°C overnight. The sections were next incubated with biotinylated Goat anti-Rabbit IgG secondary antibody (Vector Laboratories, Cat# BA-1000) diluted 1:500 in PBS at RT for 30 min and finally the signal was detected using HRP-Streptavidin (Vector Laboratories, Cat# SA-5004) as described above.

4.2.10 β-Galactosidase histochemistry

In Chapter 6, specific Cre mice were crossed to *R26R* Cre reporter line for analyses of recombination events. To visual the activity of Cre in tissues where the recombination event took place, β-Gal or LacZ histochemistry was performed as follows: Harvested embryos were fixed in 4% PFA, 0.8% Glutaraldehyde, 0.02% NP40, and 1 mM $MgCl_2$ in PBS for 1 hour. After briefly washing in PBS, embryos were then stained overnight at 37°C in 400 µg/ml X-gal, 0.1 mM $MgCl_2$, 20mM Potassium Ferrocyanide, and 20 mM Potassium Ferricyanide in PBS. Stained embryos were photographed and stored in 4% PFA in PBS at 4°C.

4.2.11 Chromatin Immunoprecipitations (ChIP)

Studies in Chapter 5, examined whether Pbx, Hox, and other proteins indeed bind to regulatory elements of important limb genes. Formaldehyde cross-linking and ChIP from E10.5 mouse limb buds were performed according the

protocol of P. Farnham's Lab (http://genomics.ucdavis.edu/farnham/protocols/tissues.html), with the following modifications: to disaggregate tissues, the samples were forced through 18 G and 20 G needles using a syringe, the cells were then fixed for 15 min with 1% Formaldehyde at RT, and the reaction was quenched with 0.125 M Glycine/PBS for 5 min. The cross-linked material was sonicated for 15 times, for 25 sec each to obtain an average fragment length of 500-1000 bp. Immunoprecipitations were performed with 10 µl of Protein G-Agarose (KPL) and blocked twice with 1 µg/ml Salmon Sperm DNA (Sigma) and 1 µg/ml Bovine Serum Albumin, initially for 2 hours, then overnight. The chromatin was precleared by adding 20 µl of Protein G-Agarose for two hours, and incubated with 5 µg of the respective specific antisera, or with 5 µg of anti-Flag (F3165, Sigma) antibody as a control. Incubations were performed overnight at 4°C. The following primers were used for PCR amplifications (42 cycles):

*mShh*E1, 5'-CTTTGATTTGAAGTCCTGGC-3';

*mShh*E2, 5'-ACTGAGGGGAAAAGTCATC-3';

*mShh*C1, 5'-TCAAGAGAGATCAACAAAAG-3';

*mShh*C2, 5'-TTGGACTCAAGTCCAGAC-3'.

4.2.12 Electrophoretic mobility shift assay (EMSA)

Studies in Chapter 5 focused on whether specific Hox proteins can bind to regulatory elements of genes critical for limb bud outgrowth. EMSA was utilized to understand the nature of such binding. The GST-Hoxd13HD fusion protein was produced in *E.coli*, purified according to established methods and analyzed

by SDS PAGE and Coomassie staining. The protein was diluted in 13 ml of D-buffer (20% Glycerol, 20 mM KCl, 2 mM $MgCl_2$, 0.2 mM EDTA, 0.5 mM DTT) and pre-incubated with 100 ng Poly-(dI-dC) in a total volume of 20 ml 1X binding buffer (0.1 M KCl, 2 mM $MgCl_2$, 4 mM Spermidine, 0.1 mg/ml Bovine Serum Albumin) for 15 min on ice. 30000 cpm of the ^{32}P labeled probes were added to the samples and incubated for 30 min on ice. Reactions were separated on a 6% Polyacrylamide gel in 0.5% TBE, dried, and exposed to Kodak X-omat R film at -80°C.

4.2.13 Cell culture and transfection

Studies in Chapter 5 also examined whether Pbx and Hox can activate transcription in cell cultures possessing critical control regions for known limb developmental regulators. Accordingly, P19 mouse embryonic carcinoma cells were cultured in Minimum Essential Medium Alpha supplemented with 10% Fetal Calf Serum, 2 mM L-glutamine, 100 U/ml Penicillin, and 100 µg/ml Streptomycin. Transfections were carried out by CaPO4 precipitation. In a typical experiment, 5 µg of reporter plasmid, 2.5-5.0 µg of expression construct and 0.1 µg of CMV-Beta-gal (Clontech) as an internal control, were used per 6 cm dish. Forty-eight hours after transfection, the cells were washed, lysed, and assayed for Luciferase and Beta-Galactosidase expression as previously described (Brendolan et al., 2005).

4.2.14 Photo-documentation

All whole-mount and slide *in situ* hybridization, immunohistochemistry, skeletal preparation, and gross morphology experiments were visualized using a Retiga-2000XR digital camera and Leica Dissection scope setup with Q Capture software run on a Mac OS 10.4.1 computer platform. Typically, processed embryos were first submerged in PBS in a 60 mm petris dish with 1.2 % Agarose, pinned, and imaged with both transmitted and incidental light. Images were then saved typically in Q Capture as tiff files and optimized using Adobe Photoshop software. All panels were then arranged using both Canvas 9.0 and Adobe Illustrator graphic design software.

Figures and Tables

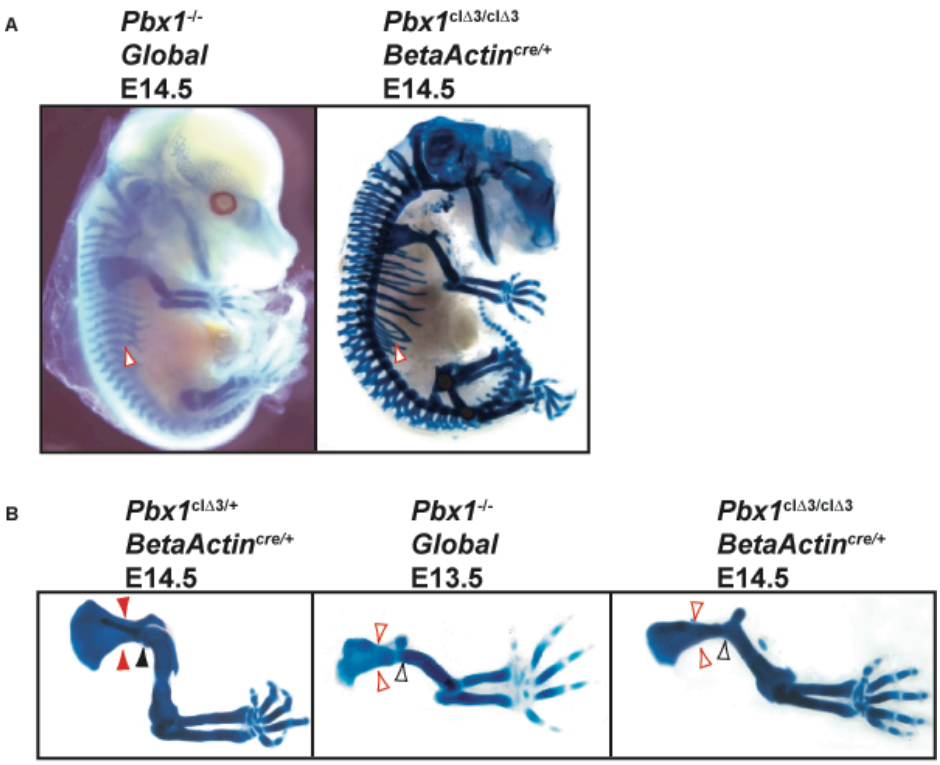

Figure 4.1. Conditional inactivation of *Pbx1* allele (in a homozygous state) using a ubiquitously-specifically expressed Cre transgene under the *Beta Actin* promoter.

Alcian Blue staining reveals that at E14.5, the conditionally inactivated *Pbx1* embryo generated using the Beta Actin Cre fully recapitulates the global loss of *Pbx1* generated using traditional gene targeting. For example, both embryos have rib fusions (empty light-shaded arrowheads). (B) A comparison of the global and conditional mutant forelimb to the wildtype forelimb demonstrates that each displays a fusion of the proximal humerus (empty dark shaded and dark shaded arrowheads, respectively) to the scapula and a superior to inferior reduction in the scapular blade (empty light shaded and light shaded arrowheads, respectively). Proximal (left); Anterior (top).

Figure 4. 2. Proportion of *Pbx* compound mutant embryos recovered per genotype and gestational day (E8.5 to E13.5) from Summer 2001 to Fall 2005.

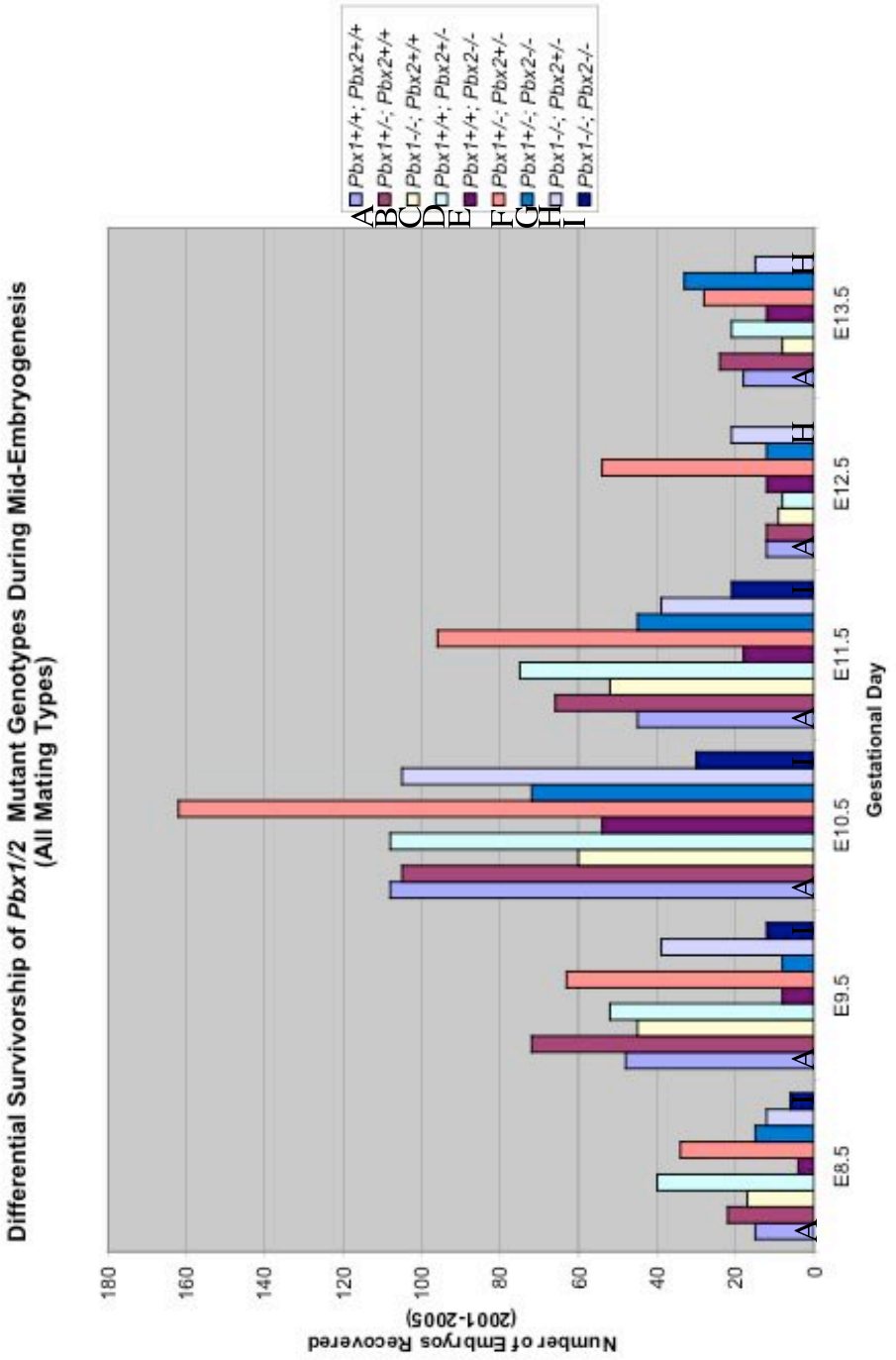
Differential Survivorship of Pbx1/2 Mutant Genotypes During Mid-Embryogenesis
(All Mating Types)
Number of Embryos Recovered
(2001-2005)
Gestational Day
E8.5
E9.5
E10.5
E11.5
E12.5
E13.5
0
20
40
60
80
100
120
140
160
180
A Pbx1+/+; Pbx2+/+
B Pbx1+/-; Pbx2+/+
C Pbx1-/-; Pbx2+/+
D Pbx1+/+; Pbx2+/-
E Pbx1+/+; Pbx2-/-
F Pbx1+/-; Pbx2+/-
G Pbx1+/-; Pbx2-/-
H Pbx1-/-; Pbx2+/-
I Pbx1-/-; Pbx2-/-

Intercrosses of *Pbx1* $^{+/-}$ *;Pbx2* $^{+/-}$ Mice

(Summer 2001-Fall 2005)

Genotype	E8.5	E9.5	E10.5	E11.5	E12.5	E13.5	Totals
Pbx1+/+; Pbx2+/+	15	48	108	45	12	18	246
Pbx1+/-; Pbx2+/+	22	72	105	66	12	24	301
Pbx1-/-; Pbx2+/+	17	45	60	52	9	8	191
Pbx1+/+; Pbx2+/-	40	52	108	75	8	21	304
Pbx1+/+; Pbx2-/-	4	8	54	18	12	12	108
Pbx1+/-; Pbx2+/-	34	63	162	96	54	28	437
Pbx1+/-; Pbx2-/-	15	8	72	45	12	33	185
Pbx1-/-; Pbx2+/-	12	39	105	39	21	15	231
**Pbx1-/-; Pbx2-/-*	6	12	30	21	0	0	69
Totals	165	347	804	457	140	159	2072

* E10.5 and 11.5 embryos were resorbed and were most unusable.

Table 4.1. Exact counts of *Pbx* compound mutant embryos acquired per genotype per gestational day from timed-mating (Summer 2001-Fall 2005).

Chapter 5: *Pbx1* and *Pbx2* Are Required for Distal Limb Patterning via Their Hierarchical Control of *Hox* Spatial Distribution and *Shh* Expression

5.1 Introduction

Vertebrate limb development occurs along the proximal-distal (P-D; e.g., shoulder to fingertip), anterior-posterior (A-P; e.g., thumb to little finger), and dorsal-ventral (D-V; e.g., back of hand to palm) axes (reviewed by Niswander, 2003; Tickle, 2003). As discussed in Chapter 3, these axes are established through molecular networks beginning when the limbs bud out of the flank and continuing with the organization of signaling centers, such as the ZPA (reviewed by Pearse and Tabin, 1998). Continued outgrowth and patterning of the distal limb bud requires the establishment of a molecular feedback loop between the ZPA and the AER. Critical to the development of this interaction is the expression *Shh* in the ZPA (Riddle et al., 1993) and of *Fgf*s in the AER (Sun et al., 2002). Shh signaling establishes the A-P axis of the limb (Chiang et al., 2001) and leads to the formation of distal limb elements of the posterior zeugopod (i.e., ulna and fibula) and digits of the autopod (Harfe et al., 2004).

As of yet, the molecular triggers that activate *Shh* expression are mostly unknown, although a few candidate genes have been proposed. Recall that *Hand2* has been shown to act upstream of *Shh*, as it is expressed early in the limb mesenchyme while *Hand2*$^{-/-}$ embryos lack *Shh* expression (Charite et al., 2000). Likewise, *Hox* genes (reviewed by Krumlauf, 1994; Capecchi, 1997; Deschamps and van Nes, 2005) have been more recently proposed as upstream regulators of *Shh* (Zakany et al., 2004) and determinants of A-P and P-D axis

formation (Kmita et al., 2005). For example, prior to *Shh* onset, the early collinear expression of *Hox* genes in limb bud mesenchyme leads to the posterior accumulation of *Hox* transcripts in the ZPA (Zakany et al., 2004; Tarchini and Duboule, 2006). Furthermore, their ectopic expression leads to ectopic *Shh* transcription (Charite et al., 1994; Stratford et al., 1997; Knezevic et al., 1997; Zakany et al., 2004). Finally, in vertebrates, functional ablation of multiple 5' *Hox* genes leads to distal limb truncations partially mediated by the lack of *Shh* (Kmita et al., 2005; reviewed in Chapter 3).

While the early phase of *Hox* expression appears essential for *Shh* onset in the ZPA, the dynamic expression of *Hox* genes throughout limb bud development aids in patterning elements along the entire P-D axis. Indeed, dramatic patterning alterations occur in limb skeletal elements of specific developmental modules in mice where multiple paralogous *Hox* genes have been genetically ablated, suggesting an internal functional redundancy within paralogous groups (Condie and Capecchi, 1994; Davis et al., 1995; Davis and Capecchi, 1996; Fromental-Ramain et al., 1996a-b; Wellik and Capecchi, 2003). These findings highlight that *Hox* genes act as global regulators of both axial and limb skeletal patterning throughout development.

As reviewed in Chapter 3, the present understanding of Hox protein function is that they exert their roles partially through the aid of cofactors, such as Pbx TALE homeodomain proteins (Burglin, 1997; 1998), that increase Hox DNA binding specificity and selectivity (reviewed by Mann and Chan, 1996; Mann and Affolter, 1998; Moens and Selleri, 2006). Pbx proteins, when forming complexes

with Hox proteins, are further known to lead to the transcriptional regulation of *Hox* genes themselves (Popperl et al., 1995; Maconochie et al., 1996; 1997; Jacobs et al., 1999; Ferretti et al., 2000). However, recent findings strongly suggest that Pbx proteins can also function more broadly in a Hox-independent manner (Knoepfler et al., 1999; Berkes et al., 2004; Moens and Selleri, 2006).

Recently, the roles of *Pbx* genes have been elucidated in organogenesis and skeletal development. Indeed, *Pbx1* was found to be required for proximal limb patterning (Selleri et al., 2001). Specifically, in *Pbx1*$^{-/-}$ mouse embryos, skeletal structures of the limb girdles (i.e., scapula and pelvis) and proximal limb stylopod (i.e., humerus and femur) that normally express nuclear *Pbx1* at early developmental stages, are malformed, while, in contrast, their distal limb elements and joints appear normal. These findings parallel the role of *Exd* (the *Drosophila Pbx* homolog; Peifer and Weischaus, 1990; Rauskolb et al., 1993) in governing proximal domains of the fly appendage, where its expression is restricted (Mercader et al., 1999). Conversely, more recently, *Pbx2* or *Pbx3* loss was found to not affect skeletal or limb phenotype (Rhee et al., 2004; Selleri et al., 2004).

In this chapter several important insights into *Pbx* gene expression and function are uncovered. First, that early (E7.5-E9.25), *Pbx1* and *Pbx2* are co-expressed in the vertebrate limb field and that later (E.925-E11.5), *Pbx2* is expressed throughout the limb mesenchyme, while *Pbx1* is expressed only proximally. Second, by exploiting a *Pbx1;Pbx2* loss-of-function mouse model

(i.e., where the dosages of both *Pbx1* and *Pbx2* are concurrently lost or reduced), that decreasing *Pbx2* dosage in the complete absence of *Pbx1* does indeed affect limb development more severely than the loss of *Pbx1* or *Pbx2* alone. In fact, compound *Pbx1*;*Pbx2* embryos, in addition to their proximal limb defects, exhibit the appearance of novel and severe distal limb abnormalities; *Pbx1*$^{-/-}$;*Pbx2*$^{+/-}$ embryos display dramatic loss of distal hindlimb elements; whereas *Pbx1*$^{-/-}$;*Pbx2*$^{-/-}$ embryos lack limbs altogether. Third, it is established, on several experimental levels, that in vertebrates' patterning of the distal limb is genetically regulated by *Pbx1* and *Pbx2*, at least in part, through their hierarchical control of *Hox* spatial distribution and *Shh* expression.

5.2 Results

5.2.1 Loss of *Pbx1* and *Pbx2* caused not only proximal but also distal fore- and hindlimb defects

Double heterozygous *Pbx*$^{+/-}$;*Pbx2*$^{+/-}$ mice were intercrossed to generate progeny with different compound genotypes (see Chapter 4). Axial and limb skeletal abnormalities were evident only in *Pbx1*$^{-/-}$;*Pbx2*$^{+/+}$ (Selleri et al., 2001), *Pbx1*$^{-/-}$;*Pbx2*$^{+/-}$ and *Pbx1*$^{-/-}$;*Pbx2*$^{-/-}$ compound embryos (Fig. 5.1). *Pbx1*$^{-/-}$;*Pbx2*$^{-/-}$ embryos died at E9.5/10.5 during the period critical for limb bud initiation, due to multiple organogenesis defects. They displayed extreme delays in axial, craniofacial, and limb development. Chapter 6 further discusses their morphology and development (Fig. 5.1A). In this chapter the focus is on limb development in *Pbx1*$^{-/-}$;*Pbx2*$^{+/-}$ (hereafter described as *Pbx1/2 Mut*) embryos (Fig.

5.1A). *Pbx1/2 Mut* survived until E13.5/14.5 and exhibited drastic exacerbations of the *Pbx1*$^{-/-}$ axial and proximal limb defects (Selleri et al., 2001; see Chapter 3) and novel distal phenotypes (Fig. 5.1A-C).

Fore- and hindlimb development in *Pbx1/2 Mut* embryos was differently affected, specifically with respect to the timing and extent of limb bud malformations during early development. *Pbx1/2 Mut* forelimbs at E9.5 already appeared malformed with buds that were P-D shortened (data not shown). At E10.5 (Fig. 5.1A), forelimb bud size remained small, when compared to forelimbs and hindlimbs of all other genotypes, except *Pbx1*$^{-/-}$*;Pbx2*$^{-/-}$ embryos. However, by E11.5 and E12.5 (Fig. 5.1B) forelimb buds increased in size and achieved some dimensional and morphological characteristics resembling normal buds; specifically, a more A-P expansion, reminiscent of, but not identical to, the wildtype pattern. While this improvement continued until E13.5 (i.e., their day of lethality) (Fig. 5.1C) forelimbs still exhibited strong alterations in gross morphology; they displayed a shortened zeugopod and hypoplastic (i.e., A-P reduced) autopod. Furthermore, they projected approximately ninety degrees perpendicular to the body wall, a situation uncharacteristic of wildtype embryos, suggesting that stylopodial development and early limb rotation were also compromised (data not shown).

The *Pbx1/2 Mut* hindlimb exhibited a different pattern of morphological development. Early, at E10-E10.5, hindlimbs still exhibited relatively normal A-P and P-D morphology (Fig. 5.1A) despite the typical half-day delay in hindlimb development. By E11.5, obvious defects in A-P and distal limb development

became apparent, which by E12.5 (Fig. 5.1B) and E13.5 (Fig. 5.1C) became extremely exacerbated. At E13.5, hindlimbs appeared rudimentary and lacked a true A-P patterned autopod (Fig. 5.1C). Interestingly, although quite malformed, hindlimbs were still oriented properly with respect to the body axis.

Analysis of skeletal development from E12.5 to 13.5 in *Pbx1/2 Mut* embryos demonstrated that both proximal and distal limb elements were malformed and/or lacking in both fore- and hindlimbs (Fig. 5.2). In fact, these defects were evident prior to the earliest stages of skeletogenesis when mesenchymal cells coalesced into condensations. In forelimbs at E12.5 (Fig. 5.2A), the expression of *Sox9*, a marker for mesenchymal condensation (Wright et al., 1995), revealed a general mis-patterning across most developmental modules. For example, condensations for the humerus of the stylopod were reduced as well as those observed for the radius and ulna of the zeugopod (Fig. 5.2A). In addition, forelimb autopodia displayed only three central intact rudimentary digital condensations while condensations corresponding to digits one and five were absent and/or rudimentary at best (Fig. 5.2A).

Cartilage preparations at E12.5, as visualized by Alcian Blue staining, more clearly demonstrated the alterations in the humerus and adjoining pectoral girdle (Fig. 5.2B). The condensations giving rise to the scapula were completely unorganized and/or missing as discussed in Chapter 7. With respect to the stylopod, the humerus was highly contorted. Proximally, it remained fused to the “scapular” mass. In addition, the condensation for the deltoid tuberosity was mis-patterned in that it lied more proximally in the limb field than what was typically

observed in wildtype forelimbs. By E13.5, *Pbx1/2 Mut* forelimbs and girdles were more clearly dysmorphic, but possessed most of their cartilaginous elements (Fig. 5.2C). The scapular defect observed at E12.5 became more exacerbated at E13.5 (as discussed in Chapter 6). The residual "scapular" mass remained strongly fused laterally to the humeral head and possessed an adjoining, anteriorly oriented skeletal element likely representing a duplicated humeral head. Interestingly, the humerus also had a shaft that was thickened and grossly contorted, and possessed a cartilaginous anlagen mimicking a hypertrophic deltoid tuberosity (Fig. 5.2C). This particular structure also extended proximo-anteriorly, giving the entire humerus a bifurcated appearance with two proximal facing heads (Fig. 5.2C). In the zeugopodial regions, both elements of the forelimb were present, albeit moderately shortened and bowed. In the autopod, only rudimentary carpals remained proximally adjacent to three central metacarpal/ phalangeal rays, while most elements were either absent and/or rudimentary for digits one and five (Fig. 5.2C).

Pbx1/2 Mut hindlimb skeletogenesis proceeded with comparable alterations proximally, but more drastic malformations distally. Analysis of *Sox9* expression at E12.5 (Fig. 5.2A) demonstrated that condensations for stylopodial (i.e., femur) and anterior zeugopodial (i.e., tibia) elements were present, whereas condensations for the posterior zeugopod (i.e., fibula) and autopod were missing (Fig. 5.2A). Detection of early cartilaginous condensations at the same gestational day by Alcian Blue staining, more clearly demonstrated proximal hindlimb defects (see Fig. 5.2B). Accordingly, pelvic girdle defects were evident

(discussed in Chapter 7) and as in the forelimb, the femoral condensation also remained shortened and thickened and appeared fused to the residual pelvic element. No proximo-anterior duplications of the femoral head were observed in any skeletal preparations. By E13.5 (Fig. 5.2C), the pelvic girdle defects remained (discussed in Chapter 7) and the femur was still fused to this structure and also severely truncated and grossly thickened. The only remaining hindlimb zeugopodial element appeared as a tibia, albeit only slightly dysmorphic, whereas the posterior forming fibula was absent, as were all autopodial elements, except for one single extremely rudimentary digital ray (Fig. 5.2C).

This residual digital ray possessed cartilaginous elements whose allocation to tarsals, metatarsals, and/or phalanges could not be discerned. This digit most likely represented number one, although this assignment is, at best, tentative. For example, as discussed in Chapter 4, observations of *Pbx1/2 Mut* hindlimbs on increasingly Blackswiss backgrounds (Fig. 5.3) demonstrated a phenotypic amelioration whereby additional digits appeared, most likely of more posterior nature, and produced a cleft between them and a residual looking digital ray element reminiscent of digit one. Unfortunately, current reagents, such as *Cre-ROSA* fate-mapping system (i.e., similar to that employed in Chapter 6), that serve to specifically label the anterior cellular populations that give rise to digits one and two have not yet been established. The use of the *Shh Cre-ROSA* system (Harfe et al., 2004) was considered given that it serves to fate-map specific populations of cells that give rise to digits. However, since this mapping strategy only determines the fate of cells for the posterior three digits (i.e., as

only the three most posterior digits form from once expressing ZPA *Shh* cells), it was not useful for these analyses. Thus, the assignment of the rudimentary ray to either digit 1 or 2 remains unclear until newer methods can be established.

The drastic loss of the fibula and digits in the *Pbx1/2 Mut* hindlimb strongly resembled the condition seen in *Shh* knockout embryos (Chiang et al., 2001; Kraus et al., 2001) and *HoxA/HoxD* (Kmita et al., 2005). With respect to the former, *Pbx1/2 Mut* hindlimbs did indeed display a more severe phenotype as they lacked nearly all digits and alterations throughout the limb, a condition not observed in *Shh* knockout limbs. With respect to the latter, the loss of *HoxA/HoxD* did result in truncations with complete loss of digits, however, such alterations were evident in both elements of the zeugopod. This condition is not phenocopied in *Pbx1/2 Mut* hindlimbs, as one zeugopodial element, i.e., the tibia, remained relatively normal.

5.2.2 *Pbx1*, *Pbx2*, and *Pbx3* mesenchymal expression during limb development was dynamic

In order to determine how specific spatio-temporal differences in *Pbx1* and *Pbx2* limb expression underlie such abnormalities, *in situ* hybridization was performed on wildtype embryos with *Pbx1* and *Pbx2* specific probes. In addition, Di Giacomo et al. (2006) also demonstrated that *Pbx3* is dynamically expressed during limb development and thus an understanding of its expression patterns here will aid in discussion of *Pbx1/2* mutant phenotypes and their underlying genetic networks.

5.2.2.1 Early *Pbx* gene expression in limbs (E8.5-11.0)

Pbx1 expression was first detected at E7.5 (data not shown) to E8.5 (Fig. 5.4A) in LPM and thus, throughout the regions that gave rise to future limb bud prominences. Between E8.5 and E9.5, as limb bud induction and initial outgrowth commenced, *Pbx1* transcripts became more proximal in the forming bud and were lost distally in the mesenchyme (Fig. 5.4A). At E9.5-11, *Pbx1* transcripts remained in flank and proximal limb bud mesenchyme (Fig. 5.4B), albeit expanded distally in the bud's anterior domains. *Pbx2* was also first detected throughout flank mesenchyme at E7.5 (data not shown) to E8.5 (Fig. 5.4A). During limb bud induction and initial outgrowth from E8.5 to E9.5, *Pbx2* transcripts acquired a more distal domain, such that by E9.5 and E9.75 they were particularly intense distally (Fig. 5.4A). From E10.5 to E11, *Pbx2* expression remained distal, although upon sectioning and performing immunohistochemistry, it appeared to occupy a peripheral rim along the distal limb bud and was absent from the central limb mesenchymal core (Fig. 5.4B and inset). *Pbx3* expression was unique, in that it remained present in the flank of early (E9.5) embryos (Fig. 5.4B), but shortly after became restricted only to the forelimb bud until E11.0 when transcripts again became evident in the hindlimb. With respect to the forelimb proper, *Pbx3* was first expressed in the proximal-anterior domain of the limb bud at E9.0-E9.5 and remained anteriorly until E11.0 (Fig. 5.4B). Hindlimb expression of *Pbx3* once again became evident after E11 although in a significantly reduced manner compared to both *Pbx1* and *Pbx2* (Fig. 5.4B).

Interestingly, transcripts for *Pbx1, Pbx2,* and *Pbx3* were shown to overlap several times during early limb development. Specifically, they co-localized early (E8.5) in the flank and in the limb anlagen (Fig. 5.4C), while later (E9.5-11), all three co-localized along the forelimb's proximal-anterior domains along a strip of mesenchyme just distal to the bud/flank proximal articulation (Fig. 5.4C). In the developing hindlimb region, only *Pbx1* and *Pbx2* co-localized in the developing flank and limb bud a pattern that remained until *Pbx3* commenced at E11 (Fig. 5.4C). Overall, the early expression patterns, herein described, suggest a scenario where *Pbx1*, *Pbx2,* and *Pbx3* provide an overlapping and complementary "code" along the entire P-D limb axis (Fig. 5.4C). The ramifications of this finding are discussed below and also in Chapter 8.

5.2.2.2 Later limb *Pbx* gene expression (E11-12)

At the first appearance of a morphologically identifiable autopod (E11-11.75, Fig. 3.4), expression of all *Pbx* then changed dynamically where they became restricted to the anterior and posterior mesenchyme proximal to the autopod (Fig. 5.4B-C). This pattern was quite evident in the forelimb for all three genes while in the hindlimb transcripts for *Pbx1* and *Pbx2* appeared much stronger than *Pbx3*. During later autopod formation (i.e., during handplate and footplate maturation), *Pbx1*, *Pbx2,* and *Pbx3* co-localized in the interdigital mesenchyme (data not shown), suggesting that these three factors play important roles in later digit maturation and morphology (Di Giacomo et al., 2006).

Of note, *Pbx1* and *Pbx2* expression was also analyzed at different time points in *Pbx2*$^{-/-}$ and *Pbx1*$^{-/-}$ limb buds, respectively. At E10.5, *Pbx1* (Fig. 5.5) in *Pbx2*$^{-/-}$ fore- and hindlimbs displayed a slightly broader expression domain but remained relatively proximal, whereas *Pbx2* expression (Fig. 5.6) in *Pbx1*$^{-/-}$ and *Pbx1/2 Mut* limbs remained unaltered in these experiments, thus indicating that *Pbx1* and *Pbx2* do not markedly control each other's expression. This finding indicates that the loss or reduction of one *Pbx* gene is not normally rescued by an up-regulation of another, at least in terms of its spatial expression and intensity (i.e., as assessed by *in situ* hybridization). At later days such as at E11.5 (Fig. 5.5 and Fig. 5.6) no significant differences in expression of *Pbx1* and *Pbx2* were apparent in these reciprocal experiments. *Pbx3* expression was also analyzed in limbs deficient for *Pbx1* or *Pbx2*, as well as in the *Pbx1/2 Mut* (*Pbx1*$^{-/-}$*;Pbx2*$^{+/-}$*)*. No differences in *Pbx3* expression were observed in single knockouts for *Pbx1* and *Pbx2* when compared to their wildtype controls (E10.5-E11.5; data not shown) although in the *Pbx1/2 Mut*, a posteriorization of the *Pbx3* expression domain was identified in the forelimb at E10.5-11.0 (Fig. 5.7 and Chapter 7). These latter data suggest that a genetic interaction may have been evident in the forelimb bud domain in the relative absence of *Pbx1* and *Pbx2*.

5.2.3 In *Pbx1/2 Mut* limbs, early anterior and posterior mesenchymal patterning remained relatively preserved

In order to ascertain how and when skeletal malformations became evident in *Pbx1/2 Mut* limbs, *in situ* hybridization studies were carried out at different gestational days to examine for changes in A-P gene expression and thus whether the mechanisms that establish limb bud axes and outgrowth were altered. Therefore, the first *in situ* hybridizations were performed at the initial stages of limb bud outgrowth.

As reviewed in Chapter 3, starting from early gestational days prior to *Shh* onset (i.e., prior to E9.75 in the forelimb and E10.25 in the hindlimb), a mutual genetic antagonism has been shown to exist between *Gli3* in the anterior limb mesenchyme and *Hand2* in the posterior mesenchyme (te Welscher et al., 2002). In addition, *Hand2* has been shown to be genetically required to restrict *Alx4* anteriorly (te Welscher et al., 2002). These genetic interactions subdivide the early limb bud into anterior and posterior domains. In addition, *Twist* is also expressed anteriorly in limb bud development and has been shown to be involved in early A-P patterning and modulation of later Shh signaling in the limb bud (O'Rourke et al., 2002). While marked morphological alterations were observed in *Pbx1/2 Mut* forelimbs prior to E10.5 (Fig. 5.1A), no gross perturbations of *Alx4*, *Hand2*, and *Gli3* expression were detected in distal forelimb buds (Fig. 5.8A). Similarly, *Twist* remained expressed anteriorly. At E10.5, normal transcript levels and expression of *Alx4*, *Gli3,* and *Hand2* in *Pbx1/2 Mut* hindlimbs were detected (Fig. 5.8B), although in the latter there appeared to have been a slight proximal reduction in signal, the significance of which remains to be determined. These data indicate that the anterior and

posterior domains of the hindlimb mesenchyme were initially preserved and are in agreement with the normal hindlimb morphology also present at this day (Fig. 5.1A). In addition, *Twist* was expressed normally in hindlimbs further suggesting a normal mesenchymal expression of A-P prepatterning genes (Fig. 5.8B). Overall, normal A-P limb domains were present in the early limb buds of *Pbx1/2 Mut* embryos.

5.2.4 *Pbx1* and *Pbx2* were required for normal *Shh* expression in the limb ZPA

The early subdivision of the limb into A-P domains sets the initial patterning conditions that, with the aid of *HoxA* and *HoxD* transcription factors (Zakany et al., 2004), help drive the formation of the ZPA and the distal limb. Additionally, *Hand2* and *Alx4* have already been described as having upstream and parallel affects, respectively, on the spatial distribution of *Shh* expression in the ZPA (see Chapter 3). Given similarities between the *Pbx1/2 Mut* hindlimb phenotype and the defects reported in *Shh*-deficient embryos (Chiang et al., 2001; Kraus et al., 2001), *Shh* expression was examined in compound *Pbx1;Pbx2* limbs (Fig. 5.9). In the forelimb (Fig. 5.9A), the timing and duration of *Shh* expression occurred normally (E9.75 to E11.75), and was not delayed in its termination. Despite this temporal consistency, levels of *Shh* expression were considerably lower than observed in wildtype. The expression of *Shh* in *Pbx1/2 Mut* hindlimbs (Fig. 5.9B) was significantly different. Recall, that normal *Shh* expression in hindlimbs commences around E10-10.25 and declines at E11.75-

12.0. *Shh* was never detected throughout *Pbx1/2 Mut* hindlimb development, as represented at E10.5 and 11.5 (Fig. 5.9B). Furthermore, later days of gestation were examined (E12-E13.5) and *Shh* expression was never detected, indicating that *Shh* expression was absent and not merely delayed (Fig. 5.9C). In addition, this absence could not be attributed to either a global *Shh* down-regulation or to a delay in posterior embryonic development, as both *Pbx1/2 Mut* cloaca and notochord developed normally and displayed normal *Shh* expression (Fig. 5.9D).

As discussed in Chapter 3, *Patched* and *Gli1* are considered downstream of *Shh* and are normally activated at strong levels upon *Shh* initiation. Interestingly, in hindlimbs, low levels of *Ptc* and *Gli1* (readouts of hedgehog signaling; reviewed in Chapter 3) were observed at E10.75 (Fig. 5.10A), suggesting that a minimal and transient wave of *Shh* activity likely occurred. *Gli1* was examined at later days and no expression was observed (data not shown). In contrast to the hindlimb, in *Pbx1/2 Mut* forelimbs, where *Shh* expression was reduced yet present, *Ptc and Gli1* were still expressed (Fig. 5.10B), indicating that *Shh* absence was hindlimb-specific.

As elaborated in Chapter 3, the AER can have specific influences on *Shh* expression when AER formation and function are completely abrogated via either experimental removal or loss of multiple signaling molecules (i.e., Fgf4 and Fgf8). Therefore, AER function was assayed using several different informative markers. Prior to *Shh* onset, *Fgf8* expression was present in both fore- and hindlimbs, and with respect to the latter, its expression remained posterior and distal (Fig. 5.11A). This finding indicates that critical AER signals are present

prior to *Shh* onset; and therefore, that *Shh* loss in the *Pbx1/2 Mut* hindlimb cannot necessarily be explained by a dysfunctional AER.

Fgf4 expression was also examined at E10.25 (see Fig. 5.11B) and at later days at E11, as it is a direct readout of Shh signaling. Therefore, studying its expression patterns in mutant versus wildtype embryonic limbs provided a means to assess the overall reduction and loss of *Shh* in fore- and hindlimbs, respectively. In forelimbs at both days, *Fgf4* was lost (E10.25) and/or detected (E11, Fig. 5.11B), although its central distal expression in the AER was lost. These data are coincident with both the reduction but presence of *Shh* as well as the overall dysmorphology of the forelimb prior to Shh signaling (see Chapter 6 for more detailed analysis). In the hindlimb at both days, *Fgf4* was only slightly expressed along the most posterior portion of the AER, an area that is directly adjacent to the ZPA (Fig. 5.11B). This specific result demonstrates that the AER was capable of "comprehending" signals from *Shh* cascade, and that a residual Shh wave of signaling may have occurred.

CD44 is a transmembrane glycoprotein that serves to present FGF signals from AER cells to receptors on subjacent cells. Additionally, CD44 has a demonstrated role in maintaining the growth promoting function of the AER and in this manner serves as an excellent marker for AER "healthiness" and function (Sherman et al., 1998). CD44 distribution was relatively preserved in both *Pbx1/2 Mut* fore and hindlimbs (Fig. 5.11C), although both AER possessed a light anterior reduction. In the *Pbx1/2 Mut* hindlimb, CD44 expression occurred relatively normally in the posterior AER, thus indicating that AER function was

normal, at least until E10.5, and thus was unlikely responsible for *Shh* absence (Fig. 5.9B). This result was further corroborated by the findings that AER-specific markers, such as *Dlx6* (Robledo et al., 2002), remained unperturbed in *Pbx1/2 Mut* posterior fore- and hindlimbs (Fig. 5.11D). In addition, such data is in agreement with the expression of *Fgf8* at this time (Fig. 5.11A). Overall, these data demonstrate that the posterior AER function was preserved before *Shh* onset [note: a detailed analysis of other genes involved in AER formation and function is also presented in Chapter 6]. On the other hand, at E11.5, well after *Shh* initiation, expression of *Fgf8* and several other genes (Fig. 5.9B and see Chapter 6) was patchy in *Pbx1/2 Mut* hindlimbs and resembled the pattern reported for *Shh*-deficient embryos (Chiang et al., 2001; Kraus et al., 2001).

In *Drosophila*, proximal appendage localization of *Hth* and *Exd* (homologs of vertebrate *Meis* and *Pbx*, respectively), has been shown to antagonize or repress hedgehog signaling (see Mercader et al., 1999). In this manner, *Hth/Exd* are important for influencing both the A-P and P-D axes of the fly appendage. In vertebrates, *Meis1* and *Meis2* are also expressed proximally, thus implicating them in a similar role in P-D axis establishment (Capdevila et al., 1999). Intriguingly, normal proximal limb identity was observed in *Pbx1/2 Mut* limbs (Fig. 5.12), as both *Meis 1* and *Meis2* remained unchanged throughout early to mid limb development. This indicates that P-D limb outgrowth proceeded relatively normally, at least until E11 and that the observed *Shh* decrease (forelimbs) and absence (hindlimbs) were most likely not due to direct repression of *Shh* by *Meis*.

To examine whether genes downstream of Shh signaling were disrupted in *Pbx1/2 Mut* limbs, *in situ* hybridizations were performed for multiple genes at several days post-*Shh* onset (i.e., after E10.25). *Gremlin* (Scherz et al., 2004), *Bmps*, and *Fgf4* (Niswander, 2003) are involved in a Shh-Fgf feedback positive loop critical for ZPA and *Shh* maintenance (see Chapter 3). Analyses of *Gremlin* demonstrate a considerable reduction of signaling in both *Pbx1/2 Mut* fore- and hindlimbs at E10.75-11 (Fig. 5.13A). In addition, as reported (Scherz et al., 2004), Gremlin and Shh protein seem to antagonize one another producing two discrete domains in the anterior and posterior limb domains, respectively. Indeed, as demonstrated in the *Pbx1/2 Mut* hindlimb bud, *Gremlin* expression is posteriorized into the region where "*Shh*" expression should be, and thus is in agreement with those reported observations. *Bmp2* and *Bmp4* were also examined at the time of *Shh* onset in both *Pbx1/2 Mut* fore- and hindlimbs. In forelimbs, both *Bmp2* and *Bmp4* were slightly altered in their most anterior and posterior AER domains (Fig. 5.13B, data not shown). In *Pbx1/2 Mut* hindlimbs, *Bmp* loss was considerable and nearly absent (Fig. 5.13B, data not shown). On the other hand, as mentioned above, *Fgf4* expression was present in the forelimb buds, albeit altered, and in hindlimbs, it was slightly visible in the posterior AER (Fig. 5.11B).

Shh expression has also been shown to lie upstream of other genes such as *Hand2*, *Gli3* (te Welscher et al., 2002), and *Tbx2/3* (Gibson-Brown et al., 1998; Suzuki et al., 2004; see Chapter 3). While *Hand2* expression remained unaltered prior to Shh signaling in both fore- and hindlimb buds (Fig. 5.8), at later

gestational days (E10.75-11) (Fig. 5.14A) *Hand2* was markedly down-regulated in hindlimbs, but not forelimbs (data not shown), further confirming *Shh* absence in mutant hindlimbs. *Gli3* expression also remained normally expressed in *Pbx1/2 Mut* forelimbs (data not shown) whereas in hindlimbs it was markedly posteriorized indicating the lack of Shh signaling posteriorly (Fig. 5.14B and Chapter 7). Interestingly, the observed expression patterns of *Hand2* and *Gli3* strongly resembled those observed patterns in mice lacking *Shh* (Chiang et al., 2001; Kraus et al., 2001) as well as *HoxA/HoxD* (Kmita et al., 2005). Analyses of *Tbx2* (data not shown) and *Tbx3* (Fig. 5.14C), genes expressed each in the anterior and posterior mesenchyme, demonstrate a comparable alteration in posterior hindlimb mesenchyme (Fig. 5.14C). In addition, both show that anterior patterning is altered with *Shh* loss, perhaps suggesting the involvement of *Tbx* and a gene responsive to *Shh* in an anterior genetic interaction. On the other hand, loss of *Tbx* anterior domain may be related to disruptions in *Shh*-independent pathways (see below and Chapter 6). Overall, taking into consideration the plethora of data presented above, all of these findings establish that *Pbx1* and *Pbx2* were required in the mesenchyme of the developing limb for *Shh* expression in the ZPA.

5.2.5 *Pbx* and *Hand2* may control *Shh* through parallel pathways; *Shh* and *Pbx* did not form a cross regulatory loop

As mentioned in Chapter 3, *Hand2* has been demonstrated to be upstream of *Shh* expression, specifically, as *Hand2*$^{-/-}$ embryos lack *Shh*

expression (Charite et al., 2000). In the context of the early *Pbx1/2 Mut* hindlimb, *Shh* was absent but *Hand2* remained well expressed (Fig. 5.8A), suggesting that *Pbx1* and *Pbx2* were upstream of *Shh* but not necessarily of early *Hand2* expression. In this manner, *Hand2* may still lie upstream of *Pbx,* which in turn, appears upstream of *Shh* signaling. Alternatively, *Pbx* and *Hand2* may regulate *Shh* via separate pathways or cooperatively. To understand the genetic relationships between *Pbx, Hand2,* and *Shh*, *Pbx* expression was examined in *Hand2*$^{-/-}$ embryos (Fig. 5.15).

Specifically, *Pbx1* expression in *Hand2*$^{-/-}$ forelimbs remained proximal, although a slight distal expansion of the signal was discovered in posterior domains (Fig. 5.15A). *Pbx2* expression was also found to be normal at this day in the forelimb (Fig. 5.15B). In hindlimbs, *Pbx* expression also remained relatively normal (data not shown), although accurate hindlimb analyses, specifically for *Pbx2* expression, were hampered by the poor growth and posterior developmental delay in *Hand2*$^{-/-}$ embryos, as well as their lethality at E10.5 (Charite et al., 2000). Unfortunately, as *Hand2*$^{-/-}$ embryos die at E10-10.5, it was impossible to examine *Pbx* expression at later stages. Overall, these results indicate that neither *Hand2* nor *Pbx* significantly control each other's genetic expression and therefore, that they each likely control *Shh* either through parallel pathways or in unison. However, one cannot rule out the possibility that Pbx and Hand2 interact post-translationally to regulate Shh expression. Future work will clarify this distinction.

Given that *Hand2*, *Shh*, and *Hox* appear to form a regulatory loop in limb development, wherein *Hand2* lies both up- and downstream of *Shh* (Zakany et al., 2004), *Pbx1, Pbx2,* and *Shh* were also examined to see if they form a similar regulatory loop. While *Shh* was found to be absent in *Pbx1/2 Mut* hindlimbs (and reduced in *Pbx1/2 Mut* forelimbs) analyses of *Shh*-deficient embryos revealed relatively unperturbed *Pbx1* and *Pbx2* expression (Fig. 5.16), despite their abnormal limb morphology. Specifically, *Pbx1* expression remained proximal in fore- and hindlimbs lacking *Shh* (Fig. 5.16A); and *Pbx2* expression remained relatively distal despite the presence of marked apoptosis in distal limb domains (Fig. 5.16B)(Chiang et al., 2001). These findings argue against a cross regulatory loop (i.e., where each gene control the others expression) between *Shh* and *Pbx1* and *Pbx2* in limb development.

5.2.6 *Hox* gene expression, prior to and after, *Shh* onset was spatially perturbed or absent in *Pbx1/2 Mut* limbs

Recently, early *Hox* expression in limb mesenchyme has been suggested to be crucial for *Shh* activation and for the specification of A-P and P-D axis formation (Zakany et al., 2004; Kmita et al., 2005; Tarchini and Duboule, 2006). Given the lack of *Shh* expression throughout *Pbx1/2 Mut* hindlimb development and its marked down-regulation in *Pbx1/2 Mut* forelimbs, *HoxA* and *HoxD* expression was examined in all compound mutant limbs. Intriguingly, the expression of all analyzed *Hox* were severely reduced or absent in the future

Shh-expressing domains of early *Pbx1/2 Mut* hindlimbs (E10.25-10.5), despite their relatively normal morphology at this gestational day (Fig. 5.17; *Hoxa10* and *Hoxd10,* data not shown). In contrast, the expression of most *Hox* remained in the ZPA of *Pbx1/2 Mut* forelimbs, although overall *Hox* expression was slightly altered (Fig. 5.18). In addition, in forelimbs, multiple *Hox* were either up-regulated (e.g., *Hoxa9* and *Hoxd9*) or severely down-regulated and/or absent (e.g., *Hoxa13* and *Hoxd13*), suggesting a multifaceted, complex, hierarchical control of *Hox* gene expression by *Pbx* family members. Finally, *Hox* expression was unaltered in limbs of all other compound mutant genotypes (data not shown), including key controls such as $Pbx1^{-/-};Pbx2^{+/+}$ and $Pbx1^{+/-};Pbx2^{-/-}$.

Given the suggested regulatory loop wherein *Shh* regulates digit patterning via its purported control of autopod-specific 5' *Hox* "reverse" collinearity (Zakany et al., 2004) and the observed defects in *Pbx1/2 Mut* digit patterning, *Hox* expression was also examined at later gestational days such as at E11.5 (Figs. 5.19 and 5.20). 5' *HoxD* expression was reduced in somite matched *Pbx1/2 Mut* hindlimb bud anterior domains, while 5' *HoxA* gene expression remained normal (Fig. 5.19; *Hoxa10* and *Hoxd10,* data not shown). This altered *HoxD* expression pattern was similar, but not identical, to that reported in *Shh*-deficient mice (Chiang et al., 2001). Additionally, in these mutant hindlimbs, the proximal-most expression domain of several *Hox* was reduced both anteriorly and in terms of overall signal intensity (Fig. 5.19). The implications of such loss are discussed below. With respect to *Pbx1/2 Mut* forelimb expression, only a slight anterior alteration of 5' *HoxD* expression, but

not 5' *HoxA* expression (Fig. 5.20; *Hoxa10*, *Hoxd10*, and *Hoxd12,* data not shown) was detected, and this is coincident with the observed reduction in *Shh* expression. Therefore, in the context of reduced *Pbx1* and *Pbx2* dosage, the mechanisms underlying the spatial regulation of *HoxA* versus *HoxD* gene expression differ during autopod development.

5.2.7 Hox proteins bound *in vivo* to, and activated transcription through, the *Shh* long-range limb enhancer

To ascertain whether *Shh* expression was directly regulated by Hox and/or Pbx protein in developing limb buds, their *in vivo* binding to an evolutionarily conserved *Shh* regulatory region (*Shh*E) was tested. This *Shh*E has been shown to be sufficient to direct the correct spatio-temporal expression of *Shh* within developing mouse limbs (Lettice et al., 2003; see Chapter 3). Chromatin Immunoprecipitation (ChIP) analyses (Orlando et al., 1997) were performed on E10.5 mouse fore- and hindlimb bud cells, using specific antisera against Hoxd10, Hoxd13, and Pbx (Fig. 5.21). The enrichment for genomic DNA fragments containing the *Shh*E sequence was verified by PCR amplification. As shown (Fig. 5.21A), a significant enrichment was observed for both the anti-Hoxd10 and anti-Hoxd13 antisera in forelimb as well as in hindlimb bud immunoprecipitated chromatin, indicating that these HoxD proteins are indeed bound to the long-range *Shh* limb regulatory element *in vivo*. No enrichment was observed using a non-specific control antibody (Fig. 5.21A). Using an antiserum

against all Pbx isoforms, Pbx protein was also found to bind *in vivo* to this *Shh* regulatory element in limb bud cells (Fig. 5.21A). The specificity of the observed binding of Hoxd10, Hoxd13, and Pbx to the *Shh*E was further verified by the lack of enrichment on a genomic region located upstream to this enhancer (Fig. 5.21A). As an additional control, Hoxd13 binding to the *Shh*E was analyzed at E13.5 when *Shh* expression had ceased in limb buds. No binding was detected at this gestational day (Fig. 5.21B).

Subsequently, to determine which Pbx family member co-localized with *Shh* in limb buds, *in situ* hybridization and immunohistochemistry were carried out. Notably, *Pbx2* was the only *Pbx* family member that co-localized with *Shh* in the ZPA, as it is expressed throughout the limb bud (Fig. 5.4). Double *in situ* hybridization and immunohistochemistry experiments on adjacent limb bud sections more clearly demonstrate the overlap of Pbx2 protein and *Shh* mRNA (Fig. 5.22). In contrast, two-color *in situ* hybridization experiments, where *Shh* was visualized as a dark shaded signal and *Pbx1* as a light-shaded signal, revealed that *Pbx1* does not co-localize with *Shh*, even in the absence of *Pbx2* (Fig. 5.23). These results were further corroborated by findings obtained by immuno-histochemistry whereby Pbx1 and Pbx2 proteins were detected on adjacent limb bud sections, after *Shh* expression had been visualized by *in situ* hybridization (data not shown). In these latter analyses, Pbx1 remained cytoplasmic distally in the limb prior to *Shh* expression, however, given that the half-life of Pbx1 is unknown it remains unclear whether or not some residual Pbx1 nuclear protein remained in future Shh-expressing cells. Finally, it was

recently uncovered that *Pbx3* was not expressed in hindlimbs (Fig. 5.4; Di Giacomo et al., 2006) and reported findings in the literature demonstrated that *Pbx4* was present only in the testes (Wagner et al., 2001). In conclusion, at this time, *Pbx2* appears the only *Pbx* family member that co-localized with *Shh*, and was thus responsible for the observed binding to the *Shh*E.

As the *Shh*E contains at least eleven different putative sites for Abd-B like Hox proteins, it was analyzed using electrophoretic mobility shift assay (EMSA) to test for the *in vitro* binding ability of HoxD proteins. Hoxd13 binding was tested using seven oligonucleotide probes spanning 450 bp of the ShhE. Indeed, four of these were efficiently bound (Fig. 5.24), confirming the results obtained by ChIP *in vivo*.

The functional significance of the observed *in vivo* binding of Hoxd10, Hoxd13, and Pbx2 to the *Shh*E was next tested in transient transfection assays using P19 embryonal carcinoma cells. A luciferase reporter construct (pT81*Shh*E) was generated, which contained a 745 bp fragment representing the complete long-range *Shh*E element (Lettice et al., 2003). Co-transfection of the *Shh*E reporter with expression constructs for Hoxd9, Hoxd10, and Hoxd13 resulted in significant transcriptional activation above the reporter's basal activity in this cellular system (Fig. 5.25). The expression of Pbx2, conversely, had virtually no affect on the reporter's activity (Fig. 5.25) and the co-expression of Pbx2 with Hoxd9, Hoxd10, or Hoxd13 did not significantly alter their activation of the reporter construct (Fig. 5.25). This finding is consistent with the non-essential function of Pbx2 throughout embryonic development (Selleri et al., 2004). Taken

together, these results show that HoxD proteins were able to bind *in vivo* to the *Shh* long-range limb enhancer in limb bud cells and could activate transcription through this regulatory element in cultured cells, suggesting that they directly controlled *Shh* expression.

5.2.8 The attenuated expression of *Shh* in *Pbx1/2 Mut* hindlimbs in different genetic backgrounds influenced digit formation and onset of appearance

As discussed above, on C57BL/6 background, *Pbx1/2 Mut* hindlimbs possessed a rudimentary digit 1(?) and lacked digits 2-5, indicative of the loss of Shh signaling during limb development. However, following observations that limb phenotype of the *Pbx1/2 Mut* embryo appeared ameliorated upon introducing an outbred Blackswiss background, crosses were established to ascertain the degree of amelioration and the effects that improved Shh signaling have on digit number and identity. As shown (Fig. 5.3), digit number improved to two upon introducing, at most, half genetic background of Blackswiss. In addition, digit number one had not yet appeared.

Upon further backcrossing of hybrid C57BL/6/Blackswiss double heterozygous *Pbx1;Pbx2* to Blackswiss and then mating double heterozygous individuals to each other (therefore at least 3 crosses to Blackswiss) digit number improved to two posterior digits and the presence of an anterior digit, possibly digit 1. This latter finding suggests that the observed phenotypic amelioration may not have come about only via more robust Shh signaling, but also via Shh-

independent mechanisms responsible for forming digit 1. Whole Mount *in situ* hybridizations on limbs (personal observations, data not shown) from each set of mutants revealed that *Shh* expression indeed became more evident in embryos possessing increased Blackswiss backgrounds, a point which corroborated well the finding in digit improvement.

Comparison of proximal tarsal morphologies and their relative positions to their respective digital rays indicates that the two main digits that formed in the first hybrid cross were digits 2 and 3. Furthermore, the continued development of the more posterior digit (i.e., the more intense Alcian Blue staining and increased chondrogenic size) suggests that this element, digit 3, was first to form. This finding is in agreement with those reported by both Ahn and Joyner (2004) and Harfe et al. (2004). In addition, it appeared that digit one formed after these two more posterior digits, suggesting that in a pure C57BL/6 *Pbx1/2 Mut* hindlimb, the rudimentary digital ray may not necessarily have been digit 1 but digit 2 or 3. Interestingly, in this model knockout system, the next digit that formed on Blackswiss backgrounds was digit 2, a finding not in agreement with those reported. Indeed, the lack of formation of the posterior digits 4 and 5 are in agreement with those findings of Harfe et al. (2004) that the most posterior digits form under maximal and sustained exposure to Shh signaling in the ZPA.

5.2.9 *Pbx1/2 Mut* limb development proceeded in the absence of marked alterations to cellular proliferation and apoptosis

In order to determine whether differences in gene expression and gross morphology between wildtype and *Pbx1/2 Mut* limbs resulted from defects in cellular behaviors such as proliferation and apoptosis (cell death), BrdU and Caspase3 were carried out as described in Chapter 4. Analyses of cell proliferation revealed that limb mesenchymal BrdU counts were not altered in *Pbx1/2 Mut* limbs as no statistically significant differences were observed between wildtype and *Pbx1/2 Mut* fore and hindlimbs (treated separately) at any day of gestation analyzed (E9.5-E12.5), as depicted for E9.5 (Fig. 5.26). Therefore, observed alterations in gene expression occurred in the absence of detectable changes in cell proliferation. Similarly, staining for Caspase3 did not reveal any statistically significant differences in cell death between fore- and hindlimbs of wildtype and *Pbx1/2 Mut* embryos at E9.5 and E11.5, although at both E11.5 and E12.5, slight increases in apoptosis were observed in *Pbx1/2 Mut* hindlimbs in a region subapical to the AER (Fig. 5.27). This degree of apoptosis was not severe and in no way matched that which was reported in *Shh*$^{-/-}$ limbs (see below for discussion). Overall, the marked loss of gene expression throughout *Pbx1/2 Mut* limb development appeared to be occurring outside significant changes in cell behaviors such as proliferation and cell death.

5.3 Discussion

5.3.1 *Pbx1* and *Pbx2* are required for proximal and distal limb patterning

The observed results establish that, while *Pbx1* is required for proximal limb patterning (Selleri et al., 2001), *Pbx1* and *Pbx2* share overlapping functions

in proximal as well as distal limb development. In this respect, the fundamental roles of *Pbx1* and *Pbx2* are underscored by the finding that *Pbx1*$^{-/-}$;*Pbx2*$^{-/-}$ embryos did not form limbs. Nevertheless, by decreasing *Pbx2* dosage to one allele on a *Pbx1* null background a mouse model was generated where limb development could be studied in depth. Accordingly, *Pbx1/2 Mut* embryos died earlier *in utero* than single *Pbx1*$^{-/-}$ embryos and had limbs with more drastic skeletal defects. Furthermore, compared to those present in single *Pbx1*$^{-/-}$ embryos, axial skeletal defects were also worsened in *Pbx1/2 Mut* embryos (Fig. 5.28). Overall, these results establish that *Pbx1* and *Pbx2* genetically interact in axial and appendicular skeletal development.

The observed phenotypes of *Pbx1/2 Mut* forelimb versus hindlimb distal limb morphologies varied. Distal hindlimb defects were more severe than those observed in the forelimb; specifically, the fibula and digits were missing, whereas in the forelimb the ulna and most digits were present, albeit malformed. While the presence of different expression levels of *Pbx1* and *Pbx2* in forelimb versus hindlimb could explain the variability in the phenotype expressivity, gross differences in their expression by *in situ* hybridization or immunohistochemistry were never detected. Instead, the less severe distal phenotype of the *Pbx1/2 Mut* forelimb is more consistent with the recent finding that the highly related family member *Pbx3* was expressed only in the forelimb up to E11.5 (Fig. 5.4; Di Giacomo et al., 2006). Finally, the overlapping expression of *Pbx3* proximally with *Pbx1* and *Pbx2* in the limb mesenchyme, may also explain why forelimb but not hindlimb development, is relatively spared in the *Pbx1/2 Mut* embryo. In

addition, it supports the findings that forelimb buds but not hindlimb buds eventually form in *Pbx1*$^{-/-}$;*Pbx2*$^{-/-}$ mutants (see Chapter 6).

Of importance, except for *Pbx1*$^{-/-}$ (Selleri et al., 2001), *Pbx1*$^{-/-}$;*Pbx2*$^{-/-}$, and *Pbx1/2 Mut* embryos, all other compound genotypes lacked limb defects and alterations in gene expression. These findings highlight the primary role of *Pbx1* and the critical impact that *Pbx1* and *Pbx2* (as well as *Pbx3*) spatio-temporal expression patterns have on limb development. Indeed, the early co-localization of *Pbx1* and *Pbx2* in lateral plate and limb field mesoderm *(*with *Pbx3)* appears critical for distal limb development. Interestingly, the finding of normal gene expression levels for early mesenchymal markers in *Pbx1*$^{-/-}$ or *Pbx2*$^{-/-}$ embryos (data not shown) suggest that *Pbx* interaction and/or cooperation is more important and furthermore, that their loss collectively from the early limb field and perhaps later during bud onset, may be essential to driving limb outgrowth.

Concomitantly, the later proximal versus distal restrictions of *Pbx1 (*and *Pbx3)* and *Pbx2*, respectively, suggest a scenario where these genes provide a dynamic spatio-temporal “code” along the entire P-D limb axis. It is during this period, that Pbx may or may not be operating with Hox on target gene activation. While analyses of the *Shh* enhancer suggest that Pbx are upstream of Hox rather than cooperating biochemically with Hox to drive *Shh* expression, Pbx2 binding to this element perhaps indicates an otherwise unknown functional role of Pbx in *Shh* activation. Future work will investigate these specific roles of Pbx (and Hox) during later limb development (see below).

5.3.2 *Pbx* requirement for distal limb patterning is, at least in part, mediated by *Shh* control; posterior digital loss is a consequence of *Shh* absence

The *Pbx1/2 Mut* distal limb phenotype markedly resembles those observed in embryos lacking *Shh* (Chiang et al., 2001; Krause et al., 2001) and *HoxA/HoxD* (Zakany et al., 1997; Kmita et al., 2005). These similarities are particularly evident in the *Pbx1/2 Mut* hindlimb, which initially exhibits relatively normal morphology and A-P patterning until E10.25-10.5 (the time of *Shh* onset in the hindlimb) but subsequently lacks *Shh* expression. *Shh* absence is further supported by the marked reduction in all genes involved in Shh-Fgf feedback signaling, such as *Gremlin, Bmps*, *Fgf4,* as well as genes involved in *Shh* maintenance (i.e., *Twist*) and other downstream factors, such as *Tbx2*, *Tbx3*, and *Hand2*. Furthermore, the marked posterior expansion of *Gli3* and the severe reduction of 5' *HoxD* gene expression, as also documented in $Shh^{-/-}$ embryos (Chiang et al., 2001; Kraus et al., 2001), not only indicates *Shh* absence but supports models where Shh is upstream of the "reverse" co-linearity observed for *5' HoxD* expression during autopod development.

In this model, it remains unclear as to whether Shh operates through Gli3 in regulating *HoxD* "reverse" collinearity, whether it directly activates *HoxD* gene expression, or if it has a dual function. It is currently understood, via studies on the direct interaction of 5' HoxD and Gli3 proteins (Chen et al., 2004) that their ratio across the limb bud regulates digit pattern and identity. In this context, posterior digital loss in the *Pbx1/2 Mut* hindlimb appears to be mediated by *Shh* absence and its differential affects on *Gli3* and 5' *HoxD* expression. The

specifics of such effects remain unclear. In *Pbx1/2 Mut* hindlimbs, the loss of Shh protein should lead to disruption of the Gli3 activator/repressor gradient, as cells that normally should harbor Shh protein do not and as a result no counterbalance to Gli3 posterior repression is present. In this manner, Gli3 repression of 5'*HoxD* gene activation may ensue, leading to a situation where the most 5' *HoxD* (e.g., *Hoxd13*) have the most reduced anterior domains, while more 3' members of this *HoxD* gene group (e.g., *Hoxd10*) remain expressed posteriorly, but with a slightly greater anterior extent. This observed loss corresponds to those expected as reported by Kmita et al. (2003), where the distance of individual Hox promoters to the digital enhancer element determines *Hox* gene activation and transcriptional efficiency. In this context, Gli3 has been suggested to act as a major repressor of transcriptional efficiency of this element (Tarchini and Duboule, 2006). On the other hand, if Shh activation of *HoxD* "reverse" collinearity is direct (i.e., it leads to the direct activation of the digital enhancer), then the reduced and posteriorly restricted *HoxD* levels observed during *Pbx1/2 Mut* autopod formation may reflect direct *Shh* loss. Given the complexity of Shh signaling in the limb, most likely the observed *HoxD* expression alterations at E11.5, reflect at least both of these processes. It is important to note that regardless of Shh direct or indirect effects on *HoxD* expression, *HoxA* gene expression was less affected in *Pbx1/2 Mut* hindlimbs further demonstrating the specific effects on Shh on *HoxD* expression and digit formation.

These exact scenarios do not necessarily hold for the *Pbx1/2 Mut* forelimb, which already appears malformed at early gestational days (E9.5-E10.5) but harbors residual *Shh* expression (and relatively normal levels of most downstream genes) throughout development. Intriguingly, despite their altered morphology, *Pbx1/2 Mut* forelimbs still possessed normal anterior and posterior distal expression domains for *Alx4*, *Hand2*, and *Gli3* prior to Shh signaling, suggesting a relative robusticity in A-P prepatterning. It is not surprising, when taken in this context, that forelimbs display less severe digit malformations and/or losses. In fact, the loss of digit five in *Pbx1/2 Mut* forelimbs conforms to the expectation that the most posterior digits form under the influence of maximum and sustained Shh signaling (Ahn and Joyner, 2004; Harfe et al., 2004). Interestingly, the loss of digit one in *Pbx1/2 Mut* forelimbs likely occurs via the disruption of *Shh*-independent pathways that underlie the early morphological abnormalities occurring prior to *Shh* onset (See below and Chapter 6).

Digital loss in the *Pbx1/2 Mut* fore- versus hindlimbs does share some commonalities that when analyzed could have bearing on the timing and sequence of digit formation in normal and mutant embryos. In both *Pbx1/2 Mut* fore- and hindlimbs posterior digit 5 fails to form. This digit loss coincides with alterations in the levels of maximum Shh signaling experienced in each limb. Next, in both limb contexts, digits 2 and 3 appear in the absence of digit 1, a situation highlighted by the analyses of C57BL/6:Blackswiss mice. These results suggest that these posterior elements normally form before digit 1, though whether this is an important mechanistic relationship remains unclear, given that

only the posterior four digits appear under the influence of Shh signaling. However, it does further corroborate the common dogma that the mechanisms underlying (pre-axial) digit one formation partially differ from those mechanisms governing (post-axial) posterior digit formation. Next, with respect to the *Pbx1/2 Mut* hindlimb, digit 3 appears the first to form and therefore, appears to support those results (Ahn and Joyner, 2004) that suggest that it is the most sensitive to Shh signaling. Interestingly, digit 5 is reported to be the next most sensitive digit, and it did not form in all *Pbx1/2 Mut* hindlimbs, regardless of the genetic background studied. Therefore, if normal post-axial digits form in the sequence 3-5-4-2, then distal and posterior limb patterning in *Pbx1/2 Mut* may be more markedly affected and earlier than that which can be explained solely by the absence of *Shh*. Certainly the major down-regulation of *Tbx2* and *Tbx3* along with the severe alterations in *Hox* may be quite important influences on this disruption in digit formation sequence. Overall, these results suggest that loss of *Shh* in the posterior mesenchyme may be just one contemporaneous consequence of the loss of *Pbx1* and *Pbx2* on distal limb patterning; and that *Hox* alterations (prior to and after *Shh* onset) may have more severe consequences on limb mesenchymal patterning than previously understood.

Interestingly, the above analysis of digit formation indicates that digit one may not necessarily be the residual digit remaining in *Pbx1/2 Mut* hindlimbs. If this is the case, then it coincides with the observed loss of digit one in *Pbx1/2 Mut* forelimbs. In both limb contexts, then, digit loss may be at best partially mediated by the disruption of Shh signaling. However, disruption of Shh

signaling may in turn have downstream effects on *Hox* gene expression that may lead to anterior digit loss. In this context, the most anterior extent of *Hoxd13* and *Hoxa13* gene expression has been correlated with digit one morphogenesis (Zakany et al., 1997; Kmita et al., 2002). In both *Pbx1/2 Mut* fore and hindlimbs, loss of anterior expression for *Hoxd13*, via Shh loss, may lead to digit one loss particularly if it is associated with reduction of *Hoxa13* expression. In the hindlimb, it is difficult to determine whether the anterior extent of *Hoxa13* expression overlaps with the "digit one" zone given the highly altered morphology of the limb. In the forelimb, *Hoxa13* expression is slightly reduced anteriorly. Therefore, digit one loss in forelimbs may be attributed to alterations in *Hox*, particularly if the loss of *Hoxd13* is enough to mediate the phenotype. These results suggest that other mechanisms may also drive digit one loss in the *Pbx1/2 Mut* limbs. Some of these mechanisms are discussed in Chapter 6.

5.3.3 *Pbx1/2* and *Hand2* may genetically regulate each other; *Pbx1*, *Pbx2*, and *Shh* do not form a genetic regulatory loop

Analyses on *Shh*, *Hand2*, and *Pbx1;Pbx2* compound mutant embryos, additionally establish that *Pbx1* and *Pbx2* hierarchically control *Shh* expression in the ZPA and that this process is independent of regulation by *Hand2* (Charite et al., 2000). These results demonstrate that *Pbx* and *Hand2* likely control *Shh* through parallel pathways and therefore influence distal limb development in similar, but not identical ways. However, the possibility that Hand2 controls Pbx, or vice versa at the post-translational level, and therefore controls *Shh*

expression, cannot be ruled out and future experiments must focus on this issue. Lastly, in light of the known regulatory interactions among *Hand2*, *Shh*, and *Hox* in limb development, wherein *Hand2* lies both up- and downstream of *Shh* (Zakany et al., 2004), the reported observations that *Pbx1* and *Pbx2* remain relatively unaltered in *Shh*-deficient embryos further argue against a cross regulation between *Shh* and *Pbx1* and *Pbx2* in limb development.

5.3.4 *Pbx1* and *Pbx2* hierarchical control of *Hox* spatial distribution mediates *Shh* expression in the limb

In *Pbx1/2 Mut* hindlimbs, expression was severely perturbed for all 3' and 5' *HoxA* and *HoxD* genes analyzed, especially in posterior domains, while in forelimbs, the alterations varied depending on the *Hox* paralog. These alterations occurred in mutant limbs that exhibited relatively normal early A-P patterning. Therefore, *Pbx1* and *Pbx2* act upstream of *Hox* in a manner that appears to occur independently from known molecular regulators required for the establishment of early A-P asymmetry. Furthermore, this *Hox* control occurs early, perhaps in the limb field, because expression of both 3' and 5' *HoxA* and *HoxD* are already altered at the onset of limb development.

The mechanisms by which *Pbx* hierarchically control and maintain *Hox* spatial distribution in early limb mesenchyme remain elusive. *Pbx* requirements in auto- and/or cross-regulatory interactions (Popperl et al., 1995; Popperl et al., 2000; Jacobs et al., 1999; Ferretti et al., 2000; Waskiewicz et al., 2002), or their cooperative roles with other transcription factors upstream of *Hox* (Berkes et al.,

2004; reviewed by Sagerstrom 2004; Moens and Selleri, 2006) may have bearings.

Indeed, with respect to the assertion that Pbx may be required for Hox auto-cross regulation, it cannot be excluded that Pbx might directly regulate *Hox* collinearity, given the co-expression of *Pbx1* and *Pbx2* with 3' *Hox* in the flank and early limb buds (with *Pbx3*) (compare Fig. 5.4 and Figs. 5.17 and 5.18). Accordingly, the early collinear activation of *HoxD* in the limb has been suggested to reside under the control of a 3' region called the ELCR (Spitz et al., 2001; Tarchini and Duboule, 2006). It has been demonstrated that the distance of an individual *HoxD* promoter/gene to this element regulates the A-P spatial extent and temporal onset and duration of its expression in the limb. Specifically, at the onset of bud outgrowth (E9.0-9.5), 3' *Hox* located nearest to the ELCR are activated first and have the greatest A-P distributions in the early limb field, whereas, more 5' *Hox* are transcribed later and have increasingly posterior restrictions (Tarchini and Duboule, 2006). In addition, at later days of gestation (E11-11.5) after bud formation (i.e. at the onset of autopod formation and *HoxD* "reverse" collinearity), proximal expression of 5' *Hox* is maintained and is under the same control as at earlier days.

Various molecular inputs are believed to exist in this early regulatory network (pictured in Fig. 5.29) specifically reported for the activation of 3' members via auto-regulatory networks on *Hox* gene specific promoters, and reported for the activation of *HoxD* members via distance effect studies (as described in Tarchini and Duboule, 2006). In addition, while the ELCR remains

unknown, such a regulatory region must have binding sites for activator/repressor complexes for its regulation. In this latter regard, a preliminary review of the upstream region of *Hoxd1* was conducted and several putative Pbx binding sites were identified within a specific and narrow base range (data not shown). Future studies will focus on this region as one particular genomic area that may drive *Hox* expression.

In light of this potential regulation, *HoxD* expression in *Pbx1/2 Mut* limbs is, indeed, heavily effected and corresponds to specific alterations that are predicted if ELCR function was disrupted. Specifically, *Hoxd9* and *Hoxd10* expression is posteriorly reduced across the hindlimb, while *Hoxd12* and *Hoxd13* expression is lost completely. These data are in line with those reported by Tarchini and Duboule (2006) where they demonstrated that by increasing the distance of 3' *Hox* to the ELCR, expression became delayed (i.e. activated later) and spatially posteriorized in the early limb bud. Additional evidence comes from the analyses of *Hox* expression during early autopod formation (i.e., at E11.0-11.5). Tarchini and Duboule (2006) specifically note that the most anterior extent of the proximal expression domains of 5' *Hox* are reduced in cases when the activation of *Hox* is delayed via experimentally increasing their distance to the ELCR. In *Pbx1/2 Mut* hindlimbs at E11.5, all examined *Hox* had their most anterior proximal expression domains considerably reduced in manner that became more severe, the more 5' the *Hox* gene analyzed (light shaded empty arrows in Fig. 5.19). Finally, these reductions were observed in hindlimbs that do not display alterations in cellular proliferation and cell death, indicating that

Pbx regulation of *Hox* is real and not an artifact of a known defect in cellular behavior.

Expression of *HoxD* in *Pbx1/2 Mut* forelimbs also conforms to those expected via the disruption of early *Hox* collinearity. Indeed, *Hox* expression becomes exceedingly worse the further 5' the *Hox* in the cluster, ultimately demonstrated by the complete loss of expression for *Hoxd13*. Later at E11.5, the proximal expression domains for these *Hox* genes are slightly altered spatially and slightly reduced in intensity compared to wildtype limbs. These early and late reductions are not as severe as observed in hindlimbs, a point attributed to the presence of *Pbx3* throughout forelimb bud development.

Regardless of the possibility that Pbx regulates *Hox* expression via ELCR control, Pbx known cofactor relationships with 3' Hox may have very important ramifications on auto-regulation with Hox of *HoxD* gene collinearity. Additionally, Pbx/Meis and other heterodimeric (see Chapter 3) complexes have more recently been shown to drive gene expression, leading to the possibility that multi-protein complexes drive *Hox* gene expression. However, as of this point in time, *Pbx1* and *Pbx2* (and *Pbx3*) are indeed upstream of *Hox* expression in the early limb, the very mechanisms of which must be explored in future studies.

With respect to Hox regulation of *Shh* expression, the absence of *Shh* expression in the *Pbx1/2 Mut* hindlimb ZPA, therefore, is well in keeping with the severe spatial perturbations of multiple *Hox* genes in posterior hindlimb domains. On the other hand, in the *Pbx1/2 Mut* forelimb, *Shh* regulation by *Hox* requires

Pbx1 and *Pbx2* only in part, as the reduction in *Shh* expression coincided with a less severe alteration in posterior *Hox* localization. Therefore, *Hox* localization to the forelimb ZPA appears to require additional factors, with one potential candidate being *Pbx3*, whose expression only in the forelimb partially overlaps with *Pbx1* and *Pbx2* in the mesenchyme (Di Giacomo et al., 2006).

To investigate the possibility that Hox directly regulates *Shh* expression, several analyses were performed. Indeed, several 5' HoxD proteins were shown here to bind *in vivo* to the *Shh* long-range enhancer (Lettice et al., 2003) at a gestational stage when *Shh* was expressed, but not at a later stage when *Shh* expression had waned. These results provide strong evidence in favour of the proposed direct involvement of Hox proteins in the control of early *Shh* expression (Zakany et al., 2004; Kmita et al., 2005). Furthermore, several HoxD proteins were able to activate transcription through this regulatory element in cell culture, suggesting that *Shh* expression might be, indeed, controlled in an overlapping and/or synergistic manner by various 5' Hox proteins.

In agreement with the non-essential function of Pbx2 throughout embryonic development (Selleri et al., 2004), Pbx2 was found to be bound to the *Shh*E but not able to activate or cooperate with Hox proteins in transcriptional activation through this element. The *in vivo* binding of Pbx2 to the *Shh*E is therefore functionally unessential within the *Pbx1/Pbx2-Hox-Shh* regulatory network as assessed in the cellular assay utilized. It may, however, represent a "mark" for the possible recruitment of other yet uncharacterized transcription factors, as was reported in the case of the *myogenin* promoter (Berkes et al.,

2004; reviewed by Sagerstrom, 2004). This role for Pbx may be particularly important if Pbx acts with Hox as “selector” genes (see Chapter 8).

However, before conclusions can be drawn, several essential aspects of the transcriptional activation analyses must be addressed. First, as the molecular environment of P19 cells (the cellular assay utilized) may be quite different from limb bud cells *in vivo*, the observed transcriptional activation through this *Shh* enhancer element could be considered an artifact. However, unlike limb bud mesenchymal cells, where high levels of Pbx and Hox are expressed and may interfere with reporter activity, P19 cells possess only low levels of Pbx and Hox until Retinoic Acid (RA) treatment, and therefore should be quite responsive to Pbx and Hox construct activity. In the studies conducted here, RA was not applied and therefore the P19 cell system may be a more useful tool to demonstrate the effects of Pbx and Hox on *Shh*E reporter activity. Therefore, future work may be needed to address this issue, as such is pertinent to the use of limb versus non-limb cell culture studies in developmental biology.

Second, it is possible that for Pbx2 to have a direct and significant influence on Shh transcriptional activation in the presence (or even the absence) of Hox, other partner proteins must be co-expressed with Pbx2 in these assays. Indeed, transcriptional activating complexes containing Pbx and other proteins such as Meis or Prep for example, may participate in the activation of transcription through this enhancer element. Interestingly, Meis1 and Meis2 do not co-localize with Pbx2 and Shh *in vivo* and therefore most likely are not potential candidate cofactors in this regard. Another candidate cofactor is Prep2

and while this cofactor has an expression domain that does overlap with Shh and Pbx2 (data not shown), its protein signal in the distal limb bud, as detected via immunohistochemistry, is cytoplasmic and not nuclear and therefore, most likely does not aid directly in Shh transcriptional activation. Other, as of yet, unknown cofactors may also aid in transcriptional activation with Pbx2, but currently they remain the topic of future research. Regardless of these criticisms, the data presented above, are important as they indicate that Pbx2 alone cannot activate transcription and that if complexes are critically important for Shh activation, they must involve Hox. Overall, these data indicate the primary role of *Pbx2* is at this time exerted in concert with *Pbx1* in hierarchically controlling *Hox* spatial expression.

The findings that multiple Hox proteins are recruited to the *Shh* limb enhancer are consistent with the observation that single deletions of specific *Hox* genes do not produce dramatic phenotypes (Capecchi, 1997) resembling the loss of *Shh*. Indeed, the *Pbx1/2 Mut* mouse model reveals that multiple *Hox* transcripts must synergistically act *in vivo* in the ZPA for proper and sustained *Shh* activation, as corroborated by previous reports on mice with *Hox* cluster deletions (Zakany et al., 2004; Kmita et al., 2005). The findings that mis-expression of single *Hox* genes (*Hoxb8* or *Hoxd12*) in anterior limb domains caused ectopic *Shh* activation (Charite et al., 1994; Stratford et al., 1997; Knezevic et al., 1997), are not in contrast with these findings, given the relaxed DNA-binding specificity of Hox proteins and the high expression levels obtained

in mis-expression experimental settings. Overall, *Pbx1* and *Pbx2*-dependent *Hox* spatial perturbation in the posterior limb appears to have an equally drastic effect on *Shh* onset as does the disruption of early temporal *Hox* collinearity (Zakany et al., 2004) and the complete ablation of HoxA/HoxD function (Kmita et al., 2005). However, the possibility that additional triggers and/or inputs might concomitantly function *in vivo* in a multifaceted control of *Shh* transcription cannot be ruled out.

5.3.5 Proximal mesenchymal interactions of *Pbx1* and *Pbx2* may drive mouse limb outgrowth

As compound *HoxA/HoxD* mutants possess limb truncations (Kmita et al., 2005) and *Hox* genes are known to synergistically pattern all limb elements (Davis et al., 1995; Davis and Capecchi, 1996; Fromental-Ramain et al., 1996a-b; Wellik and Capecchi, 2003), they govern limb outgrowth. Similarly, as *Pbx1* and *Pbx2* genetic interactions likely occur in early limb field mesenchyme, where they co-localize, they appear to have critical bearings on overall limb outgrowth, especially in view of their control of *Hox* spatial distribution. Accordingly, stylopod, zeugopod, and autopod elements were grossly mis-patterned even at the onset of mesenchymal condensation, suggesting that early *Hox*-dependent patterning alterations underlie the *Pbx1/2 Mut* defects. Furthermore, compound *Pbx1*;*Pbx2* homozygous loss results in the absence of limbs, suggesting that a complete disruption of the *Hox* code occurs in early limb development. In light of the Early Specification Model (ESM) for limb patterning (Dudley et al., 2002), it is therefore suggested that interactions of *Pbx* genes early in outgrowth may drive

specification and patterning of distal limb elements. Limb mesenchyme-specific *Pbx* inactivation will test this scenario (see Chapter 6 for discussion).

The analyses of skeletal development of the fore- and hindlimbs of *Pbx1/2 Mut* embryos strongly demonstrate that skeletogenesis is disrupted prior to mesenchymal condensation formation. As *Hox* genes are expressed before and throughout skeletogenesis and compound knockouts of *Hox* gene paralogs produce dramatic yet compartmentalized alterations in the skeleton, their roles in the etiology of *Pbx1/2 Mut* fore- and hindlimb development must be addressed. In this manner, the specific skeletal abnormalities observed in *Pbx1/2 Mut* limbs can also be understood via the interpretation that *Pbx1/2* mesenchymal expression creates an overlapping code that may influence Hox both as upstream regulators and also as potential ancillary cofactors. This viewpoint is specifically interesting considering that *Hox* expression and skeletal morphology are both grossly altered in *Pbx1/2 Mut* embryos in different ways in fore- and hindlimbs.

With respect to stylopod development, the lack of well-defined wildtype-like expression for *Hoxa9-11* and *Hoxd9-11* in the developing *Pbx1/2 Mut* limb from E9.5-11.5 indicates that cells within proximal domains may not have been subjected to definitive gradients of Hox signals. Furthermore, the strong nuclear localization of Pbx1 in the proximal anterior limb field with Hoxa9, Hoxd9, Hoxa10, and Hoxd10 suggest a basis for their interaction and involvement in the development of the humerus and femur. In fact, even single *Pbx1*$^{-/-}$ embryos form misshapen humeri and *Hoxa9;Hoxd9* double compound mutants possess

alterations in humeral shaft shape. Ablations of *Hoxa10*;*Hoxd10* also result in patterning defects more distal in these elements (Carpenter et al., 1997; Chen and Capecchi, 1997). Interestingly, when compared to the humerus, the morphology of the femur in these compound *Hox* mutants was not as affected, a point that may have resulted from the overlapping and unique hindlimb-specific expression of *Hoxc9-11* (Tarchini and Duboule, 2006). In *Pbx1/2 Mut* limbs, throughout all gestational days analyzed, *Hox9* and *Hox10* paralogs were significantly altered in both fore and hindlimbs. In forelimbs, the unique and highly expanded *Hoxa9* and *Hoxd9* expression observed during early forelimb bud formation (i.e., E9.5 and 10.5)(Fig. 5.18) and their subsequent dysregulation later (i.e., E11.5)(Fig. 5.20) coincides well with the strong A-P displacement/curvature of the humeral shaft (Fig. 5.2C). In hindlimbs, expression of *Hoxa9* and *Hoxd9* were different in that they were severely down-regulated throughout early limb development (Fig. 5.17) and accordingly, femoral size and morphology were truncated and indistinct (Fig. 5.2C). Overall, the distortion of the humerus and truncation of the femur may be indicative of the differential distribution of *Hox* expression throughout both limb buds and over time.

The altered morphology of both elements of the *Pbx1/2 Mut* forelimb zeugopod (i.e., radius and ulna)(Fig. 5.2C) may correspond to earlier *Hoxd11* and *Hoxd12* expression (E10.5 and E11.5) pattern changes in the mutant (Figs. 5.18 and 5.20). Normally, at E10.5 both *Hoxd11* and *Hoxd12* overlap in the posterior domain of the limb bud while at E11.5 *Hoxd11* and *Hoxd12* are

expressed in the forelimb differently, with the former present in two separate proximal and distal domains and the latter present only distally. During these two critical periods, both *Hox* are believed to be involved in patterning of zeugopodial elements and this role is shown to be the result of the early *Hox* collinearity (Tarchini and Duboule, 2006; Tarchini et al., 2006). In fact, compound mutant embryos for these particular homologs possess drastic alterations in radii and ulnae (Davis and Capecchi, 1994); specifically, both elements show strong size reductions as their cartilaginous rudiments form but fail to grow longitudinally. In the *Pbx1/2 Mut* forelimb, the presence of both the radius and ulna may reflect that these Hox paralogs were present, although somewhat altered early in development. Of course, ulna morphology in the *Pbx1/2 Mut* forelimb has been discussed in view of *Shh* absence (also see below).

In the *Pbx1/2 Mut* hindlimb (Fig. 5.2C), the lack of a fibula appears directly mediated by *Shh* absence as supported by the phenotype seen in *Shh*-deficient mutants. More recently, fate-mapping studies by Harfe et al. (2004), Scherz et al. (2004), and Ahn and Joyner (2004) demonstrate that cells that at one time express *Shh* expand and give rise to the distal posterior structures of the zeugopod such as the distal ulna and fibula (see Chapter 3). Interestingly, even *Shh*-deficient embryos possess rudimentary proximal zeugopodial cartilages and therefore complete fibular loss in *Pbx1/2 Mut* hindlimbs may result from the simultaneous and severe alteration of *Shh* as well as *Hoxd11* and *Hoxd12* expression. Specifically, *Hoxd11* expression was severely down-regulated at

E10.5 and E11.5, while *Hoxd12* was absent at E10.5 and only residual at E11.5 (Figs. 5.17 and 5.19). In addition, as discussed above, the anterior extent of the proximal expression domains were quite reduced. Therefore, it is quite possible that cells giving rise to proximal fibula condensation require sustained Hox presence. Interestingly, the tibia, the anterior oriented zeugopodial element appeared relatively normal in morphology despite alterations in *Hox* expression, suggesting that tibia condensation formation is subjected to additional factors and/or may be more sensitive to Hox presence (i.e. only low Hox levels are essential for their formation) than other structures. Clearly, more research is needed to understand the etiology of tibia condensation formation.

The E13.5 *Pbx1/2 Mut* forelimb autopod possessed most of its skeletal elements although many were dysmorphic and lacked true terminal phalanges (Fig. 5.2C). Those elements that were completely missing included the metacarpals and phalanges of digit 1 and 5. At early days (i.e., E11.5) there were minimal differences in *Hox* gene expression as compared to wildtype littermates for most *Hox* paralogs analyzed, although there are some important differences (Fig. 5.20). For example, there was a reduction in the anterior domain of *Hoxd11-13* expression and a coincident and complete loss of digit 1 formation, suggesting that anterior Hox function may critically underlie anterior digit condensation formation. Compound mutants for *Hoxa13/Hoxd13*, *Hoxd10-13,* and *HoxA/HoxD* all demonstrate severe alterations in forelimb autopod formation including the loss of well defined metacarpal and phalangeal rays for digit 1 and 5. Digit 5 reduction, as mentioned, appears to be a direct

consequence of *Shh* absence. Alternatively, and as mentioned above, Hox and Shh-independent effects may be attributed to digit 1 loss.

Conversely, in the *Pbx1/2 Mut* hindlimb, the autopod was practically missing, with the exception of one residual condensational ray (black arrow head in Fig. 5.2C). Concordantly, *Hoxd13* expression at E10.5 was absent and only remained as a small stub along the posterior domain of the limb at E11.5 (Figs. 5.17 and 5.19). These findings are in agreement with those reported in *Shh*-deficient mice, where *Hoxd13* is reduced similarly. This expression pattern may reflect a partial loss of mesoderm in the anterior and medial region of the autopod and/or a real down-regulation of this gene in the anterior limb. With respect to the latter, *Hoxd10, Hoxd11*, and *Hoxd12* are also reduced anteriorly, although not entirely absent, as was reported for their expression in *Shh*-deficient limbs. In this manner, their ameliorated expression pattern when compared to that seen in *Shh*-deficient embryos, may indeed reflect low level transient Shh-activity and, therefore, highlight the important role that Shh has on 5' *HoxD* gene "reverse" collinear activation (as discussed above). On the other hand, as noted above, perhaps the loss of anterior expression of 5' *HoxD* is more directly related to alterations in cell proliferation or cell death. Both *Hox* and *Shh* have been implicated in influencing cell proliferation (Duboule, 1994), although analyses of cell proliferation in the *Pbx1/2 Mut* limb did not reveal any significant perturbation in cell proliferation (Fig. 5.26). Therefore, simultaneous loss of *Shh* and reduced 5' *Hox* gene expression does not appear to have a severe influence of proliferation in the *Pbx1/2 Mut* limb and in this manner, may not explain the

observed loss of 5' *HoxD* expression anteriorly. Interestingly, while *Shh*-deficient limbs display marked apoptosis, apoptosis in *Pbx1/2 Mut* hindlimbs was only minimal and may reflect the transient *Shh* wave of expression (Fig. 5.27). In addition, no severe anterior zone of apoptosis was identified in the *Pbx1/2 Mut* hindlimb from E9.5 through E11.5 that could explain the reported *Hox* loss anteriorly and therefore, there appears to be no real loss of cellular tissue in that region. Overall, these data highlight the role that *Shh* has on regulating *5'HoxD* gene "reverse" collinearity and in this regard mediating the phenotype observed *in Pbx1/2 Mut* hindlimbs.

Despite their similarities to *HoxA/HoxD* and *Shh* mutant phenotypes, the *Pbx1/2 Mut* limb defects are indeed more severe than the former. Therefore, these results do not completely negate other concomitant scenarios involving disruptions of different networks that govern limb patterning. For example, as suggested in recent studies (Kmita et al., 2005), *Hox* genes may sustain distal limb bud growth by ensuring proper AER function. Similarly, *Pbx1* and *Pbx2*, via spatial control of *Hox*, may allow for the proper AER function required to maintain *Shh* expression. Three factors, however, argue in favor of the primary role of *Pbx1* and *Pbx2* in *Shh* control, independent of their potential AER function (as discussed in Chapter 6): (1) the relatively normal *Pbx1/2 Mut* hindbud morphology, AER morphology, and observed AER gene expression prior to *Shh* onset; (2) the finding that ectopic *Hox* expression triggers *Shh* transcription (Charite et al., 1994; Stratford et al., 1997; Knezevic et al., 1997; Zakany et al.,

2004); and (3) the strong resemblance of *Pbx1/2 Mut* hindlimb phenotype to those specifically reported in *Shh* (Chiang et al., 2001; Kraus et al., 2001) as well as *HoxA/HoxD* absence (Kmita et al., 2005). However, the roles of *Pbx* in limb development may resemble those in spleen genesis, where *Pbx1* hierarchically controls all known pathways required for spleen development (Brendolan et al., 2005). The next chapter focuses on some of these additional and potential roles.

5.4 Summary of *Pbx/Hox/Shh* interaction in the limb mesenchyme and the skeletal defects reported *in Pbx1/2 Mut* limbs

As demonstrated in Fig. 5.30, *Pbx1* and *Pbx2* appear to have very early upstream effects on the expression of many genes involved in limb development. What appears to be most critical in mediating the limb phenotype, specifically in lieu of Pbx function in mesenchyme, is their control of early *Hox* expression. Pbx control of *Hox* in turn mediates *Shh* expression which leads to severe alterations in distal limb patterning. At the same time, disruption of early *Hox* expression and/or the loss of Pbx as potential cofactors with Hox, leads to skeletal alterations from the scapula/pelvis through to the autopod. Details of these interactions are discussed in the legend of Fig. 5.30 and also in subsequent chapters.

Figures

Figure 5.1. Gross morphology of *Pbx1/2* compound mutant embryos.

(A) At E10.25 (and E10.5), *Pbx1*$^{-/-}$;*Pbx2*$^{+/-}$ (Mut) embryos exhibit abnormal morphology and appear delayed. Their forelimbs are P-D shortened and A-P dysmorphic, while their hindlimbs appear relatively normal versus wildtype (WT). *Pbx1*$^{-/-}$;*Pbx2*$^{-/-}$ embryos are severely delayed versus WT, exhibiting striking morphological abnormalities, including the lack of limbs. All WT and mutant limbs are enlarged on the right hand-side of the embryos, some outlined by dashed lines. Also, both WT and Mut *hindlimbs* are shown at two gestational days in adjacent enlargements, while *Pbx1*$^{-/-}$;*Pbx2*$^{-/-}$ limbs are shown at E11 to demonstrate rudimentary forelimb bud formation (lower magnification). (B) At E12.5, forelimbs of Mut embryos developmentally improve but still remain anterior-posteriorly dysmorphic and proximal-distally truncated, while hindlimb buds begin to display the complete loss of distal mesenchyme and a severely anterior-posteriorly reduced autopod. (C) At E13.5, Mut embryos are smaller than WT with abnormal morphology. Their forelimbs display shorter zeugopodia (short light shaded arrow) versus WT (long light shaded arrow) and dysmorphic autopodia (short dark shaded arrow) versus WT (long dark shaded arrow), whereas their hindlimbs exhibit rudimentary autopodia (short light shaded arrow) versus WT (long light shaded arrow). Proximal (left); anterior (top); FL, Forelimb; HL, Hindlimb.

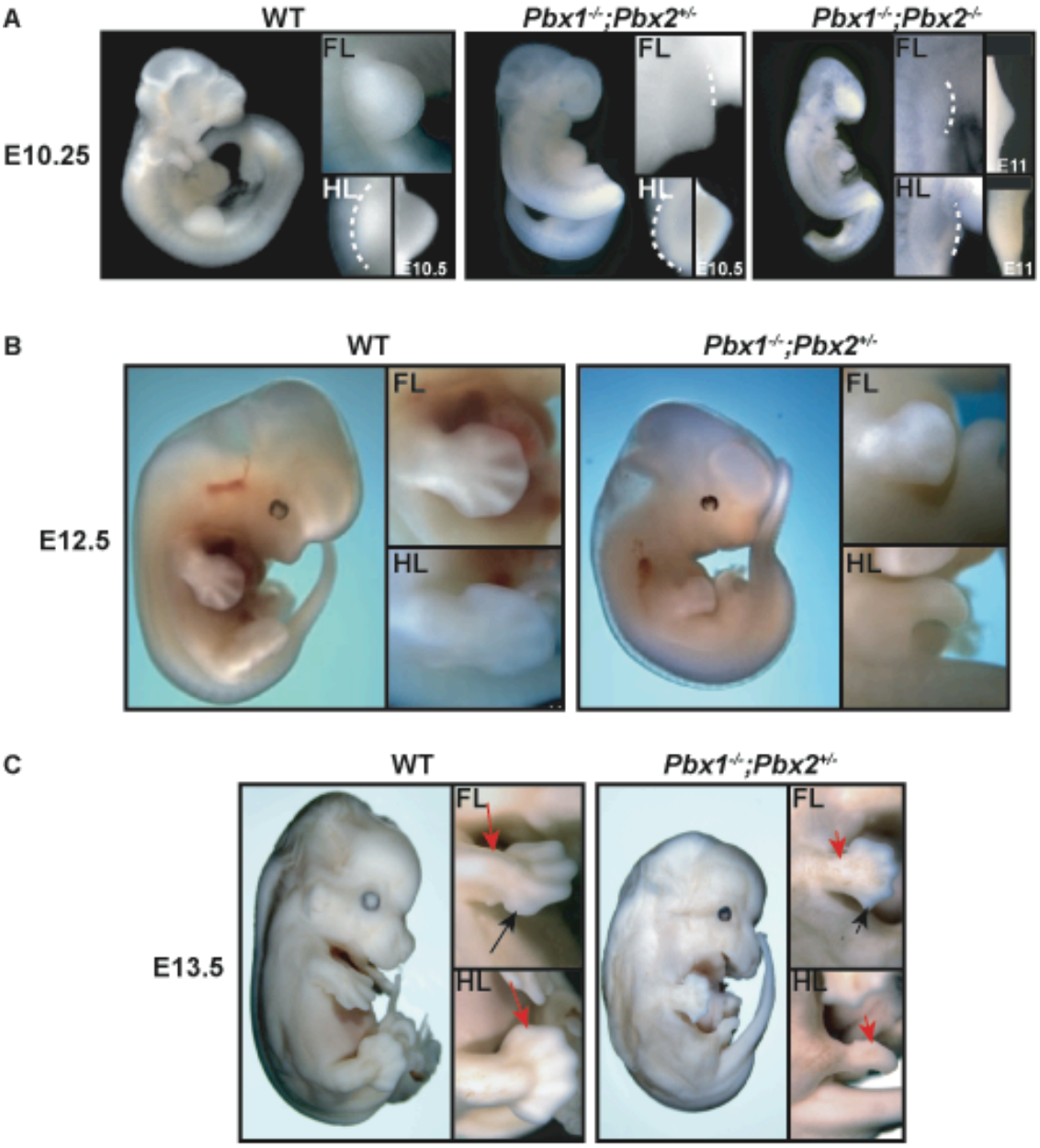
A
WT
Pbx1-/-;Pbx2+/-
Pbx1-/-;Pbx2-/-
E10.25
FL
HL
E10.5
E11
B
WT
Pbx1-/-;Pbx2+/-
E12.5
FL
HL
C
WT
Pbx1-/-;Pbx2+/-
E13.5
FL
HL

Figure 5.2. Limb skeletal morphology of *Pbx1/2* compounds embryos.

(A) At E12.5, *Sox9* expression indicates that *Pbx1*$^{-/-}$;*Pbx2*$^{+/-}$ (Mut) forelimb mesenchymal condensations for digit 1 (empty light shaded arrowhead) and 5 (empty dark shaded arrowhead) are rudimentary versus WT. In Mut hindlimbs, digit (empty light shaded arrowhead) and fibula condensations (empty dark shaded arrowhead) are absent versus WT (dark shaded arrow). (B) At E12.5, unlike WT (light shaded arrow), Mut scapular anlagen is reduced (light shaded arrowhead) and the humerus dysmorphic with a hypertrophic anlagen reminiscent of a deltoid tuberosity (dark shaded arrowheads). In Mut, the pelvis is virtually absent except for one element (empty dark shaded arrowhead) that may be a rudimentary ischium versus WT (long dark shaded arrow). (C) At E13.5, unlike WT (light shaded arrow), Mut scapula (inset) is dysmorphic (light shaded arrowhead) and the humeral head is fused to it and duplicated medially (double dark shaded arrowhead), more severely than in *Pbx1*$^{-/-}$;*Pbx2*$^{+/+}$ mutants (arrowheads). In Mut hindlimbs, only a rudimentary anlagen reminiscent of an ischium (open dark shaded arrowhead) remains fused to the dysmorphic femur (light shaded arrow), more severely than in *Pbx1*$^{-/-}$;*Pbx2*$^{+/+}$ mutants (arrowheads). The Mut forelimb zeugopod (ra and ul) appears shortened (short dark shaded arrows), while the Mut hindlimb zeugopod (ti and fi) lacks the fibula (open light shaded arrowhead), versus WT (light shaded arrow). The Mut forelimb autopod exhibits three central digits, with digit 1 (open light shaded arrowhead) and 5 (open dark shaded arrowhead) absent or rudimentary. The Mut hindlimb autopod lacks all digits (dashed light shaded rectangle) except one rudimentary ray (open dark shaded arrowhead; inset) compared to WT. fe, femur; fi, fibula; hu, humerus; pg, pelvic girdle; ra, radius; sc, scapula; ti, tibia; ul, ulna.

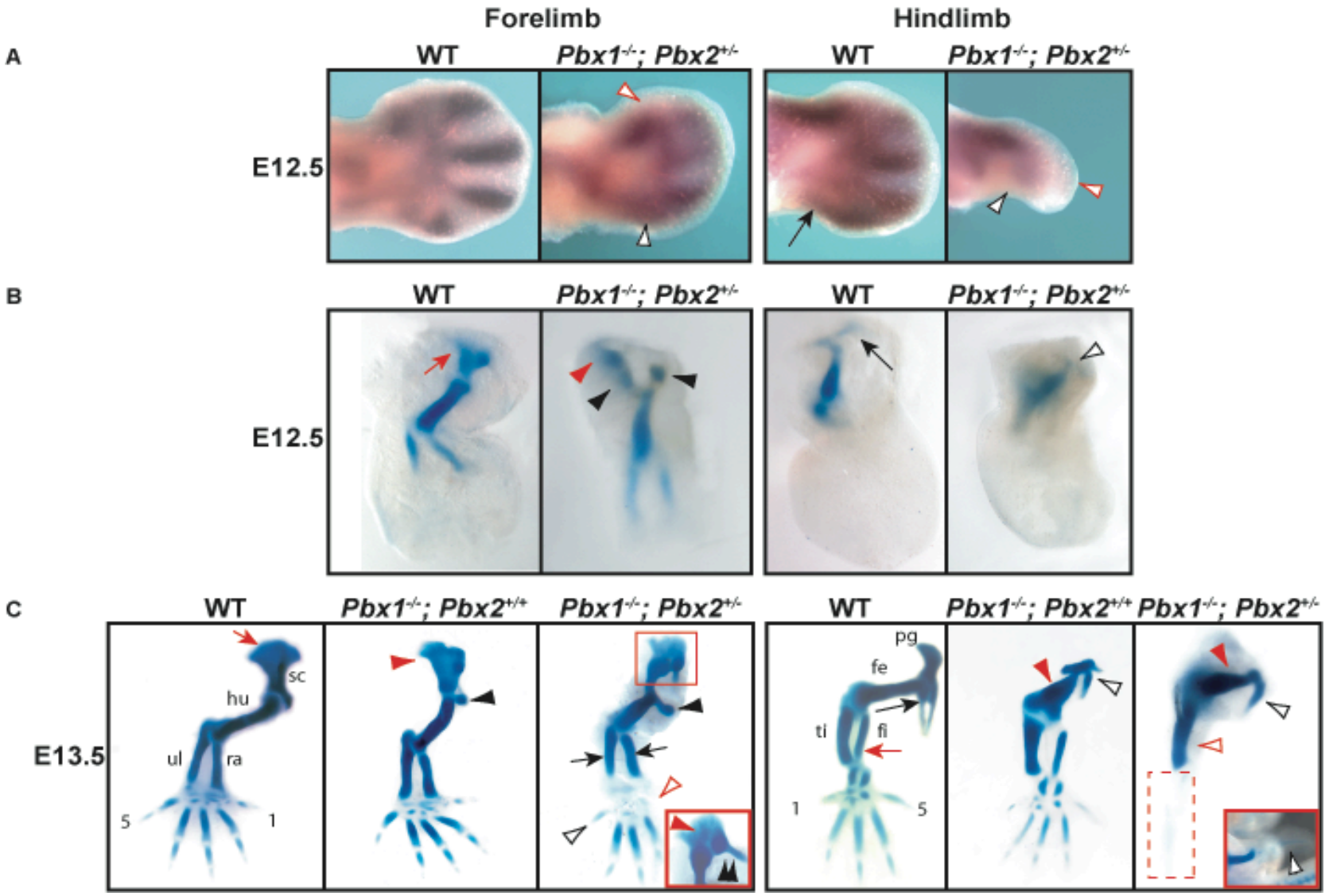
Forelimb
Hindlimb
A
WT
Pbx1-/-; Pbx2+/-
WT
Pbx1-/-; Pbx2+/-
E12.5
B
WT
Pbx1-/-; Pbx2+/-
WT
Pbx1-/-; Pbx2+/-
E12.5
C
WT
Pbx1-/-; Pbx2+/+
Pbx1-/-; Pbx2+/-
WT
Pbx1-/-; Pbx2+/+
Pbx1-/-; Pbx2+/-
E13.5
sc
hu
ul
ra
5
1
pg
fe
ti
fi
1
5

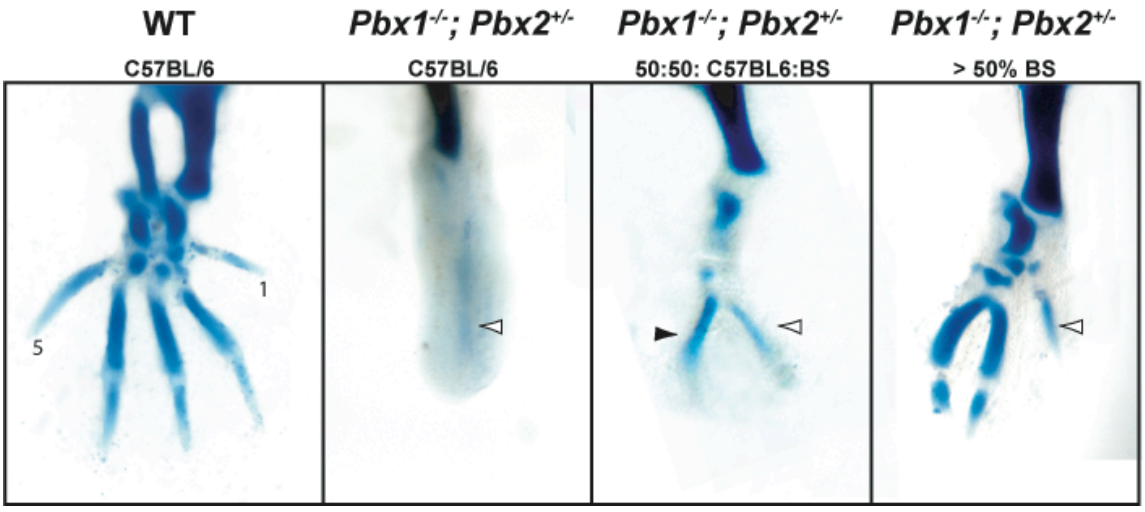

Figure 5.3. Amelioration of the *Pbx1*$^{-/-}$;*Pbx2*$^{+/-}$ hindlimb phenotype on increasingly Blackswiss genetic backgrounds.

On a C57BL/6 genetic background, only one rudimentary digital ray forms in the *Pbx1*$^{-/-}$;*Pbx2*$^{+/-}$ (Mut) hindlimb (empty dark shaded arrowhead). However, as the genetic background of these mutants is comprised of equal percentages of Blackswiss (BS) and C57BL/6, additional digits begin to form, first with the addition of digit 3 (dark shaded arrowhead) followed by digit 2 (empty dark shaded arrowhead). Finally, as the percentage of Blackswiss exceeds that of C57BL/6 in the mutants, additional digits (empty dark shaded arrowhead, right panel) possibly representing digit one, form. These data call into question whether the rudimentary digital ray that forms on a pure C57BL/6 genetic background is indeed digit 1.

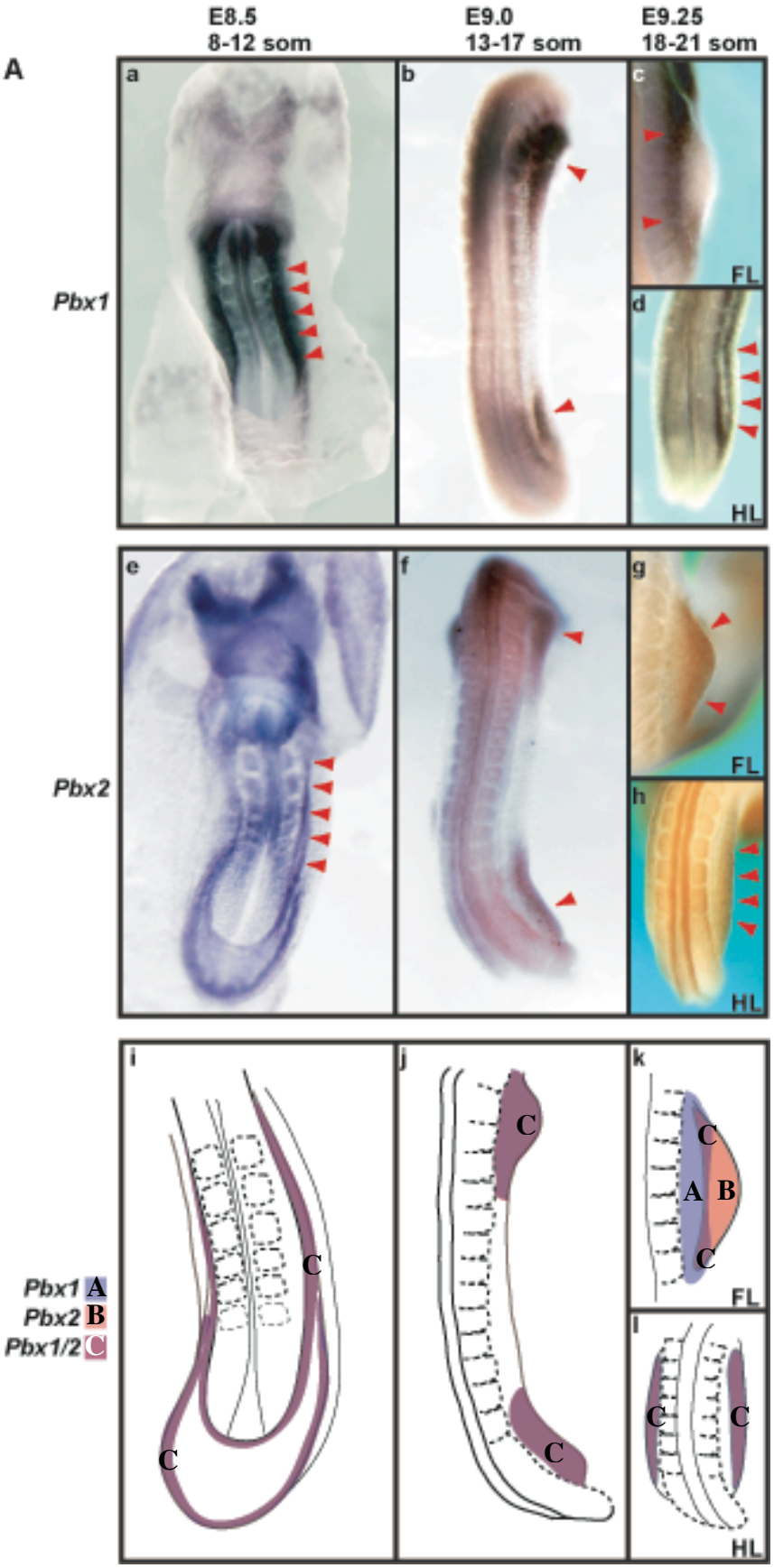
A
E8.5
8-12 som
E9.0
13-17 som
E9.25
18-21 som
a
b
c
d
FL
HL
Pbx1
e
f
g
h
FL
HL
Pbx2
i
j
k
l
C
A
B
C
C
C
C
C
C
C
FL
HL
Pbx1 A
Pbx2 B
Pbx1/2 C

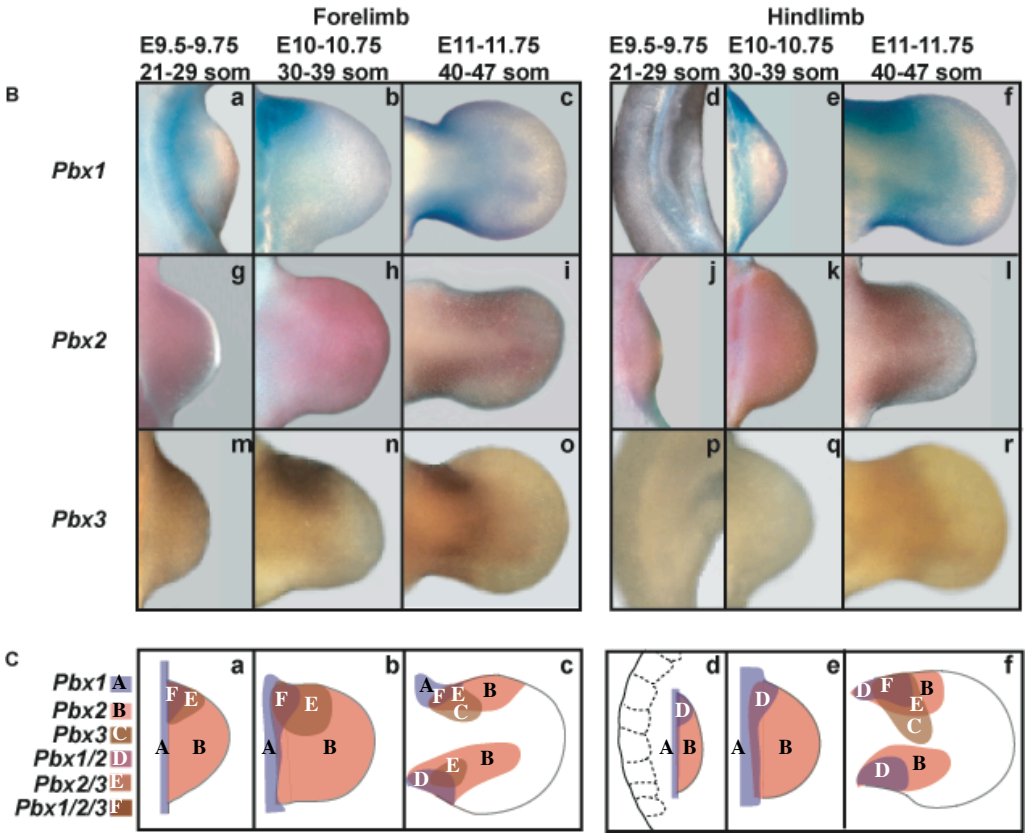

Figure 5.4. *Pbx1/2/3* expression during limb development.

(A)(a,e,i) At E8.5, *Pbx1* (a) and *Pbx2* (e) co-localize (i) in lateral plate-intermediate mesoderm (light shaded arrows). (b,f,j) At E9, *Pbx1* (b) and *Pbx2* (f) co-localize (j) in the early limb fields (light shaded arrows). (c,g,k) At E9.25, while overlapping proximally (k), *Pbx1* (c) and *Pbx2* (g) forelimb expression domains become mostly complementary, being proximal and distal, respectively (light shaded arrows). (d,h,l) At E9.25, *Pbx1* (d) and *Pbx2* (h) hindlimb expression domains remain overlapping (l) (light shaded arrows). (B) At E9.5-10.75, *Pbx1* (a-b; d-e) is expressed in proximal forelimbs and hindlimbs and mostly anteriorly, while *Pbx2* (g-h; j-k) distally and throughout the limb. Contemporaneously, *Pbx3* (m-n; p-q)) is only expressed proximal and anteriorly in forelimbs and not at all in the hindlimbs. At E11-11.75, *Pbx1* (c, f) is still expressed proximally in limbs, but localized anteriorly and posteriorly in the mesenchyme proximal to the autopod. Similarly, *Pbx2* (i,l) expression becomes restricted to this domain, albeit more broadly. *Pbx3* (o,r) is also expressed in the similar domains in the forelimbs and is only beginning to be expressed in the hindlimbs at this day. (C) Diagrams depicting dynamic expression of *Pbx1*, *Pbx2,* and *Pbx3;* and overlapping domains of all three *Pbx* at different gestational days (a-f). These schemata represent summaries of the expression patterns present at the gestational time-points indicated by the somite range at the top of each panel. See text for explanation. Proximal (left); anterior (top); FL, Forelimb; HL, Hindlimb; Som, Somites.

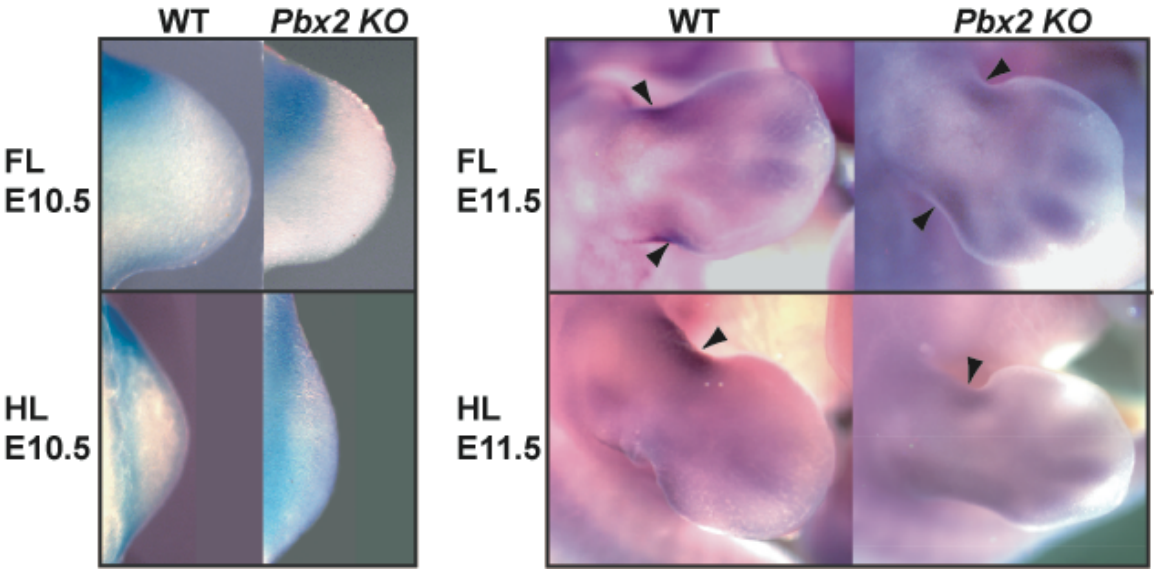

Figure 5.5. *Pbx1* expression in Wildtype (WT) and *Pbx2*$^{-/-}$ (KO) limbs.

Pbx1 expression remains mostly unchanged in E10.5 and E11.5 *Pbx2* KO limbs. Black arrowheads indicate expression. Proximal (left); anterior (top); FL, Forelimb; HL, Hindlimb.

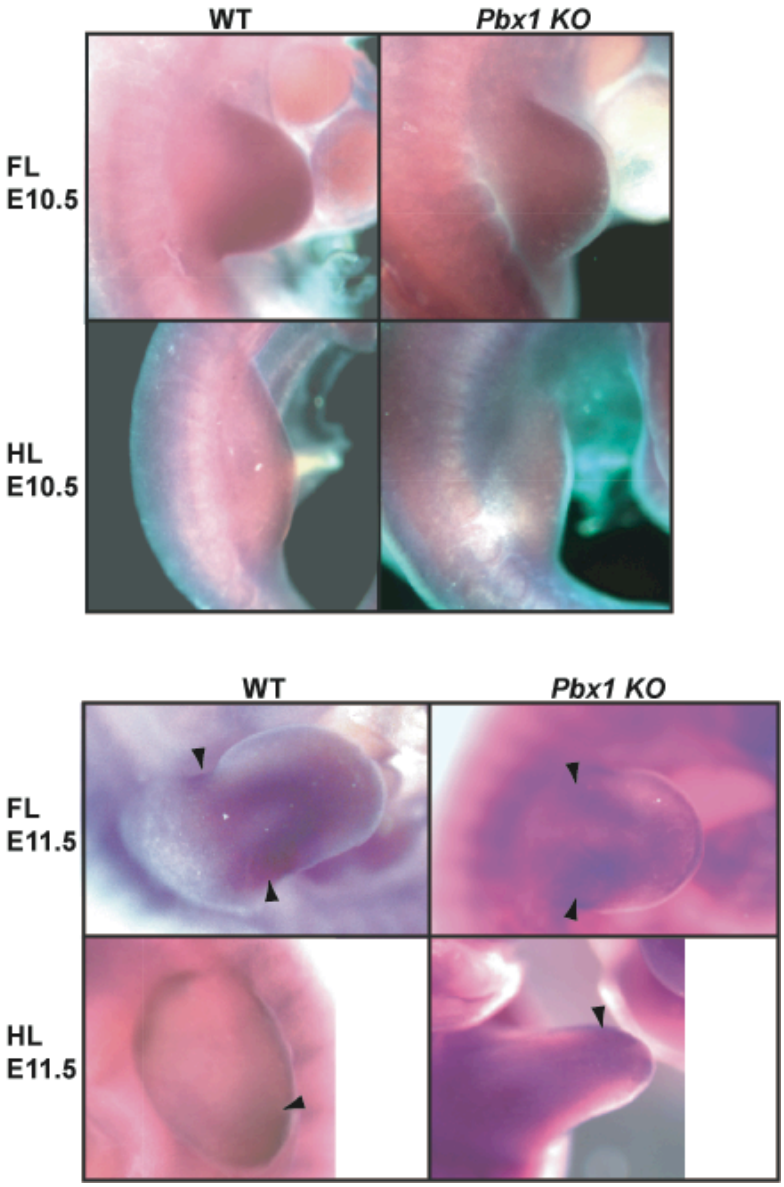

Figure 5.6. *Pbx2* expression in Wildtype (WT) and *Pbx1*$^{-/-}$ (KO) limbs.

Pbx2 expression remains mostly unchanged in E10.5 and E11.5 *Pbx1* KO limbs. Black arrowheads indicate expression in the lower panel. Proximal (left); anterior (top); FL, Forelimb; HL, Hindlimb.

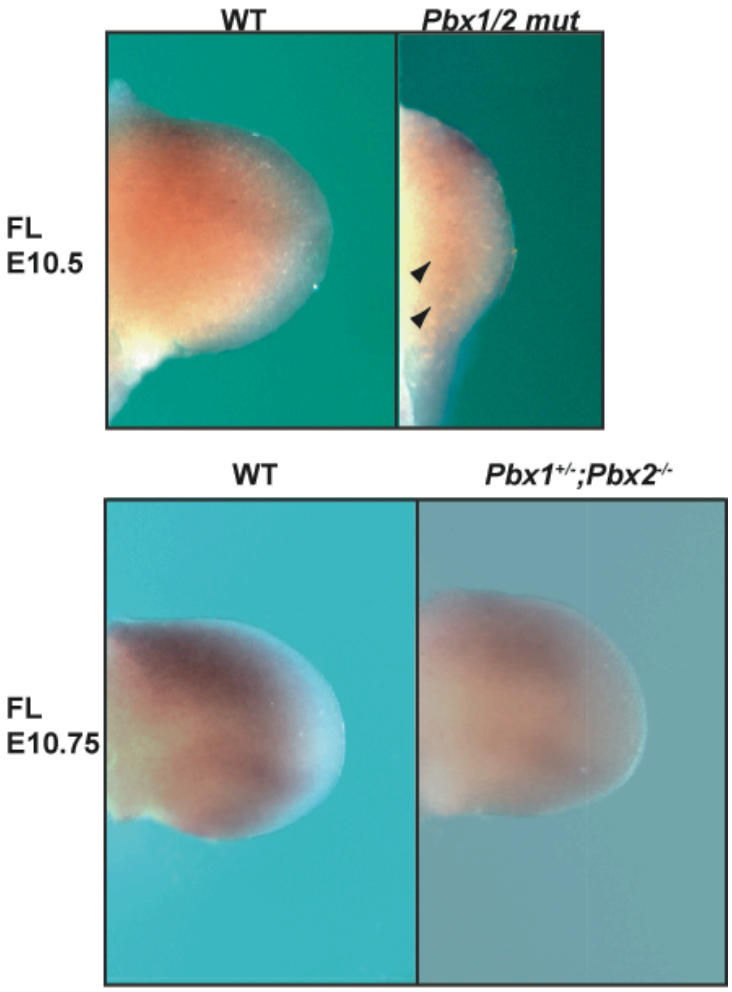

Figure 5.7. *Pbx3* expression in Wildtype (WT) and *Pbx1*$^{-/-}$;*Pbx2*$^{+/-}$ (*Pbx1/2 Mut*) and *Pbx1*$^{+/-}$;*Pbx2*$^{-/-}$ forelimbs.

Pbx3 expression is posteriorized along a proximal strip of mesenchyme in the forelimb bud of E10.5 *Pbx1/2 Mut* embryos. However, in the reciprocal genotype, its expression remains mostly unchanged at E10.75 in forelimbs. Black arrowheads indicate expression. Proximal (left); anterior (top); FL, Forelimb; HL, Hindlimb.

Figure 5.8. Mesenchymal gene expression in *Pbx1*$^{-/-}$;*Pbx2*$^{+/-}$ (Mut) limbs.

(A) Despite the dysmorphology of the Mut forelimb bud, mesenchymal gene expression remains relatively unperturbed in Mut forelimbs at and directly after *Shh* onset. *Alx4* and *Hand2* are relatively unperturbed in Mut forelimbs at *Shh* onset, indicating that until E10.5 their mesenchyme is rather normally patterned anteriorly to posteriorly. *Gli3* has a slight posteriorization of its signal, potentially reflecting the reduced Shh signaling at this time-point. *Twist* expression remains anterior although the entire Mut forelimb bud is dysmorphic. (B) *Alx4*, *Hand2*, *Gli3,* and *Twist* are relatively unperturbed in Mut hindlimbs at *Shh* onset, indicating that until E10.5 their mesenchyme is rather normally patterned anteriorly to posteriorly. Proximal (left); anterior (top); FL, Forelimb; HL, Hindlimb.

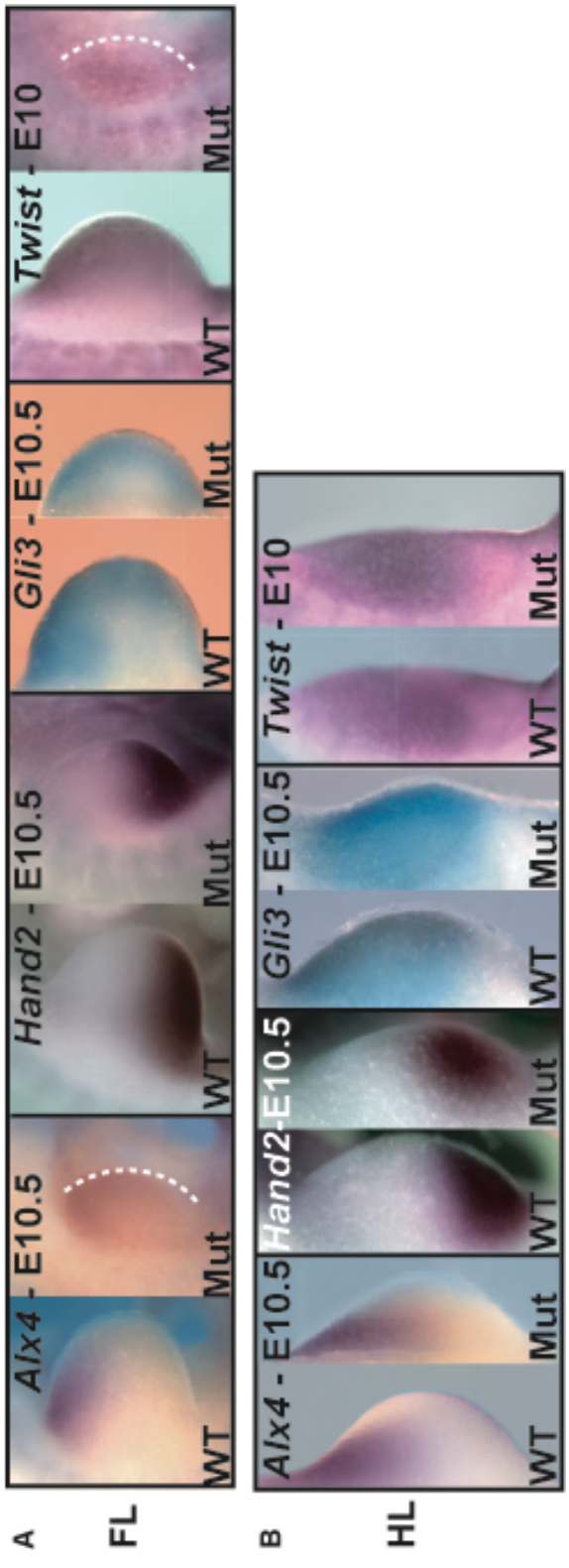
A
FL
Alx4 - E10.5
WT
Mut
Hand2 - E10.5
WT
Mut
Gli3 - E10.5
WT
Mut
Twist - E10
WT
Mut
B
HL
Alx4 - E10.5
WT
Mut
Hand2-E10.5
WT
Mut
Gli3 - E10.5
WT
Mut
Twist - E10
WT
Mut

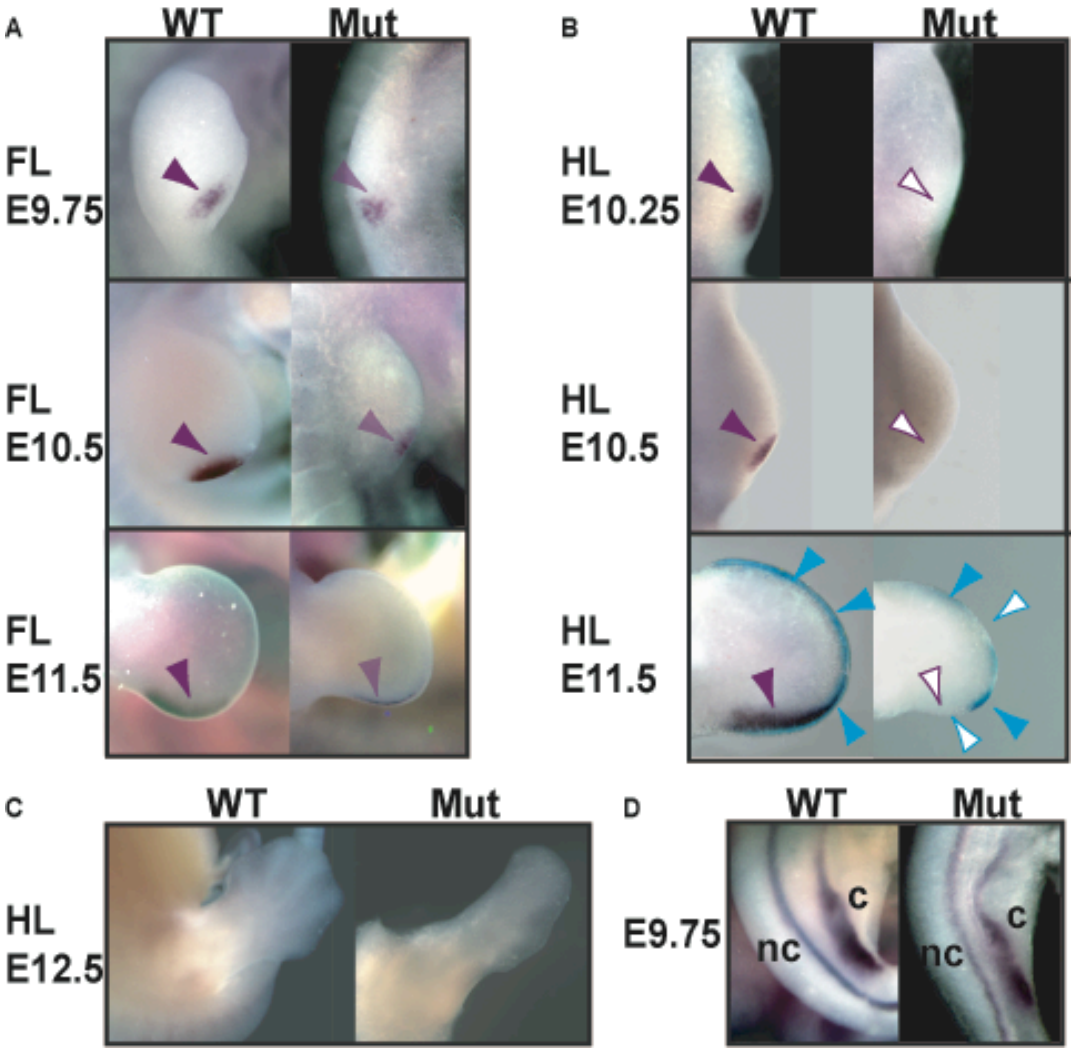

Figure 5.9. Expression of *Shh* in *Pbx1*$^{-/-}$;*Pbx2*$^{+/-}$ (Mut) embryos.

(A) *Shh* expression is present throughout forelimb development in Mut embryos, albeit reduced, suggesting that *Shh* absence is hindlimb-specific. Dark shaded arrows indicate normal expression while light shaded arrows indicate reduced expression. (B) *Shh* expression is absent throughout Mut hindlimb development, as represented at E10.5 and E11.5. At E11.5, *Shh* absence (empty dark shaded arrowhead) in Mut hindlimbs is associated with a similar and expected alteration in *Fgf8* expression (empty light shaded arrowheads), versus WT hindlimbs (normal *Shh* expression indicated by solid dark shaded arrowhead and *Fgf8* by light shaded arrowheads). (C) *Shh* expression is not delayed as E12.5-12.75 Mut hindlimbs lack *Shh* as do WT controls. (D) Normal *Shh* expression in Mut cloaca (c) and notochord (nc) demonstrates that the lack of *Shh* is not global in the absence of *Pbx1* and *Pbx2* and that the posterior region that gives rise to hindlimb buds develops normally. (B) Proximal (left); anterior (top); c, cloaca; FL, Forelimb; HL, Hindlimb; nc, notochord.

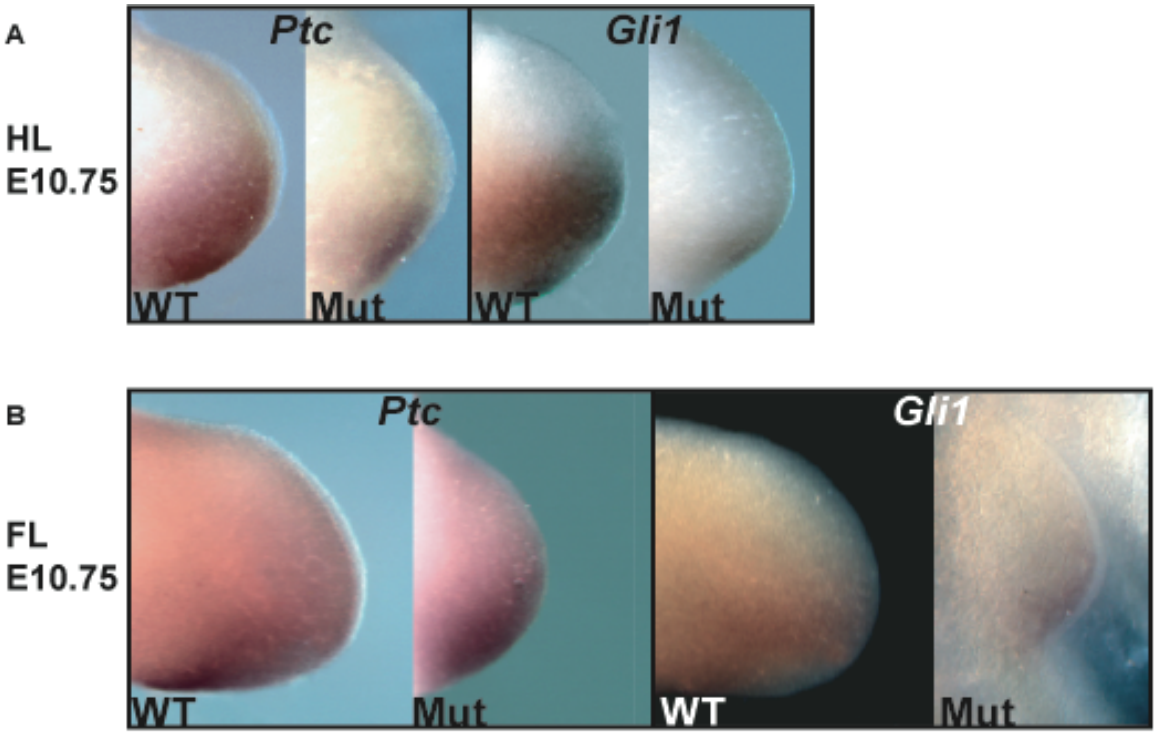

Figure 5.10. Expression of *Ptc and Gli1* in *Pbx1*$^{-/-}$;*Pbx2*$^{+/-}$ (Mut) limbs.

(A) Albeit reduced, *Ptc* and *Gli1* are present at E10.75 in Mut hindlimbs suggesting minimal and transient *Shh* activity. (B) Forelimb expression of *Ptc* and *Gli1* is also reduced in Mut but persists well after *Shh* onset at E9.75. Proximal (left); anterior (top); FL, Forelimb; HL, Hindlimb.

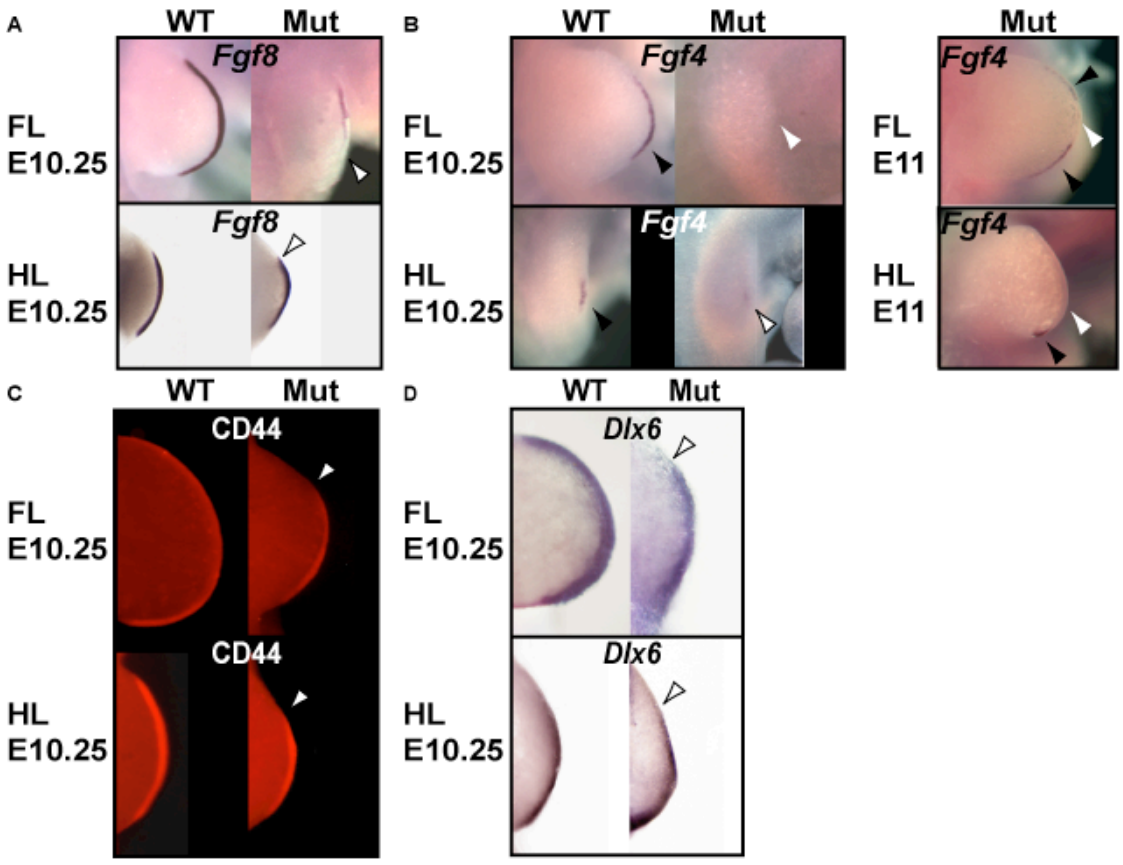

Figure 5.11. Expression of AER markers in *Pbx1*$^{-/-}$;*Pbx2*$^{+/-}$ (Mut) limbs.

(A) *Fgf8* expression is reduced posteriorly in Mut forelimbs and anteriorly in Mut hindlimbs at E10.25, the latter that indicates that posterior AER signaling remains intact at *Shh* onset. (B) At E10.25, *Fgf4* expression is severely altered in both forelimbs and hindlimbs, although in the latter, a minimal and transient signal can be detected indicating an initial *Shh* wave. At E11, *Fgf4* expression is stronger in Mut forelimbs except for a central distal reduction while in hindlimbs only a minimal posterior expression remains. These findings support the observations that *Shh* expression in the forelimbs commences while in hindlimbs it is minimal and transient. (C) The relatively preserved CD44 distribution in E10.5 Mut limbs suggests that AER development proceeds relatively normally up to this gestational day, despite slight anterior alterations and smaller bud sizes. (D) Likewise, the unperturbed posterior expression of the AER-specific marker *Dlx6* in E10.5 Mut limbs indicates that the posterior AER is preserved before *Shh* onset. Dark shaded arrowheads indicate normal expression. In all panels, empty dark shaded arrowheads indicate reduced and/or spatially perturbed expression. Light shaded arrowheads indicate the lack of expression. Proximal (left); anterior (top); FL, Forelimb; HL, Hindlimb.

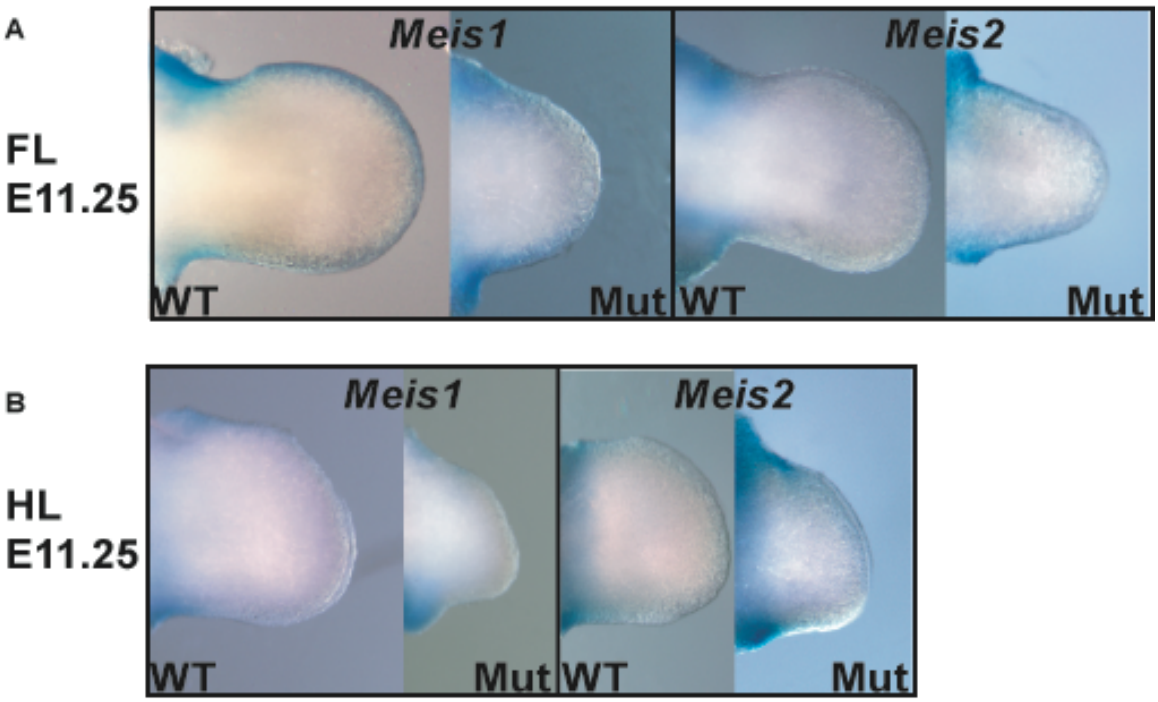

Figure 5.12. Expression of proximal mesenchymal markers in *Pbx1*$^{-/-}$;*Pbx2*$^{+/-}$ (Mut) limbs.

(A-B) *Meis1* and *Meis2* are unperturbed in Mut limbs (E11.25), suggesting that proximal limb domains remain relatively intact. Proximal (left); anterior (top); FL, Forelimb; HL, Hindlimb.

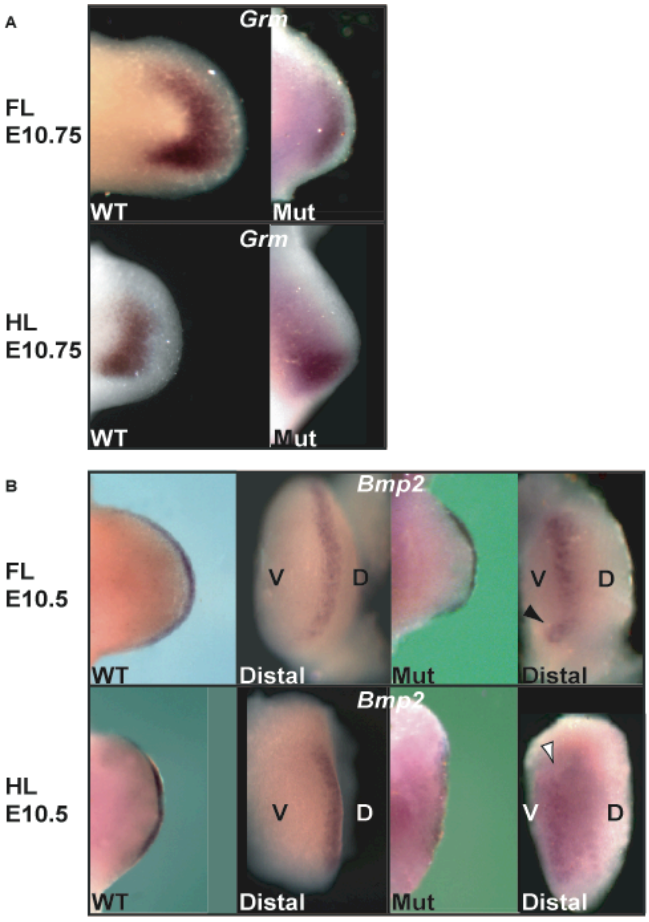

Figure 5.13. *Gremlin* and *Bmp2* expression in *Pbx1*$^{-/-}$;*Pbx2*$^{+/-}$ (Mut) limbs.

(A) In both Mut fore- and hindlimbs at E10.75, *Grm* is extended posterior-distally, although in the latter it lies directly adjacent to the posterior-most ectoderm. These findings reflect the forelimb reduction and hindlimb absence of *Shh* in the ZPA (Scherz et al., 2004). (B) In E10.75 Mut forelimbs *Bmp2* expression remains intact, although is slightly ventralized along the posterior AER (dark shaded arrowhead). In Mut hindlimbs, *Bmp2* expression is less organized and is reduced anteriorly from the developing AER (empty dark shaded arrowhead). Proximal (left); anterior (top); FL, Forelimb; HL, Hindlimb.

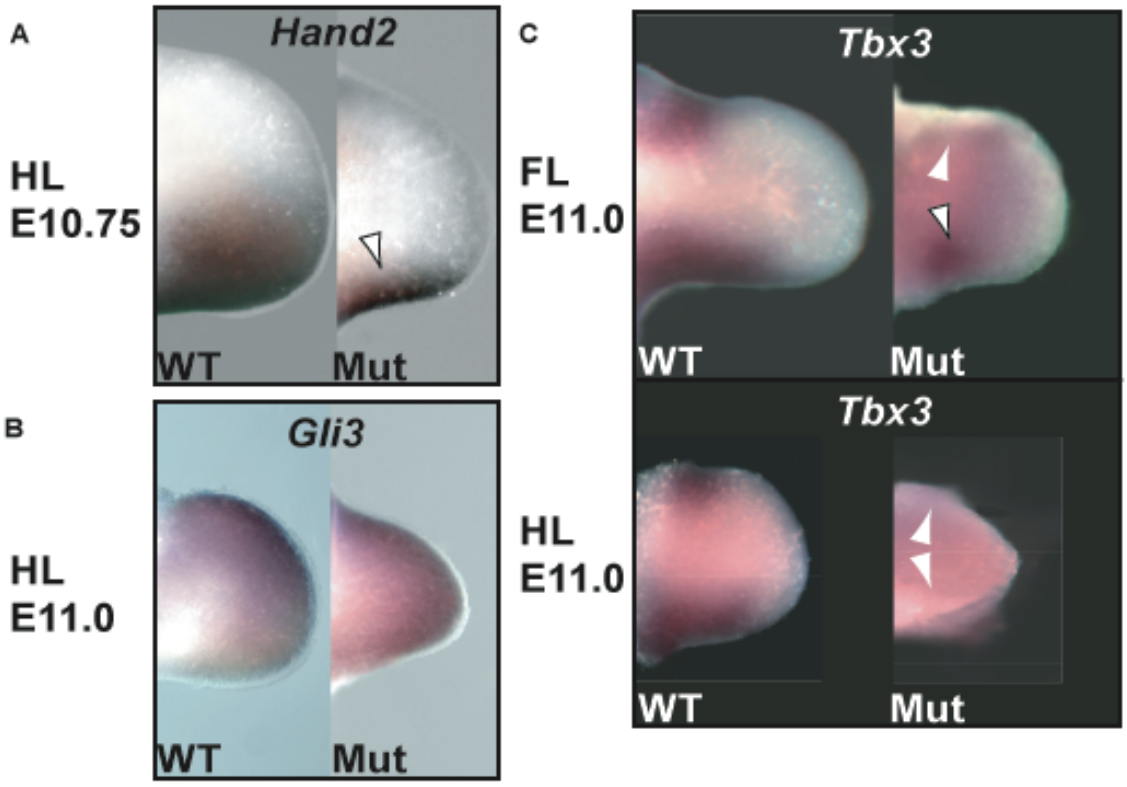

Figure 5.14. Expression of mesenchymal genes after *Shh* onset in *Pbx1*$^{-/-}$ *;Pbx2*$^{+/-}$ (Mut) limbs.

(A-B) *Hand2* is reduced and *Gli3* diffused throughout Mut hindlimbs (E10.75, E11.0, respectively), resembling expression patterns in mice lacking *HoxA/HoxD* (Kmita et al., 2005) and suggesting an A-P patterning defect in the absence of sustained *Shh* activity. Empty dark shaded arrowhead indicates reduced expression. (C) Expression of *Tbx3* is lost anteriorly and reduced posteriorly in Mut forelimbs, while in Mut hindlimbs *Tbx3* expression is lost altogether. Empty dark shaded arrowhead indicates reduced expression, while empty or white arrowheads indicate the lack of expression. Proximal (left); anterior (top); FL, Forelimb; HL, Hindlimb.

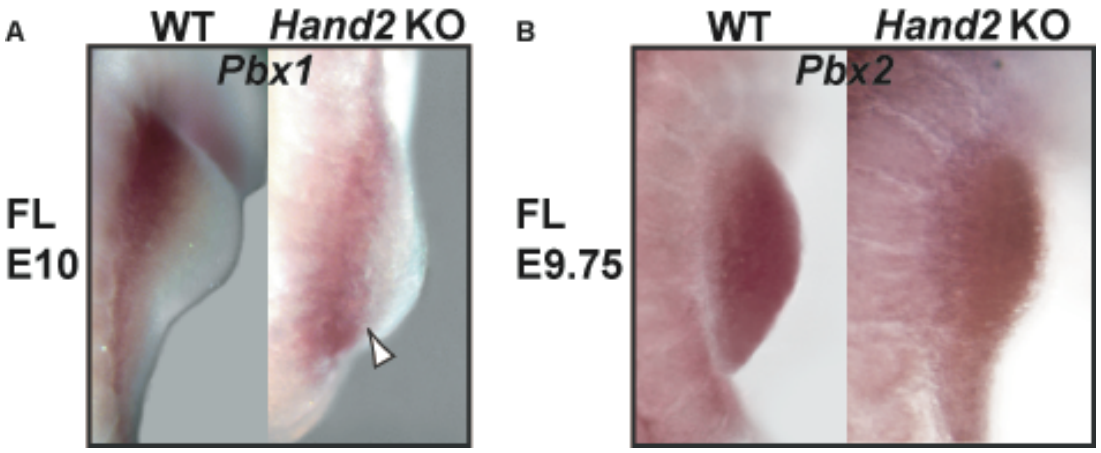

Figure 5.15. *Pbx* and *Hand2* likely control *Shh* through parallel pathways.

(A) At E10, *Pbx1* remains proximally expressed and mostly unperturbed in *Hand2*$^{-/-}$ (KO) forelimbs (left panel), albeit a modest expansion of its expression domain is observed posteriorly (empty dark shaded arrowhead). (B) At E9.75, *Pbx2* is relatively unperturbed in *Hand2* KO forelimbs (30X view) compared to WT controls (20X view). The differing magnifications provide an indication of the body size defects in *Hand2* KO embryos. These results indicate that *Pbx1/2* are not downstream of *Hand2* in limb development. FL, Forelimb.

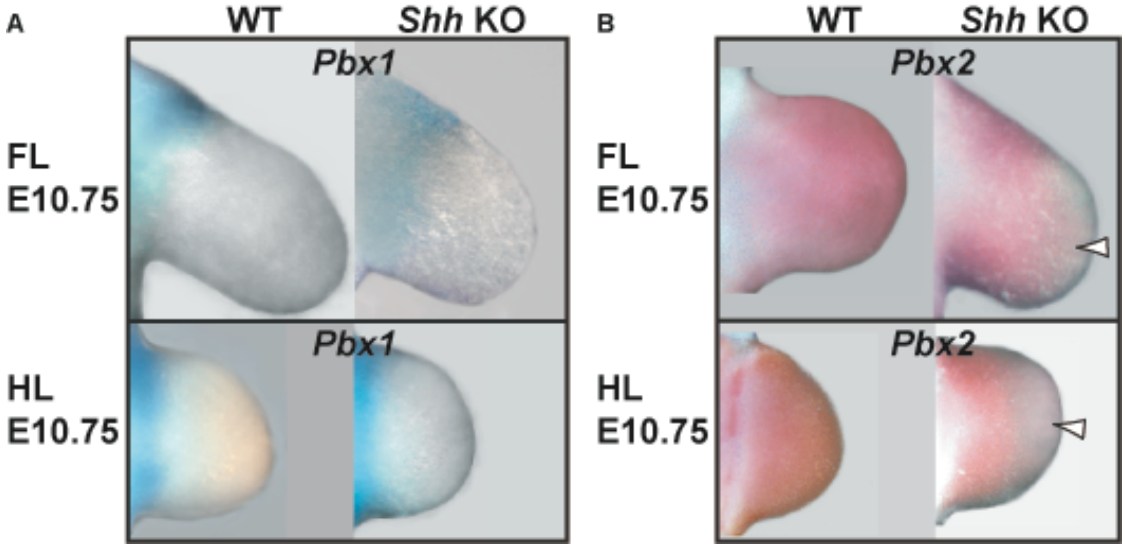

Figure 5.16. *Pbx1/2* expression in *Shh*$^{-/-}$ (KO) limbs.

(A-B) *Shh*-deficient (KO) embryos reveal relatively unperturbed *Pbx1* and *Pbx2* expression at E10.75, despite their abnormal limb morphology and presence of marked apoptosis in distal domains (empty dark shaded arrowheads) (Chiang et al., 2001). This reported apoptosis likely causes a slight decrease of *Pbx2* signal in the middle and distal limb bud. Proximal (left); anterior (top); FL, Forelimb; HL, Hindlimb.

Figure 5.17. *Hox* expression in Early *Pbx1*$^{-/-}$;*Pbx2*$^{+/-}$ (Mut) hindlimbs.

Hox expression (E10.25-10.5) is absent or reduced in somite matched Mut hindlimb posterior domains before, or at, *Shh* onset, despite their relatively normal morphology. Black empty arrowheads indicate lack of posterior expression (*Hoxa9*, *Hoxa11*, *Hoxd9*). Light shaded empty arrowhead indicates reduced posterior expression (*Hoxd11*). Light shaded arrowheads indicate absence of expression (*Hoxa13*, *Hoxd12, Hoxd13*). Diagrams depict summaries of expression data across two time-points (E10.25 and E10.5): *Hox* expression domains are represented by lines with text specifying the particular gene as displayed in their respective *in situ* hybridization panels. Dashed domains in Mut indicate reduced *Hoxd11* expression, whereas missing domains reflect complete absence of expression (*Hoxa13*, *Hoxd12, Hoxd13*). Proximal (left); anterior (top).

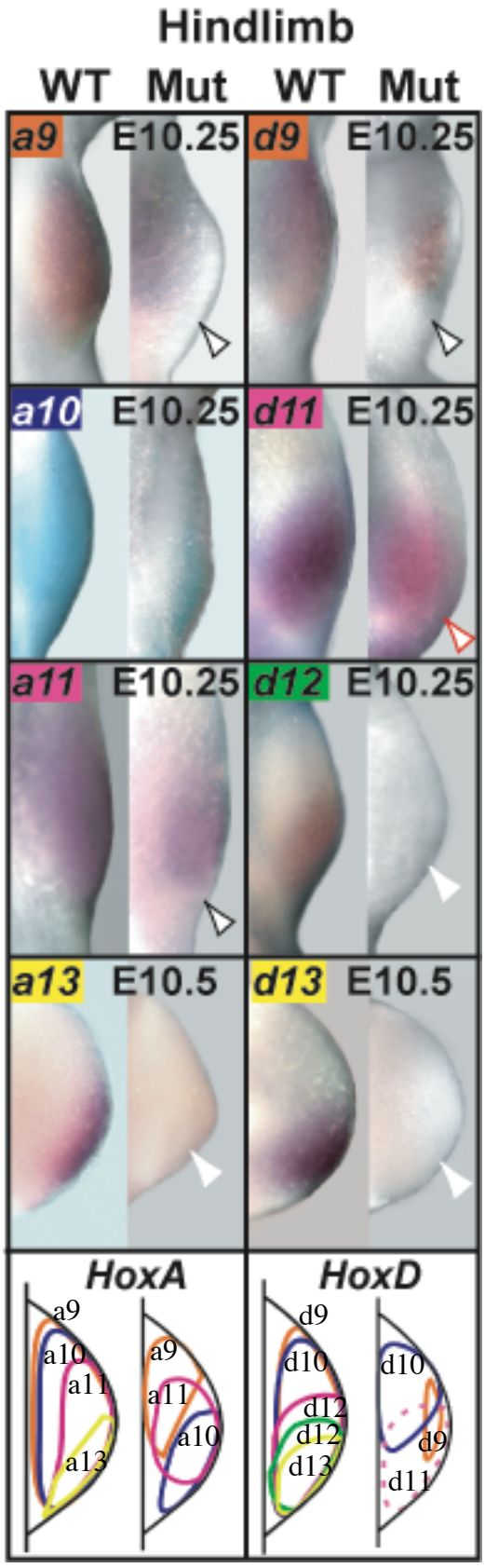
Hindlimb
WT
Mut
WT
Mut
a9
E10.25
d9
E10.25
a10
E10.25
d11
E10.25
a11
E10.25
d12
E10.25
a13
E10.5
d13
E10.5
HoxA
a9
a10
a11
a13
a9
a11
a10
HoxD
d9
d10
d12
d12
d13
d10
d9
d11

Figure 5.18. *Hox* expression in early *Pbx1*$^{-/-}$;*Pbx2*$^{+/-}$ (Mut) forelimbs.

In situ hybridization of 3' and 5' *HoxA* and *HoxD* expression in E10-10.75 WT and Mut forelimbs at, and/or following, *Shh* onset. Expression of *Hoxa9-a11* and *Hoxd9-d12* remains similar to WT forelimbs in that their transcripts lie within the domain of *Shh* expression. In addition, *Hoxa9* and *Hoxd9* expression is markedly up-regulated (black arrowheads) throughout the early forelimb bud, while expression of *Hoxa13* and *Hoxd13* (E10.75) are absent (light shaded arrowheads) from the forelimb bud. Diagrams on the right of each expression profile depict summaries of expression data across several time-points (E10 to E10.75): *Hox* expression domains are represented by lines specifying each gene as displayed in their respective *in situ* hybridization panels. Thicker solid lines in Mut depict increased and expanded *Hoxa9* and *Hoxd9* domains. Dashed domains in Mut indicate reduced *Hoxd10* and *Hoxa11* expression, whereas missing domains reflect complete absence of expression (*Hoxa13* and *Hoxd13*). Proximal (left); anterior (top).

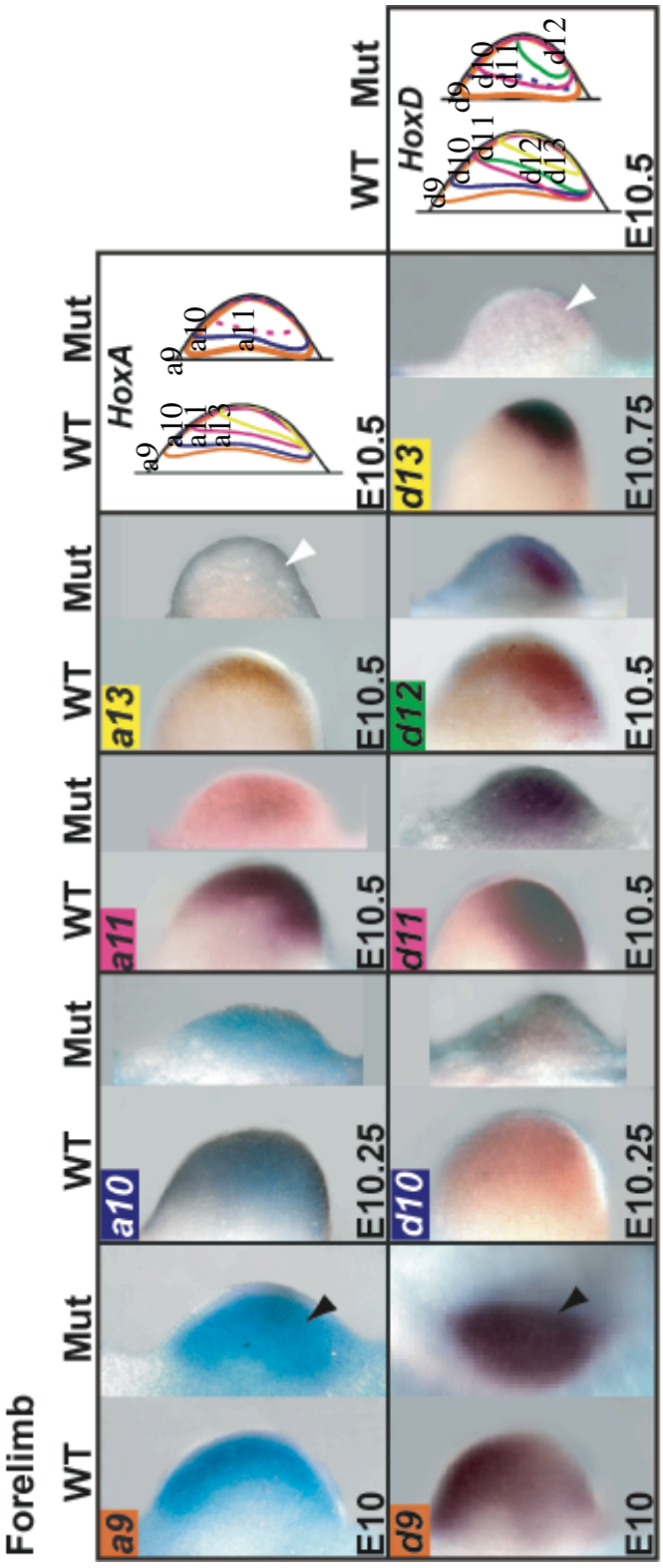
Forelimb
WT
Mut
WT
Mut
WT
Mut
WT
Mut
WT
Mut
a9
a10
a11
a13
HoxA
a9
a10
a11
a13
a9
a10
a11
E10
E10.25
E10.5
E10.5
E10.5
WT
Mut
d9
d10
d11
d12
HoxD
d9
d10
d11
d12
d13
E10
E10.25
E10.5
E10.5
E10.75
E10.5

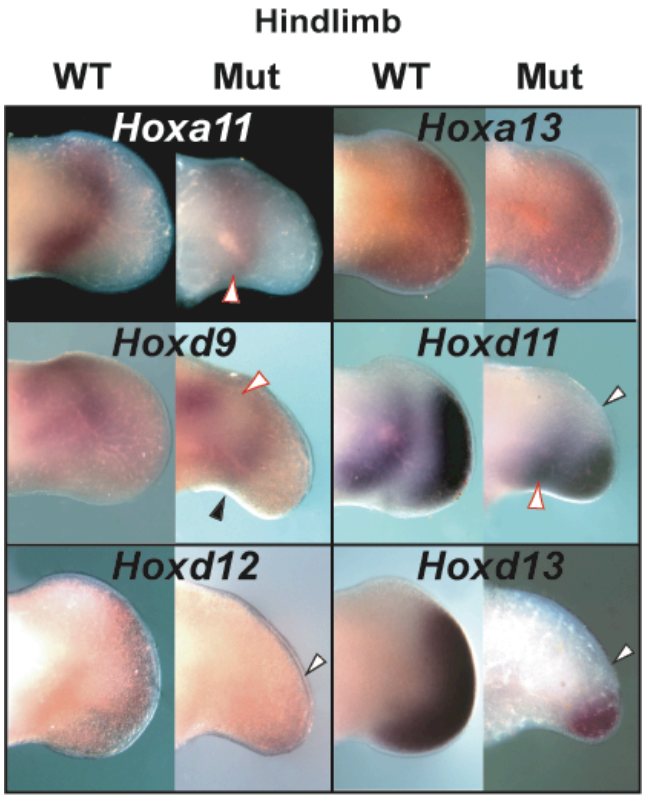

Figure 5.19. *Hox* expression in E11.5 *Pbx1*$^{-/-}$;*Pbx2*$^{+/-}$ (Mut) hindlimbs.

5' *HoxA* (*Hoxa11* and *Hoxa13*) expression (E11.5) remains relatively unperturbed distally in Mut hindlimbs, although there is a proximal-posterior reduction in *Hoxa11* at this day (empty light shaded arrowhead). This latter finding points toward an alteration in early collinear expression of *HoxA* in the limb. Distal *HoxD* (*Hoxd9, Hoxd11, Hoxd12,* and *Hoxd13*) expression is severely reduced anteriorly (dark shaded empty arrowheads). In addition, *Hoxd9* proximal-anterior expression is reduced and patchy (light shaded empty arrowhead) while it is expanded posteriorly in the limb bud (dark shaded arrowhead). Finally, *Hoxd11* proximal domain of expression is severely reduced (empty light shaded arrowhead) compared to WT limbs at this day. This finding is indicative of an alteration to early *HoxD* collinearity Proximal (left); anterior (top).

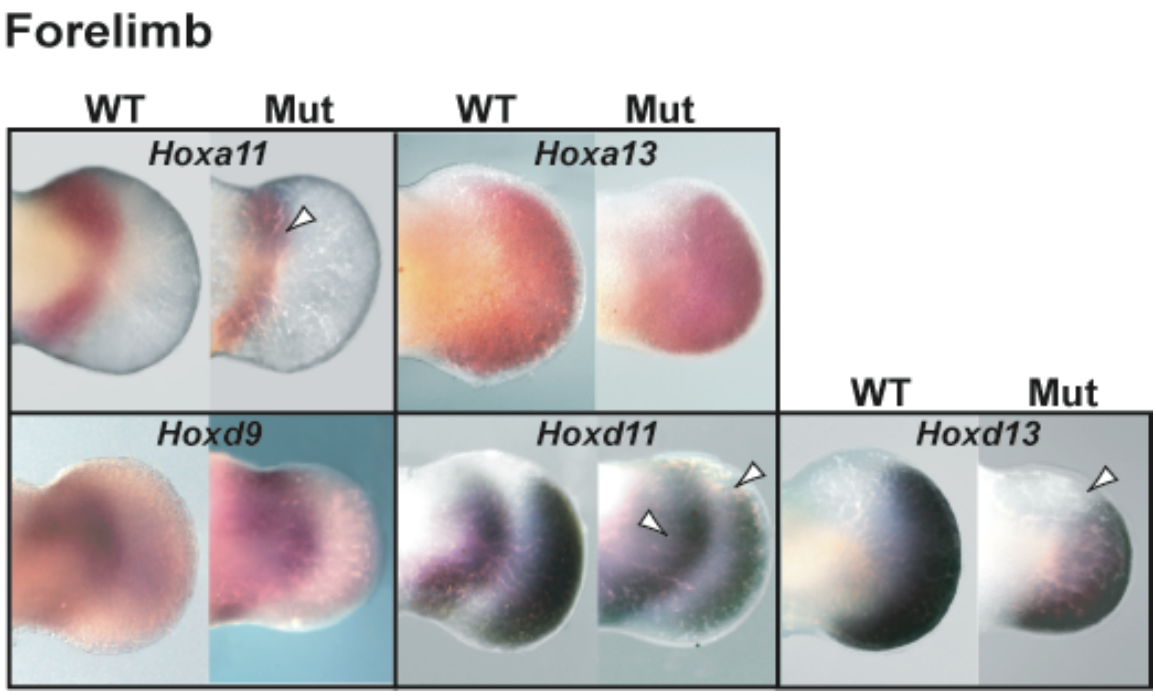

Figure 5.20. *Hox* expression in E11.5 *Pbx1*$^{-/-}$;*Pbx2*$^{+/-}$ (Mut) forelimbs.

5' *HoxA* (*Hoxa11* and *Hoxa13*) expression remains relatively unperturbed in Mut forelimbs, although there is a slight reduction in signal of *Hoxa11* (empty dark shaded arrowhead) when compared to WT. While 3' *HoxD* (*Hoxd9*) expression is present, distal 5' *HoxD* (*Hoxd11* and *Hoxd13*) expression is reduced anteriorly and is weaker proximally in signal intensity (dark shaded empty arrowheads). Proximal (left); anterior (top).

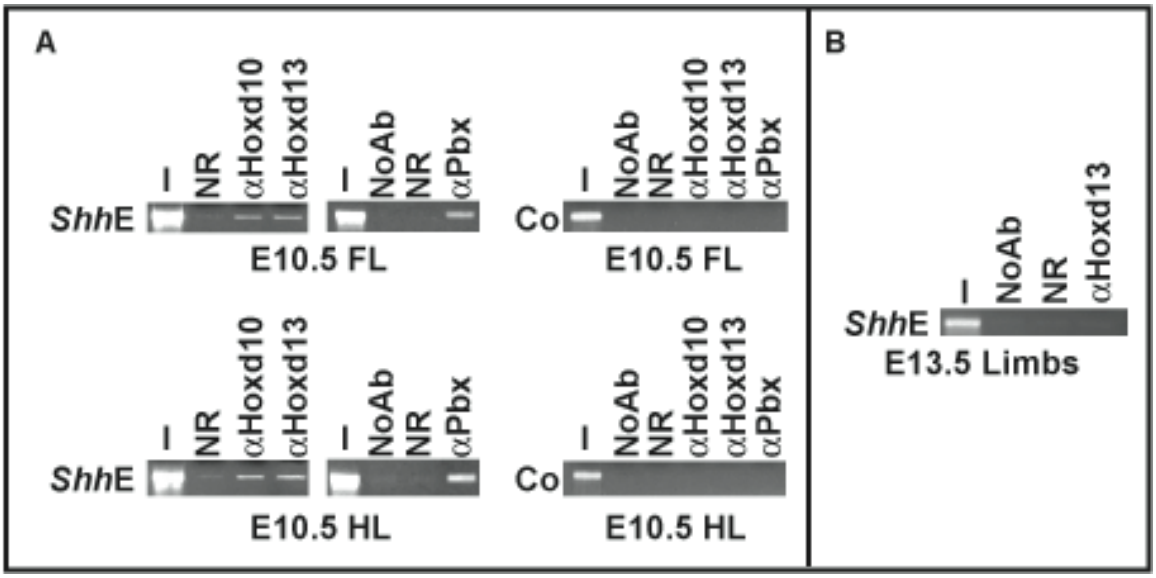

Figure 5. 21. Co-immunoprecipitation assay (ChIP).

(A-B) HoxD proteins are bound to the *Shh* limb enhancer (*Shh*E). (A) ChIP analyses on E10.5 mouse fore- and hindlimbs, using specific anti-Hoxd10 (αHoxd10), anti-Hoxd13 (αHoxd13), and anti-Pbx (αPbx) antisera, demonstrate their direct *in vivo* binding to the mouse *Shh*E. A 424 bp fragment of the *Shh*E was amplified by PCR. No PCR amplification of a 373 bp negative-control region (Co) located 1400 bp upstream of this enhancer was detected using E10.5 limb chromatin. Representative reactions of all PCR amplifications, done in triplicate, are shown. (B) ChIP on pooled E13.5 limbs using the αHoxd13 antiserum revealed no amplification of the *Shh*E. Co, control; FL, forelimb; HL, hindlimb; I, input chromatin; NoAb, no antibody-control resin; NR, non-specific control antibody.

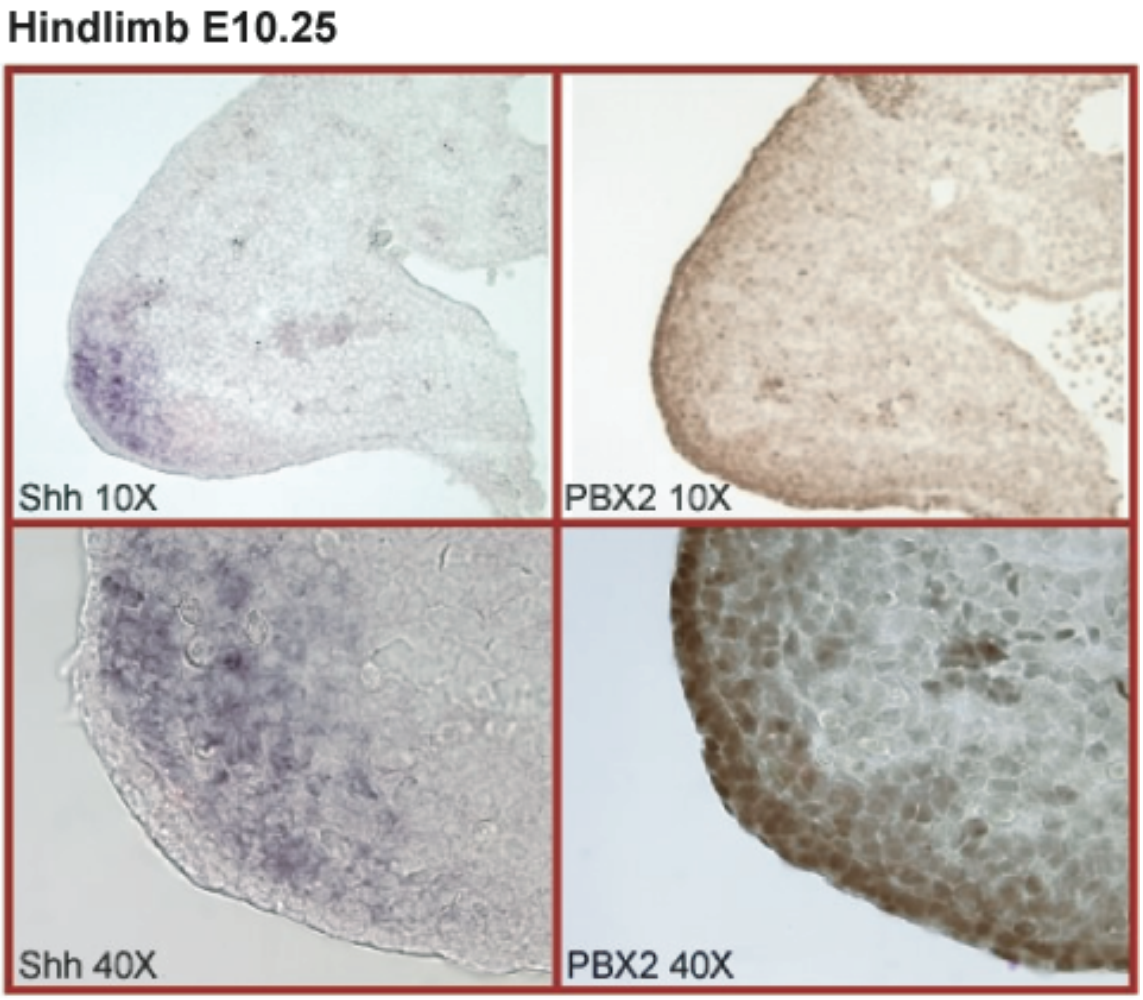

Figure 5.22. *Shh* and Pbx2 co-localization in the hindlimb at E10.25.

Shh expression (two right panels with 10X and 40X magnifications), as first detected using *in situ* hybridization, can be seen in the distal and posterior hindlimb mesenchyme. Subsequently, Pbx2 distribution (two left panels with 10X and 40X magnifications), as detected using immunohistochemistry with specific Pbx2 antibodies, can be seen to co-localize with *Shh* in these two adjacent sections.

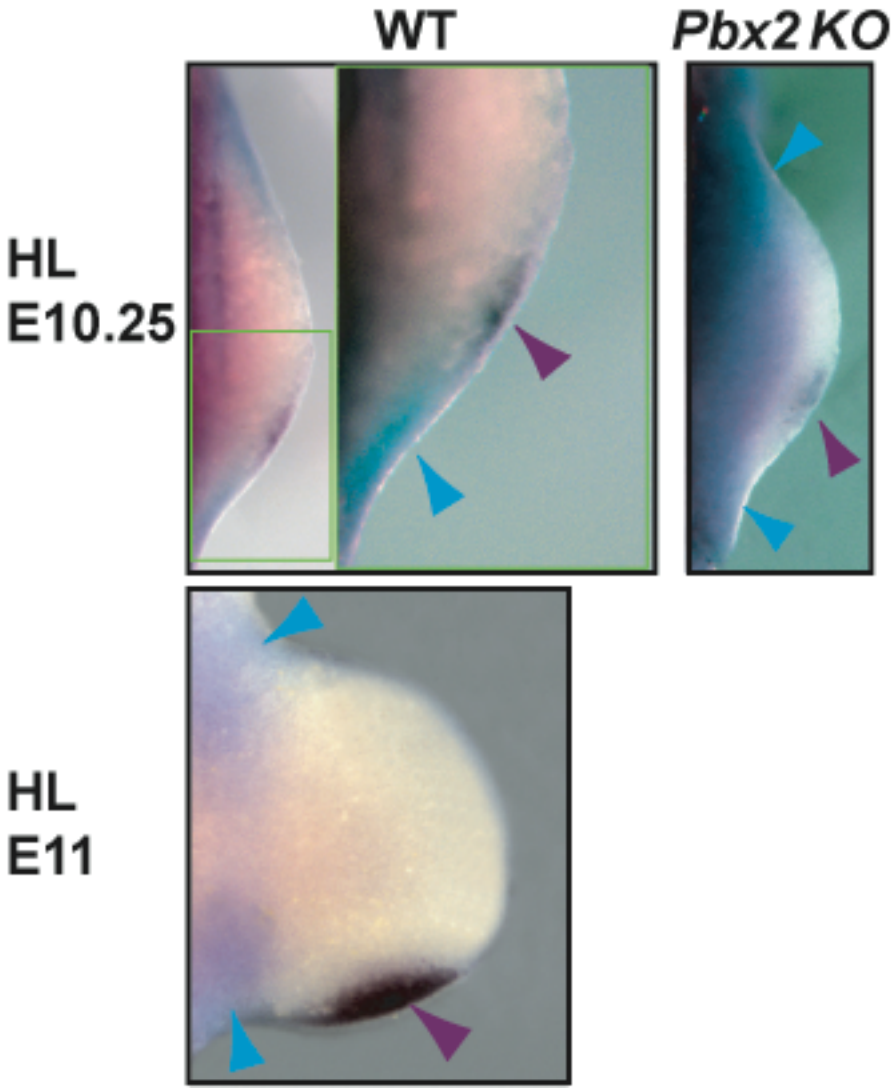

Figure 5.23. *Shh* and *Pbx1* do not co-localize in the hindlimb at E10.25 and E11.0.

At E10.25 and E11, *Pbx1* (denoted by light shaded domains and arrowheads) and *Shh* (denoted by dark shaded domains and arrowheads) mRNA transcripts, as detected using two-color *in situ* hybridization, do not co-localize in WT and *Pbx2*$^{-/-}$ (KO) hindlimbs. Proximal (left); anterior (top); HL, Hindlimb.

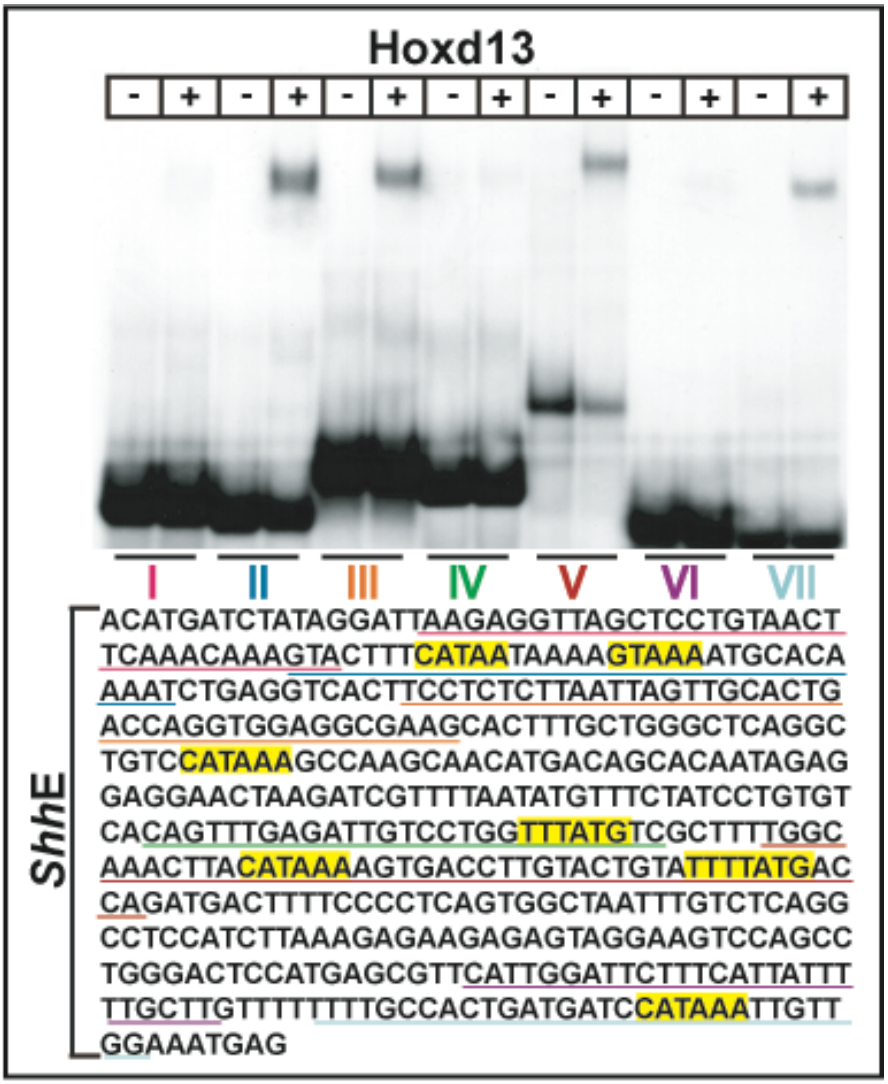

Figure 5.24. Electrophoretic Mobility Shift Assay (EMSA).

EMSA using seven different oligonucleotide probes (indicated by different shaded lines within the sequence of the ShhE; bottom) spanning a region of 450 bp. Specific binding of Hoxd13 is detected with probes II, III, V, and VII.

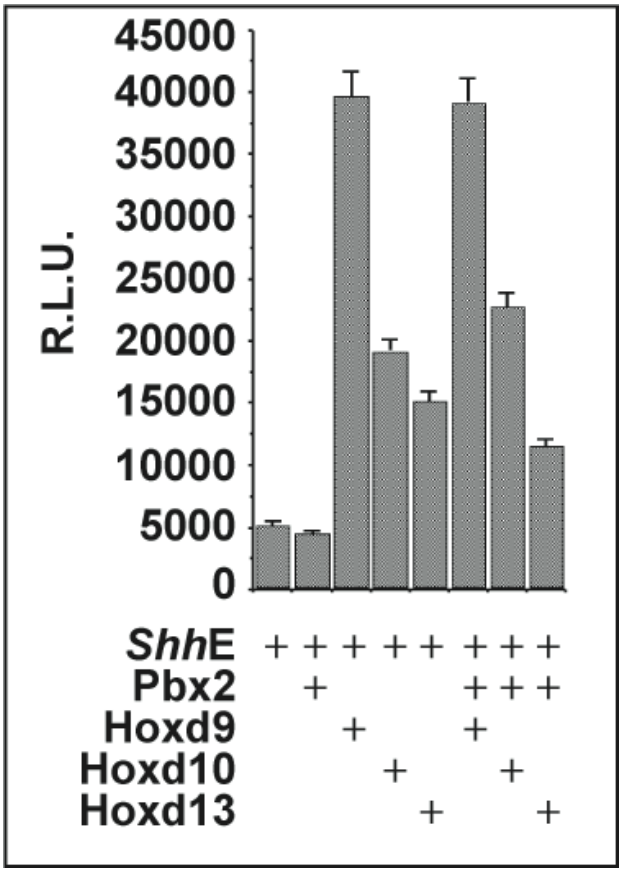

Figure 5.25. Transient transfection assays in P19 carcinoma cells.

HoxD proteins can activate transcription from the *Shh*E (8-fold for Hoxd9, 4-fold for Hoxd10, and 3-fold for Hoxd13) in P19 embryonal carcinoma cells. Luciferase activity, in arbitrary units (R.L.U.), was assayed from extracts of transiently transfected P19 cells. Co-transfection assays were performed in the presence (+) of the indicated expression vectors encoding Pbx2, Hoxd9, Hoxd10, and Hoxd13 and with a luciferase reporter construct (pT81m*Shh*E) containing the *Shh*E. Bars represent the mean ± SEM of at least four independent experiments.

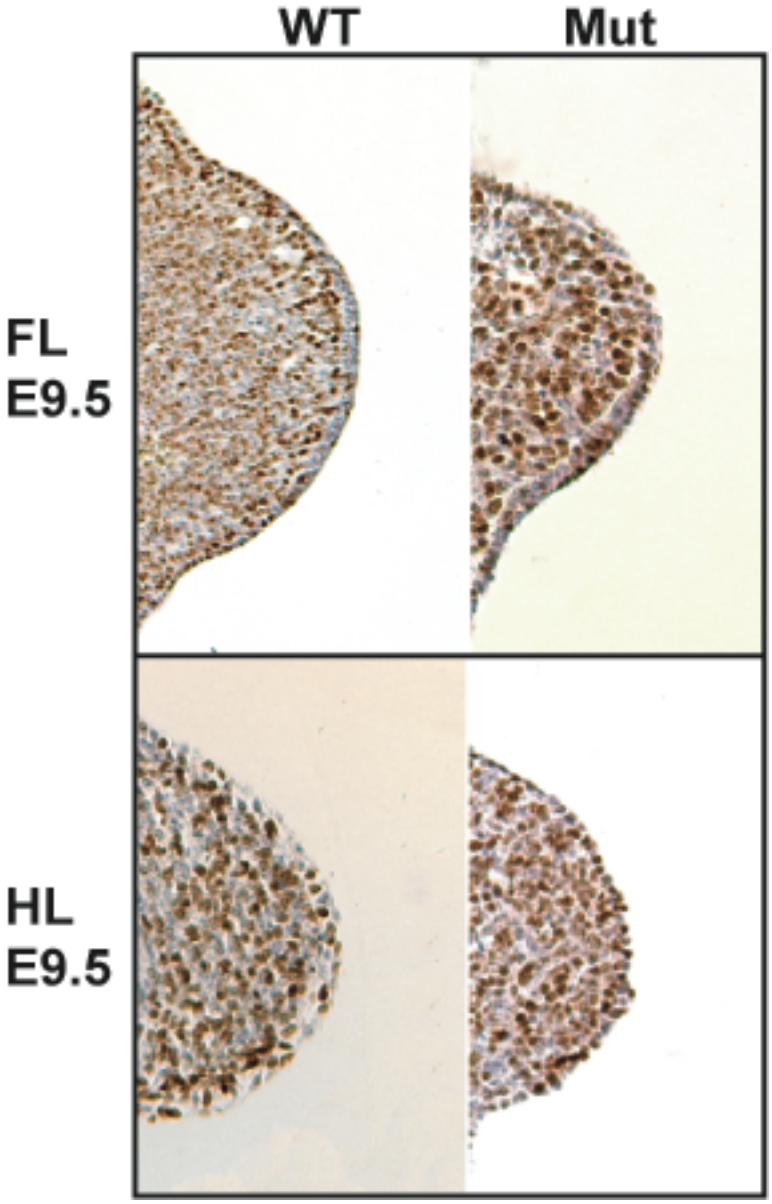

Figure 5.26. BrdU analyses in *Pbx1*$^{-/-}$; *Pbx2*$^{+/-}$ (Mut) limbs.

As represented at E9.5, no significant differences were detected in the proliferation of cells between WT and *Pbx1*$^{-/-}$; *Pbx2*$^{+/-}$ (Mut) forelimbs and hindlimbs. Proximal (left); anterior (top); FL, Forelimb; HL, Hindlimb.

Figure 5.27. Caspase3 analyses in *Pbx1*$^{-/-}$; *Pbx2*$^{+/-}$ (Mut) limbs.

As represented at three different gestational time-points, abnormal levels of cellular apoptosis via Caspase3 staining, were not detected in Mut forelimbs, despite their abnormal morphology and reduced Shh signaling. Conversely, while no abnormal level of apoptosis was detected prior to *Shh* onset in Mut hindlimbs, after onset, at E11.5 and E12.5, appreciable levels of apoptosis could be detected. On the left for each genotype are 10X magnifications, while on the right are the 40X magnification insets of the boxes present in the 10X view. Proximal (left); anterior (top); FL, Forelimb; HL, Hindlimb.

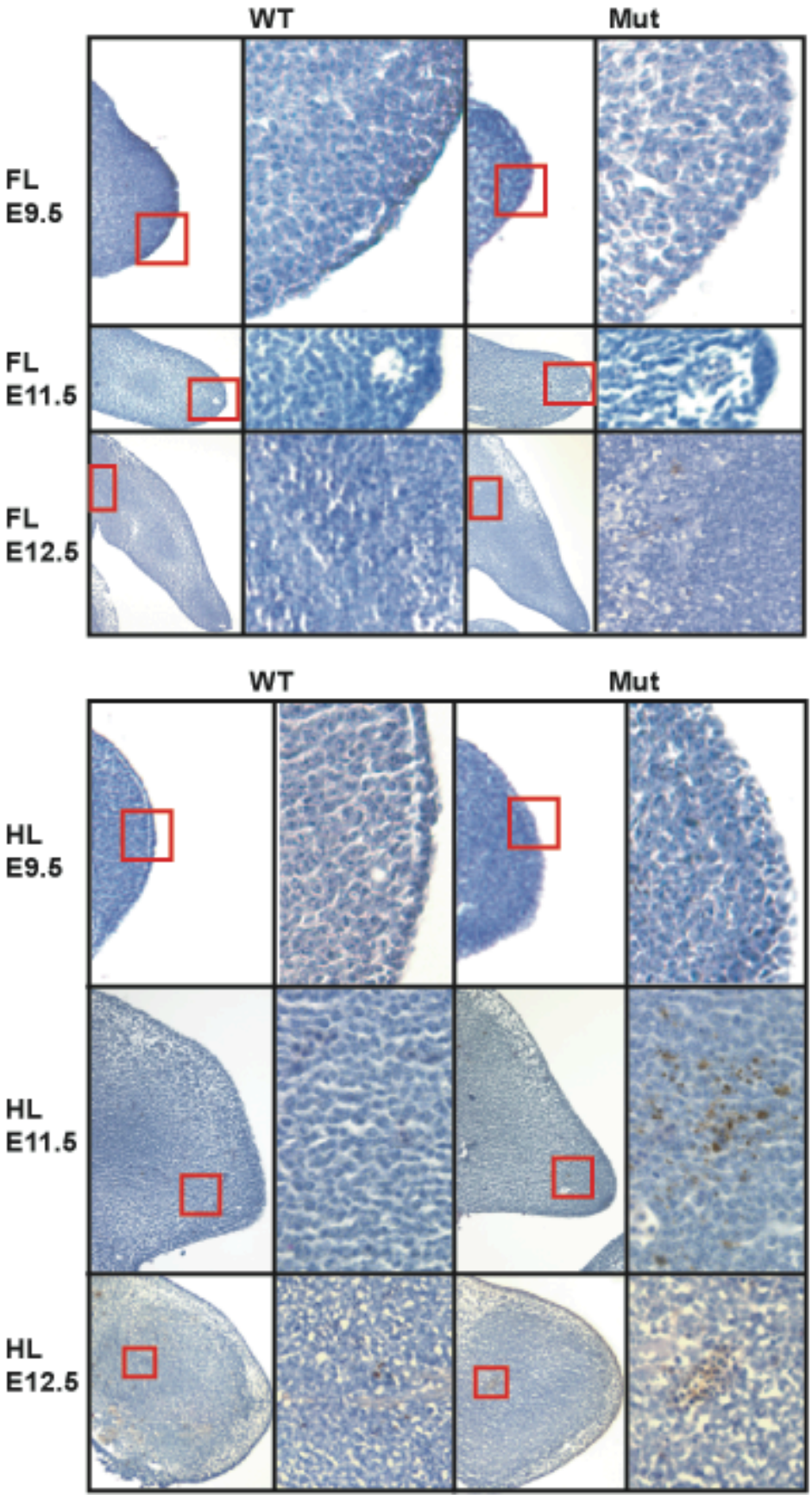
WT
Mut
FL
E9.5
FL
E11.5
FL
E12.5
WT
Mut
HL
E9.5
HL
E11.5
HL
E12.5

Figure 5. 28. Axial malformations in the *Pbx1/2* mutant embryos at E13.5.

(A-C) Alcian Blue staining of E13.5 littermates reveals axial defects in *Pbx1*$^{-/-}$*;Pbx2*$^{+/+}$ and *Pbx1*$^{-/-}$*;Pbx2*$^{+/-}$ (Mut) embryos. When compared to WT (A), *Pbx1*$^{-/-}$*;Pbx2*$^{+/+}$ embryos (B) display marked skeletal defects as reported by Selleri et al., 2001. Such malformations include the thinning of the spinous processes of C1 and C2 (B1) (black empty arrowheads) and the fusion of rudimentary ribs (B4)(light shaded empty arrowheads) compared to WT (black arrowheads in A1; light shaded arrowheads in A4). Mut embryos (C) display a drastic alteration of the *Pbx1*$^{-/-}$*;Pbx2*$^{+/+}$ (B) phenotype and the appearance of novel axial defects, specifically compared to *Pbx1*$^{-/-}$*;Pbx2*$^{+/+}$ (B) and WT embryos (A). Specifically, when compared to *Pbx1*$^{-/-}$*;Pbx2*$^{+/+}$ embryos (B1) spinous processes of the Mut cervical region (C1) are thinned and attenuated (black empty arrowheads in each panel). In addition, spinous processes of the more caudal cervical vertebrae (C1) also are thinned (empty light shaded arrowheads) compared to WT (A1) (light shaded arrowheads). In both the cervical thoracic region, the vertebral bodies of Mut embryos (C2-C3 empty light shaded arrowheads) are more cranio-caudally flattened when compared to WT (A2-A3 light shaded arrowheads). In the thoracic region of Mut embryos (C4), ribs remain rudimentary (double empty light shaded arrowheads) and lack an intrinsic axial level identity (indicated by a "?") specifically compared to WT (A4)(light shaded arrowheads), and more extreme than observed in *Pbx1*$^{-/-}$*;Pbx2*$^{+/+}$ embryos (B4)(empty light shaded arrowheads). In the lumbar-sacral axial region of Mut embryos (C5), their transverse processes are thinned and lose the typical angulation (empty light shaded arrowhead) seen in both *Pbx1*$^{-/-}$*;Pbx2*$^{+/+}$ (B5) and WT embryos (A5)(light shaded arrowheads) at this day. Finally, the development of the caudal region of Mut embryos (C6) appears delayed as the number of vertebral bodies which form is less than *Pbx1*$^{-/-}$*;Pbx2*$^{+/+}$ (B6) and WT embryos (A6).

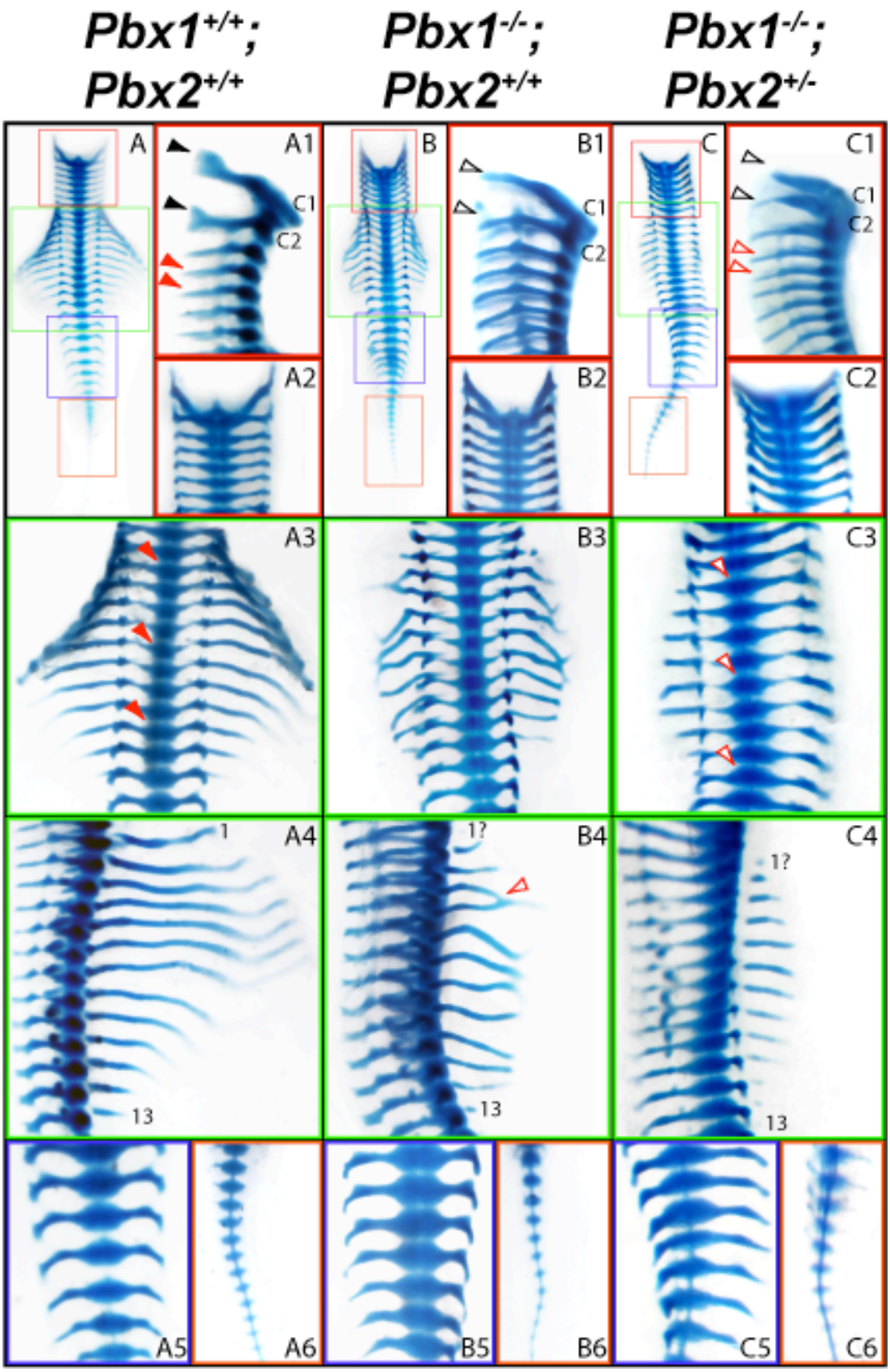
Pbx1+/+; Pbx2+/+
Pbx1-/-; Pbx2+/+
Pbx1-/-; Pbx2+/-
A
A1
C1
C2
A2
B
B1
C1
C2
B2
C
C1
C1
C2
C2
A3
B3
C3
A4
1
13
B4
1?
13
C4
1?
13
A5
A6
B5
B6
C5
C6

Figure 5.29. *Pbx1/2* and the control of *Hox* expression.

(A-C) Diagram of Pbx/Hox/Shh regulatory interactions during limb development. (A) *Pbx1/2* lie upstream of early *Hox* collinear expression during hindlimb development (dashed arrow) and may directly control *Hox* expression (dark arrow) via an interaction with the purported 3' ELCR (left-most rectangle). Hox proteins may cooperate in this activation either directly with Pbx as a complex (oval with "Hox" above solid black line) or indirectly (solid curved to dashed line with a "?") via their role upstream of binding factors. Such Hox auto-regulation has been shown for several of its 3' *Hox* promoters (small dashed curved arrow) (Popperl et al., 1995; 2000). Regardless of the manner of activation, *Hox* activation proceeds 3' (i.e., *Hoxd1*) to 5' (i.e. *Hoxd13*) (depicted by the longest arrow), such that 3' *Hox* are typically activated first (as they are closest to the ELCR) and are expressed throughout the limb bud, whilst 5' *Hox* are activated later (as they are furthest from the ELCR) and are restricted to the posterior limb domains. In addition, as demonstrated by Tarchini and Duboule (2006), the increasingly posterior restriction of 5' *Hox* appears to result to their increasing proximity to an antagonistic domain (circle) located 5' of *Hoxd13* that appears to regulate spatial expression (inhibitory T-line) during this early collinear phase. Finally, an intronic region (box with "i") located between *Hoxd4* and *Hoxd8* may provide a spacing mechanism to regulate spatio-temporal *Hox* expression. (B) Simplified model depicts the overlapping genetic hierarchical roles of *Pbx1* and *Pbx2* in controlling *Hox* spatial distribution and Hox recruitment to the limb *Shh*E. In addition, Pbx2, albeit not functionally essential within this network, is also recruited to this enhancer in limb cells. Intensity of the lighter shade of Pbx2 correlates with its functional relevance. (C) Diagram depicts the control of late *Hox* "reverse" collinear expression during autopod development. In this model, a 5' global control region (GCR, right-most rectangle) activates 5' *Hox* (*Hoxd13-Hoxd9*) with decreasing transcriptional efficiency (the shorter the curved arrow the greater the efficiency) and no longer influenced by the antagonistic domain (shaded circle just 5' of Hoxd13) and the ELCR (shaded left-most rectangle). The mechanisms that activate "reverse collinearity" via control of the digital enhancer in the GCR remain elusive but appear downstream of Shh (arrow with "?"). Squares in (A) and (C) present regulatory elements and individual *Hox* genes, while square with "i" depicts introns and circles depict antagonistic domains. Rectangles in (B) represent *Shh* regulatory regions (smaller) and *Shh* gene promoter (larger). All diagrams are not drawn to scale.

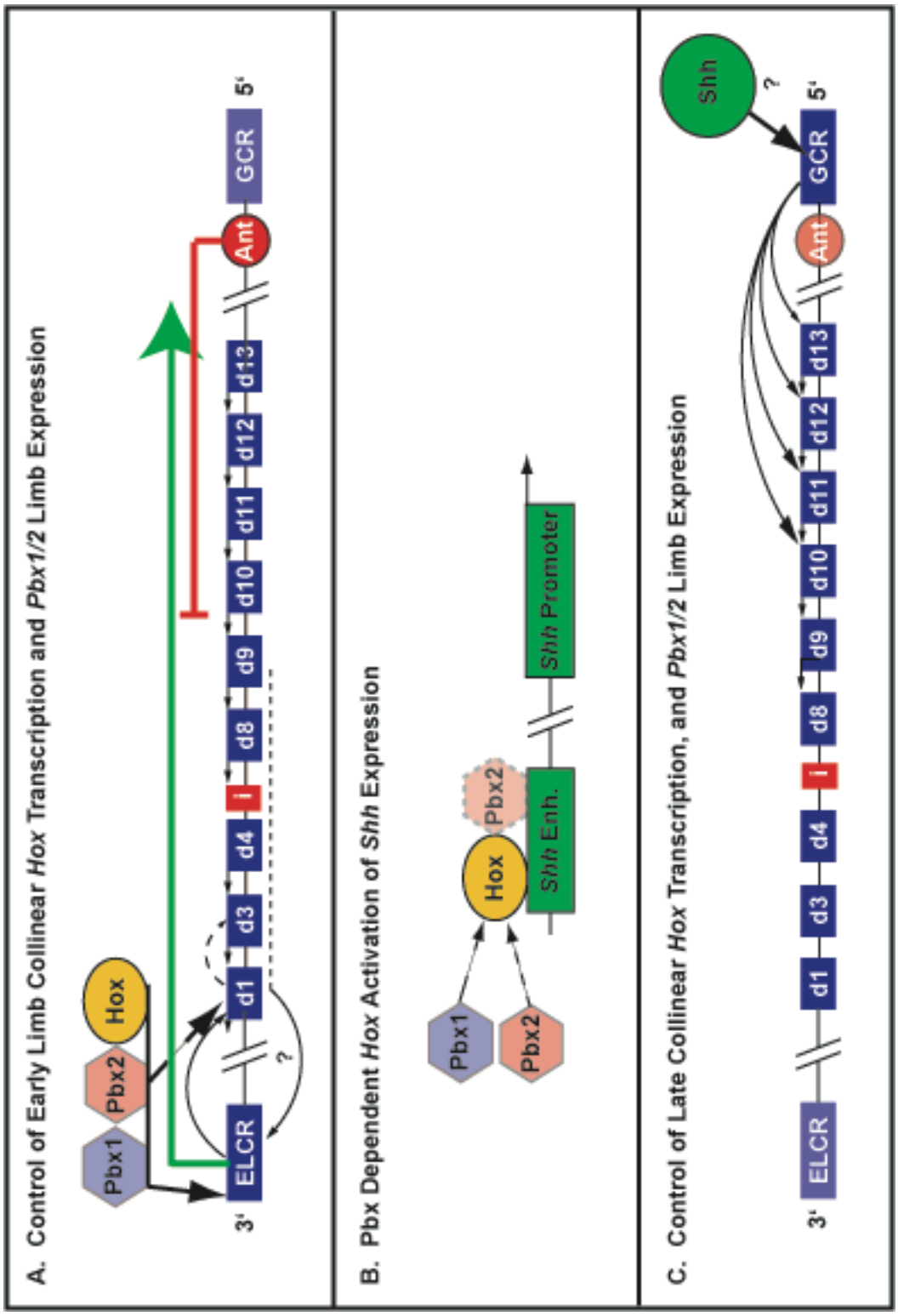
A. Control of Early Limb Collinear Hox Transcription and Pbx1/2 Limb Expression
Hox
Pbx2
Pbx1
3'
ELCR
d1
d3
d4
i
d8
d9
d10
d11
d12
d13
Ant
GCR
5'
?
B. Pbx Dependent Hox Activation of Shh Expression
Pbx1
Pbx2
Hox
Pbx2
Shh Enh.
Shh Promoter
C. Control of Late Collinear Hox Transcription, and Pbx1/2 Limb Expression
Shh
?
3'
ELCR
d1
d3
d4
i
d8
d9
d10
d11
d12
d13
Ant
GCR
5'

Figure 5.30. Model of Pbx action upstream of Hox and the activation of *Shh*.

(A) *Pbx-dependent Hox transcription*. Diagram displays the co-localization of *Pbx1/2* (a) in the early limb field at (E9.5) and their lowered transcript distribution (a') in the *Pbx1*$^{-/-}$*; Pbx2*$^{+/-}$ (Mut) hindlimb at this day. Also, at this day, *Pbx1/2* co-localize with 3' *Hox* in this domain in WT (b) and subsequently in their loss, 3' *Hox* expression decreases (b') in Mut. At E10 (right diagram), while normally, *Pbx1/2* lie upstream of *Hox* (c) leading to the posterior accumulation of 3'and 5' *Hox* transcripts in the future ZPA, in Mut, lowered *Pbx* expression (lighter shaded of each respective domain) leads to altered and/or lost *Hox* transcript localization (c'). (B) *Hox-dependent Shh activation.* Diagram illustrates the requirement of *Pbx1* (a), *Pbx2* (b) and *Pbx1* and *Pbx2* (c) for controlling the positioning of 5' *Hox* (i.e., *HoxA/HoxD*, d) to future *Shh*-expressing domain (e). At E10.25, in Mut limbs, *Hox* expression remains partially external to and mostly reduced (d') in the ZPA, and *Shh* activation does not occur (the posteriorly located X). (C) *Shh-dependent Hox transcription.* Diagram depicts a refinement of a previous model (Zakany et al., 2004) and highlights that *Shh* loss, due to early *Pbx1* and *Pbx2* perturbation, leads to partial disruption of 5' *HoxD* "reverse" collinearity (a in WT versus a' in Mut), but not of 5' *HoxA* expression (b in WT versus b' in Mut). Proximal (left); anterior (top). HL, Hindlimb.

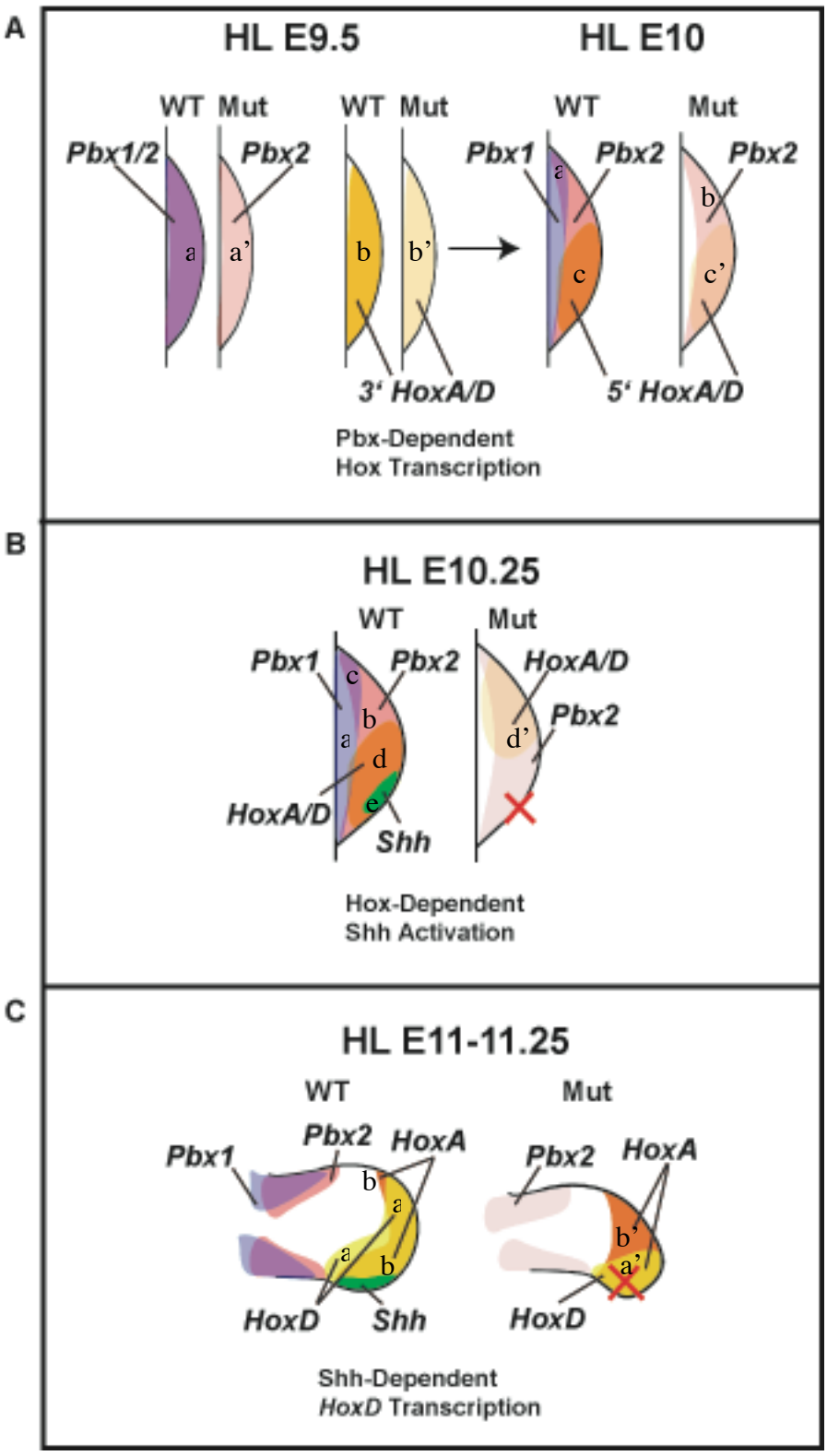
A
HL E9.5
HL E10
WT
Mut
WT
Mut
WT
Mut
Pbx1/2
Pbx2
Pbx1
Pbx2
Pbx2
a
a'
b
b'
a
b
c
c'
3' HoxA/D
5' HoxA/D
Pbx-Dependent
Hox Transcription
B
HL E10.25
WT
Mut
Pbx1
Pbx2
HoxA/D
Pbx2
c
b
a
d
d'
HoxA/D
e
Shh
Hox-Dependent
Shh Activation
C
HL E11-11.25
WT
Mut
Pbx1
Pbx2
HoxA
Pbx2
HoxA
b
a
a
b
b'
a'
HoxD
Shh
HoxD
Shh-Dependent
HoxD Transcription

Chapter 6: Differentiating *Pbx* Ectodermal Versus Mesenchymal Roles During Limb Development

6.1 Introduction

As reviewed in Chapter 3, the development of the limb requires precise molecular interactions between the mesenchyme and the ectoderm covering the bud. Indeed, abrogation of gene expression in either of these tissues severely compromises the functionality of the other tissue and leads to defects in limb bud outgrowth. With respect to the ectoderm, induction of the limb field mesenchyme as well as the transformation of columnar into pseudostratified epithelium of the AER depends on the expression of several genes, such as *Fgf4*, *Fgf8, Wnt7a,* and *En1*. Compound mutants for these genes lack limbs, or have limbs with mis-patterned and reduced numbers of skeletal elements and/or possess defects in AER morphogenesis (Niswander, 2003). Likewise, the expression of mesenchymal-specific genes, such as *Fgf10*, *Tbx* (i.e., *Tbx4* and *Tbx5*), *Wnt*, among others, leads to the initiation of limb bud outgrowth; while their experimental deletion results in the disruption of the mesenchymal-epithelial tissue interaction and partial to complete limb agenesis (Min et al., 1998; Sekine et al., 1999; Agarwal et al., 2003; Hill et al., 2006).

The concerted action of these mesenchymal and ectodermal expressed genes facilitates the patterning of skeletal elements across all limb compartments. Part of this action revolves around each gene's role in early induction, whereas another aspect concerns their involvement in establishing the ZPA-AER positive feedback loop (Niswander, 2003). Still another aspect may be

their direct involvement (i.e., as several are transcription factors) in the patterning of skeletal elements in a cell autonomous manner. To help determine their role in limb development, data from their experimental deletion must be addressed in relation to the current models of skeletal element cell fate specification. For example, if viewed from the perspective of the Early Specification (ES) Model (see Chapter 3), many of these genes may be functioning in the early limb field to specify cells destined to become skeletal elements from every compartment (Dudley et al., 2002). In this case, a component of their effects on patterning would occur primarily early during limb field specification. On the other hand, according to the Progress Zone (PZ) Model, their roles may be in governing the formation of the PZ and thus facilitating the time-dependent specification and patterning of skeletal elements throughout bud formation (reviewed in Niswander, 2003; Chapter 3).

As introduced in Chapter 5, because *Pbx1*$^{-/-}$*;Pbx2*$^{-/-}$ embryos die early *in utero* between E9.5-E10.0, a study of *Pbx1*$^{-/-}$*; Pbx2*$^{+/-}$ (*Pbx1/2 Mut*) embryos was conducted to explore the consequences of partial *Pbx* loss on limb development. Accordingly, it was demonstrated that, besides other functions, *Pbx* are genetically upstream of *Hox* and *Shh* (and ZPA formation), and hence zeugopodial and autopodial patterning and morphogenesis. However, the question still remains as to how the total loss of *Pbx* influences limb bud development as well as skeletal element specification and patterning. Indeed, preliminary data (presented in Chapter 5 and below) demonstrate that despite their early lethality (i.e., at critical limb developmental stages), double

homozygous mutants lack well developed limbs, indicating that *Pbx* are critical in bud formation and perhaps during early skeletal element specification and patterning.

An essential aspect of deciphering the role(s) of Pbx during limb formation concerns the model employed to understand the skeletal element cell fate specification. On the one hand, if viewed under the PZ Model, Pbx would function either during the development of the major limb signaling centers (e.g., ZPA and AER) and/or in the cell autonomous events leading to time-dependent specification of skeletal elements of each compartment. In this case, the early lethality of double homozygous mutants would occur contemporaneously with the stage when the initial cellular specification of stylopodial skeletal elements occurs; and the mis-patterning and distal loss of skeletal elements observed in *Pbx1/2 Mut* embryos would reflect defects in the development of the PZ and/or in the cell autonomous events leading to skeletal element specification across all compartments. In either case, it still remains unclear how total Pbx loss influences the later time-dependent patterning of zeugopodial and autopodial skeletal elements.

On the other hand, if Pbx role is thought of with respect to the ES Model, it could be argued that the overlap of *Pbx* early in the limb field is responsible for either governing epithelial-mesenchymal interactions critical for early specification and/or the *sensu stricto* early specification of skeletal elements into unique prepatterned domains. In this case, the lack of limbs in double homozygous mutants would reflect extreme defects in early limb induction, the

loss of specific prepatterned compartments, or both; whereas the mis-patterning across all fore- and hindlimb compartments, as observed in *Pbx1/2 Mut* embryos, would reflect early *Pbx* loss from the limb field and its subsequent effects on the formation of prepatterning domains.

With respect to Pbx potential role as viewed under the ES Model, it may be possible to assess how specific loss of these genes alters skeletal element specification and patterning at early stages (i.e., because all three limb compartments are believed to be specified prior to double homozygous lethality). Unfortunately, the current state of experimental expertise does not permit this accurate determination, as markers that specifically label stylopodial, zeugopodial, and autopodial precursors are not available. However, to at least understand how *Pbx* loss impacts the function of early ectoderm and mesenchyme (e.g., at the time of initial limb outgrowth), an examination of gene expression in both mutant double homozygous and *Pbx1/2 Mut* embyos can be conducted. In this manner, an overall assessment of the functionality of several of the limbs signaling centers and domains in these mutants could serve as a relatively good proxy for understanding how complete global (and partial) *Pbx1/Pbx2* loss affects early limb development. Such data can then be re-examined to see if they have consilience with either specification model.

In addition to the use of global knockout mice (i.e., as described above and in Chapter 5), the ability to conditionally inactivate a gene in a tissue-specific manner and/or at an exact time period during embryogenesis offers a technique to determine how gene loss impacts a specific developmental system

(Lewandoski, 2001). Recently, a novel targeting construct for *Pbx1* has been completed (i.e., *Pbx1* "floxed" as described in Chapter 4), which allows for its specific deletion from tissues possessing Cre recombinase activity under the promoter of an endogenously expressed gene. When homozygous *Pbx1* "floxed" embryos (i.e., $Pbx1^{cl/cl}$) are generated on a $Pbx2^{-/-}$ background, and crossed to a Cre line, an assessment can be made on how *Pbx* gene loss in specific tissues and time periods impinges on normal limb development. Furthermore, since inactivation of *Pbx1* can occur in tissue-specific manner (i.e., from one domain or tissue type only), complications that arise from both global loss of *Pbx* in all tissues and *in utero* lethality can be prevented.

Utilizing the global and conditional *Pbx1* alleles (each on a $Pbx2^{-/-}$ background), studies outlined in this chapter further demonstrate how *Pbx* loss impacts development of the limb. Accordingly, this chapter is divided into two sections. Section 6.2.1 focuses on the finding that, in addition to their mesenchymal expression, *Pbx1* and *Pbx2* are also highly expressed in the ectoderm. This section next concentrates on the molecular and morphological phenotypes of the early limb bud in global $Pbx1^{-/-}$; $Pbx2^{-/-}$ embryos. In this manner, studies described here provide a preliminary answer to the question of how specific gene networks and early limb signaling centers are affected by the global loss of *Pbx*. In the context of this strategy, forelimb and hindlimb development is assessed. Section 6.2.2 focuses on the morphological phenotypes of the limb skeletons of conditionally inactivated *Pbx1;Pbx2* compound mutant embryos. By utilizing Cre recombinase in ectodermal versus

mesenchymal tissue domains, studies here preliminarily address the question of how *Pbx* loss in these specific tissues affects limb development. Given that the early (E8-E11.0) hindlimb domain exhibits *Pbx1* and *Pbx2* expression only, whereas the forelimb domain additionally possesses *Pbx3* expression, studies here have focused on the hindlimb-specific inactivation of *Pbx* to simplify and more clearly understand how *Pbx* loss impacts limb development. In addition, by utilizing this Cre-Lox technology (Dymecki, 1996; Nagy, 2000; Lewandoski, 2001; Kwan, 2002), the early *in utero* lethality caused by the global homozygous loss of *Pbx1* and *Pbx2* during development has been circumvented. Finally, the results from both of these sets of studies and their ramifications on understanding skeletal element specification are analyzed in a discussion (Section 6.3) at the end of the chapter.

6.2 Results

6.2.1 The Morphological and molecular phenotypic characterization of global *Pbx1;Pbx2* loss on early limb development

6.2.1.1 Ectoderm and AER expression of *Pbx* genes

Recall from the previous chapter that *Pbx1* and *Pbx2* are dynamically expressed in the IM/LPM and bud mesenchyme during limb development (Fig. 5.4A). As limb outgrowth and patterning relies on epithelial-mesenchymal interactions, expression of *Pbx1*, *Pbx2*, and *Pbx3* was also examined in ectodermal tissues of the developing limb buds. *In situ* hybridization experiments mostly failed to detect *Pbx1*, *Pbx2*, and *Pbx3* mRNA transcripts in the developing

AER, even at stages when the AER is well formed. In those experiments that proved relatively informative, *Pbx1* and *Pbx2* expression was detected, albeit at extremely low levels, in both the AER and ventral ectoderm (Fig. 6.1). *Pbx3* was never detected in the AER or ectoderm covering the limb in any *in situ* hybridization experiments. As mentioned in Chapter 5, *Pbx4* is expressed only in the testes (Wagner et al., 2001).

More compelling data on the presence of Pbx in the limb field ectoderm and AER comes from studies on their protein localization (Fig. 6.2). As demonstrated, both Pbx1 (Fig. 6.2A) and Pbx2 (Fig. 6.2B) were detected in the limb ectoderm and AER by standard immunohistochemistry and immunofluorescence at stages such as at E10.5. In addition, Pbx1 (Fig. 6.2c) and Pbx2 (data not shown) were found at E9.0-9.5 in the early ectoderm indicating that their proteins were co-expressed prior to the completion of AER compaction. Pbx3 was never detected by immunohistochemistry in the ectoderm or AER (Fig. 7.2B) indicating that it is most likely absent from these tissues during development.

6.2.1.2 Morphological defects in limbs of mutant *Pbx1;Pbx2* double homozygous embryos

As discussed last chapter, *Pbx1/2 Mut* embryos have drastic defects in both forelimbs and hindlimbs, while embryos completely lacking both *Pbx1* and *Pbx2* (i.e., *Pbx1*$^{-/-}$*; Pbx2*$^{-/-}$) do not form well-developed limbs (Fig. 5.1). In *Pbx1/2 Mut* embryos, forelimbs were relatively less effected than hindlimbs (Fig. 5.1 and

5.2), a point attributed to the potential role of Pbx3 in the limb mesenchyme during early development. Indeed, in late surviving *Pbx1*$^{-/-}$*; Pbx2*$^{-/-}$ embryos, forelimb initiation occurred but then ceased, indicating that while Pbx3 was present it may not have been sufficient to allow limbs to form in the absence of total Pbx1 and Pbx2 loss (Fig. 5.1A). In these embryos, rudimentary forelimb buds were present but were very much reduced in size even when compared to those found in early E9.5 embryos. In contrast, even in late surviving *Pbx1*$^{-/-}$*; Pbx2*$^{-/-}$ embryos, hindlimbs did not appear to be morphologically visible (Fig. 5.1A), although molecular data suggests that limb specification/induction may have been initialized (see below).

6.2.1.3 Limb field specification appears slightly altered in *Pbx* compound mutants

Given their early lethality between E9.5 and E10.5 and delay in posterior somitogenesis (see Chapter 7) it has been difficult to ascertain whether forelimbs and hindlimbs are formed at the proper axial levels in *Pbx1*$^{-/-}$*; Pbx2*$^{-/-}$ embryos. Unfortunately, the extreme tissue malformations and necrosis that occurred in these early embryos makes it difficult to delineate somite boundaries and to study *Hox* expression patterns along the embryonic axis. Studies on *Pbx1/2 Mut* embryos provide some evidence that forelimb and hindlimb buds may not have formed at their proper axial levels. For example, axial level expression of *Hoxc6* was slightly rostralized with respect to the forelimb bud specifically when compared to that seen in wildtype embryos at E10.5 (Fig. 7.10B). This shift may

indeed have resulted in a change in forelimb bud location, but future work using conditional inactivation should help elucidate whether this was the case.

6.2.1.4 Limb induction was initiated in *Pbx1;Pbx2* mutants

The extreme limb defects observed in *Pbx1*$^{-/-}$*; Pbx2*$^{-/-}$ embryos raises the question of whether the induction of forelimb and hindlimb bud development occurred normally. Recall from Chapter 3, that one of the first important mechanisms for limb field induction is the expression of *Tbx5* in the presumptive forelimb mesenchyme and that of *Tbx4* in the presumptive hindlimb mesenchyme (Agarwal et al., 2003). Indeed, in knockout embryos for both of these genes, forelimbs and hindlimbs fail to form. Furthermore, in both limb contexts, *Fgf10* expression, which is a critical component of the Fgf/Wnt feedback cycle that underlies ectodermal-mesenchymal interactions in the limb, was altered (Kawakami et al., 2001; Agarwal et al., 2003; Barrow et al., 2003).

In situ hybridization experiments were performed for several of these markers to ascertain a molecular basis for the loss of limbs in mutant *Pbx* double homozygous embryos. *Tbx4* and *Tbx5* expression was analyzed in all *Pbx1;Pbx2* compound genotypes using littermate and non-littermate somite-matched controls (Fig. 6.3). As demonstrated, *Tbx4* expression occurred in the presumptive hindlimb field in all genotypes analyzed including in *Pbx1*$^{-/-}$*; Pbx2*$^{-/-}$ embryos (Fig. 6.3A). Furthermore, at E11.0, hindlimbs of *Pbx1/2 Mut* embryos possessed relatively normal distal expression of *Tbx4* although at this day expression was also found within the embryonic flank (Fig. 6.3B). These results

indicate that despite the developmental delay in *Pbx1*$^{-/-}$*; Pbx2*$^{-/-}$ embryos, a critical early limb field marker was maintained. Moreover, these data suggest that perhaps in compound mutants limb bud outgrowth is delayed such that cells do not progress (migrate or expand) into the limb field proper.

Tbx5 expression was also examined given the defects seen in forelimb development in both *Pbx1/2 Mut* and *Pbx1*$^{-/-}$*; Pbx2*$^{-/-}$ embryos. Accordingly, when compared to somite-matched and littermate controls, early *Pbx1*$^{-/-}$*; Pbx2*$^{-/-}$ embryos displayed a lack of expression of *Tbx5* in the limb field domains (Fig. 6.3C). The basis for this loss remains unclear as it may have resulted from the extreme cranial/thoracic level defects identified in these mutants and the apparent ablation of tissue that occurred with necrosis in these specimens due to their early *in utero* lethality. However, *Tbx5* expression was also reduced in *Pbx1/2 Mut* embryos suggesting that part of the forelimb phenotype was in fact mediated by a reduction in *Tbx5* during limb outgrowth (Fig. 6.3D).

Unfortunately, when *Fgf10* expression was examined in *Pbx1*$^{-/-}$*; Pbx2*$^{-/-}$ embryos it was difficult to detect as limb buds either did not form or when they did, as in late surviving embryos, they were extremely necrotic (Fig. 6.4A). *Fgf10* expression, however, was also examined from E9.5-E10.5 in *Pbx1/2 Mut* embryos and interestingly in both fore- and hindlimbs its expression was delayed and weakened compared to somite-matched littermates (Fig. 6.4A-C). These data are in partial agreement with the findings of *Tbx* expression and indicate that limb development was retarded (see discussion).

6.2.1.5 Early AER gene expression was altered in *Pbx1*$^{-/-}$*; Pbx2*$^{-/-}$ mutants

A downstream consequence of Tbx and Fgf10 activity in the limb field mesenchyme is the activation of *Fgf8* expression in the developing pre-AER and AER (see Chapter 3). Interestingly, despite the presence of *Fgf8* expression in the developing hindbrain region of mutant double homozygous embryos at 30 somites (at E10) (Fig. 6.5A), its expression was grossly reduced in the developing ectoderm of their limb buds, particularly when compared to somite-matched and littermate control embryos (Fig. 6.5). Specifically, *Fgf8* expression was extremely reduced, yet present, in the developing forelimb bud AER at 30 somites, a pattern that coincided with the extremely reduced limb bud size of these mutants (Fig. 6.5B). On the other hand, *Fgf8* was absent from the developing hindlimb bud of *Pbx1*$^{-/-}$*; Pbx2*$^{-/-}$ mutants, coincident with their lack of hindlimb development (Fig. 6.5C).

6.2.1.6 Ectodermal markers were severely reduced in *Pbx1/2 Mut* embryos during fore- and hindlimb bud development

To compensate for the early lethality of *Pbx1*$^{-/-}$*; Pbx2*$^{-/-}$ mutants as well as to identify the potential influence that *Pbx* loss has on AER gene expression, several markers critical for AER function and limb skeletogenesis were examined in the *Pbx1/2 Mut* embryos. These data should provide some evidence as to whether concomitant pathways were disrupted in the absence of *Pbx1* and *Pbx2;* and in addition, should provide some insight into the potential role that *Pbx3* plays in ameliorating development of the forelimbs as compared to hindlimbs.

As mentioned in Chapter 3, it is becoming clear that a significant degree of functional redundancy exists among genes expressed in the AER and that it is only after experimental deletion of multiple family members that phenotypic defects become evident. In this regard, expression of multiple *Dlx* and *Msx* genes were examined in *Pbx1/2 Mut* embryos, as their concomitant loss or reduction (i.e., as in compound *Msx1;Msx2*, and *Dlx5;Dlx6* mutants) has been shown to result in limb defects (Robledo et al., 2002; Lallemand et al., 2005; Kraus and Lufkin, 2006). Unfortunately, their expression patterns could not be examined in *Pbx1*$^{-/-}$*; Pbx2*$^{-/-}$ embryos given that they become expressed at approximately the time of death of these embryos.

Examination of *Dlx2* expression at E10.5 in *Pbx1/2 Mut* and control littermate embryos also revealed alterations in forelimb and hindlimb domains (Fig. 6.6A,B). In *Pbx1/2 Mut* embryonic forelimbs, *Dlx2* expression was reduced from the most anterior and posterior domains of the AER and was more diffuse dorsal-ventrally unlike the tight expression seen in wildtype forelimbs (Fig. 6.6A). This same pattern of expression was observed in *Pbx1/2 Mut* hindlimbs, although the degree of posterior loss was much more extreme (Fig. 6.6B). Furthermore, this gene's expression was lost from the distal-most posterior ventral surface of the limb, but remained in the anterior surface, a condition which mirrors that seen also for *Engrailed 1* expression (see below).

Analyses of *Dlx5* and *Dlx6* expression at this same gestational day (E10.5, data not shown) and later (E11.25) (Fig. 6.6C,D) revealed a similar pattern of alteration in *Pbx1/2 Mut* embryos. In *Pbx1/2 Mut* forelimbs (Fig. 6.6C), *Dlx5*

expression was lost from the most anterior and posterior boundaries of the AER, as also seen for *Dlx2*. In addition, its abnormal expression indicates that the AER may have been slightly concave ventral-dorsally (Fig. 6.6C). Expression of *Dlx5* in the mutant hindlimb at E11.25 was absent posteriorly, remained anteriorly, and showed an AER undergoing greater compaction then that seen at E10.5 (Fig. 6.6D). Expression of *Dlx6* in the posterior AER, however, remained well expressed in both forelimbs and hindlimbs of *Pbx1/2 Mut* embryos at E10.5 (Fig. 5.11).

Analyses of *Msx1* and *Msx2* expression also revealed unique alterations in these mutants. Normally, *Msx1* is expressed (e.g., at E10.5-E11.5) in both the AER and underlying distal mesenchyme (Fig. 6.7). Interestingly, at these days, *Msx1* expression (Fig. 6.7; data not shown) appeared up-regulated in the *Pbx1/2 Mut* fore and hindlimb mesenchyme. In the *Pbx1/2 Mut* forelimb mesenchyme expression was also distalized compared to the wildtype control. With respect to its D-V distribution, *Msx1* appeared more widely expressed in this domain as compared to the wildtype pattern (Fig. 6.7A). Finally, in the *Pbx1/2 Mut* hindlimb, there was a considerable up-regulation of *Msx1* in the anterior domain of the distal mesenchyme, and a severe down-regulation in the posterior mesenchyme (Fig. 6.7B).

Msx2 has a unique pattern of expression in wildtype embryos, in that its hindlimb AER and ventral ectoderm expression occurs earlier, relative to overall limb bud development, than in forelimbs (Fig. 6.8). In addition, *Msx2* expression is also found in the subjacent distal limb mesenchyme. At E10.5, *Msx2*

expression was normally absent from the *Pbx1/2 Mut* forelimb AER although its mesenchymal expression was greatly reduced when compared to that seen in wildtype (Fig. 6.8A). Furthermore, it was reduced more anteriorly than posteriorly in these mutant forelimbs. In hindlimb buds, where AER expression is typically present, *Msx2* expression was absent except from the most anterior region, where it was reduced (Fig. 6.8B). In this manner, this expression recapitulated that seen for other AER markers. Finally, analysis of the ventral extent of *Msx2* expression revealed that it was slightly expanded ventral-anteriorly (cranially) in *Pbx1/2 Mut* hindlimbs as compared to wildtype hindlimbs (Fig. 6.8B).

Expression of *Msx2* was also examined at later days (E11.0-11.5) to determine if the same abnormal patterns remained, worsened, or ameliorated. Strikingly, *Msx2* expression in the forelimb AER of *Pbx1/2 Mut* embryos never initiated (Fig. 6.8C). In addition, in a manner similar to that seen at E10.5, *Msx2* expression in the anterior mesenchyme remained absent or down-regulated and yet was expressed, albeit at lower levels, in the posterior mesenchyme (Fig. 6.8C). In the AER of *Pbx1/2 Mut* hindlimbs (at E11.5), *Msx2* was absent (or extremely reduced) despite its presence in the subjacent mesenchyme (Fig. 6.8D). In addition, its reduction in the mesenchyme corresponded to that which was seen at E10.5, with its specific down-regulation in the posterior domain (Fig. 6.8D). Overall, the expression patterns that emerge are quite complicated, suggesting that *Pbx* loss in fore- and hindlimb AER and mesenchyme differentially impacted *Msx* gene expression.

6.2.1.7 Dorsal-ventral patterning was altered in *Pbx1/2 Mut* embryos

Given that most genes involved in D-V patterning are also critical for AER formation, the expression of several key regulators was examined in *Pbx1/2 Mut* embryos to identify possible disruptions in these pathways [note: as most known D-V patterning genes are detectable by *in situ* hybridization once limb buds have initialized, their expression could not be studied in *Pbx1*$^{-/-}$*; Pbx2*$^{-/-}$ embryos]. An early marker of ventral polarity and of cells that migrate ventrally to compact to form the AER is *Engrailed1* (*En1*) (see Chapter 3). In *Pbx1/2 Mut* limbs, *En1* expression at E10.25 displayed a specific alteration that mirrored the loss of *Msx* and *Dlx* in these domains (Fig. 6.9). In forelimbs, *En1* expression was reduced in the most anterior and posterior domains of the ventral AER region (Fig. 6.9A). In hindlimbs, a specific down-regulation of *En1* was observed in the posterior ectoderm on the ventral side of the limb (Fig. 6.9B). Interestingly, these specific alterations of *En1* expression were not exactly observed in somite regions, which displayed a unique pattern of reduction. For example, while *En1* expression remained well intact in the developing somites at the forelimb level, its expression became reduced more posteriorly along the axis (Fig. 6.9C,D).

To examine if a similar disruption of dorsal fate occurred in *Pbx1/2 Mut* limbs, the dorsal ectodermal marker *Wnt7a* was examined. Besides extreme difficulty in probe generation and also in its detection, preliminary results demonstrate that *Wnt7a* expression at E10.5 was slightly decreased in *Pbx1/2 Mut* limbs (data not shown). At E11, *Wnt7a* expression became more severely down-regulated in the ectoderm of the posterior region of the forelimb (Fig.

6.10A). Likewise, *Wnt7a* expression was reduced in the dorsal ectoderm of the *Pbx1/2 Mut* hindlimb (Fig. 6.10B), indicating that the molecular mechanisms regulating and maintaining dorsal ectoderm identity became disrupted in these mutants.

Given the difficulties with using the *Wnt7a* probe, an additional dorsal marker was utilized. Normally, while *Lmx1b* transcripts are present in the dorsal mesenchyme, specifically from E10.5 to E11.5, earlier they are found throughout the limb mesenchyme. In addition, *Wnt7a* signaling has been shown to perpetuate and restrict *Lmx1b* expression in the dorsal mesenchyme after its ventral domain is reduced (see Chapter 3). At E10.75, *Lmx1b* expression was restricted to the dorsal mesenchyme of *Pbx1/2 Mut* forelimbs indicating that Wnt signaling was present (Fig. 6.11A). Interestingly, its expression appeared up-regulated in the posterior region of the dorsal mesenchyme. Despite these alterations in *Wnt7a* and *En1*, the D-V interface as demarcated by *Lmx1b* expression, remained intact (Fig. 6.11A). *Lmx1b* expression was also present in hindlimbs at E10.75 and potentially up-regulated compared to somite-matched wildtype and littermate controls (Fig. 6.11B). This potential up-regulation was present throughout the dorsal limb field and not necessarily restricted to the posterior region as was seen in the forelimb. Initially, it was considered that there was a ventral up-regulation of *Lmx1b* in the posterior *Pbx1/2 Mut* hindlimb bud. However, considering that *Lmx1b* is first expressed throughout the limb mesenchyme and later becomes restricted dorsally, analyses of limb buds of similar size were examined to determine the nature of this observation (Fig.

6.11B). Accordingly, *Lmx1b* was similarly expressed in a small ventral posterior and anterior domain in size-controlled buds suggesting that the expression observed in the *Pbx1/2 Mut* posterior limb bud was normal, yet delayed, and not that of up-regulation (Fig. 6.11B). Overall, while ectodermal signals appeared slightly disrupted at these days gestation, D-V mesenchymal patterning remained relatively intact.

6.2.1.8 Genes involved in the formation of the proximal to distal Fgf-RA gradient were disrupted in the absence of *Pbx1* and *Pbx2*

As the expression of numerous AER genes was altered in *Pbx1/2 Mut* embryonic limbs an attempt was made to examine if such alterations were commensurate with changes in gene expression within the early limb bud mesenchyme. While the expression of many mesenchymal genes such as *Hox* was altered early in *Pbx1/2 Mut* limbs (Chapter 5) additional markers were examined to gauge the extent of the effects of *Pbx* loss on limb outgrowth. A critical factor that both leads to and also reflects the activation of genes in the AER and mesenchyme, is the balance of Fgf signals emanating from the AER and retinoic acid (RA) signals coming from the proximal limb field mesenchyme (see Chapter 3). Specifically, changes in this balance have been argued to mediate the developmental progression of all three axes (Yashiro et al., 2004). As a measure of RA distribution in the limb, the expression of the gene *Cyp26B1* was examined, as this gene encodes an enzyme that degrades RA distally in the early bud (Fig. 6.12). At E10, *Cyp26B1* expression was extremely reduced in

Pbx1/2 Mut forelimb buds and absent in hindlimb buds (Fig. 6.12A,B). At E10.5, expression was also absent from hindlimb buds, further suggesting that enzymes that regulate RA degradation are disrupted by the absence of *Pbx1* and *Pbx2* (Fig. 6.12C). Given that in the mesenchyme and ectoderm numerous Fgfs were also severely reduced, it appears as though the Fgf-RA balance was markedly altered in *Pbx1/2 Mut* (and perhaps *Pbx1*$^{-/-}$;*Pbx2*$^{-/-}$) limbs.

6.2.2 The morphological and molecular phenotypic characterization of conditional *Pbx1/Pbx2* loss on limb development (conditional inactivation of *Pbx* in the AER versus limb mesenchyme)

6.2.2.1 Overview

As discussed above, *Pbx1* and *Pbx2* are expressed in the developing ectoderm and AER as well as in the limb field mesoderm and bud mesenchyme. Their dual expression presents a problem in understanding the roles of Pbx during limb bud outgrowth, i.e., it is extremely difficult to assess whether Pbx1 and Pbx2 proteins drive limb bud outgrowth and patterning via their roles in the mesenchyme, in the ectoderm, or in both. While it is possible that they play roles in both tissues, abrogation of their function in one specific tissue may result in phenotypic consequences. This situation is likely given that, for example, mesenchymal gene expression in *Pbx1/2 Mut* embryos was drastically altered in domains where *Pbx1* and *Pbx2* are co-expressed early. Furthermore, the observed binding of Pbx to the *Shh* limb enhancer in the mesenchyme (see Chapter 5) makes probable that *Pbx* deletion from this tissue should result in

phenotypic consequences. Therefore, conditional inactivation of *Pbx* from mesenchymal and ectodermal tissues has been employed to examine the effects of their deletion in these specific domains on limb development.

6.2.2.2 Conditional inactivation of *Pbx1* in the mesenchyme from E9.5 to birth

Since only *Pbx1* and *Pbx2* are expressed during hindlimb bud outgrowth until E11.0-11.5 (i.e., before *Pbx3* expression), their inactivation should allow for an assessment of how *Pbx* loss impacts limb development. To this end, the Cre-Lox technology was employed (Dymecki, 1999, Nagy, 2000; Lewandoski, 2001; Kwan, 2002), specifically utilizing a mesenchyme-specific Cre and a conditional or "floxed" *Pbx1* allele (i.e., $Pbx1^{cI\Delta 3/cI\Delta 3}$) as described in Chapter 4. The specific Cre recombinase was driven under the promoter of *Tbx4* (i.e., $Tbx4^{cre}$, courtesy of T. Jessell), a gene whose normal expression initializes at E9.5 and is limited to the hindlimb mesenchyme (Gibson-Brown et al., 1996).

To assess the spatio-temporal extent of Tbx4 Cre activity, $Tbx4^{cre/cre}$ homozygous mice were crossed to the Cre reporter line *R26R* (Soriano, 1999) as described in Chapter 4. This strategy provided a way to assess when and where Cre activity was capable of excising *Pbx1* "floxed" alleles in cells where they were co-expressed. Accordingly, during limb bud outgrowth, Tbx4 Cre was present throughout the limb mesenchyme, a pattern that continued throughout later hindlimb development after mesenchymal condensation formation (Fig. 6.13A).

A comparison of the spatio-temporal extent of Tbx4 Cre activity with that of the endogenous expression patterns of *Tbx4* revealed discrepancies in their distributions in the hindlimb. Specifically, the proximal extent of Cre activity was reduced and more distal when compared to *Tbx4* mRNA expression at E9.5 and E10.5 (Fig. 6.13B,C). In addition, both ROSA GFP and β-galactosidase detection revealed a reduction in the anterior to posterior extent of Cre activity (Fig. 6.13B). This situation presented a possible problem specifically since *Pbx1* was normally expressed throughout the proximal and anterior limb fields and excision of the *Pbx1* "floxed" allele may have been incomplete in these partially "non-overlapping" domains.

To assess the efficiency of Cre mediated recombination in domains where *Pbx1* and Tbx4 Cre co-localized, anti-Pbx1 immunohistochemistry was performed on transverse limb sections spanning several axial levels for embryos where the recombination event took place (i.e., $Pbx1^{cl\Delta 3/cl\Delta 3}$; $Pbx2^{-/-}$; $Tbx4^{cre/+}$ or $Pbx1^{cl\Delta 3/cl\Delta 3}$; $Pbx2^{-/-}$; $Tbx4^{cre/+}$) or where it did not (i.e., $Pbx1^{cl/cl}$; $Pbx2^{-/-}$; $Tbx4^{+/+}$). In all axial level comparisons, the extent of excision, as determined by that lack of nuclei staining anti-Pbx1 positive, was slightly more proximal for those specimens undergoing the recombination event (Fig. 6.14). For example, at a mid-transverse level positive cells in the control were present more distally then that which was evident in the recombinant limb (Fig. 6.14). This study revealed that the Tbx4 Cre was capable of excising *Pbx1* in regions where both overlap.

However, these analyses also revealed that a large domain of Pbx1 positive cells, which lied proximal to the domain of Tbx4 Cre activity, still

persisted in the limb (Fig. 6.14). Therefore, this analysis, performed at E10.75, revealed that regardless of the degree of excision at earlier days, when their respective domains more significantly overlapped, Pbx1 remained present in the proximal-most limb domain Since *Pbx1* has been shown to be a proximal limb marker (Selleri et al., 2001) and *Pbx1*$^{-/-}$ embryos have proximal limb defects, this Cre has failed to delete *Pbx1* in its most proximal and presumably "important" domain. Therefore, this Cre is not useful for deciphering how early loss of Pbx1 (and Pbx2) effects limb bud development. Yet, given that *Pbx1* and *Pbx2* are additionally expressed throughout later limb development (Fig. 5.4B), this degree of excision may still be significant to demonstrate Pbx cooperative functions during later limb development, particularly after E10.

Regardless of the degree of distal excision of *Pbx1*, analyses of the phenotypes of *Pbx1*$^{cI\Delta 3/cI\Delta 3}$*; Pbx2*$^{+/-}$*; Tbx4*$^{cre/+}$ and *Pbx1*$^{cI\Delta 3/cI\Delta 3}$*; Pbx2*$^{-/-}$*; Tbx4*$^{cre/+}$ embryos at several developmental stages revealed no observable differences in gross and skeletal tissue patterning and morphogenesis of the hindlimb when compared to appropriate control embryos. For example, at E14.5, both recombinant mutant and control specimens had normal hindlimb gross (Fig. 6.15) and skeletal morphologies (Fig. 6.16), including proper digit numbers and similar degrees of joint formation. Newborn hindlimb element morphology was also examined to see if late excision of *Pbx1* affected limb development. Analyses of newborn (P=0) skeletal morphology (data not shown) revealed no phenotypic defects in hindlimb patterning and morphogenesis in mutant and control

specimens, once again revealing that the loss of *Pbx* in this system did not impact normal limb development.

To compensate for the possibility that Cre excision was inefficient and, by doing so, further reducing the dosage of *Pbx1* in the developing limb, these same experiments were performed on embryos that additionally possessed one copy of the *Pbx1* global null allele (i.e., $Pbx1^{cI\Delta 3/-}$; $Pbx2^{+/-}$; $Tbx4^{cre/+}$ and $Pbx1^{cI\Delta 3/-}$; $Pbx2^{-/-}$; $Tbx4^{cre/+}$). Once again, analyses of embryos at E14.5 (data not shown) and P0 (Fig. 6.17) revealed no observable phenotypic defects in hindlimb patterning and morphogenesis. For example, at P0, hindpaws possessed all normal volar pads and five digits indicating that Pbx1 and Pbx2 were dispensable for their formation (Fig. 6.17). Furthermore, patterning of all elements of the girdle, stylopod, zeugopod, and autopod was normal (Fig. 6.18).

6.2.2.3 Conditional inactivation of *Pbx1* in the ventral ectoderm and AER

Since *Pbx1* and *Pbx2* are co-expressed in the developing ectoderm and AER of the forelimb and hindlimb (Fig. 6.2) their complete inactivation from these domains should allow for an assessment of how *Pbx* loss impacts limb development. In a similar manner to their partial mesenchymal inactivation, the Cre-Lox technology was again employed (Dymecki, 1999, Nagy, 2000; Lewandoski, 2001; Kwan, 2002), however, this time an ectodermal Cre was used along with the conditional or "floxed" *Pbx1* allele (i.e., $Pbx1^{cI\Delta 3/cI\Delta 3}$) as described in Chapter 4. The specific Cre recombinase was driven under the promoter of

Msx2 (i.e., *Msx2*^{cre}, courtesy of M. Lewandoski), a gene whose expression was present in the ventral limb bud ectoderm and AER at the onset of bud formation.

To assess the spatio-temporal extent of Msx2 Cre activity, *Msx2*$^{cre/+}$ mice were crossed to the Cre reporter line *R26R* (Soriano, 1999) as described above. An important consideration in using this specific *Msx2*^{cre} line was that the endogenous expression of *Msx2* occurred earlier during hindlimb bud development (relative to limb bud progression) than that of the forelimb, and therefore, a Cre driven under its promoter should have affected hindlimb development more efficiently. During early limb outgrowth (E9.25), Msx2 Cre was present in the lateral and ventral ectoderm of the forelimb bud and hindlimb field, a pattern that continued throughout limb development (Fig. 6.19A,B).

A close examination of the spatio-temporal extent of Msx2 Cre activity to that of the endogenous expression patterns for the *Msx2* gene revealed precise approximation in the limb (Fig. 6.19C). Specifically at E10.0, *Msx2* mRNA transcripts were localized along the ventral ectoderm and AER cells of the hindlimb bud, a pattern nearly identical to that detected for Cre activity in these domains. Furthermore, there was a significant decrease in Cre activity along the dorsal ectoderm of both limb bud types, indicating that this Cre is specific to the ventral ectoderm as reported (Lewandoski et al., 2000). The congruence between *Msx2* mRNA expression and Msx2 Cre activity suggested that this Cre should have been sufficient to excise *Pbx1* in the ventral ectoderm and AER domains of the hindlimb.

To assess the efficiency of Msx2 Cre recombination in domains where *Pbx1* and Msx2 Cre co-localized, anti-Pbx1 immunohistochemistry was performed on transverse limb sections for embryos where the recombination event took place (i.e., $Pbx1^{cl\Delta 3/cl\Delta 3}$; $Pbx2^{+/-}$; $Msx2^{cre/+}$ and $Pbx1^{cl\Delta 3/cl\Delta 3}$; $Pbx2^{-/-}$; $Msx2^{cre/+}$) and where it did not (i.e., $Pbx1^{cl/cl}$; $Pbx2^{-/-}$; $Msx2^{+/+}$). In all axial level comparisons, the extent of excision in the hindlimb, as determined by that lack of nuclei staining anti-Pbx1 positive, was efficient in specimens undergoing the recombination event (Fig. 6.20). For example, at all transverse limb levels at E10.5, positive staining nuclei were absent from the ventral ectoderm in the majority of the AER cells in recombinant mutants while strong staining nuclei were present ventrally in the AER in control (non-recombinant) limbs. Furthermore, while mutant ventral cells exhibited excision, dorsal ectodermal cells remained strongly positive for anti-Pbx1 mirroring the pattern in control limbs and also following closely the pattern expected by the restricted ventral activity of Cre recombinase (Fig. 6.19). Therefore, these data demonstrate that Pbx1 was excised from the ventral AER and AER domains where it potentially functioned along with Pbx2.

While the efficiency of ventral excision was high in the hindlimb, it appeared much lower, as expected, in the forelimb (Fig. 6.21). For example, at E10.5, forelimb ventral ectoderm and AER displayed more positive anti-Pbx1 cells than seen for the hindlimb. However, the degree of excision increased towards the medial-most domain of the forelimb bud ventral ectoderm (Fig. 6.21).

These differences between fore- and hindlimb excision appear to relate to the timing and spatial extent of Cre activity, as discussed above (Fig. 6.19A,B).

Interestingly, regardless of the degree of *Pbx1* excision in the ventral ectodermal and AER, analyses of the phenotypes of *Pbx1*$^{cl\Delta 3/cl\Delta 3}$*; Pbx2*$^{+/-}$*; Msx2*$^{cre/+}$ and *Pbx1*$^{cl\Delta 3/cl\Delta 3}$*; Pbx2*$^{-/-}$*; Msx2*$^{cre/+}$ embryos at several developmental stages revealed no observable differences in hindlimb gross and skeletal patterning and morphogenesis compared to control (non-recombinant) specimens. For example, at E12.75 (Fig. 6.22) and E13.0 (data not shown), both mutant and control specimens possessed normal hindlimb gross (Fig. 6.22A) and skeletal (Fig. 6.22B,C) morphologies, including proper digit numbers and similar degrees of joint formation. At E14.5, patterning and morphogenesis of all limb elements and joints were normal indicating that the ventral ectodermal loss of *Pbx* from the forming limb bud did not have overt soft tissue (Fig. 6.23) or skeletal morphological consequences (Fig. 6.24; forelimb data not shown).

Given that *Pbx* (*Pbx1-3*) and *Msx2* additionally co-localized in the interdigital mesenchyme of the limb (data not shown) and that AER gene expression has also been shown to influence later digital formation, newborn hindlimb element morphology was also examined to see if late excision of *Pbx1* (on a *Pbx2*$^{-/-}$ background) affected development. Analyses of newborn (P=0) gross (Fig. 6.25) and skeletal (Fig. 6.26; forelimb data not shown) morphology revealed no phenotypic defects in hindlimb patterning and morphogenesis in mutant and control specimens.

To compensate for the possibility that Cre excision was inefficient and, by doing so, further reducing the dosage of *Pbx1* in the developing limb, these same experiments were performed on embryos that possessed one copy of the *Pbx1* global null allele (i.e., *Pbx1*$^{cI\Delta 3/-}$*; Pbx2*$^{+/-}$*; Msx2*$^{cre/+}$ and *Pbx1*$^{cI\Delta 3/-}$*; Pbx2*$^{-/-}$*; Msx2*$^{cre/+}$). Once again, analyses of these embryos at E14.5 (Fig. 6.27) and P0 (data not shown) revealed no observable phenotypic defects in limb patterning and morphogenesis. For example, at P0, the ventral surface of the hindlimb and forelimb possessed all normal volar pads and five digits indicating that Pbx1 and Pbx2 were dispensable for their formation. Furthermore, patterning of all elements of the girdle, stylopod, zeugopod, and autopod was normal (data not shown).

The only low penetrant phenotypes identified in these mutant mice (i.e., *Pbx1*$^{cI\Delta 3/-}$*; Pbx2*$^{-/-}$*; Msx2*$^{cre/+}$) were slight edema and smaller overall body size (Fig. 6.27). Both of these defects may have resulted from a low occurrence of germline deletion of *Pbx1* by Msx2 Cre, as has been reported for the interaction of other conditionally inactivated alleles with this Cre (Lewandoski et al., 2000). These mild phenotypes slightly recapitulated those seen in single global *Pbx1*$^{-/-}$ embryos.

6.3 Discussion

6.3.1 *Pbx* genes exhibit complex expression patterns in vertebrates that underlie intricate roles during embryogenesis

The studies on *Pbx* gene expression and protein localization as presented in this thesis, demonstrate novel and more complex spatio-temporal patterns in vertebrate compared to invertebrate appendages. For example, there are no reports that in flies Exd occupies epithelial tissue layers covering the wing or leg imaginal disc (Pueyo and Couso, 2005). In contrast, in vertebrates, Pbx1 and Pbx2 are found in both the surface ectoderm and the AER (Fig. 6.2), and therefore, they lie on both sides of the mesenchymal-epithelial network critical for limb outgrowth. Furthermore, their observed binding to *Fgf8* (unpublished results) and *Shh* regulatory regions (Chapter 5) suggest that Pbx proteins directly interact with important mesenchymal and ectodermal genes. Interestingly, it has been observed in amphibians (Mercader et al., 2005) and even mouse (unpublished results) that Meis proteins are also present in the ectoderm and AER of the limb. Therefore, Pbx and Meis cofactors may cooperate in this tissue to drive gene expression and/or Meis may be required for Pbx translocation to the nuclei of ectoderm and AER cells. Overall, when compared to that seen in invertebrates, vertebrates display increasing levels of complexity in the expression patterns, and perhaps functionality, of both Pbx and Meis proteins in the limb (see Chapter 3).

These studies on Pbx (and Meis/Prep2) localization in both limb mesenchyme and ectoderm may also reflect the importance of these TALE proteins in the development of many other organ systems, specifically those that require epithelial-mesenchymal interactions. For example, in craniofacial development, Pbx1, Pbx2, and Pbx3 are present in both the facial mesenchyme

and ectoderm where they play critical roles in the regulation of Fgf-Wnt signaling and the development of the lip and palate (Ferretti, Selleri, unpublished results). In fact, compound mutant *Pbx1;Pbx2* and *Pbx1;Pbx3* embryos, where *Pbx1* has been either globally or conditionally inactivated from the facial ectoderm reveal severe clefting of the face and lip, a phenotype that recapitulates that seen in human cleft lip patients (Ferretti, Selleri, unpublished results). Similarly, during spleen development, *Pbx1* and *Pbx2* are found in both the mesenchyme and splenic capsule, a mesothelial layer surrounding the spleen. Inactivation of *Pbx1* from the splenic mesenchyme results in partial to complete spleen agenesis (Brendolan, Selleri, unpublished results).

6.3.2 *Pbx1/Pbx2* effects on limb bud induction and outgrowth reflect complex hierarchical relationships with the Tbx family of transcription factors

It has been proposed that *Tbx5* and *Tbx4* in the forelimb and hindlimb, respectively, serve to initialize limb bud outgrowth and execute a genetic program established by a cranial to caudal axial *Hox* code (Minguillon et al., 2005). Once activated, both *Tbx* genes appear to partially execute their effects via their direct control of *Fgf10* expression in the limb bud mesenchyme (Agarwal et al., 2003). In addition, *Tbx5* has been demonstrated to regulate Wnt signaling (Takeuchi et al., 2003) early during bud outgrowth and therefore Tbx may mediate limb bud formation via their upstream control of multiple pathways.

Importantly, it has been demonstrated above using global compound *Pbx1*;*Pbx2* mutants that the expression of *Tbx5* and *Tbx4* is affected differently by the loss of *Pbx* in their respective limb domains. For example, *Tbx5* expression was severely reduced in both *Pbx1*$^{-/-}$*; Pbx2*$^{-/-}$ and *Pbx1*$^{-/-}$*; Pbx2*$^{+/-}$ forelimbs (Fig. 6.3). Thus, in the forelimb, *Pbx* appears to lie upstream of *Tbx5.* Furthermore, early in forelimb development there was a reduction of *Fgf10* expression, a known direct target of Tbx5 (Agarwal et al., 2003). Therefore, as *Pbx* lie genetically upstream of *Tbx5*, as these data indicate, then they are one of the earliest known regulators of *Tbx5* expression and forelimb bud initiation. At the same time, that Pbx may function more directly upstream of Fgf10 remains a possibility (see below and Fig. 6.28).

Unlike that proposed for the forelimb, *Pbx* does not appear to act genetically upstream of *Tbx* during hindlimb bud initiation, as *Tbx4* was normally expressed in both *Pbx1*$^{-/-}$*; Pbx2*$^{-/-}$ and *Pbx1*$^{-/-}$*; Pbx2*$^{+/-}$ hindlimb buds. Interestingly, despite its normal limb bud expression, *Tbx4* was also partially expressed in the proximal flank unlike that found in wildtype domains (Fig. 6.3). This finding suggests that the regulation of hindlimb bud outgrowth in the absence of *Pbx* is compromised with important effects on the mesenchymal cell population expressing *Tbx* genes. In support of this view is the additional finding that the expression of *Fgf10* in early *Pbx1*$^{-/-}$*;Pbx2*$^{+/-}$ hindlimbs (Fig. 6.4) was reduced and delayed. Therefore, it is a possible that *Pbx* regulates limb bud outgrowth partially through their effects on Fgf10 signaling, independent of any effect on Tbx4.

With respect to all three of these molecular factors and their roles during early limb bud induction, several scenarios can be envisioned (Fig. 6.28): (A) *Pbx* and *Tbx4* mediate *Fgf10* expression (and function) in the hindlimb through parallel genetic networks; (B) *Tbx4* lies upstream of *Pbx* (and *Fgf10*) during hindlimb bud outgrowth; (C) *Pbx* and *Tbx4* cooperate in a complex biochemical regulation of *Fgf10* in the limb bud mesenchyme; and/or (D) *Pbx* and *Tbx4* cross-regulate each other in the limb via their effects on *Fgf10*, the ectoderm, and/or other unknown target genes. With respect to (A) and (B), studies of *Pbx* expression in *Tbx4* and *Tbx5* homozygous mutant embryos should aid in clarifying the proposed hierarchical relationships between *Pbx* and *Tbx*. In regards to (C), as the *Fgf10* promoter has been recently characterized and assessed with respect to Tbx binding and regulation (Agarwal et al., 2003), similar analyses can be conducted for Pbx and whether it can also bind to this regulatory region. Finally, conditional inactivation of *Pbx* during early limb bud outgrowth can aid in identifying the complex relationships between these factors and how they potentially cross-regulate each other during mesenchymal-ectodermal interactions (D).

6.3.3 *Pbx* are upstream of gene expression in the preAER and AER

Despite the normal posterior expression of *Fgf8* in early *Pbx1/2 Mut* fore- and hindlimb buds (Fig. 5.11), its expression was either reduced or absent in *Pbx1*$^{-/-}$*; Pbx2*$^{-/-}$ forelimb and hindlimb buds, respectively, indicating that early ectodermal function was significantly abrogated by the loss of *Pbx* (Fig. 6.5).

This alteration of *Fgf8* expression in the double homozygous mutant was associated with severely reduced forelimb buds and hindlimb buds that morphologically did not develop past the initialization stage. Importantly, the reduction and loss of *Fgf8* expression in the limbs did not reflect a global down-regulation, specifically since the mid-brain to hindbrain transition still demonstrated near normal *Fgf8* expression (Fig. 6.5). Interestingly, in addition to the loss of *Fgf8*, *Pbx1/2 Mut* limbs displayed numerous alterations in the expression of several other AER genes, such as those of the *Dlx* and *Msx* family of transcription factors (Figs. 6.6-6.8).

Notably, several of these reductions in ectodermal gene expression in *Pbx1;Pbx2* compound mutants were observed early at stages prior to *Shh* initiation, indicating that a component of their down-regulation was due to alterations during the initial stage of mesenchyme-ectoderm interaction. While at this point in time it is tempting to explain these reductions as resulting from problems in limb bud induction (see previous section) and alterations in mesenchymal signaling to the ectoderm, the fact that *Pbx* are expressed in both of these tissue types complicates the matter. On the one hand, it is possible that *Pbx* loss specifically from the ectoderm led to these reductions in AER and ectodermal gene expression. This cell autonomous role for Pbx could be the case given that they (and their partner proteins Meis1 and Meis2) are co-localized in the early ectoderm and have preliminary been shown to bind to a *Fgf8* regulatory element (unpublished results). On the other hand, it is also possible that the abrogation of limb bud initiation (i.e., via the reduction in Fgf10

signaling and/or some other pathway in the mesenchyme, see below), led to a disruption in the mesenchymal component of this induction process and to the loss of ectodermal gene expression. In this case, a cell non-autonomous role for Pbx would be paramount. Regardless, at this time, it is clear that *Pbx1* and *Pbx2* are hierarchical factors that partially regulate ectodermal gene expression in the early (pre-Shh) limb bud.

Another pathway that influences ectodermal gene expression and is effected by the loss of *Pbx* in the limb is RA signaling. In the limb, RA is normally highest in the proximal domain and lowest in the distal domain (Reijntjes et al., 2003; Yashiro et al., 2004). This gradient is maintained by the actions of RaldH2 and Cyp26B1 enzymes in the mesenchyme, the latter of which degrades RA and lowers its distal concentration (Abu-Abed et al., 2002). In *Pbx1/2 Mut* embryos, the expression of *Cyp26B1* was severely down-regulated, suggesting that the RA gradient remained high distally. Interestingly, in studies on chick limbs, ectopic application of high levels of RA has been shown to lead to apoptosis (Jiang and Kochhar, 1992; 1993); yet, in *Pbx1/2 Mut* embryos distal apoptosis was not marked during or after the stage when *Cyp26B1* was found to be down-regulated (see Chapter 5). Therefore, the levels of RA in the *Pbx1/2 Mut* limb may not have been sufficiently high to cause distal truncation via apoptosis. However, distal limb reductions/absences in *Pbx1;Pbx2* mutants may have been mediated by a concurrent lowering of the concentrations (and altering the balance) of both Fgf and RA in the limb; specifically lower for each in the distal hindlimb bud. This

balance, when altered, as demonstrated in *Fgf10*$^{-/-}$ (Min et al., 1998; Sekine et al., 1999), *RaldH2*$^{-/-}$ (Mic et al., 2004), and *Cyp26B1*$^{-/-}$ (Yashiro et al., 2004) embryos, ultimately leads to truncations in the limb and for several of these mutants, simultaneous effects on preAER and AER gene expression and formation (Yashiro et al., 2004). Overall, ectodermal gene expression could be altered in *Pbx1/2* mutants via Pbx concerted consequences on Fgf and RA signaling in the mesenchyme and the ectoderm.

6.3.4 *Pbx* are upstream of D-V axis determination and AER formation in the limb

Since *Pbx1*$^{-/-}$*; Pbx2*$^{-/-}$ embryos died early in utero, it was not possible to determine whether their limbs exhibited significant morphological and molecular alterations along the D-V axis. Intriguingly, the partial loss of *Pbx* from the fore- and hindlimb fields in *Pbx1/2 Mut* embryos did result in molecular D-V alterations, which suggests that skeletal element identity may have been modified. However, such molecular alterations did not translate into gross morphological transformations in E13.5 mutant embryos; although this stage may have been to early for such an assessment.

The specific molecular changes observed in *Pbx1/2 Mut* limbs were evident in the expression of ectodermal genes such as *En1*, *Msx*, and *Wnt7a*, and the mesenchymal gene, *Lmx1b*. Each expression pattern was slightly different from that seen in wildtype embryos, specifically along the D-V boundary in the ectoderm and subjacent mesenchyme. For example, *En1* expression was

lost from the posterior ventral hindlimb ectoderm and *Lmx1b* was slightly ventralized in this domain at the same stage (compare Fig. 6.9 to 6.11). Interestingly, the forelimb displayed a more dramatic alteration in *En1* as both the anterior and posterior regions of the ventral ectoderm lacked expression, whereas this change was not coupled with an alteration in the mesenchymal expression of *Lmx1b*. These data suggest that *Pbx* differentially affect gene expression in the different limb types as was already demonstrated in Chapter 5 and discussed above with respect to *Tbx* expression. As both *En1* and *Lmx1b* are critical for the delineating the D-V axis and also for providing the proper D-V identity to mesenchymal cells during skeletal element patterning (i.e., null mice for these genes display drastic D-V patterning alterations, Loomis et al., 1996; Chen et al., 1998b; Chen and Johnson, 2002; Adamska et al., 2004; Murcia et al., 2004), Pbx may function upstream and direct patterning along this axis. In this regard, as their expression is along the entire ectoderm, Pbx may serve as general transcription factors that aid in establishing networks of gene expression along each domain, possibly by cooperating with different factors in the dorsal versus ventral ectoderm, or via an affect on ectoderm cell differentiation and/or survival. At the same time the concept that *Pbx* mesenchymal expression leads to ectodermal gene alteration cannot be ruled out.

That Pbx play critical roles in the ectoderm is supported by the additional findings that *Msx and Dlx* gene expression are highly altered in this tissue in *Pbx1/2 Mut* limbs (Figs. 6.6-6.8). Specifically, the expression of most of these genes is drastically reduced and/or spatially altered in both the forelimb and

hindlimb ectoderm prior to and after *Shh* expression. Concomitantly, as *En1*, *Msx1*/*Msx2*, and *Wnt7a* are critical for AER formation (i.e., as single null and compound mutants for these genes display AER defects, Cygan et al., 1997; Parr et al., 1998; Loomis et al., 1996; Adamska et al., 2004; Murcia et al., 2004; Lallemand et al., 2005), their unique patterns of absence and spatial alteration in *Pbx1/2 Mut* limbs suggests a disruption in AER formation. For example, in hindlimb buds the expression of *Msx*, *Dlx*, and *En1* in the AER was not only posteriorly absent but anteriorly diffused. Furthermore, the expression of all examined *Msx* and *Dlx* (as well as *Bmp2*, Fig. 5.13) demonstrate that hindlimb AER expressing cells were not directly aligned along a D-V midline axis but bowed along the most anterior and posterior domains. Subsequently, this angulation was also seen in the subjacent mesenchymal expression of *Lmx1b*. These data may indicate that AER cells did not compact correctly along the D-V interface, as at later days (i.e., E11 and E11.5) the ectodermal expression of all of genes is restricted to the AER proper and thus serves as a proxy of AER formation and shape. Despite these alterations, such changes did not necessarily correspond to complete disruptions in signaling, as *Fgf8* expression is relatively normal in most of the AER prior to the loss of *Shh*.

At present, *Pbx* appear to act upstream of the expression of several genes (i.e., *En1* and *Msx*) that operate to concurrently guide AER formation (and function) and D-V patterning. As discussed in Chapter 3, these specific genes (i.e., *En1* and *Msx*) are additionally downstream of Bmp signaling in the limb. While AER gene expression (including *Bmp*) and formation ensued in the

hindlimb of *Pbx1/2 Mut* embryos (albeit in an abnormal manner), the failure to form a limb in the complete absence of *Pbx1* and *Pbx2* may further evince Pbx hierarchical control of Bmp signaling. Thus, hindlimb loss in double homozygous mutants may be the result of mesenchymal and/or ectodermal signaling disruptions of both the Bmp → En1 (D-V determining) pathway as well as the Bmp → Msx (AER formation) pathway (see Chapter 3). In this manner, complete loss of *Pbx* from the hindlimb may phenocopy that observed for the conditional inactivation of *BmpR1A* in the hindlimb ectoderm (Ahn et al., 2001). Finally, as specific anterior and posterior loss of *En1* and *Msx* were also observed in the *Pbx1/2 Mut* forelimbs, the presence of Pbx3 as a redundant factor functioning during forelimb outgrowth may ameliorate Bmp signaling and facilitate at least partial limb outgrowth. A hypothesis borne out of this work is that *Pbx* lies genetically upstream of early Bmp signaling in the presumptive limb field. Future work on *Pbx* conditional inactivation in the pre-limb mesenchyme will help experimentally test this hypothesis and understand Pbx roles in both pathways.

6.3.5 Late *Pbx1* and *Pbx2* mesenchymal expression is dispensable for limb development

Earlier in the chapter, it was demonstrated that the conditional inactivation of *Pbx1* (on a *Pbx2*$^{-/-}$ background) from the distal mesenchyme results in normal hindlimb bud development and skeletal patterning. Specifically, Cre driven under the promoter of *Tbx4* in the hindlimb bud was sufficient to excise *Pbx1* from its distal-most limb domain, and yet no proximal or distal skeletal patterning

alterations were evident at early days such as E14.5. In this manner and according to the PZ model, Pbx proteins most likely do not influence skeletal patterning within the Progress Zone as in this mouse model, they were excluded from this domain at least after E10.5, when zeugopodial and autopodial patterning takes place. Furthermore, if distal limb patterning and growth of the limb's skeletal elements are Hox dependent (see Chapter 3), then according to that ascribed in the PZ Model, this specific Hox-dependent patterning may not rely on Pbx ancillary role; i.e., that Hox can mediate patterning via their control of target genes in absence of Pbx cofactor binding. However, this scenario does not exclude the possibilities that Pbx hierarchical regulation of *Hox,* as demonstrated in Chapter 5, governs distal limb patterning via their early mesenchymal roles, or that Pbx "mark" regulatory elements of genes early in the limb field to facilitate their later transcriptional activation or repression (see Chapter 8).

Before accepting these interpretations, several caveats still remain. First, while immunohistochemistry experiments demonstrated that *Pbx1* was excised distally, it may be that residual low-level nuclear Pbx1 protein was still present and stable in this domain from earlier stages prior to Tbx4 Cre activity. Currently, the half-life of Pbx1 protein is unknown and it remains possible that even low-level concentration is enough for proper function. Second, the possibility still holds that excision by Tbx4 Cre was not efficient enough, although the absence of nearly all Pbx1 protein distally as in $Pbx1^{cI\Delta 3/-}$; $Pbx2^{-/-}$; $Tbx4^{cre/+}$ embryos and newborn pups should compensate for distal excision deficiency. Third, with

respect to later skeletal element patterning, if domains of Pbx1 reside outside the domain of Tbx4 Cre then its function would only partially be compromised. Fourth, the presence of *Pbx3* in the hindlimb mesenchyme after E11 may partially compensate for the loss of *Pbx1* and *Pbx2* from this domain and therefore ameliorate the morphological consequences.

At present, these findings strongly support the hypothesis that the later *Pbx1* and *Pbx2* distal-most expression domains (i.e., after E9.5/10.5) are not essential for limb bud formation. That the proximal-most cellular domain of *Pbx1*, not excised by Tbx4 Cre, may potentially serve as a pool of cells that compensate for the distal loss of Pbx1 activity still remains a possibility. This scenario could be likely given the suggested roles of Pbx in controlling cell proliferation and differentiation (see Chapter 3). At this point in time, however, Pbx1 immunohistochemistry provides no evidence for the distal migration of Pbx1 positive cells, as all cells distal to this positive domain, lack nuclear Pbx1 protein (Fig. 6.14).

Importantly, these data, acquired from the use of the *Tbx4*^{cre} line as a specific deleter of *Pbx1* from distal limb domains, indirectly support, the hypothesis borne out of the findings in Chapter 5, that Pbx function early in the limb field to execute its effects on limb bud outgrowth and skeletal patterning. These early stages/domains of *Pbx* gene expression and suggested function (i.e., specifically for the hindlimb) exist before the activity of Tbx4 Cre. If viewed under the ES model, *Pbx* gene expression in the early limb field (i.e., prior to its abrogation by Tbx4 Cre) would lie within the reported zones of early stratified,

prepatterned cells that eventually become under the influence of the limbs major signaling centers and expand to become skeletal elements (Dudley et al., 2002). Since these early domains also overlap with Hox, then the action of Pbx, as not only upstream regulatory factors but as Hox ancillary factors, remains possible.

Future experiments that ensure the complete absence of *Pbx1* and *Pbx2* from both the proximal and distal limb should help specifically address the ES and PZ models and Pbx functionality. Experiments are currently underway to explore Pbx early functions using an inducible *Hoxb6*^{creER} line that displays strong Cre activity in complete overlapping domains with *Pbx1* from E7.5 (i.e., during gastrula stages) to E10.5 (i.e., to mid- to late hindlimb development) (Mackem, unpublished results).

6.3.6 The ventral ectodermal and AER expression of *Pbx1* and *Pbx2* are dispensable for normal limb development after E10

It has been specifically demonstrated that the conditional inactivation of *Pbx1* (on a *Pbx2*$^{-/-}$ background) from the ventral preAER and AER cells, using a *Msx2*^{cre} mouse line, results in normal embryonic and newborn hindlimb skeletal development. These data suggest that, at the time of deletion and onwards, Pbx has no essential functions in these ectodermal tissues. Interestingly, Sun et al. (2002) have demonstrated utilizing this same *Msx2*^{cre} line that the conditional inactivation of *Fgf4* and *Fgf8* from these cells results in complete limb agenesis. Therefore, Pbx deletion from these same tissues and at this stage of development does not affect the functionality of Fgf signaling, as such would

have resulted in limb dysmorphogenesis. In fact, even partial loss of Fgf signaling (i.e., the deletion of *Fgf8* only using this *Msx2^{cre}* line; Lewandoski et al., 2000) results in limb stylopodial defects and such alterations were not observed in conditional *Pbx1;Pbx2* embryos at comparable gestational days. Regardless of this finding, the possibility still exists that Pbx upstream role on Fgf signaling (as suggested above) occurs at earlier stages in development (i.e., prior to its deletion by this Cre).

Interestingly, Kimmel et al. (2000) utilizing an inducible *Msx2^{creER}* line demonstrated that the AER specifically derives from ectodermal cells that express both *En1* and *Msx2* (and later express *Fgf8*). In fact, as discussed in Chapter 3, the AER forms in the mouse from the ventral ectoderm (Niswander, 2003). Based on visual comparisons of the *Msx2^{creER}* and *Msx2^{cre}* lines, it appears that both reported Cre activities were essentially similar spatially and temporally. If such is the case, then from E9.75 onwards, Pbx1 and Pbx2 are not acting in these ventral ectodermal cells in a manner to promote their formation into the AER, specifically because Pbx loss using the *Msx2^{cre}* line from this cell population (i.e., at these same days) results in normal limb bud patterning and no evident defects in AER formation (data not shown). To date, skeletal defects have been observed in all mutants that display severe or even mild AER malformations, including many mutants produced using either *Msx2^{cre}* line (see Chapter 3). Therefore, if Pbx are involved in AER formation and function, as the data acquired from global mutant embryos suggests, then their action may be before and/or during preAER cell migration and/or compaction (i.e., before or

during the time period of their deletion by Msx2 Cre). At the same time, their presence in the dorsal ectoderm may be of great importance (see below) .

Similar to the use of the *Tbx4*^{cre} line, several caveats still remain before accepting these results. First, as mentioned it is possible that only very low concentrations of Pbx are essential for their functions in the limb ectoderm. In this way, incomplete or inefficient deletion could result in some residual Pbx protein. However, the lack of limb defects in *Pbx1* $^{cI\Delta 3/-}$*; Pbx2*$^{-/-}$*; Msx2*$^{cre/+}$ embryos and newborn pups provided one means to lower overall Pbx dose and in these mutants no defects were observed. A second concern is that *Pbx1* and *Pbx2* are expressed in the ventral ectoderm prior to the activity of Msx2 Cre and in this way may provide either residual Pbx (stabilized and/or not yet degraded) protein for their early limb roles, or again be present in an early cell population that sufficiently provided cell descendants to the limb ectoderm. Unfortunately, at this time a mouse line harboring an earlier active Cre, specifically restricted to the entire ectoderm of the prelimb field, is not known to exist.

Finally, an important concern regarding the interpretation of Pbx ectodermal roles during limb bud outgrowth centers on the finding that while Msx2 Cre was sufficient to delete *Pbx1* from the ventral ectoderm, it was unable to delete it from the dorsal ectoderm. While the dorsal ectoderm is important for AER formation as well as P-D, D-V, and A-P skeletal element patterning, no known mouse mutant for the dorsal limb ectoderm (or mesenchyme) displays complete agenesis of the limb. For example, even though *Wnt7a*$^{-/-}$ embryos display D-V and A-P patterning defects, all three main limb compartments

possess most elements, many of which are normal (Cygan et al., 1997; Parr et al., 1998). However, since *Wnt7a* is expressed at the onset of limb bud formation (i.e., at E9.5), its genetic abrogation may not be a good indicator of the effects of ectodermal gene perturbation on initial limb bud outgrowth. In other words, the action of Wnt7a may be too "late" for an assessing the importance of the dorsal ectoderm during early mouse limb bud initiation. In this respect, both *Bmpr1a* (Ahn et al., 2001) and *β-Catenin* (Soshnikova et al., 2003) mutants, which lack functional protein from nearly the entire posterior ectoderm (at E9.5), display complete to partial hindlimb skeletal element absence, respectively. In addition, tissue deletion experiments in chicks in which the pre-limb ectoderm is removed prior to bud emergence demonstrate that the entire ectoderm overlying the limb field is essential to initialize limb bud and skeletal element formation (see Chapter 3). Therefore, it still remains possible that *Pbx* presence in the entire pre-limb field ectoderm (i.e., prior to the action of Msx2 Cre) is required for normal limb development.

6.4 Summary

In conclusion, an abundance of evidence has been presented that suggest that the actions of Pbx during limb bud formation are early, perhaps during the initial stage of induction. The findings that early ectodermal and mesenchymal gene expression are significantly reduced and/or absent demonstrate that Pbx hierarchically regulate many critical genetic pathways involved in limb bud formation. Such upstream roles include their control of the initiation of P-D, A-P

and D-V axis establishment and later skeletal patterning, as evinced by the severe loss and reduction of genes known to be upstream of these processes.

Figures

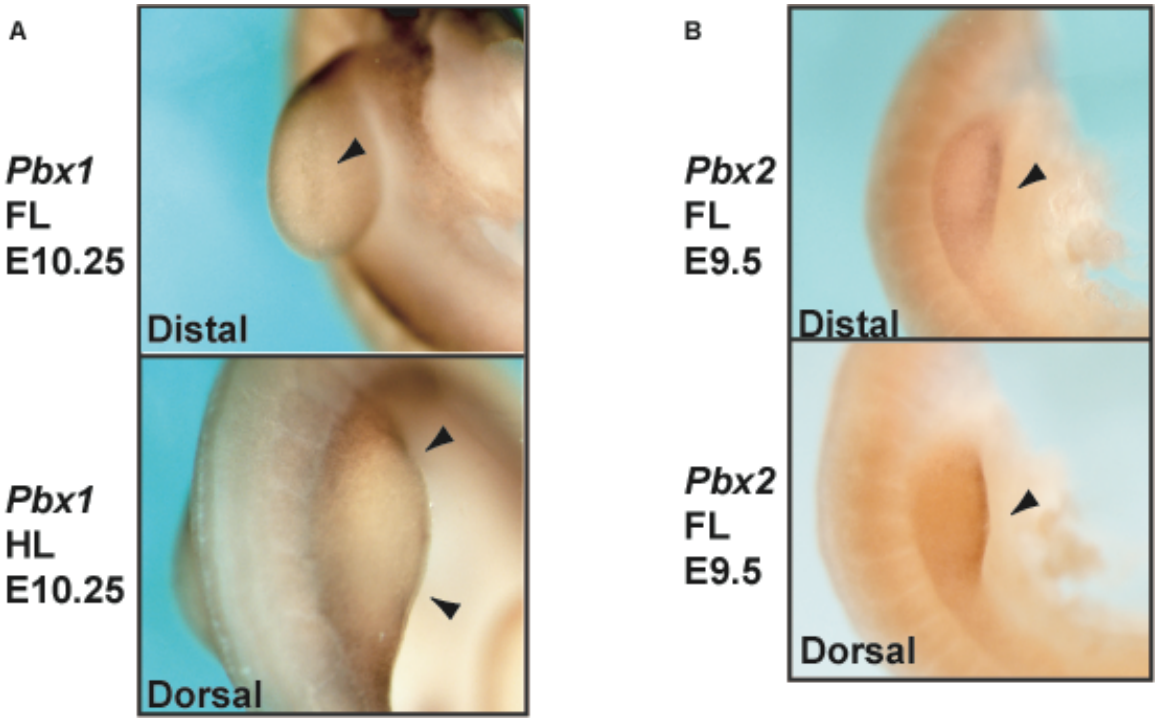

Figure 6.1. *Pbx1* and *Pbx2* expression in the limb ectoderm and AER.

(A) *In situ* hybridization at E10.25 revealed that *Pbx1* was expressed in the distal forelimb AER and distal hindlimb preAER ectoderm and AER (dark arrowhead). (B) At E9.5, *Pbx2* was expressed in the ventral ectoderm and pre-AER in the forelimb (dark arrowheads). Proximal (left); anterior (top); FL, Forelimb; HL, Hindlimb.

Figure 6.2. Pbx1 and Pbx2 proteins co-localization in the ectoderm and AER.

(A) Immunohistochemistry at E10.5 revealed that Pbx1 protein was present in the ventral (light shaded arrowhead) and dorsal ectoderm (light shaded arrowhead) and the AER (dark shaded arrowhead) of the fore- and hindlimbs. (B) At E10.5, Pbx2 protein was present in the ventral (light shaded arrowhead) and dorsal ectoderm (light shaded arrowhead) and the AER (dark shaded arrowhead) of fore- and hindlimbs. (C) At E9.5, Pbx1 was also present in the ectoderm surrounding the limb and body (dark shaded arrowheads). (A, B) left to right: 4X, 10X, 20X, 20X fluorescence immunohistochemistry. (C) 4X. Proximal (left); dorsal (top); FL, Forelimb; HL, Hindlimb.

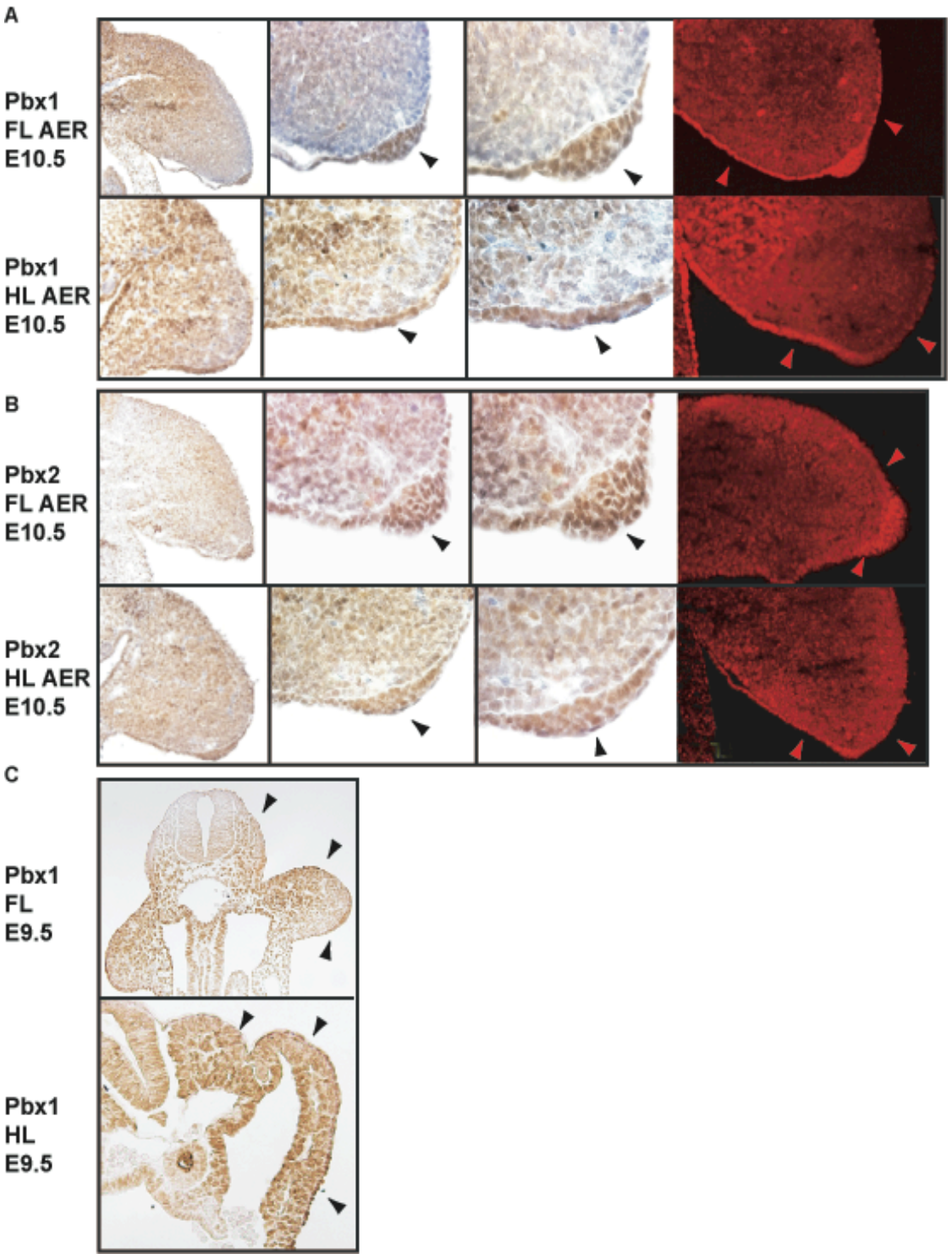
A
Pbx1
FL AER
E10.5
Pbx1
HL AER
E10.5
B
Pbx2
FL AER
E10.5
Pbx2
HL AER
E10.5
C
Pbx1
FL
E9.5
Pbx1
HL
E9.5

Figure 6.3. *Tbx4/Tbx5* expression in *Pbx1*$^{-/-}$;*Pbx2*$^{-/-}$ and *Pbx1*$^{-/-}$;*Pbx2*$^{+/-}$ embryos.

(A) *In situ* hybridization revealed that despite the lack of morphologically visible hindlimb buds, *Tbx4* remained well expressed (black arrowheads) in *Pbx1*$^{-/-}$;*Pbx2*$^{-/-}$ (19 som.) embryos compared to somite-matched WT (18 som.) and littermate WT (34 som.) embryos. Littermate WT control embryos were included (in A and C) to demonstrate that *Pbx1*$^{-/-}$;*Pbx2*$^{-/-}$ embryos were delayed in somitogenesis. (B) *Tbx4* remained well expressed in *Pbx1*$^{-/-}$;*Pbx2*$^{+/-}$ hindlimb buds at E11; however mRNA transcripts were detected in the flank of these embryos (black arrowheads) when they were typically absent in the flank of WT embryos (empty black arrowheads) at this same day. (C) *Tbx5* was not detected in the forelimb region of E10.75 *Pbx1*$^{-/-}$;*Pbx2*$^{-/-}$ embryos (19 som.)(empty black arrowhead) unlike that in somite-matched WT (18 som.) and littermate WT controls (36 som.) (black arrowhead). However, such a loss could have been due to the severe necrosis in the anterior/cranial region of these embryos. (D) *Tbx5* expression was markedly reduced in E10.25 and E10.5 *Pbx1*$^{-/-}$;*Pbx2*$^{+/-}$ hindlimb buds (light shaded arrowheads) compared to that seen in somite-matched WT embryos (dark shaded arrowheads) at this same day. Proximal (left); anterior (top); FL, Forelimb; HL, Hindlimb; Som., Somites.

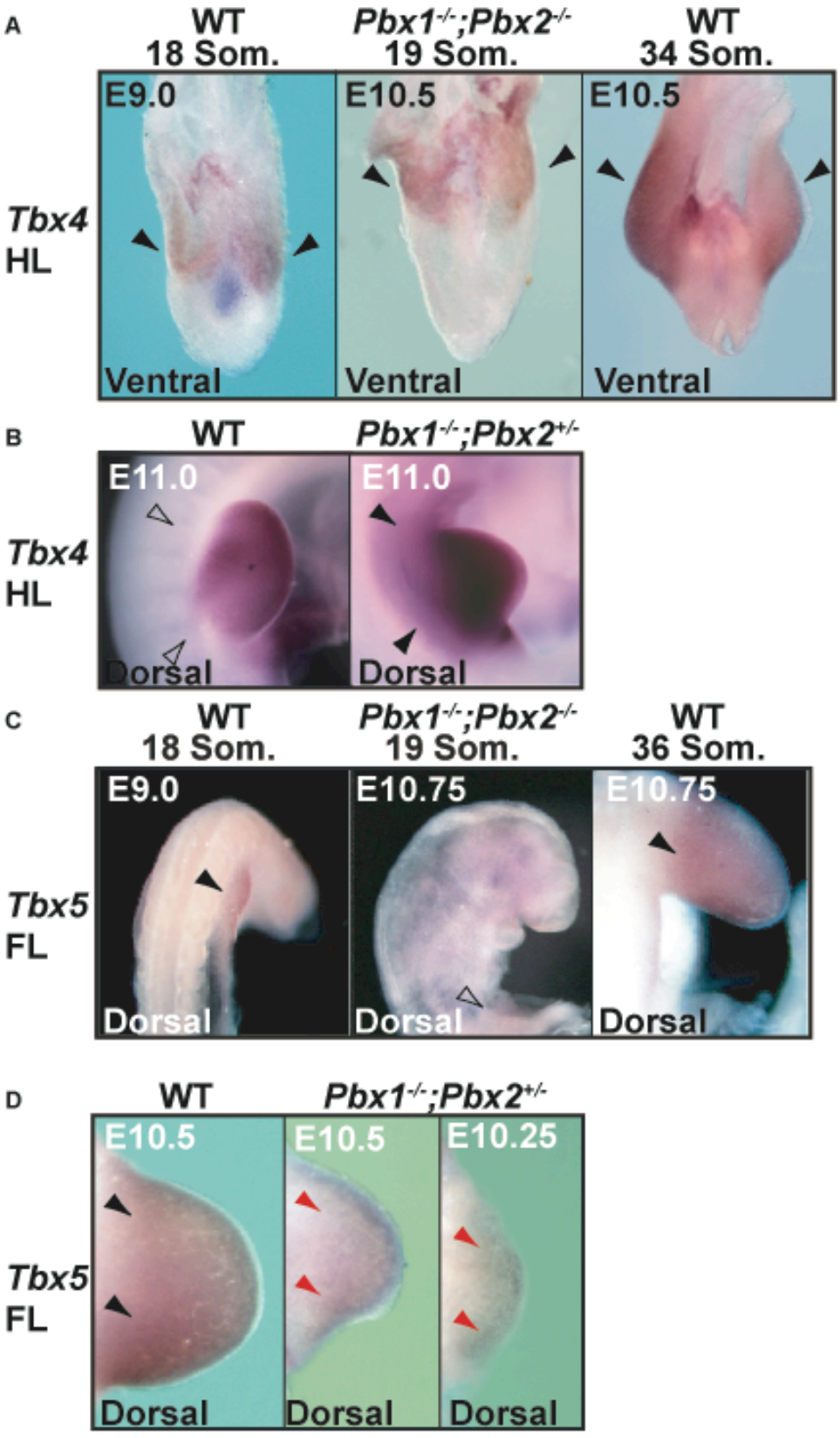
A
WT
18 Som.
Pbx1-/-;Pbx2-/-
19 Som.
WT
34 Som.
E9.0
E10.5
E10.5
Tbx4
HL
Ventral
Ventral
Ventral
B
WT
Pbx1-/-;Pbx2+/-
E11.0
E11.0
Tbx4
HL
Dorsal
Dorsal
C
WT
18 Som.
Pbx1-/-;Pbx2-/-
19 Som.
WT
36 Som.
E9.0
E10.75
E10.75
Tbx5
FL
Dorsal
Dorsal
Dorsal
D
WT
Pbx1-/-;Pbx2+/-
E10.5
E10.5
E10.25
Tbx5
FL
Dorsal
Dorsal
Dorsal

Figure 6.4. *Fgf10* expression was markedly reduced in *Pbx1*$^{-/-}$;*Pbx2*$^{+/-}$ limbs.

(A) *In situ* hybridization at E9.5 revealed that *Fgf10* expression was reduced in the forelimb of *Pbx1*$^{-/-}$;*Pbx2*$^{+/-}$ embryos (light shaded arrowhead) and was absent in the forelimb field of *Pbx1*$^{-/-}$;*Pbx2*$^{-/-}$ embryos (empty dark shaded arrowhead) when compared to WT embryos (dark shaded arrowhead). (B) At E10, *Fgf10* was barely visible in the hindlimb of *Pbx1*$^{-/-}$;*Pbx2*$^{+/-}$ embryos (light shaded arrowhead) compared to somite-matched WT embryos (dark shaded arrowhead). (C) At E10.5, *Fgf10* was reduced and diffused in the fore- and hindlimb buds of *Pbx1*$^{-/-}$;*Pbx2*$^{+/-}$ embryos (light shaded arrowheads) when compared to WT embryos (dark shaded arrowheads). Proximal (left); anterior (top); FL, Forelimb; HL, Hindlimb.

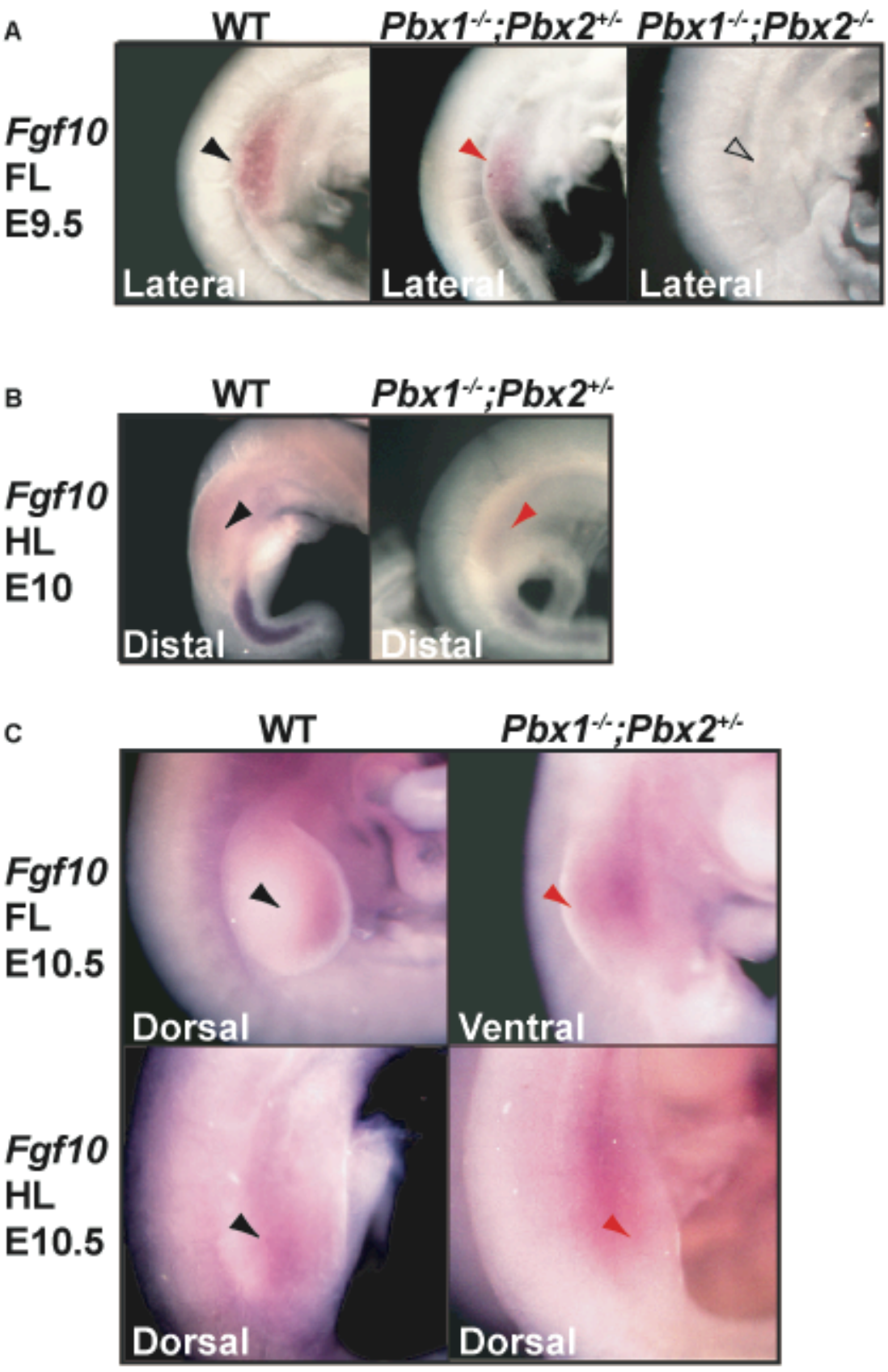
A
WT
Pbx1-/-;Pbx2+/-
Pbx1-/-;Pbx2-/-
Fgf10
FL
E9.5
Lateral
Lateral
Lateral
B
WT
Pbx1-/-;Pbx2+/-
Fgf10
HL
E10
Distal
Distal
C
WT
Pbx1-/-;Pbx2+/-
Fgf10
FL
E10.5
Dorsal
Ventral
Fgf10
HL
E10.5
Dorsal
Dorsal

Figure 6.5. *Fgf8* expression was markedly reduced and absent in *Pbx1*$^{-/-}$*;Pbx2*$^{-/-}$ fore- and hindlimbs, respectively.

(A) *In situ* hybridization at E11 revealed that *Fgf8* expression remained mostly unchanged (black arrowhead) at the mid- to hind-brain transition in *Pbx1*$^{-/-}$*;Pbx2*$^{-/-}$ embryos (30 som.) compared to somite-matched E10 WT (30 som.) and littermate E11 WT (44 som.) embryos (black arrowheads). Littermate WT control embryos were included (in A-C) to demonstrate that *Pbx1*$^{-/-}$*;Pbx2*$^{-/-}$ embryos were delayed in somitogenesis. (B) *Fgf8* expression was barely visible in *Pbx1*$^{-/-}$*;Pbx2*$^{-/-}$ forelimb buds (light shaded arrowhead) compared to somite-matched WT and littermate WT forelimb buds (dark shaded arrowheads). (C) *Fgf8* expression was absent is *Pbx1*$^{-/-}$*;Pbx2*$^{-/-}$ hindlimb buds (empty black arrowhead) compared to somite-matched WT and littermate WT hindlimb buds (black arrowheads). Dorsal (left); anterior (top); FL, Forelimb; HL, Hindlimb; Som., Somites.

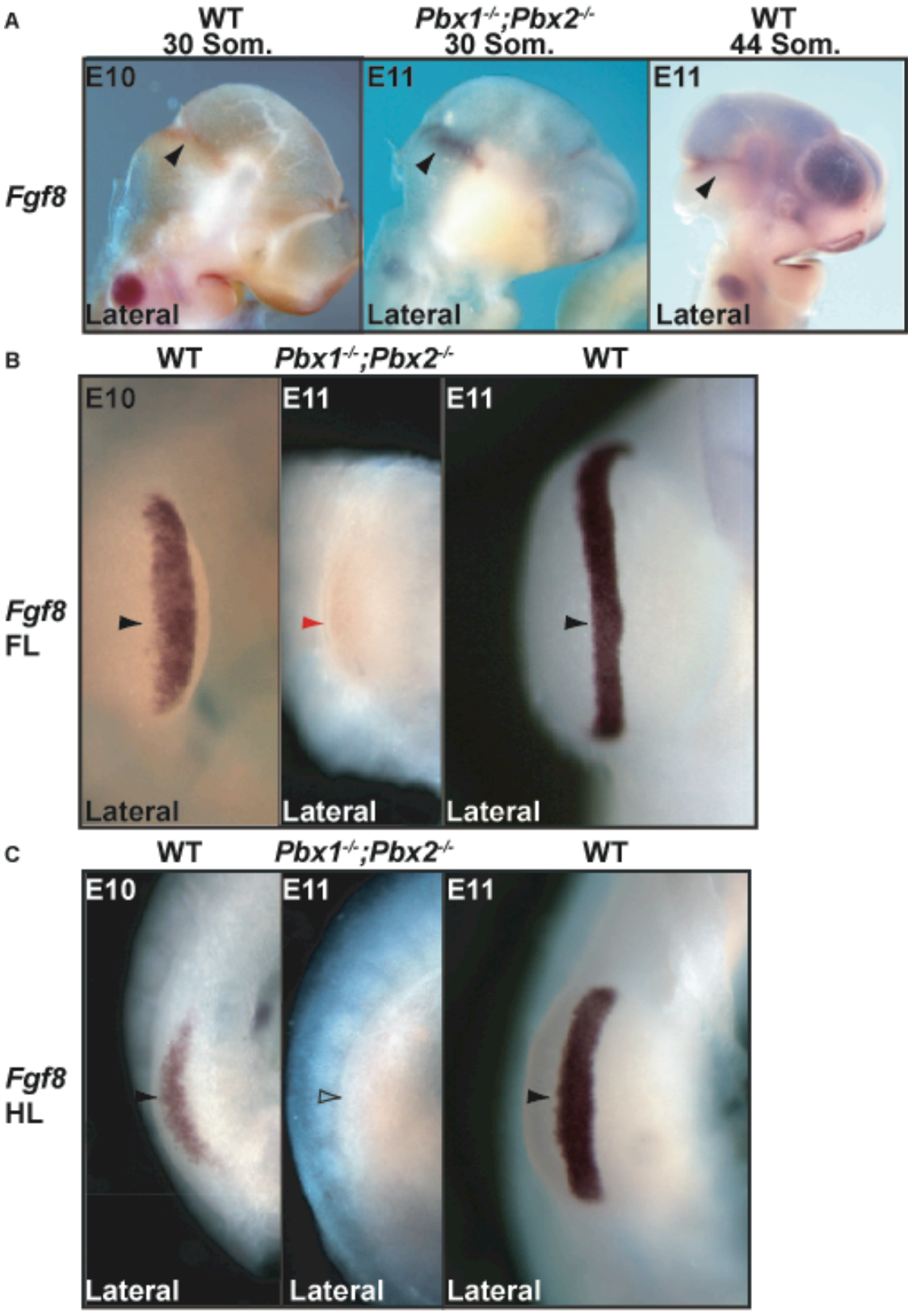
A
WT
30 Som.
Pbx1-/-;Pbx2-/-
30 Som.
WT
44 Som.
Fgf8
E10
E11
E11
Lateral
Lateral
Lateral
B
WT
Pbx1-/-;Pbx2-/-
WT
Fgf8
FL
E10
E11
E11
Lateral
Lateral
Lateral
C
WT
Pbx1-/-;Pbx2-/-
WT
Fgf8
HL
E10
E11
E11
Lateral
Lateral
Lateral

Figure 6.6. *Dlx* expression was highly altered in *Pbx1*$^{-/-}$;*Pbx2*$^{+/-}$ limb buds.

(A) *In situ* hybridization at E10.5 revealed that *Dlx2* expression was reduced in the anterior and posterior domains of the AER of *Pbx1*$^{-/-}$;*Pbx2*$^{+/-}$ forelimbs (light shaded arrowheads) compared to WT forelimbs (dark shaded arrowheads) as shown in both dorsal and distal views . (B) At E10.5, *Dlx2* expression was markedly reduced in the anterior ectoderm (light shaded arrowheads) and lost from the posterior domains of the AER and ectoderm (empty dark shaded arrowheads) of *Pbx1*$^{-/-}$;*Pbx2*$^{+/-}$ hindlimbs compared to WT hindlimbs (dark shaded arrowheads). (C) At E11.25, *Dlx5* expression was absent from the anterior and posterior domains of the AER of *Pbx1*$^{-/-}$;*Pbx2*$^{+/-}$ forelimbs (empty dark shaded arrowheads) compared to WT forelimbs (dark shaded arrowheads). (D) At E11.25, *Dlx5* expression was absent in the anterior and posterior domains of the AER and ectoderm (empty dark shaded arrowheads) of *Pbx1*$^{-/-}$;*Pbx2*$^{+/-}$ hindlimbs compared to WT hindlimbs (dark shaded arrowheads). Furthermore, the AER appeared not as tightly compacted in the mutant when compared to WT. In dorsal view, Proximal (left); anterior (top); FL, Forelimb; HL, Hindlimb.

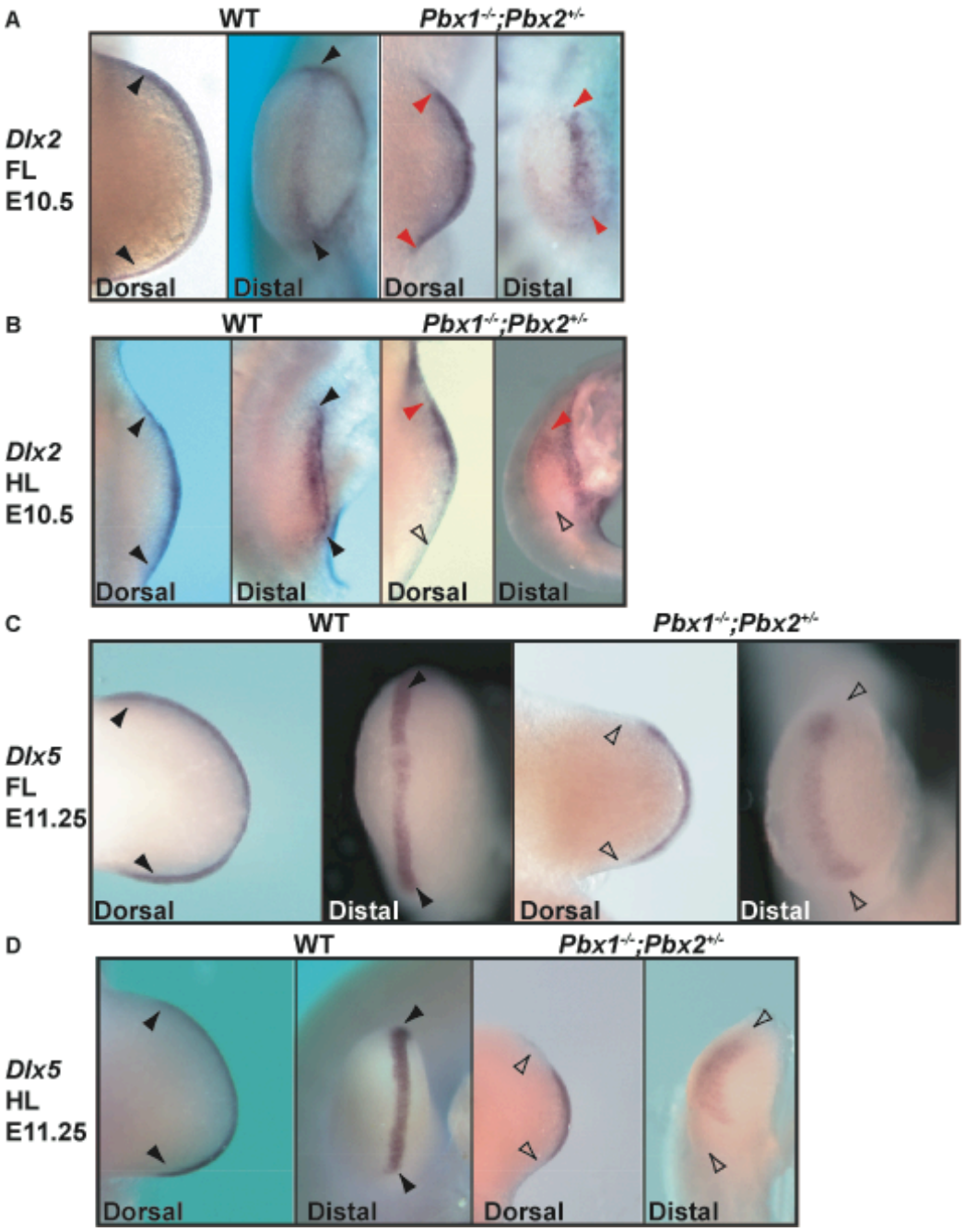
A
WT
Pbx1-/-;Pbx2+/-
Dlx2
FL
E10.5
Dorsal
Distal
Dorsal
Distal
B
WT
Pbx1-/-;Pbx2+/-
Dlx2
HL
E10.5
Dorsal
Distal
Dorsal
Distal
C
WT
Pbx1-/-;Pbx2+/-
Dlx5
FL
E11.25
Dorsal
Distal
Dorsal
Distal
D
WT
Pbx1-/-;Pbx2+/-
Dlx5
HL
E11.25
Dorsal
Distal
Dorsal
Distal

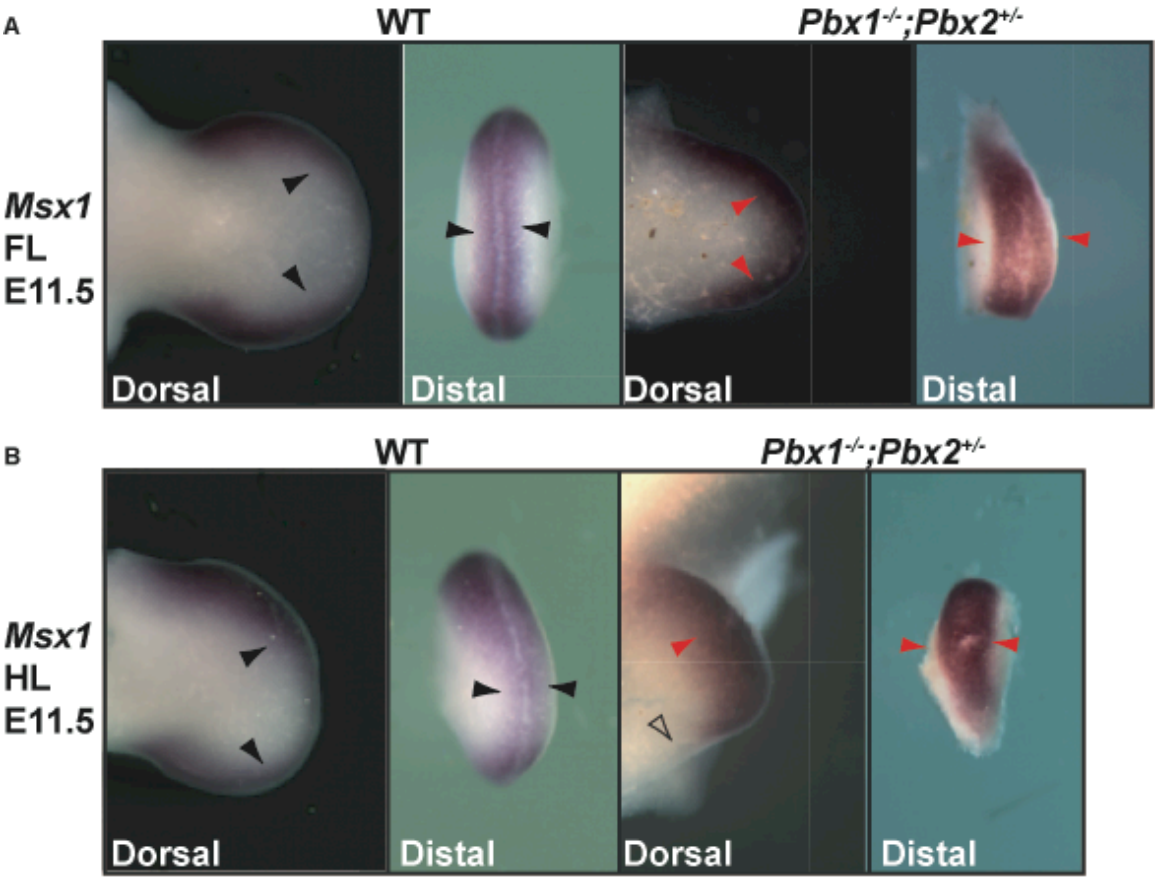

Figure 6.7. *Msx1* expression was markedly altered in *Pbx1*$^{-/-}$;*Pbx2*$^{+/-}$ limbs.

(A, B) *In situ* hybridization at E11.5 revealed that *Msx1* expression was up-regulated and expanded dorsal-ventrally in the distal mesenchyme of the *Pbx1*$^{-/-}$;*Pbx2*$^{+/-}$ fore- and hindlimb (light shaded arrowheads) when compared to WT limbs (dark shaded arrowheads). Furthermore, in *Pbx1*$^{-/-}$;*Pbx2*$^{+/-}$ hindlimbs, *Msx1* expression was lost along the most posterior border (empty dark shaded arrowhead) when compared WT hindlimbs (dark shaded arrowheads). In dorsal view, Proximal (left); anterior (top); FL, Forelimb; HL, Hindlimb.

Figure 6.8. Expression of *Msx2* was differently effected in the AER versus mesenchyme in *Pbx1*$^{-/-}$;*Pbx2*$^{+/-}$ limbs.

(A) *In situ* hybridization at E10.5 revealed that *Msx2* expression remained absent from the AER (dark shaded arrowheads) but was reduced in the mesenchyme (light shaded arrowheads) in *Pbx1*$^{-/-}$;*Pbx2*$^{+/-}$ forelimb buds when compared to WT limbs (dark shaded arrowheads) at standard and high magnification views. (B) In *Pbx1*$^{-/-}$;*Pbx2*$^{+/-}$ hindlimbs, *Msx2* was reduced from the anterior AER (light shaded arrowhead) and lost from the posterior AER (empty dark shaded arrowhead) compared to WT limbs (dark shaded arrowheads). Furthermore, ventral view demonstrates an increased anterior expression of *Msx2* (three dark shaded arrowheads) compared to WT (dark shaded arrowhead). (C) At E11, *Msx2* expression remained absent from the *Pbx1*$^{-/-}$;*Pbx2*$^{+/-}$ forelimb AER (empty dark shaded arrowhead) despite its presence in the WT control (dark shaded arrowheads). Furthermore, it was reduced in posterior mesenchyme (light shaded arrowhead) and lost from anterior mesenchyme (empty dark shaded arrowhead) in mutant hindlimbs compared to controls (dark shaded arrowheads for AER and mesenchyme). (D) At E11, *Msx2* expression remained absent from the AER (empty dark shaded arrowhead), reduced in the anterior mesenchyme (light shaded arrowhead) and was lost from the posterior mesenchyme of *Pbx1*$^{-/-}$;*Pbx2*$^{+/-}$ hindlimbs compared to WT hindlimbs (dark shaded arrowheads for AER and mesenchyme). In dorsal view, Proximal (left); anterior (top); FL, Forelimb; HL, Hindlimb.

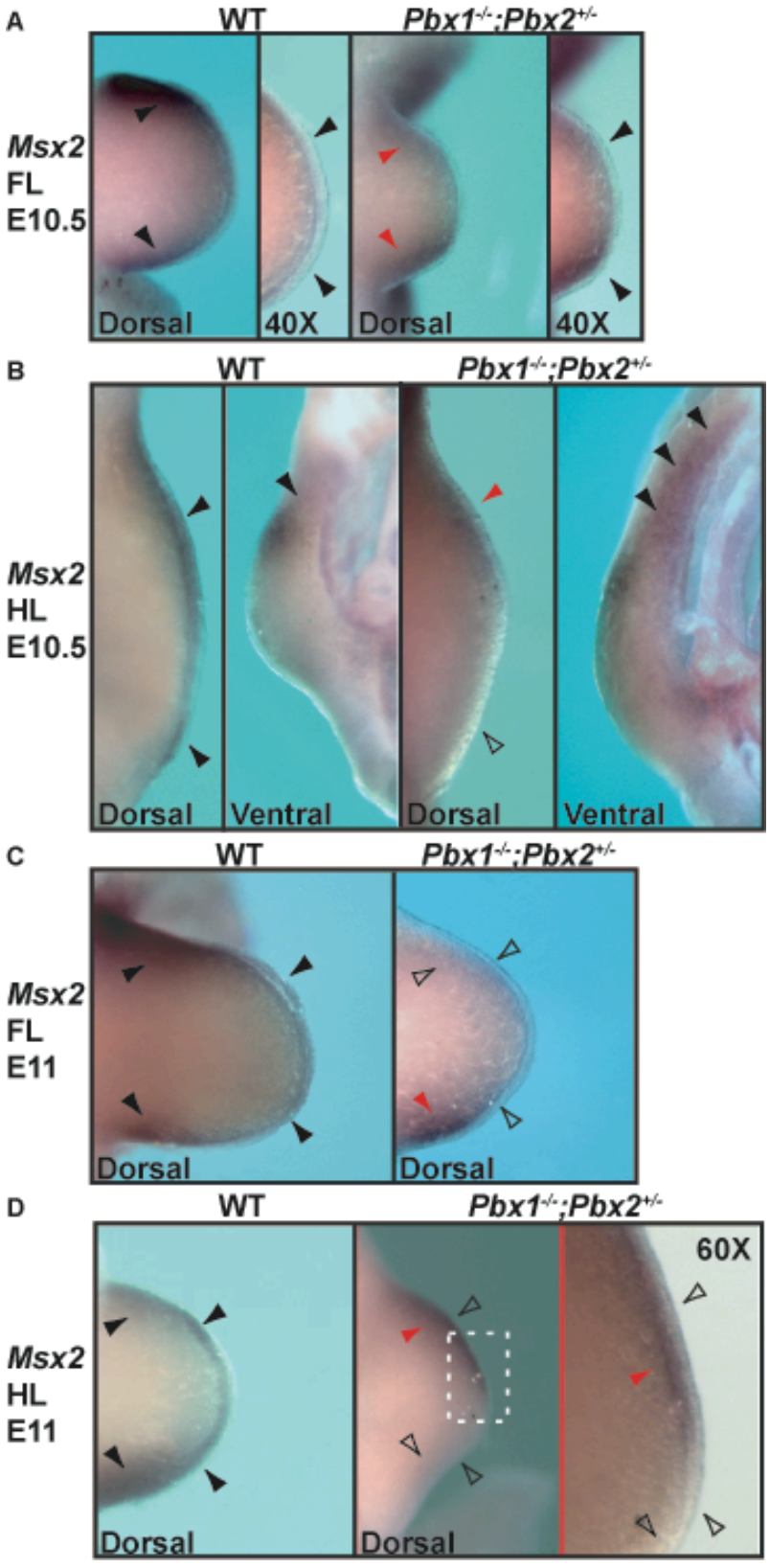
A
WT
Pbx1-/-;Pbx2+/-
Msx2
FL
E10.5
Dorsal
40X
Dorsal
40X
B
WT
Pbx1-/-;Pbx2+/-
Msx2
HL
E10.5
Dorsal
Ventral
Dorsal
Ventral
C
WT
Pbx1-/-;Pbx2+/-
Msx2
FL
E11
Dorsal
Dorsal
D
WT
Pbx1-/-;Pbx2+/-
Msx2
HL
E11
60X
Dorsal
Dorsal

Figure 6.9. *En1* expression was intricately altered *Pbx1*$^{-/-}$;*Pbx2*$^{+/-}$ embryos.

(A) *In situ* hybridization at E10.25 revealed that *En1* expression was absent from the distal, anterior and posterior ventral ectoderm in *Pbx1*$^{-/-}$;*Pbx2*$^{+/-}$ embryos (empty black arrowheads) compared to controls (black arrowheads). (B) In *Pbx1*$^{-/-}$;*Pbx2*$^{+/-}$ hindlimbs at E10.25, *En1* expression was only lost from the posterior ventral ectoderm (empty black arrowhead) compared to control (black arrowhead). (C) Despite the reduction in *En1* expression, the somites at the level of the forelimb displayed normal levels of *En1* (black arrowheads in mutant and control). (D) This conservation of expression, however, was not maintained posteriorly at the hindlimb somite level, as *En1* expression was markedly reduced (light shaded arrowheads) to lost (empty dark shaded arrowheads) in mutant embryos compared to controls (dark shaded arrowheads). Anterior (top); FL, Forelimb; HL, Hindlimb.

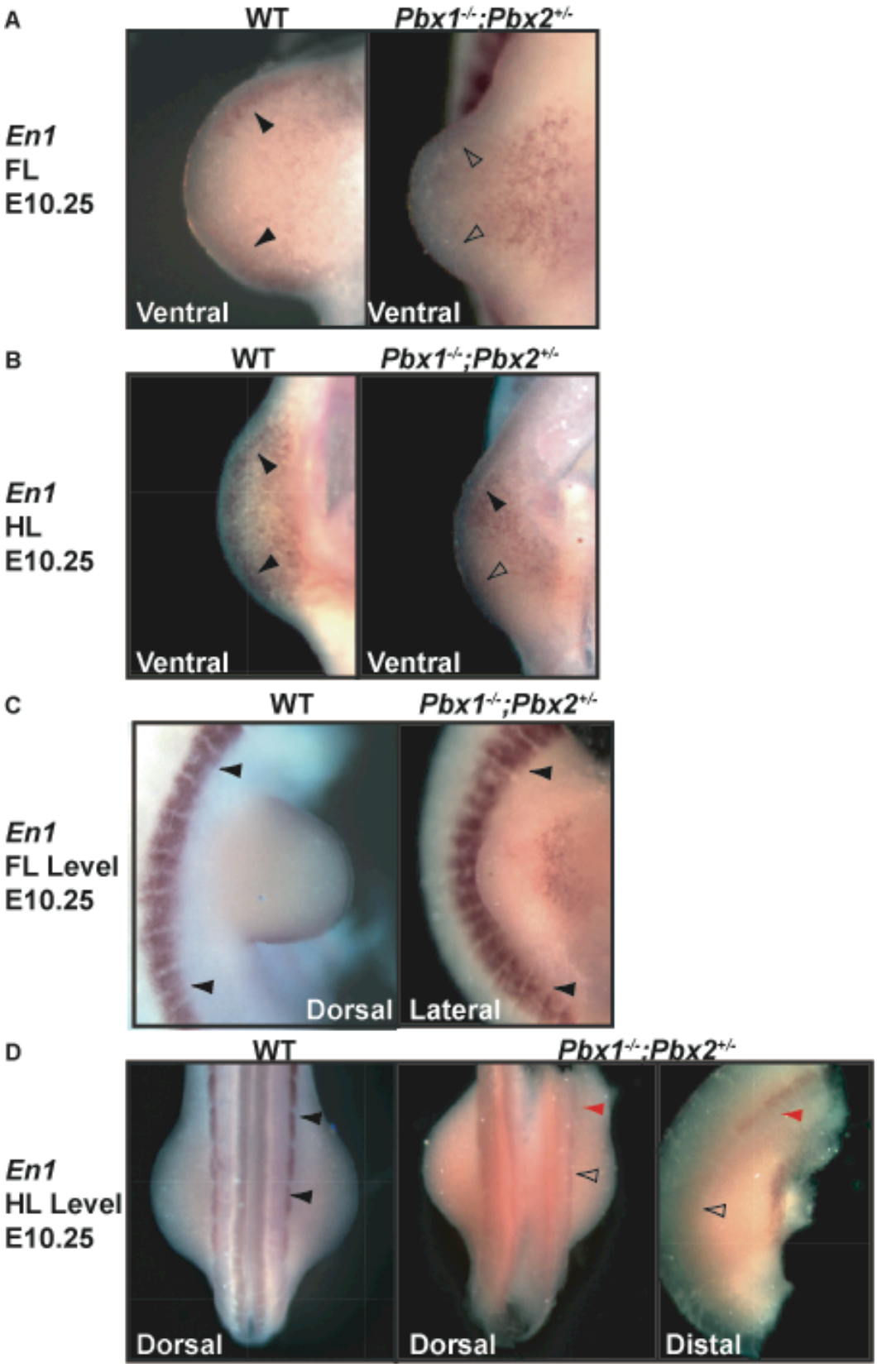
A
WT
Pbx1-/-;Pbx2+/-
En1
FL
E10.25
Ventral
Ventral
B
WT
Pbx1-/-;Pbx2+/-
En1
HL
E10.25
Ventral
Ventral
C
WT
Pbx1-/-;Pbx2+/-
En1
FL Level
E10.25
Dorsal
Lateral
D
WT
Pbx1-/-;Pbx2+/-
En1
HL Level
E10.25
Dorsal
Dorsal
Distal

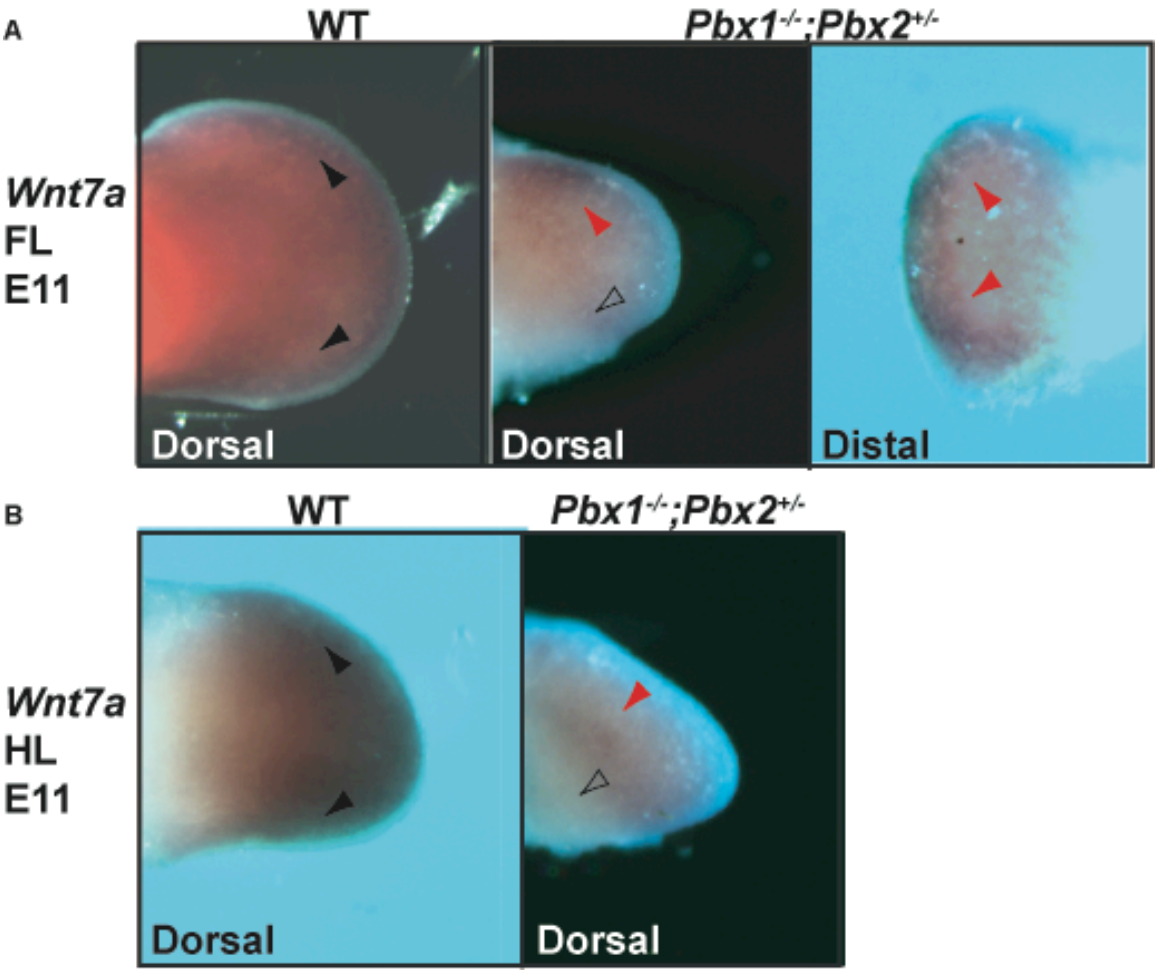

Figure 6.10. *Wnt7a* expression was down-regulated in *Pbx1*$^{-/-}$;*Pbx2*$^{+/-}$ limbs.

(A, B) *In situ* hybridization at E11 revealed that *Wnt7a* expression was reduced in the fore- and hindlimb anterior dorsal ectoderm (light shaded arrowhead, also shown in forelimb distal view) and lost in the posterior dorsal ectoderm (empty dark shaded arrowhead), compared to WT limbs (dark shaded arrowheads). Proximal (left); anterior (top); FL, Forelimb; HL, Hindlimb.

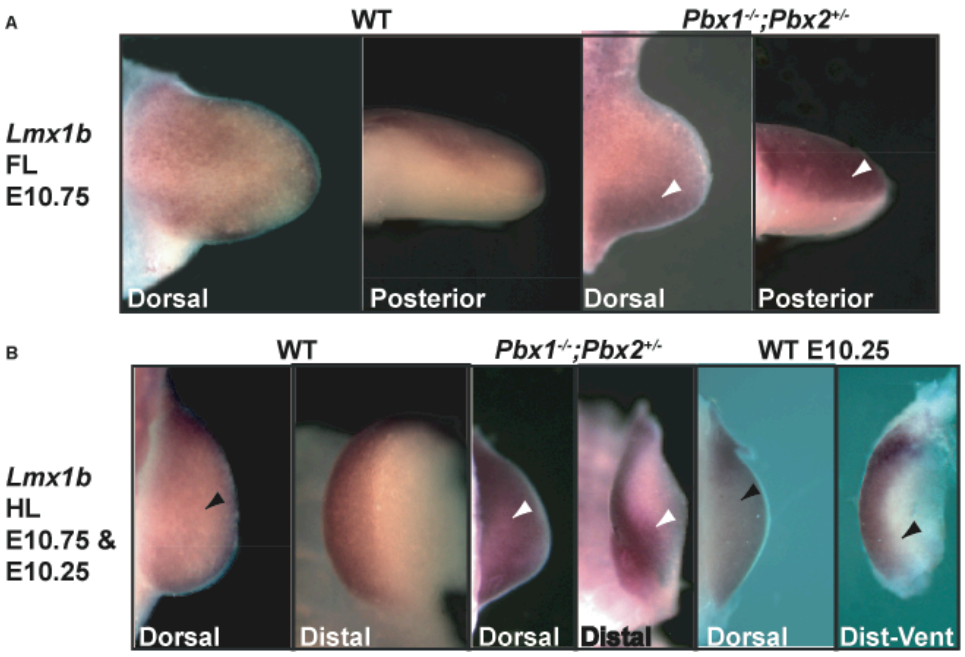

Figure 6.11. *Lmx1b* expression remained preserved in *Pbx1*$^{-/-}$*;Pbx2*$^{+/-}$ limbs.

(A) *In situ* hybridization at E10.75 revealed that *Lmx1b* expression remained intact and delineated the D-V mesenchymal border in mutant and WT forelimbs; although in the mutant, it was up-regulated in the posterior dorsal mesenchyme (light shaded arrowhead in dorsal and distal views of *Pbx1*$^{-/-}$*;Pbx2*$^{+/-}$). (B) In *Pbx1*$^{-/-}$*;Pbx2*$^{+/-}$ hindlimbs at E10.75, *Lmx1b* expression was also severely up-regulated (light shaded arrowhead in mutant dorsal view) compared to both somite-matched WT control (left) and size-corrected WT control (right) limb buds (dark shaded arrowheads in both controls). Also, while there was a ventral expansion of the *Lmx1b* expression domain in the mutant (light shaded arrowhead in distal view), it may have reflected a delay in this genes dorsalization, as suggested by still ventral expression of *Lmx1b* in the size-corrected hindlimb bud (left; dark shaded arrowhead in distal-ventral view). In dorsal view, Proximal (left), anterior (top); FL, Forelimb; HL, Hindlimb.

Figure 6.12. *Cyp26B1* expression was reduced in *Pbx1*$^{-/-}$;*Pbx2*$^{+/-}$ limbs.

(A) *In situ* hybridization at E10 revealed that *Cyp26B1* expression was severely reduced in *Pbx1*$^{-/-}$;*Pbx2*$^{+/-}$ forelimbs (light shaded arrowhead) compared to WT forelimbs (dark shaded arrowhead). (B, C) At E10 and E10.5, *Cyp26B1* expression was never detected in the distal *Pbx1*$^{-/-}$;*Pbx2*$^{+/-}$ mutant hindlimb (empty dark shaded arrowheads) compared to the WT hindlimb (dark shaded arrowheads) suggesting that the molecular regulation of the RA-Fgf gradient was critically altered. Proximal (left); anterior (top); FL, Forelimb; HL, Hindlimb.

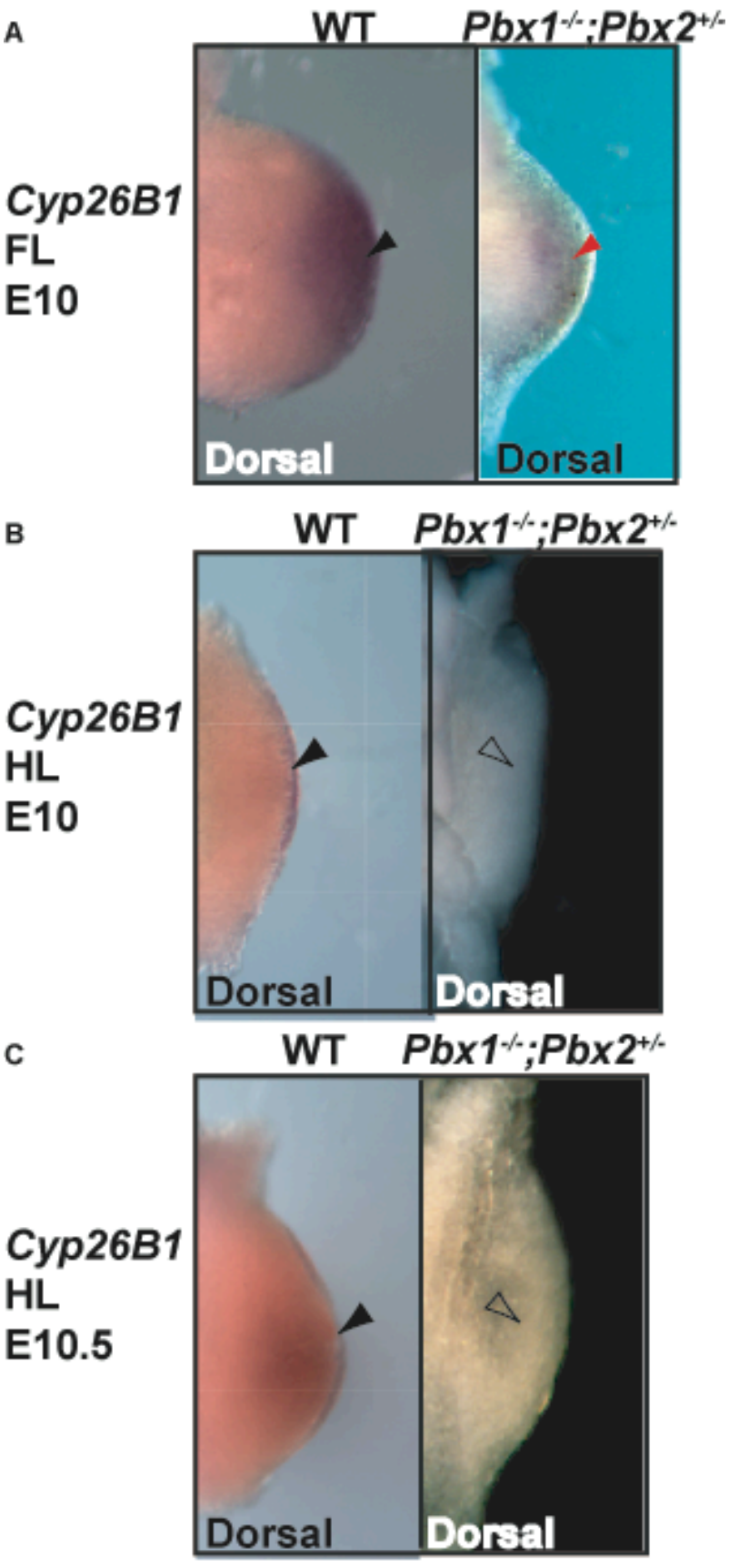
A
WT
Pbx1-/-;Pbx2+/-
Cyp26B1
FL
E10
Dorsal
Dorsal
B
WT
Pbx1-/-;Pbx2+/-
Cyp26B1
HL
E10
Dorsal
Dorsal
C
WT
Pbx1-/-;Pbx2+/-
Cyp26B1
HL
E10.5
Dorsal
Dorsal

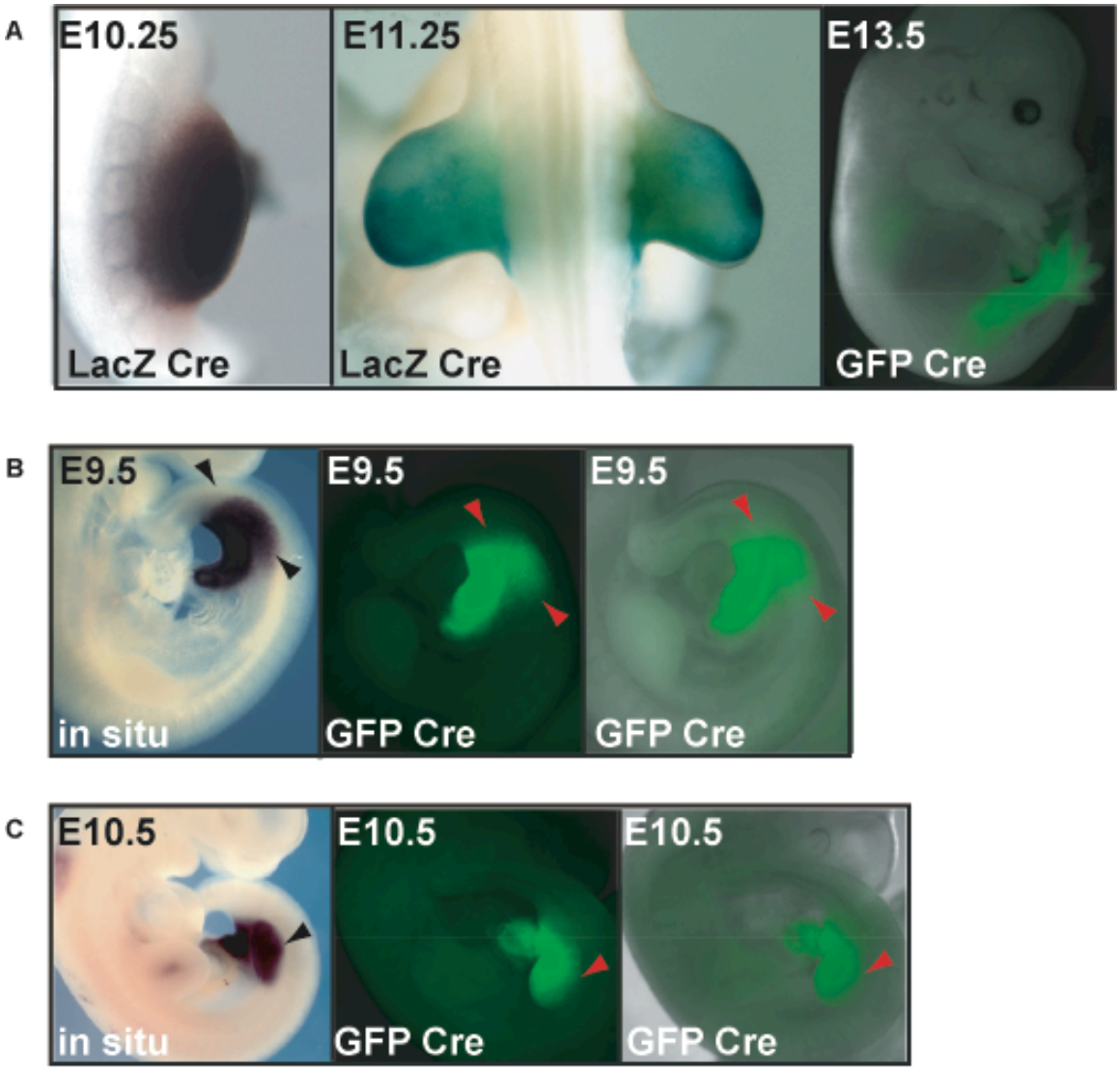

Figure 6.13. Tbx4 Cre activity during hindlimb development.

Tbx4$^{cre/cre}$ mice were crossed to the Cre reporter line *R26R* as described in Chapter 4. (A) LacZ staining and GFP detection in early (E10.25, LacZ, dark stain), middle (E11.25, LacZ, dark stain), and later (E13.5, GFP, dark stain) limb bud development. Cre was present in the distal limb bud mesenchyme (at E10.25-E11.25) and in the limb mesenchyme (at E13.5). (B) At E9.5, a comparison of *Tbx4 in situ* hybridization with Tbx4 Cre activity as assessed by GFP detection indicated that the anterior to posterior extent of Cre activity (light shaded arrowheads) was reduced compared to mRNA transcript distribution (dark shaded arrowheads). (C) At E10.5, a similar comparison indicated that the proximal extent of Cre activity (light shaded arrowheads) was reduced compared to mRNA transcript distribution (dark shaded arrowheads). Panels (B, C) were adapted from those provided by Naiche Adler. In (A) Proximal (left); anterior (top). In (B, C) Proximal (right); Anterior (bottom) FL, Forelimb; HL, Hindlimb.

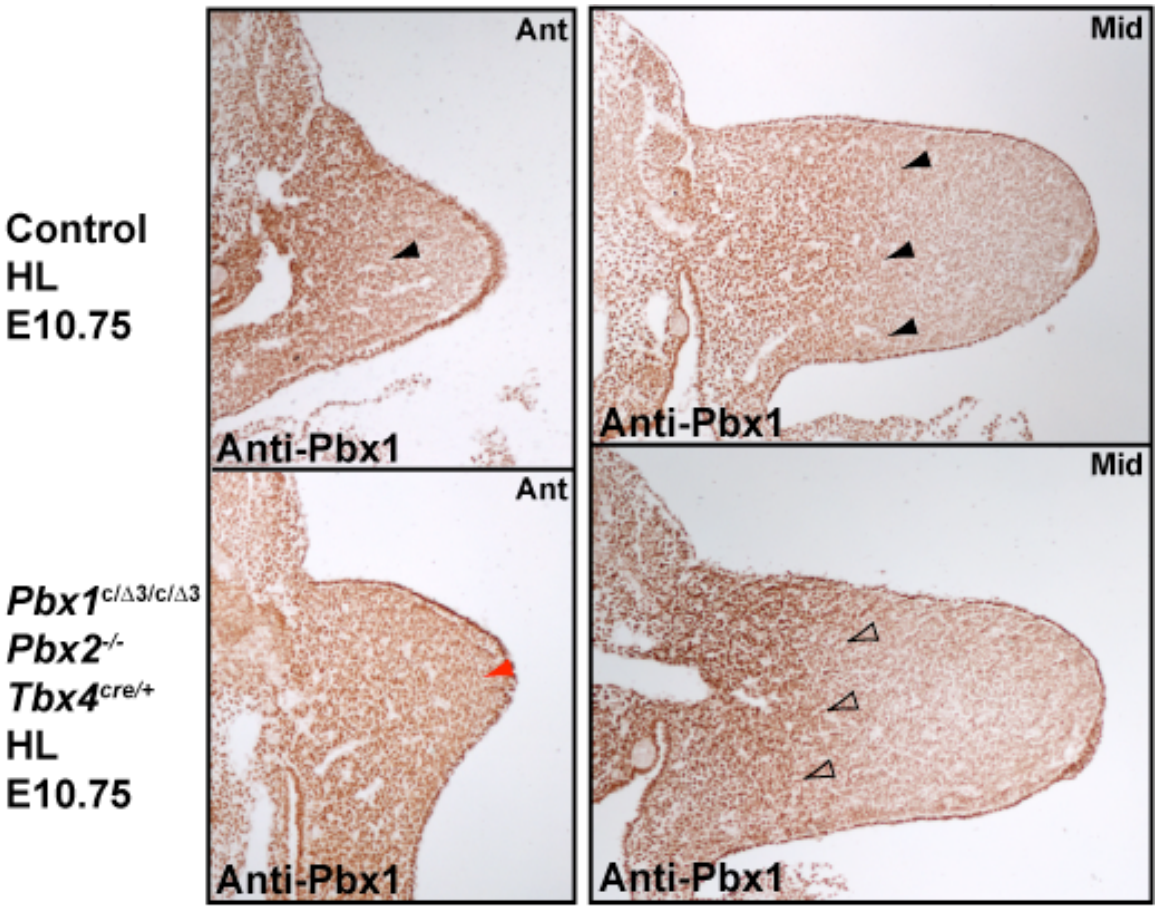

Figure 6.14. Efficiency of excision of *Pbx1* "floxed" allele by Tbx4 Cre during hindlimb development.

Pbx1 immunohistochemistry on E10.75 transverse sections revealed that at anterior (Ant) levels the Tbx4 Cre was unable to efficiently excise *Pbx1* in recombinant limbs (light shaded arrowhead) (control section at this level simply demonstrates that Pbx1 nuclear distribution can be proximalized). At mid-limb levels (Mid), Tbx4 Cre was capable of excising *Pbx1* most distal domain (compare locations of empty dark shaded arrowheads in recombinant limb to the dark shaded arrowheads in the control) although a large proximal domain of Pbx1 localization remained in the recombinant limb. Proximal (left); anterior (top); HL, Hindlimb.

Figure 6.15. Gross morphology of E14.5 *Pbx1*$^{cI\Delta3/cI\Delta3}$; *Pbx2*$^{+/-}$; *Tbx4*$^{cre/+}$ and *Pbx1*$^{cI\Delta3/cI\Delta3}$; *Pbx2*$^{-/-}$; *Tbx4*$^{cre/+}$ mutant embryos was normal.

At E14.5, despite the distal excision of *Pbx1* in the hindlimb, recombinant mutants lacked any visible signal of gross morphological alteration. Proximal (left); anterior (top); FL, Forelimb; HL, Hindlimb.

Control
E14.5
FL
HL
Pbx1cIΔ3/cIΔ3
Pbx2+/-
Tbx4cre/+
E14.5
FL
HL
Pbx1cIΔ3/cIΔ3
Pbx2-/-
Tbx4cre/+
E14.5
FL
HL

Figure 6.16. Skeletal morphology of E14.5 *Pbx1*$^{cI\Delta 3/cI\Delta 3}$; *Pbx2*$^{-/-}$; *Tbx4*$^{cre/+}$ mutant embryos was normal.

At E14.5, Alcian Blue staining revealed that despite the distal excision of *Pbx1* in the hindlimb, recombinant mutants lacked any visible signal of skeletal alteration. Recombinant mutant and control embryos displayed similar degrees of morphological development in the overall embryo (A,B), the hindlimb (C,D), the femoral-acetabular joint and pelvis (E,F), the femoral-tibial joint (G,H), and the pes (I,J). Panels (C-H): Proximal (right); anterior (top); Panels (I,J): Proximal (top); anterior (right); FL, Forelimb; HL, Hindlimb.

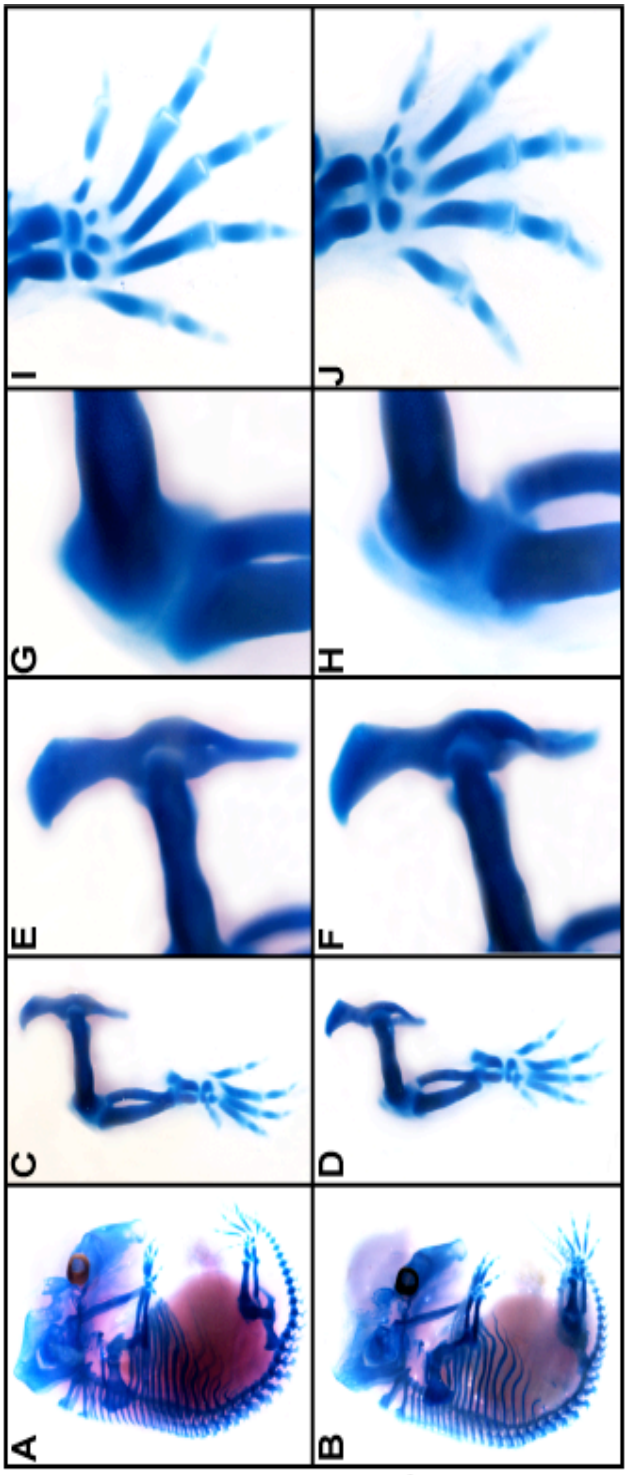
A
C
E
G
I
B
D
F
H
J
Control
E14.5
Pbx1cIΔ3/cIΔ3 ;
Pbx2-/- ;
Tbx4cre/+
E14.5

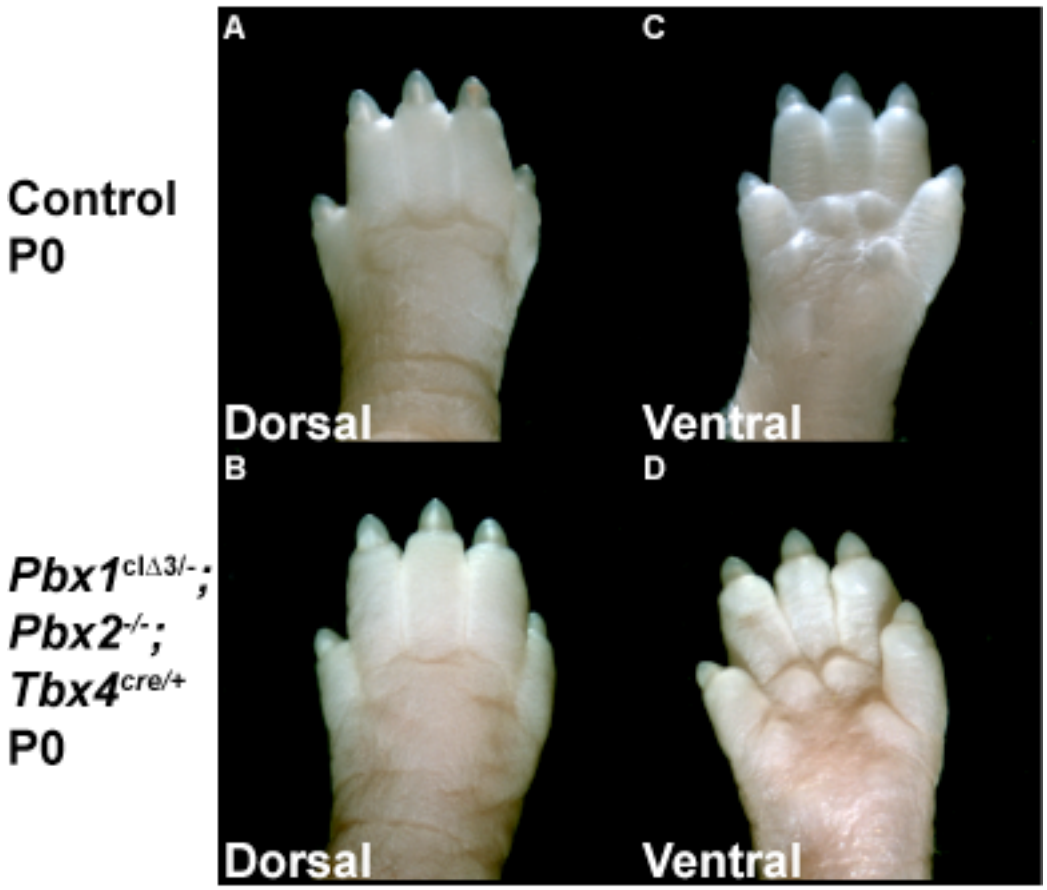

Figure 6.17. Gross morphology of the pes of newborn (P0) *Pbx1*$^{cI\Delta 3/-}$; *Pbx2*$^{-/-}$; *Tbx4*$^{cre/+}$ mutant embryos was normal.

To reduce the dosage of *Pbx1* further, the *Pbx1* global null allele was introduced to the recombinant genotype. Despite the distal excision of *Pbx1* in the hindlimb and the additional loss of *Pbx1* via this global allele, newborn mutant hindlimbs, specifically pes (B,D), displayed no overt morphological anomalies when compared to controls (A,C). Proximal (bottom); right pes shown.

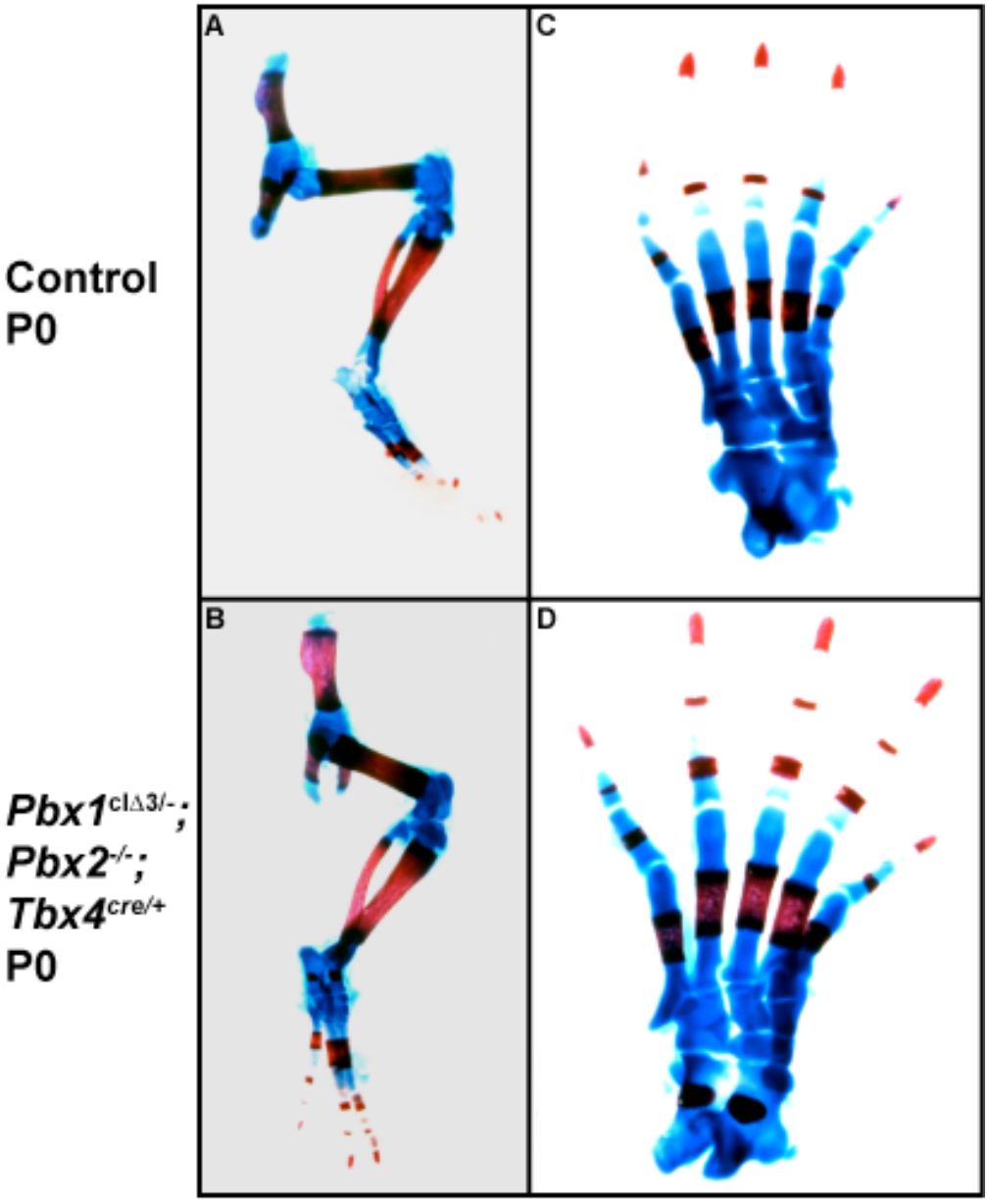

Figure 6.18. Skeletal morphology of the hindlimb and pes of newborn (P0) *Pbx1*$^{cI\Delta 3/-}$; *Pbx2*$^{-/-}$; *Tbx4*$^{cre/+}$ mutant embryos was normal.

To reduce the dosage of *Pbx1* further, the *Pbx1* global null allele was introduced to the recombinant genotype. Alcian Blue and Alizarin Red staining revealed that despite the distal excision of *Pbx1* in the hindlimb and the additional loss of *Pbx1* via this global allele, newborn mutant hindlimbs (B), specifically pes (D), displayed no overt skeletal anomalies when compared to controls (A,C). See text for details, right pes shown.

Figure 6.19. Msx2 Cre activity during limb development.

Msx2$^{cre/cre}$ mice were crossed to the Cre reporter line *R26R* as described in Chapter 4. (A-C) LacZ staining (dark staining on limb) for detection of Msx2 Cre activity from E9.25 to E10.25 during limb bud development. (A) Msx2 Cre was present in the ventral ectoderm (at E9.25) and in the developing AER (from E9.5-E10.25) of the forelimb bud. (B) Msx2 Cre was present in the ventral ectoderm (from E9.25-E9.5) and AER (at E10.25, ventral view) of the developing hindlimb bud. (C) Comparison of *Msx2 in situ* hybridization (black arrowheads) with Msx2 Cre activity (black arrowheads) demonstrates a close approximation between the two. Proximal (left); anterior (top); FL, Forelimb; HL, Hindlimb.

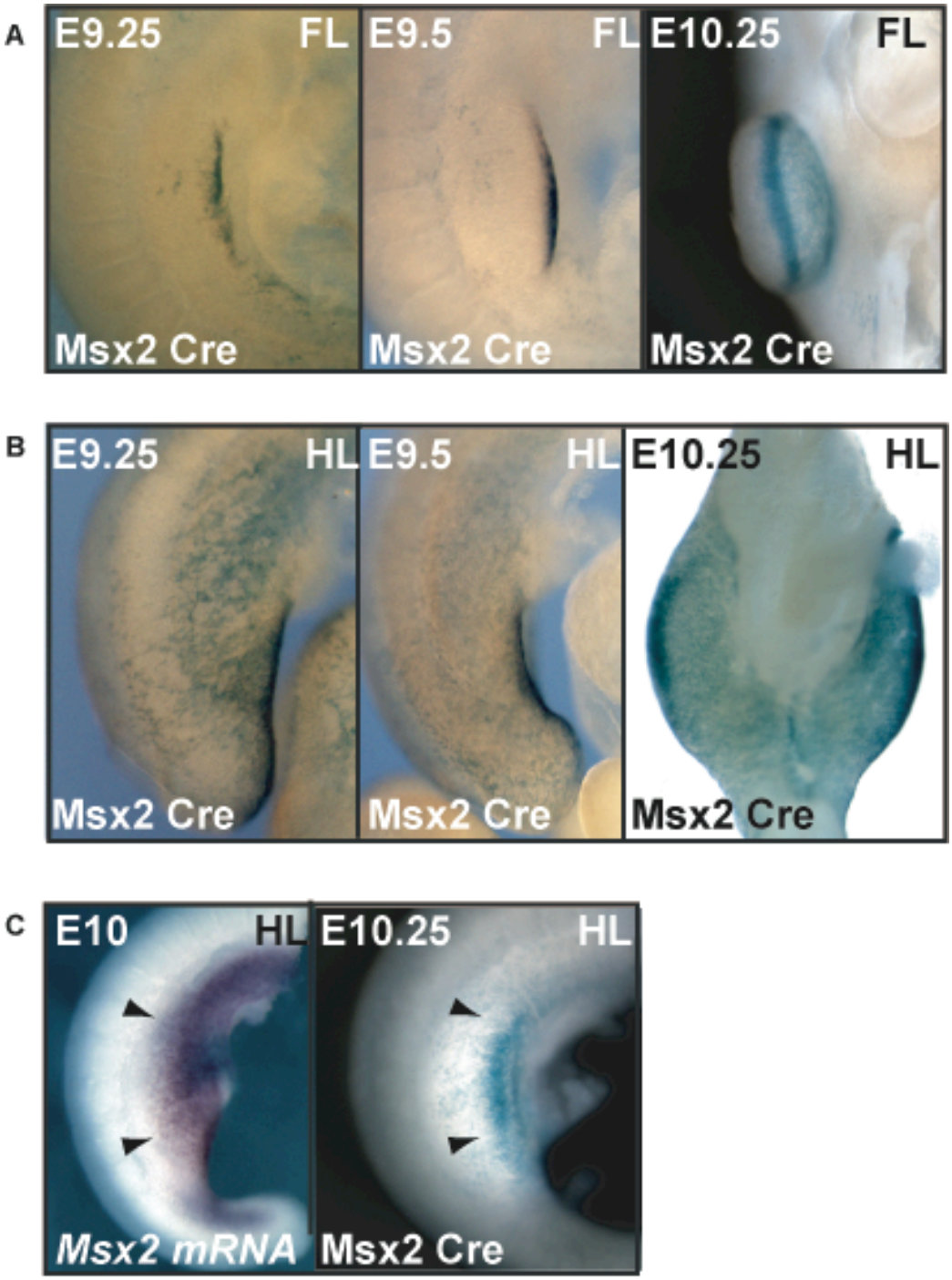
A
E9.25
FL
Msx2 Cre
E9.5
FL
Msx2 Cre
E10.25
FL
Msx2 Cre
B
E9.25
HL
Msx2 Cre
E9.5
HL
Msx2 Cre
E10.25
HL
Msx2 Cre
C
E10
HL
Msx2 mRNA
E10.25
HL
Msx2 Cre

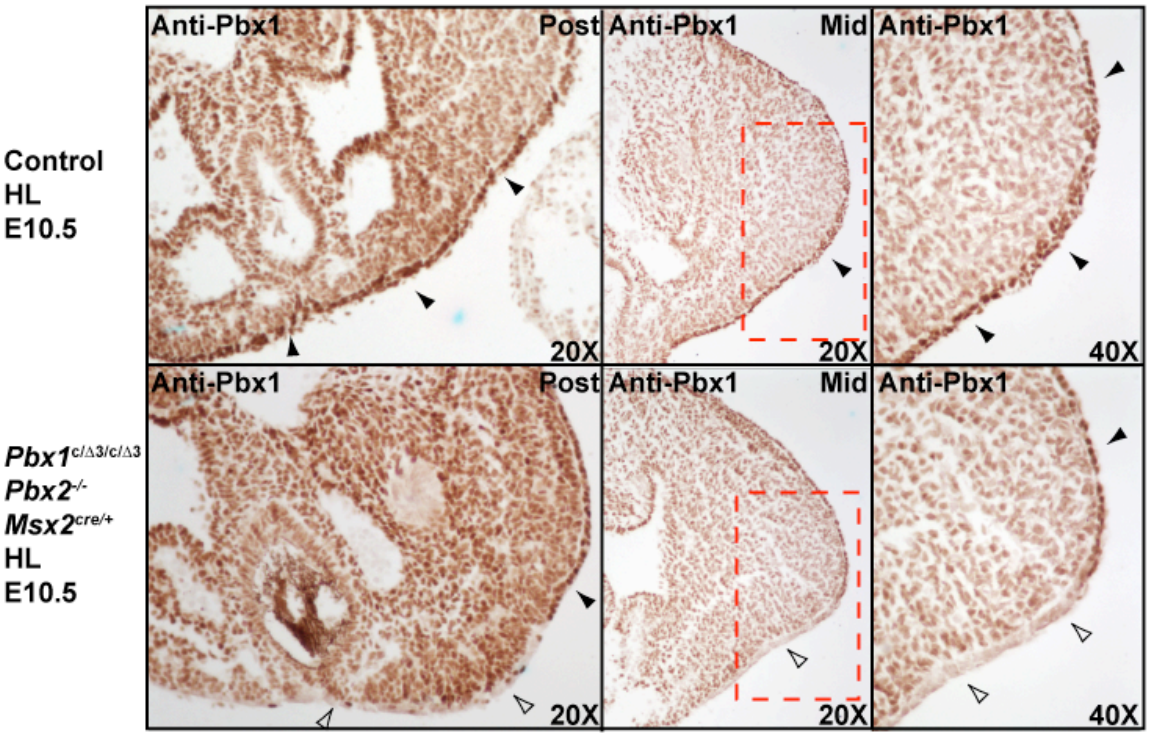

Figure 6.20. Efficiency of excision of *Pbx1* "floxed" allele by Msx2 Cre during hindlimb development.

Pbx1 immunohistochemistry on E10.5 transverse sections revealed that Msx2 Cre was able to efficiently excise *Pbx1* in the ventral ectoderm of recombinant limbs (empty black arrowheads) compared to control limbs (black arrowheads). At posterior levels (Post), excision was marked in both the limb and axial ventral ectoderm. At mid-limb levels (Mid), excision was present in the ventral ectoderm and ventral AER (empty black arrowheads in 20X and 40X inset). However, Pbx1 protein remained in the dorsal ectoderm of the recombinant mutant (black arrowheads) as expected since the Msx2 Cre was not active in this domain. Proximal (left); dorsal (top); HL, Hindlimb.

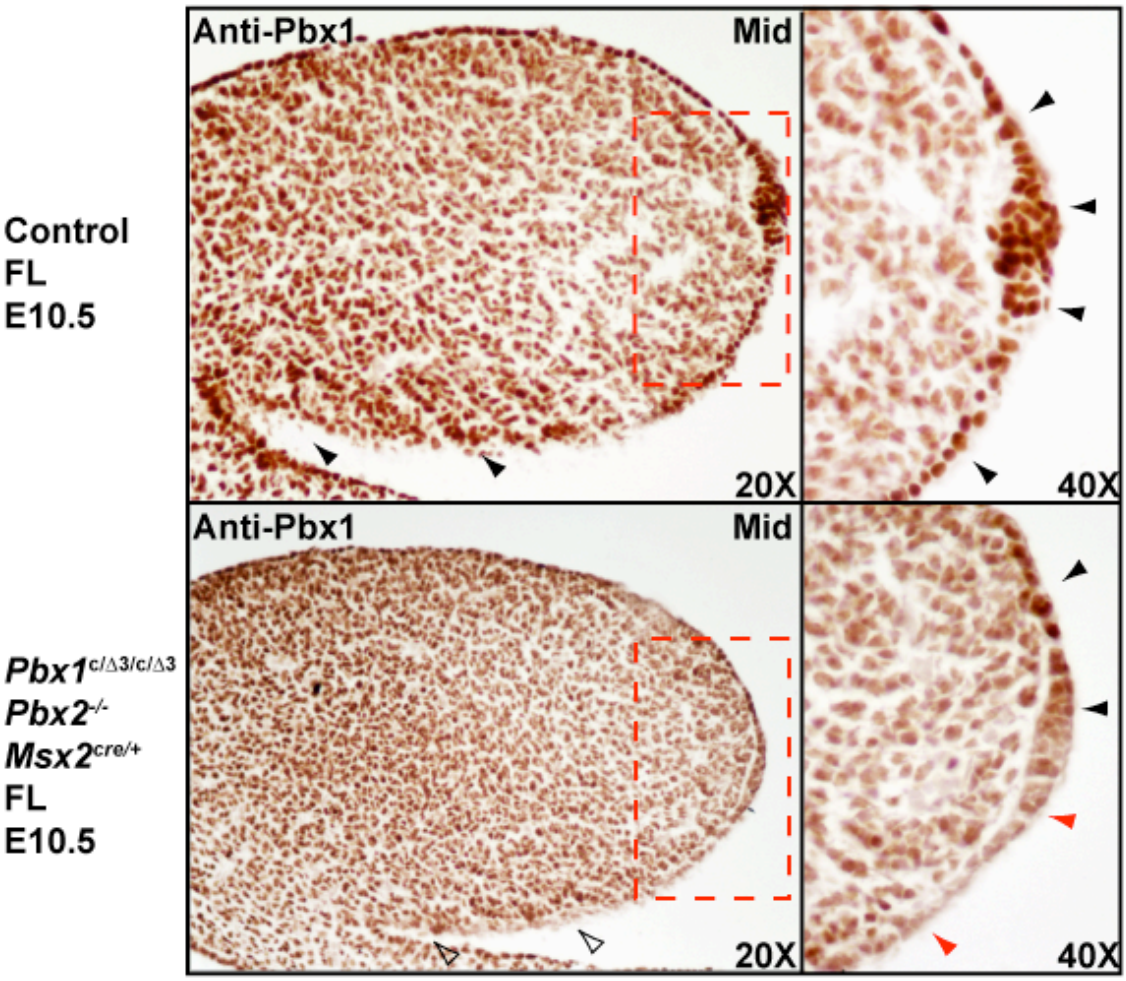

Figure 6.21. Efficiency of excision of *Pbx1* "floxed" allele by Msx2 Cre during forelimb development.

Pbx1 immunohistochemistry on E10.5 transverse sections revealed that Msx2 Cre was inefficient in excising *Pbx1* in the ventral AER of recombinant forelimbs (light shaded arrowheads in 40X inset) compared to control (dark shaded arrowheads). This partial excision was evident specifically when compared to the dorsal presence of Pbx1 in the mutant limb (dark shaded arrowheads). At this mid-limb level (Mid), excision did become more pronounced proximally in the recombinant mutant ventral ectoderm (empty dark shaded arrowheads in 20X view) compared to controls (dark shaded arrowhead). This relative inefficiency related to the later onset of Msx2 Cre in the forelimb versus hindlimb domain. Proximal (left); dorsal (top); FL, Forelimb.

Figure 6.22. Gross morphology of E12.75 *Pbx1*$^{cI\Delta 3/cI\Delta 3}$; *Pbx2*$^{+/-}$; *Msx2*$^{cre/+}$ and *Pbx1*$^{cI\Delta 3/cI\Delta 3}$; *Pbx2*$^{-/-}$; *Msx2*$^{cre/+}$ mutant embryos was normal.

(A) At E12.75, despite the distal excision of *Pbx1* in the ventral ectoderm and AER of the hindlimb (and partial excision in the ventral ectoderm and AER of the forelimb) recombinant mutants lacked any visible sign of gross morphological alteration. (B, C) At E12.75, Alcian Blue staining revealed that both mutant fore- and hindlimbs displayed similar degrees of skeletal development compared to control embryos. Proximal (top); anterior (right); FL, Forelimb; HL, Hindlimb.

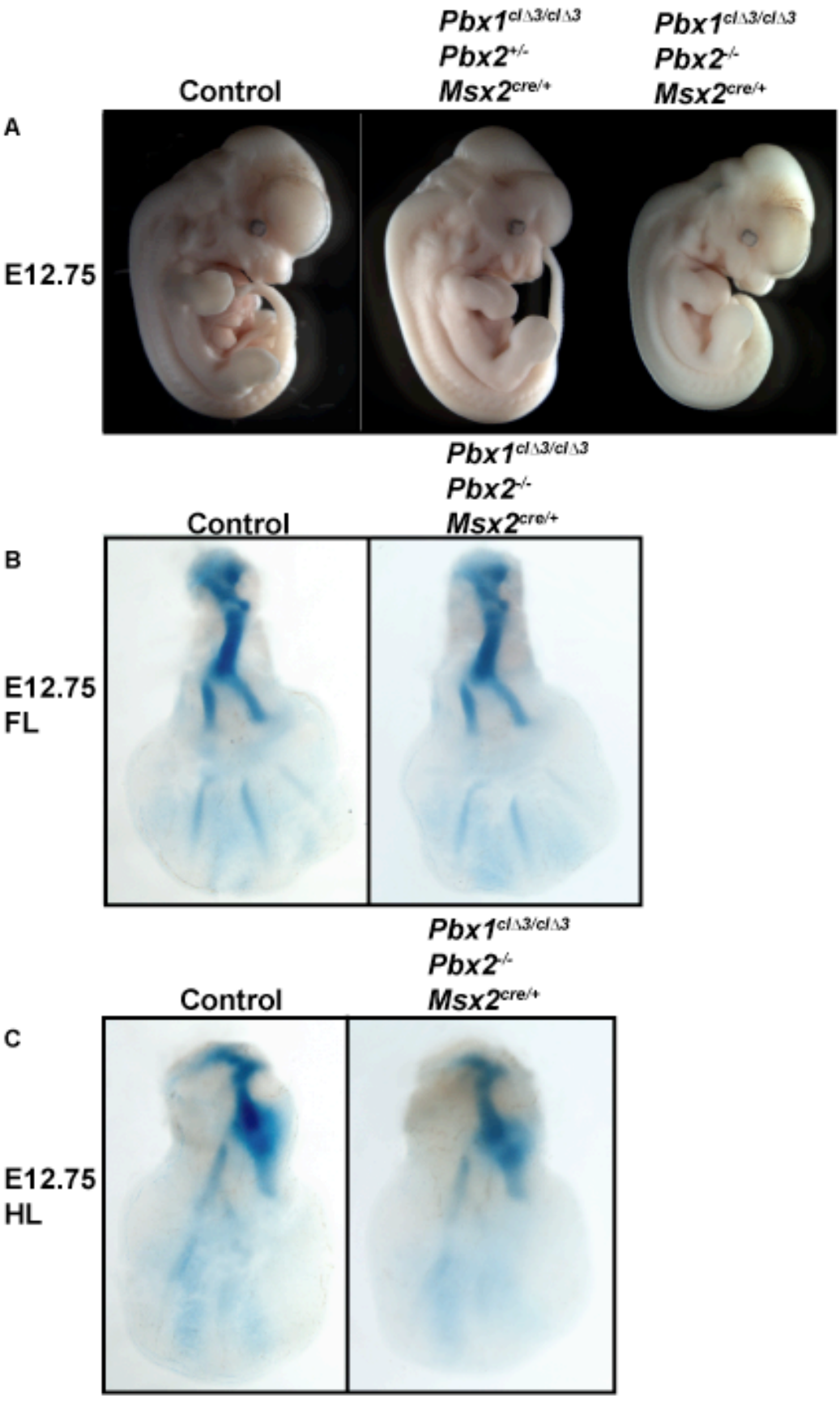
Control
Pbx1cIΔ3/cIΔ3
Pbx2+/-
Msx2cre/+
Pbx1cIΔ3/cIΔ3
Pbx2-/-
Msx2cre/+
A
E12.75
Control
Pbx1cIΔ3/cIΔ3
Pbx2-/-
Msx2cre/+
B
E12.75
FL
Control
Pbx1cIΔ3/cIΔ3
Pbx2-/-
Msx2cre/+
C
E12.75
HL

Figure 6.23. Gross morphology of E14.5 *Pbx1*$^{cI\Delta3/cI\Delta3}$; *Pbx2*$^{+/-}$; *Msx2*$^{cre/+}$ and *Pbx1*$^{cI\Delta3/cI\Delta3}$; *Pbx2*$^{-/-}$; *Msx2*$^{cre/+}$ mutant embryos was normal.

At E14.5, despite the distal excision of *Pbx1* in the ventral ectoderm and AER of the hindlimb (and partial excision in the ventral ectoderm and AER of the forelimb) recombinant mutants lacked any visible sign of gross morphological alteration. Proximal (left); anterior (top); FL, Forelimb; HL, Hindlimb.

Control
E14.5

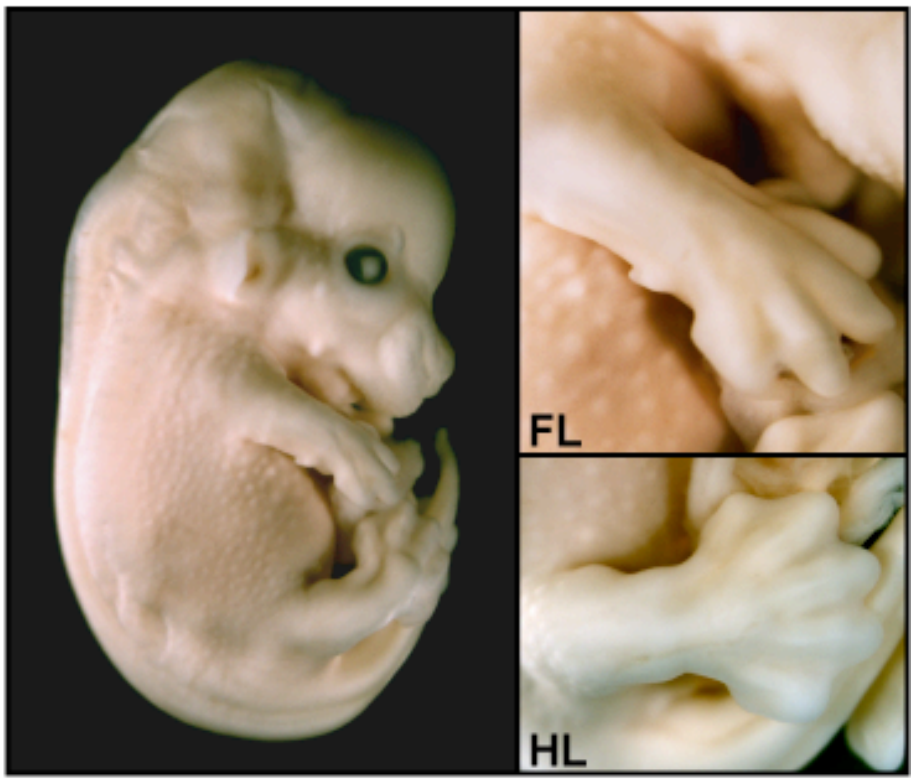

Pbx1$^{cl\Delta3/cl\Delta3}$
Pbx2$^{-/-}$
Msx2$^{cre/+}$
E14.5

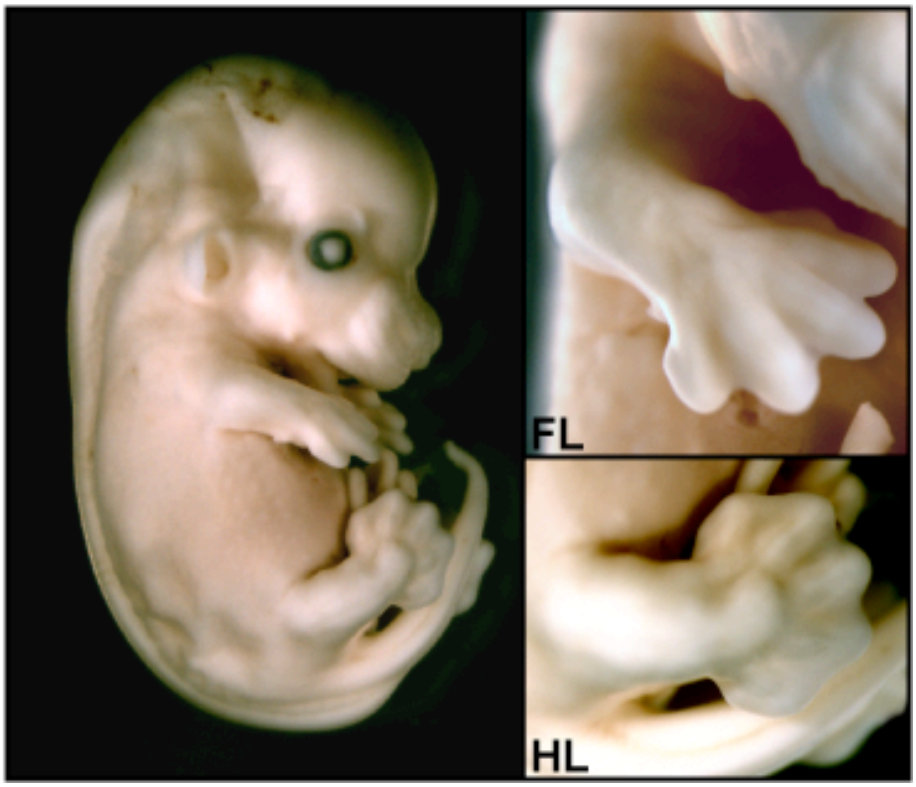

Figure 6.24. Skeletal morphology of E14.5 *Pbx1*$^{cI\Delta 3/cI\Delta 3}$; *Pbx2*$^{-/-}$; *Msx2*$^{cre/+}$ mutant embryos was normal.

At E14.5, Alcian Blue staining revealed that despite the distal excision of *Pbx1* in the ventral ectoderm and AER of the hindlimb (and partial excision in the ventral ectoderm and AER of the forelimb) recombinant mutants lacked defects in the development of overall embryo (A,B), the hindlimb (C,D), the femoral-acetabular joint and pelvis (E,F), the femoral-tibial joint (G,H), and the pes (I,J). Panels (C-H): Proximal (right); anterior (top); Panels (I,J): Proximal (top); anterior (right).

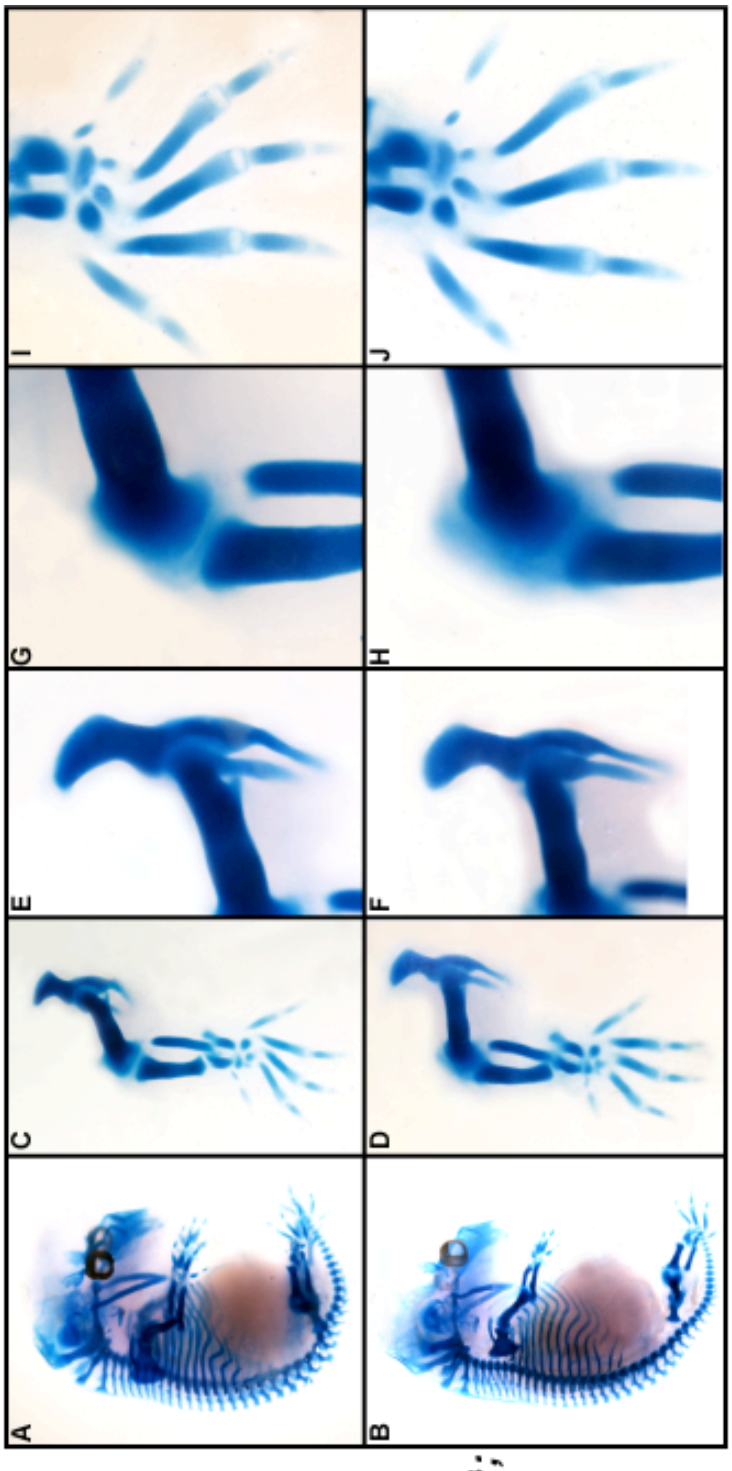
A
C
E
G
I
B
D
F
H
J
Control
E14.5
Pbx1cIΔ3/cIΔ3; Pbx2-/-; Msx2cre/+
E14.5

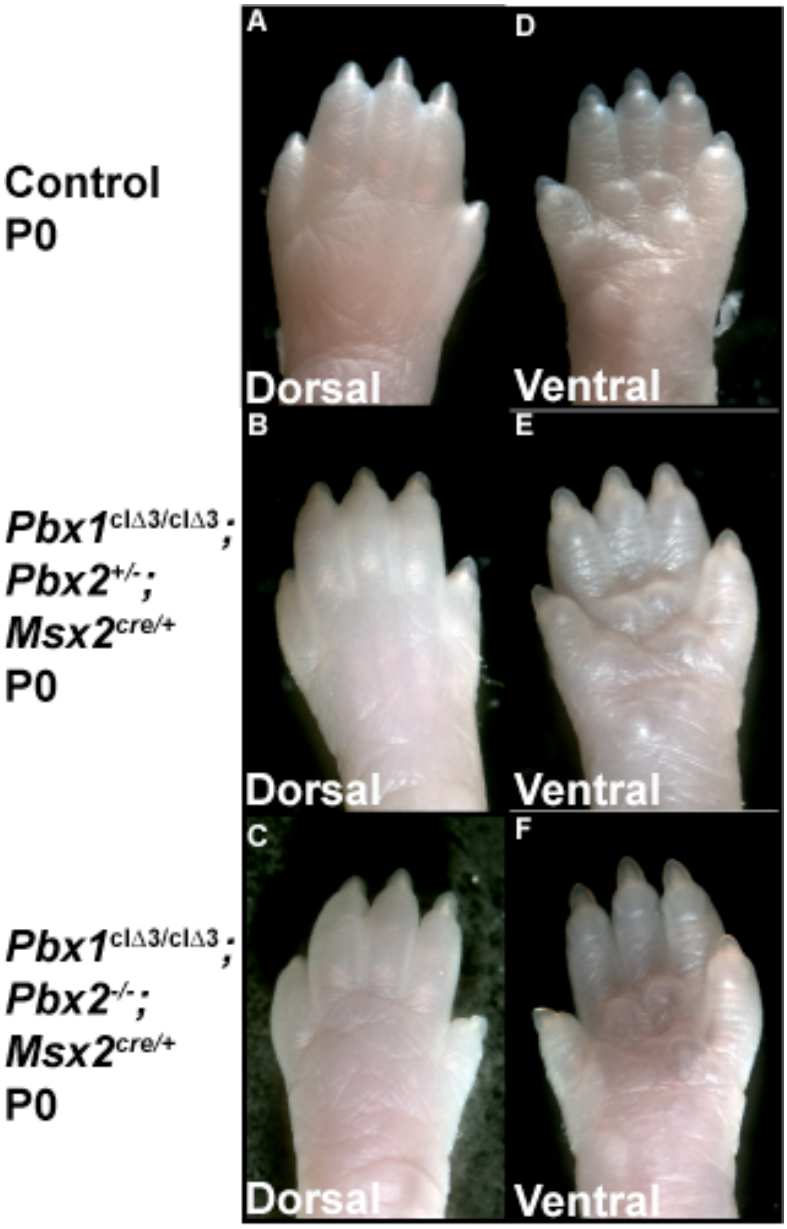

Figure 6.25. Gross morphology of the hindpaws of newborn (P0) *Pbx1*$^{cI\Delta3/cI\Delta3}$*; Pbx2*$^{+/-}$*; Msx2*$^{cre/+}$ and *Pbx1*$^{cI\Delta3/cI\Delta3}$*; Pbx2*$^{-/-}$*; Msx2*$^{cre/+}$ mutant embryos was normal.

The dorsal (B,C) and ventral (E,F) surfaces of recombinant hindpaws were phenotypically normal when compared to control hindpaws (A,D) indicating that the loss of *Pbx1* from the ventral ectoderm did not effect overt D-V patterning of the limb. Proximal (bottom); left hindpaw shown.

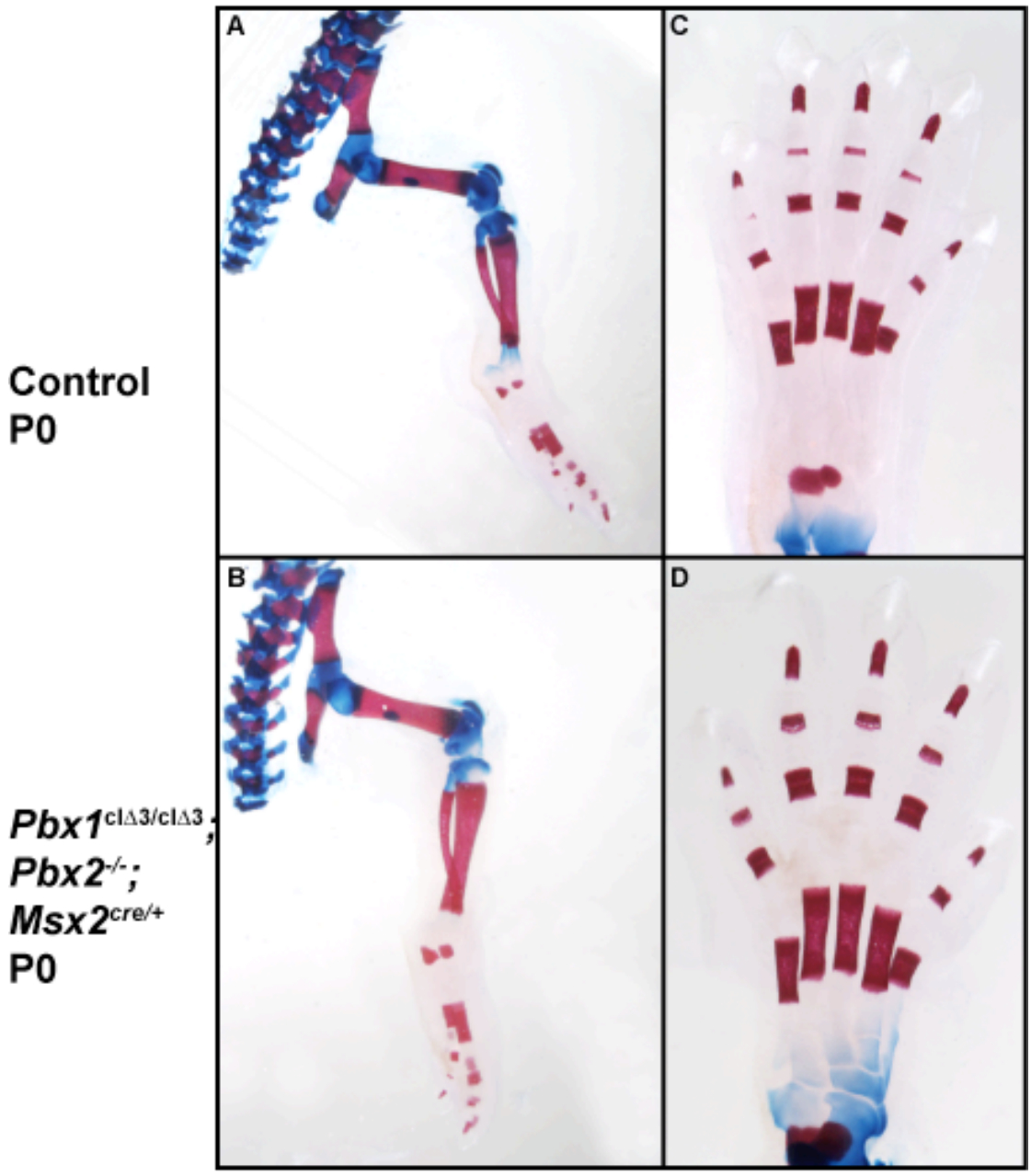

Figure 6.26. Skeletal morphology of the hindlimb and pes of newborn (P0) *Pbx1*$^{cI\Delta3/cI\Delta3}$; *Pbx2*$^{-/-}$; *Msx2*$^{cre/+}$ mutant embryos was normal.

Alcian Blue and Alizarin Red staining revealed that despite the excision of *Pbx1* in the ventral ectoderm of the hindlimb, newborn mutants (B,D) displayed no overt skeletal anomalies when compared to controls (A,C). See text for details. left pes shown.

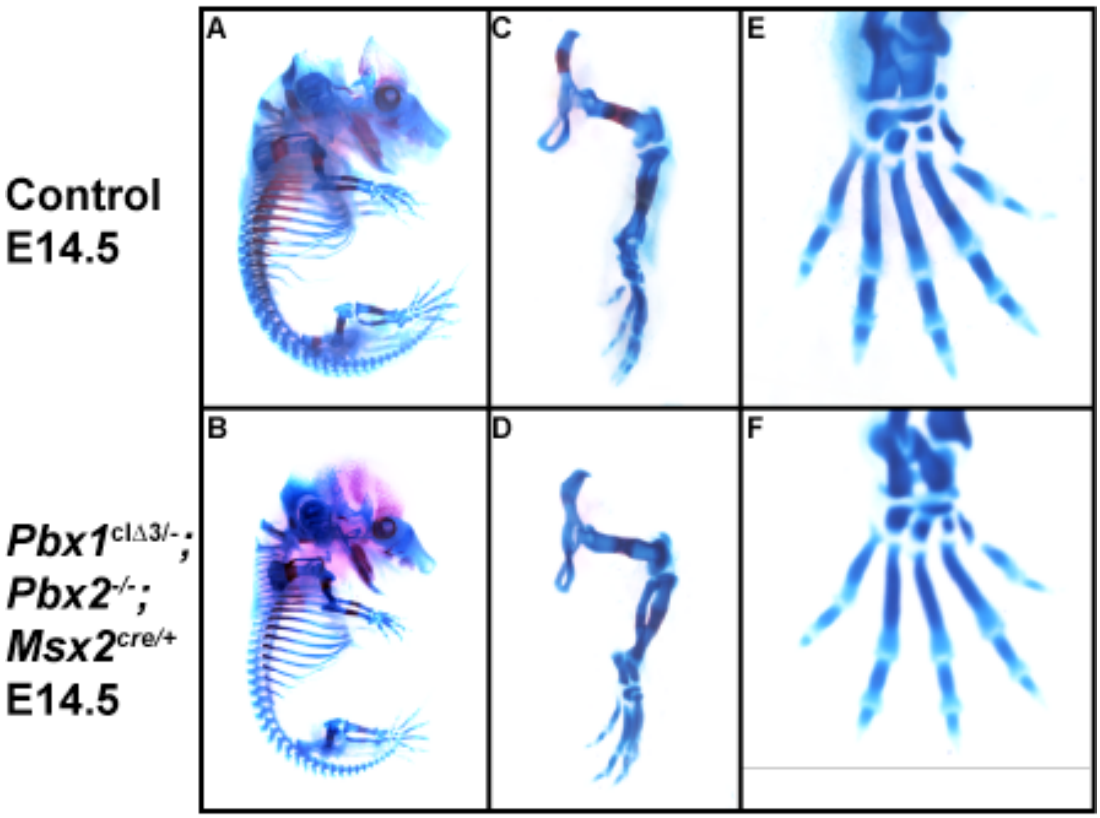

Figure 6.27. Skeletal morphology of E14.5 *Pbx1*$^{cI\Delta 3/-}$; *Pbx2*$^{-/-}$; *Msx2*$^{cre/+}$ mutant embryos was normal.

To reduce the dosage of *Pbx1* further, the *Pbx1* global null allele was introduced to the recombinant genotype. Alcian Blue and Alizarin Red staining revealed that despite the distal excision of *Pbx1* in the hindlimb and reduced *Pbx1* dosage, at E14.5, recombinant mutants lacked any visible skeletal dysmorphology in the overall embryo (B), the hindlimb (D), and the pes (F) compared to control embryos (A,C,E). The only overt phenotype was a reduced overall body-size (B) compared to controls (A). See text for details. Panels (C,D): Proximal (left); Panels (E,F): Proximal (top); anterior (right).

Figure 6.28. Scenarios of Pbx control of early limb development.

Model depicts several hypotheses and scenarios for Pbx early roles in limb development, specifically with respect to Tbx and Fgf activity. Based on current data, at least three hypotheses can put forth for Pbx roles in the early forelimb (circles 1-3) and four hypotheses for the early hindlimb. (1) depicts *Pbx* known genetic hierarchical role on *Tbx5* and *Fgf10* in the forelimb, although whether its effect on *Fgf10* expression is direct (and thus in parallel to Tbx5, long curved arrow) or indirect (through Tbx5) remains unclear. (2) as a subset of this first hypothesis (indicated by dashed vertical line) if Pbx affects *Fgf10* expression directly, it may do so in parallel with Tbx5 by directly activating the *Fgf10* promoter. (3) depicts a cell non-autonomous role for Pbx on *Fgf10* expression as Pbx would operate through Fgf8 (for example) in the ectoderm (lettering on right) to perpetuate its signaling in the mesenchyme (curved arrows from ectoderm to mesenchyme). (4) depicts Pbx known genetic role in affecting Fgf10 expression in parallel to that of Tbx4 in the hindlimb field. (5) as a subset of this hypothesis (indicated by dashed vertical line) Pbx may directly bind to the *Fgf10* promoter, as has been shown for Tbx4. (6) depicts the possibility that Pbx resides downstream of Tbx4 during early hindlimb development. (7) depicts a similar relationship as in (3) whereby Pbx role in the ectoderm on Fgf8 (lettering on right) is to drive *Fgf10* expression in the underlying mesenchyme (curved arrow from ectoderm to mesenchyme). Proximal (left); anterior (right).

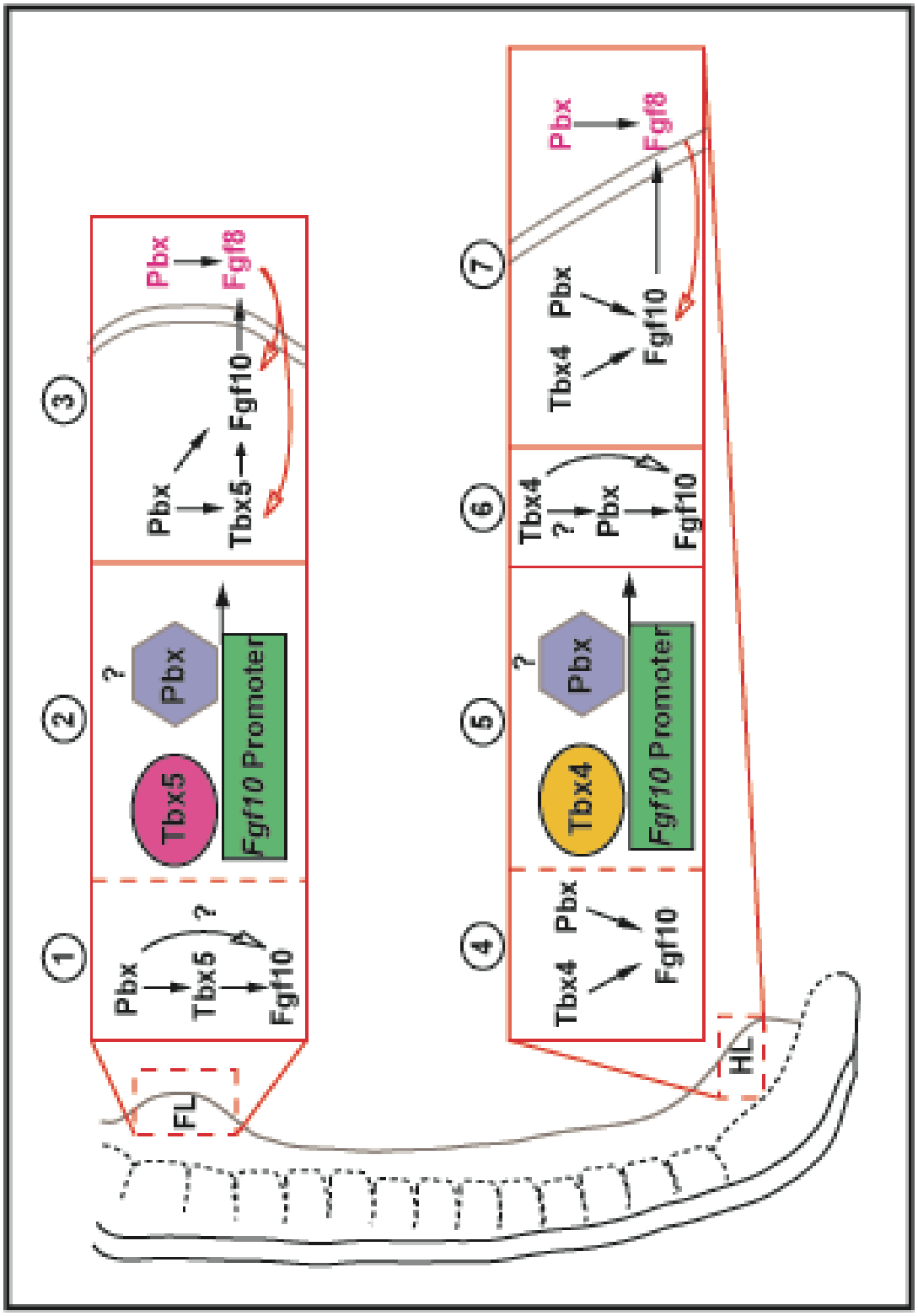
1
Pbx
Tbx5
?
Fgf10
2
Tbx5
?
Pbx
Fgf10 Promoter
3
Pbx
Tbx5
Fgf10
Pbx
Fgf8
4
Tbx4
Pbx
Fgf10
5
Tbx4
?
Pbx
Fgf10 Promoter
6
Tbx4
?
Pbx
Fgf10
7
Tbx4
Pbx
Fgf10
Pbx
Fgf8
FL
HL

Chapter 7: *Pbx* and the Development of the Pectoral and Pelvic Girdle

7.1 Introduction

As a composite bone, the vertebrate scapula arises from several distinctive tissues during development. As reviewed in Chapter 3, cells from the dorsal-lateral dermomyotome of the somite as well as the medial somatopleure of the LPM and anterior proximal limb form structures of the scapular blade and neck/head, respectively (Huang et al., 2000). Recently, it has been demonstrated that post-otic neural crest (PONC) cell derivatives also participate in scapula formation, where they aid in forming musculo-skeletal connections (Matsuoka et al., 2005). While these three tissues give rise to the scapula, the pelvic girdle has been suggested to form only from the somatopleuric mesoderm (Chevallier, 1977). Interestingly, common factors involved in the regulation of both girdles are signals emanating from the somatopleure and the ectoderm as it has been shown that disruptions to either of these signaling domains result in girdle malformations and absences (Malashichev et al., 2005; Huang et al., 2006).

Thus far, it has been demonstrated that *Pbx* genes and their protein products are present in various tissues, specifically, those involved in limb development. In addition to these domains, *Pbx* genes are expressed in several of the tissues discussed above, which indicate that they may be involved in girdle formation. Specifically, *Pbx1* and *Pbx2* have been demonstrated to share overlapping expression domains within the ectoderm of the pre-limb and limb field (including the AER) (Figs. 6.1 and 6.2) as well as within the LPM and limb

bud mesoderm (Fig. 5.4). *Pbx3* on the other hand, has only been shown to co-localize with *Pbx1* and *Pbx2* in the anterior forelimb mesenchyme from E9.5 to E12.5 and in the hindlimb mesenchyme after E11.0 (Fig. 5.4). As presented below *Pbx* genes also share overlapping domains in both the somatopleuric mesoderm as well as the dermomyotome of the somite.

As the expression of *Pbx* significantly overlap within several of these tissue domains it is of great importance to identify whether and how they genetically interact during the formation of the scapula and pelvis. Since, it has already been introduced that *Pbx1/2 Mut* embryos possess striking scapular and pelvic defects (Fig. 5.2), it is equally important to understand whether such defects occur in other compound Pbx genotypes. Accordingly, compound *Pbx1;Pbx3*, *Pbx2;Pbx3,* and *Pbx1;Pbx2;Pbx3* mutant embryos have been generated to determine the extent of genetic interaction among *Pbx* family members. In addition, in those genotypes that display marked defects, a molecular characterization has been performed to understand how loss of Pbx function specifically impacts known genetic pathways involved in girdle development.

This chapter is divided into several sections, each focused on some aspect of *Pbx* involvement in girdle formation. Section 7.2.1 focuses on novel expression patterns of *Pbx1*, *Pbx2*, and *Pbx3* in tissues that critically aid in forming the scapular and pelvic girdles. In this section, specific focus is on early somatopleuric mesoderm and dermomyotomal expression of these genes and the distribution of their proteins. Section 7.2.2 presents data on the

morphological defects in the scapular girdle of *Pbx* compound mutants and the molecular basis of their phenotypes. In this regard, analyses of gene expression for known developmental regulators of scapular formation have been conducted using only *Pbx1;Pbx2* mutant embryos. Section 7.2.3 presents data on the morphological defects in the pelvic girdles of *Pbx* compound mutants and provides a limited molecular characterization for the basis of these malformations. As with the scapular girdle, specific focus is the molecular characterization of compound *Pbx1;Pbx2* mutant pelvic girdles. Finally, the developmental significance of these findings is highlighted in a discussion (Section 7.3) that follows at the end of the chapter.

7.2 Results

7.2.1 Novel domains of TALE gene expression and protein localization during girdle development

7.2.1.1 *Pbx* and *Meis* expression during scapula formation

As discussed above, the scapula forms from the derivatives of the dermomyotome, the somatopleure, and to a lesser extent the PONC. Therefore, *Pbx* expression was examined in each of these tissues, save the PONC, since its contribution becomes evident only later in development, specifically after the *in utero* lethality of compound *Pbx1;Pbx2* mutants.

At early stages during mesoderm formation, specifically from E8.5 to E9.25, *in situ* hybridization reveals that *Pbx1* and *Pbx2* were present in the IM/LPM and embryonic flank that directly underlie the ectoderm (Fig. 5.4A), while

Pbx3 was absent from this domain (data not shown). Section *in situ* hybridization (and immunohistochemistry) on transverse sections at later days (e.g., E10.5 and E11) reveals a similar pattern in that only *Pbx1* and *Pbx2* were present in somatopleuric mesoderm (Fig. 7.1), specifically, in anterior to posterior domains just proximal to, and including, the limb field. Whole mount *in situ* hybridization (Fig. 5.4B) also clearly reveals that at the onset of limb formation (E9.5), all three *Pbx* strongly co-localized in the proximal and anterior-most domain of the bud, a region that has been shown in chicks to be fated to scapular and stylopodial skeletal elements (see Chapter 3). This pattern continued until E11.0-11.5 when the expression of all three genes occupied a more distal domain. Therefore, with respect to the mesoderm, all three *Pbx* overlap only within the limb bud proper and not the somatopleure.

Immunohistochemistry at these same stages also reveals that Pbx1 and Pbx2 were present in the overlying ectoderm of the early limb bud as well as the ectoderm surrounding the body proper (Figs. 6.2 and 7.2). Specifically, Pbx1 and Pbx2 proteins were found in both the ventral and dorsal body wall ectoderm, while Pbx3 was not present in these tissues (Fig. 7.2 and data not shown).

Novel expression patterns were also identified for all three *Pbx* genes from E9.5 to E11, where they are found in the paraxial mesoderm of the developing somites (Fig. 7.2). *Pbx* genes were expressed in the developing somites, early (at E8.5-9.5, Figs. 5.4A and 7.2B), and after they divided into their dorsal and ventral halves (data not shown). In addition, all three Pbx strongly co-localized in the dermomyotome of the dorsal-lateral somite, a critical region involved in

scapular formation (Fig. 7.2). Finally, after E11, Pbx were also present in the ventral-medial portion of the somite, specifically throughout the sclerotome, as well as in their mesenchymal derivatives that give rise to the transverse processes and centra of the vertebrae (Capellini, Di Giacomo, Selleri, in preparation).

Immunohistochemistry and *in situ* hybridization for several Pbx partners, specifically from the Meinox family, reveals that they also occupied very similar domains during limb and girdle development. For example, *Meis1* and *Meis2*, but not *Meis3* were present in the proximal forelimb and specifically co-localized with all three *Pbx* in their most anterior domain (Fig. 5.12). As discussed in Chapter 6, *Meis* were also present in the overlying ectoderm (data not shown), implicating them in epithelial-mesenchymal interactions and perhaps even during early scapular patterning and morphogenesis. Finally, preliminary analyses demonstrate that Prep1 co-localized with Pbx in the developing dermomyotomal domain of the somite (Fig. 7.2C). These data suggest that Meinox proteins may functionally cooperate with Pbx to regulate gene expression, control the nuclear importation of Pbx (Bethelsen et al., 1999), and/or have additional Pbx-independent roles in several tissues important for scapular development.

7.2.1.2 *Pbx* and *Meis* expression during posterior axis and pelvic formation

The patterns of expression identified at hindlimb levels for *Pbx1* and *Pbx2* remained extremely similar to those identified above. Both of these genes and their proteins occupied overlapping domains in the IM/LPM and early limb bud

from E8.5-9.25 (Fig. 5.4A), and after in the somatopleuric mesoderm (Fig. 7.1) as well as in the anterior-proximal domain of the limb field from E9.5 to E11.5 (Fig. 5.4B). *Pbx3* expression was absent from both the somatopleure (Fig. 7.1) and also the anterior-proximal hindlimb domain until at least E11.0, when it became only faintly expressed (Fig. 5.4B). In a similar fashion, *Pbx1* and *Pbx2* occupied the posterior body and limb field ectoderm (including AER) during pelvic development, while *Pbx3* remained absent from these tissues (Fig. 6.1). In terms of their somite expression, all three *Pbx* co-localized early at E9.5 to E11.5, and after during sclerotomal and dermomyotomal differentiation (Fig. 7.2 and data not shown). Finally, a cursory analysis of Meinox gene expression reveals similar patterns to those described above for the forelimb (Fig. 7.2 and data not shown).

7.2.2 Morphological and molecular phenotypes of the scapula in compound *Pbx* mutants

7.2.2.1 Morphological defects in compound *Pbx1;Pbx2* mutants

Scapular defects were evident in only two *Pbx1;Pbx2* compound mutant genotypes, *Pbx1*$^{-/-}$*; Pbx2*$^{+/-}$ (i.e., *Pbx1/2 Mut*) and *Pbx1*$^{-/-}$*; Pbx2*$^{+/+}$ (Fig. 5.2B,C). As initially reported by Selleri et al. (2001) and expanded upon here, in *Pbx1*$^{-/-}$*; Pbx2*$^{+/+}$ embryos the scapular blade was reduced in the anterior (superior) to posterior (inferior) dimension with a residual spinous process and reduced acromion (Fig. 5.2C). With respect to the scapular head and neck, single *Pbx1* null embryos possessed an obliterated glenoid cavity with a subsequent fusion of this domain to the head of the humerus (Fig. 5.2C). In addition, the proximal

coracoid process was either greatly expanded, or reduced and replaced by a proximally shifted deltoid tuberosity (Fig. 5.2C).

In *Pbx1/2 Mut* forelimbs and girdles, several of the *Pbx1* null defects were exacerbated and novel defects have become evident. Cartilage preparations at E12.5, as visualized by Alcian Blue staining, clearly demonstrated alterations in the humerus and adjoining pectoral girdle (see Fig. 5.2B). The condensations giving rise to the scapula and proximal humerus were completely unorganized and/or missing; specifically, scapular blade chondrogenesis was reduced suggesting that earlier mesenchymal condensation and patterning events were disrupted. Furthermore, there was a complete loss of the acromion process and an obliterated glenoid fossa. The humerus was highly contorted and proximally it remained fused to the “scapular” mass. In addition, the condensation for the deltoid tuberosity was mis-patterned in that it lied more proximal in the limb field than what was typically observed in wildtype forelimbs.

By E13.5, *Pbx1/2 Mut* girdles and proximal limbs were more clearly dysmorphic, but possessed most of their cartilaginous elements (Fig. 5.2C). The scapular blade defects observed at E12.5 were more exacerbated at E13.5, as the blade itself remained extremely rudimentary. Specifically, the proximal to distal dimension of the blade was markedly reduced compared to both single *Pbx1* null and wildtype embryos at this day. Also, there was a complete absence of the scapular spine and acromion process. The residual “scapular” mass remained strongly fused laterally to the humeral head and possessed an adjoining, anteriorly oriented skeletal element likely representing a duplicated

humeral head and scapular head/neck. Interestingly, the humerus also had a shaft that was thickened and grossly contorted, and possessed a cartilaginous anlagen mimicking a hypertrophic deltoid tuberosity (Fig. 5.2C). This particular structure also extended proximal-anteriorly, giving the entire humerus a bifurcated appearance with two proximal facing heads (Fig. 5.2C). Overall, the defects observed in *Pbx1/2 Mut* scapula and proximal limb suggests that loss of function of both of these genes results in alterations in several tissue types, specifically, the somatopleure and dermomyotome.

7.2.2.2 Compound *Pbx1;Pbx3* mutants and their forelimb and girdle morphological defects

Intercrosses of *Pbx1* and *Pbx3* mice were performed as described in Chapter 4 to determine whether, like *Pbx2*, loss of *Pbx3* impacts scapular formation. Analyses of limited numbers of progeny to date indicate that *Pbx1*$^{-/-}$*; Pbx3*$^{-/-}$ embryos died early *in utero* before E9.0 and thus could not be used for this study, while *Pbx1*$^{-/-}$*; Pbx3*$^{+/-}$ embryos died approximately between E13.5-14.5 (data not shown, Ferretti, Selleri, unpublished results). Only two genotypes (*Pbx1*$^{-/-}$*; Pbx3*$^{+/+}$ and *Pbx1*$^{-/-}$*; Pbx3*$^{+/-}$) displayed abnormalities in axial and appendicular skeletal structures.

Pbx1$^{-/-}$*; Pbx3*$^{+/-}$ embryos (hereafter, called *Pbx1/3 Mut*) possessed striking rib and vertebral malformations that phenocopied those identified in *Pbx1/2 Mut* embryos (data not shown and Fig. 5.28). With respect to the appendicular skeleton, these embryos have normal distal fore- and hindlimbs, evinced by the

normal expression of genes such as *Shh* and *Fgf8* during critical limb developmental stages (Fig. 7.3). However, they possessed differing severities of proximal limb defects for the fore- and hindlimbs (Fig. 7.4). The proximal forelimb and pectoral girdle of *Pbx1/3 Mut* phenocopied that seen for *Pbx1/2 Mut* embryos (Fig. 7.4A). The pectoral girdle of *Pbx1/3 Mut* embryos at E13.5 displayed a marked P-D reduction and disorganization of the scapular blade including the loss of the spine and acromion process (Fig. 7.4A). There was also an anterior duplication of the humeral head and scapular neck/head and the fusion of it to the scapular blade (and a subsequent obliteration of the glenoid cavity) (7.4A). Furthermore, the head and shaft of the proximal humerus were contorted as seen in *Pbx1/2 Mut* embryos and the deltoid tuberosity displayed variable fusion and elongation (Fig. 7.4A).

7.2.2.3 Compound *Pbx2;Pbx3* and triple heterozygous *Pbx1;Pbx2;Pbx3* mutants and their lack of limb and girdle morphological defects

As both *Pbx1/2 Mut* and *Pbx1/3 Mut* embryos have marked skeletal phenotypes, intercrosses between $Pbx2^{+/-}$; $Pbx3^{+/-}$ males and females were established to examine whether compound *Pbx2;Pbx3* mutant mice possessed limb and girdle defects (see Chapter 4). To this end, all compound genotypes exhibited normal girdle, forelimb, and hindlimb morphologies (data not shown). However, several embryos of distinctive genotypes died at, or before birth, presumably due to problems associated/exacerbated with the loss of *Pbx3* (Ferretti, Selleri, unpublished results), specifically since $Pbx2^{-/-}$ mice live to old

age and lack any known abnormalities. Similarly, generation of *Pbx1*$^{+/-}$*;Pbx2*$^{+/-}$*; Pbx3*$^{+/-}$ embryos was carried out to determine the extent of genetic interaction among all three Pbx family members expressed in scapular forming tissues (data not shown, Ferretti, Selleri, unpublished results). Since these triple heterozygote embryos died *in utero*, analyses of more complex genotypes could not be carried out. Nevertheless, in these specific mutants, defects in limb and girdle development were not evident. Therefore they were not characterized from a molecular perspective.

7.2.2.4 The molecular basis of the *Pbx1/2 Mut* scapular defects

The drastic malformations of *Pbx1/2 Mut* and *Pbx1/3 Mut* scapula and proximal forelimb skeletons suggest that multiple genetic and molecular pathways are altered by the absence of these *Pbx* genes. The basis for this assertion is the dual findings that early at E12.5, scapular blade, neck, and head skeletal elements were grossly mis-patterned and that each of these elements derives from distinctive tissues. With respect to the latter, scapular blade formation requires that epithelial tissues originating from the dermomyotome receive signals from the somatopleure and overlying dorsal ectoderm for their proper differentiation into scapular mesenchyme (Huang et al., 2006). Concurrently, elements of the neck and head derive solely from the somatopleure and, currently are understood to receive patterning signals from ectoderm and somatopleure (Huang et al., 2006). Therefore, to understand the basis for the *Pbx1/2 Mut* scapular phenotypes, several marker genes were

examined for each of these tissues and signaling domains. At this point in time, analyses were conducted only on *Pbx1/2 Mut* embryos, as *Pbx1/3 Mut* embryos were not available. Future work will examine the expression of some or all of the marker genes on *Pbx1/3 Mut* embryos, as it is possible that its phenotype reflects alterations in different molecular pathways.

7.2.2.4.1 Early mesenchymal condensation of scapular blade, head, and neck structures was altered in *Pbx1/2 Mut* embryos

The finding that the E12.5 *Pbx1/2 Mut* scapula and proximal humerus were markedly mis-patterned indicates that earlier mesenchymal formation and/or the allocation of position information were grossly disrupted in these mutants. To assess scapular mesenchymal condensation in *Pbx1/2 Mut* embryos, *Sox9* expression was examined at E12 (Fig. 7.5). *Sox9 in situ* hybridization revealed that the scapular blade anlagen was absent from the inferior (posterior) blade-forming domain (i.e., infraspinatous) and markedly disorganized and reduced in the superior (anterior) (i.e., supraspinatous) blade-forming domain. In addition, the mesenchyme that gave rise to the presumptive spine and acromion process was markedly reduced, if not absent. Finally, at this stage, the mesenchyme of the scapular neck/head and the humerus formed one continuous and thin tissue, a pattern that was not evident in wildtype proximal limb and scapular domains, as there appeared two separate condensations for these two elements (Fig. 7.5).

7.2.2.4.2 Expression of genes critical for scapular blade formation were altered in *Pbx1/2 Mut* embryos

To address whether the assignment of positional information and differentiation of scapular blade progenitors were altered in *Pbx1/2 Mut* embryos, several markers were examined at stages (at E10.5 and E11.5) prior to the formation of mesenchyme condensation. Analysis of the expression at E10.5 of *Emx2*, a transcription factor that is required for overall blade formation (Pelligrini et al., 2001), demonstrates that it was significantly reduced, if not absent, from the proximal domain of the *Pbx1/2 Mut* forelimb field (Fig. 7.6A). This pattern of expression continued to E11.5 when the *Emx2* signal became stronger and evident only in the most anterior and posterior domains of the scapular field (Fig. 7.6B). These data suggest that the activation of *Emx2* is delayed in *Pbx1/2 Mut* forelimbs.

The interaction of several Aristaless family genes (*Cart1*, *Alx3*, *Alx4*, and *Tbx15*) and the zinc finger protein-encoding gene *Gli3* has recently been demonstrated to pattern the scapular blade (Kuijper et al., 2005; see Chapter 3). Expression of these genes was examined in *Pbx1/2 Mut* embryos at E10.5 and E11.5 to determine the extent of mis-patterning among the different blade domains. *Tbx15* expression at E10.5 was severely reduced in the proximal and anterior domains of the *Pbx1/2 Mut* forelimb field, a pattern not identified in wildtype or single *Pbx1*$^{-/-}$ embryos (Fig. 7.7A). These data, along with *Emx2* expression, indicate that either early patterning mechanisms of the central scapular blade and/or the migration/specification of mesenchymal-scapular

forming cells were highly altered in *Pbx1/2 Mut* forelimbs. Interestingly, while the expression of *Tbx15* was grossly reduced at E10.5, at E11.5 it was present at normal and/or increased levels (Fig. 7.7B). Specifically, *Tbx15* was expressed in a strong continuous band across the presumptive blade, stylopod, and zeugopod, a pattern that was similar to that observed for *Sox9*. This pattern, however, was very different from that seen in wildtype forelimbs, where separate condensations were identifiable for the scapula and humerus (Fig. 7.7B). In addition to these abnormal patterns, *Tbx15* was also ectopically expressed along a ventral region of the mid-limb, a pattern that may reflect the mis-specification of cells destined to form stylopodial and zeugopodial skeletal elements (Fig. 7.7B).

Tbx15 has been shown to genetically interact with *Alx3*, *Alx4*, and *Cart1* in patterning the superior scapular blade (i.e., the supraspinatous), and with *Gli3* in patterning the inferior scapular blade (i.e., the infraspinatous) (Kuijper et al., 2005). At E10.5, expression of *Alx3* and *Alx4* was present in the anterior-proximal domain in *Pbx1/2 Mut* forelimbs as in wildtype forelimbs, however, each was abnormally expanded into the proximal and distal limb (Fig. 7.8A and data not shown). Interestingly, it has been suggested that the distal limb domains of both *Alx3* and *Alx4* expression are unessential for scapular morphogenesis, but are more important for digital patterning (te Welscher et al., 2002). Therefore, the expansion into this distal domain in *Pbx1/2 Mut* forelimbs may not have bearing on the observed scapular blade defects. However, at E11.5, *Alx4* was slightly expanded proximally into the limb/flank boundary, and additionally up-

regulated in the flank mesoderm (Fig. 7.8B), suggesting that superior blade morphogenesis was altered.

Next, *Cart1* expression was examined at E10.5 (data not show), E11 (Fig. 7.9A), and E11.75 (Fig. 7.9B) and never detected in the proximal-anterior and ventral-proximal domain of the *Pbx1/2 Mut* forelimb. Interestingly, in *Pbx1*$^{-/-}$ embryos, *Cart1* expression was reduced but present (Fig. 7.9B), suggesting that *Pbx1* and *Pbx2* affect *Cart1* expression directly perhaps in a dose-dependent manner. Finally, while the proximal domain of *Cart1* was absent in *Pbx1/2 Mut* forelimbs, its distal domain at the zeugopodial-autopodial junction remained (Fig. 7.9B), albeit reduced, suggesting that Pbx differentially affects *Cart1* expression in different domains. Overall, when viewed in the context of the observed alterations in *Tbx15*, *Alx3*, and *Alx4* expression, superior blade patterning and morphogenesis were greatly altered in *Pbx1/2 Mut* forelimbs at very early stages.

To examine how patterning and morphogenesis of the inferior scapular blade of *Pbx1/2 Mut* embryos were altered, both *Tbx15* (see above) and *Gli3* were examined. At E10.5 (Fig. 7.8C) and E11.5 (data not shown), *Gli3* expression in the proximal-anterior forelimb was reduced, particularly along its posterior extent, suggesting that the assignment of positional information to migrating mesenchymal cells was altered. This specific domain was also reduced at E10.5 for *Tbx15* in *Pbx1/2 Mut* forelimbs (Fig. 7.7A) suggesting that their concomitant loss at this stage either reflects the absence of an early progenitor mesenchymal cell population, or led to mis-patterning of this population along the A-P axis of the presumptive blade region.

7.2.2.4.3 Expression of genes involved in scapular head, neck, and acromion progenitors were altered in *Pbx1/2 Mut* embryos

Given the drastic alterations in the neck/head and acromion regions of *Pbx1/2 Mut* scapula, the expression of several genes known to be involved in their morphogenesis was examined. As these elements largely derive from tissues of the somatopleure and proximal limb field, *Hox* gene expression was examined at early stages of forelimb development. In general, all observed *Hox* were grossly altered (mis-expressed, up-regulated, and/or absent) in their expression, supporting the view that overall mesenchymal patterning in presumptive pectoral element domains was strongly affected in these mutants and that *Pbx* lie genetically upstream of *Hox* expression in the embryo. For example, expression of *Hoxc6* at E10.75 and E11 was posteriorly diffused and reduced when compared to the wildtype pattern (Fig. 7.10A,B). Furthermore, there was a loss of D-V delineation of *Hoxc6* along the superior border of the limb and flank (Fig. 7.10A). *Hoxc6* was previously shown to be important for glenoid and scapular head formation (Oliver et al., 1990), therefore, mis-expression of *Hoxc6* may have led patterning alterations in the mesenchyme and the loss or gain of skeletal identities. Similarly, other 3' and 5' *Hox* were markedly altered in *Pbx1/2 Mut* forelimb domains during periods when skeletal patterning is argued to occur (Fig. 5.18). For example, both *Hoxa9* and *Hoxd9* were drastically up-regulated and anteriorly mis-expressed, while more 5' members, such as *Hoxa10* and *Hoxd10* were significantly down-regulated during early limb bud development (Fig. 5.18). These data demonstrate that gene

expression in the mesenchyme of the very early limb bud, specifically in domains known to give rise to scapular head and neck regions, was severely altered in *Pbx1/2 Mut* forelimbs.

As mentioned in Chapter 5, *Pbx3* expression in the anterior forelimb may be ameliorating the severity of the morphological defects seen in *Pbx1/2 Mut* embryos. Therefore, the expression of *Pbx3* was also examined in *Pbx1/2 Mut* forelimbs to identify whether its spatial domain was altered (Fig. 7.11). Indeed, in these forelimb buds, *Pbx3* expression at E10.5 (Fig. 7.11A) and E11.25 (Fig. 7.11B) was diffused posteriorly, although at the later day the degree of posteriorization was not as severe. In addition, *Pbx3* was also altered in the flank mesoderm, directly adjacent to the proximal limb field (Fig. 7.11B). These data suggest that the regulation of *Pbx3* in the forelimb/pectoral field is specific and sensitive to the presence/absence of *Pbx1* and *Pbx2*. Such alterations in expression are consistent with the overall disorganization of mesenchymal gene expression at these time-points in *Pbx1/2 Mut* forelimbs (see Chapter 5).

Pax1 has been demonstrated to pattern the scapular spine and the acromion process (Timmons et al., 1994; Wilm et al., 1998) and may additionally have interactive roles with *Hox* to pattern more distal head and neck structures (Aubin et al., 2002). Examination of *Pax1* at E11.5 (Fig. 7.12) demonstrates that it was reduced in its anterior and ventral extent, suggesting that acromion process and scapular neck/head specification is severely abrogated in the *Pbx1/2 Mut* forelimb. In fact, examination of *Pbx1/2 Mut* skeletal preparations and *Sox9* expression at this day, demonstrated not only the loss of a complete

spine but of any mesenchymal structure arising laterally from the presumptive blade domain (Figs. 7.4 and 7.5).

As most limb-specific genes have been shown to be diffused, up-regulated, or down-regulated during early *Pbx1/2 Mut* forelimb development, additional examination of “non-limb” markers was conducted. Such an examination may provide additional insight into how alterations in different domains (other than the limb) affect overall limb development. For example, *Scleraxis* (*Scx*), a gene expressed in presumptive tendon progenitor cells that originate in the somite (Schweitzer et al., 2001), was examined for differences in expression in *Pbx1/2 Mut* and control embryos. Expression of *Scx* at E10.5 in *Pbx1/2 Mut* was severely reduced (Fig. 7.13A) in the mid-proximal limb and along the somites. Similar to several other markers discussed above, *Scx* expression in single *Pbx1*$^{-/-}$ embryonic forelimbs appeared up-regulated in both of these domains specifically when compared to compound *Pbx1/2 Mut* and wildtype controls (Fig. 7.13A). *Scx* expression in *Pbx1/2 Mut* forelimbs at E11.5 recovered but remained both disorganized in the proximal domain and reduced in its distal extent (Fig. 7.13B). These data indicate that somite and limb expression of *Scx* is sensitive to *Pbx* dosage.

7.2.3 Morphological and molecular defects in the pelvic girdle of compound *Pbx* Mutants

7.2.3.1 Morphological defects in compound *Pbx1;Pbx2* mutants

As shown (Fig. 5.2B,C), pelvic defects were evident in only two *Pbx1;Pbx2* compound mutant genotypes, *Pbx1/2 Mut* and *Pbx1*$^{-/-}$*; Pbx2*$^{+/+}$. As reported by Selleri et al. (2001), the pelvis of *Pbx1*$^{-/-}$*; Pbx2*$^{+/+}$ embryos was as reduced overall in size and each of its three adjoining (fused) elements was moderately dysmorphic. The most rostral element, the ilium, was reduced in its medial to lateral breadth and truncated cranial-caudally. Recent observations on *Pbx1*$^{-/-}$ mice on increasing C57Bl/6 backgrounds (i.e., at least ten generations) demonstrate that often the iliac cartilage was missing (Fig. 5.2C). The pubis and ischium were similarly reduced in overall dimensions and neither articulated with one another along their caudal extent (Fig. 5.2C).

In *Pbx1/2 Mut* hindlimbs and pelvic girdles, novel defects have become evident. Cartilage preparations at E12.5 clearly depict the alterations in the femur and adjoining pelvic girdle (see Fig. 5.2B). The condensations that gave rise to the girdle and proximal femur were severely reduced and/or missing; specifically, only a small rudiment of cartilaginous anlagen was present in the domain of the future pelvis suggesting that early patterning events were disrupted. The femur was also drastically reduced in size and not well structured as in wildtype embryos.

By E13.5, *Pbx1/2 Mut* proximal limbs were more clearly dysmorphic, and their girdles lacked most of their elements (Fig. 5.2C). The only remaining

fragment appeared as an ischium. This assignment was based on relative anatomical location, size, and orientation; as for example, the element was found in a similar posterior position to that which was recently reported for the chick (Malashichev et al., 2005). This residual fragment also remained fused to a femoral shaft that was also reduced in size. Overall, the defects observed in *Pbx1/2 Mut* pelvic and proximal hindlimb domains suggest that loss of function of both of these genes results in alterations in the somatopleure, as pelvic structures at this point are known only to arise from this tissue (Chevallier, 1977).

7.2.3.2 Compound *Pbx1;Pbx3* mutants and their hindlimb and girdle morphological defects

Pbx1/3 Mut embryos, as assessed at E13.5 by Alcian Blue and Alizarin Red staining, possessed pelvic alterations that mimicked those found in severely affected *Pbx1*$^{-/-}$ embryos (Compare Fig. 7.4B to Fig. 5.2C). Specifically, their ilia were missing entirely, though at a moderate penetrance (Fig. 7.4B). Both the ischium and pubis were present, however they also did not articulate along their most caudal extent (Fig. 7.4B). Finally, as in *Pbx1*$^{-/-}$ embryos, the femur remained fused to these pelvic elements (Fig. 7.4B). These data are in agreement with the lack of *Pbx3* from the hindlimb somatopleure (Fig. 7.1), the early anterior limb bud (Fig. 5.4B) and ectoderm (Fig. 7.2B) and suggest that *Pbx3* does not play a role in early pelvic morphogenesis and patterning.

7.2.3.3 The molecular basis of *Pbx1/2 Mut* pelvic defects

Given the absence of novel pelvic phenotypes in *Pbx1/3 Mut* embryos (i.e., when compared to single *Pbx1* null embryos), molecular characterization was conducted only on *Pbx1/2 Mut* hindlimb and posterior regions. The drastic alterations to *Pbx1/2 Mut* pelvic girdle and proximal hindlimb skeletons indicate that the molecular pathways involved in somatopleuric mesoderm patterning and differentiation into chondrogenic tissues were altered. Interestingly, as *Pbx1* and *Pbx2* are additional found in the ectoderm overlying the pelvic field (to the exclusion of *Pbx3*); and early removal of the ectoderm results in agenesis of the pelvis (Malashichev et al., 2005), Pbx may play important roles in both tissues. Therefore, several marker genes were examined to ascertain a molecular basis for the observed phenotype and to determine how these tissue domains were disrupted in *Pbx1/2 Mut* embryos.

7.2.3.3.1 Early mesenchymal condensations of pelvic structures were altered in *Pbx1/2 Mut* embryos

To assess pelvic mesenchymal condensation in *Pbx1/2 Mut* embryos, *Sox9* expression was examined at E12 (Fig. 7.14). *Sox9 in situ* hybridization revealed that the pelvic mesenchyme for domains which give rise to the superior and inferior portions of the ilium, as well as the ischium and pubis were mostly absent and/or reduced to extremely small centers (Fig. 7.14). In addition, the mesenchyme that gave rise to the proximal femur was markedly reduced, if not absent.

7.2.3.3.2 Expression of genes involved in the specification of the ilium, ischium, and pubis formation were altered in *Pbx1/2 Mut* embryos

Several molecular markers of ilium formation were examined at stages (E10.5 and E11.5) prior to the formation of mesenchyme condensation. Analysis of the expression of *Emx2*, a gene required for iliac blade formation (Pellegrini et al., 2001), demonstrates that at E10.5 it was significantly reduced, if not absent, from the proximal domain of the hindlimb field (data not shown). This pattern continued to E11.5, when *Emx2* mRNA transcripts were present in only the most anterior domain of the hindlimb/flank region (Fig. 7.15). More posteriorly, *Emx2* expression became less evident along the flank. These data suggest that the activation of *Emx2* was not only delayed in specific regions of *Pbx1/2 Mut* embryos, but also extremely down-regulated throughout iliac specification. *Fgf10* expression was also examined in the hindlimb domains from E9.5 through E10.5 (Fig. 6.4B,C) and was reduced compared to wildtype limbs. As *Fgf10* mutants also lack ilia (Sekine et al., 1999), its delayed expression in *Pbx1/2 Mut* hindlimbs suggests that an overall delay in mesenchymal formation during presumptive pelvic development has occurred.

Expression of *Alx3* and *Alx4* was examined in *Pbx1/2 Mut* embryos at E10.5 and E11.5 to determine the extent of mis-patterning among the different presumptive pubic and ischial domains (Figs. 5.8B and 7.16A; *Alx3,* personal observations). Interestingly, their expression remained intact in the anterior proximal limb field specifically when compared to wildtype controls. *Cart1*

expression was also examined at E11.5 and found reduced in *Pbx1*$^{-/-}$ embryos and absent in *Pbx1/2 Mut* pelvic domains (data not shown). These findings are in agreement with those observed in the forelimb domain.

While the genetic interaction of *Gli3* and *Tbx15* is not essential for patterning of the pelvis (Kuijper et al., 2005), an evaluation of their expression can aid in assessing how the mesenchyme of the entire posterior limb field and girdle was patterned. Subsequently their expression was analyzed in the hindlimb domains of *Pbx1/2 Mut* embryos at E10.5 and E11 (and E11.5). Recall from Chapter 5 that while *Gli3* is normally expressed anteriorly prior to *Shh* expression (Fig. 5.8B), after *Shh* loss in *Pbx1/2 Mut* hindlimbs *Gli3* became drastically posteriorized at E11 (Figs. 5.14B and 7.16B). In addition, at this day there was a reduction in the most posterior extent of the anterior expression domain (Fig. 7.16B). With respect to *Tbx15*, both single *Pbx1* null and *Pbx1/2 Mut* hindlimbs displayed a posteriorization in its expression at E10.5, indicative of a global alteration in mesenchymal A-P patterning (Fig. 7.17A). Interestingly, in a similar manner to that seen at E10.5 (and quite unlike the pattern found in wildtype hindlimbs), at E11.5 *Tbx15* became strongly expressed in the distal posterior portion and to a lesser extent along the middle zeugopodial portion of the limb indicating (along with other mesenchymal markers) once again that the mesenchyme is globally mis-patterned in the entire hindlimb domain (Fig. 7.17B). These data are corroborated by the findings that *Sox9* expression was highly disorganized in the proximal hindlimb and lost in the flank (Figs. 5.2A and 7.14).

A marker of tendon progenitor cell specification was also analyzed to determine if limb and pelvic tendon formation were grossly mis-patterned. *Scx* expression was drastically posteriorized in *Pbx1/2 Mut* limbs at E10.5 demonstrating that the axial level of tendon precursor cell migration was highly altered (Fig. 7.18A). A similar posterior pattern was observed at E11.5, though a more anterior domain of *Scx* expression was also evident (Fig. 7.18B). *Scx* was additionally reduced in the zeugopodial domain and occupied a more posterior position unlike that seen in wildtype hindlimbs (Fig. 7.18B). Taken together with observations on *Gli3* and *Tbx15* expression, these data demonstrate a strong disorganization and posteriorization of identity in the limb mesenchyme. These data are in agreement with those findings on mesenchymal gene expression presented in Chapter 5.

The expression of *Pax1*, a marker for the anterior proximal hindlimb and pubis domains as well as the developing sclerotome along the A-P embryonic axis (Timmons et al., 1994), was also examined at E11.5. Unlike the wildtype pattern, *Pax1* was absent entirely from *Pbx1/2 Mut* hindlimbs (Fig. 7.19A). Interestingly, as viewed by whole mount *in situ* hybridization, its flank expression, between the anterior extent of the forelimb and the posterior extent of the hindlimb, was severely reduced if not absent, suggesting a global down-regulation of *Pax1* (Fig. 7.19B).

Finally, *Pbx3* expression at E11-11.5 was examined to determine if there was a similar spatial alteration to that observed in the forelimb region. In *Pbx1/2 Mut* hindlimbs, *Pbx3* was normally and faintly expressed in its anterior domain

(data not shown). However, unlike the wildtype pattern, *Pbx3* remained slightly expressed in the anterior proximal limb field and flank, and was slightly reduced in the mid-posterior domain.

7.3 Discussion

7.3.1 *Pbx1* emerges as paramount in the determination of limb and girdle formation

The above analyses on scapula and pelvic development demonstrate that while *Pbx1;Pbx2* and *Pbx1;Pbx3* mutants have drastic skeletal defects, *Pbx2;Pbx3* mutants remain phenotypically normal. Therefore, in the context of the proposed hypothesis of the genetic redundancy and overlapping function between Pbx family members during limb and girdle development, it appears as though the dosage of *Pbx1* is most critical, at least initially, to produce an abnormal skeletal phenotype. This scenario is supported by the findings that: (1) single *Pbx2* and *Pbx3* null mice lack abnormal girdle and limb phenotypes; (2) the loss of *Pbx2* or *Pbx3* on a *Pbx1* null background, strongly exacerbates the *Pbx1* null proximal limb and girdle phenotype in domains already affected by the loss of *Pbx1*; (3) embryos with complementary genotypes such as $Pbx1^{+/-}; Pbx2^{-/-}$ and $Pbx1^{+/-}; Pbx3^{-/-}$ display normal girdles and limbs; and (4) both *Pbx1/2 Mut* and *Pbx1/3 Mut* embryos display similar vertebral and rib malformations (Capellini, Di Giacomo, Selleri, in preparation), which appear as extreme exacerbations of a *Pbx1* null axial phenotype and arise from somitic domains expressing all three *Pbx* (Fig. 5.28). Interestingly, the phenotypic consequence

of overall *Pbx* family gene loss is not simply additive because even triple *Pbx1*$^{+/-}$; *Pbx2*$^{+/-}$; *Pbx3*$^{+/-}$ embryos lack proximal limb, girdle, and axial skeletal defects (data not shown; Ferretti, Selleri, unpublished results). Thus, these results indicate that *Pbx1* synergizes with *Pbx2* and *Pbx3* to pattern the mammalian pectoral and pelvic girdle, however, in manner that may reflect differences in the spatio-temporal expression of these genes and/or biochemical activities.

7.3.2 *Pbx* are hierarchical upstream factors of scapula development

The finding that *Pbx* are expressed in multiple tissues, each of which participates in scapular formation, makes it extremely difficult to discern when and where their functions are most important. It is apparent that components of the entire scapula (i.e., blade and head/neck) were grossly reduced and altered in *Pbx1/2 Mut* (and *Pbx1/3 Mut*) embryos indicating that partial *Pbx* loss from multiple tissues may be responsible for the observed malformations. And, as discussed in the next three sections, different genetic and molecular pathways have been specifically altered in distinct domains where Pbx function has been reduced. Currently, it is unclear, how the complete loss of *Pbx* affects scapula development. On the one hand, such a loss may result in more drastic morphological alterations coupled with absences of only particular domains (i.e., head versus blade). This scenario is particularly possible if several of the genetic pathways (discussed below) already affected by partial *Pbx* loss in multiple tissues are more strongly (and differentially) disrupted by complete *Pbx* absence. On the other hand, complete *Pbx* loss may also result in scapula agenesis. This

scenario could result from *Pbx* loss from all tissue types critical for scapular formation, or from select tissues essential early in the process.

With respect to complete scapula agenesis, it is interesting that only single homozygous *Tbx5* null mice have been demonstrated to display this phenotype. Specifically, structures of the blade, head, and neck do not form in mice lacking Tbx5 function (see Chapter 3). Interestingly, it has already been reported in Chapter 6 (Fig. 6.3), that *Tbx5* expression is severely reduced in *Pbx1/2 Mut* and *Pbx1*$^{-/-}$*; Pbx2*$^{-/-}$ forelimbs. These data suggest that if *Pbx* lies upstream of *Tbx5* then the partial alterations of blade, head, and neck in *Pbx1/2 Mut* may have resulted from a disruption of Tbx5 function. However, given the uncertainty as to when, where, and how Tbx5 functions to promote scapula formation (i.e. whether it promotes the somatopleuric induction of the dermomyotome, promotes somatopleuric mesoderm differentiation into scapular structures, acts within the proximal limb bud, or is involved in all three, see Chapter 3), it remains unclear whether *Tbx5* loss alone is enough to explain the malformations identified in *Pbx1/2 Mut* embryos. For example, since *Pbx* expression is present in several additional tissue types that lack *Tbx5* expression and that these tissues (i.e., the ectoderm and dermomyotome) are critical early, it may well be that scapula formation was already compromised in *Pbx1/2 Mut* embryos prior to any role of Tbx5. Future work will clarify these relationships.

7.3.3 *Pbx* are hierarchical upstream factors of scapular blade morphogenesis

As demonstrated, the scapular blade is highly dysmorphic and rudimentary in *Pbx1/2 Mut* and *Pbx1/3 Mut* mouse embryos (Fig. 7.4). These defects were shown to occur early, before the formation of scapular blade mesenchyme (Fig. 7.5). Recently, it has been demonstrated in chick that *Emx2* functions upstream of *Sox9* expression and thus blade mesenchymal condensation. Specifically, *Emx2* is argued to specify a zone of tissue that eventually expresses *Sox9* upon its down-regulation (Huang et al., 2006). This work has been supported by research on *Emx2*$^{-/-}$ mouse embryos that lack scapular blade mesenchymal condensations and chondrogenesis (Pellegrini et al., 2001). In *Pbx1/2 Mut* embryos, the expression of both of these genes was highly reduced and spatially altered in very distinctive domains. For example, the early preliminary stages of *Emx2* expression were absent (at E10.5) while later (at E11.5) weak expression that was concentrated only in the most anterior and posterior domains of the blade progenitor tissue became evident (Fig. 7.6). In turn, *Sox9* expression was highly reduced at E12 across the entire region and markedly absent (Fig. 7.5) in and around the domain where *Emx2* was not expressed at earlier time points. Given that some residual *Pbx* remains in this mutant genotype, and that *Pbx3* is present in the anterior proximal limb domain, it is argued here that *Pbx* are genetically upstream of *Emx2* and *Sox9* expression in scapular blade morphogenesis; and that blade morphogenesis is disrupted early prior to *Emx2* expression in *Pbx1/2 Mut* embryos.

Concomitant with the early disruption of blade morphogenesis, markers for both the superior and inferior blade were down-regulated in *Pbx1/2 Mut* forelimbs. Interestingly, *Cart1*, a gene whose role is to specify superior blade development (Kuijper et al., 2005), is reduced in the presumptive scapula domain of single *Pbx1*$^{-/-}$ embryos (Fig. 7.9). This finding is in agreement with the significant superior reduction in blade formation in this mutant (Selleri et al., 2001 and Fig. 5.2C). In *Pbx1/2 Mut* forelimbs, *Cart1* is completely absent (Fig. 7.9) which indicates that its expression is dependent on the dosage of *Pbx* and thus perhaps is a direct target of *Pbx* during scapula formation. Interestingly, this same loss in *Cart1* expression is evident in *Pbx1*$^{-/-}$*; Emx2*$^{+/-}$ embryos with severe blade defects (data not shown, Zappavigna, Capellini, Selleri, unpublished data) indicating that: (1) both Emx2 and Pbx may cooperate to regulate *Cart1* expression; and/or (2) early blade morphogenesis may be a prerequisite for *Cart1* expression. Another critical point in both of these experiments is that the presence of the remaining *Pbx* (i.e., residual *Pbx2* and *Pbx3*) is unable to ameliorate or prevent the loss of *Cart1* expression. Therefore, *Pbx* may lie directly upstream of *Cart1*, or at this point may reside upstream of overall blade formation which subsequently affects *Cart1* expression. Finally, the finding that some superior-specifying genes like *Alx3* and *Alx4* are present, yet unorganized (Fig. 7.8), complicates the picture and may explain why some aspect of the most distal blade remains in *Pbx1/2 Mut* forelimbs.

As superior blade markers were altered in *Pbx1/2 Mut* proximal forelimbs, so too were inferior and central blade markers. The genetic interaction between

Gli3 and *Tbx15* produces a severe scapular phenotype, which in the double homozygous state presents as a completely absent inferior blade (i.e., giving the superior blade a long bone like appearance)(Kuijper et al., 2005). In *Pbx1/2 Mut* embryos, the expression of both of these genes was reduced early (Figs. 7.6 and 7.7A), and when present later was highly unorganized compared to wildtypes (Figs. 7.7B and data not shown). Specifically, *Gli3* expression was lost from the proximal aspect of the presumptive scapular-forming domain, and only slightly posteriorized distally, consistent with the reduction of *Shh* in the forelimb of *Pbx1/2 Mut* embryos. Likewise, *Tbx15* was reduced is this proximal anterior domain. A strong possibility may be that the reduction of blade progenitor cells in this proximal domain led to the loss and/or reduction in the expression of these genes. In this context, *Pbx* still emerges upstream of blade formation. A summary of Pbx hierarchical role in scapular blade and neck/head morphogenesis is presented in Figures 7.20 and 7.21.

7.3.4 Evidence suggests that dermomyotomal function of Pbx underlies their roles in blade morphogenesis

The scapular blade defects in *Pbx1/2 Mut* (and perhaps in *Pbx1/3 Mut*) embryos appear to result from a failure in progenitor cell specification, differentiation, and/or migration to blade-forming regions. An understanding of the spatio-temporal function of Pbx in scapular blade morphogenesis remains unclear given that *Pbx* are expressed in at least three tissues that in aid in its formation. First, *Pbx1* and *Pbx2* are expressed in the overlying somitic and limb

ectoderm; and recent work has highlighted the importance of signaling from this tissue for the induction of several critical scapular blade-forming genes, including *Emx2.* In these studies, Ehehalt et al. (2004) have further indicated that Wnt signaling may play critical roles in this regard. At this time, conditional inactivation of *Pbx* from the dorsal ectoderm in mice can satisfactorily address this concern. Conditional inactivation of *Pbx* in the ectoderm, as performed in Chapter 6, occurred late in forelimb development and only ventrally. Therefore, inactivation would need to be accomplished by a Cre active in the entire ectoderm. Importantly, the inactivation of *Pbx* from the facial ectoderm suggests that *Pbx* are upstream of Wnt/Fgf signaling interactions (data not shown; Ferretti, Selleri, unpublished results). These findings may be of great significance to understanding the general functions of *Pbx* in the entire ectoderm (as well as mesenchyme).

Second, *Pbx1* and *Pbx2* are also expressed in the developing LPM (Fig. 5.4A) and in the somatopleure (Fig. 7.1) whereas all three (including Pbx3) are co-expressed in the proximal anterior limb (Fig. 5.4B). While these tissues contribute to the scapular head and neck, the somatopleure has also been shown to signal to the epithelial cells of the dermomyotome and lead to both their cellular differentiation into mesenchyme and their migration from this tissue (Wang et al., 2005). Therefore, *Pbx* inactivation from the somatopleure and the anterior limb should help determine if blocking its function in this tissue disrupts blade morphogenesis. Interestingly, the partial loss of *Pbx1* in the distal-most portion of this domain, as achieved by the Tbx4 Cre, resulted in normal scapular

blade, neck, and head patterning. However, such deletion was inefficient and incomplete to truly shed light on the proximal limb role of *Pbx* in blade formation. Current investigation into a forelimb field-specific Cre is under way and its use may help clarify *Pbx* roles in the somatopleure and proximal anterior limb.

Third, *Pbx* have also been shown to be highly expressed in the dermomyotome proper (Fig. 7.2), which has been specifically demonstrated to give rise to the scapular blade (Huang et al., 2000). Several preliminary observations and findings point to Pbx role in this tissue, as being most critical in governing normal scapular blade morphogenesis. First, all three *Pbx* are co-expressed in this domain (Fig. 7.2) and *Pbx1/2 Mut* and *Pbx1/3 Mut* embryos possess severe, near identical blade defects (Fig. 7.4). Recall, that besides this dermomyotomal domain, *Pbx3* only co-localizes with *Pbx1* and *Pbx2* in the proximal anterior limb, as it is absent from the LPM, somatopleure, and ectoderm. Currently, it is unclear which scapular components this limb tissue contributes to, although, since it is derived directly from the LPM, it may only give rise to proximal humeral and distal scapular head/neck elements. This limb domain will have to be examined further using conditional *Pbx* mutants, to determine if deletion of *Pbx* from this tissue alone contributes to scapular blade defects. Indeed, the dermomyotomal expression (and perhaps function) of all three *Pbx* is a novel and important finding, specifically since no other gene (or set of genes) known to be expressed in this domain results in scapular blade defects when experimentally deleted. Furthermore, Pbx partner proteins, such as Prep1, are highly present in the dermomyotome (Fig. 7.2) suggesting that they interact

with Pbx to execute its genetic and molecular effects on scapular blade development.

Second, loss of *Pbx* also leads to sclerotomal and myotomal alterations (i.e., *MyoD* expression is reduced, data not shown), suggesting that Pbx functions heavily in somite differentiation. Interestingly, the recent discovery of a fourth domain of the somite, called the syndetome (Brent et al., 2003), also impacts the understanding of Pbx functions during blade formation. *Scleraxis*, a marker of the syndetome and of its progenitor cell populations that give rise to tendons (Schweitzer et al., 2001), was significantly down-regulated and delayed in *Pbx1/2 Mut* forelimbs, hindlimbs, and somite-derived flank domains (Figs. 7.13 and 7.18). These data suggest that all four somite cell populations are affected by the loss of Pbx.

Third, recent data demonstrates that the development of axial vertebral structures in *Pbx1/2 Mut* embryos (Capellini, Di Giacomo, Selleri, in preparation) was grossly altered and that a component of this alteration results from a partial disruption of *Pax1* expression during somite differentiation. In the development of vertebrae, *Pax1* expression is critical for the formation and condensation of the sclerotomal mesenchyme that gives rise to the vertebral centra (Peters et al., 1999). Importantly, *Pax1* has also been demonstrated to be a critical factor for dermomyotomal differentiation into mesenchyme, as when it is severely down-regulated (by blocking Bmp signals from the somatopleure) blade formation is disrupted (Wang et al., 2005). In both the somitic and limb domains of *Pbx1/2 Mut* embryos, *Pax1* expression is reduced, if not absent (specifically in the

hindlimb and posterior flank) (Figs. 7.12, 7.19 and data not shown). This *Pax1* down-regulation therefore may signify that an overall delay in somite differentiation has occurred in these mutants. It also suggests that *Pax1* may be a target of Pbx, as other *Pax* genes have been recently shown (Zhang et al., 2006).

Fourth, *Pbx1*$^{-/-}$*;Pbx2*$^{-/-}$ mice are significantly delayed with respect to somitogenesis, a disruption whose molecular basis at this time remains unclear. *Pbx1*$^{-/-}$*; Pbx2*$^{-/-}$ embryos consistently displayed reduced somite numbers compared to wildtype embryos of the same gestational day (Figs. 6.3 and 6.5). Interestingly, while this defect was found in double homozygous mutants, *Pbx1/2 Mut* embryos possessed approximately normal to slightly lower somite numbers, which suggests that overall *Pbx1/Pbx2* dose is critical in this regard. Therefore, Pbx functions in somitogenesis and somite differentiation may be the basis of the scapular blade defects.

Fifth, both axial and limb expression of *Hox* are slightly and/or grossly altered, respectively, in *Pbx1/2 Mut* embryos at E10.5/E11.0 (Figs. 5.17, 5.18, and 7.10). As mutations in *Hox* genes have been shown to significantly alter the fate of cells within somites (i.e., vertebral bodies which arise from the somites with altered *Hox* expression domains show homeotic transformations, e.g., Favier and Dolle, 1997; Chen et al., 1998a) disruption in their expression patterns in *Pbx* mutants suggests that specification of the dermomyotome (and of the somite proper) may be disrupted. If *Pbx* are conditionally inactivated in the somite field, using an early Cre, then analyses can ensue to test whether, like the

limb, *Pbx* are upstream of axial *Hox* expression. Such data would definitely aid in understanding a disruption in dermomyotomal cell specification and alteration. Currently, use of triple homozygous *Pbx* mice, whereby *Pbx1* and *Pbx3* are conditionally inactivated on a *Pbx2* null background, are being sought to answer this complex question.

7.3.5 *Pbx* lie upstream of scapular neck, head and acromion formation

The abnormal skeletal morphology of the scapular neck and head as well as the absence of the acromion in *Pbx1/2 Mut* and *Pbx1/3 Mut* embryos indicates that an overall disruption in somatopleuric and proximal limb mesodermal cell patterning occurred. Appropriately, analyses of several of the known molecular markers involved in early somatopleuric and forelimb bud patterning revealed that they were drastically altered in *Pbx1/2 Mut* embryos. For example, specific *Hox* genes, such as *Hoxc6*, that have been demonstrated to be involved in scapular neck/head patterning (Oliver et al., 1990), were spatially altered in these mutants (Fig. 7.10). In addition, other *Hox* genes, not typically thought of as "scapula patterning genes" such as *Hoxa9-10* and *Hoxd9-10* were strikingly mis-expressed, up-regulated, and/or down-regulated in these mutant limbs during critical patterning stages (Fig. 5.18). While these *Hox* are argued to pattern stylopodial structures (see Chapter 3), their dysregulation and mis-expression into more anterior scapular forming domains may have significant bearing on understanding the duplication of the humeral head and the loss of identity of the glenoid cavity. In this manner, Pbx upstream hierarchical role on *Hox* expression

in the LPM and limb bud may indeed be the basis for these defects, or their role as Hox cofactors may be of equal importance. Conditional inactivation of *Pbx* from this somatopleuric domain should help elucidate whether they are upstream of *Hox* expression.

Regardless of this suggested regulatory and/or biochemical interaction between Pbx and Hox, other functions for Pbx may also aid in explaining the distal scapular neck/head phenotype. It has been shown in Chapters 5 and 6 that several genes critically involved in both proximal to distal limb bud outgrowth and RA signaling were drastically down-regulated in *Pbx1/2 Mut* embryos. For example, *Cyp26B1* was down-regulated in the *Pbx1/2 Mut* forelimb (Fig. 6.12), possibly the result of a disruption in limb mesenchymal outgrowth (i.e., via a reduction or delay in *Fgf10* expression) and/or AER signaling (i.e., via a reduction of several AER-specific genes). Yashiro et al. (2004) has shown that experimental deletion of *Cyp26B1* (i.e., in *Cyp26B1*$^{-/-}$ embryos) results in the failure to completely degrade RA in the limb (with higher overall RA levels) and abrogation in P-D limb bud outgrowth. Interestingly, in these mutants, there are also malformations in distal scapular head and neck structures, while those of the proximal blade remain relatively normal. As discussed in Chapter 3, ectopic application of RA in chick limbs results in both the expansion of *Hoxc6* domain and scapular head and neck duplications (Oliver et al., 1990). Also, RA has been consistently shown to lead to an up-regulation of *Hox* gene expression when applied to the limb (Charite et al., 1994). However, in these experiments the levels of RA may have greatly exceeded its endogenous level in the limb and

even those reported in *Cyp26B1*$^{-/-}$ embryos. Therefore, tentatively, the marked skeletal malformations in *Pbx1/2 Mut* forelimb girdles, including duplications of somatopleuric-derived structures, may be partially explained by alterations in RA and their direct or indirect affects on *Hox* gene expression and patterning. In this manner, RA influence may be only part of the reason for these skeletal malformations, as the phenotypes of *Cyp26B1*$^{-/-}$ embryos differ from that seen in both *Pbx1/2 Mut* (and *Pbx1/3 Mut*) embryos and in experiments in chick on ectopic RA application. In addition, *Hox* gene expression in *Cyp26B1*$^{-/-}$ embryos is reduced and not necessarily up-regulated (Yashiro et al., 2004). Therefore, other mechanisms are at work in *Pbx* mutants and must be examined.

7.3.6 *Pbx* are upstream of pelvic girdle formation

While the *Pbx1/2 Mut* scapular malformations reflect a complex etiology, which include disruptions in the formation of both its dermomyotomal and somatopleuric components, the observed pelvic girdle defects in these mutants may only reflect alterations to the somatopleure. This situation may be particularly the case, since as of yet, only somatopleuric tissues are argued to give rise to the three skeletal elements of the pelvis (i.e., the ilium, pubis, and ischium) (Chevallier, 1977).

Malashichev et al. (2005) have recently demonstrated that the skeletal elements of the pelvis form in a distinctive sequence, beginning with the ilium, followed by the pubis, and finally the ischium. Using tissue deletion experiments in chicks these authors have additionally demonstrated that pelvic formation

requires signaling from both the limb mesenchyme as well as the ectoderm. For example, ablation of the limb mesenchyme prior to Stage 18 results in pelvic malformations. In addition, removal of the ectoderm over the pre-limb field and the presumptive pelvic forming domain (i.e., during Stage 12-18) results in either near complete agenesis of all girdle elements (i.e., at Stage 12 all elements except a small residual cranial portion of the ilium were absent) or severe girdle malformations (i.e., before Stage 18 there were varying degrees of ilium malformation as well as pubis and ischium loss). However, loss of ectoderm at stages prior to Stage 12 was not possible given the nature of posterior ectodermal formation. Finally, in these ectoderm deletion experiments, loss of skeletal elements did not simply mirror the reverse order of their formation; rather in the majority of experiments, the pubis was most often affected, the ischium was only completely affected when ectoderm was removed at Stage 12 (and not after), and the ilium was never completely absent. Malashichev et al. (2005: 195) therefore conclude, “that the influence of the ectoderm on the development of the various pelvic elements is differential.”

Interestingly, their study also indicates that the specification of pelvic skeletal elements occurs before limb bud outgrowth, which suggests that a prepatterning stage exists for the girdle as has been already proposed for the limb (Dudley et al., 2002). Several lines of evidence in mouse support this assertion, specifically as they relate to how mutations in known limb regulators affect girdle formation. One of the earliest hindlimb bud inducers, *Tbx4*, has been shown to be critical for limb bud outgrowth, as *Tbx4*$^{-/-}$ embryos lack

hindlimbs (Agarwal et al., 2003). Given their early lethality, other *Tbx4* conditional mutants demonstrate that pelvic girdle elements form, albeit abnormally, suggesting that *Tbx4* lies partially downstream of this process and/or that its effects do not impinge entirely on the spatial domain of pelvic development. Interestingly, Tbx4 has been suggested to be an upstream factor capable of directly driving *Fgf10* expression (Agarwal et al., 2003; Minguillon et al., 2005); and *Fgf10* mutants lack limbs as well as a near complete absence of the pelvic girdle (Min et al., 1998; Sekine et al., 1999). These data suggest that the pelvic forming function of Fgf10 lies partially independent of its influence from Tbx4. Since Tbx4 activity is commensurate with limb bud outgrowth, these data suggest that a prepatterning stage exists for elements of the pelvic girdle early in the hindlimb field. Finally, this work is partially supported by studies on *Pitx1*$^{-/-}$ embryos that possess alterations to only the ilium and the complete loss of the hindlimb (Marcil et al., 2003; Minguillon et al., 2005). With respect to Pitx1 function, it may be that while it is hierarchically upstream of *Tbx4*, its “pelvic” function lies in an earlier restricted spatio-temporal domain. Future work must clarify some of the spatial and temporal relationships among these genes and their effects on pelvic girdle formation.

In *Pbx1/2 Mut* embryos hindlimbs are both drastically truncated and malformed across each developmental module and the pelvis is reduced to only one element that has been interpreted here to be a residual ischium (Fig. 5.2C). These skeletal defects and absences are occurring prior to mesenchymal formation, as *Sox9* and *Emx2* expression were absent and/or extremely

reduced/delayed in most of the proximal hindlimb field during development (Figs. 7.14 and 7.15). Moreover, in chick and mouse, *Pax1* expression has been demonstrated to demarcate the mesenchymal domain for the pubis as well the cranial acetabular anlagen prior to chondrogenesis (Timmons et al., 1994; Malashichev et al., 2005), and in *Pbx1/2 Mut* hindlimbs its expression is completely absent (Fig. 7.18). Furthermore, the proximal and distal mesenchyme at early stages of limb bud outgrowth appears mis-patterned as evinced by the reduction of most *Hox* genes (Fig. 5.17), the spatial alterations to *Tbx15* (Fig. 7.17) and *Gli3* (Fig. 7.16), and the loss of *Cart1* (data not shown), the last of which has been shown important for the proper formation of the pubis-ischial caudal articulation (Kuijper et al., 2005). Therefore, as most known markers that have been shown to aid in the specification of specific pelvic structures (e.g., ilium vs. pubis) are absent; and as many are upstream of mesenchymal condensation, it may be that *Pbx* operates extremely early in the development of the hindlimb and the pelvic girdle.

Additional evidence that supports an early Pbx role comes from studies on early gene expression patterns (e.g., at E9.0-9.5) in *Pbx1/2 Mut* and *Pbx1*$^{-/-}$*; Pbx2*$^{-/-}$ embryos. For example, in all *Pbx1;Pbx2* compound mutants, *Tbx4* expression is present (Fig. 6.3) yet *Fgf10* expression in the *Pbx1/2 Mut* is delayed and reduced (Fig. 6.4), suggesting that the loss of most elements of the pelvic girdle may be partially mediated by an effect on *Fgf10* expression, independent of the role of Tbx4 on the activation of this gene. In other words, both Tbx4 and Pbx may govern *Fgf10* expression via different pathways

(involving or not involving different spatial domains). However, the delay and reduction in *Fgf10* is partial which may explain why some residual pelvic element forms (i.e., that at some later stage *Fgf10* expression is strong enough to permit the molecular cascade that gives rise to the ischium). It is possible that early disruptions in the expression of these particular genes in mouse roughly parallels the very early stage removal of the limb mesenchyme in chicks, which results in the absence of nearly all pelvic structures. In this case, these domains of mesenchymal ablation may correlate with domains of *Fgf10*, *Tbx4* and *Pbx1/Pbx2* co-localization. In either case, these data do also support the notion of a differential regulation of different pelvic elements.

If the somatopleure is the only tissue which gives rise to the cartilaginous elements of the pelvis, then the study of Pbx protein function in this domain as well as within the posterior limb ectoderm will be of great significance towards deciphering some of the major molecular mechanisms guiding pelvic girdle formation. As mentioned above, many of the genes that are altered in their expression patterns in *Pbx1/2 Mut* embryos are of mesenchymal, specifically somatopleuric and limb bud, origin. Their alteration indicates a cell autonomous role of Pbx in driving pelvic girdle formation, as *Pbx1* and *Pbx2* are highly expressed in these domains. However, a cell non-autonomous role for Pbx could also be suggested given that Fgf10 is a signaling molecule which functions within the mesenchyme and between it and the ectoderm to drive limb bud outgrowth. In this case, the loss of Pbx from the somatopleure may directly affect Fgf/Wnt signaling and again reflect the potential role of Pbx in controlling early epithelial-

mesenchymal interactions. Figure 7.22 depicts of model of proposed Pbx function during pelvic girdle development.

An equally important role for Pbx could be within the ectoderm, where both Pbx1 and Pbx2 are present during embryogenesis. Their loss from the early ectoderm could explain the complete abrogation of hindlimb bud formation in *Pbx1*$^{-/-}$*; Pbx2*$^{-/-}$ embryos as well as the severe malformations/absences in pelvic and limb formation in *Pbx1/2 Mut* embryos. In this manner, their deletion from the early posterior embryonic ectoderm (i.e., prior to limb bud outgrowth) would approximately but not entirely mimic the earliest deletion of the ectoderm in chick. Deletion of Pbx from this domain using an ectoderm-specific Cre may be the only way to test Pbx affects in this tissue on pelvic girdle formation. Investigation into such a Cre is currently underway.

Finally, it may be that deletion of *Pbx* from the ectoderm or the mesenchyme alone is not sufficient to completely abrogate pelvic girdle development as identified in *Pbx1/2 Mut* embryos. This scenario is possible, particularly if Pbx function on both sides of the epithelial-mesenchymal network required for pelvic girdle and limb bud formation. Indeed, the loss of the specific girdle elements in this mutant does not completely recapitulate that seen in mesenchymal and ectodermal deletion experiments as performed in chick nor in mouse mutants lacking genes which specifically affect pelvic morphogenesis. In fact, in comparison to most of these reported phenotypes, the *Pbx1/2 Mut* phenotype appears worse, with nearly the complete absence of all elements, save one residual fragment. Therefore, this extreme phenotype may reflect the

concurrent loss of critical functional domains in both the ectoderm and the mesenchyme. In support of this view is the overall finding that *Pbx* lies upstream of many genes involved in both limb and girdle development. Future work on *Pbx* inactivation in distinct tissues at exacting times will help clarify Pbx tissue-specific functions (if they exist) in these tissues and additionally may clarify Pbx hierarchical roles on gene expression during pelvic patterning and morphogenesis. In addition, such a strategy may lead to the discovery of specific pathways involved in the development of individual pelvic elements.

7.4 Summary

Pbx genes have been shown in this chapter to lie upstream of various processes involved in scapular and pelvic morphogenesis. With respect to the scapula, Pbx roles in the dermomyotome and somatopleure act to shape the scapular blade, while their roles in the somatopleure (and LPM) and proximal anterior forelimb bud drive head/neck and acromion formation. In addition, Pbx roles in the early pre-AER ectoderm cannot be ruled out. For both presumptive domains of the scapula, Pbx act early prior to mesenchymal formation and directly impinge on genetic networks as shown in Fig. 7.20 and 7.21. A similar situation is found during pelvic morphogenesis, but here their function in the ectoderm and/or somatopleure is paramount. Figure 7.22 highlights Pbx role in the formation of this structure.

Figures

Figure 7.1. *Pbx* expression in the somatopleuric mesoderm.

(A,B) *In situ* hybridization of *Pbx1*-, *Pbx2*-, *Pbx3*-specific probes, and Pbx1 immunohistochemistry on transverse sections of WT embryonic limbs. (A) At E11, *Pbx1* and *Pbx2* were expressed in the somatopleure of the forelimb and hindlimb (dark shaded arrowheads) while *Pbx3* was only expressed at extremely faint transcript levels in this domain in both limb types (light shaded arrowheads). (B) At E10.5, immunohistochemistry revealed that Pbx1 was present in the somatopleure (and ectoderm) of fore- and hindlimbs. In (B), two different forelimb views are shown on the top: an anterior (Ant) and middle-limb (Mid) view. In (B), two different magnifications are shown for the hindlimb on the bottom: a 10X view (left) and a 40X view (right). In all panels, Proximal (left); dorsal (top); FL, Forelimb; HL, Hindlimb.

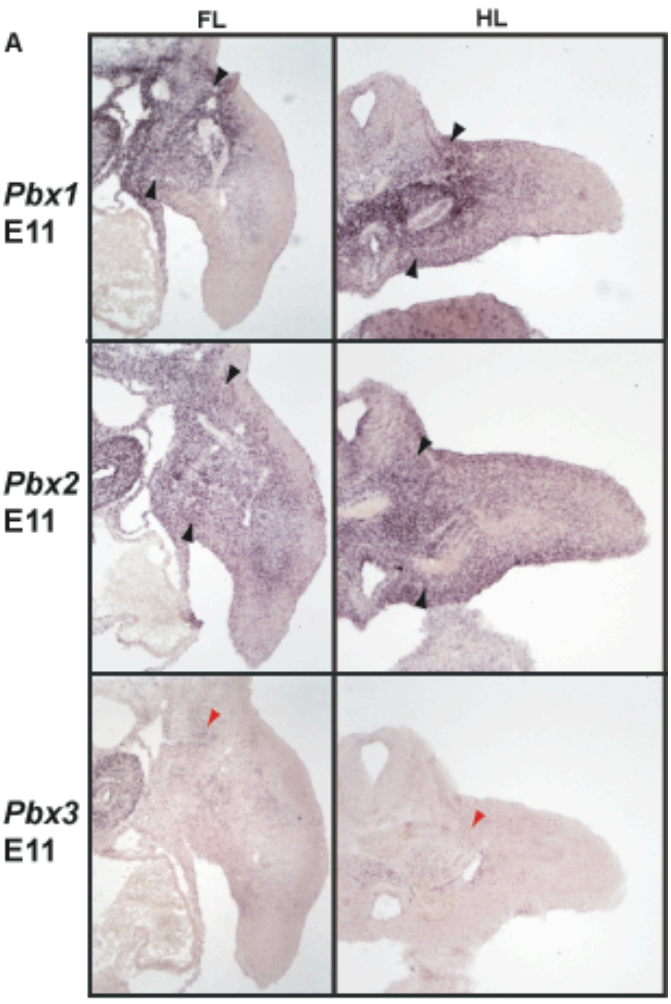
A
FL
HL
Pbx1
E11
Pbx2
E11
Pbx3
E11

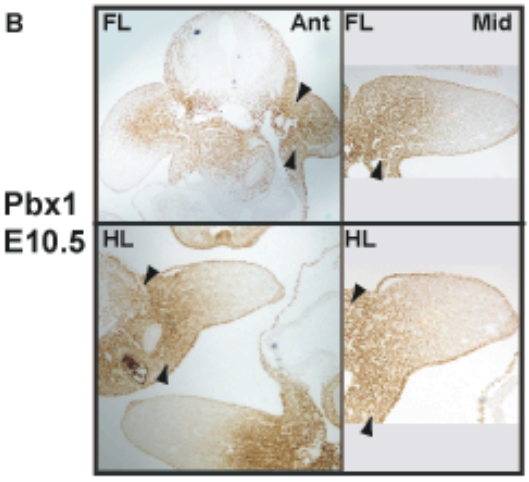
B
FL
Ant
FL
Mid
Pbx1
E10.5
HL
HL

Figure 7.2. Pbx and other TALE proteins co-localized in the dermomyotome during scapula development.

(A-C) Pbx immunohistochemistry on transverse sections of WT embryos at different gestational days. (A) At E11, Pbx1 and Pbx2 protein co-localized in the dermomyotome (upper dark shaded arrowheads) and the anterior limb bud (lower dark shaded arrowheads) during fore- and hindlimb bud development. (B) At E9.5, Pbx3 protein was present in the developing dermomyotome (dark shaded arrowheads) and was absent from the early ectoderm of the hindlimb field (empty dark shaded arrowhead points to thin epithelial tissue along lateral aspect of limb field). (C) At E10.5, the TALE proteins Pbx2 and Prep1 strongly co-localized in the dermomyotome (lateral dark shaded arrowheads), suggesting their involvement in both this tissue's maturation and role during scapular blade formation. These proteins also co-localized in the notochord (midline dark shaded arrowheads). Proximal (left); dorsal (top); FL, Forelimb; HL, Hindlimb.

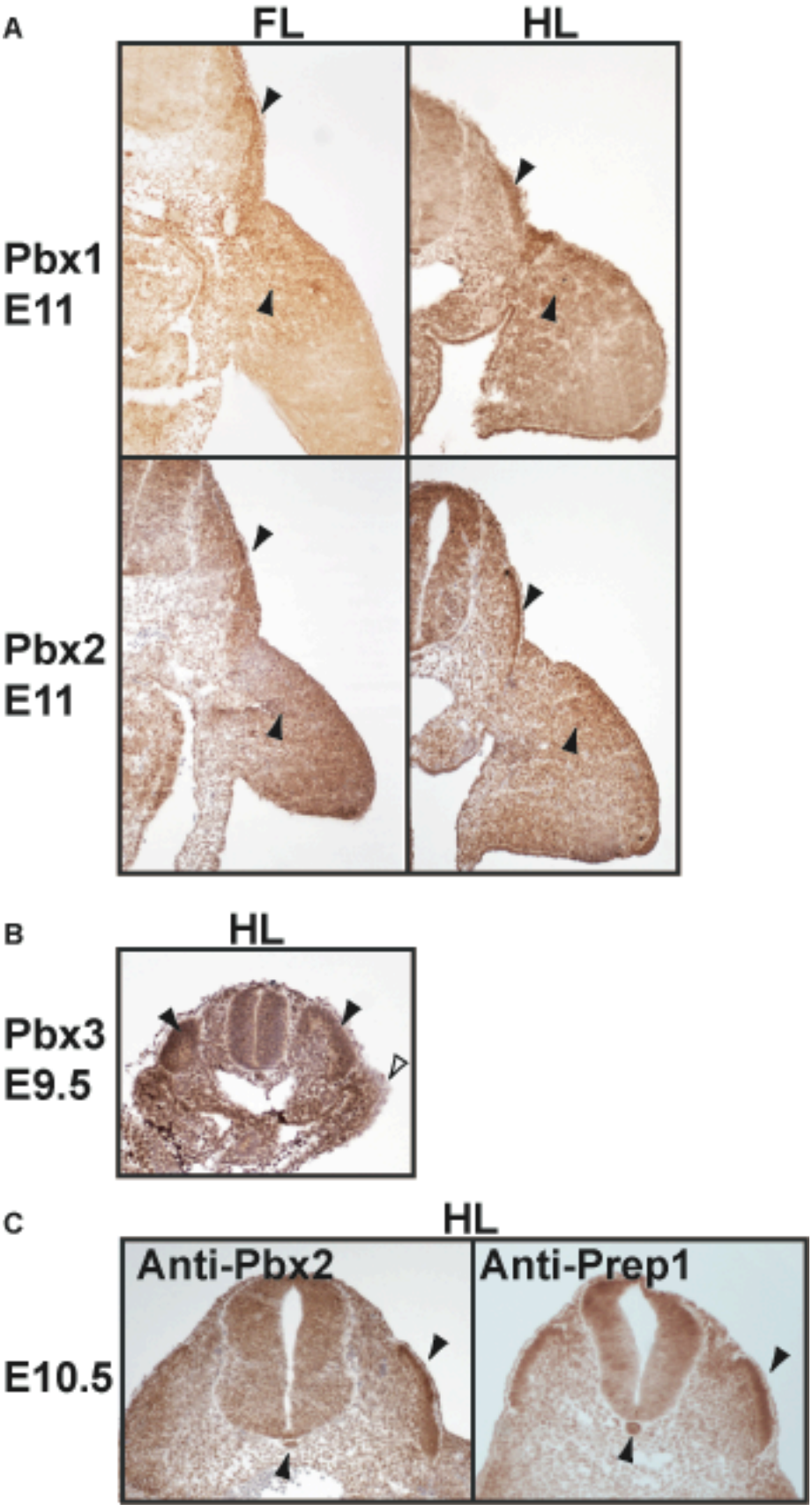
A
FL
HL
Pbx1
E11
Pbx2
E11
B
HL
Pbx3
E9.5
C
HL
Anti-Pbx2
Anti-Prep1
E10.5

Figure 7.3. *Fgf8* and *Shh* were normally expressed in *Pbx1*$^{-/-}$;*Pbx3*$^{+/-}$ embryos during limb development.

(A) *In situ* hybridization At E10.5 demonstrated that *Fgf8* remained normally expressed in *Pbx1*$^{-/-}$;*Pbx3*$^{+/-}$ fore- and hindlimb bud AER, coincident with the lack of distal limb defects in embryos harboring this genotype [note: smaller limb bud size in mutant phenocopied that seen in single *Pbx1* null embryos at this gestational day]. (B) At E11.5, *Shh* remained well expressed in *Pbx1*$^{-/-}$;*Pbx3*$^{+/-}$ fore- and hindlimb buds indicating that ZPA function was intact. Proximal (left); anterior (top); FL, Forelimb; HL, Hindlimb.

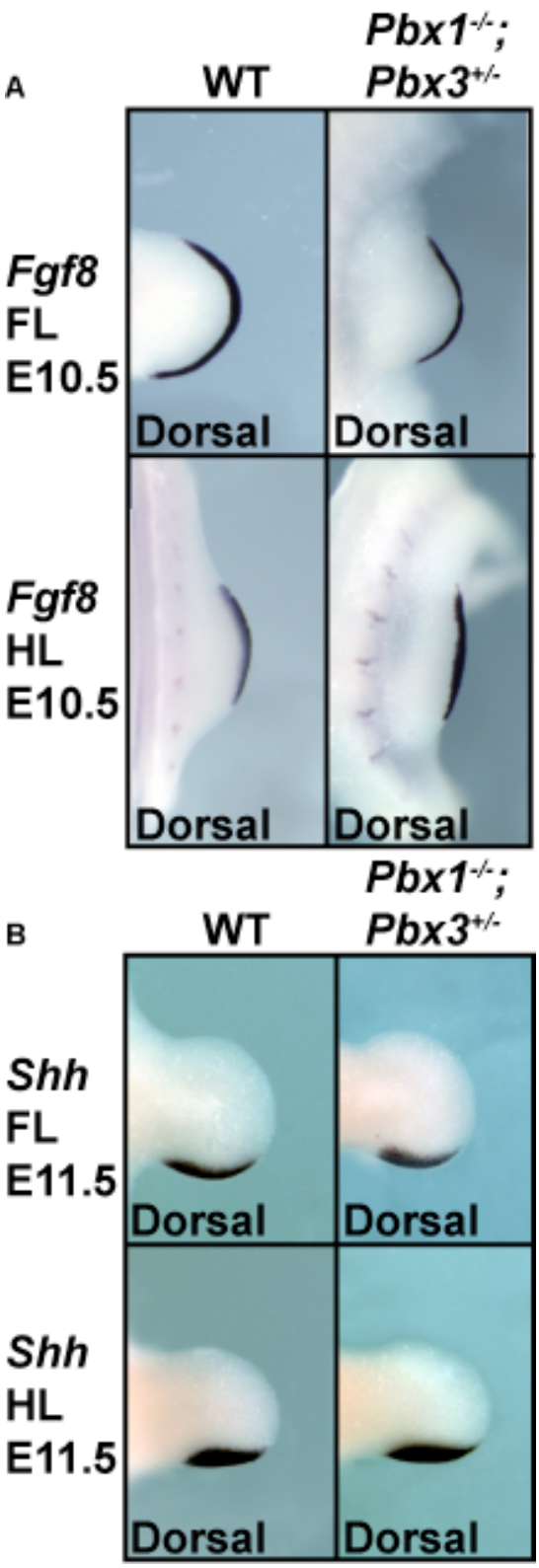
A
WT
Pbx1-/-; Pbx3+/-
Fgf8 FL E10.5
Dorsal
Dorsal
Fgf8 HL E10.5
Dorsal
Dorsal
B
WT
Pbx1-/-; Pbx3+/-
Shh FL E11.5
Dorsal
Dorsal
Shh HL E11.5
Dorsal
Dorsal

Figure 7.4. Comparative limb skeletal morphology of *Pbx1$^{-/-}$;Pbx2$^{+/-}$* and *Pbx1$^{-/-}$;Pbx3$^{+/-}$* embryos.

(A) At E13.5, the abnormal phenotypes of *Pbx1$^{-/-}$;Pbx2$^{+/-}$* and *Pbx1$^{-/-}$;Pbx3$^{+/-}$* forelimbs, as demonstrated by Alcian Blue staining, were nearly identical in the proximal stylopodial and scapular domains. Specifically, when compared to WT (dark and light shaded arrows, respectively), the deltoid tuberosity remained fused to the humeral shaft (dark shaded arrowheads), the scapular blade was reduced proximally (light shaded arrowheads in inset), and the scapular head/humeral head was duplicated anteriorly (double dark shaded arrowheads in inset) in both mutant genotypes. Note that the distal *Pbx1$^{-/-}$;Pbx3$^{+/-}$* forelimb was phenotypically normal indicating that loss of Pbx3 had a different affect on limb bud development than Pbx2. (B) At E13.5, while the *Pbx1$^{-/-}$;Pbx2$^{+/-}$* mutant hindlimb was grossly affected both distally and proximally (i.e., there was only one rudimentary ischial fragment in the pelvic girdle, dark shaded arrowhead), *Pbx1$^{-/-}$;Pbx3$^{+/-}$* hindlimb and pelvic girdle defects phenocopied those seen for single *Pbx1$^{-/-}$* embryos at this day (see Fig. 5.2), indicating that *Pbx3* may not have been involved in the formation of these structures. Specifically, this mutant's pelvic girdle consisted of both pubic and ischial elements (dark shaded arrowheads) but not the ilium (empty dark shaded arrowhead), as was normally present in WT embryos (dark shaded arrow). Proximal (top); anterior (right); fe, femur; fi, fibula; hu, humerus; pg, pelvic girdle; ra, radius; sc, scapula; ti, tibia; ul, ulna.

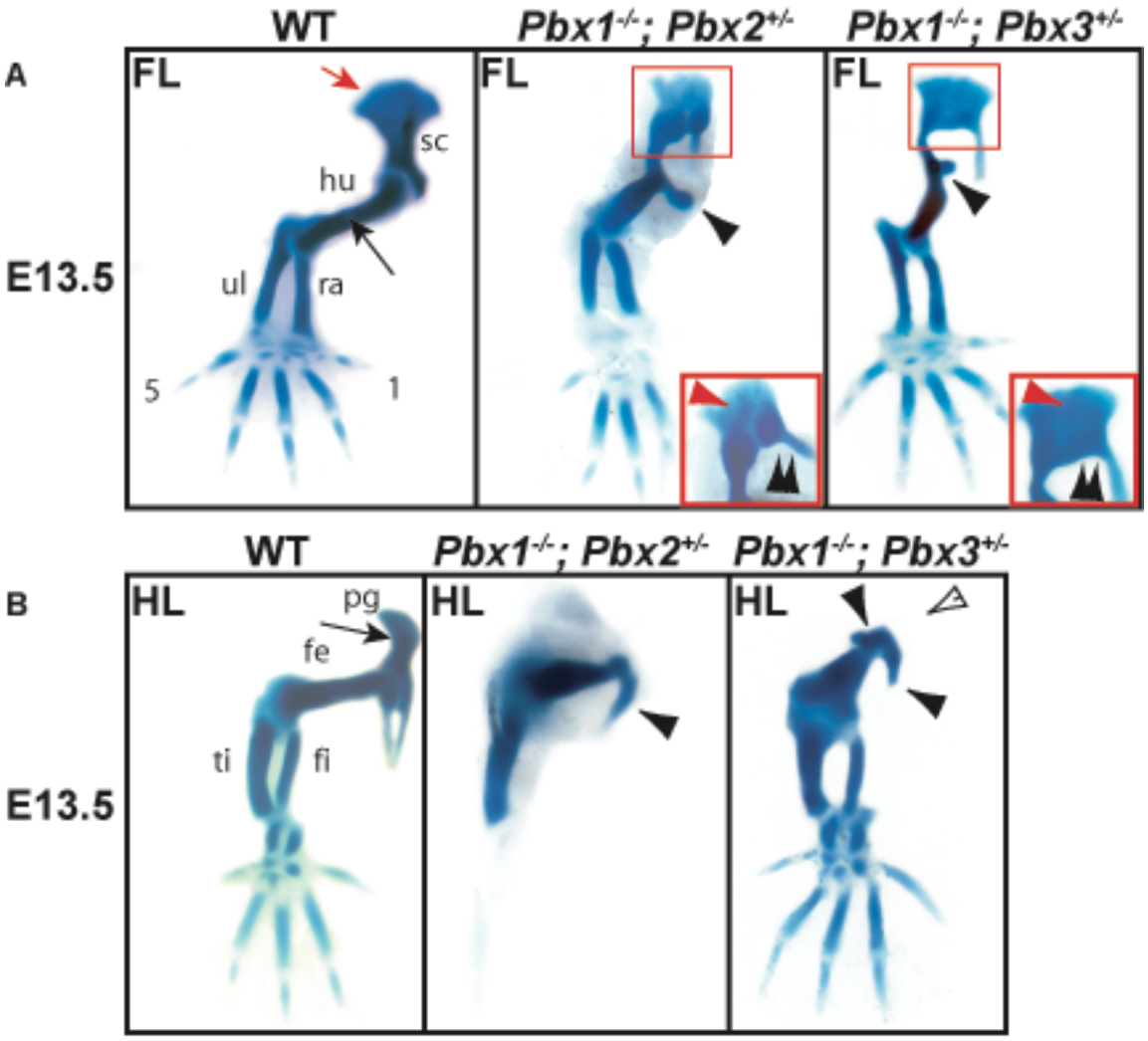
WT
Pbx1-/-; Pbx2+/-
Pbx1-/-; Pbx3+/-
A
E13.5
FL
sc
hu
ul
ra
5
1
FL
FL
WT
Pbx1-/-; Pbx2+/-
Pbx1-/-; Pbx3+/-
B
E13.5
HL
pg
fe
ti
fi
HL
HL

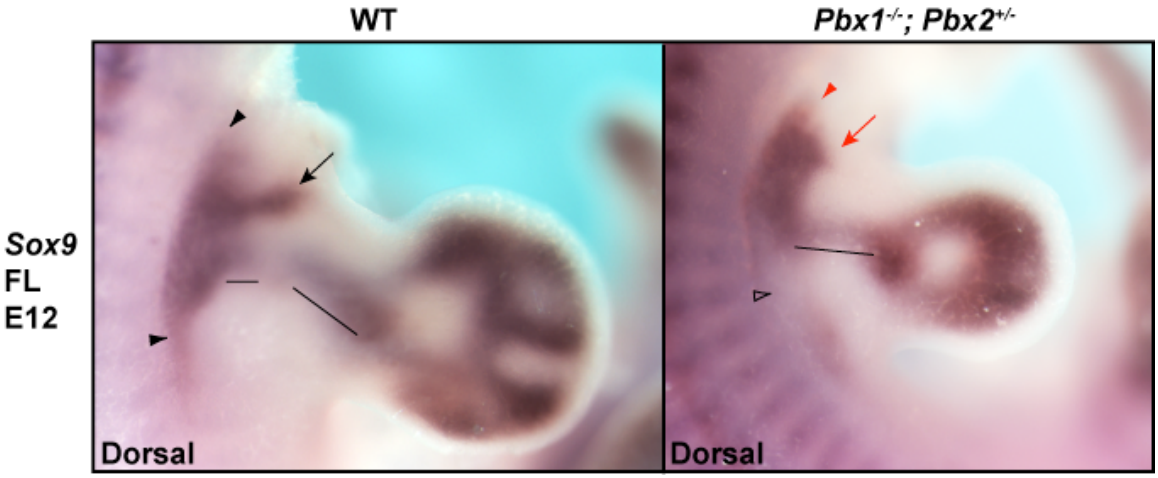

Figure 7.5. *Sox9* expression was markedly absent and disorganized in the presumptive scapula domain of *Pbx1*$^{-/-}$;*Pbx2*$^{+/-}$ forelimbs.

In situ hybridization at E12 revealed that *Sox9* expression was reduced in the anterior (light shaded arrowhead) and absent from the posterior (caudal) (empty dark shaded arrowhead) presumptive blade domains in *Pbx1*$^{-/-}$;*Pbx2*$^{+/-}$ forelimbs compared to WT forelimbs (anterior and posterior dark shaded arrowheads, respectively). In addition, the mesenchymal condensation that normally gave rise to the acromion process in WT (dark shaded arrow) was lost in the mutant (light shaded arrow). Finally, in the mutant forelimb, *Sox9* expression was continuous from the scapular anlagen through the distal zeugopodial domain (continuous dark line), a pattern not identified in WT forelimbs (broken dark line). Proximal (left); anterior (top); FL, Forelimb.

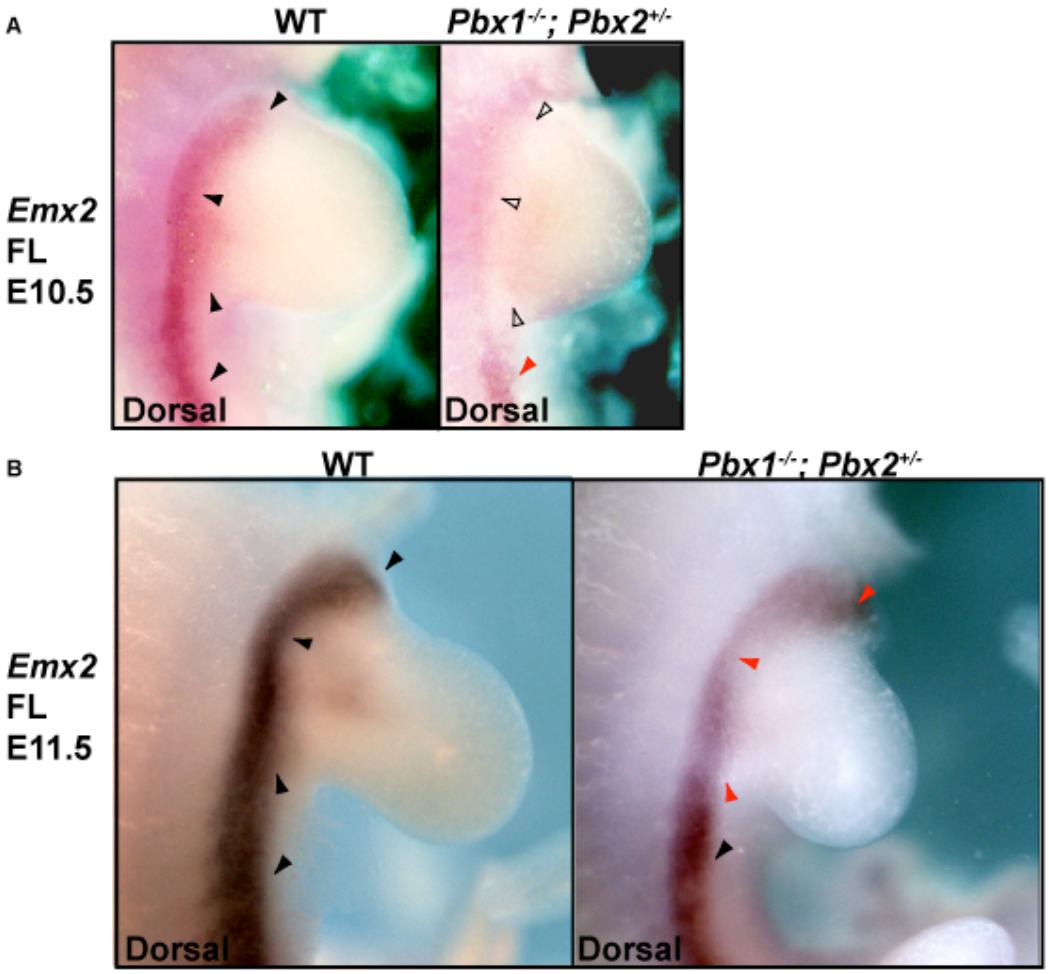

Figure 7.6. *Emx2* expression was reduced in the presumptive scapular blade domain of *Pbx1*$^{-/-}$;*Pbx2*$^{+/-}$ forelimbs.

(A) *In situ* hybridization at E10.5 revealed that *Emx2* expression was reduced, if not absent, from the entire presumptive blade domain of *Pbx1*$^{-/-}$;*Pbx2*$^{+/-}$ forelimbs (empty dark shaded arrowheads) as compared to WT forelimbs (dark shaded arrowheads). However, this loss was limited to the blade domain, as *Emx2* expression was present, yet reduced, in the mutant interlimb flank (light shaded arrowhead) as compared to WT (dark shaded arrowhead). (B) At E11.5, much of the blade expression of *Emx2* was present, though reduced in mutant (light shaded arrowheads) compared to WT forelimbs (dark shaded arrowheads), suggesting that blade mesenchymal formation was delayed in the absence of *Pbx1* and *Pbx2*. Furthermore, the intensity of *Emx2* expression differed along the axial level of the forelimb bud. Finally, its flank expression was relatively restored in the mutant (dark shaded arrowhead) compared to WT embryos (dark shaded arrowheads) Proximal (left); anterior (top); FL, Forelimb.

Figure 7. 7. *Tbx15* expression was markedly delayed and disorganized in *Pbx1*$^{-/-}$;*Pbx2*$^{+/-}$ forelimbs.

(A) *In situ* hybridization at E10.5 revealed that *Tbx15* expression was markedly reduced in the distal limb (light shaded arrowhead) and essentially absent in the proximal limb (empty dark shaded arrowhead) of mutant forelimb buds as compared to WT (dark shaded arrowheads in each respective domain indicate normal expression). Furthermore, its expression in single *Pbx1* null embryos appeared up-regulated and expanded (light shaded arrowheads) when compared to WT (dark shaded arrowheads). (B) At E11.5, *Tbx15* was strongly expressed, yet in a highly disorganized pattern, in the mutant anterior and middle proximal limb bud (light shaded arrowheads) but was lost from the posterior proximal bud (empty dark shaded arrowhead) specifically compared to WT (dark shaded arrowheads). Finally, when viewed superiorly (lower panels), in the mutant zeugopodial region, there was an ectopic ventral expression domain of *Tbx15* (light shaded arrowhead) when compared WT forelimbs (dark shaded arrowhead) Proximal (left); anterior (top); FL, Forelimb.

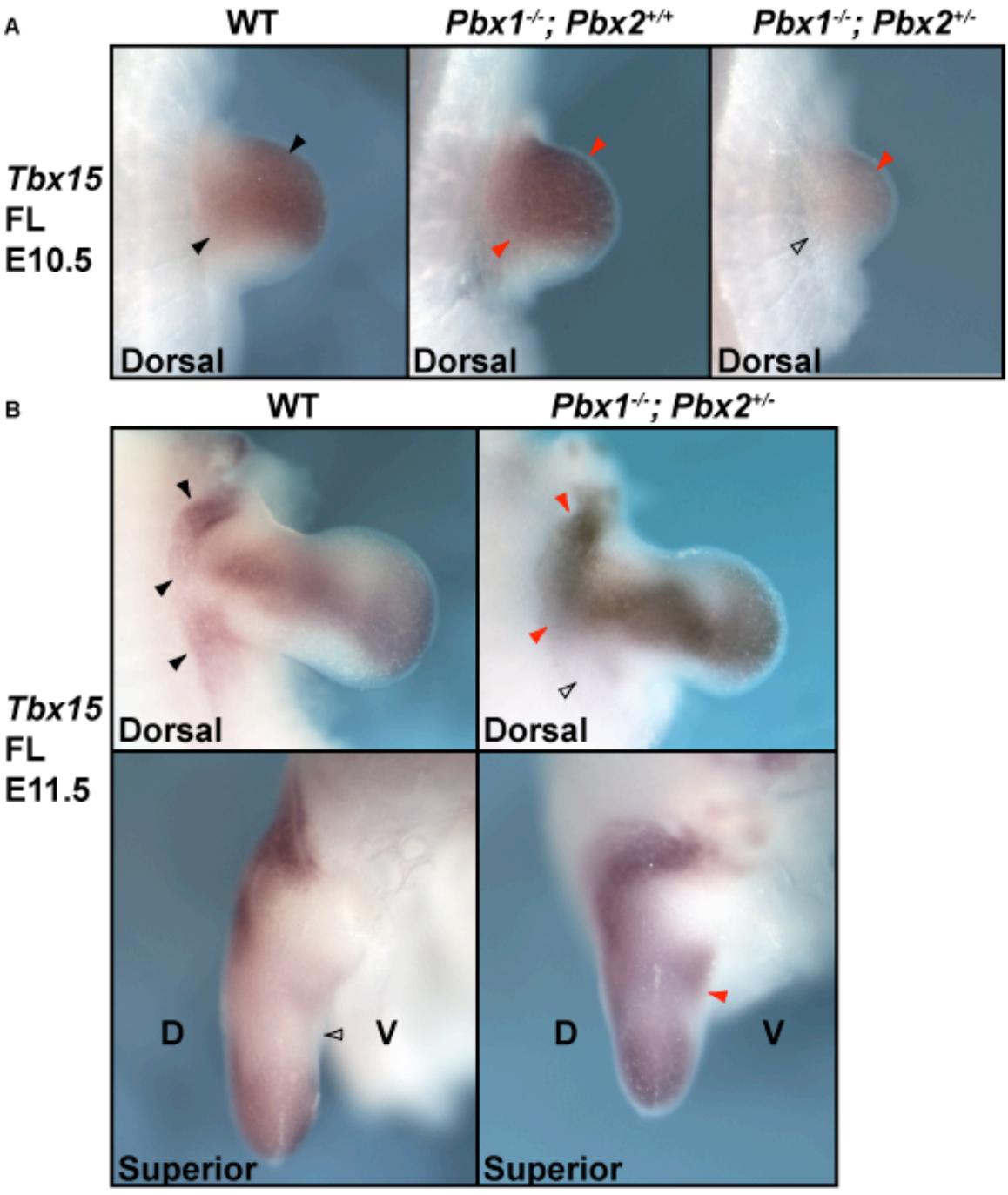
A
WT
Pbx1-/-; Pbx2+/+
Pbx1-/-; Pbx2+/-
Tbx15
FL
E10.5
Dorsal
Dorsal
Dorsal
B
WT
Pbx1-/-; Pbx2+/-
Tbx15
FL
E11.5
Dorsal
Dorsal
D
V
D
V
Superior
Superior

Figure 7.8. Expression of *Alx4* and *Gli3* were spatially altered in the presumptive scapular domain of *Pbx1*$^{-/-}$;*Pbx2*$^{+/-}$ forelimbs.

(A) *In situ* hybridization at E10.5 revealed that *Alx4* expression was spatially diffused in the proximal and distal *Pbx1*$^{-/-}$;*Pbx2*$^{+/-}$ forelimb (light shaded arrowheads) compared to WT (dark shaded arrowheads). (B) At E11.5, this diffused expression pattern in the mutant partially remained in the proximal (light shaded arrowheads in limb) but not distal (dark shaded arrowhead) limb compared to WT (dark shaded arrowhead). Interestingly, *Alx4* was additionally up-regulated in the flank region of the mutant forelimb (light shaded arrowheads) compared to WT (dark shaded arrowhead), indicating that gene expression in the somatopleuric mesoderm was highly altered by the loss of *Pbx1* and *Pbx2*. (C) At E10.5, the distal limb expression of *Gli3* was posteriorized (light shaded arrowhead) as expected given the concurrent reduction of *Shh* in the ZPA. However, the proximal anterior domain of *Gli3* expression was also absent in the mutant (empty dark shaded arrowhead) compared to the WT pattern (dark shaded arrowhead), indicating that markers for the presumptive inferior scapular blade were altered in the absence of *Pbx*. Proximal (left); anterior (top); FL, Forelimb.

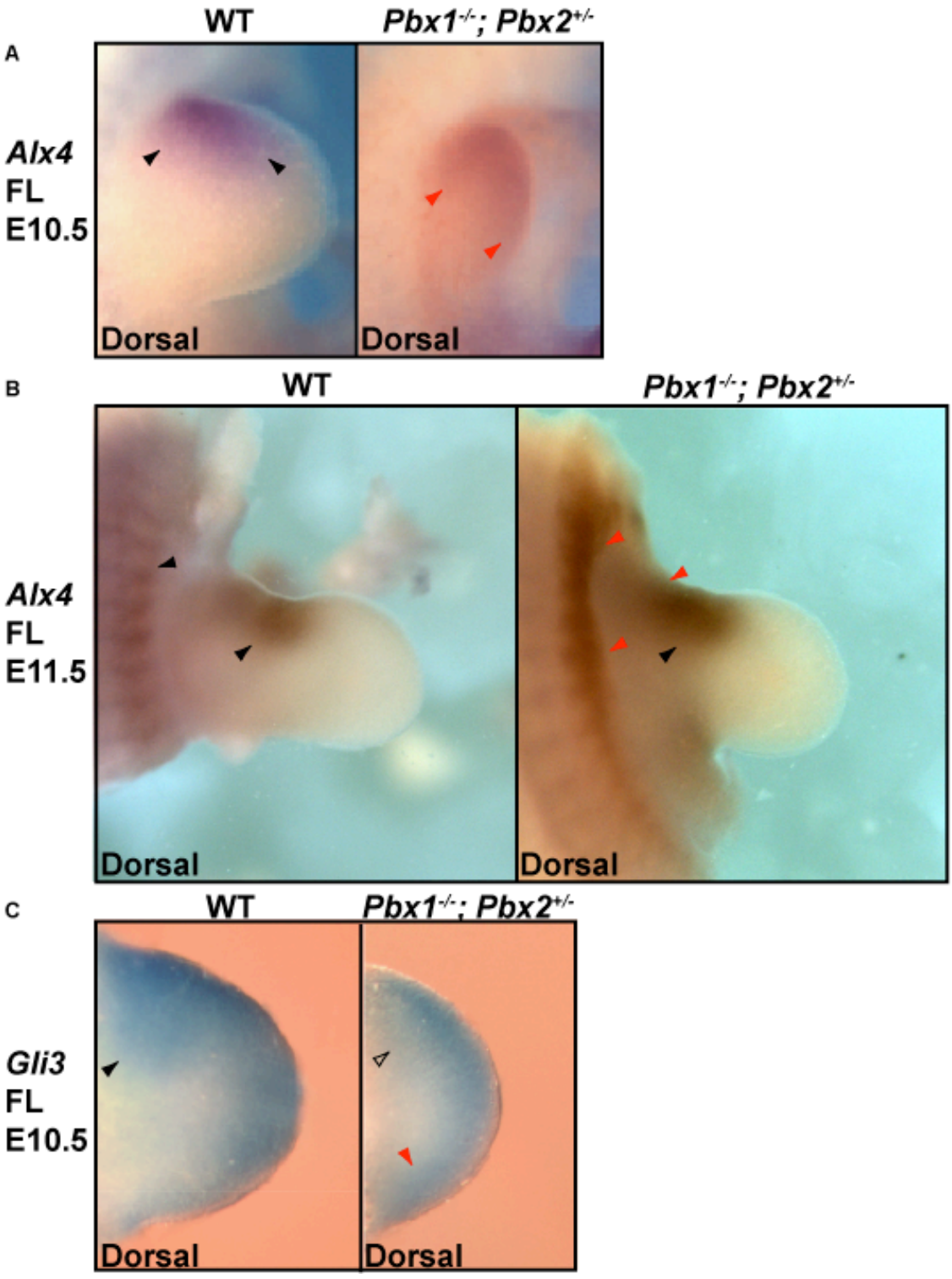
A
WT
Pbx1-/-; Pbx2+/-
Alx4
FL
E10.5
Dorsal
Dorsal
B
WT
Pbx1-/-; Pbx2+/-
Alx4
FL
E11.5
Dorsal
Dorsal
C
WT
Pbx1-/-; Pbx2+/-
Gli3
FL
E10.5
Dorsal
Dorsal

Figure 7.9. *Cart1* expression was reduced in the presumptive superior scapular blade domain of *Pbx1*$^{-/-}$;*Pbx2*$^{+/-}$ forelimbs.

(A,B) *In situ* hybridization at E11 and E11.75 revealed that *Cart1* expression was absent from the superior and proximal anterior forelimb/flank boundary in *Pbx1*$^{-/-}$;*Pbx2*$^{+/-}$ embryos (empty dark shaded arrowheads in both views) compared to WT (dark shaded arrowheads in both views). (B) At E11.75, despite this reduced proximal expression, *Cart1* expression remained weak, but present, in the mid-limb domain of the mutant (light shaded arrowheads in both views) compared to WT (dark shaded arrowheads in both views) indicating that *Pbx* genetic effects on *Cart1* expression may have been tissue-specific. In addition, the reduction of *Cart1* in both fields in single *Pbx1* null forelimbs (light shaded arrowheads in both views) suggests that this gene may be a direct target of Pbx during scapular development. Proximal (left or top); anterior (top or out of page); FL, Forelimb.

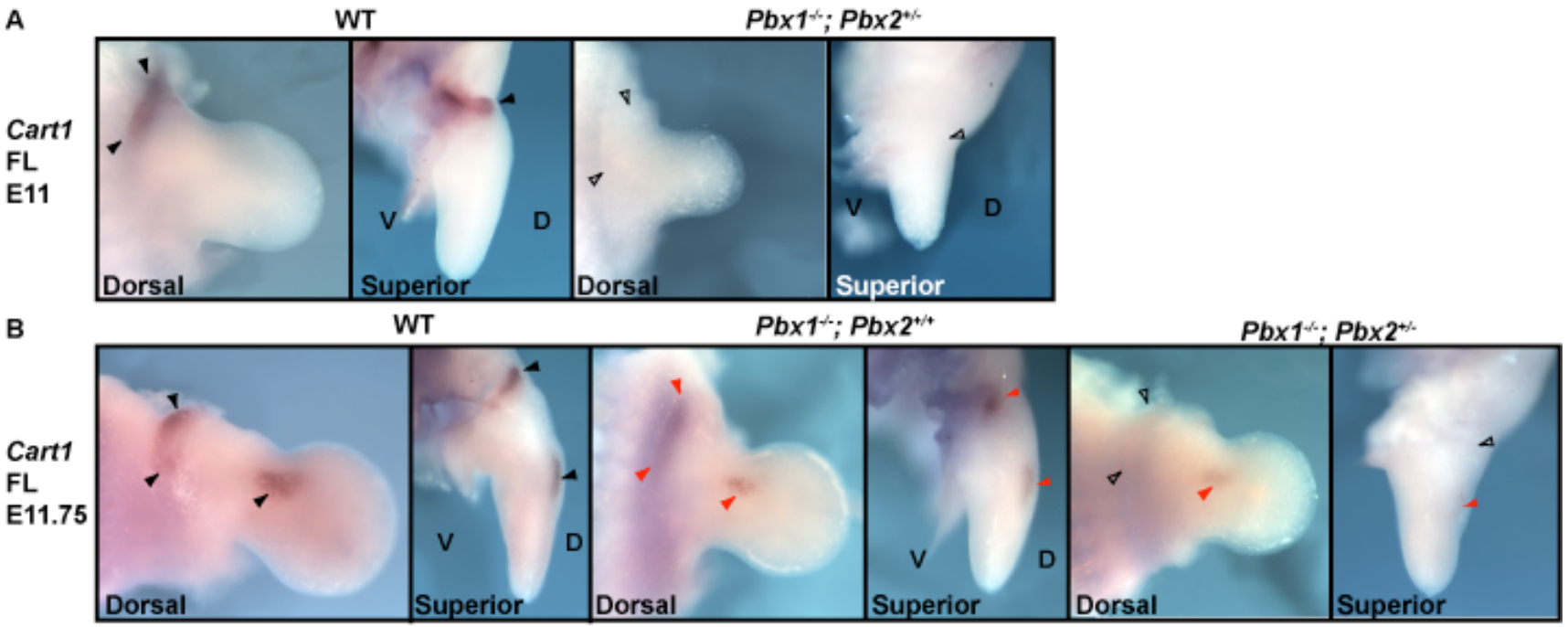
A
WT
Pbx1-/-; Pbx2+/-
Cart1
FL
E11
V
D
Dorsal
Superior
Dorsal
Superior
B
WT
Pbx1-/-; Pbx2+/+
Pbx1-/-; Pbx2+/-
Cart1
FL
E11.75
V
D
Dorsal
Superior
Dorsal
Superior
Dorsal
Superior

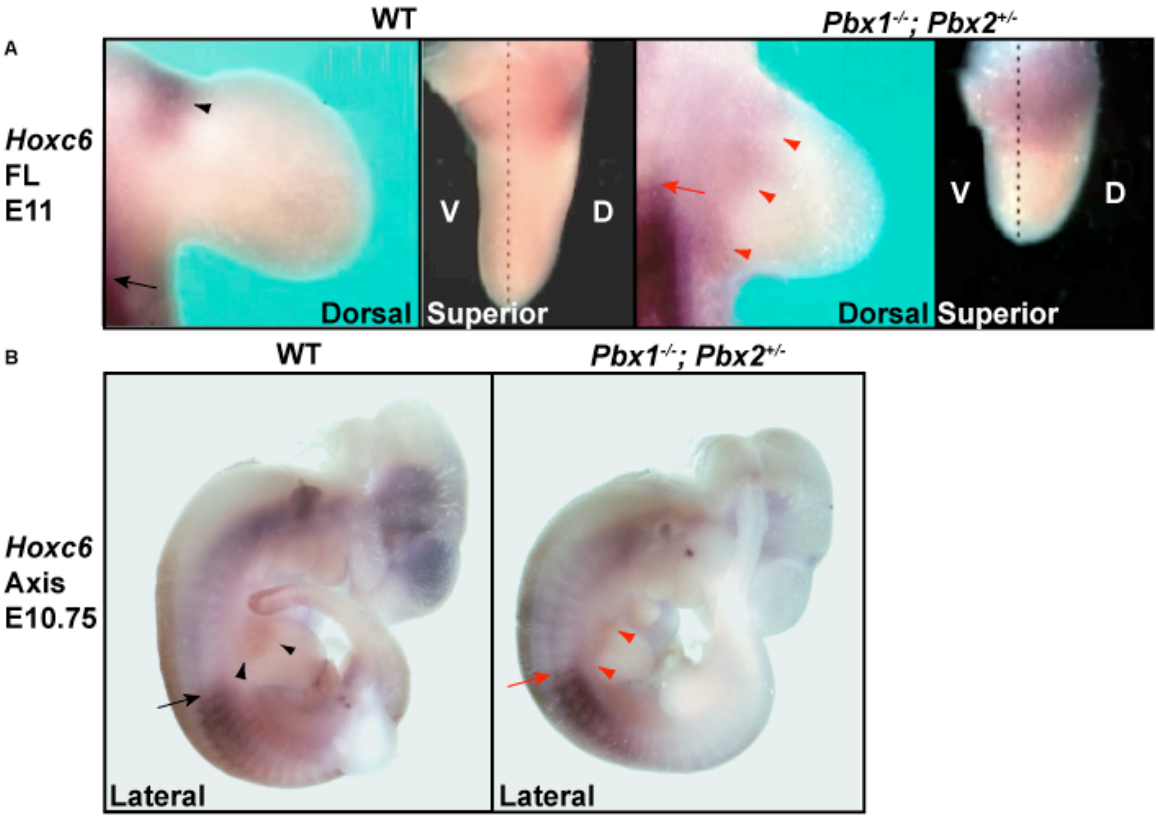

Figure 7.10. *Hoxc6* expression was spatially diffused and shifted in *Pbx1*$^{-/-}$ *;Pbx2*$^{+/-}$ embryos.

(A) *In situ* hybridization at E11 revealed that *Hoxc6* expression was reduced and diffused posteriorly and across the D-V proximal limb in mutant embryos (light shaded arrowheads) compared to WT (dark shaded arrowhead) indicating that the somatopleuric domain which gave rise to scapular head/neck was altered in the absence of *Pbx1* and *Pbx2*. (B) This same pattern was seen at E10.75 in the forelimb of the WT (dark shaded arrowheads) and mutant (light shaded arrowheads). Importantly, the complex hierarchical control of *Hox* expression by *Pbx* as identified for the limb may extend to the control of axial *Hox* expression, as *Hoxc6* was rostralized in its cranial extent in mutants (light shaded arrow in flank demarcates rostral shift; also shown in panel A, light shaded arrow) compared to WT (dark shaded arrow on flank demarcates normal *Hoxc6* expression boundary; also shown in panel A, dark shaded arrow). Finally, these data suggest that somite level specification may have been altered, and thus the position of the forelimb bud with respect to the axis. Proximal (left); anterior (top); FL, Forelimb.

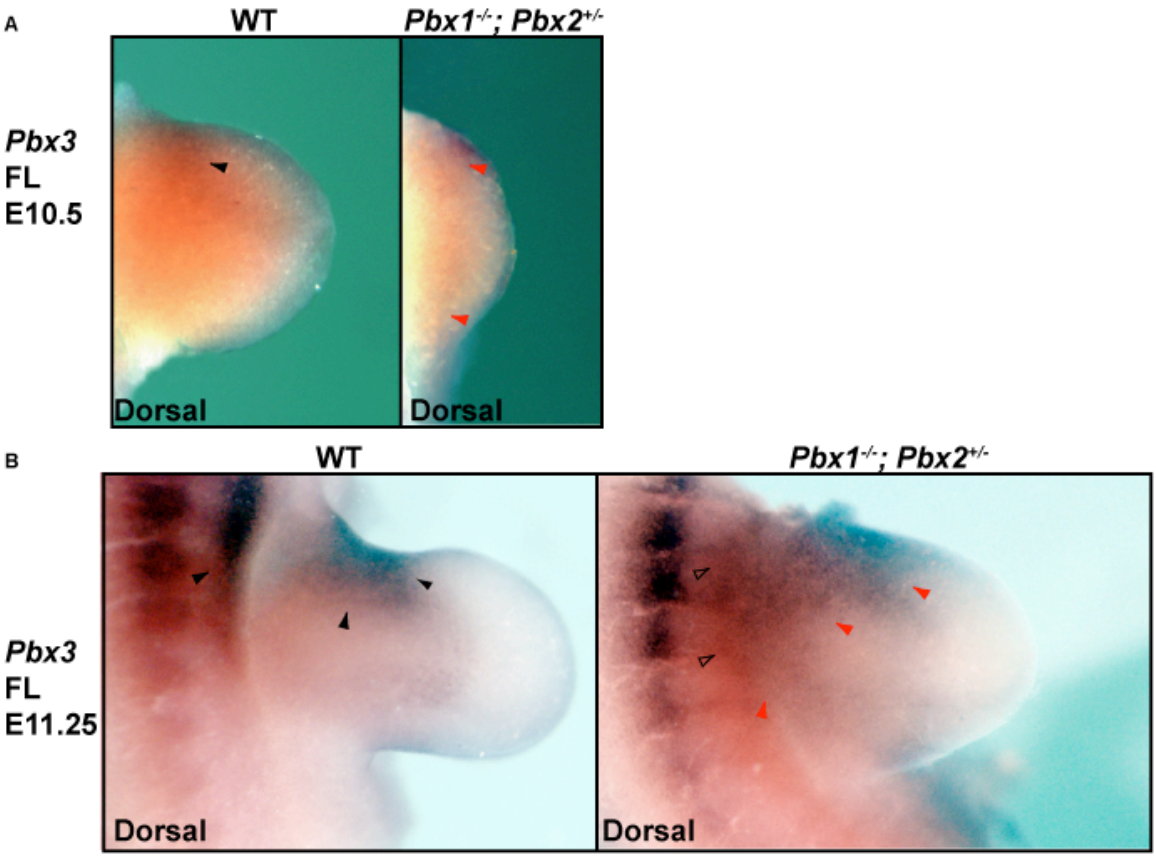

Figure 7.11. *Pbx3* expression was spatially altered in *Pbx1*$^{-/-}$;*Pbx2*$^{+/-}$ forelimbs.

(A) *In situ* hybridization at E10.5 revealed that *Pbx3* expression was posteriorized along the proximal limb in mutant (light shaded arrowheads) versus WT (dark shaded arrowhead), indicating that the limb mesenchyme was grossly mis-patterned in the absence of *Pbx1* and *Pbx2*. (B) At E11.25, *Pbx3* remained disorganized and slightly posteriorized in *Pbx1*$^{-/-}$;*Pbx2*$^{+/-}$ forelimbs. Furthermore, *Pbx3* was markedly reduced in the flank/proximal limb boundary of mutants (empty dark shaded arrowheads) versus WT (dark shaded arrowhead). Proximal (left); anterior (top); FL, Forelimb.

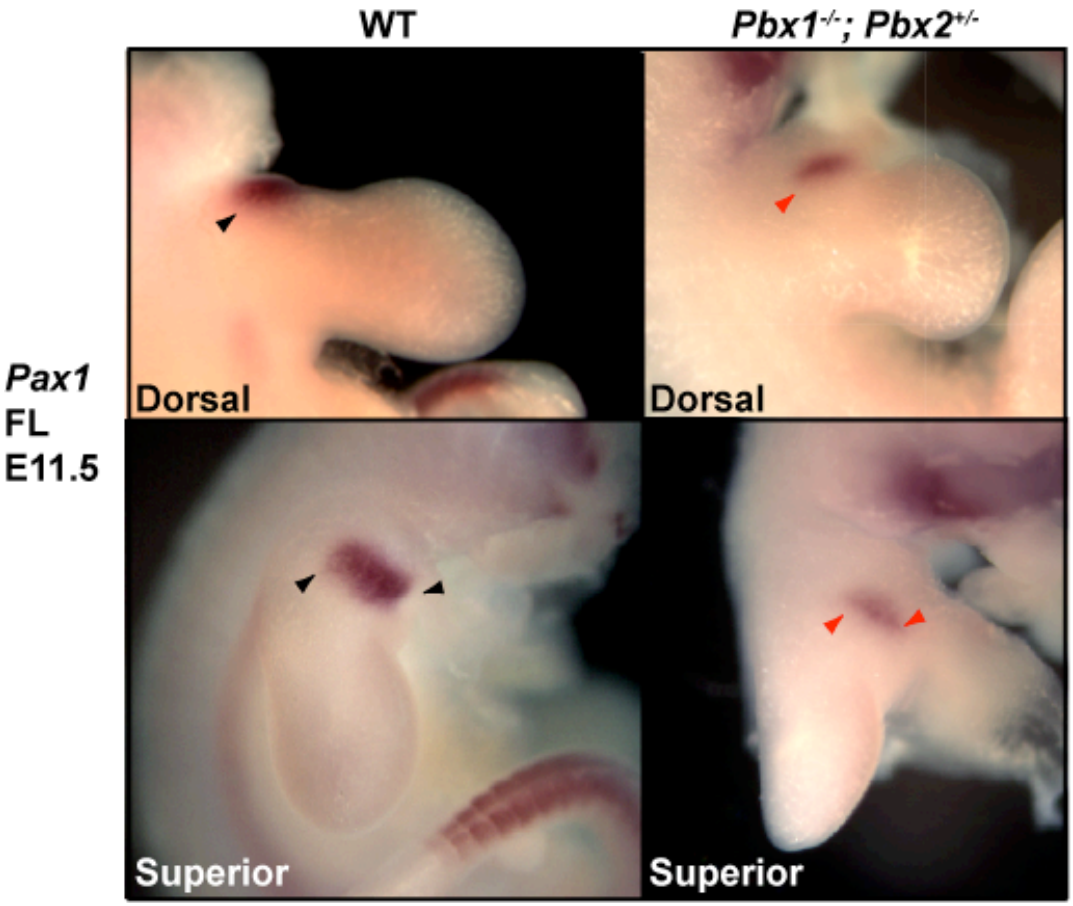

Figure 7.12. *Pax1* expression was markedly reduced in *Pbx1*$^{-/-}$;*Pbx2*$^{+/-}$ forelimbs.

(A) *In situ* hybridization at E11.5 revealed that *Pax1* expression was severely reduced in *Pbx1*$^{-/-}$;*Pbx2*$^{+/-}$ forelimbs (light shaded arrowheads in both views) compared to WT (dark shaded arrowheads in both views), indicating that the presumptive acromion process anlagen was either reduced and/or mis-patterned. In top panels, Proximal (left); anterior (top); In bottom panels, Proximal (top); anterior (top-right); FL, Forelimb.

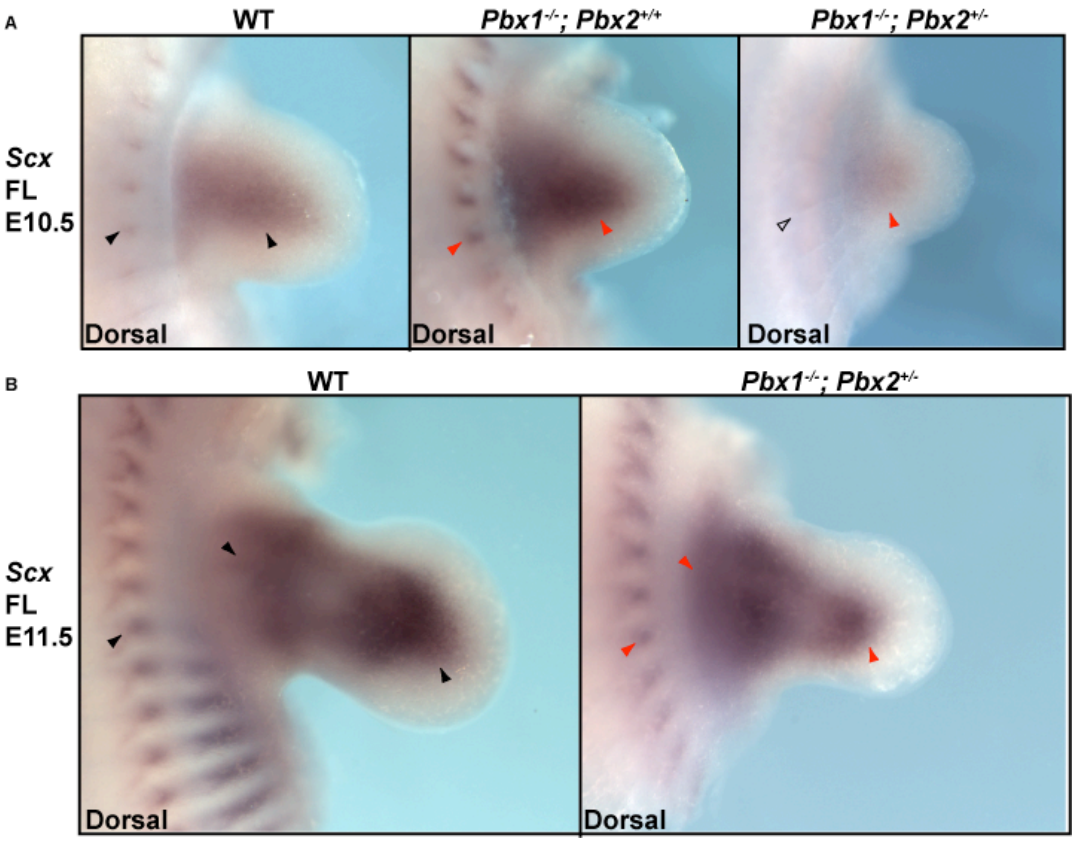

Figure 7.13. Expression of the tendon progenitor marker, *Scx*, was delayed and spatially altered in *Pbx1*$^{-/-}$;*Pbx2*$^{+/-}$ forelimbs.

(A) *In situ* hybridization at E10.5 revealed that *Scx* expression was severely reduced in the mutant forelimb (light shaded arrowhead) and absent from the mesenchymal derivatives of the somites (empty dark shaded arrowhead) compared to WT controls (dark shaded arrowheads in both domains). Furthermore, in single *Pbx1*$^{-/-}$forelimbs (center), *Scx* appeared up-regulated (light shaded arrowheads in both domains). (B) Despite the earlier reduction, at E11.5, *Scx* appeared reduced only in the distal limb (light shaded arrowhead) and somites (light shaded arrowhead), and slightly spatially disorganized in the proximal limb/flank (light shaded arrowhead) compared to WT (dark shaded arrowhead in each respective domain). Proximal (left); anterior (top) FL, Forelimb.

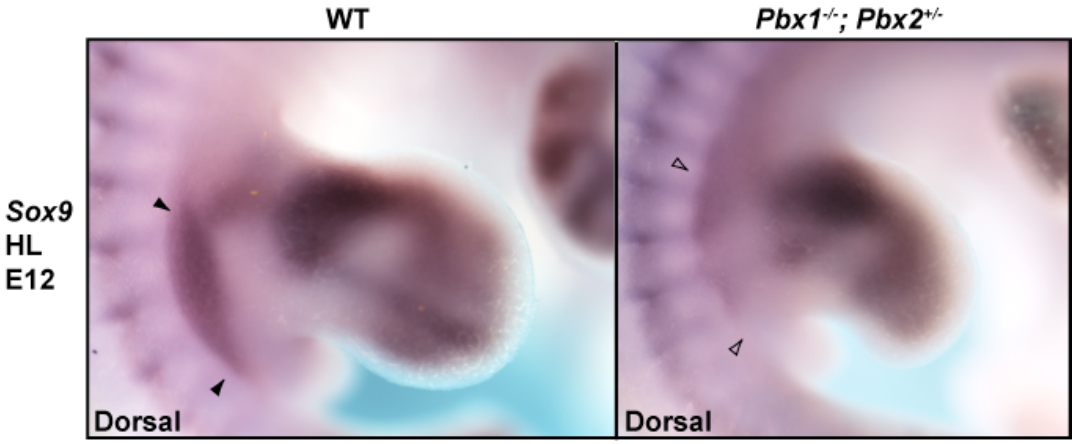

Figure 7.14. *Sox9* expression was absent from the presumptive pelvic domain of *Pbx1*$^{-/-}$;*Pbx2*$^{+/-}$ hindlimbs.

In situ hybridization at E12 revealed that *Sox9* expression was absent from the anterior (empty dark shaded arrowhead along flank) and posterior (empty dark shaded arrowhead along flank) presumptive pelvic domain in *Pbx1*$^{-/-}$;*Pbx2*$^{+/-}$ mutants compared to WT (anterior and posterior dark shaded arrowheads, respectively) indicating that mesenchymal condensations did not form. Proximal (left); anterior (top); HL, Hindlimb.

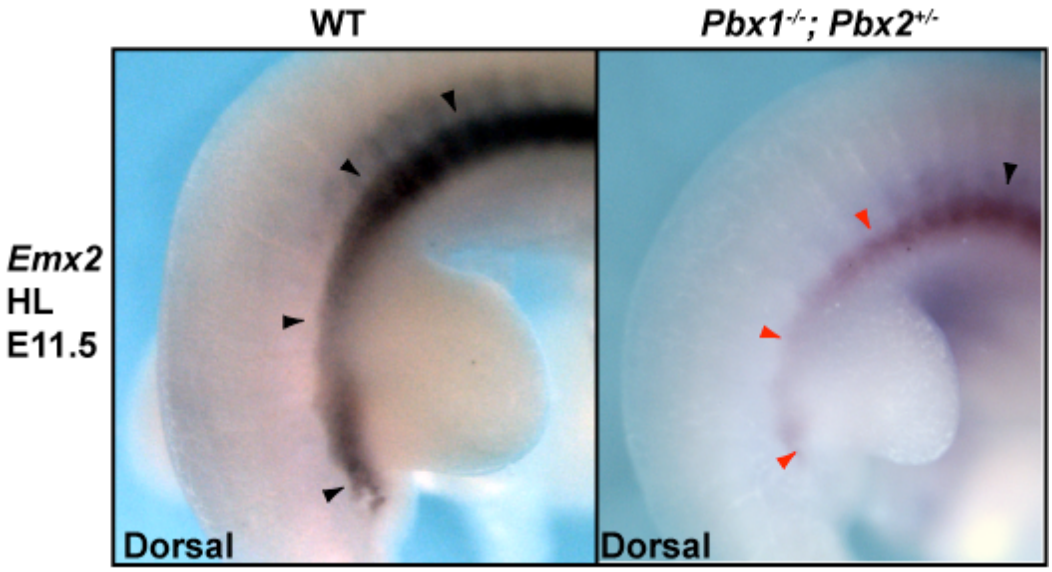

Figure 7.15. *Emx2* expression was reduced in the presumptive pelvic girdle domain of *Pbx1*$^{-/-}$;*Pbx2*$^{+/-}$ hindlimbs.

In situ hybridization at E11.5 revealed that *Emx2* expression was reduced in the mutant proximal hindlimb/flank (light shaded arrowheads) compared to WT (dark shaded arrowheads). Furthermore, such expression became weaker along more posterior axial levels, but remained expressed in the interlimb flank domain (dark shaded arrowhead) compared to WT (dark shaded arrowheads). Proximal (left); anterior (top); HL, Hindlimb.

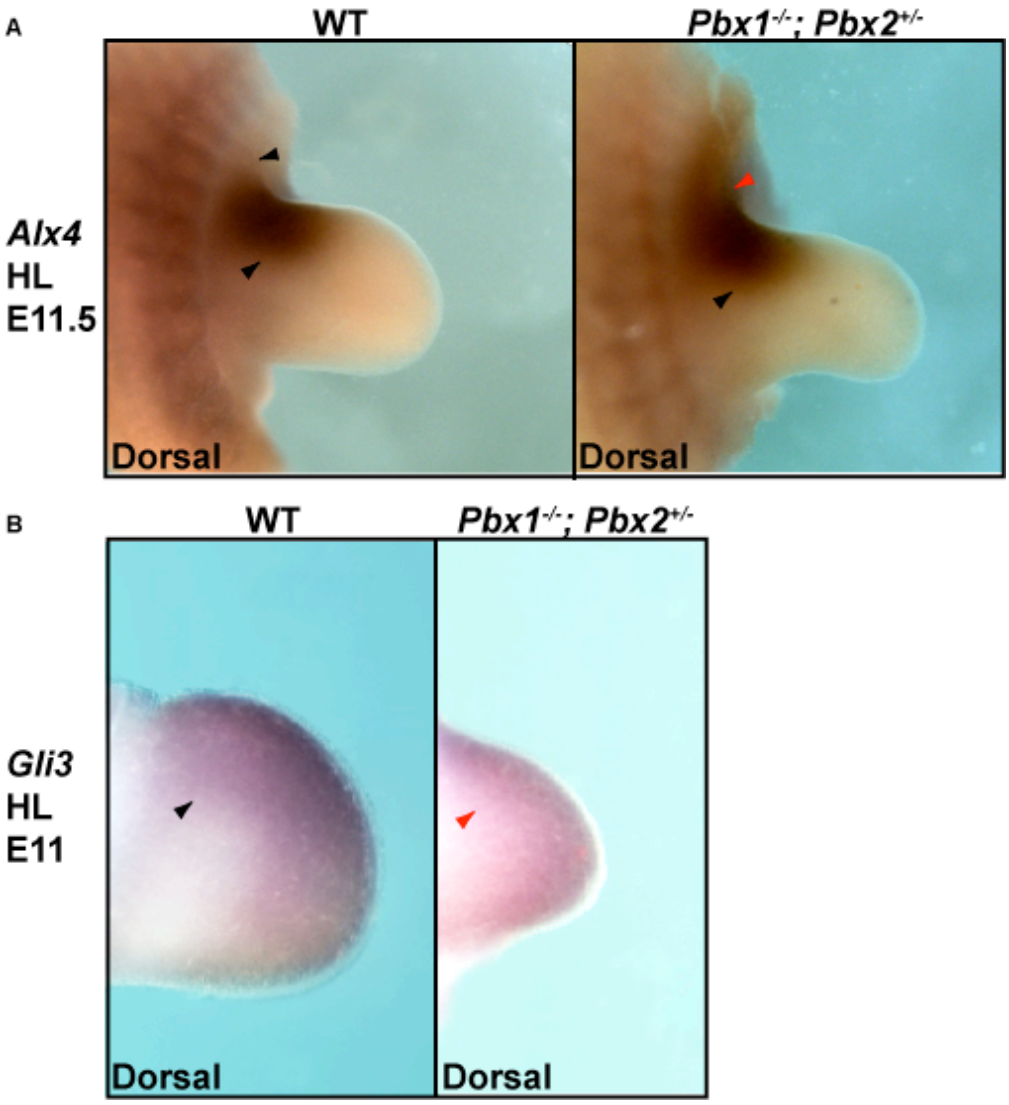

Figure 7.16. Expression of *Alx4* and *Gli3* were slightly spatially altered in the presumptive pelvic domain of *Pbx1*$^{-/-}$;*Pbx2*$^{+/-}$ hindlimbs.

(A) *In situ* hybridization at E11.5 revealed that *Alx4* expression was spatially extended into the proximal *Pbx1*$^{-/-}$;*Pbx2*$^{+/-}$ hindlimb/flank (light shaded arrowhead) but remained normal in the limb (dark shaded arrowhead) compared to WT (dark shaded arrowheads in these respective domains). (B) At E11, the distal limb expression of *Gli3* was posteriorized as expected given the loss of *Shh* from the ZPA. However, its proximal anterior domain was also slightly reduced in the mutant (light shaded arrowhead) compared to WT (dark shaded arrowhead), indicating that markers for the presumptive pelvic girdle were altered in the absence of *Pbx*. Proximal (left); anterior (top); HL, hindlimb.

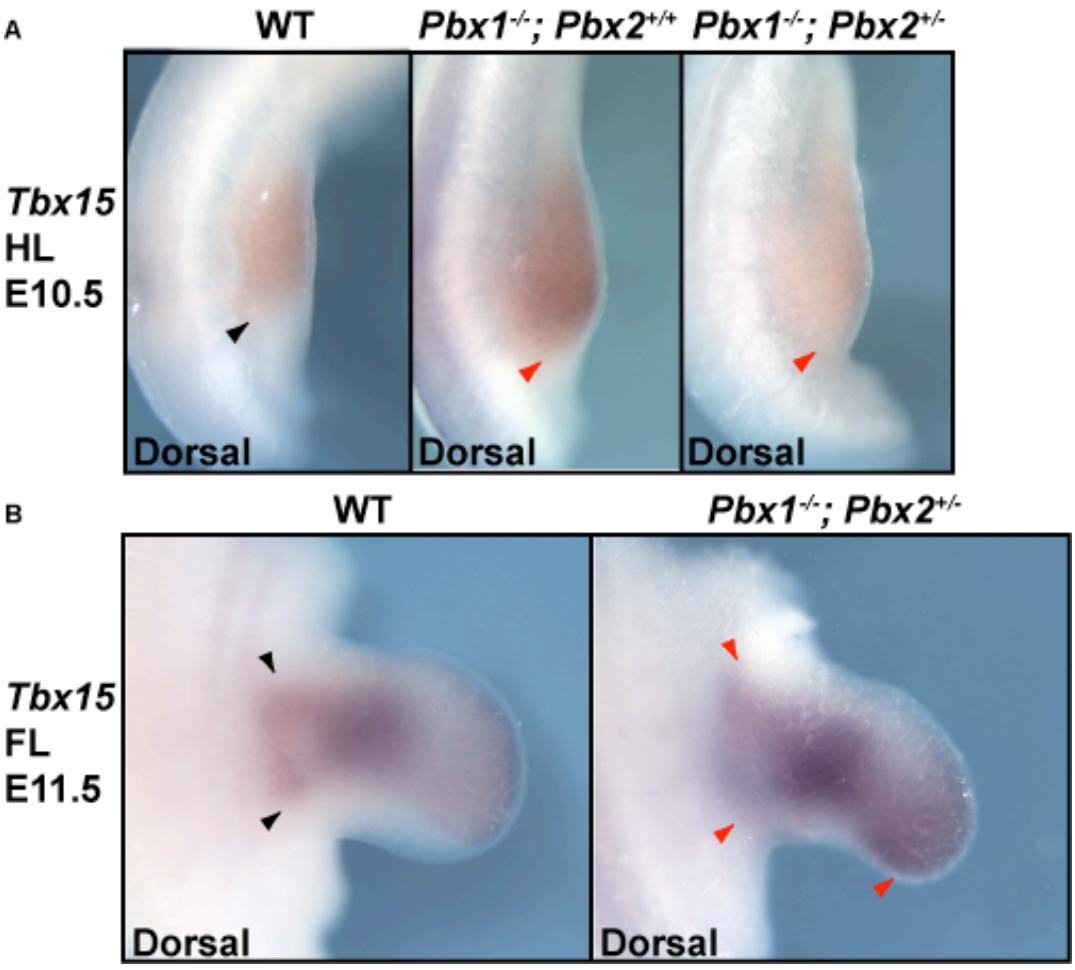

Figure 7.17. *Tbx15* expression was spatially altered in *Pbx1*$^{-/-}$;*Pbx2*$^{+/-}$ hindlimbs.

(A) *In situ* hybridization at E10.5 revealed that *Tbx15* expression was posteriorized into the distal mutant hindlimb bud (light shaded arrowhead) compared to WT (dark shaded arrowhead). Furthermore, its expression in single *Pbx1* null embryos appeared up-regulated and also posteriorly expanded (light shaded arrowhead) when compared to WT (dark shaded arrowhead). (B) At E11.5, *Tbx15* was strongly expressed in the distal limb (light shaded arrowhead) and slightly expanded anteriorly and posteriorly in the proximal limb (light shaded arrowheads) compared to WT (dark shaded arrowheads). Proximal (left); anterior (top); HL, Hindlimb.

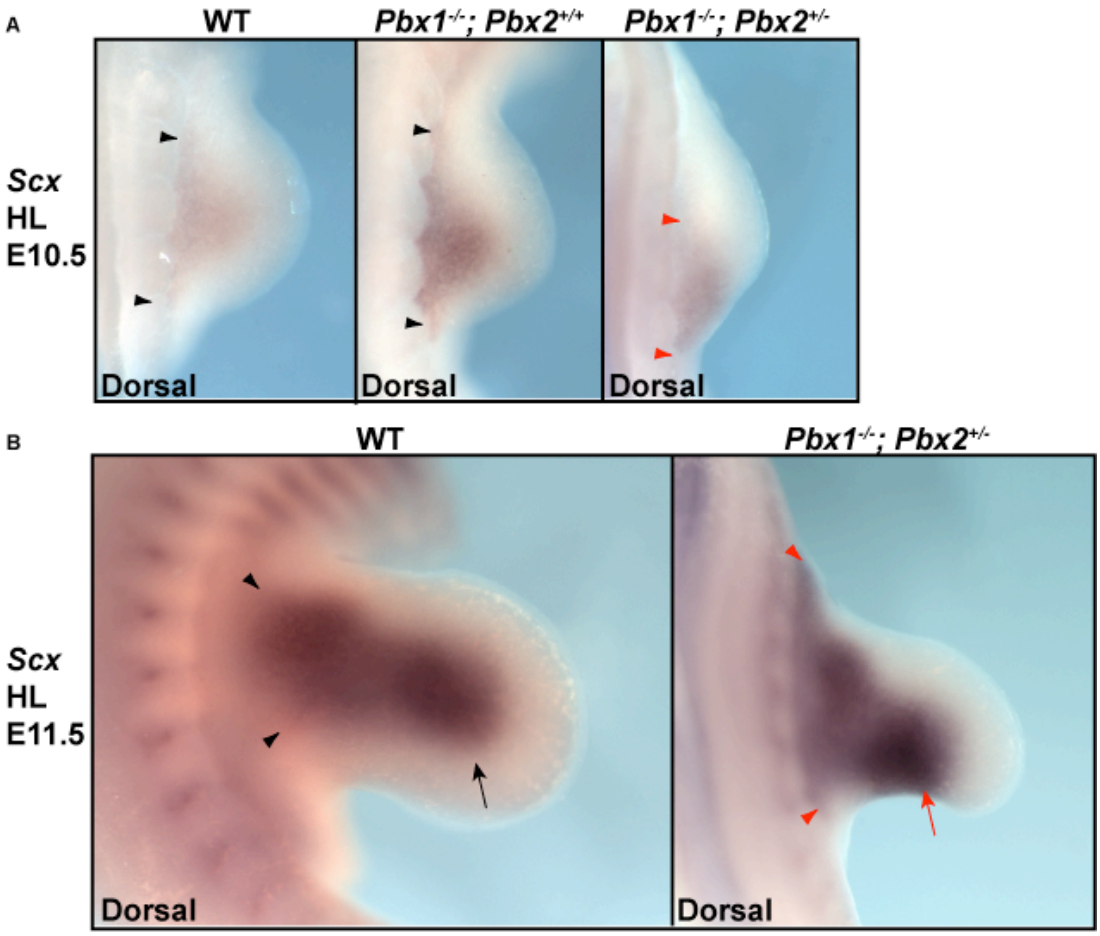

Figure 7.18. Expression of the tendon progenitor marker, *Scx,* was posteriorized in *Pbx1*$^{-/-}$;*Pbx2*$^{+/-}$ hindlimbs.

(A) *In situ* hybridization at E10.5 revealed that *Scx* expression was posteriorized in the mutant hindlimb (light shaded arrowheads) compared to WT (dark shaded arrowheads). Furthermore, in single *Pbx1*$^{-/-}$ hindlimbs, *Scx* appeared slightly up-regulated (dark shaded arrowheads) compared to WT. (B) Despite the earlier reduction, at E11.5, levels of *Scx* expression were normal. However, its expression domain was still posteriorized in the distal limb (light shaded arrow); and additionally occupied a large anterior to posterior domain in the proximal limb (light shaded arrowheads) compared to WT (dark shaded arrow and dark shaded arrowheads, respectively). Proximal (left); anterior (top); HL, Hindlimb.

Figure 7.19. *Pax1* expression was absent from the presumptive pelvic field and interlimb flank mesoderm of *Pbx1*$^{-/-}$;*Pbx2*$^{+/-}$ embryos.

(A) *In situ* hybridization at E11.5 revealed that *Pax1* expression was absent from the proximal anterior domain of *Pbx1*$^{-/-}$;*Pbx2*$^{+/-}$ hindlimbs (empty dark shaded arrowheads in both views) compared to WT (dark shaded arrowheads in both views), indicating that the presumptive pubic domain mesenchyme was absent or mis-patterned. (B) At E11.5, *Pax1* expression was reduced in the mutant throughout the interlimb flank mesoderm (long light shaded arrow) and in the somite domains proximal to the hindlimb (short light shaded arrow) compared to WT (long and short dark shaded arrows, respectively). Posterior expression then resumed in the tail region of both embryos. In (top A), proximal (top); anterior (top-right); In (bottom A), proximal (top); anterior (out of page); HL, Hindlimb.

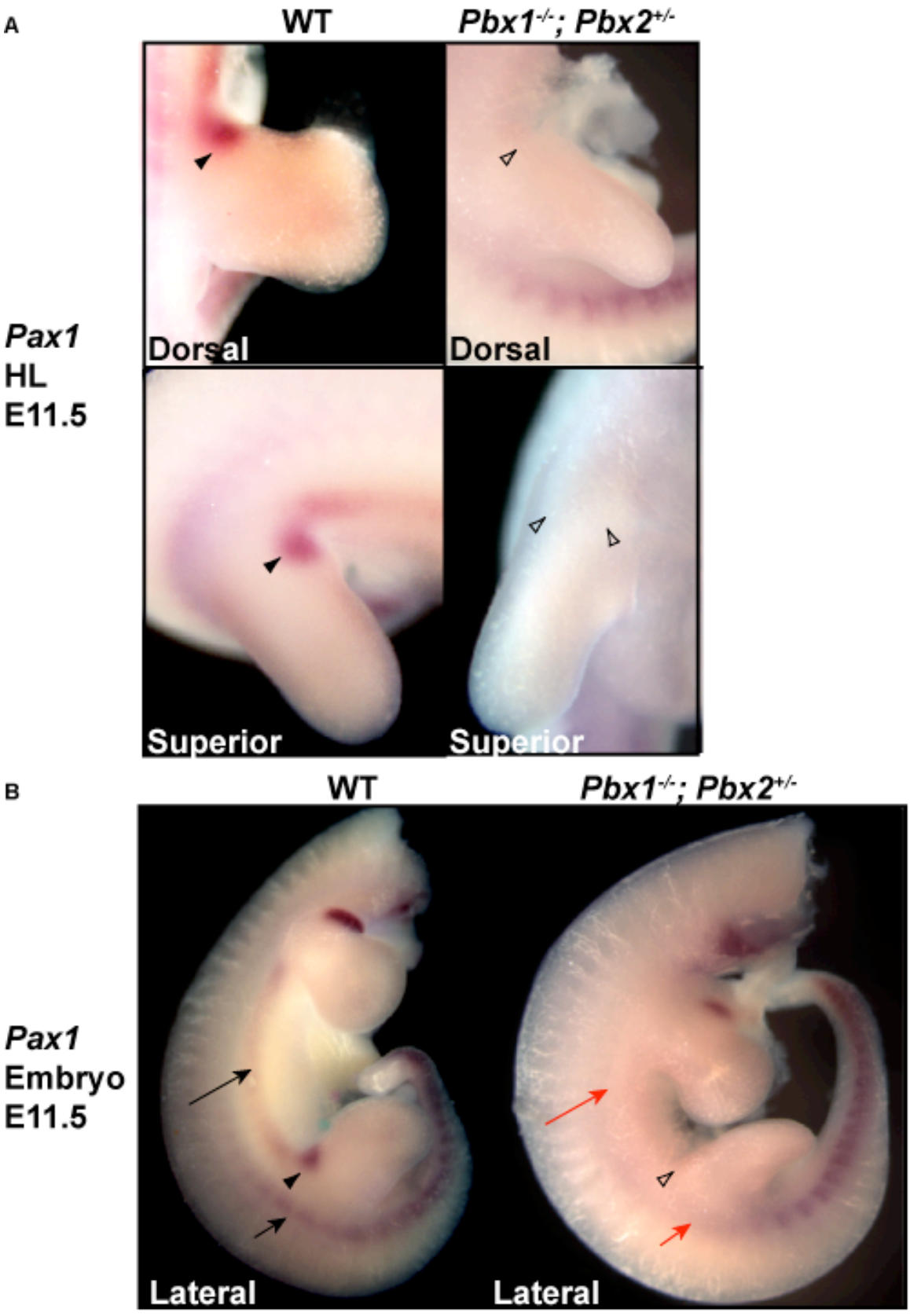
A
WT
Pbx1-/-; Pbx2+/-
Pax1
HL
E11.5
Dorsal
Dorsal
Superior
Superior
B
WT
Pbx1-/-; Pbx2+/-
Pax1
Embryo
E11.5
Lateral
Lateral

Figure 7.20. Pbx roles in scapular blade development (A,B).

(A) In WT at E9.0, Pbx has a role upstream of axial *Hox* expression, which aids in providing axial level identity to all dermomyotomal cells (a) including an axial domain (b) giving rise to the scapular blade (on right shown at E13.5). The shaded "a" domain also depicts the normal *Pbx* expression in this tissue, suggesting a cell-autonomous role for Pbx in dermomyotomal specification. In *Pbx1*$^{-/-}$*;Pbx2*$^{+/-}$ embryos (A, bottom), *Pbx* and *Hox* expression is reduced and the latter is spatially altered (compared *Hoxc6* expression levels, slanted horizontal lines), leading to a reduction in blade progenitors and the relative absence of the blade in this mutant (b' shade in dysmorphic scapular blade on left). (B) represents a model of a transverse section at the level of the anterior forelimb bud at approximately E10 that, depicts overlapping *Pbx* expression in critical tissues that signal and/or give rise to presumptive scapular blade progenitors, and several scenarios regarding Pbx roles during blade formation (see legend for expression domains). In left box, Pbx1/2/3 roles within the dermomyotome may act through Pax1 or more directly to aid in the specification of blade mesenchyme and/or the epithelial to mesenchymal conversion required for progenitor cell formation. Concurrently, Pbx1/2 in the ectoderm (lighter shaded text) may signal through Fgf/Wnt (X?) to promote dermomyotomal epithelial to mesenchymal transformation. In middle box, Pbx1/2 roles in the somatopleure may act through Tbx5 and signaling molecules (X?) to promote Pax1 up-regulation and dermomyotomal differentiation. In right box, Pbx1/2/3 act upstream of genes responsible for providing positional information (*Cart1*, *Tbx15*, *Gli3*) to blade progenitors and those involved in pre-mesenchymal formation (*Emx2*) and condensation (*Sox9*); although it remains unclear as to whether the reduction in patterning genes, as observed in *Pbx* mutants, result from disruptions in early blade forming processes that lead to the absence of scapular progenitor cells. Also it remains unclear as to the interactions between sets of genes along each pathway (e.g., between *Emx2* and *Cart1, Tbx15,* and *Gli3*). In (A) anterior (top); dorsal (left/out-of-page); distal (right); in (B) dorsal (top); distal (right). AL, anterior proximal limb; BE, Body Ectoderm; Cond., Condensation; D, Dermomyotome; Diff., Differentiation; DL, Distal Limb; LE, Limb Ectoderm; Mig., Migration; Nc, Notochord; Sc, Pat., Patterning; Scleratome; So, Somatopleure.

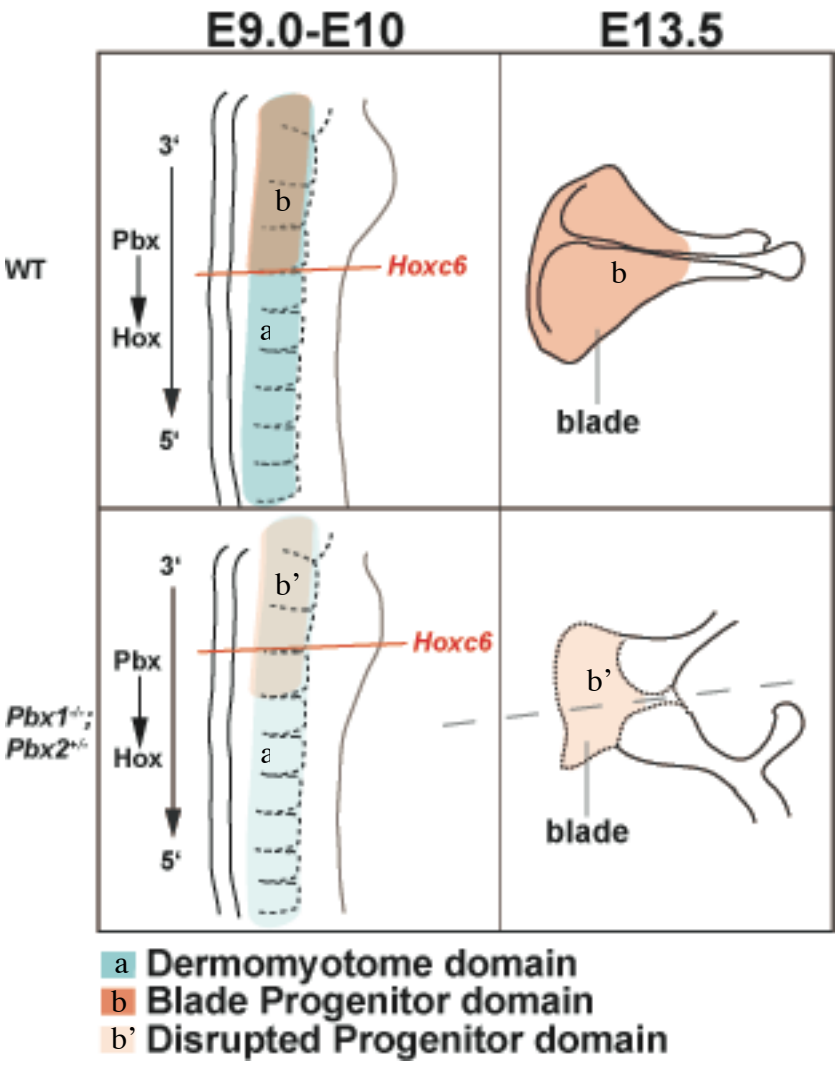
E9.0-E10
E13.5
WT
3'
Pbx
Hox
5'
b
a
Hoxc6
b
blade
Pbx1+/-;
Pbx2+/-
3'
Pbx
Hox
5'
b'
a
Hoxc6
b'
blade
a Dermomyotome domain
b Blade Progenitor domain
b' Disrupted Progenitor domain

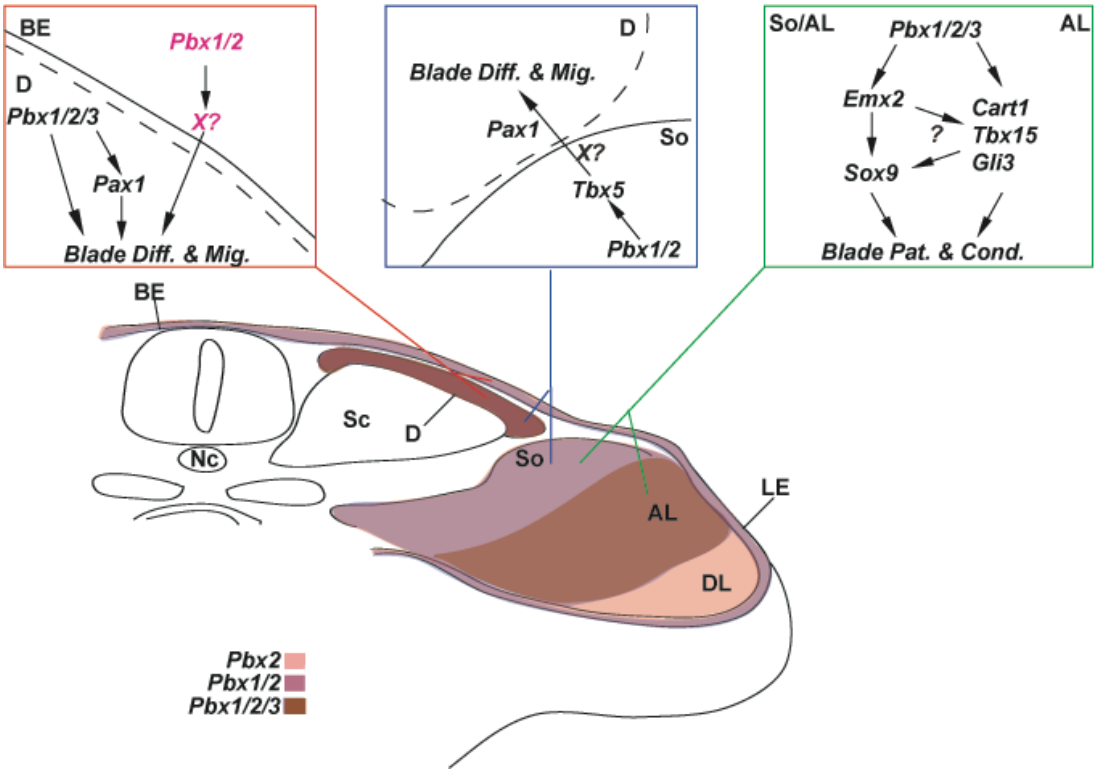
BE
Pbx1/2
D
Pbx1/2/3
X?
Pax1
Blade Diff. & Mig.
D
Blade Diff. & Mig.
Pax1
X?
So
Tbx5
Pbx1/2
So/AL
Pbx1/2/3
AL
Emx2
Cart1
?
Tbx15
Sox9
Gli3
Blade Pat. & Cond.
BE
Sc
D
Nc
So
LE
AL
DL
Pbx2
Pbx1/2
Pbx1/2/3

Figure 7.21. Pbx roles in scapular neck/head development.

Model depicting Pbx roles during normal scapular neck/head patterning and the consequences of *Pbx* loss on this patterning process. (Top) in WT, *Hoxa9*/*Hoxd9* (E9.5-11.5, “a”) and *Hoxc6* (E10-E11.5,”b”) are expressed in the anterior limb, specifically in domains roughly adjacent to, and overlapping (“c”) with a region that has been fated to give rise to the future proximal humerus and scapular neck/head (shown on the right panel with same letter designations). (Bottom) in *Pbx1*$^{-/-}$*;Pbx2*$^{+/-}$ mutants, *Hoxa9*/*Hoxd9* are strongly up-regulated and spatially anteriorized early (E9.5-E10.5, “a’ “) and *Hoxc6* is spatially expanded both posteriorly (E10-11.5,”b“) and also along the dorsal-ventral anterior limb surface (as shown at E11, “c” expanded overlapping domain). Given that both *Hox* have roles in scapular neck/head and humeral patterning, the observed morphological alterations observed in these mutants (right panel), such as duplications of the scapular neck/head and humerus, appear to correspond to alterations in their gene expression. At E9.5, E10-10.5, and E13.5, proximal (left); anterior (top); at E11-11.5, dorsal (D, left); ventral (V, right); proximal (top).

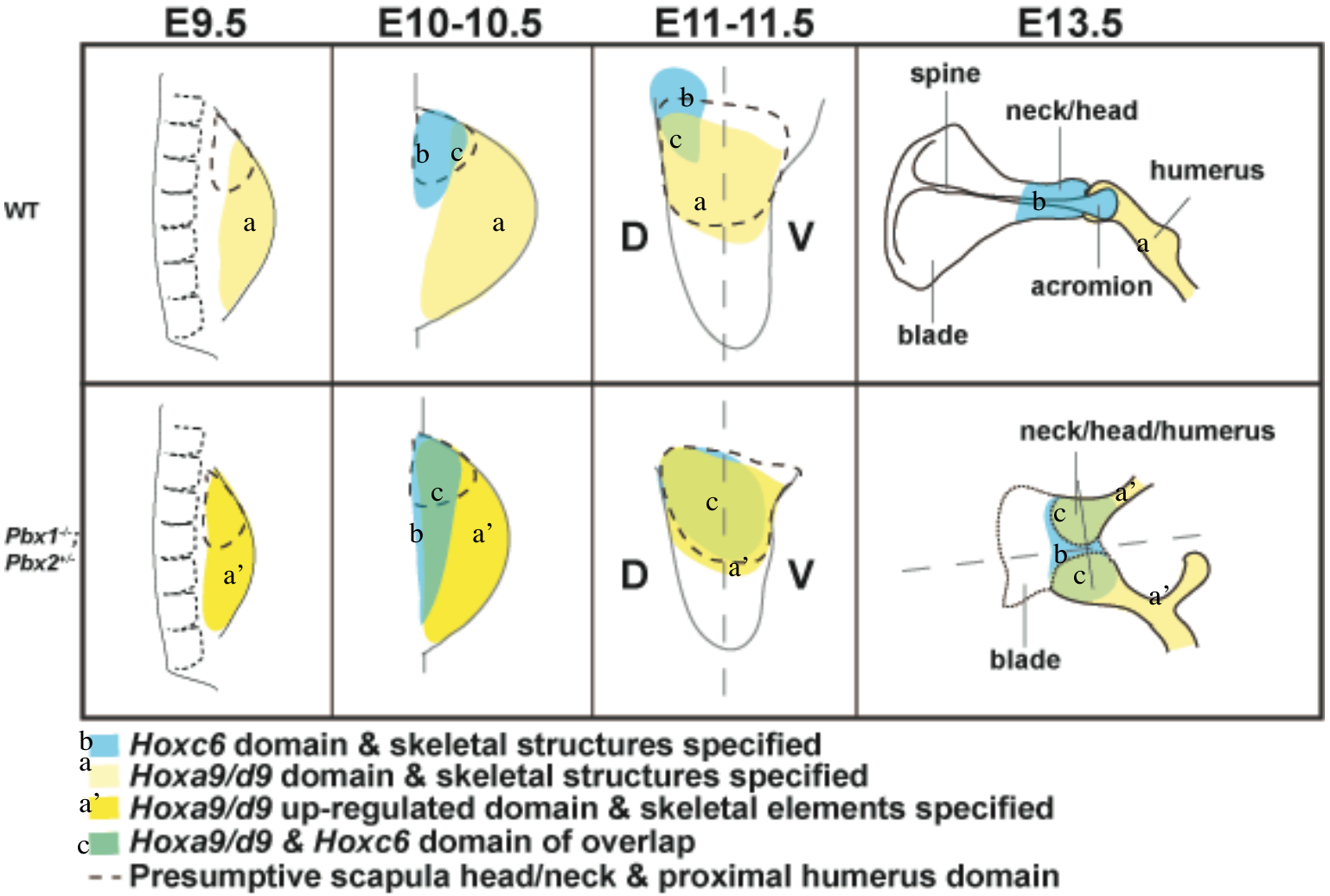
E9.5
E10-10.5
E11-11.5
E13.5
WT
Pbx1-/-;
Pbx2+/-
a
b
c
a'
D
V
spine
neck/head
humerus
acromion
blade
neck/head/humerus
b Hoxc6 domain & skeletal structures specified
a Hoxa9/d9 domain & skeletal structures specified
a' Hoxa9/d9 up-regulated domain & skeletal elements specified
c Hoxa9/d9 & Hoxc6 domain of overlap
Presumptive scapula head/neck & proximal humerus domain

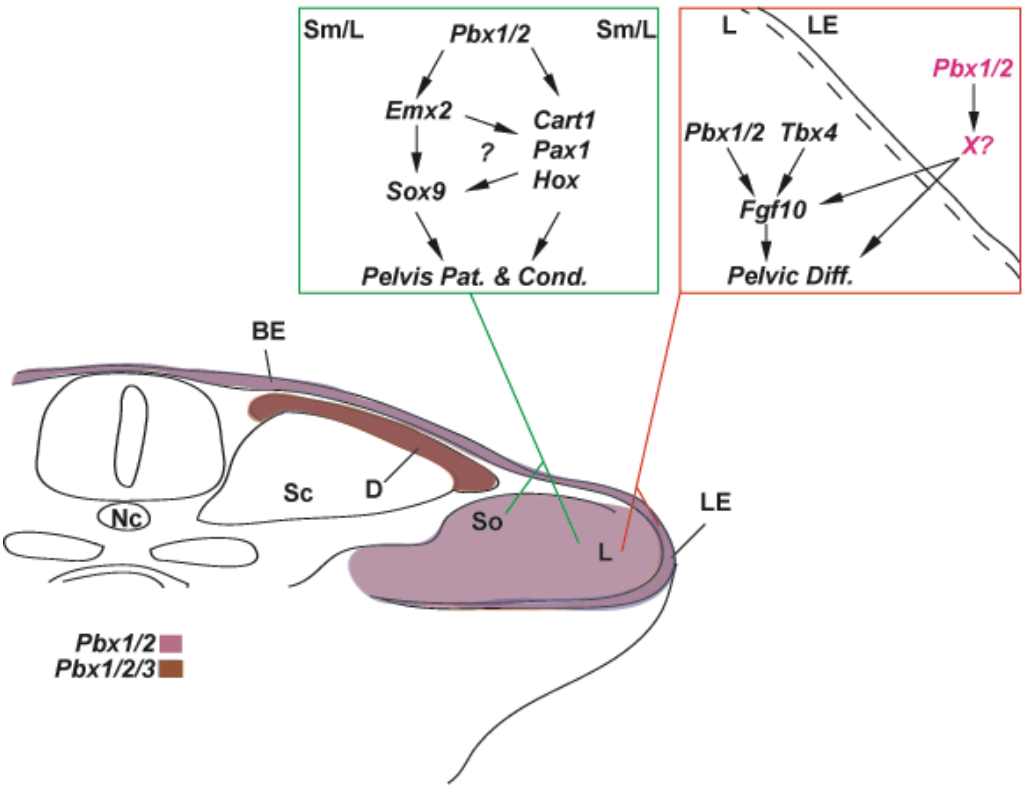

Figure 7.22. Pbx roles in pelvic development.

A model of a transverse section at the level of the mid-hindlimb bud at approximately E10 that, depicts overlapping *Pbx* expression in critical tissues (designated by different shades) that signal and/or give rise to presumptive pelvic progenitors, and several scenarios regarding Pbx roles during pelvic formation (see legend for expression domains). In left box, Pbx1/2 within the somatopleure and proximal limb act upstream of genes responsible for providing positional information (*Cart1*, *Pax1*, *Hox?*) to pelvic progenitors and those genes involved in pre-mesenchymal formation (*Emx2*) and condensation (*Sox9*); although it remains unclear if the reduction in patterning gene expression, as observed in *Pbx* mutants, results from disruptions in early pelvic forming processes that lead to the absence of pelvic progenitor cells. Also it remains unclear as to the interactions between sets of genes along each pathway (e.g., between *Emx2* and *Cart1, Tbx15,* and *Gli3*). In right box, Pbx1/2 act in parallel to Tbx4 to activate *Fgf10* expression leading to pelvic progenitor cell specification and differentiation. Concurrently, Pbx1/2 roles in the ectoderm (lighter shaded text) on Fgf/Wnt (X?) signaling may lead to *Fgf10* expression and pelvic specification and differentiation. In (B) dorsal (top); distal (right). BE, Body Ectoderm; Cond., Condensation; D, Dermomyotome; Diff., Differentiation; L, Limb; LE, Limb Ectoderm; Nc, Notochord; Pat., Patterning; Sc, Scleratome; So, Somatopleure.

Chapter 8: Conclusions and Evolutionary Implications

8.1 Summary of thesis research

The analyses conducted for this thesis have demonstrated that *Pbx* genes have overlapping roles during limb and girdle development. This general hypothesis has been shown in the limb where Pbx loss of function in the mesenchyme and ectoderm resulted in drastic exacerbations of the previously reported phenotype of *Pbx1*$^{-/-}$ embryos (Selleri et al., 2001). Specifically, *Pbx1*$^{-/-}$*;Pbx2*$^{+/-}$ (i.e., *Pbx1/2 Mut*) embryos displayed severe manifestations of the *Pbx1*$^{-/-}$ proximal limb phenotype, i.e., the humerus was grossly contorted, potentially duplicated, and fused to the scapula, while the femur was rudimentary, truncated, and fused to the pelvis (Fig. 5.2). These exacerbations were also seen in other (non-limb) overlapping Pbx domains such as along the axis, where vertebrae and ribs were more affected than observed in *Pbx1*$^{-/-}$ embryos (Fig. 5.28). Concomitantly, novel defects were revealed specifically for the distal limb, a region that was unaffected in single *Pbx1*$^{-/-}$ and *Pbx2*$^{-/-}$ embryos; i.e., there were zeugopodial alterations, such as the dysmorphology of the radius and ulna in the forelimb and the loss of the fibula in the hindlimb; and autopodial alterations, such as the dysmorphology and loss of digits 1 and 5 in the forelimb, and the near complete loss of all digits in the hindlimb (Fig. 5.2). Further support for their overlapping and novel functions during limb development comes from studies on compound *Pbx1*$^{-/-}$*;Pbx2*$^{-/-}$ mutants that lack limbs altogether (Fig. 5.1).

If the nature of *Pbx* genetic interaction is addressed with respect to the domains where they spatially overlap, then the early limb field mesenchyme (Fig.

5.4A) and/or preAER ectoderm (Figs. 6.1 and 6.2), constitute the tissues where Pbx most likely functionally cooperate during limb development. In support of this view, compound *Pbx1/2 Mut* and *Pbx1*$^{-/-}$*;Pbx2*$^{-/-}$ embryos display disruptions in the expression of many genes known to govern the initial stages of limb development. In addition, *Pbx1*$^{-/-}$*;Pbx2*$^{-/-}$ hindlimbs develop as minor prominences even before embryonic *in utero* lethality, and *Pbx1*$^{cI\Delta 3/-}$*;Pbx2*$^{-/-}$*;Tbx4*$^{cre/+}$ as well as *Pbx1*$^{cI\Delta 3/-}$*;Pbx2*$^{-/-}$*;Msx2*$^{cre/+}$ embryos at all developmental stages after the initial excision of the *Pbx1* allele (at E10) lacked any phenotypic defects. While some caveats still exist for this last interpretation (see Chapter 6), these data strongly indicate that the critical developmental functions of Pbx during patterning and morphogenesis are early during the stage of limb bud initiation and outgrowth.

When these findings are analyzed with respect to that of other compound mutant embryos, such as *Pbx1*$^{-/-}$*;Pbx3*$^{+/-}$ (i.e., *Pbx1/3 Mut*), *Pbx1*$^{+/-}$*;Pbx3*$^{-/-}$, *Pbx2*$^{-/-}$*;Pbx3*$^{+/-}$, *Pbx2*$^{+/-}$*;Pbx3*$^{-/-}$, and *Pbx1*$^{+/-}$*;Pbx2*$^{+/-}$*;Pbx3*$^{+/-}$, it becomes apparent that *Pbx3* may not directly affect patterning of the distal limb. In this regard it is interesting that *Pbx3* is not present in the ectoderm or LPM (data not shown). The only limb domain where these three *Pbx* significantly overlap is the anterior proximal forelimb bud (Fig. 5.4B), which has been fated in chicks to give rise to the scapular neck/head and proximal humerus (see Chapter 3). Appropriately, in *Pbx1/3 Mut* embryos, this specific domain is affected (and phenocopies are seen in *Pbx1/2 Mut* embryos) and not that of the distal limb (Fig. 7.4). Therefore, the

proposed genetic interaction between *Pbx1*, *Pbx2*, and *Pbx3* in scapular neck/head and humeral patterning may be within this domain.

The finding that several other compound mutants (i.e., *Pbx1*$^{+/-}$*;Pbx2*$^{+/-}$*, Pbx1*$^{+/-}$*;Pbx2*$^{-/-}$*, Pbx1*$^{+/-}$*;Pbx3*$^{+/-}$*, Pbx1*$^{+/-}$*;Pbx3*$^{-/-}$*, Pbx2*$^{+/-}$*;Pbx3*$^{+/-}$*, Pbx2*$^{-/-}$*;Pbx3*$^{+/-}$*, Pbx2*$^{+/-}$*;Pbx3*$^{-/-}$, and *Pbx1*$^{+/-}$*;Pbx2*$^{+/-}$*;Pbx3*$^{+/-}$) lack limb defects also suggests that the absence of these genes from specific tissues at exact times cause their phenotypes rather than a change in the overall quantity of Pbx in the limb. Furthermore, while it has not yet been demonstrated quantitatively that individual Pbx are present at different levels in limb tissues, no marked up-regulation was observed (i.e., for *Pbx1* in *Pbx2*$^{-/-}$ embryos or *Pbx2* and *Pbx3* in *Pbx1*$^{-/-}$, *Pbx1*$^{-/-}$*;Pbx2*$^{+/-}$, and all other compound mutant controls) by *in situ* hybridization and immunohistochemistry suggesting that loss (or even normal control) of a particular Pbx is not rescued (or normally regulated) by the differential up-regulation of another family member.

Of significance is the finding that the pectoral girdles of *Pbx1/2 Mut* and *Pbx1/3 Mut* embryos also display severe morphological alterations above those seen in single *Pbx1*$^{-/-}$, *Pbx2*$^{-/-}$, and *Pbx3*$^{-/-}$ embryos (with the latter two genotypes being phenotypically normal)(Fig. 7.4). Specifically, the scapular blade was reduced in all dimensions in both compound mutants compared to its superior-inferior reduction observed in single *Pbx1*$^{-/-}$ embryos (Selleri et al., 2001; Fig. 7.4). In addition, all elements of the scapular neck/head and proximal humerus were mis-patterned and partially duplicated in both compound mutants. With respect to the pelvis, the phenotype of single *Pbx1*$^{-/-}$ mutants (i.e., the absence of

the ilium and the slight dysmorphology of the pubis and ischium) was significantly worsened only in *Pbx1/2 Mut* embryos (i.e., most elements were absent save one residual ischial fragment) (Fig. 7.4). The lack of an additional pelvic phenotype in *Pbx1/3 Mut* embryos above that observed in single *Pbx1*$^{-/-}$ embryos can be attributed to the lack of *Pbx3* in the posterior embryonic domains that give rise to the presumptive pelvic girdle and proximal hindlimb.

Unlike the limb, understanding the temporal and spatial requirements of *Pbx* genetic interaction in the formation of the pectoral girdle is more complicated. This difficulty is due to the findings that while all three *Pbx* co-localize only in the anterior proximal limb (i.e., in the presumptive scapular neck/head and proximal humerus domain) (Fig. 5.4B) and the dermomyotome (i.e., in the presumptive scapular blade progenitor population) (Fig. 7.2), *Pbx1* and *Pbx2* additionally co-localize in the body and limb ectoderm (Fig. 6.2) and the somatopleuric mesoderm (i.e., in the presumptive neck/head domain) (Fig. 7.1). Therefore, it may be presumptuous to state at this time, that the similarities in the neck/head and blade morphologies of *Pbx1/2 Mut* and *Pbx1/3 Mut* embryos result from the loss of *Pbx1* and *Pbx2*, and *Pbx1* and *Pbx3* from each domain where all three overlap. In other words, since tissues like the ectoderm and somatopleure also have noted roles in signaling to and from the dermomyotome (Wang et al., 2005; Huang et al., 2006), it is unclear whether loss of *Pbx1* and *Pbx2* from these domains results in a phenocopy of that seen for the loss of *Pbx1* and *Pbx3*. Future work will help clarify this issue.

With respect to the limb proper, it is evident that *Pbx1* and *Pbx2* regulate hindlimb patterning and outgrowth, roles that can be attributed to their early expression in the presumptive hindlimb LPM (Fig. 5.4A). Concomitantly, the failure to form an intact forelimb bud in the complete absence of *Pbx1* and *Pbx2* indicates that *Pbx3* may not be critical for rescuing P-D outgrowth, although the finding that forelimb elements are ameliorated in their degree of mis-patterning (when compared to the hindlimb) in *Pbx1/2 Mut* embryos indicates that *Pbx3* may rescue some of the patterning functions of this gene family. Interestingly, *Pbx3* expression in this specific mutant was posteriorized (i.e., it occupied an anterior to posterior domain, Fig. 7.11) as opposed to the more restricted anterior limb domain as observed in wildtype embryos. This finding may indicate that Pbx3 functioned (in the *Pbx1/2 Mut* embryo) in the patterning of elements of the entire limb and/or to help initialize proper mesenchymal gene expression, such as the activation of *Hox*. Accordingly, the finding that *Pbx1/3 Mut* embryos lack distal defects (Fig. 7.4) may reflect that *Pbx1* and *Pbx2* are normally found predominately in an overlapping manner throughout the early limb field, to the exclusion of *Pbx3*. Conversely, the concurrent loss of *Pbx1* and *Pbx3* does not result in the same pattern defects because of the more restricted spatio-temporal expression of the latter's domain.

Given Pbx's early influence in limb development, at least two scenarios can be envisioned for their roles in specification and patterning: (1) Their role may be in controlling an initial cellular population of naïve mesenchyme prior to the specification process. This role may specifically be evident since Pbx

inactivation after E10 had no effect on patterning, and according to the PZ Model distal limb patterning occurs continuously and after this gestational day (see Chapter 3). In this regard, the alterations to the limb compartments as seen in *Pbx1/2 Mut* embryos would reflect disruption of the early pre-specified population and its response to an altered *Hox* and *Shh* molecular coordinate system. (2) With respect to the ES Model, the action of Pbx could be as above (1) and/or during the early specification of the cellular progenitors of the limbs three compartments (see Chapter 3). Accordingly, the alterations seen in *Pbx1/2 Mut* embryos would reflect a disruption in the specification domains of the limb, including a global alteration in mesenchymal patterning via the loss of *Hox*, ultimately leading to the disruption of the limbs signaling centers, such as the ZPA and the AER with concurrent effects on later limb patterning.

8.2 Model of *Pbx* roles during limb and girdle development

All the data thus far presented suggest a role for Pbx in the early mesoderm and/or the ectoderm in governing several critical aspects of limb and girdle development. As mentioned in Chapter 6, it is possible that Pbx involvement in regulating epithelial-mesenchymal interactions are critical in this regard. For example, limb bud induction requires initial signaling between the mesoderm and ectoderm, via an Fgf10 to Fgf8 feedback loop, respectively (see Chapter 3). *Pbx* regulation of this epithelial-mesenchymal interaction, via a control on their underlying molecular networks, may facilitate this loop that eventually leads to early cell-fate specification and to formation of the ZPA, AER,

and DE. Concurrently, through their effects on these networks, and promoting later epithelial-mesenchymal interactions in the limb they may continue limb bud patterning and outgrowth (i.e., between the ZPA and AER). Finally, their involvement in these tissue interactions underscores their fundamental roles in scapular and pelvic development. Figure 8.1 presents a general model that depicts Pbx roles during the regulation of limb and girdle development, although the specifics on Pbx function in both structures are provided in Figures 5.29-30 and 6.28 (limb), and Figures 7.20-22 (girdle).

According to this model, *Pbx* would act as "selector" genes like *Hox* that permit the progression of cells down particular pathways of specification and lineage commitment. Initially, Pbx may first bind to sites along various regulatory elements (e.g. enhancers) of multiple genes and by doing so would "mark" these sites for later transcriptional regulation (i.e., activation or repression). As Sagerstrom (2004: 737) argues, Pbx may act as pioneers that "penetrate repressive chromatin and "mark" specific genes for activation." This process of "marking" has also been regarded as genetic "potentiation" as the action on DNA would prime and/or potentiate (i.e., make possible) future gene transcription (Nelson, 2004). These binding properties would then allow other "selectors," such as Hox to form complexes with Pbx (and Meis or other factors), cause conformational changes to chromatin structure, and transcriptionally activate/repress target genes. This process may be particularly relevant to specification and patterning if specific Hox (and other cofactor combinations) that are recruited to these Pbx "marked" elements provide positional information to

progenitor cells. In this manner, early specification (i.e., prepatterning) may literally be synonymous with the initial "marking" of cells for later regulation, as prescribed above. In other words, the initial segregation of cells into the limbs three compartments (i.e., as argued under the ES Model) would rely on Pbx "marking" function with other proteins also capable of delineating tags. These functions are not unlikely given the recent findings by Berkes et al. (2004) who demonstrated that Pbx is bound to several MyoD-dependent regulatory elements prior to muscle cell differentiation. Furthermore, data presented in this thesis demonstrated that Pbx and Hox proteins not only bind to the *Shh* long-range enhancer at multiple binding sites along this element (Figs. 5.21 and 5.24) but that Hox were then capable of driving transcription through this element (Fig. 5.25). Finally, while not presented, preliminary evidence suggests that Pbx is bound to an *Fgf8* regulatory element in the limb ectoderm (data not shown).

In the presumptive limb and girdle, Pbx are present in overlapping domains that span nearly the entire mesodermal and ectodermal fields. In this manner, they may serve to "mark" numerous genes in the mesoderm and ectoderm to respond and cooperate with specific combinations of Hox (and other proteins) to carry out their "selector" gene functions. In this way, their "marks" may serve to coordinate differentiation of bone, muscle, and other soft tissues in a highly regulative fashion (e.g. as they derive partially from mesoderm), a process also dependent on the proper activation of *Hox* and execution of its dynamic spatio-temporal code during the development of these structures (Carroll et al., 2005). Concomitantly, the possibility that Pbx "marks" *Hox*

regulatory regions (i.e., ELCR, individual promoters, etc.) for activation remains a strong possibility, as *Hox* activation is altered in *Pbx* mutant mice and since *Hox* can auto- and cross-regulate its own transcription with Pbx (see Chapter 3).

8.3 *Pbx* roles in evolution

As discussed in Chapter 1 comparisons of gene sequence data for structural coding regions of *Pbx* homologs indicate that they are quite evolutionarily conserved among Metazoan taxa (Moens and Selleri, 2006). For example, vertebrates such as mice and humans, and invertebrates, such as the fly, share at least 90% identity in coding regions for each respective *Pbx* ortholog. This degree of homology is even higher on the protein sequence level. The high conservation among Pbx1 orthologs is also matched, though to a lesser extent, among the other orthologs (e.g., Pbx2 across different vertebrates) and even between homologs (e.g., between Pbx1 and Pbx2 in vertebrates), which suggest that in terms of general functionality, these proteins have remained conserved over the course of Metazoan evolution (Moens and Selleri, 2006). However, it is possible that *cis*- and *trans*-regulation of *Pbx* has changed throughout evolution leading to changes in the spatio-temporal expression of these genes and their functional domains. Unfortunately, these regulatory elements for *Pbx* remain unknown.

Regardless of this limitation, it is important to address if there exists functional differences in Pbx across different Metazoan taxa, and how such differences relate to morphological divergence and specialization. At the same

time, while comparative data on *Pbx* gene expression and function in mammals, specifically primates, are missing and most likely will never be obtained through traditional methods (as employed in this thesis), knowledge on Pbx function during limb and girdle development can be used to address issues of modularity and the manner in which variation is generated by developmental systems. This knowledge can serve as a framework for interpreting evolutionary changes in primate limb and girdle morphology. The remainder of this chapter focuses on these aims.

8.3.1 Comparative developmental genetics of *Pbx*

8.3.1.1 *Pbx* roles in proximal-distal limb patterning in vertebrates and invertebrates

Comparisons of the expression of *Pbx* and its invertebrate ortholog, *Exd*, indicate some similarities and differences that may stem from common heritage as well as from functional constraints during evolution (Fig. 8.2). For example, *Exd* is expressed in the proximal wing and leg of the fly imaginal disc, an ectodermal tissue critical for proximal appendage patterning (Rauskolb et al., 1995; Capdevila et al., 1999; Mercader et al., 1999). While *Exd* is expressed in various other fly embryonic body tissues, it has not been reported to be expressed in the epithelial-like cap surrounding the imaginal disc. Thus, *Exd* may not be important for regulating tissue-to-tissue interactions in the appendage. Conversely, *Pbx1* is expressed in both the vertebrate limb mesenchyme, a tissue of mesodermal origin, and also in the surface ectoderm

surrounding the limb and embryo proper (Selleri et al., 2001; this thesis). Thus, *Pbx1* may be required for mesenchymal-epithelial interactions during limb development. In addition, the finding that *Pbx1* and *Exd* are present in ectoderm may indicate a conserved expression domain for members of this gene family. As other *Pbx* genes have been discovered only in vertebrates, their domains of expression (i.e., such as both the proximal (*Pbx3*) and early and late distal (*Pbx2*) limb mesenchyme expression) suggest that additional domains and/or shifts in *Pbx* expression have occurred during vertebrate evolution and are equally important in limb patterning and morphogenesis.

Interestingly, this appearance of novel *Pbx* expression domains in vertebrate appendages is coupled with the novel expression of other proteins that Pbx partially rely on for proper function. For example, as in the fly where *Hth* is expressed proximally with *Exd* in the ectoderm (Rauskolb et al., 1995; Capdevila et al., 1999; Mercader et al., 1999), in the mouse, *Meis1* and *Meis2* are also proximally expressed in limb mesenchyme with *Pbx1* (Mercader et al., 1999). In addition, both *Meis* genes are expressed in the ectoderm and AER with *Pbx1* and *Pbx2* (data not shown). Furthermore, Pbx2 and Prep1 proteins additionally co-localize in the distal limb mesenchyme, while in flies the distal appendage is devoid of nuclear Exd and Hth protein (data not shown). These comparative data indicate that *Pbx/Exd* and *Meis/Hth* may have shared a common evolutionary heritage in the ectoderm and later in the limb mesenchyme of vertebrates. Future work will have to clarify these relationships.

From an evolutionary point of view, the observed co-localization of both Pbx/Exd and Meis/Hth indicates that their functions (and the domains that underlie them) may have co-evolved during Metazoan evolution due to constraints placed on them by such functional cooperativity. For example, one of their conserved functions certainly involves Meis/Hth ability to control the nuclear importation of Pbx/Exd (see Moens and Selleri, 2006). In a similar fashion, since Pbx/Exd and Meis/Hth co-expression results in their ability to form dimeric and trimeric complexes (with or without Hox) that are critical for the regulation of numerous target genes, such a constraint may have limited functions of these proteins in domains where they overlap (see Moens and Selleri, 2006). This is particularly important if Pbx (and Meis) function upstream of numerous pathways involved in generating an appendage and its constitutive parts. Regardless of these potential constraints, it is evident that Pbx can function in Meis-independent manners, which suggests that some divergence has occurred (Moens and Selleri, 2006).

The findings on *Pbx* gene function in this thesis indicate that the mechanisms of P-D and A-P limb patterning may have also departed from flies and accordingly are not necessarily conserved from invertebrates to vertebrates (Fig. 8.2). Unlike in vertebrates (Capecchi, 1997), the fly leg P-D axis develops independently of *Hox* . In the fly, *Exd* and *Hth* (the homolog of vertebrate *Meis*) are restricted to proximal limbs (Rauskolb et al., 1995; Capdevila et al., 1999; Mercader et al., 1999) and *Exd* is required for specification of proximal, but not distal, limb identities (Gonzales-Crespo et al., 1998). This process occurs

partially through their repression of (and thus restriction of) Distaless (Dll) distally (see Pueyo and Couso, 2005). Mutations in fly *Exd* result in homeotic transformations without altering the expression patterns of *Hox* genes themselves, thereby indicating that Exd can act as an ancillary co-factor to Hox proteins (Peifer and Weischaus, 1990; Rauskolb et al., 1993; 1995). In addition, the roles of Hth and Exd serve to antagonistically restrict hedgehog signaling to distal domains leading to P-D and D-V axis establishment (Abu-Shaar and Mann, 1998; Gonzalez-Crespo et al., 1998).

In vertebrates, the situation is different where patterning of distal limb structures is also *Pbx1* and *Pbx2* (and *Pbx3*) dependent (Fig. 8.2). Part of this vertebrate innovation may lie in *Pbx1* and *Pbx2* (and *Pbx3*) interaction in early limb field mesenchyme and possibly also in later *Pbx2* localization to distal limb domains. Unlike in flies, loss of *Pbx1* and *Pbx2* causes drastic alterations in the homologs of *Dll*, *Dlx,* as well as on *Hox* gene expression, pointing to a primary role of *Pbx* as upstream hierarchical regulators of *Hox* genes in vertebrate limbs. This latter vertebrate novelty indeed has crucial bearings on *Shh* regulation, as well as on the origins of morphological complexity of distal appendages in tetrapods. In this manner, *Pbx* regulation of *Hox* expression appears to lead to *Shh* activation, not repression as reported in flies.

8.3.1.2 Conservation of general Pbx function during fin and limb evolution

The genetic mechanisms that regulate limb and fin bud outgrowth appear quite conserved across distantly related vertebrates such as tetrapods (i.e.,

sarcopterygians) and teleost fish (i.e., actinopterygians) (Carroll et al., 2005). For example, in both groups, *Tbx* homologs in the early bud mediate proximal to distal outgrowth through their effects on *Fgf* expression and on ectodermal-mesenchymal interactions between either the limb bud mesenchyme and AER, or the fin mesenchyme and the apical ectodermal fold (AEF)(Chapman et al., 1996; Ahn et al., 2002; Garrity et al., 2002; Ng et al., 2002; Agarwal et al., 2003; Rallis et al., 2003; Takeuchi et al., 2003). In addition, *Hox* and *Shh* are also expressed in the early field of each bud type (Sordino et al., 1996; Hinchliffe, 2002; Carroll et al., 2005). While these data are particularly true in comparisons of mouse, chick and zebrafish, whether they hold for more primitive taxa remains to be seen. Recent data on other finned and limbed vertebrates suggests that some slight divergences have occurred (Shapiro et al., 2003; Stopper and Wagner, 2005; Tanaka et al., 2002; 2005).

In contrast to the relative conservation in molecular mechanisms of early bud formation, later mechanisms involved in distal limb and fin development are less conserved and more divergent. For example, in zebrafish as in other actinopterygians not all *Hox* are expressed in a 5' to 3' "reverse" anterior to posterior gradient as found in tetrapods. This departure has been cited as critical for the morphological development of the tetrapod autopodium, including the marked specialization of this structure as seen in mammals, for example (Sordino et al., 1996; Shubin et al., 1997; Carroll et al., 2005).

Comparative studies on *Pbx* (*pbx*) expression and function in the fin and limb have bearing on understanding the nature of the development of these

respective structures, their evolutionary histories, and whether they have been conserved or became divergent. Accordingly, in zebrafish, *pbx4* is expressed in the pectoral fin bud, and its loss, as in *Lazarus* mutants, results in the disruption of the embryonic fin entirely (Popperl et al., 2000). This is evinced by the complete loss of morphologically visible buds and also the absence of *tbx5.1* expression (homolog of the mammalian *Tbx5*). In these mutants, given the absence of the fin bud, *hox* and *shh* are not initiated (Popperl et al., 2000). At this point in time, the expression of other *pbx* homologs has not been reported in the fin proper or to have roles during fin bud outgrowth.

In the mammalian condition, as seen in this thesis, hindlimb buds do not form in the complete absence of multiple *Pbx* and forelimb buds only partially initialize (i.e., the likely result of *Pbx3* presence; Fig. 5.4B). In addition, in *Pbx1/2 Mut* and *Pbx1*$^{-/-}$*;Pbx2*$^{-/-}$ forelimbs, *Tbx5* expression is drastically down-regulated and the bud is greatly compromised prior to *Shh* expression (Figs. 6.3 and 5.1). Therefore, there appears a striking similarity in these early fin and limb bud programs with respect to the overall Pbx function. However, what becomes apparent is that mammals (and perhaps, tetrapods in general) have developed multiple *Pbx* genes and expression domains that strongly co-localize in these early limb domains. Furthermore, this redundancy is not trivial but has become important as it ensures that P-D outgrowth, *Hox* expression, *Shh* activation, and "reverse" *HoxD* collinear activation (critical for autopodial patterning and morphogenesis) occur in embryos that lose function of any single Pbx member. This integration between *Shh* activation and the control of "reverse" *HoxD*

collinearity is critical as it ensures the proper spatio-temporal distribution of Hox protein during digit patterning and morphogenesis. As observed in this thesis, *Pbx* loss spatially alters both processes and results in the loss of mammalian pentadactly.

While it may be safe to argue on a fundamental level that Pbx roles are strongly conserved between finned and limbed ancestors, the presence of multiple *Pbx* in the limb and in distinctive tissues (e.g., in ectoderm versus mesenchyme; in the anterior limb; in the proximal versus distal limb; in the forelimb versus hindlimb), may indicate that Pbx functions have become divergent (and/or specialized) from that seen in finned organisms such as the zebrafish, where *pbx* appears expressed only in the proximal fin mesenchyme. Future experiments using conditional *Pbx* mice should aid in sorting out some of these roles.

8.3.2 Incorporating *Pbx* into Evo-Devo models on primate limb and girdle evolution

8.3.2.1 Limb modularity and *Pbx*

In Chapter 2, several topics were introduced that are specifically relevant for addressing evolutionary changes in the primate limb and girdle. The first topic was that of modularity, or the idea that an organism (or one of its parts) consists of “a collection of elements whose intrinsic behaviors and functional interactions yield a mechanistic explanation of an identifiable developmental process or transformation (Von Dassow and Monroe; 1999: 313).” With respect

to the limb, several modules can be envisioned: (1) a module comprising each limb compartment; (2) a module comprising the limbs traditional signaling centers (i.e., ZPA, AER, and DE); and (3) a module comprising Hox territories.

It is important to address how knowledge on Pbx function in the limb modifies the understanding of these modules, their interactions, their relative autonomy, as well as their role(s) during limb development and evolution. With respect to the first modular system (#1), because *Pbx* has an early role in the limb field, suggests that for their influence to be developmentally and/or evolutionarily significant they would act to influence limb compartmentalization early, either at the time of their initial specification and/or by affecting a cell population that later becomes specified. *Pbx* intrinsic expression in the mesenchyme and influence on early 3' and 5' *Hox* gene expression may be of fundamental importance to this specification process. At the same time, Pbx roles as an important Hox cofactor in these early cell populations may have additional ramifications on the regulation of downstream Hox targets (see below).

With respect to the second modular (#2) system, Pbx proteins have been shown to orchestrate the development of these signaling centers and also to facilitate their interaction. Chapter 5 has demonstrated that *Pbx* upstream role on *Hox* establishes *Shh* expression and ZPA function, and that loss of the ZPA formation, as in *Pbx1/2 Mut* embryos disrupts its interaction with the other submodules; e.g., the loss of *Shh* in the ZPA of the *Pbx1/2 Mut* hindlimb resulted in a change from the near normal *Fgf8* expression in the AER (prior to Shh onset) to its patchy expression. Chapter 6 has demonstrated that Pbx are found

in the AER and DE and that global loss of *Pbx* from the ectoderm is commensurate with reductions in expression of multiple AER genes.

In view of developmental modularity as reflected by Hox territories (3) (put forth for the forelimb by Reno et al., in press), *Pbx* were not reported to be expressed in the perichondrium (i.e., where *Hox* expression supports the definition of the above modules) although they are expressed in the growth plate proper; and *Pbx1*$^{-/-}$ embryos undergo precocious hypertrophy of their chondrocytes (Selleri et al., 2001). Therefore, *Pbx* cell-autonomous influence on cartilage development may occur during chondrocyte differentiation and maturation at the growth plate. In addition, by not being known to typically form complexes with Hoxd11-13, and since as most of these perichondrial modules are defined by these specific 5' Hox, Pbx may not cooperate directly in complexes (with Hox) to regulate their perichondrial gene targets. As a result, understanding Pbx-Hox cofactor relationships may not provide additional insight into the modular growth of these territories via a direct cell autonomous role in the perichondria.

However, an examination of several of these Hox territories indicates that they may have also been affected by the loss of Pbx, as observed in *Pbx1/2 Mut* embryos. For example, Reno et al. (in press) identified one developmental module as a domain corresponding to the combinatorial forelimb expression of *Hoxa13* and *Hoxd10-13* and evinced by strong morphometric correlations among length measurements of the posterior metacarpals of digits 2-5 in all primates studied. In *Pbx1/2 Mut* forelimbs, all of these *Hox* were affected early and during

the autopod-specific “reverse” collinearity stage (i.e., the result of reduced *Shh* expression in the forelimb, respectively). In addition, dysmorphologies were evident in all four posterior digits in the forelimb. In another example, Reno et al. (in press) identified a second developmental module as defined by the presence of the overlapping anterior expression of *Hoxa13* and *Hoxd13* and a lack of statistical correlation between the length of forelimb digit number one and that of the remaining four posterior digits. Interestingly, in *Pbx1/2 Mut* forelimbs, digit one was lost and there was an observed reduction in both *Hoxd13* and *Hoxa13* in the most anterior domain of the autopodium prior to the formation of this digit. At the same time, the remaining four posterior digits were present.

These examples indicate that Pbx can influence the morphology of individual skeletal elements within several Hox modules prior to the time point when each respective module is argued to be functionally active or required. These effects may stem from a disruption of *Hox* collinearity in *Pbx1/2 Mut* embryos and its effects on *Hox* target gene functionality in these domains (i.e., as sufficient amounts of Hox protein may have been absent and thus unable to trigger target gene activation), or from an alteration in presumptive cell populations which give rise to the specified mesenchymal anlagen and cartilage domains that express specific *Hox* genes and execute their genetic and biochemical effects (i.e., as cell lineages may have been removed early in the limb that normally are activated by Hox in the perichondrium). Finally, if *Pbx* acts as a “selector” gene and marks elements for transcriptional regulation (i.e.,

activation/repression) then the loss of Pbx may lead to a lack of “potentiation” necessary for later Hox targeting.

The basis for this re-examination of modularity in the limb has been to demonstrate that Pbx may function early to set the modular cascades in motion and by doing so may influence modular activity even after their expression has ceased. If Pbx (and/or some other factor) acts as a “selector” gene and is able to influence all three types of developmental modules, then it may be necessary that all three of these modules be viewed as spatio-temporal overlapping submodules within the limb developmental system. In other words, that each has a quasi-autonomy that may not necessarily be easily identified given the interplay of early specification and patterning events on later aspects of development. Indeed, Reno et al.’s (in press) intention of exploring Hox modularity by studying intraspecific variation was to demonstrate that modular patterns could be deciphered from such analyses and that they arise via phenotypic selection on the organism. Accordingly, the idea that Hox modules emerge via selection on an aspect of a developmental system indicates that deeper, upstream pathways, may also be selected over the course of primate evolutionary history. In this manner, patterns of morphometric covariation may also reflect the earlier action of selector genes like Hox and Pbx. Clearly, understanding how selector genes influence morphometric variation will be an important bridge for deciphering if variations that have arisen via their modulation have been selected for over the course of an organism’s evolutionary history.

8.3.2.2 Girdle modularity and *Pbx*

To date, there have been limited studies exploring the issue of modularity in the primate girdle. Young (2004) has examined aspects of integration and modularity in ape scapula by performing morphometric studies on these primates and a cercopithecoid outgroup. He demonstrated that: (1) there exists at least two, if not three, developmental modules in the scapula, as determined by patterns of covariation in these structures across different primates; (a) a blade/spine/acromion module, (b) a glenoid module; and (c) a coracoid module; (2) these modules approximately correspond to patterns of known developmental gene activity during scapula development in mice and chicks; (3) in general, traits comprising the blade and acromion, and to a lesser extent the glenoid, are highly integrated in primates suggesting a strong developmental interconnection; (4) the coracoid module is that part of the scapula that exhibits more independence (is less integrated) which reflects its separate developmental evolutionary history; and (5) in primates the degree of variation in the scapula closely follows two distinct patterns of locomotor/positional behavior: quadrupedalism and suspensory locomotion.

With respect to (5) Young (2006), conducted more extensive analyses across many haplorhine primates to explore differences and similarities in covariation structure between suspensory and quadrupedal primates. The results of this study further support the findings above, specifically that primates, which are more quadrupedal, possess limited scapular shape variation when

compared to those that engage more in suspensory locomotion (i.e., in these primates, scapular shape variation was twice as high as those that practice quadrupedalism). Of critical importance is the additional finding that scapular variation does not change throughout postnatal ontogeny (i.e., it does not increase nor decrease within primate species) and that embryonic factors establish these initial patterns of variation.

Examining Pbx roles during scapular formation serves as a basis to test if Young (2004; 2006) modules are supported from a developmental genetics perspective. *Pbx* genes have been shown to influence the development of all scapular components, a point attributed to their ubiquitous expression. Though it remains uncertain if the significant cause of the blade defects in *Pbx* compound mutants results from Pbx absence from the somatopleure and/or dermomyotome, that blade and spine formation were altered in both *Pbx1/2 Mut* and *Pbx1/3 Mut* embryos suggests that dermomyotomal expression is most paramount in influencing the formation of these structures. If this is the case, then the observed patterns of covariation structure for this module in primates has a genetic basis with respect to *Pbx*. Interestingly, the absence of *Pbx1* and *Pbx2* but not *Pbx3* from the somatopleuric mesoderm, can account for the alteration to the glenoid (i.e., head/neck) and acromion domains in *Pbx1/2 Mut* embryos, but not for the same alterations in *Pbx1/3 Mut* embryos. The basis for developmental integration of these two modules (i.e., blade/spine and glenoid modules) may lie in the proximal anterior limb bud where all three *Pbx* are present, or depend solely on *Pbx1* which is expressed in the somatopleure and

anterior limb and that which affects the development of this structure when abrogated alone (i.e., *Pbx1*$^{-/-}$ embryos have the loss of the gleno-humeral joint indicating that patterning of these specific structures are altered). In this regard, there may be a basis, from a developmental perspective, for increased covariation between measurements of the blade, spine, and glenoid. Finally, the relative independence of the scapular coracoid process from that of the remaining structures may reflect the presence of all three *Pbx* in the anterior proximal blade, specifically if all three *Pbx* are needed to execute tissue-specific patterns of gene transcription in this module. In this manner, they may cooperate with different suites of transcription factors, including Hox, to select developmental programming of this structure.

8.3.2.3 Modularity, gene regulation, variation, and *Pbx*

An understanding of modularity and how modular systems (and submodules) interact offers a way to envision how phenotypic variation is generated in developmental systems such as the limb (Raff,1996; Schlosser and Wagner, 2004). As Pbx and the networks they participate in are critical for normal limb and girdle development several mechanisms can be examined that may shed light on how variation is generated by way of Pbx modulation.

First, a cross species examination of *Pbx cis*-regulatory elements may provide clues as to how Pbx function has been modified by different taxa. If regulatory element divergence is identified between taxa, it may indicate that the expression and functional domains of these genes has been modulated. *Cis*-

regulatory element divergence may take the form of; overall changes in sequence identity (across the entire element), specific changes within enhancer elements that reflect the loss or gain of binding sites for specific proteins, duplications or deletions of enhancer elements, positional changes between enhancers and other regulatory elements such as promoters, and modifications to the promoters themselves. Second, the examination of trans-acting regulatory factors (i.e., transcription factors) between taxa may provide an additional means of understanding changes in Pbx function. If trans-regulatory divergence is identified then the activities of *Pbx* enhancers and/or promoters may be modified (i.e., a direct influence via their protein to DNA interaction), and/or Pbx may be spatio-temporally removed from normal functional domains (i.e., due to changes in protein to protein interaction). For example, if modifications were found to Meis and Prep, which aid in the nuclear localization of Pbx, and/or to Hox themselves, then changes in their ability to bind with Hox to other target genes would be affected. Third, the examination of Pbx (and Hox) target sequences may help identify not only the major factors involved in the morphological divergence between two organisms harboring such differences, but also highlight when and where during development the modulation of Pbx (and/or Hox) function occurred. The potential changes in target genes themselves include; the gain and/or loss of enhancer sequences or binding sites for Pbx (and Hox), and also changes in the spatial position of these downstream elements to other control regions and how Pbx impinges on their interaction.

The types of modifications discussed above, if capable of altering Pbx function, may result in real changes in cell biological properties. Such downstream consequences could constitute alterations in cell proliferation, apoptosis, size, density, migration, communication, differentiation, matrix production, and mesenchymal condensation formation, among others.

Subtle modulations to these properties should produce real variations in the developmental system that have systemic and/or localized consequences depending on when and where they occur. For example, if they occur early then overall organ (i.e., limb) size and/or patterns of integration between developmental modules may occur. If they occur later (and in more spatio-temporally restricted domains) then variations may arise within modules or in submodule interactions. In this light, if selection favors one particular aspect of a regulatory modulation, it may have consequences on modular (or submodular) components that are genetically and/or functionally interconnected. For example, in the discussion on bat wing development (Chapter 2), selection in favor of an enlarged autopodial handplate (and the molecular mechanisms driving such) may have resulted in distal ulnar reduction. Likewise, selection may favor an upstream effect, as for example, the up-regulation of many genes expressed in the bat perichondria (see Chapter 2) may stem from a *cis*- or *trans*-regulatory change in one factor that binds to the enhancers of multiple genes expressed in these domains.

8.3.2.4 Mechanisms generating morphological variation via the *Pbx-Hox-Shh* limb developmental network

Before addressing several examples of primate limb variation it is important to address how the specific model of Pbx-Hox-Shh function in the limb and girdle may be modified by several of the mechanisms addressed above. This approach will offer a way to then critically evaluate how primate limb variation can be generated by Pbx and Hox developmental functions in the limb.

It has been discussed that *Hox* expression in limbs is regulated by two control regions: an ELCR, 3' of the *HoxD* cluster, which drives the initial spatio-temporal expression of *Hox* in limbs; and a later, digital enhancer contained within the GCR, 5' of the cluster, which drives autopod-specific *Hox* expression (see Fig. 5.29). According to Tarchini and Duboule (2006) it is the early collinear expression that aids in the morphogenesis and patterning of stylopodial and zeugopodial structures and *Shh* activation, while it is later "reverse" collinearity that leads to autopodial, specifically digital ray, development.

In both instances, the position of individual *Hox* promoters to these two control regions appears critical in driving specific *Hox* expression. With respect to the ELCR, the further 5' a *Hox* promoter is located, the more posterior and temporally delayed its expression will be compared to more 3' members. At the same time, there exists an early 5' region functionally coupled to the ELCR, but apparently independent of the GCR, that also aids in antagonizing early collinear expression. Tarchini and Duboule (2006) provide additional evidence that *Hox* expression is promoter independent with respect to the ELCR, meaning that

transcriptional activation efficiencies do not change from one promoter to the next along the cluster. This latter aspect is quite different from that seen between individual 5' *Hox* promoters and the GCR, where it has been demonstrated that 3' *Hox* (i.e. *Hoxd9-10*) when repositioned under the influence of the GCR, have lower transcriptional efficiencies when compared to 5' *Hox* (i.e., *Hoxd11-13*) that normally reside closer to this element (Kmita et al., 2002).

The current views on *Hox* promoter function and their relationships to these control regions have provided some interesting insights into the mechanisms that underlie morphological evolution. Tarchini and Duboule (2006) and Freitas and Cohn (2006) have noted that from an evolutionary standpoint the development of external control regions (i.e., elements which lie 3' and 5' of the *HoxD* cluster, such as those described above) governing sequential *Hox* expression was adaptive and perhaps a necessary outcome of the cluster organization. Accordingly, development of enhancers within the *HoxD* cluster may have been problematic as if they were modified they may affect expression of *Hox* in domains other than the limb. In other words, that because cluster organization is relatively ancient (as evinced by phylogenetic studies of *HoxA-D* cluster evolution, Carroll et al., 2005), and was initially required for specification along the cranial to caudal regions of the embryo, internal alterations to the overall control of the cluster (i.e., in the form of internal enhancer elements) would result in disruptions in axial *Hox* expression and specification. These phylogenetic and functional constraints may have allowed for a greater likelihood of evolving regulatory regions outside of the cluster and accordingly, such

enhancers may have provided an initial source of functional asymmetry in *Hox* control (Tarchini and Duboule, 2006; Tarchini et al., 2006).

If this last aspect is the case, then evolution of morphology via direct alterations in *Hox* control could be envisioned as resulting from at least three mechanisms: (1) genetic changes to these control regions proper (including upstream changes to its transcriptional regulatory molecules)(Figs. 8.3 and 8.4); (2) genetic changes in the positioning of individual *Hox* promoters specifically with respect to these external control regions, as well as changes in transcriptional efficiencies of the individual promoters themselves (Figs. 8.5-8.7); and (3) changes in Hox protein function (i.e., alterations in Hox specificity to target genes).

With respect to these three potential mechanisms, Pbx functions and alterations thereof, may indeed underlie morphological and patterning alterations in limbs over the course of evolution. Specifically, delays in *Pbx* expression may result in spatio-temporal modifications in *Hox*, particularly if Pbx controls *Hox* collinearity directly. This scenario could be quite interesting considering the most recent view that besides providing positional or patterning information to skeletal elements, Hox transcription factors are critical regulators of overall limb growth, as well as growth of the limbs individual components (i.e., consider double *Hoxa11; Hoxd11* homozygous mutants which show alterations in zeugopodial growth; Davis and Capecchi, 1994). In addition, since Pbx complexes with other partner proteins have been shown to regulate 3' *Hox* promoter activity (see Chapter 3), then altering *Pbx* expression may affect individual *Hox* promoter

activity. This select and temporal-specific control could result in compartmental-specific alterations in morphology since different *Hox* pattern separate elements. Figures 8.3 and 8.4 discuss some of the types of limb modifications that may be predicted from altering early *Hox* collinearity, directly.

The second mechanism revolves around the experimental findings that the spacing of *Hox* promoters to the ELCR and GCR is critical to individual *Hox* gene regulation (see Chapter 3). If evolutionary mechanisms have altered these relationships, then the spatio-temporal control of *Hox* activation may have been changed which may have led to morphological shifts. In this regard, the presence of an intronic region between *Hoxd4* and *Hoxd8* (Tarchini and Duboule, 2006) may act as an important spacing mechanism controlling the activation of *Hoxd8-Hoxd13* versus those of the more 3' members, and in buffering against the antagonistic effects of the early 5' region controlling early *Hox* expression. Future work must determine if changes in the length of the intronic region do indeed affect *Hox* expression and resultant morphology. As intronic regions are not typically considered under intense selection (Carroll et al., 2005), mutations resulting in sequence length changes may be critical in the generation of variation in limb morphologies, particularly in lieu of *Hox* upstream role as growth promoting agents (Davis and Capecchi, 1996; Goff and Tabin, 1997). Figures 8.5 through 8.7 discuss some of the types of limb modifications that may be predicted from these positional alterations.

Finally, since one of Pbx functions is to cooperate with Hox, and regulate their *in vivo* binding to target DNA sequences, then alterations in Pbx spatio-

temporal protein distribution over the course of development may translate to modifications in Hox function and target specificity. This scenario has obvious implications to evolution as subtle variations in Pbx (and thus Hox) localization may provide for slight morphological alterations, which would then serve as the template for selection. In addition, modifications to binding sites of Hox and/or Pbx target genes offers another mechanism of divergence.

At this point, several examples are discussed to illustrate how understanding modularity, *cis*- and *trans*-regulation, and Pbx function during limb and girdle development can account for the potential generation of variation in primate appendages. For sake of simplicity, specific focus is on the use of the *Pbx-Hox-Shh* model addressed above.

8.3.2.5 Examples in primates

8.3.2.5.1 Changes in digit proportionality and specialization

As discussed in Chapter 2, primates display considerable variation in the lengths of each of their digital rays. Much of the work by Reno et al. (in press) has focused on the use of Hox modularity to understand the origins of this variation. Of several examples they discuss, two specific cases of digit proportionality have been chosen to illustrate how an understanding Pbx and Hox, and their role in development can be used to interpret the origins and maintenance of digit variation in primates. In the first case, they have addressed how different digital proportions among apes, specifically gibbons, reflect alterations in Hox modularity. By examining patterns of intraspecific covariation in

the distal ape limb, they argue that gibbon thumb length may well have increased over the course of evolution as a result of selection in favor of longer posterior digits and distal zeugopodial elements, the results of which reflect modification to a developmental Hox module for these domains. Accordingly, the underlying developmental module governing this morphological pattern includes territories for *Hox13* paralogs and *Hoxd11*; and spatio-temporal changes in these genes may have facilitated growth changes in the perichondria of the gibbon autopod and zeugopod.

It is of interest that these developmental modules may have an earlier basis during the assignment of positional information in the early limb bud and its pleiotropic affects on the execution on downstream target genes (i.e., of Hox and their targets in the perichondrium). Evolutionarily, one way to obtain an increase in overall *Hox* expression may have been to up-regulate and/or heterochronically shift the expression of *Shh* in the limb to earlier stages, and/or make the 5' *Hox* "reverse" collinearity more sensitive to overall up-regulation by one or more upstream factors (i.e., by up-regulating a transcription factor capable of binding to each regulatory element). One genomic way to increase 5' Hox sensitivity to up-regulation would be to shift the distance of these *Hox* promoters to the 5' located GCR and digital enhancer (e.g., Fig. 8.7). These changes would bring all 5' *Hox* closer to this regulatory element and as the individual *Hox* promoters are sensitive to this distance, earlier and stronger transcriptional activation may be achieved. However, while this up-regulation for the 5' group of *Hox* would certainly alter autopodial *Hox* expression (Kmita et al., 2002; 2005) it may not

have bearing on earlier *Hoxd11* zeugopodial expression, as this domain appears to relate to an earlier mechanism in *Hox* collinearity control. In this regard, another possibility to obtain coordinated up-regulations of *Hox* spanning different collinearity periods or episodes may be to systematically up-regulate early *Hox* collinearity which may lead to earlier *Shh* activation and thus earlier 5' *Hox* autopodial expression (Figs. 8.3 and 8.4). Another possibility would be to separately change early *Hoxd11* expression and then also change later 5' *Hox* collinearity. However, the more parsimonious view would be to change one regulatory domain.

The second case, concerns a relatively opposite pattern, that of digit reduction in specific primates such as *Ateles* and *Colobus*. As mentioned in Chapter 2, both genera possess unique distal limb morphologies (i.e., they possess elongated posterior digits, greatly reduced and residual anterior "thumb" digits, and concurrently lack the distal zeugopod length increases seen in other primates). Reno et al. (in press) discuss several different scenarios of *Hox* alteration that may explain the phenotype but favor one particular, i.e., that perhaps modification to the control of *Hox13* genes (i.e., *Hoxd13* and *Hoxa13*) may be sufficient to cause thumb reduction in these primates. For instance, the reduction of Hox13 proteins across the entire autopod where other Hox (i.e., Hoxd10-12) are endogenously present would allow these Hox proteins to compete for targets more efficiently and increase growth of the posterior four digits, as experimental evidence in chicks suggests (Goff and Tabin, 1997). Also, a decrease in Hox13 paralog level would explain the observed reduction in

digit one, specifically since digit one development is sensitive to Hox13 paralog level, as it is lost, for example, in *Hoxa13*$^{+/-}$ (*Hd* mutant) mice (Morlock et al., 1996).

Interestingly, *Pbx1/2 Mut* embryos display unique forelimb alterations, such that the remaining posterior digits 2-5 are present but that digit 1 is missing, and that such changes were commensurate with alterations in *Hox* expression (see above). While this is an experimental case, presumably altering *Shh* onset even slightly as in the forelimb of these mutants, may have farther-reaching effects on digit one outgrowth (i.e., in its effects on later *Hox* "reverse" collinearity). In this manner, *Pbx* control of *Hox* and *Shh* could be one potential mechanism, as well as would be changes in *Shh* expression directly or also to 5' *Hox* "reverse" collinearity as described above (e.g., Fig. 8.7). Finally, as digit 1 morphogenesis also depends on early anterior mesenchymal patterning events (see Chapter 3), alterations to anterior limb ectodermal-mesenchymal interactions may have been significant places that led to variation in digit and limb formation.

8.3.2.5.2 Differences in intralimb proportionality

The potential to modify Hox and Shh activity via Pbx may influence patterns of covariation seen across proximal to distal elements of a single limb and aid in explaining the different intralimb proportions identified across primates. For example, apes display different patterns of skeletal element proportionality across the limbs major compartments. Gibbons, which typically have the longest

forelimbs, possess elongations in each limb compartment with particular size increases in the zeugopod and autopod. In chimps and gorillas, these length changes are not as drastic nor are they present in the stylopod as they are in gibbons. Patterns of length increases across the distal two compartments has been argued by Reno et al. (in press) to reflect evolutionary changes in Hox activity among different ape lineages (see Chapter 2).

Interestingly, given the knowledge on how Pbx controls early *Hox* collinearity, *Shh*, and thus on later *Hox* "reverse" collinearity, several additional scenarios could be envisioned to coordinate an up-regulation of growth across all of these domains, specifically in gibbons versus other apes. One possibility is that heterochronic shifts in early *Hox* gene collinearity may have led to up-regulations of stylopodial and zeugopodial growth targets and to earlier *Shh* activation and *Hox* "reverse" collinearity (e.g., Figs. 8.3 and 8.4). This mechanism could be via up-regulation of Pbx or its partners, though this is only one possibility, as modifications to several upstream targets may also have significant effects.

Another possibility is a genomic modification to the intronic region between *Hoxd4* and *Hoxd8*, which through partial reduction in intron size (not necessarily under selection) may reposition these 5' promoters (for *Hoxd8-d13*) closer to the 3' ELCR without altering 5' spatial relationships to the GCR (e.g., Fig. 8.5). Movement of individual promoters in the 3' direction would lead to earlier onset of all 5' *Hox* (i.e., those centromeric to the deletion)(Tarchini and Duboule, 2006), *Shh* (Tarchini et al., 2006) and an overall up-regulation of Hox

activity in presumptive stylopodial and zeugopodial domains (i.e., recall that 3' *Hox* such as *Hoxd9* and *Hoxd10* pattern stylopodial elements, Carpenter et al., 1997; Chen and Capecchi, 1997, while 5' *Hox* such as *Hoxd11* and *Hoxd12* pattern zeugopodial elements, Davis et al., 1995; Boulet and Capecchi, 2002). Concurrently, the earlier activation of *Shh* should trigger earlier 5' "reverse" *Hox* collinearity leading to increases in *Hox* expression in autopodial domains. Interestingly, recently it was demonstrated that only repositioning of 5' *HoxD* (i.e., *Hoxd10-13*) is enough to alter *Shh* activation (Tarchini et al., 2006). Therefore, in this context, a repositioning would lead to earlier activation of specific and important *Hox* activation, both critical for *Shh* initiation and the patterning of skeletal elements across each developmental module. Another possibility would be an up-regulation of a regulator of Hox, which is able to bind to all promoters equally (e.g., Fig. 8.4). This may be particularly possible since *Hox* genes (and their promoters) arose through duplication (Carroll et al., 2005) and may share common transcription factor binding domains.

Distal limb variation, among ape forelimbs, for example, may result from mutations in this intronic region (e.g., Fig. 8.5) or in intergenic DNA regions between individual *Hox* genes (e.g., Fig., 8.6). Such mutations may result in subtle limb variations that become selected for during the gradual development of the distinctive locomotive abilities of these different primates. One potential problem with this viewpoint is that such genomic repositions may lead to concurrent changes in both forelimbs and hindlimbs. In this manner, it may be more parsimonious to argue that the up-regulation of forelimb specific

hierarchical regulators plays a specific role in these limb variations or that there are different forelimb versus hindlimb regulatory elements (for *Hox*) that have evolved and diverged separately to accommodate specific genomic changes.

8.3.2.5.3 Forelimb versus hindlimb specializations

Tarsiers, for example, exhibit unique forelimb versus hindlimb adaptations that reflect functional divergence of these limb types during locomotive and positional behaviors (Fleagle, 2001). In the forelimb, the middle three digital rays display length increases while carpal elements remain small and “carpal-like”, adaptations that probably arose for improved grasping during vertical clinging and capturing prey. In the hindlimb, digital rays are also long, specifically compared to other haplorhines and strepsirrhines but so too are several tarsal elements (i.e., calcaneous and talus). Furthermore, they also display length increases in the hindlimb zeugopodial elements. All of these traits appear as adaptations to leaping.

With respect to the morphological differences in tarsier forelimb versus hindlimb skeletal elements, several evolutionary scenarios could be envisioned, which relate to both alterations in *Hox* expression and function as well as to changes in factors that are limb-type specific. One simple scenario involves a change in the *cis*- and *trans*-regulation of the *HoxC* cluster expression and function, which may have important ramifications on affecting hindlimb but not forelimb element patterning and growth (i.e., *HoxC* genes are expressed in the hindlimb only, see Chapter 3). In this regard, while it is known that in mice

deletion of individual *HoxC* genes or of the entire cluster does not result in hindlimb defects, over-expression of *Hoxc11* results in fibular absence (Papenbrock et al., 2000). These results indicate that HoxC does have the potential to modulate patterning in this limb type and it may do so by out competing other HoxA and HoxD where they overlap. The question then arises as to why *HoxC* deletion results in no phenotype in mice? One answer may be that mice lack extreme differences in their forelimbs and hindlimbs (as seen in other mammals) and have not evolved HoxC functional requirements in these domains. On the other hand, perhaps the loss of HoxC can be co-opted in mice by other Hox. This latter situation is likely given the overlapping functions of Hox on *Shh* transcription (see Chapter 3).

Another scenario is that during tarsier evolution, heterochronic and heterotropic shifts in hindlimb-specific *HoxA* and *HoxD* expression, into domains corresponding to the fields of the presumptive posterior tarsal elements (such as the calcaneous) have been positively selected. One possibility is that either a hindlimb specific regulator has been modified, or that 5' *Hox* genes have been repositioned with respect to the GCR, both of which may have lead to slight proximalization of the late "reverse" *HoxD* expression into tarsal zones (e.g., Fig. 8.7). This situation may be analogous to that described for the bat distal wing (see Chapter 2). Another possibility is that upstream *cis*- regulatory changes in early *Hox* collinearity (via a hindlimb specific factor) led to a distal shift of early collinear expression into domains of the forming tarsal region and/or led to shifts in the assignment of positional information to presumptive tarsal-forming cells

(e.g., Fig. 8.3). As tarsiers also exhibit the increased length of the distal zeugopod and the subsequent fusion of the tibia to the fibula, perhaps these changes are coordinated by earlier distalization signals in these domains. In this regard, since *Pbx* lies upstream of early *Hox* collinearity and that only *Pbx1* and *Pbx2* are present in the hindlimb, shifts in their regulation may be more influential in hindlimb morphological divergence, while alterations in forelimbs may be buffered by the presence of *Pbx3*.

Another scenario is that as tarsiers also experienced forelimb digital length specializations, coordinated changes in overall distal 5' *Hox* expression may have demarcated both limb types, via the up-regulation of a single ubiquitous factor or modification to the genomic organization and spacing of the *Hox* cluster itself. Concomittantly, hindlimb specialization may have resulted from additional shifts in other *Hox* genes at subsequent times. For example, if 5' *Hox* are up-regulated via the repositioning of 5' *Hox* closer to the digital enhancer (see Fig. 8.7), then overall anlagen size may have been differentially affected along with changes in down-stream target growth genes. Shifts in *HoxD* in both limb types due to genomic repositioning may have lead to *HoxC* domain shifts (i.e., because the cells that express *HoxD* have changed in number, size, position, etc.) that produced coordinated changes in distal zeugopodial and autopodial domains. In this manner, subtle variation in this integrated network, specific to the hindlimb and not the forelimb, may have resulted in overall patterning rearrangements that were selected for (or against).

This latter type of gross change in networks has been demonstrated experimentally as limb-specific “selector” genes may shift morphological determination during early pathways. For example, if *Pitx1* (i.e., a gene upstream of hindlimb identity) is ectopically mis-expressed in the proximal forelimb field a shift in genetic programming occurs to make a hindlimb-like structure in this field (Marcil et al., 2003; Minguillon et al., 2005). Likewise, in the development of vertebral types (e.g., cervical, thoracic, etc.), vertebral identities shift due to changes in axial level *Hox* expression domains (e.g., Condie and Capecchi, 1994; Kostic and Capecchi, 1994; Horan et al., 1995; Favier et al., 1996; Fromental-Ramain et al., 1996a; Chen et al., 1997; de la Cruz et al., 1999; van den Akker et al., 2001; Wellik and Capecchi, 2003). These shifts in limb and vertebral type identities are not restricted to hard tissue but also to muscle and nervous tissue, as has been most recently shown for *Pitx1* mutants (DeLaurier et al., 2006).

8.3.2.5.4 Differences in the scapular girdle

Young (2006) has demonstrated that variation in primate scapular morphology is determined prenatally, as patterns of variation across this element’s modules did not drastically increase or decrease during ontogeny for the numerous primates examined. However, he did indicate that the lack of such a postnatal change might stem from the canceling effects of increasing neuro-muscular control and environmental factors during ontogeny. He also demonstrated that primates engaging in suspensory locomotion display more

scapular shape variation then those practicing quadrupedalism. Accordingly, the scapula in suspensory primates is triangular with broader dimensionality along the superior to inferior domains and narrower proximally-distally, while in quadrupedal primates this element shows reduced dimensionality in the superior to inferior dimension and has been expanded proximal-distally. Also the angle of the spine and acromion process to that of the superior-inferior axis of the blade is more oblique in suspensory forms while in quadrupedal forms it is more perpendicular to this same axis (i.e., the spine and acromion lie almost parallel to the P-D axis of the blade). These changes are also accompanied modifications to the shape of the glenoid and the coracoid process that permit movement and/or stabilization of the shoulder joint (Oxnard, 1967; 1977; Larson, 1993; 1998; Fleagle, 2001).

Given the high degree of integration between the blade and spine, and partially with the glenoid, it may be that changes in the size and shape of the initial anlagen led to some of these morphological differences between quadrupedal and suspensory primates. Shifts in axial level *Hox* expression may alter the patterning of blade progenitors that eventually migrate to the scapular blade domains. Concurrently, shifts in somatopleure-dermomyotomal interaction caused by modifications to somatopleuric gene expression (e.g., *Pbx*, *Tbx*, *Hox*) may alter the number and fate of cells giving rise to the blade. Interestingly, as the somatopleure itself is critically involved in forming neck and glenoid domains gene expression changes in this domain may have cascading effects on the entire scapula.

At this point only a few genes, such as *Tbx5* and *Pbx*, have been shown to simultaneously affect blade/spine and glenoid domains (see Chapter 3). Furthermore, it was demonstrated in this thesis that *Pbx* most likely lie upstream of *Tbx5* expression in adjacent somatopleuric and limb domains. In this manner, subtle variations in *Pbx* gene expression (via *cis*- and *trans*-regulatory changes in each gene) may have resulted in shifts in somatopleuric patterning and dermomyotomal differentiation in coordinated ways. For example, loss of *Pbx1* entirely as in *Pbx1*$^{-/-}$ mice results in reductions of the superior inferior blade dimensions, while coordinated loss with other *Pbx* results also in changes in the proximal to distal extent of blade formation. In both cases, alterations are made in the head and neck as well. Given the newly discovered and potential upstream roles of Pbx on numerous genes involved in morphological formation of all domains of the scapula, subtle shifts in early Pbx function may aid in coordinating downstream modifications on multiple domains and genetic networks. The differences in morphology, as seen in quadrupedal versus suspensory primates, suggests that correlated changes in multiple tissue domains has occurred during evolution, and thus, it may be more parsimonious to argue that selection has favored morphologies that result from shifts in early fields of growth (thus altering all scapular domains), rather than morphologies that result from the independent acquisition of mutations influencing each domain, and each conferring a fitness advantage.

With respect to variation within different functional domains of the scapula, the finding that blade and glenoid/humeral domains are both subjected to all

three *Pbx* indicate that patterns of variation may vary independently by way of different effects of *cis*- and *trans*-regulatory *Pbx* influences on downstream targets in both domains. In this manner, if *Pbx* behaves like a "selector" gene it could trigger suites of differential gene activation in these distinct domains, by interacting with different cofactors and signaling pathways, or by having separate inputs on its own or in downstream target gene promoter and enhancer elements. Indirect evidence that supports this upstream role is the finding that the scapular neck and humeral head are duplicated in *Pbx1/2 Mut* and *Pbx1/3 Mut* embryos (Fig. 7.4) and that such changes are associated with the early mis-expression of *Hoxc6*, *Hoxa9*, and *Hoxd9* (Figs. 7.10 and 5.18).

8.3.2.5.5 Integration of girdle and limb evolution

Humans and apes, such as chimpanzees and gorillas, display variation in the numbers of vertebrae, in the shape and orientation of the pelvis (e.g., in the shape of the iliac blades), and in proximal femoral head/neck orientation and size, aspects of the skeletal biology that has been argued to reflect different locomotor practices (e.g., Fleagle, 2001; Lovejoy et al., 1999). For example, the chimpanzee pelvis (i.e., more similar to a quadrupedal primate) has superiorly to inferiorly tall iliac blades that lie dorsally along the coronal plane, and tall pubii and ischii. Their sacra are also superior-inferiorly tall and they possess six lumbar vertebrae. The femoral head/neck are also short and brought in close to the acetabulum (i.e., specifically compared to humans). In humans and australopithecines, such as *Australopithecus afarensis* (i.e., representative of

bipedal condition), the shape of the entire pelvis is reduced in the superior-inferior dimension, and the illia are flared laterally and aligned more in the sagittal plane. Likewise, elements of the pubis and ischium are also reduced in these dimensions and broadened. Concurrently, sacral vertebrae are wider and the number of lumbar vertebrae are reduced (i.e., to 5). Finally, the femoral neck is also longer in this same medial-lateral dimension. These observations have been known for many years, but Lovejoy et al. (1999), proposed several scenarios by which they envisioned how an understanding of development could lead to these changes.

One scenario put forth by Lovejoy et al. (1999) is that subtle shifts in the initial positional information (i.e., by changes in morphogenetic gradients) in the fields that govern pelvic morphogenesis may have occurred which if selected for could modulate the entire shape of the pelvis simultaneously. Interestingly, very few genes are known at this time to simultaneously influence shape of the pelvis and limb. Altering shape is an important component of this perspective since there have been experiments in chicks that demonstrate that axial level specification of the limb and girdle can be shifted (i.e., via bead implants) but in such experiments shape remains mostly normal (see Chapter 3). Those genes that do influence shape and normal morphogenesis are extremely critical for understanding such morphogenetic shifts and their results on morphology.

From the perspective of *Pbx* and *Hox* function during limb and girdle development there is at least two potential mechanisms for such shifts. First, Pbx was shown to be upstream of nearly all known genes critical for pelvic and

proximal limb morphogenesis. In single *Pbx1* mutants, there is a simultaneous alteration of the proximal femur and girdle, while in compound mutants for *Pbx1;Pbx2* there were more drastic effects across these domains. Furthermore, it has been demonstrated that *Pbx* influences axial level expression of *Hox* and that limb location may have been slightly altered. However, if *Pbx* acts (with *Hox*) as "selector" genes that lead to downstream changes in gene expression, then subtle shifts in *Pbx* and/or *Hox* via alterations in *cis*- and *trans*-regulatory networks may lead to coordinated changes in pelvic field and proximal limb specification. The idea that *Pbx* does behave as a "selector" gene is evinced not only by the near duplication of the humeral head in the forelimb but also by the transformation of BA1 arch derived structures into BA2 arch derived structures in *Pbx1* and *Pbx1;Pbx2* absence (Selleri et al., 2001; data not shown). Furthermore, *Pbx1/2 Mut* embryos also possess severe alterations (i.e., reductions and loss of identities; Fig. 5.28) across all vertebral domains, a phenotype partially related to shifts in axial expression of *Hox* and *Pax* (Capellini, Di Giacomo, Selleri, in preparation). Modulating, even slightly, the expression of *Pbx* in the axis, the somatopleure, and the limb, may lead to alterations in positional information in all domains and subtle variations in morphology. Another potential mechanism may relate to repositioning individual *Hox* promoters closer to their enhancers that could lead to shifts in *Hox* expression across multiple domains and to patterning alterations in both the axis and the limb simultaneously (e.g., Fig. 8.3). Overall, coordinated changes in the positional information across these domains may have led to initial patterning

variations in human ancestors that became selected for and eventually led to the pelvic and limb morphologies argued by Lovejoy et al. (e.g., 1999) to be a quintessential evolutionary pre-requisite to the modern human condition.

8.3.2.6 The evolutionary forces and generating limb diversity in primates

It has long been argued, under basic tenants of the adaptationist paradigm, that the unique skeletal attributes found in extinct and extant primates come about by selection favoring individualistic changes that arise via mutation in their encoding genes (Gould and Lewontin, 1979). For example, the morphological changes observed in the primate scapula and/or in limb proportionalities were argued, according to this view, to arise independently, each change conferring some fitness advantage and in an incremental fashion. Overtime, such additive fitness increases allowed for each specific trait to become fixed within the population. This perspective assumes that the individual attributes are under what Lovejoy et al. (1999) has called “descriptive specification,” or that individual genes control specific morphologies, and that each is under separate selective pressure. The basis for this perspective relies partially on the adherence to the theory of mass selection (Fisher, 1930) in which specific morphologies are argued to have arisen by the refinement of existing adaptations through additive genetic effects (arising by mutation) under the influence of natural selection in large, panmictic populations.

Recent emergent understanding of several aspects of developmental biology and evolution call into question the need to rely strictly on descriptive

speciation and mass selection as adequate means of describing evolutionary change in primates. From a developmental perspective, currently it is understood that patterning and morphogenesis are highly integrated and that genes that control developmental trajectories and cascades may be most critical to producing variation. As Lovejoy (1999:13247) states: "from a morphological perspective, it is important to be continuously vigilant of the fact that patterning in the limb is determined at a cellular, and not an anatomical, level. Morphology is the ultimate read-out of these complex molecular interactions." This view highlights the importance of modularity and the interconnectedness of molecular and tissue domains, as well as that individual genes do not determine specific skeletal morphologies. From an evolutionary perspective, shifts in developmental fields (via spatio-temporal changes in gene regulation) may be subtle enough to modify various aspects of morphology in such a way as to not be detrimental, but perhaps neutral, and by doing so provide new variations into the environment on which selection can act.

From an evolutionary perspective, small population size and stochastic effects of evolutionary forces (i.e., genetic drift, founder effect, bottleneck) may also have been equally important for generating morphological novelty and diversity during primate evolution. Shifting-Balance theory, as proposed by Wright (1932), argues that adaptive novelties (variations) arise in small, subdivided populations as a result of mutation, epistasis, pleiotropy, and the context dependence of allelic effects as well as the combinatorial action of local natural selection, random genetic drift, and migration on underlying population

genetic structure. These mechanisms may have provided initial variations upon which both localized selection in small populations have operated to initially shape primate morphologies. With respect to Shifting-Balance theory, if primate communities spanning specific geographic domains became isolated and experienced periods of intra-deemic mating (i.e., inbreeding) then the possibility exists that neutral mutations (e.g., in intronic regions and/or *cis*- and *trans*-regulatory elements) may have occurred, that developmental systems became slightly modified, and that overall levels of allelic polymorphism may have been reduced. Upon contact with other primate groups, rapid morphological divergence may have been established due to the genetic interactions between genetically diverse populations, as proposed by Wright (1932). Such rapid morphological variation would then have been subjected to localized selection in the same environments that allowed for the re-establishment of contact. Appropriately then, long term selection on these morphologies (as proposed by Fisher, 1930), may have further aided in fixing these morphological variants (and their underlying genetic structure) in large populations.

There has been some evidence presented in this thesis that indicates that the generation of variation during development critically depends on the differences in overall polymorphic levels between inbred and outbred populations, and in this manner, offers some support for the idea of the context dependence of allelic effects as suggested under Shifting-Balance theory. For example, the generation of *Pbx1/2 Mut* embryos on a “relatively” purebred genetic background (C57BL/6) showed the complete loss of all digits save one

rudimentary digital ray (Fig. 5.3). The C57BL/6 line is considered a “relatively” pure genetic background, since initially the gene targeting strategy for *Pbx* employed a different line (129SV) and only after was backcrossed to C57BL/6 for at least ten generations. Backcrossing to C57BL/6 aided in reducing the overall degree of genetic polymorphism (i.e., at all loci) that subsequently permitted higher degrees of penetrance and expressivity (i.e., it became permissive and allowed the loss of a particular genes function to be consistently visible).

Interestingly, when these *Pbx1;Pbx2* mice were crossed once to an outbred Blackswiss line that displays high degrees of polymorphism, the *Pbx1/2 Mut* hindlimb phenotype became slightly ameliorated, specifically with respect to digit number (Fig. 5.3). When progeny of this first cross were mated to this outbred line again, even higher degrees of amelioration were identifiable in the hindlimb. This amelioration was observed despite that both *Pbx1/2 Mut* C57BL/6 and *Pbx1/2 Mut* C57BL/6;Blackswiss embryos possessed the same numbers and configurations of the null mutations for these *Pbx*. These data indicate that allelic polymorphisms (i.e., potential modifier alleles) present in this outbred population resulted in genetic interactions that buffered against the severe effects of the loss of the *Pbx* genes during hindlimb development. Furthermore, and perhaps as equally important, these variations were evident only in the distal hindlimb, as phenotypic defects in the proximal hindlimb, the entire forelimb, and the axial skeleton all remained relatively the same. This finding indicates that allelic polymorphism in the outbred strain had specific effects on one

developmental module (i.e., hindlimb) independent of any noticeable affects on other modules.

While the effects of the genetic interactions between these two lines were noticeable owing largely to the presence/absence of identifiable elements, situations in nature are quite different as organisms often vary metrically. Furthermore, the levels of polymorphism identified in C57BL/6 mice may be extremely restricted, while in nature the degrees of polymorphism may not approach these low levels. However, the degree of polymorphism in nature may be enough to lead to subtle changes in skeletal element size and morphology that serve as initial sources of variation for future selective environments.

Above all else, this example serves to illustrate the manner of how modulation in development may come about via genetic differences in small relatively isolated (genetically speaking) populations, and how such has the potential to translate into morphological variation. If morphological variations can arise during development by the interactions of diverse polymorphic populations, which have remained relatively isolated from each other for long time periods, then understanding this process from a developmental perspective is necessary and directly applicable to deciphering the tempo and mode of morphological evolution. Future work will concentrate on how variation is generated during prenatal development.

8.4 Future directions

The studies conducted here have opened several new avenues of potential research in developmental biology as well as in primate evolutionary biology. As many of the proposed experiments in developmental biology are discussed in Chapters 5-7 they are not discussed here further. It is sufficient to state that conditional inactivation studies are underway and will clarify the spatio-temporal roles of *Pbx* during limb and girdle development.

Future experiments following more closely to those prescribed under an Evo-Devo perspective will involve the use of mouse developmental systems, bioinformatics, comparative primate genomics, as well as *in vitro* methods such as tissue culture experiments. Interestingly, only recently have developmental systems been used to explore the origins of variation in populations. In this regard, experiments will aim to examine how the conditional loss of critical "selector" genes (such as Pbx) results in morphometric differences in skeletal morphology in embryonic and postnatal mice. Many of the protocols for examining morphometric variation have been utilized to investigate limb morphology in mouse models lacking specific gene or combinatorial gene functions. For example, in a collaborative study involving the author, Vidal et al. (2006) examined the morphometric differences in length and width of forelimb skeletal elements in mice lacking critical cell-cycle genes. These studies demonstrate that upon their experimental deletion, disruption of the cell-cycle, resulted in morphometric variation in mice. Similar experiments will be carried out using conditional *Pbx* mutants to examine how their spatio-temporal deletion

results in limb metric variation. This will be performed on several different genetic backgrounds to examine the effects of overall levels of allelic polymorphism on morphological variation.

Coupled with these analyses will be examinations of *cis*- and *trans*-regulatory elements governing Pbx and Hox in mice and, once identified, in primates, which display distinct limb and girdle morphologies. In this regard, if differences can be identified with respect to either individual *Hox* or *Pbx* promoters or for enhancer elements such as the *Hox* ELCR and GCR then tests can be carried out using transgenic mice harboring primate regulatory elements, in a similar fashion to that performed for bats by Cretekos et al. (submitted). Likewise, comparisons of multiple *cis*- and *trans*-regulatory elements upstream of early modular development versus downstream during limb element growth, across different primates, may help determine the nature of developmental evolution in specific primate lineages and gain insight into how some of the complex morphologies have co-evolved during primate evolution. Techniques such as bioinformatics and comparative primate genomics should aid in this process. Finally, studies examining how specific changes in regulatory elements during limb development, specifically if they are found for *Hox* and *Pbx* (and other upstream patterning genes), affect cell behaviors can be accomplished *in vitro* (i.e., in cell cultures such as micromass). Such *in vitro* systems may help identify how modifications alter downstream cellular behaviors such as cell-to-cell communication, adhesion, differentiation, proliferation, death, among others, as they are critical to the process of morphogenesis and the generation of

morphological variation. Overall, these techniques will offer a powerful way to integrate an understanding of genetic evolution, with that of morphology (linking more clearly genotype to phenotype) using model systems, techniques that cannot be performed on primates because above all else, their highly endangered status among mammals.

Figures

Figure 8.1. Model of *Pbx* roles during limb and girdle development.

Line drawings of embryonic limb and limb/girdle regions from E8.5 to E11.75 with each day subdivided into forelimb (top) and hindlimb (bottom) components. Brief roles of Pbx are depicted for the limb (see Fig. 5.29-5.30 and 6.28 for details), whereas for the girdle only cursory outlines are presented (see Figs. 7.20-7.22 for details). Black arrows indicate pathways demonstrated in this thesis while lighter shaded arrows depict hypothetical interactions. At E8.5 and E9.0 (1) depicts the Pbx role upstream of axial *Hox* expression, which aids in providing axial level identity to dermomyotomal cells giving rise to the scapular blade and in specifying the limb location along the axis (e.g., indicated by the level of *Hoxc6* expression posterior to the forelimb). The normal population of dermomyotome (light shade along the axis) is specified by axial *Hox* expression, with a specific anterior subpopulation (darker shade anteriorly) specified by a unique, combinatorial, and still unknown 3' *Hox* pattern. The lighter shaded domain also constitutes the normal *Pbx* expression in this tissue, indicating a cell-autonomous role for Pbx in dermomyotomal specification. At E9.0, (2a) and (2b) during fore- and hindlimb field specification, respectively, Pbx facilitate early mesenchymal interactions through their limb specific affects on Tbx, which in the forelimb domain (also see Figs. 6.28 and 7.20B) and hindlimb domain (also see Figs. 6.28 and 7.22) drastically influence girdle and limb development. At E.9.25 (3a) and (3b) depict Pbx roles in facilitating mesenchymal-ectodermal interactions through their effects on Tbx, Fgf10, and 3' Hox in the mesenchyme and also on Fgf8 and Bmp in the ectoderm (lighter shaded text). These interactions allow for the proper cell signaling to and from the mesoderm and ectoderm and aids in establishing mesenchymal cell populations (specified or not) that eventually give rise to the different compartments of the limb and girdle. At this early stage cellular distance is small across the field and, therefore, early signaling molecules (i.e., Fgfs, Wnts) help establish initial specified zones for the girdle and individual limb compartments. At E9.5-9.75, (4a) and (4b) depict Pbx roles on maintaining the coordinated signaling loop between Fgf10 and Fgf8, its influence on *Hox* and therefore, on *Shh* expression in the forelimb. At E10-10.75, (5a) and (5b) depict a similar ongoing role for Pbx in the hindlimb and on their upstream control of *Hox* and thus *Shh* activation. In the both limb types, *Shh* activation is one required mechanism for the establishment of the ZPA to AER feedback loop. At E11.0-E11.75, (6a) and (6b) depict that the ongoing ZPA to AER feedback loop continues and aids in patterning the skeletal elements of the autopod through the control of 5' *Hox* "reverse" collinearity. Pbx may not play a direct activating role in this regard, although certainly their early influence is required for this later phase of *Hox* activation. See text for a continued discussion of Pbx later roles in the limb and girdle. Proximal (left); anterior (top); FL, Forelimb; HL, Hindlimb.

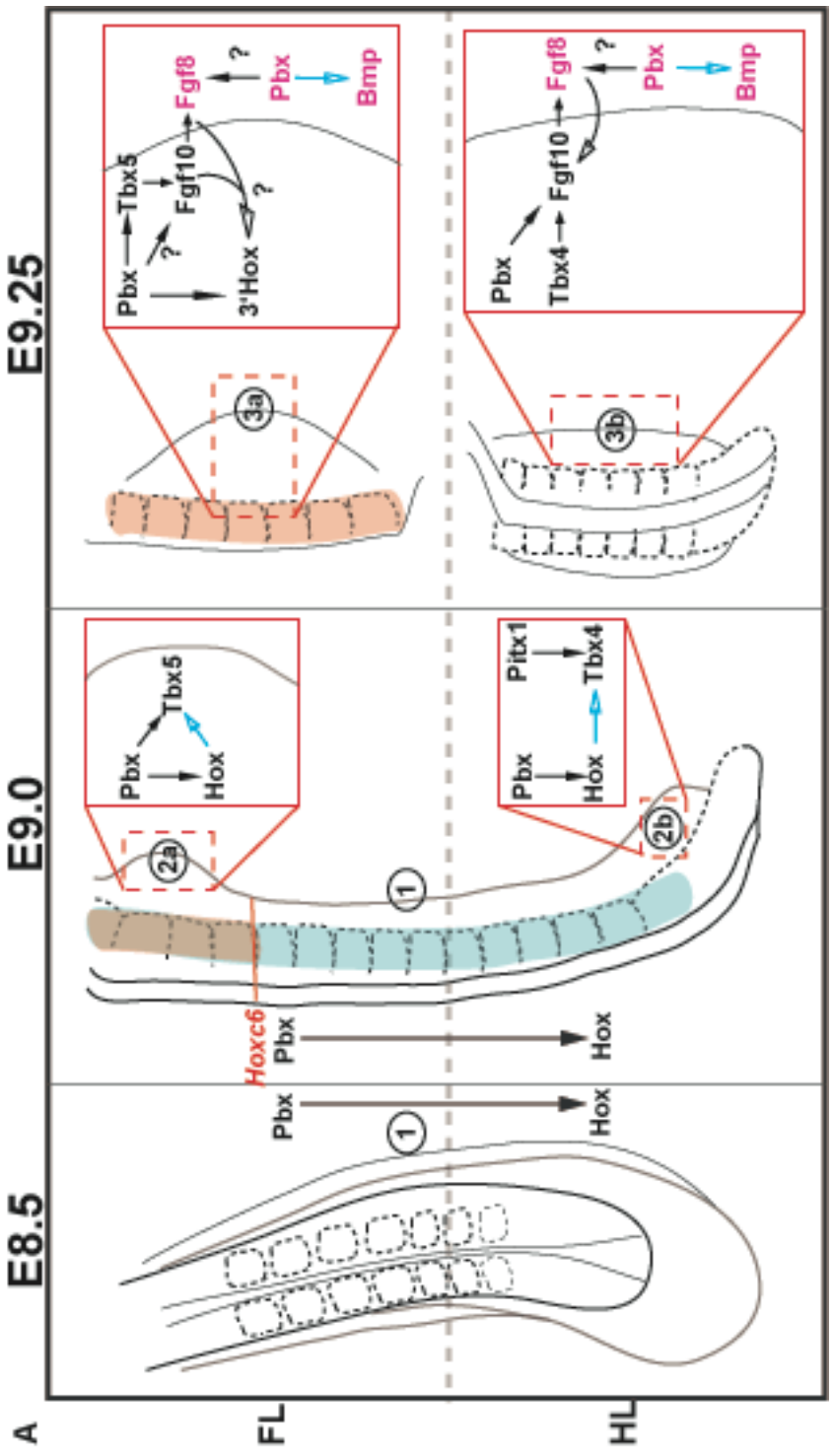
A
FL
HL
E8.5
E9.0
E9.25
Pbx
Hox
Hoxc6
1
2a
2b
3a
3b
Tbx5
Fgf10
Fgf8
Bmp
Tbx4
Pitx1
3'Hox
?

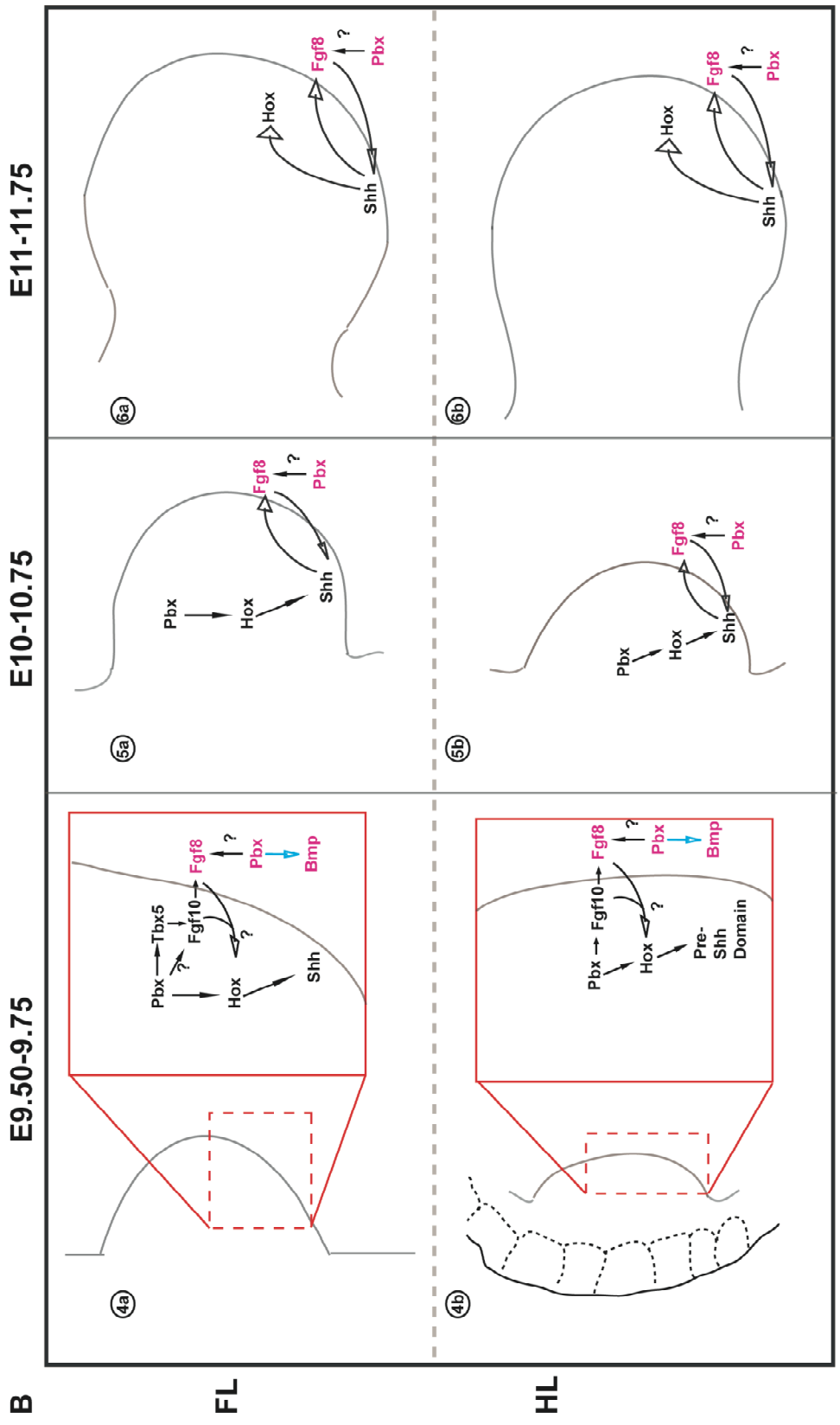
B
E9.50-9.75
E10-10.75
E11-11.75
FL
HL
4a
4b
5a
5b
6a
6b
Pbx
Tbx5
Fgf10
Fgf8
Pbx
Bmp
Hox
Shh
Pre-
Shh
Domain

Figure 8.2. Comparative *Pbx* and *Exd* expression and function in vertebrate and invertebrate appendage development.

Figure depicts comparative Exd/Pbx-mediated, invertebrate (left panels) and vertebrate (right panels) proximal-distal appendage development. Light shaded text denotes ectodermal gene expression while dark shaded text denotes mesenchymal (mesoderm) gene expression. During early appendage development (top), Exd (and Hth, not shown) restrict Dll signaling distally in the invertebrate ectoderm setting up distinct proximal and distal zones. This pattern is different in vertebrates where Pbx in the mesenchyme and/or ectoderm are, at this time, shown to be upstream of the Dll homologs, Dlx. Furthermore, the entire limb is Pbx positive. During mid-appendage development (middle), Hh signaling in the invertebrate posterior ectoderm acts to repress Exd (Hth) to proximal domains and activates other genes distally (not shown), further establishing and compartmentalizing proximal and distal domains. Also, Exd does not appear to be upstream of invertebrate Hox activation in the limb. In vertebrates, Pbx in the limb mesoderm hierarchically regulate Hox, which leads to Shh transcription (not repression) and facilitates later distal patterning. Finally, once adult limb morphology is approximately obtained only the proximal domains of the invertebrate limb are specified by Exd (Hth) activating roles, whereas the entire vertebrate limb requires Pbx functionality. Proximal (left); anterior (top).

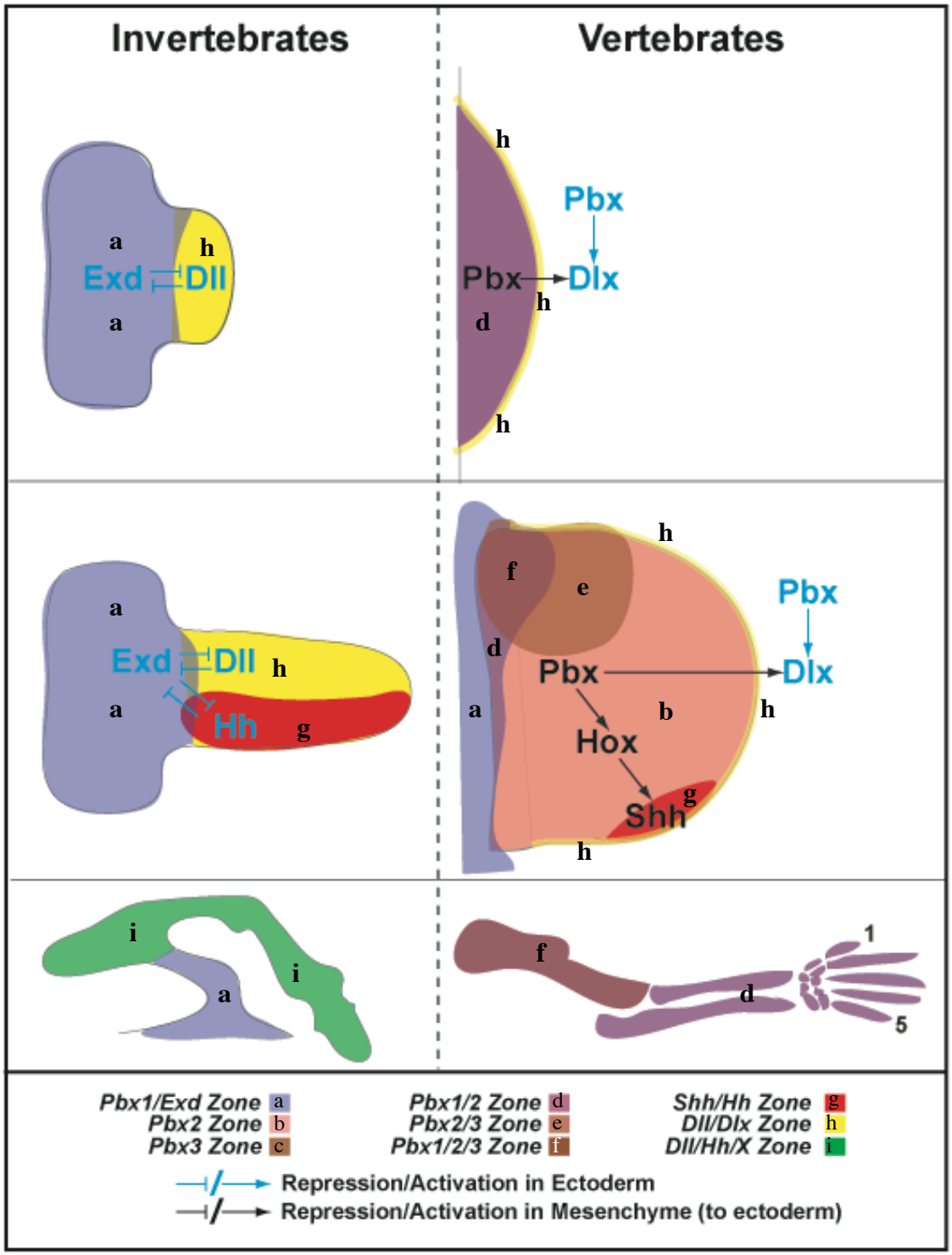
Invertebrates
Vertebrates
a
h
Exd
Dll
a
h
Pbx
Pbx
Dlx
h
d
h
a
h
Exd
Dll
h
a
Hh
g
h
f
e
Pbx
d
Pbx
Dlx
a
b
h
Hox
g
Shh
h
i
i
a
f
d
1
5
Pbx1/Exd Zone a
Pbx2 Zone b
Pbx3 Zone c
Pbx1/2 Zone d
Pbx2/3 Zone e
Pbx1/2/3 Zone f
Shh/Hh Zone g
Dll/Dlx Zone h
Dll/Hh/X Zone i
Repression/Activation in Ectoderm
Repression/Activation in Mesenchyme (to ectoderm)

Figure 8.3. Evolutionary model of *Hox-Shh* modulation during limb development: Heterochronic shifts in early *Hox* collinear activation.

Model depicts the developmental ramifications of altering the onset of early *Hox* collinearity on limb development and morphology. Along the x-axis lies the 3' to 5' *HoxD* cluster organization with individual genes (e.g., d1) and intronic region (i) along with the ELCR and GCR regulatory elements. The y-axis represents the timing of onset of early *Hox* collinearity (and *Shh* activation). The depiction of early collinearity (also shown at E9 and E10 limb stages) corresponds to the skeletal elements specified on the right (e.g., humerus/radius/ulna). Likewise, *Shh* expression (via *Hoxd9-d13* activation), shown as a line underscoring the Hox cluster along the x-axis and during limb bud development (as a dark posteriorly located domain at E10), also corresponds to the skeletal elements that Shh signaling/progenitors directly pattern (e.g., ulna and posterior four digits, the shaded skeletal elements in the skeletal diagram on the right). Finally, *Shh* activation leads to "reverse" *Hox* collinearity (via the GCR function), depicted in different shades in the E11.5 limb bud (lines depict anterior extent of a specific *Hox* activation domain) and corresponding to the skeletal elements that are patterned by this *Hox* phase (e.g., all elements of the autopod, digits 1-5). In this model, normal Hox-based patterning and growth occurs at T=0 (middle) when collinear activation leads to *Shh* activation and late *Hox* "reverse" activation leading to a population average morphology. However, if initial variations arise in early collinearity where it is precociously activated (i.e., at T=-1, bottom) by way of *cis*-regulatory changes at the ELCR (black arrowhead), then *Shh* will be activated earlier and so would late *Hox* collinearity. These changes would lead to an overall spatio-temporal up-regulation of Hox/Shh throughout the duration of proximal-distal and anterior-posterior limb patterning and growth; variations that if selected for would lead to longer elements across all limb compartments in species-specific manners. On the other hand, if there is a temporal delay in early collinearity (i.e., at T=+1, top) skeletal elements may be reduced in size due to a general reduction in Hox and its effects on growth targets. In all illustrations, Proximal (left); anterior (top).

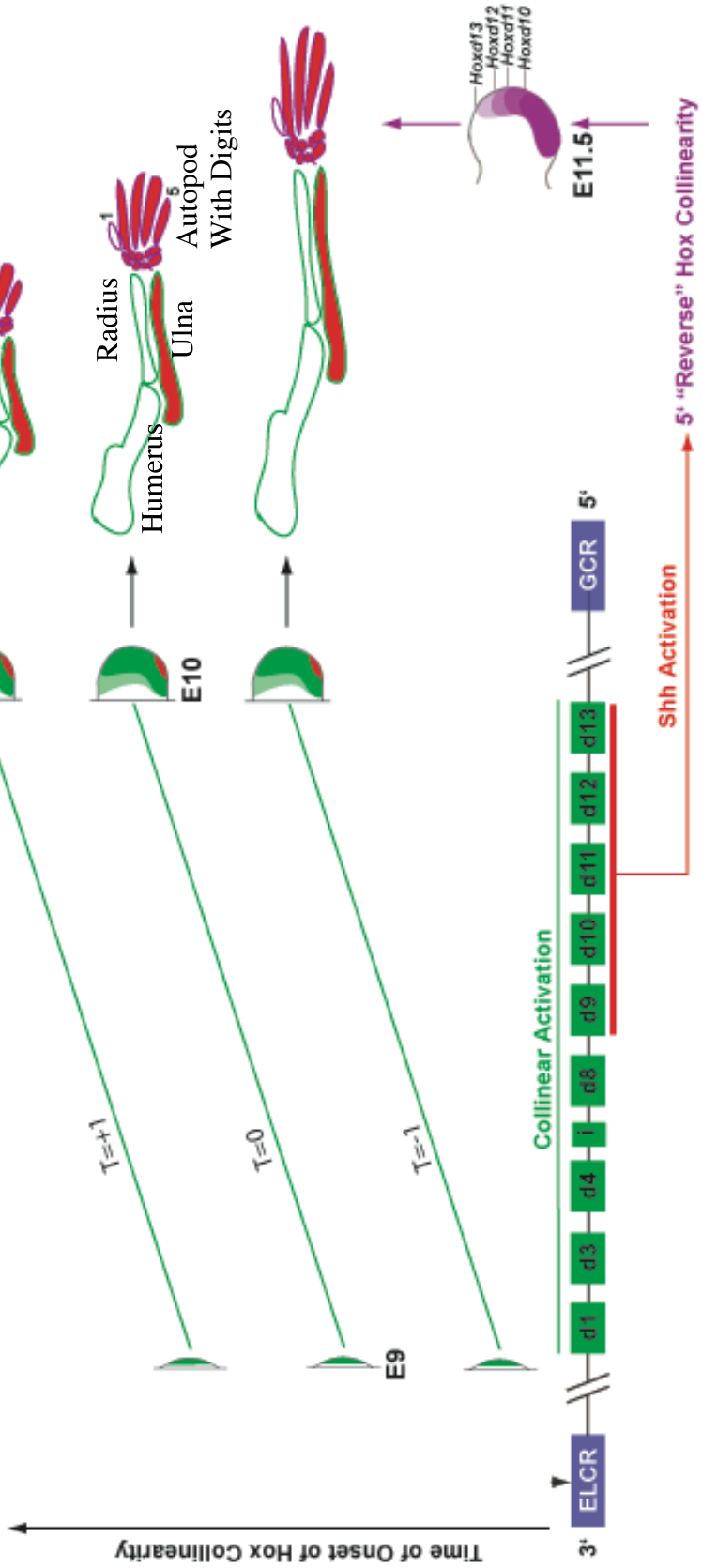
Hoxd13
Hoxd12
Hoxd11
Hoxd10
E11.5
5' "Reverse" Hox Collinearity
Shh Activation
Collinear Activation
5'
GCR
d13
d12
d11
d10
d9
d8
I
d4
d3
d1
ELCR
3'
Time of Onset of Hox Collinearity
T=+1
T=0
T=-1
E9
E10
Humerus
Radius
Ulna
1
5
Autopod
With Digits

Figure 8.4. Evolutionary model of *Hox-Shh* modulation during limb development: Heterochronic rate shifts in early collinear *Hox* expression.

Model depicts the developmental ramifications of altering the rate of early *Hox* collinearity and individual gene transcription on limb development and morphology. See Fig. 8.3 for a description of figure properties. In this model, normal Hox-based patterning and growth occurs as shown in middle leading to a population average morphology. However, if initial variations arise in early collinearity where it is activated at a faster rate and up-regulated (top line with steeper slope) by way of *cis*- or trans-regulatory changes at individual *Hox* promoters (e.g., black arrowhead at d1) for example, then *Shh* will be activated earlier and so would late *Hox* collinearity. These changes would also result in longer limb dimensions across all limb compartments. The opposite may be true for overall reductions in *Hox* transcription across all (or even individual) promoters (bottom line). Proximal (left); anterior (top).

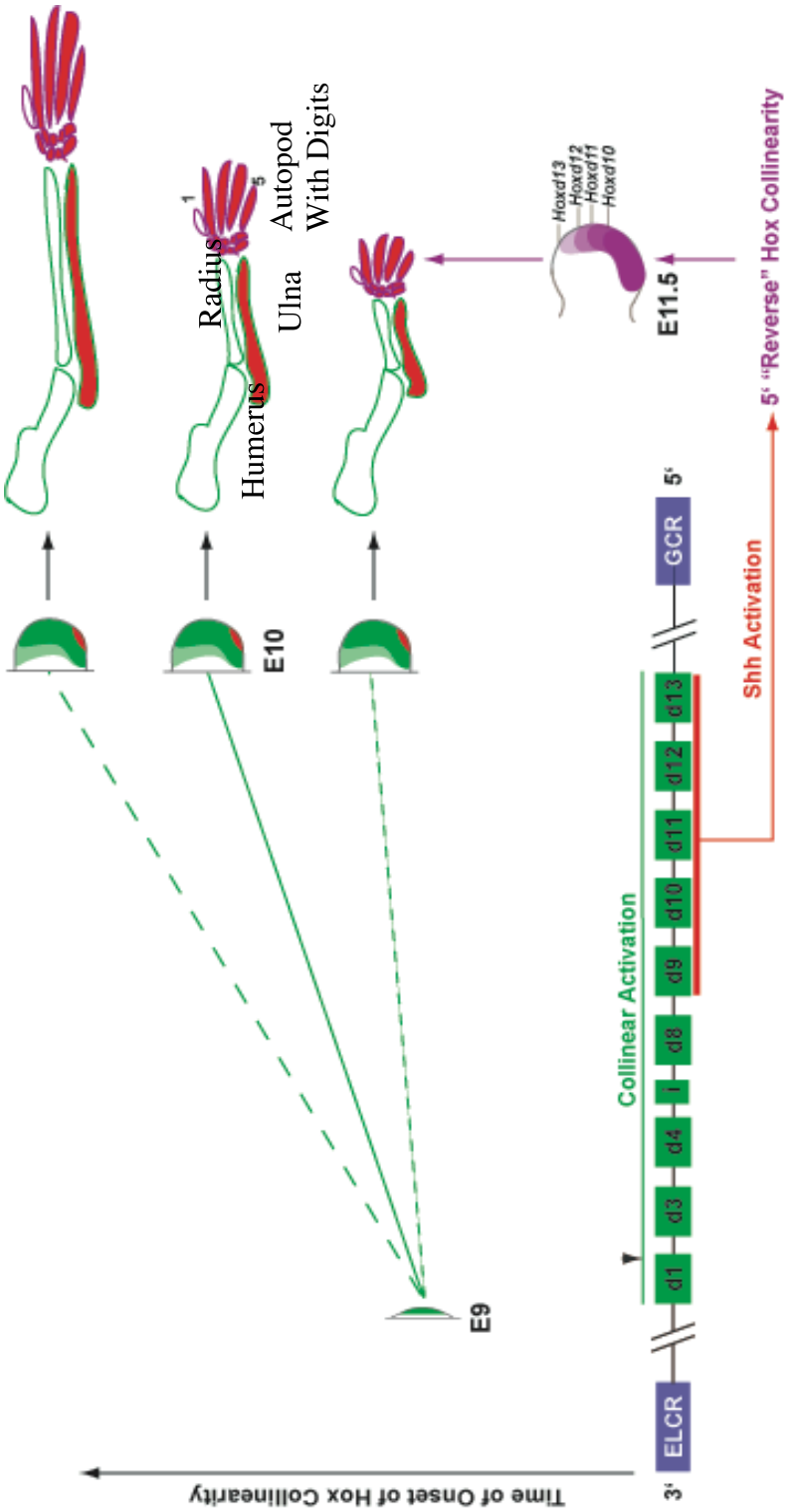
Autopod
With Digits
Radius
Ulna
Humerus
1
5
E10
E9
E11.5
Hoxd13
Hoxd12
Hoxd11
Hoxd10
5' "Reverse" Hox Collinearity
Shh Activation
Collinear Activation
ELCR
GCR
5'
3'
d1
d3
d4
I
d8
d9
d10
d11
d12
d13
Time of Onset of Hox Collinearity

Figure 8.5. Evolutionary model of *Hox-Shh* modulation during limb development: Heterochronic and heterotopic shifts in early collinear *Hox* activation via genomic repositioning.

Model depicts the developmental ramifications of altering the genomic positions of individual *Hox* genes to the ELCR and thus how gene-specific positional changes modify early collinearity, individual gene transcription, as well as limb development and morphology. These repositions would not alter 5' *Hox* distances to the GCR. See Fig. 8.3 for a description of figure properties. In this model, normal Hox-based patterning and growth occurs as shown in the middle panel leading to a population average morphology. However, as in top panel, if initial DNA variations arise (e.g., via mutational deletion) in the intronic region (black arrowhead) such that all 5' *Hox* genes are repositioned nearer to the ELCR, then earlier and more anterior activation of early 5' *Hox*, *Shh*, and late "reverse" *Hox* expression may occur leading to overall increases in limb length. On the other hand, as in bottom panel, if these individual 5' genes are moved further away from the ELCR (e.g., via intronic DNA duplication), a temporal and spatial delay in these *Hox* may ensue, ultimately leading to shorter elements across all limb domains. Proximal (left); anterior (top).

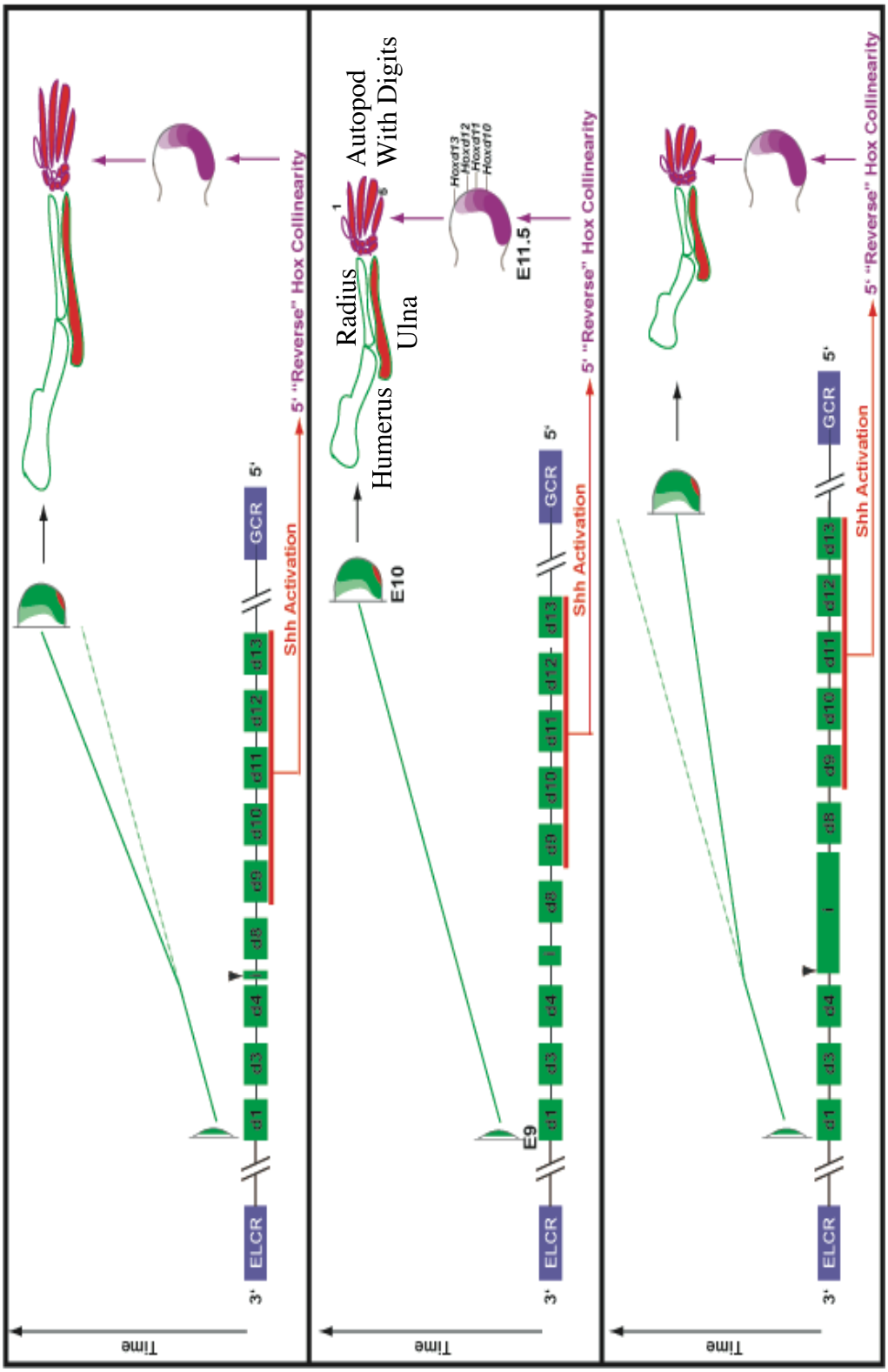
Autopod
With Digits
Radius
Ulna
Humerus
E10
E11.5
E9
Hoxd13
Hoxd12
Hoxd11
Hoxd10
ELCR
GCR
5'
3'
Shh Activation
5' "Reverse" Hox Collinearity
Time

Figure 8.6. Evolutionary model of *Hox-Shh* modulation during limb compartment development: Heterochronic and heterotopic shifts in early collinear *Hox* activation via genomic repositioning.

Model depicts the developmental ramifications of altering the genomic positions of individual *Hox* genes to the ELCR and thus how gene-specific positional changes modify early collinearity, individual gene transcription, and compartmental-specific changes in limb development and morphology. These repositions would alter 3' Hox (up to Hoxd10) distances to the GCR. See Fig. 8.3 for a description of figure properties. In this model, normal Hox-based patterning and growth occurs as shown in the middle panel leading to a population average morphology. As in the top panel, if initial DNA variations arise (i.e., via mutational deletion) in the intergenic DNA between *Hoxd10* and *Hoxd11* (black arrowhead) such that 5' *Hox* genes (i.e., *Hoxd11* to *Hoxd13*) are repositioned nearer to the ELCR (top), then activation of early and specific 5' *Hox* (i.e., *Hoxd1* to *Hoxd10*) may occur normal without altering the expression of *Hoxd9* and *Hoxd10*, 3' of the change. This change would facilitate normal patterning of the stylopod (e.g., humerus). However, earlier activation may ensue for *Hoxd11* to *Hoxd13* leading to up-regulation of *Hox* in zeugopodial domains (i.e., radius and ulna) and increases in growth of this compartment. At the same time, *Shh*, and late "reverse" *Hox* expression may occur earlier leading to overall increases in available Hox for growth targets and thus autopodial length. On the other hand, as in the bottom panel, if *Hoxd11* to *Hoxd13* are positioned further away from the ELCR (e.g., via an intergenic DNA duplication, black arrowhead), a temporal and spatial delay in these *Hox* may ensue, ultimately leading to shorter elements across all limb domains because of a reduction in Hox proteins available to growth targets. Proximal (left); anterior (top).

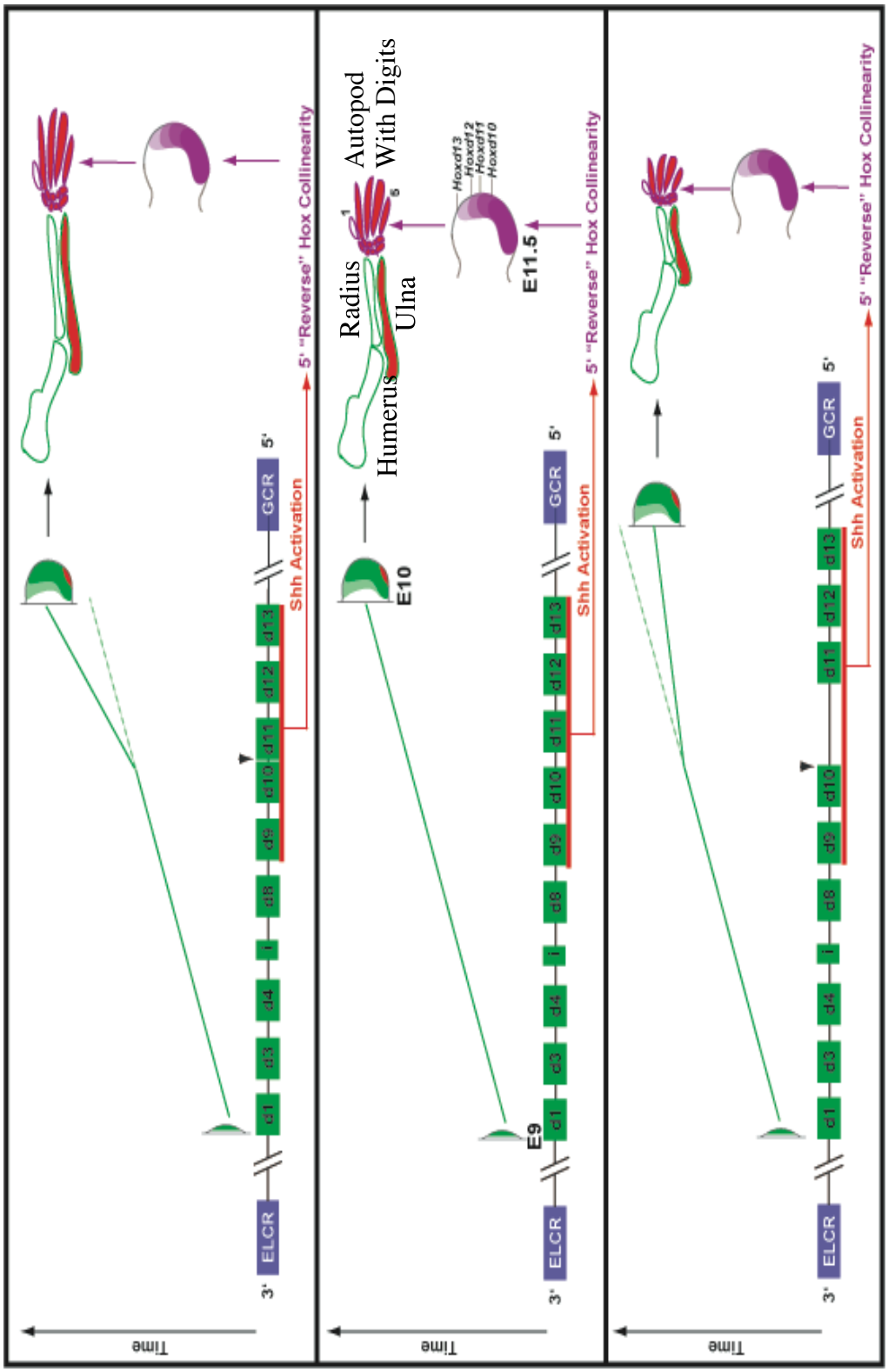
Time
3'
ELCR
d1
d3
d4
i
d8
d9
d10
d11
d12
d13
GCR
5'
Shh Activation
5' "Reverse" Hox Collinearity
E9
E10
E11.5
Radius
Ulna
Humerus
Autopod
With Digits
1
5
Hoxd13
Hoxd12
Hoxd11
Hoxd10

Figure 8.7. Evolutionary model of *Hox-Shh* modulation during limb compartment development: Heterochronic and heterotopic shifts in late collinear *Hox* activation via genomic repositioning.

Model depicts the developmental ramifications of altering the genomic positions of individual *Hox* genes to the GCR and thus how gene-specific positional changes modify late *Hox* collinearity, individual gene transcription, and compartmental-specific changes in limb development and morphology. These repositions would not alter 3' distances to the ELCR and thus in these instances normal early collinear activation, and thus patterning and growth of stylopodial and zeugopodial structures would occur. See Fig. 8.3 for a description of figure properties. In this model, normal Hox-based patterning and growth occurs as shown in the middle panel leading to a population average morphology. However, as in the top panel, if initial DNA variations arise (i.e., via mutational deletion) in the intergenic DNA between *Hoxd13* and the GCR (black arrowhead), bringing all *Hox* genes closer to this regulatory element, then activation of late and specific 5' *Hox* may occur earlier (right). Additionally, as each *Hox* gene promoter is sensitive to this distance, an overall up-regulation of autopodial *Hox* expression may occur, leading to autopod-specific elongations in the skeleton (note overall increased anterior-posterior levels of *Hox* transcript distribution in E11.5 forelimb model, right, as indicated by changes in shading and the large upward facing arrow). On the other hand, as in the bottom panel, if overall *Hox* cluster distance is increased from the GCR (e.g., via an intergenic DNA duplication), a temporal and spatial delay in late *Hox* collinearity may ensue, ultimately leading to shorter elements across all limb domains because of a reduction in Hox proteins available to growth targets (note overall decreased anterior-posterior levels of Hox transcript distribution in E11.5 forelimb model, right, as indicated by changes in shadinf and the large downward facing arrow). Of specific interest is that in this latter model, the most anterior extent of *Hoxd13* expression level would be reduced perhaps resulting in digit one reductions. Proximal (left); anterior (top).

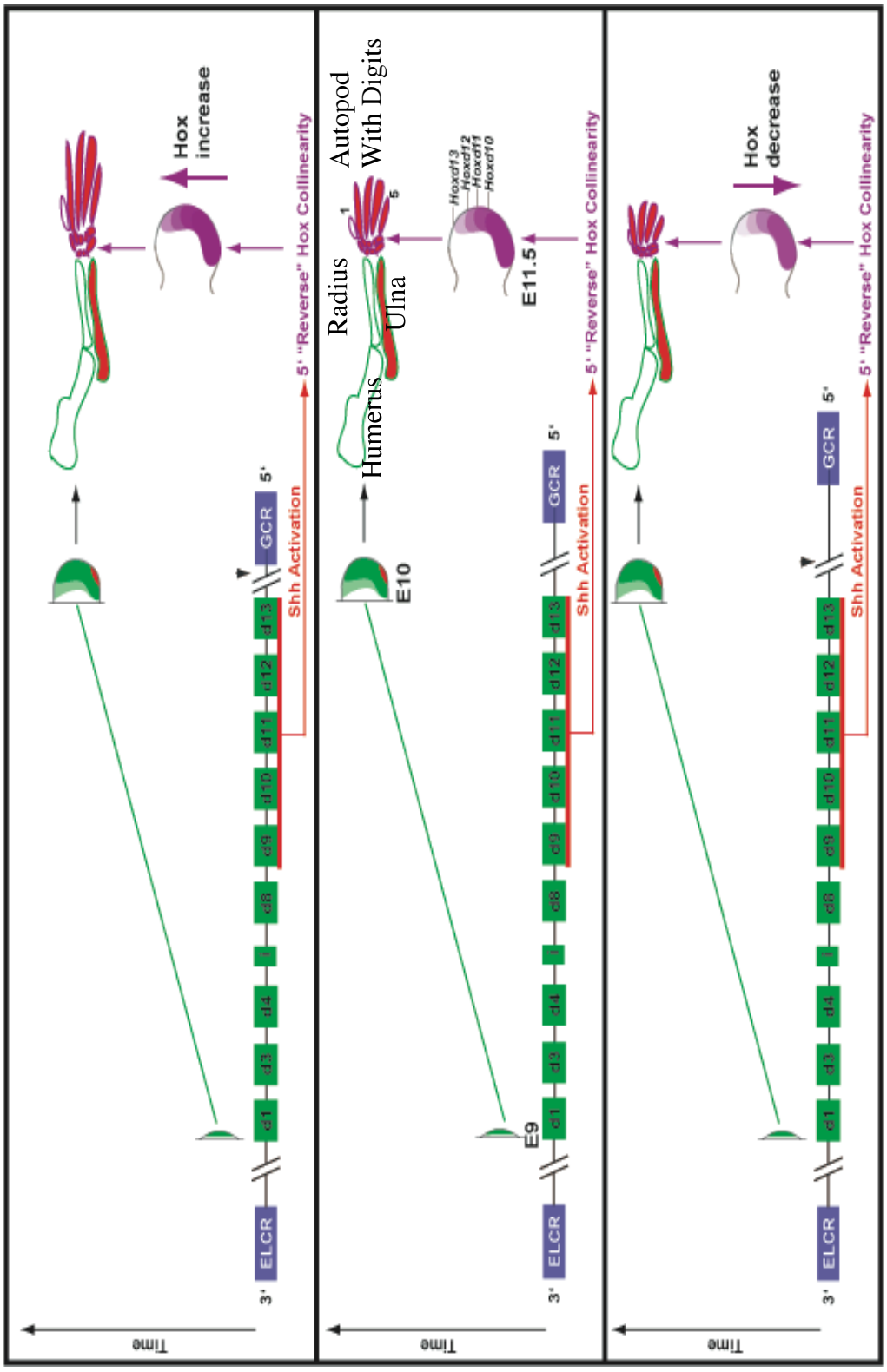
Hox increase
5' "Reverse" Hox Collinearity
Shh Activation
GCR
5'
ELCR
3'
d1
d3
d4
d8
d9
d10
d11
d12
d13
Time
Autopod With Digits
Radius
Ulna
Humerus
E10
E11.5
Hoxd13
Hoxd12
Hoxd11
Hoxd10
E9
Hox decrease

Appendix I

mRNA probe	Selected Reference	Compliments of:
Alx3	Beverdam et al. (2001)	Hubrecht Laboratory
Alx4	Beverdam et al. (2001)	Hubrecht Laboratory
Bmp2	Lyons et al. (1989)	K. Andersons Laboratory
Bmp4	Lyons et al. (1989)	K. Andersons Laboratory
Cart1	Beverdam et al. (2001)	F. Meijlink Laboratory
Cyp26b1	MacLean et al. (2001)	K. Andersons Laboratory
Dlx2	Robinson et al. (1991)	J. Rubenstein Laboratory
Dlx5	Simeone et al. (1994)	J. Rubenstein Laboratory
Dlx6	Simeone et al. (1994)	J. Rubenstein Laboratory
Emx2	Boncinelli et al. (1993)	K. Andersons Laboratory
En-1	Joyner et al. (1985)	K. Andersons Laboratory
Fgf4	Niswander and Martin (1992)	K. Andersons Laboratory
Fgf8	Crossley and Martin (1995)	K. Andersons Laboratory
Fgf10	Tagashira et al. (1997)	K. Andersons Laboratory
Gli3	Walterhouse et al. (1993)	D. Srivastava Laboratory
Grem	Zuniga et al. (1999)	L. Niswander Laboratory
Hand2	Charite et al. (2000)	D. Srivastava laboratory
Hoxa9	Dolle et al. (1989)	M. Capecchi Laboratory
Hoxa10	Dolle et al. (1989)	J. Belmonte Laboratory
Hoxa11	Dolle et al. (1989)	J. Belmonte Laboratory
Hoxa13	Dolle et al. (1989)	P. Gruss Laboratory
Hoxc6	Sharpe et al. (1988)	K. Andersons Laboratory
Hoxd9	Dolle et al. (1989)	M. Capecchi Laboratory
Hoxd10	Dolle et al. (1989)	J. Belmonte Laboratory
Hoxd11	Dolle et al. (1989)	L. Niswander Laboratory
Hoxd12	Dolle et al. (1989)	J. Belmonte Laboratory
Hoxd13	Dolle et al. (1989)	D. Duboule Laboratory
Lmx1b	Riddle et al. (1995)	K. Andersons Laboratory
Meis1	Nakamura et al. (1996)	J. Belmonte Laboratory
Meis2	Nakamura et al. (1996)	J. Belmonte Laboratory
Msx1	Monaghan et al. (1991)	R. Maas Laboratory
Msx2	Monaghan et al. (1991)	L. Niswander Laboratory
MyoD	Sassoon et al. (1989)	C. Fan Laboratory
Pax1	Walther et al. (1991)	K. Andersons Laboratory
Pax9	Wallin et al. (1993)	C. Fan Laboratory
Pbx1	Capellini et al. (2006)	H. Popperl Laboratory
Pbx2	Capellini et al. (2006)	H. Popperl Laboratory
Pbx3	Di Giacomo et al. (2006)	H. Popperl Laboratory
Ptc	Goodrich et al. (1996)	A. McMahon Laboratory
Scx	Cserjesi et al. (1995)	F. Meijlink Laboratory
Shh	Echelard et al. 1993)	A. McMahon Laboratory
Sox9	Wright et al. (1995)	R. Behringer Laboratory
Tbx2	Chapman et al. (1996)	V. Papaioannou Laboratory
Tbx3	Chapman et al. (1996)	V. Papaioannou Laboratory
Tbx4	Chapman et al. (1996)	V. Papaioannou Laboratory
Tbx5	Chapman et al. (1996)	V. Papaioannou Laboratory
Tbx15	Agulnik et al. 1998	F. Meijlink Laboratory
Twist	Wolf et al. (1991)	K. Andersons Laboratory
Wnt7a	Bui et al. (1997)	K. Andersons Laboratory

Glossary of Terms*

Activation (activate): The turning on or initiation of the transcription of a gene.

Analogy (analogous): A functional similarity among nonhomologous organs.

Apical ectodermal ridge (AER): A pseudostratified columnar epithelial layer situated along the anterior-posterior axis at the distal limb bud in tetrapods.

Autonomy: In regards to development, when a structure develops in relative genetic isolation (i.e., outside the influence of other domains of gene expression) from other structures.

Autonomous: When cells have the intrinsic ability to differentiate by way of genes whose products affect only the differentiation or behavior of cells in which they are expressed. In contrast, in cell nonautonomous settings, the product of the gene (e.g., signaling molecules) influences the action of other cells.

Autopod: The distal portion of the vertebrate limb, including the hand/foot and digits.

Bioinformatics: The use of computer science, mathematics, and information theory to model and analyze biological systems, especially systems involving genetic material.

Canalization: The development of an organism or a particular aspect of its biology along a specific probabilistic pathway.

Chondrogenesis: The process of forming cartilage tissues during embryogenesis.

Chromosomal translocation: A chromosomal rearrangement caused by the interchange of parts between nonhomologous chromosomes.

Cis-regulatory elements: Regions of DNA or RNA that regulate the expression of genes located on that same strand.

Cofactors: In regard to DNA binding, a protein that forms dimeric or trimeric complexes with other proteins (e.g., Hox) to facilitate and improve the affinity of their DNA binding.

Compound mutant: A mouse lacking different alleles from several distinct genetic loci.

Conditional inactivation: Experimental deletion of a gene in a spatio-temporal distinct fashion typically using the Cre-Lox system.

Developmental genetics: A discipline that examines how the genotype is transformed into the phenotype.

Differentiation: The process by which a relatively naïve cell transforms into a specific cell type (with specific cell function).

Discrete functionality: In regards to genetic or biochemical function, the idea that a single molecule (e.g., gene or protein) has a specific definable role independent from any homologous family member.

Dorsal ectoderm (DE): A columnar epithelial tissue in the limb, covering the dorsal surface, which is known to express genes that determine dorsal aspects of the appendage. It is typically regarded to as a signaling center.

Dosage: The number of functional copies of a gene present in a cell's nucleus.

Ectoderm: The outer tissue layer of the animal embryo that gives rise to the epidermis and the nervous system.

Ectopic expression: Expression of a gene or protein in domains where it is normally or endogenously expressed.

Enhancer: A region of DNA that can be bound with proteins (namely, the trans-acting factors) to enhance transcription levels of genes in a gene-cluster.

Epithelial-mesenchymal interactions: Tissue interactions between two types (epithelium and mesenchyme) that often lead to the formation of an organ or structure. Often, signaling molecules play critical roles in these interactions.

Epithelium (epithelial): Sheets or tubes of connected cells.

Evolutionary Developmental (Evo-Devo) Biology: A discipline that compares the developmental processes of different animals and plants in an attempt to determine the ancestral relationship between organisms and how developmental processes evolved.

Evolvability: A concept that relates to the ability of a particular genotype to evolve new adaptive changes.

Exon: Any region of DNA within a gene that is transcribed to the final messenger RNA (mRNA) molecule, rather than being spliced out from the transcribed RNA molecule.

Functional redundancy: In regards to genetic or biochemical function, the idea that a single molecule (e.g., gene or protein) shares roles with other homologous family members.

Gene targeting: A method of artificially interfering with the action of a specific gene (typically during development).

Genotype: The specific genetic makeup of an individual at a specific genetic locus, in the form of DNA.

Heterochronic shift: A change in the timing of a developmental event. In regards to gene action, a temporal change in the initiation, duration, or termination of a gene's expression.

Heterotopic shift: A change in the spatial extent of a developmental event. In regards to gene action, a spatial change in the initiation of a gene's expression.

Histomorphogenesis: The development of histological structure and shape of histological regions.

Homeobox: A 180 base pair region of DNA encoding a particular class of DNA-binding domains.

Homeodomain protein: A protein (class) that contains a specific domain called the homeodomain encoded by the homeobox gene sequence.

Homologous recombination: The process by which two chromosomes, paired up during prophase 1 of meiosis, exchange some distal portion of their DNA. Typically this process is exploited during the production of a "knockout" mouse using gene targeting strategies.

Homology (homologous): Structures that are alike due to their common genetic heritage.

Hox genes: Homeotic, homeobox-containing genes found in linked clusters in all bilaterians.

Identity: In regards to cellular biology, a particular state of a cell as determined by its position within a morphogenetic field.

Imaginal disc: Small sets of epithelial cells that are set aside during Drosophila embryogenesis, subsequently proliferate in the larvae, and give rise to adult structures (e.g., the leg or wing).

Integration: The degree to which structures a developmentally (and/or functionally) interconnected.

Intergenic DNA: DNA sequences located between functional genes, that may or may not contain regulatory elements.

Intermediate mesoderm: Mesoderm in vertebrate embryos that give rise to the urogenital system.

Intron: Sections of DNA that will be spliced out after transcription, but before the RNA is used.

Knockout mouse: A genetically engineered mouse with one or more genes that have been made inoperable through gene targeting.

Lateral plate mesoderm: Mesoderm in vertebrate embryos that give rise to the blood, heart tissues, lining of the body cavities, and limbs.

Mesenchyme: A loosely organized group of cells that are remain relatively unconnected from one another.

Mesoderm: A middle germ layer in the embryo that is sandwiched between the endoderm (inner) and ectoderm (outer) and gives rise to various tissues including, blood, heart, kidneys, gonads, bones, and connective tissues.

Mis-expression: When a gene or protein is expressed in a domain where it is not normally expressed. Typically, mis-expression studies use bead implants or express the gene under the promoter of another gene during embryogenesis.

Model systems: A select number of organisms that possess special properties which allow them to be studied from a developmental perspective. See text.

Modularity or modular system: A system in biology that consists of relatively autonomous parts or modules.

Morphogen: A substance governing the pattern of tissue development and, in particular, the positions of the various specialized cell types within a tissue. It spreads from a localized source and forms a concentration gradient across a developing tissue.

Morphogenesis: The process by which the shapes of tissues, organs, and entire organisms develop as well as how the positions of the various specialized cell types emerge within these structures.

Morphogenetic fields: A group of cells whose position and fate are specified with respect to the same set of boundaries.

Non-coding regions: Regions of DNA that do not contain instructions for making proteins but can be involved in gene regulation or have no known function.

Organogenesis: The process by which the ectoderm, endoderm, and mesoderm develop into the organs of the organism.

Orthology (orthologous/ortholog): Homology in gene sequence that results from a speciation event: if a gene exists in a species, and that species diverges into two species, then the divergent copies of this gene in the resulting species are orthologous and each is an ortholog of the other.

Paraxial mesoderm: Mesodermal tissue in the vertebrate embryo that gives rise to the somites (and their derivatives).

Phenotype: An organisms total physical appearance and constitution or a specific manifestation of a trait, such as size, eye color, or behavior that varies between individuals. Phenotype is determined to a large extent by genotype, or by the identity of the alleles that an individual carries at one or more positions on the chromosomes. In developmental biology, often the phenotype is referred to as that which departs from normal condition.

Paralogy (paralogous/paralog): Homology in gene sequence that results from a gene duplication event: if a gene in an organism is duplicated to occupy two different positions in the same genome, then the two copies are paralogous and each is a paralog of the other

Patterning: The process by which cells in a developing embryo acquire identities that lead to well ordered spatial arrangements (patterns) of cell activities. This process occurs through genetic and epigenetic mechanisms.

Phenocopy: A manifestation of a characteristic (generally referring to a single trait) that arises under a particular environmental and/or genetic condition, which is identical to another phenotype determined by a separate environmental and/or genetic condition.

Phylotypic stage: A stage of development during which different embryos of different species look morphologically similar to each other.

Pleiotropy (pleiotropic): When a single gene influences multiple phenotypic traits.

Positional information: The instructions that are given and interpreted by cells to determine their differentiation in respect of their position relative to other parts of the organism. This concept is usually used in relation to morphogenetic fields.

Post-translational modification: A chemical modification of a protein after its translation. It is one of the later steps in protein biosynthesis for many proteins.

Progress zone (PZ): An undifferentiated population of mesenchymal cells subjacent (proximally) to the apical ectodermal ridge of the limb bud from which the successive parts of the limb are laid down in a proximodistal sequence.

Promoter: A region of DNA upstream of the coding region of a gene to which RNA polymerase binds before initiating gene transcription.

Regulative development: In regards to cellular determination, the concept that cell fate is determined by the process of cell-cell interactions as they occur during development.

Repression (repress): Inhibition of the transcription of a gene by the binding of a protein (the product of a regulatory gene) to its promoter region (the transcription initiation site). Repressor proteins block RNA polymerase from binding to the promoter region, thus "switching off" the gene and preventing mRNA production.

Selector gene: A gene that controls cell-fate.

Signaling molecules: A chemical (e.g., a morphogen) involved in transmitting information between cells.

Skeletogenesis: The process of forming the cartilaginous and osseous skeleton of an organism.

Specification: During the process of deciding a cell's fate, a cell can be first specified (specification) and after determined (determination). Specification is the process involved in the initial commitment of a cell to a particular fate. This process is not permanent but can be reversible. Once specification has taken place, a cell will be partially committed to differentiate down a specific pathway if left in its normal environment. Determination is the process by which a cell's fate is sealed, that is the cell is irreversibly committed to a particular fate.

Structural-coding regions: Regions of DNA that contain instructions for making proteins.

Stylopod: the proximal-most segment of the limb proper that corresponds to the brachium (humerus or upperarm) in the forelimb and thigh (femur or upperlimb) in the hindlimb, and the associated structures composed of soft tissues (muscles, nerves and blood vessels, etc.).

Submodules: Compartments within a developmental module that have relative genetic autonomous but functionally interact within the module (e.g., the ZPA and the AER of the limb).

Target genes: Genes that lie downstream and are directly regulated (biochemically) by upstream genes and their protein products.

Transcription factors: A protein that mediates the binding of RNA polymerase and the initiation of transcription. A transcription factor may work to either stimulate or repress transcription of a gene.

Transgenic organism: Animals produced with externally introduced genes either from a different organism or the same.

Trans-regulatory elements: Molecules that may modify the expression of genes distant from the gene that was originally transcribed to create them.

Triple-acid loop extension (TALE) homeodomain proteins: A protein class characterized by an atypical homeodomain that has three extra amino acids in the homeodomain that loop out between helices I and II. Usually the three amino acids are proline-tyrosine-proline. The function of this loop is still unknown.

Zeugopod: The second segment of the paired limb (in the proximodistal direction), which includes the antebrachium (radius and the ulna) in the forelimb, and the crus (tibia and fibula) in the hindlimb, and the associated structures composed of soft tissues (muscles, nerves and blood vessels, etc.).

Zone of polarizing activity (ZPA): A small group of mesenchymal cells that is located at the posterior margin of the developing limb bud and that produces a substance (i.e., Shh), that provides positional information to the developing limb bud. It is a classical signaling center in the limb, and was originally defined as those cells in the posterior limb mesenchyme that were capable of inducing mirror-image digit duplications when placed in the anterior limb margin.

* Glossary compiled from definitions adapted from the following sources: Carroll et al. (2006); en.wikipedia.org/; Gilbert (2006); Liem et al. (2001); Moens and Selleri (2006); and www.biology-online.org/.

References

Abu-Abed, S., MacLean, G., Fraulob, V., Chambon, P., Petkovich, M. and Dolle, P. (2002). Differential expression of the retinoic acid-metabolizing enzymes CYP26A1 and CYP26B1 during murine organogenesis. *Mech Dev* **110**, 173-7.

Abu-Shaar, M., Ryoo, H. D. and Mann, R. S. (1999). Control of the nuclear localization of Extradenticle by competing nuclear import and export signals. *Genes Dev* **13**, 935-45.

Adamska, M., MacDonald, B. T. and Meisler, M. H. (2003). Doubleridge, a mouse mutant with defective compaction of the apical ectodermal ridge and normal dorsal-ventral patterning of the limb. *Dev Biol* **255**, 350-62.

Adamska, M., MacDonald, B. T., Sarmast, Z. H., Oliver, E. R. and Meisler, M. H. (2004). En1 and Wnt7a interact with Dkk1 during limb development in the mouse. *Dev Biol* **272**, 134-44.

Adham, I. M., Gille, M., Gamel, A. J., Reis, A., Dressel, R., Steding, G., Brand-Saberi, B. and Engel, W. (2005). The scoliosis (sco) mouse: a new allele of Pax1. *Cytogenet Genome Res* **111**, 16-26.

Agarwal, P., Wylie, J. N., Galceran, J., Arkhitko, O., Li, C., Deng, C., Grosschedl, R. and Bruneau, B. G. (2003). Tbx5 is essential for forelimb bud initiation following patterning of the limb field in the mouse embryo. *Development* **130**, 623-33.

Agulnik, S. I., Papaioannou, V. E. and Silver, L. M. (1998). Cloning, mapping, and expression analysis of TBX15, a new member of the T-Box gene family. *Genomics* **51**, 68-75.

Ahn, D. G., Kourakis, M. J., Rohde, L. A., Silver, L. M. and Ho, R. K. (2002). T-box gene tbx5 is essential for formation of the pectoral limb bud. *Nature* **417**, 754-8.

Ahn, K., Mishina, Y., Hanks, M. C., Behringer, R. R. and Crenshaw, E. B., 3rd. (2001). BMPR-IA signaling is required for the formation of the apical ectodermal ridge and dorsal-ventral patterning of the limb. *Development* **128**, 4449-61.

Ahn, S. and Joyner, A. L. (2004). Dynamic changes in the response of cells to positive hedgehog signaling during mouse limb patterning. *Cell* **118**, 505-16.

Allen, T. D., Zhu, Y. X., Hawley, T. S. and Hawley, R. G. (2000). TALE homeoproteins as HOX11-interacting partners in T-cell leukemia. *Leuk Lymphoma* **39**, 241-56.

Altabef, M., Clarke, J. D. and Tickle, C. (1997). Dorso-ventral ectodermal compartments and origin of apical ectodermal ridge in developing chick limb. *Development* **124**, 4547-56.

Arenkiel, B. R., Gaufo, G. O. and Capecchi, M. R. (2003). Hoxb1 neural crest preferentially form glia of the PNS. *Dev Dyn* **227**, 379-86.

Aubin, J., Lemieux, M., Moreau, J., Lapointe, J. and Jeannotte, L. (2002). Cooperation of Hoxa5 and Pax1 genes during formation of the pectoral girdle. *Dev Biol* **244**, 96-113.

Aubin, J., Lemieux, M., Tremblay, M., Berard, J. and Jeannotte, L. (1997). Early postnatal lethality in Hoxa-5 mutant mice is attributable to respiratory tract defects. *Dev Biol* **192**, 432-45.

Azcoitia, V., Aracil, M., Martinez, A. C. and Torres, M. (2005). The homeodomain protein Meis1 is essential for definitive hematopoiesis and vascular patterning in the mouse embryo. *Dev Biol* **280**, 307-20.

Balling, R. (1994). The undulated mouse and the development of the vertebral column. Is there a human PAX-1 homologue? *Clin Dysmorphol* **3**, 185-91.

Barna, M., Pandolfi, P. P. and Niswander, L. (2005). Gli3 and Plzf cooperate in proximal limb patterning at early stages of limb development. *Nature* **436**, 277-81.

Barrow, J. R., Thomas, K. R., Boussadia-Zahui, O., Moore, R., Kemler, R., Capecchi, M. R. and McMahon, A. P. (2003). Ectodermal Wnt3/beta-catenin signaling is required for the establishment and maintenance of the apical ectodermal ridge. *Genes Dev* **17**, 394-409.

Bejder, L. and Hall, B. K. (2002). Limbs in whales and limblessness in other vertebrates: mechanisms of evolutionary and developmental transformation and loss. *Evol Dev* **4**, 445-58.

Bell, E., Gasseling, M. T., Saunders, J. W., Jr. and Zwilling, E. (1962). On the role of ectoderm in limb development. *Dev Biol* **4**, 177-96.

Bell, E., Saunders, J. W., Jr. and Zwilling, E. (1959). Limb development in the absence of ectodermal ridge. *Nature* **184(Suppl 22)**, 1736-7.

Bell, S. M., Schreiner, C. M. and Scott, W. J. (1998). The loss of ventral ectoderm identity correlates with the inability to form an AER in the legless hindlimb bud. *Mech Dev* **74**, 41-50.

Berkes, C. A., Bergstrom, D. A., Penn, B. H., Seaver, K. J., Knoepfler, P. S. and Tapscott, S. J. (2004). Pbx marks genes for activation by MyoD indicating a role for a homeodomain protein in establishing myogenic potential. *Mol Cell* **14**, 465-77.

Berthelsen, J., Kilstrup-Nielsen, C., Blasi, F., Mavilio, F. and Zappavigna, V. (1999). The subcellular localization of PBX1 and EXD proteins depends on nuclear import and export signals and is modulated by association with PREP1 and HTH. *Genes Dev* **13**, 946-53.

Berthelsen, J., Viggiano, L., Schulz, H., Ferretti, E., Consalez, G. G., Rocchi, M. and Blasi, F. (1998a). PKNOX1, a gene encoding PREP1, a new regulator of Pbx activity, maps on human chromosome 21q22.3 and murine chromosome 17B/C. *Genomics* **47**, 323-4.

Berthelsen, J., Zappavigna, V., Ferretti, E., Mavilio, F. and Blasi, F. (1998b). The novel homeoprotein Prep1 modulates Pbx-Hox protein cooperativity. *Embo J* **17**, 1434-45.

Berthelsen, J., Zappavigna, V., Mavilio, F. and Blasi, F. (1998c). Prep1, a novel functional partner of Pbx proteins. *Embo J* **17**, 1423-33.

Beverdam, A. and Meijlink, F. (2001). Expression patterns of group-I aristaless-related genes during craniofacial and limb development. *Mech Dev* **107**, 163-7.

Bi, W., Deng, J. M., Zhang, Z., Behringer, R. R. and de Crombrugghe, B. (1999). Sox9 is required for cartilage formation. *Nat Genet* **22**, 85-9.

Bickmore, W. A., Mahy, N. L. and Chambeyron, S. (2004). Do higher-order chromatin structure and nuclear reorganization play a role in regulating Hox gene expression during development? *Cold Spring Harb Symp Quant Biol* **69**, 251-7.

Boncinelli, E., Gulisano, M. and Broccoli, V. (1993). Emx and Otx homeobox genes in the developing mouse brain. *J Neurobiol* **24**, 1356-66.

Borrow, J., Shearman, A. M., Stanton, V. P., Jr., Becher, R., Collins, T., Williams, A. J., Dube, I., Katz, F., Kwong, Y. L., Morris, C. et al. (1996). The t(7;11)(p15;p15) translocation in acute myeloid leukaemia fuses the genes for nucleoporin NUP98 and class I homeoprotein HOXA9. *Nat Genet* **12**, 159-67.

Bouchard, M., Souabni, A., Mandler, M., Neubuser, A. and Busslinger, M. (2002). Nephric lineage specification by Pax2 and Pax8. *Genes Dev* **16**, 2958-70.

Boulet, A. M. and Capecchi, M. R. (2002). Duplication of the Hoxd11 gene causes alterations in the axial and appendicular skeleton of the mouse. *Dev Biol* **249**, 96-107.

Boulet, A. M. and Capecchi, M. R. (2004). Multiple roles of Hoxa11 and Hoxd11 in the formation of the mammalian forelimb zeugopod. *Development* **131**, 299-309.

Boulet, A. M., Moon, A. M., Arenkiel, B. R. and Capecchi, M. R. (2004). The roles of Fgf4 and Fgf8 in limb bud initiation and outgrowth. *Dev Biol* **273**, 361-72.

Bowen, J., Hinchliffe, J. R., Horder, T. J. and Reeve, A. M. (1989). The fate map of the chick forelimb-bud and its bearing on hypothesized developmental control mechanisms. *Anat Embryol (Berl)* **179**, 269-83.

Brendolan, A., Ferretti, E., Salsi, V., Moses, K., Quaggin, S., Blasi, F., Cleary, M. L. and Selleri, L. (2005). A Pbx1-dependent genetic and transcriptional network regulates spleen ontogeny. *Development* **132**, 3113-26.

Brent, A. E., Schweitzer, R. and Tabin, C. J. (2003). A somitic compartment of tendon progenitors. *Cell* **113**, 235-48.

Brooke, N. M., Garcia-Fernandez, J. and Holland, P. W. (1998). The ParaHox gene cluster is an evolutionary sister of the Hox gene cluster. *Nature* **392**, 920-2.

Bui, T. D., Lako, M., Lejeune, S., Curtis, A. R., Strachan, T., Lindsay, S. and Harris, A. L. (1997). Isolation of a full-length human WNT7A gene implicated in limb development and cell transformation, and mapping to chromosome 3p25. *Gene* **189**, 25-9.

Burglin, T. R. (1997). Analysis of TALE superclass homeobox genes (MEIS, PBC, KNOX, Iroquois, TGIF) reveals a novel domain conserved between plants and animals. *Nucleic Acids Res* **25**, 4173-80.

Burglin, T. R. (1998). The PBC domain contains a MEINOX domain: coevolution of Hox and TALE homeobox genes? *Dev Genes Evol* **208**, 113-6.

Burglin, T. R. (2005). Homeodomain proteins. In Meyers, R.A. (ed.) *Encyclopedia of Molecular Cell Biology and Molecular Medicine.* Wiley-VCH **6**, pp.179-222.

Burke, A. C., Nelson, C. E., Morgan, B. A. and Tabin, C. (1995). Hox genes and the evolution of vertebrate axial morphology. *Development* **121**, 333-46.

Cao, R., Tsukada, Y. and Zhang, Y. (2005). Role of Bmi-1 and Ring1A in H2A ubiquitylation and Hox gene silencing. *Mol Cell* **20**, 845-54.

Capdevila, J. and Izpisua Belmonte, J. C. (2001). Patterning mechanisms controlling vertebrate limb development. *Annu Rev Cell Dev Biol* **17**, 87-132.

Capdevila, J., Tsukui, T., Rodriquez Esteban, C., Zappavigna, V. and Izpisua Belmonte, J. C. (1999). Control of vertebrate limb outgrowth by the proximal factor Meis2 and distal antagonism of BMPs by Gremlin. *Mol Cell* **4**, 839-49.

Capecchi, M. R. (1997). Hox genes and mammalian development. *Cold Spring Harb Symp Quant Biol* **62**, 273-81.

Capellini, T. D., Di Giacomo, G., Salsi, V., Brendolan, A., Ferretti, E., Srivastava, D., Zappavigna, V. and Selleri, L. (2006). Pbx1/Pbx2 requirement for distal limb patterning is mediated by the hierarchical control of Hox gene spatial distribution and Shh expression. *Development* **133**, 2263-73.

Carlson, B. M. (1975). The effects of rotation and positional change of stump tissues upon morphogenesis of the regenerating axolotl limb. *Dev Biol* **47**, 269-91.

Carpenter, E. M., Goddard, J. M., Chisaka, O., Manley, N. R. and Capecchi, M. R. (1993). Loss of Hox-A1 (Hox-1.6) function results in the reorganization of the murine hindbrain. *Development* **118**, 1063-75.

Carpenter, E. M., Goddard, J. M., Davis, A. P., Nguyen, T. P. and Capecchi, M. R. (1997). Targeted disruption of Hoxd-10 affects mouse hindlimb development. *Development* **124**, 4505-14.

Carroll, S., Grenier, J. K. and Weatherbee, S. D. (2005). *From DNA to Diversity: Molecular Genetics and the Evolution of Animal Design*, 2nd Edition. Blackwell Science; New York. pp.viii-258.

Chan, S. K., Jaffe, L., Capovilla, M., Botas, J. and Mann, R. S. (1994). The DNA binding specificity of Ultrabithorax is modulated by cooperative interactions with extradenticle, another homeoprotein. *Cell* **78**, 603-15.

Chan, S. K., Popperl, H., Krumlauf, R. and Mann, R. S. (1996). An extradenticle-induced conformational change in a HOX protein overcomes an inhibitory function of the conserved hexapeptide motif. *Embo J* **15**, 2476-87.

Chan, S. K., Ryoo, H. D., Gould, A., Krumlauf, R. and Mann, R. S. (1997). Switching the in vivo specificity of a minimal Hox-responsive element. *Development* **124**, 2007-14.

Chang, C. P., de Vivo, I. and Cleary, M. L. (1997a). The Hox cooperativity motif of the chimeric oncoprotein E2a-Pbx1 is necessary and sufficient for oncogenesis. *Mol Cell Biol* **17**, 81-8.

Chang, C. P., Jacobs, Y., Nakamura, T., Jenkins, N. A., Copeland, N. G. and Cleary, M. L. (1997b). Meis proteins are major in vivo DNA binding partners for wild-type but not chimeric Pbx proteins. *Mol Cell Biol* **17**, 5679-87.

Chang, C. P., Shen, W. F., Rozenfeld, S., Lawrence, H. J., Largman, C. and Cleary, M. L. (1995). Pbx proteins display hexapeptide-dependent cooperative DNA binding with a subset of Hox proteins. *Genes Dev* **9**, 663-74.

Chapman, D. L., Garvey, N., Hancock, S., Alexiou, M., Agulnik, S. I., Gibson-Brown, J. J., Cebra-Thomas, J., Bollag, R. J., Silver, L. M. and Papaioannou, V. E. (1996). Expression of the T-box family genes, Tbx1-Tbx5, during early mouse development. *Dev Dyn* **206**, 379-90.

Charite, J., de Graaff, W., Shen, S. and Deschamps, J. (1994). Ectopic expression of Hoxb-8 causes duplication of the ZPA in the forelimb and homeotic transformation of axial structures. *Cell* **78**, 589-601.

Charite, J., McFadden, D. G. and Olson, E. N. (2000). The bHLH transcription factor dHAND controls Sonic hedgehog expression and establishment of the zone of polarizing activity during limb development. *Development* **127**, 2461-70.

Chen, C. H., Cretekos, C. J., Rasweiler, J. J. t. and Behringer, R. R. (2005). Hoxd13 expression in the developing limbs of the short-tailed fruit bat, Carollia perspicillata. *Evol Dev* **7**, 130-41.

Chen, F. and Capecchi, M. R. (1997). Targeted mutations in hoxa-9 and hoxb-9 reveal synergistic interactions. *Dev Biol* **181**, 186-96.

Chen, F., Greer, J. and Capecchi, M. R. (1998a). Analysis of Hoxa7/Hoxb7 mutants suggests periodicity in the generation of the different sets of vertebrae. *Mech Dev* **77**, 49-57.

Chen, H. and Johnson, R. L. (2002). Interactions between dorsal-ventral patterning genes lmx1b, engrailed-1 and wnt-7a in the vertebrate limb. *Int J Dev Biol* **46**, 937-41.

Chen, H., Lun, Y., Ovchinnikov, D., Kokubo, H., Oberg, K. C., Pepicelli, C. V., Gan, L., Lee, B. and Johnson, R. L. (1998b). Limb and kidney defects in Lmx1b

mutant mice suggest an involvement of LMX1B in human nail patella syndrome. *Nat Genet* **19**, 51-5.

Chen, H., Rossier, C., Nakamura, Y., Lynn, A., Chakravarti, A. and Antonarakis, S. E. (1997). Cloning of a novel homeobox-containing gene, PKNOX1, and mapping to human chromosome 21q22.3. *Genomics* **41**, 193-200.

Chen, Y., Knezevic, V., Ervin, V., Hutson, R., Ward, Y. and Mackem, S. (2004). Direct interaction with Hoxd proteins reverses Gli3-repressor function to promote digit formation downstream of Shh. *Development* **131**, 2339-47.

Cheng, L., Alvares, L. E., Ahmed, M. U., El-Hanfy, A. S. and Dietrich, S. (2004). The epaxial-hypaxial subdivision of the avian somite. *Dev Biol* **274**, 348-69.

Chevallier, A., Kieny, M. and Mauger, A. (1977). Limb-somite relationship: origin of the limb musculature. *J Embryol Exp Morphol* **41**, 245-58.

Chiang, C., Litingtung, Y., Harris, M. P., Simandl, B. K., Li, Y., Beachy, P. A. and Fallon, J. F. (2001). Manifestation of the limb prepattern: limb development in the absence of sonic hedgehog function. *Dev Biol* **236**, 421-35.

Chiang, C., Litingtung, Y., Lee, E., Young, K. E., Corden, J. L., Westphal, H. and Beachy, P. A. (1996). Cyclopia and defective axial patterning in mice lacking Sonic hedgehog gene function. *Nature* **383**, 407-13.

Chiu, C. and Hamrick, M. W. (2002). Evolution and development of the primate limb skeleton. *Evolutionary Anthropology* **11**, 94-107.

Christen, B. and Slack, J. M. (1997). FGF-8 is associated with anteroposterior patterning and limb regeneration in Xenopus. *Dev Biol* **192**, 455-66.

Christen, B. and Slack, J. M. (1998). All limbs are not the same. *Nature* **395**, 230-1.

Cobb, J. and Duboule, D. (2005). Comparative analysis of genes downstream of the Hoxd cluster in developing digits and external genitalia. *Development* **132**, 3055-67.

Cohn, M. J., Patel, K., Krumlauf, R., Wilkinson, D. G., Clarke, J. D. and Tickle, C. (1997). Hox9 genes and vertebrate limb specification. *Nature* **387**, 97-101.

Cohn, M. J. and Tickle, C. (1996). Limbs: a model for pattern formation within the vertebrate body plan. *Trends Genet* **12**, 253-7.

Cohn, M. J. and Tickle, C. (1999). Developmental basis of limblessness and axial patterning in snakes. *Nature* **399**, 474-9.

Colosimo, P. F., Hosemann, K. E., Balabhadra, S., Villarreal, G., Jr., Dickson, M., Grimwood, J., Schmutz, J., Myers, R. M., Schluter, D. and Kingsley, D. M. (2005). Widespread parallel evolution in sticklebacks by repeated fixation of Ectodysplasin alleles. *Science* **307**, 1928-33.

Condie, B. G. and Capecchi, M. R. (1993). Mice homozygous for a targeted disruption of Hoxd-3 (Hox-4.1) exhibit anterior transformations of the first and second cervical vertebrae, the atlas and the axis. *Development* **119**, 579-95.

Condie, B. G. and Capecchi, M. R. (1994). Mice with targeted disruptions in the paralogous genes hoxa-3 and hoxd-3 reveal synergistic interactions. *Nature* **370**, 304-7.

Cooper, K. L., Leisenring, W. M. and Moens, C. B. (2003). Autonomous and nonautonomous functions for Hox/Pbx in branchiomotor neuron development. *Dev Biol* **253**, 200-13.

Core, N., Bel, S., Gaunt, S. J., Aurrand-Lions, M., Pearce, J., Fisher, A. and Djabali, M. (1997). Altered cellular proliferation and mesoderm patterning in Polycomb-M33-deficient mice. *Development* **124**, 721-9.

Cretekos, C. J., Wang, Y., Green, E. X., Martin, J. F., Rasweiler, J. J. I. and Behringer, R. R. (submitted). Transcriptional regulatory divergence modifies forelimb length between mouse and bat. *Nature.*

Cretekos, C. J., Weatherbee, S. D., Chen, C. H., Badwaik, N. K., Niswander, L., Behringer, R. R. and Rasweiler, J. J. t. (2005). Embryonic staging system for the short-tailed fruit bat, Carollia perspicillata, a model organism for the mammalian order Chiroptera, based upon timed pregnancies in captive-bred animals. *Dev Dyn* **233**, 721-38.

Crossley, P. H. and Martin, G. R. (1995). The mouse Fgf8 gene encodes a family of polypeptides and is expressed in regions that direct outgrowth and patterning in the developing embryo. *Development* **121**, 439-51.

Crossley, P. H., Minowada, G., MacArthur, C. A. and Martin, G. R. (1996). Roles for FGF8 in the induction, initiation, and maintenance of chick limb development. *Cell* **84**, 127-36.

Cserjesi, P., Brown, D., Ligon, K. L., Lyons, G. E., Copeland, N. G., Gilbert, D. J., Jenkins, N. A. and Olson, E. N. (1995). Scleraxis: a basic helix-loop-helix protein that prefigures skeletal formation during mouse embryogenesis. *Development* **121**, 1099-110.

Cygan, J. A., Johnson, R. L. and McMahon, A. P. (1997). Novel regulatory interactions revealed by studies of murine limb pattern in Wnt-7a and En-1 mutants. *Development* **124**, 5021-32.

Davenport, T. G., Jerome-Majewska, L. A. and Papaioannou, V. E. (2003). Mammary gland, limb and yolk sac defects in mice lacking Tbx3, the gene mutated in human ulnar mammary syndrome. *Development* **130**, 2263-73.

Davidson, E. H. (2001). *Genomic Regulatory Systems*. Academic Press; New York. pp.v-261.

Davis, A. P. and Capecchi, M. R. (1994). Axial homeosis and appendicular skeleton defects in mice with a targeted disruption of hoxd-11. *Development* **120**, 2187-98.

Davis, A. P. and Capecchi, M. R. (1996). A mutational analysis of the 5' HoxD genes: dissection of genetic interactions during limb development in the mouse. *Development* **122**, 1175-85.

Davis, A. P., Witte, D. P., Hsieh-Li, H. M., Potter, S. S. and Capecchi, M. R. (1995). Absence of radius and ulna in mice lacking hoxa-11 and hoxd-11. *Nature* **375**, 791-5.

de la Cruz, C. C., Der-Avakian, A., Spyropoulos, D. D., Tieu, D. D. and Carpenter, E. M. (1999). Targeted disruption of Hoxd9 and Hoxd10 alters locomotor behavior, vertebral identity, and peripheral nervous system development. *Dev Biol* **216**, 595-610.

Dealy, C. N., Roth, A., Ferrari, D., Brown, A. M. and Kosher, R. A. (1993). Wnt-5a and Wnt-7a are expressed in the developing chick limb bud in a manner suggesting roles in pattern formation along the proximodistal and dorsoventral axes. *Mech Dev* **43**, 175-86.

Dear, T. N., Colledge, W. H., Carlton, M. B., Lavenir, I., Larson, T., Smith, A. J., Warren, A. J., Evans, M. J., Sofroniew, M. V. and Rabbitts, T. H. (1995). The Hox11 gene is essential for cell survival during spleen development. *Development* **121**, 2909-15.

Dear, T. N., Sanchez-Garcia, I. and Rabbitts, T. H. (1993). The HOX11 gene encodes a DNA-binding nuclear transcription factor belonging to a distinct family of homeobox genes. *Proc Natl Acad Sci U S A* **90**, 4431-5.

DeLaurier, A., Schweitzer, R. and Logan, M. (2006). Pitx1 determines the morphology of muscle, tendon, and bones of the hindlimb. *Dev Biol* **299**, 22-34.

Deschamps, J. and van Nes, J. (2005). Developmental regulation of the Hox genes during axial morphogenesis in the mouse. *Development* **132**, 2931-42.

Di Giacomo, G., Koss, M., Capellini, T. D., Brendolan, A., Popperl, H. and Selleri, L. (2006). Spatio-temporal expression of Pbx3 during mouse organogenesis. *Gene Expr Patterns* **6**, 747-57.

Dietrich, S. and Gruss, P. (1995). undulated phenotypes suggest a role of Pax-1 for the development of vertebral and extravertebral structures. *Dev Biol* **167**, 529-48.

DiMartino, J. F., Selleri, L., Traver, D., Firpo, M. T., Rhee, J., Warnke, R., O'Gorman, S., Weissman, I. L. and Cleary, M. L. (2001). The Hox cofactor and proto-oncogene Pbx1 is required for maintenance of definitive hematopoiesis in the fetal liver. *Blood* **98**, 618-26.

Dolle, P., Dierich, A., LeMeur, M., Schimmang, T., Schuhbaur, B., Chambon, P. and Duboule, D. (1993a). Disruption of the Hoxd-13 gene induces localized heterochrony leading to mice with neotenic limbs. *Cell* **75**, 431-41.

Dolle, P., Izpisua-Belmonte, J. C., Brown, J., Tickle, C. and Duboule, D. (1993b). Hox genes and the morphogenesis of the vertebrate limb. *Prog Clin Biol Res* **383A**, 11-20.

Dolle, P., Izpisua-Belmonte, J. C., Falkenstein, H., Renucci, A. and Duboule, D. (1989a). Coordinate expression of the murine Hox-5 complex homoeobox-containing genes during limb pattern formation. *Nature* **342**, 767-72.

Dolle, P., Ruberte, E., Kastner, P., Petkovich, M., Stoner, C. M., Gudas, L. J. and Chambon, P. (1989b). Differential expression of genes encoding alpha, beta and gamma retinoic acid receptors and CRABP in the developing limbs of the mouse. *Nature* **342**, 702-5.

Dolle, P., Ruberte, E., Leroy, P., Morriss-Kay, G. and Chambon, P. (1990). Retinoic acid receptors and cellular retinoid binding proteins. I. A systematic study of their differential pattern of transcription during mouse organogenesis. *Development* **110**, 1133-51.

Dorus, S., Anderson, J. R., Vallender, E. J., Gilbert, S. L., Zhang, L., Chemnick, L. G., Ryder, O. A., Li, W. and Lahn, B. T. (2006). Sonic Hedgehog, a key development gene, experienced intensified molecular evolution in primates. *Hum Mol Genet* **15**, 2031-7.

Duboule, D. (1994a). How to make a limb? *Science* **266**, 575-6.

Duboule, D. (1994b). Temporal collinearity and the phylotypic progression: a basis for the stability of a vertebrate Bauplan and the evolution of morphologies through heterochrony. *Dev Suppl*, 135-42.

Duboule, D. (1995). Vertebrate Hox genes and proliferation: an alternative pathway to homeosis? *Curr Opin Genet Dev* **5**, 525-8.

Dudley, A. T., Ros, M. A. and Tabin, C. J. (2002). A re-examination of proximodistal patterning during vertebrate limb development. *Nature* **418**, 539-44.

Duprez, D. M., Kostakopoulou, K., Francis-West, P. H., Tickle, C. and Brickell, P. M. (1996). Activation of Fgf-4 and HoxD gene expression by BMP-2 expressing cells in the developing chick limb. *Development* **122**, 1821-8.

Dymecki, S. M. (1996). Flp recombinase promotes site-specific DNA recombination in embryonic stem cells and transgenic mice. *Proc Natl Acad Sci U S A* **93**, 6191-6.

Ebner, A., Cabernard, C., Affolter, M. and Merabet, S. (2005). Recognition of distinct target sites by a unique Labial/Extradenticle/Homothorax complex. *Development* **132**, 1591-600.

Echelard, Y., Epstein, D. J., St-Jacques, B., Shen, L., Mohler, J., McMahon, J. A. and McMahon, A. P. (1993). Sonic hedgehog, a member of a family of putative signaling molecules, is implicated in the regulation of CNS polarity. *Cell* **75**, 1417-30.

Ehehalt, F., Wang, B., Christ, B., Patel, K. and Huang, R. (2004). Intrinsic cartilage-forming potential of dermomyotomal cells requires ectodermal signals for the development of the scapula blade. *Anat Embryol (Berl)* **208**, 431-7.

Endo, T., Yokoyama, H., Tamura, K. and Ide, H. (1997). Shh expression in developing and regenerating limb buds of Xenopus laevis. *Dev Dyn* **209**, 227-32.

Fallon, J. F., Lopez, A., Ros, M. A., Savage, M. P., Olwin, B. B. and Simandl, B. K. (1994). FGF-2: apical ectodermal ridge growth signal for chick limb development. *Science* **264**, 104-7.

Favier, B. and Dolle, P. (1997). Developmental functions of mammalian Hox genes. *Mol Hum Reprod* **3**, 115-31.

Favier, B., Le Meur, M., Chambon, P. and Dolle, P. (1995). Axial skeleton homeosis and forelimb malformations in Hoxd-11 mutant mice. *Proc Natl Acad Sci U S A* **92**, 310-4.

Favier, B., Rijli, F. M., Fromental-Ramain, C., Fraulob, V., Chambon, P. and Dolle, P. (1996). Functional cooperation between the non-paralogous genes Hoxa-10 and Hoxd-11 in the developing forelimb and axial skeleton. *Development* **122**, 449-60.

Feldman, B., Poueymirou, W., Papaioannou, V. E., DeChiara, T. M. and Goldfarb, M. (1995). Requirement of FGF-4 for postimplantation mouse development. *Science* **267**, 246-9.

Fernandez-Teran, M., Piedra, M. E., Bastida, M. F. and Ros, M. (1996). Chick limbs develop without mesonephros. *Int J Dev Biol* **Suppl 1**, 251S.

Fernandez-Teran, M., Piedra, M. E., Simandl, B. K., Fallon, J. F. and Ros, M. A. (1997). Limb initiation and development is normal in the absence of the mesonephros. *Dev Biol* **189**, 246-55.

Ferretti, E., Marshall, H., Popperl, H., Maconochie, M., Krumlauf, R. and Blasi, F. (2000). Segmental expression of Hoxb2 in r4 requires two separate sites that integrate cooperative interactions between Prep1, Pbx and Hox proteins. *Development* **127**, 155-66.

Fisher, R. A. (1930). *The Genetical Theory of Natural Selection*. Oxford University Press; Oxford. pp.1-250.

Fleagle, J. G. (2001). *Primate Adaptation and Evolution*. Academic Press; New York. pp.v-596.

Freitas, R. and Cohn, M. J. (2006). Genomic regulation of Hox collinearity. *Dev Cell* **10**, 8-9.

Freitas, R., Zhang, G. and Cohn, M. J. (2006). Evidence that mechanisms of fin development evolved in the midline of early vertebrates. *Nature* **442**, 1033-7.

Fromental-Ramain, C., Warot, X., Lakkaraju, S., Favier, B., Haack, H., Birling, C., Dierich, A., Doll e, P. and Chambon, P. (1996a). Specific and redundant functions of the paralogous Hoxa-9 and Hoxd-9 genes in forelimb and axial skeleton patterning. *Development* **122**, 461-72.

Fromental-Ramain, C., Warot, X., Messadecq, N., LeMeur, M., Dolle, P. and Chambon, P. (1996b). Hoxa-13 and Hoxd-13 play a crucial role in the patterning of the limb autopod. *Development* **122**, 2997-3011.

Galant, R., Walsh, C. M. and Carroll, S. B. (2002). Hox repression of a target gene: extradenticle-independent, additive action through multiple monomer binding sites. *Development* **129**, 3115-26.

Garcia-Fernandez, J. (2005). The genesis and evolution of homeobox gene clusters. *Nat Rev Genet* **6**, 881-92.

Garrity, D. M., Childs, S. and Fishman, M. C. (2002). The heartstrings mutation in zebrafish causes heart/fin Tbx5 deficiency syndrome. *Development* **129**, 4635-45.

Gebelein, B., McKay, D. J. and Mann, R. S. (2004). Direct integration of Hox and segmentation gene inputs during Drosophila development. *Nature* **431**, 653-9.

Geduspan, J. S. and MacCabe, J. A. (1986). Evidence for the transmission of dorsoventral information to the ectoderm during the earliest stages of limb development. *Prog Clin Biol Res* **226**, 115-26.

Geduspan, J. S. and MacCabe, J. A. (1987). The ectodermal control of mesodermal patterns of differentiation in the developing chick wing. *Dev Biol* **124**, 398-408.

Geduspan, J. S. and MacCabe, J. A. (1989). Transfer of dorsoventral information from mesoderm to ectoderm at the onset of limb development. *Anat Rec* **224**, 79-87.

Gibson-Brown, J. J., Agulnik, S. I., Chapman, D. L., Alexiou, M., Garvey, N., Silver, L. M. and Papaioannou, V. E. (1996). Evidence of a role for T-box genes in the evolution of limb morphogenesis and the specification of forelimb/hindlimb identity. *Mech Dev* **56**, 93-101.

Gibson-Brown, J. J., S, I. A., Silver, L. M. and Papaioannou, V. E. (1998). Expression of T-box genes Tbx2-Tbx5 during chick organogenesis. *Mech Dev* **74**, 165-9.

Gilbert, S. F. (2006). *Developmental Biology*. Sinauer Associates Inc.; Sunderland, Mass. pp.iv-785.

Gilbert, S. F., Opitz, J. M. and Raff, R. A. (1996). Resynthesizing evolutionary and developmental biology. *Dev Biol* **173**, 357-372.

Goff, D. J. and Tabin, C. J. (1997). Analysis of Hoxd-13 and Hoxd-11 mis-expression in chick limb buds reveals that Hox genes affect both bone condensation and growth. *Development* **124**, 627-36.

Goldring, M. B., Tsuchimochi, K. and Ijiri, K. (2006). The control of chondrogenesis. *J Cell Biochem* **97**, 33-44.

Gonzalez-Crespo, S., Abu-Shaar, M., Torres, M., Martinez, A. C., Mann, R. S. and Morata, G. (1998). Antagonism between extradenticle function and Hedgehog signalling in the developing limb. *Nature* **394**, 196-200.

Goodrich, L. V., Johnson, R. L., Milenkovic, L., McMahon, J. A. and Scott, M. P. (1996). Conservation of the hedgehog/patched signaling pathway from flies to mice: induction of a mouse patched gene by Hedgehog. *Genes Dev* **10**, 301-12.

Goudet, G., Delhalle, S., Biemar, F., Martial, J. A. and Peers, B. (1999). Functional and cooperative interactions between the homeodomain PDX1, Pbx, and Prep1 factors on the somatostatin promoter. *J Biol Chem* **274**, 4067-73.

Gould, S. J. and Lewontin, R. C. (1978). The Spandrels of San Marco and the Panglossian Paradigm: A Critique of the Adaptationist Programme. *Proc R Soc London* **205**, 581-598.

Grieshammer, U., Minowada, G., Pisenti, J. M., Abbott, U. K. and Martin, G. R. (1996). The chick limbless mutation causes abnormalities in limb bud dorsal-ventral patterning: implications for the mechanism of apical ridge formation. *Development* **122**, 3851-61.

Hamburger, V. and Hamilton, H. L. (1951). A series of normal stages in the development of the chick embryo. *J Morphol* **88**, 49-92.

Hamrick, M. W. (1999). Pattern and process in the evolution of primate nails and claws. *J Human Evolution* **37**, 293-297.

Hamrick, M. W. (2001a). Development and evolution of the mammalian limb: adaptive diversification of nails, hooves, and claws. *Evol Dev* **3**, 355-363.

Hamrick, M. W. (2001b). Primate origins: evolutionary change in digital ray patterning and segmentation. *J Human Evolution* **40**, 339-351.

Hamrick, M. W. (2002). Developmental mechanisms of digit reduction. *Evol Dev* **4**, 247-248.

Han, M. J., An, J. Y. and Kim, W. S. (2001). Expression patterns of Fgf-8 during development and limb regeneration of the axolotl. *Dev Dyn* **220**, 40-8.

Hanken, J., Carl, T. F., Richardson, M. K., Olsson, L., Schlosser, G., Osabutey, C. K. and Klymkowsky, M. W. (2001). Limb development in a "nonmodel" vertebrate, the direct-developing frog Eleutherodactylus coqui. *J Exp Zool* **291**, 375-88.

Harfe, B. D., Scherz, P. J., Nissim, S., Tian, H., McMahon, A. P. and Tabin, C. J. (2004). Evidence for an expansion-based temporal Shh gradient in specifying vertebrate digit identities. *Cell* **118**, 517-28.

Harrelson, Z., Kelly, R. G., Goldin, S. N., Gibson-Brown, J. J., Bollag, R. J., Silver, L. M. and Papaioannou, V. E. (2004). Tbx2 is essential for patterning the atrioventricular canal and for morphogenesis of the outflow tract during heart development. *Development* **131**, 5041-52.

Harrison, R. G. (1918). Experiments on the development of the forelimb of Amblystoma; a self-differentiating, equipotential system. *J Exp Zool* **25**, 413-461.

Harrison, R. G. (1921). On relations of symmetry in transplanted limbs. *J Exp Zool* **32**, 1-20.

Hayashi, K. and Ozawa, E. (1995). Myogenic cell migration from somites is induced by tissue contact with medial region of the presumptive limb mesoderm in chick embryos. *Development* **121**, 661-9.

Helms, J., Thaller, C. and Eichele, G. (1994). Relationship between retinoic acid and sonic hedgehog, two polarizing signals in the chick wing bud. *Development* **120**, 3267-74.

Herault, Y., Beckers, J., Kondo, T., Fraudeau, N. and Duboule, D. (1998a). Genetic analysis of a Hoxd-12 regulatory element reveals global versus local modes of controls in the HoxD complex. *Development* **125**, 1669-77.

Herault, Y. and Duboule, D. (1997). Control of limb morphogenesis by the Hox genes. *C R Seances Soc Biol Fil* **191**, 21-7.

Herault, Y., Kmita, M., Sawaya, C. C. and Duboule, D. (2002). A nested deletion approach to generate Cre deleter mice with progressive Hox profiles. *Int J Dev Biol* **46**, 185-91.

Herault, Y., Rassoulzadegan, M., Cuzin, F. and Duboule, D. (1998b). Engineering chromosomes in mice through targeted meiotic recombination (TAMERE). *Nat Genet* **20**, 381-4.

Hill, T. P., Taketo, M. M., Birchmeier, W. and Hartmann, C. (2006). Multiple roles of mesenchymal beta-catenin during murine limb patterning. *Development* **133**, 1219-29.

Hinchliffe, J. R. (1989). Reconstructing the archetype: innovation and conservation in the evolution and development of the pentadactyl limb. In Wake D. and Roth G. (eds.) *Complex organismal functions: integration and evolution in vertebrates.* pp.171-189.

Hinchliffe, J. R. (1991). Developmental approaches to the problem of transformation of limb structure in evolution. In Hinchliffe, J.R., Hurle, J. and Summerbell D. (eds.) *Developmental patterning of the vertebrate limb*. pp.313-323.

Hinchliffe, J. R. (2002). Developmental basis of limb evolution. *Int J Dev Biol* **46**, 835-45.

Hisa, T., Spence, S. E., Rachel, R. A., Fujita, M., Nakamura, T., Ward, J. M., Devor-Henneman, D. E., Saiki, Y., Kutsuna, H., Tessarollo, L. et al. (2004). Hematopoietic, angiogenic and eye defects in Meis1 mutant animals. *Embo J* **23**, 450-9.

Hoey, T. and Levine, M. (1988). Divergent homeo box proteins recognize similar DNA sequences in Drosophila. *Nature* **332**, 858-61.

Hombria, J. C. and Lovegrove, B. (2003). Beyond homeosis--HOX function in morphogenesis and organogenesis. *Differentiation* **71**, 461-76.

Horan, G. S., Ramirez-Solis, R., Featherstone, M. S., Wolgemuth, D. J., Bradley, A. and Behringer, R. R. (1995). Compound mutants for the paralogous hoxa-4, hoxb-4, and hoxd-4 genes show more complete homeotic transformations and a dose-dependent increase in the number of vertebrae transformed. *Genes Dev* **9**, 1667-77.

Horan, G. S., Wu, K., Wolgemuth, D. J. and Behringer, R. R. (1994). Homeotic transformation of cervical vertebrae in Hoxa-4 mutant mice. *Proc Natl Acad Sci U S A* **91**, 12644-8.

Hornstein, E., Mansfield, J. H., Yekta, S., Hu, J. K., Harfe, B. D., McManus, M. T., Baskerville, S., Bartel, D. P. and Tabin, C. J. (2005). The microRNA miR-196 acts upstream of Hoxb8 and Shh in limb development. *Nature* **438**, 671-4.

Howell, A. B. (1970). *Aquatic Mammals: Their Adaptation to Life in the Water*. Dover Publications; U.S.A. pp.1-250.

Hsu, L. C., Chang, W. C. and Yoshida, A. (2000). Mouse type-2 retinaldehyde dehydrogenase (RALDH2): genomic organization, tissue-dependent expression, chromosome assignment and comparison to other types. *Biochim Biophys Acta* **1492**, 289-93.

Huang, R., Christ, B. and Patel, K. (2006). Regulation of scapula development. *Anat Embryol (Berl)* **211 Suppl 7**, 65-71.

Huang, R., Zhi, Q., Patel, K., Wilting, J. and Christ, B. (2000). Dual origin and segmental organisation of the avian scapula. *Development* **127**, 3789-94.

Hui, C. C. and Joyner, A. L. (1993). A mouse model of greig cephalopolysyndactyly syndrome: the extra-toesJ mutation contains an intragenic deletion of the Gli3 gene. *Nat Genet* **3**, 241-6.

Hunt, P. and Krumlauf, R. (1992). Hox codes and positional specification in vertebrate embryonic axes. *Annu Rev Cell Biol* **8**, 227-56.

Imokawa, Y. and Yoshizato, K. (1997). Expression of Sonic hedgehog gene in regenerating newt limb blastemas recapitulates that in developing limb buds. *Proc Natl Acad Sci U S A* **94**, 9159-64.

Jacobs, Y., Schnabel, C. A. and Cleary, M. L. (1999). Trimeric association of Hox and TALE homeodomain proteins mediates Hoxb2 hindbrain enhancer activity. *Mol Cell Biol* **19**, 5134-42.

Jaw, T. J., You, L. R., Knoepfler, P. S., Yao, L. C., Pai, C. Y., Tang, C. Y., Chang, L. P., Berthelsen, J., Blasi, F., Kamps, M. P. et al. (2000). Direct interaction of two homeoproteins, homothorax and extradenticle, is essential for EXD nuclear localization and function. *Mech Dev* **91**, 279-91.

Jiang, H. and Kochhar, D. M. (1992). Induction of tissue transglutaminase and apoptosis by retinoic acid in the limb bud. *Teratology* **46**, 333-40.

Johnson, R. L. and Tabin, C. J. (1997). Molecular models for vertebrate limb development. *Cell* **90**, 979-90.

Joyner, A. L., Kornberg, T., Coleman, K. G., Cox, D. R. and Martin, G. R. (1985). Expression during embryogenesis of a mouse gene with sequence homology to the Drosophila engrailed gene. *Cell* **43**, 29-37.

Kamps, M. P., Murre, C., Sun, X. H. and Baltimore, D. (1990). A new homeobox gene contributes the DNA binding domain of the t(1;19) translocation protein in pre-B ALL. *Cell* **60**, 547-55.

Kappen, C. and Ruddle, F. H. (1993). Evolution of a regulatory gene family: HOM/HOX genes. *Curr Opin Genet Dev* **3**, 931-8.

Kappen, C., Schughart, K. and Ruddle, F. H. (1993). Early evolutionary origin of major homeodomain sequence classes. *Genomics* **18**, 54-70.

Karsenty, G. and Wagner, E. F. (2002). Reaching a genetic and molecular understanding of skeletal development. *Dev Cell* **2**, 389-406.

Kawakami, Y., Capdevila, J., Buscher, D., Itoh, T., Rodriguez Esteban, C. and Izpisua Belmonte, J. C. (2001). WNT signals control FGF-dependent limb initiation and AER induction in the chick embryo. *Cell* **104**, 891-900.

Kilstrup-Nielsen, C., Alessio, M. and Zappavigna, V. (2003). PBX1 nuclear export is regulated independently of PBX-MEINOX interaction by PKA phosphorylation of the PBC-B domain. *Embo J* **22**, 89-99.

Kim, S. K., Selleri, L., Lee, J. S., Zhang, A. Y., Gu, X., Jacobs, Y. and Cleary, M. L. (2002). Pbx1 inactivation disrupts pancreas development and in Ipf1-deficient mice promotes diabetes mellitus. *Nat Genet* **30**.

Kimmel, R. A., Turnbull, D. H., Blanquet, V., Wurst, W., Loomis, C. A. and Joyner, A. L. (2000). Two lineage boundaries coordinate vertebrate apical ectodermal ridge formation. *Genes Dev* **14**, 1377-89.

King, M., Arnold, J. S., Shanske, A. and Morrow, B. E. (2006). T-genes and limb bud development. *Am J Med Genet A* **140**, 1407-13.

Kmita, M. and Duboule, D. (2003). Organizing axes in time and space; 25 years of collinear tinkering. *Science* **301**, 331-3.

Kmita, M., Fraudeau, N., Herault, Y. and Duboule, D. (2002a). Serial deletions and duplications suggest a mechanism for the collinearity of Hoxd genes in limbs. *Nature* **420**, 145-50.

Kmita, M., Kondo, T. and Duboule, D. (2000). Targeted inversion of a polar silencer within the HoxD complex re-allocates domains of enhancer sharing. *Nat Genet* **26**, 451-4.

Kmita, M., Tarchini, B., Zakany, J., Logan, M., Tabin, C. J. and Duboule, D. (2005). Early developmental arrest of mammalian limbs lacking HoxA/HoxD gene function. *Nature* **435**, 1113-6.

Kmita, M., van Der Hoeven, F., Zakany, J., Krumlauf, R. and Duboule, D. (2000b). Mechanisms of Hox gene collinearity: transposition of the anterior Hoxb1 gene into the posterior HoxD complex. *Genes Dev* **14**, 198-211.

Knezevic, V., De Santo, R., Schughart, K., Huffstadt, U., Chiang, C., Mahon, K. A. and Mackem, S. (1997). Hoxd-12 differentially affects preaxial and postaxial chondrogenic branches in the limb and regulates Sonic hedgehog in a positive feedback loop. *Development* **124**, 4523-36.

Knoepfler, P. S., Bergstrom, D. A., Uetsuki, T., Dac-Korytko, I., Sun, Y. H., Wright, W. E., Tapscott, S. J. and Kamps, M. P. (1999). A conserved motif N-terminal to the DNA-binding domains of myogenic bHLH transcription factors

mediates cooperative DNA binding with pbx-Meis1/Prep1. *Nucleic Acids Res* **27**, 3752-61.

Knoepfler, P. S., Calvo, K. R., Chen, H., Antonarakis, S. E. and Kamps, M. P. (1997). Meis1 and pKnox1 bind DNA cooperatively with Pbx1 utilizing an interaction surface disrupted in oncoprotein E2a-Pbx1. *Proc Natl Acad Sci U S A* **94**, 14553-8.

Knoepfler, P. S. and Kamps, M. P. (1995). The pentapeptide motif of Hox proteins is required for cooperative DNA binding with Pbx1, physically contacts Pbx1, and enhances DNA binding by Pbx1. *Mol Cell Biol* **15**, 5811-9.

Knoepfler, P. S., Sykes, D. B., Pasillas, M. and Kamps, M. P. (2001). HoxB8 requires its Pbx-interaction motif to block differentiation of primary myeloid progenitors and of most cell line models of myeloid differentiation. *Oncogene* **20**, 5440-8.

Knosp, W. M., Scott, V., Bachinger, H. P. and Stadler, H. S. (2004). HOXA13 regulates the expression of bone morphogenetic proteins 2 and 7 to control distal limb morphogenesis. *Development* **131**, 4581-92.

Kobayashi, M., Fujioka, M., Tolkunova, E. N., Deka, D., Abu-Shaar, M., Mann, R. S. and Jaynes, J. B. (2003). Engrailed cooperates with extradenticle and homothorax to repress target genes in Drosophila. *Development* **130**, 741-51.

Kochhar, D. M., Jiang, H., Harnish, D. C. and Soprano, D. R. (1993). Evidence that retinoic acid-induced apoptosis in the mouse limb bud core mesenchymal cells is gene-mediated. *Prog Clin Biol Res* **383B**, 815-25.

Koshiba-Takeuchi, K., Takeuchi, J. K., Arruda, E. P., Kathiriya, I. S., Mo, R., Hui, C. C., Srivastava, D. and Bruneau, B. G. (2006). Cooperative and antagonistic interactions between Sall4 and Tbx5 pattern the mouse limb and heart. *Nat Genet* **38**, 175-83.

Kostic, D. and Capecchi, M. R. (1994). Targeted disruptions of the murine Hoxa-4 and Hoxa-6 genes result in homeotic transformations of components of the vertebral column. *Mech Dev* **46**, 231-47.

Koussoulakos, S. (2004). Vertebrate limb development: from Harrison's limb disk transplantations to targeted disruption of Hox genes. *Anat Embryol (Berl)* **209**, 93-105.

Koussoulakos, S., Sharma, K. K. and Anton, H. J. (1990). Effect of vitamin A on wound epidermis during forelimb regeneration in adult newts. *Int J Dev Biol* **34**, 433-9.

Kraus, P., Fraidenraich, D. and Loomis, C. A. (2001). Some distal limb structures develop in mice lacking Sonic hedgehog signaling. *Mech Dev* **100**, 45-58.

Kraus, P. and Lufkin, T. (2006). Dlx homeobox gene control of mammalian limb and craniofacial development. *Am J Med Genet A* **140**, 1366-74.

Krauss, S., Concordet, J. P. and Ingham, P. W. (1993). A functionally conserved homolog of the Drosophila segment polarity gene hh is expressed in tissues with polarizing activity in zebrafish embryos. *Cell* **75**, 1431-44.

Krosl, J., Baban, S., Krosl, G., Rozenfeld, S., Largman, C. and Sauvageau, G. (1998). Cellular proliferation and transformation induced by HOXB4 and HOXB3 proteins involves cooperation with PBX1. *Oncogene* **16**, 3403-12.

Krumlauf, R. (1994). Hox genes in vertebrate development. *Cell* **78**, 191-201.

Kuijper, S., Beverdam, A., Kroon, C., Brouwer, A., Candille, S., Barsh, G. and Meijlink, F. (2005). Genetics of shoulder girdle formation: roles of Tbx15 and aristaless-like genes. *Development* **132**, 1601-10.

Kurant, E., Pai, C. Y., Sharf, R., Halachmi, N., Sun, Y. H. and Salzberg, A. (1998). Dorsotonals/homothorax, the Drosophila homologue of meis1, interacts with extradenticle in patterning of the embryonic PNS. *Development* **125**, 1037-48.

Kwan, K. M. (2002). Conditional alleles in mice: practical considerations for tissue-specific knockouts. *Genesis* **32**, 49-62.

Lallemand, Y., Nicola, M. A., Ramos, C., Bach, A., Cloment, C. S. and Robert, B. (2005). Analysis of Msx1; Msx2 double mutants reveals multiple roles for Msx genes in limb development. *Development* **132**, 3003-14.

Lanctot, C., Moreau, A., Chamberland, M., Tremblay, M. L. and Drouin, J. (1999). Hindlimb patterning and mandible development require the Ptx1 gene. *Development* **126**, 1805-10.

Lande, R. (1978). Evolutionary mechanisms of limb loss in tetrapods. *Evolution* **32**, 73-92.

LaRonde-LeBlanc, N. A. and Wolberger, C. (2003). Structure of HoxA9 and Pbx1 bound to DNA: Hox hexapeptide and DNA recognition anterior to posterior. *Genes Dev* **17**, 2060-72.

Larson, S. G. (1993). Functional morphology of the shoulder in primates. In Gebo (ed.) *Postcranial Adaptation in Nonhuman Primates.* Northern Illinois University Press; DeKalb, Illiniois. pp.45-69.

Larson, S. G. (1998). Parallel evolution in the hominoid trunk and forelimb. *Evol Anthropol* **6**, 87-99.

Laufer, E., Nelson, C. E., Johnson, R. L., Morgan, B. A. and Tabin, C. (1994). Sonic hedgehog and Fgf-4 act through a signaling cascade and feedback loop to integrate growth and patterning of the developing limb bud. *Cell* **79**, 993-1003.

Lettice, L. A., Heaney, S. J., Purdie, L. A., Li, L., de Beer, P., Oostra, B. A., Goode, D., Elgar, G., Hill, R. E. and de Graaff, E. (2003). A long-range Shh enhancer regulates expression in the developing limb and fin and is associated with preaxial polydactyly. *Hum Mol Genet* **12**, 1725-35.

Lettice, L. A., Horikoshi, T., Heaney, S. J., van Baren, M. J., van der Linde, H. C., Breedveld, G. J., Joosse, M., Akarsu, N., Oostra, B. A., Endo, N. et al. (2002). Disruption of a long-range cis-acting regulator for Shh causes preaxial polydactyly. *Proc Natl Acad Sci U S A* **99**, 7548-53.

Lewandoski, M. (2001). Conditional control of gene expression in the mouse. *Nat Rev Genet* **2**, 743-55.

Lewandoski, M., Sun, X. and Martin, G. R. (2000). Fgf8 signalling from the AER is essential for normal limb development. *Nat Genet* **26**, 460-3.

Liem, K. F., Bemis, W. E., Walker, W. F. and Grande, L. (2001). *Functional Anatomy of the Vertebrates: An Evolutionary Perspective*. Brooks Cole; England. pp.ix-701.

Lizarraga, G., Ferrari, D., Kalinowski, M., Ohuchi, H., Noji, S., Kosher, R. A. and Dealy, C. N. (1999). FGFR2 signaling in normal and limbless chick limb buds. *Dev Genet* **25**, 331-8.

Logan, C., Hornbruch, A., Campbell, I. and Lumsden, A. (1997). The role of Engrailed in establishing the dorsoventral axis of the chick limb. *Development* **124**, 2317-24.

Logan, M., Simon, H. G. and Tabin, C. (1998). Differential regulation of T-box and homeobox transcription factors suggests roles in controlling chick limb-type identity. *Development* **125**, 2825-35.

Lohnes, D., Mark, M., Mendelsohn, C., Dolle, P., Dierich, A., Gorry, P., Gansmuller, A. and Chambon, P. (1994). Function of the retinoic acid receptors

(RARs) during development (I). Craniofacial and skeletal abnormalities in RAR double mutants. *Development* **120**, 2723-48.

Lombardo, A. and Slack, J. M. (2001). Abdominal B-type Hox gene expression in Xenopus laevis. *Mech Dev* **106**, 191-5.

Longobardi, E. and Blasi, F. (2003). Overexpression of PREP-1 in F9 teratocarcinoma cells leads to a functionally relevant increase of PBX-2 by preventing its degradation. *J Biol Chem* **278**, 39235-41.

Loomis, C. A., Harris, E., Michaud, J., Wurst, W., Hanks, M. and Joyner, A. L. (1996). The mouse Engrailed-1 gene and ventral limb patterning. *Nature* **382**, 360-3.

Lopez-Martinez, A., Chang, D. T., Chiang, C., Porter, J. A., Ros, M. A., Simandl, B. K., Beachy, P. A. and Fallon, J. F. (1995). Limb-patterning activity and restricted posterior localization of the amino-terminal product of Sonic hedgehog cleavage. *Curr Biol* **5**, 791-6.

Lovejoy, C. O., Cohn, M. J. and White, T. D. (1999). Morphological Analysis of the mammalian postcranium: a developmental perspective. *PNAS* **96**, 13247-13252.

Lovejoy, C. O., Cohn, M. J. and White, T. D. (2000). The evolution of mammalian morphology; a developmental perspective. In O'Higgins, P. and Cohn, M. (eds.) *Development, Growth, and Evolution.* Academic Press; London. pp.42-55.

Lovejoy, C. O., McCollum, M. A., Reno, P. L. and Rosenman, B. A. (2003). Developmental biology and human evolution. *Ann Rev Anthropol* **32**, 85-109.

Lovejoy, C. O., Reno, P. L., McCollum, M. A., Hamrick, M. W., Meindl, R. S. and Cohn, M. J. (2001). The Evolution of Primate Hands: Growth scaling registers with posterior HOXD expression. Poster presented to the Society for Integrative and Comparative Biology, January 7th, 2001. Chicago, Illinois.

Lu, H. C., Revelli, J. P., Goering, L., Thaller, C. and Eichele, G. (1997). Retinoid signaling is required for the establishment of a ZPA and for the expression of Hoxb-8, a mediator of ZPA formation. *Development* **124**, 1643-51.

Lumsden, A. and Krumlauf, R. (1996). Patterning the vertebrate neuraxis. *Science* **274**, 1109-15.

Lyons, K. M., Pelton, R. W. and Hogan, B. L. (1989). Patterns of expression of murine Vgr-1 and BMP-2a RNA suggest that transforming growth factor-beta-like

genes coordinately regulate aspects of embryonic development. *Genes Dev* **3**, 1657-68.

Maas, R., Chen, Y. P., Bei, M., Woo, I. and Satokata, I. (1996). The role of Msx genes in mammalian development. *Ann N Y Acad Sci* **785**, 171-81.

Maas, S. A. and Fallon, J. F. (2005). Single base pair change in the long-range Sonic hedgehog limb-specific enhancer is a genetic basis for preaxial polydactyly. *Dev Dyn* **232**, 345-8.

MacCabe, J. A., Errick, J. and Saunders, J. W., Jr. (1974). Ectodermal control of the dorsoventral axis in the leg bud of the chick embryo. *Dev Biol* **39**, 69-82.

MacLean, G., Abu-Abed, S., Dolle, P., Tahayato, A., Chambon, P. and Petkovich, M. (2001). Cloning of a novel retinoic-acid metabolizing cytochrome P450, Cyp26B1, and comparative expression analysis with Cyp26A1 during early murine development. *Mech Dev* **107**, 195-201.

Maconochie, M., Nonchev, S., Morrison, A. and Krumlauf, R. (1996). Paralogous Hox genes: function and regulation. *Annu Rev Genet* **30**, 529-56.

Maconochie, M. K., Nonchev, S., Studer, M., Chan, S. K., Popperl, H., Sham, M. H., Mann, R. S. and Krumlauf, R. (1997). Cross-regulation in the mouse HoxB complex: the expression of Hoxb2 in rhombomere 4 is regulated by Hoxb1. *Genes Dev* **11**, 1885-95.

Maden, M. and Mustafa, K. (1984). The cellular contributions of blastema and stump to 180 degrees supernumerary limbs in the axolotl. *J Embryol Exp Morphol* **84**, 233-53.

Mahmood, R., Bresnick, J., Hornbruch, A., Mahony, C., Morton, N., Colquhoun, K., Martin, P., Lumsden, A., Dickson, C. and Mason, I. (1995). A role for FGF-8 in the initiation and maintenance of vertebrate limb bud outgrowth. *Curr Biol* **5**, 797-806.

Malashichev, Y., Borkhvardt, V., Christ, B. and Scaal, M. (2005). Differential regulation of avian pelvic girdle development by the limb field ectoderm. *Anat Embryol (Berl)* **210**, 187-97.

Manley, N. R., Selleri, L., Brendolan, A., Gordon, J. and Cleary, M. L. (2004). Abnormalities of caudal pharyngeal pouch development in Pbx1 knockout mice mimic loss of Hox3 paralogs. *Dev Biol* **276**, 301-12.

Mann, R. S. (1995). The specificity of homeotic gene function. *Bioessays* **17**, 855-63.

Mann, R. S. and Affolter, M. (1998). Hox proteins meet more partners. *Curr Opin Genet Dev* **8**, 423-9.

Mann, R. S. and Chan, S. K. (1996). Extra specificity from extradenticle: the partnership between HOX and PBX/EXD homeodomain proteins. *Trends Genet* **12**, 258-62.

Manzanares, M., Bel-Vialar, S., Ariza-McNaughton, L., Ferretti, E., Marshall, H., Maconochie, M. M., Blasi, F. and Krumlauf, R. (2001). Independent regulation of initiation and maintenance phases of Hoxa3 expression in the vertebrate hindbrain involve auto- and cross-regulatory mechanisms. *Development* **128**, 3595-607.

Marcil, A., Dumontier, E., Chamberland, M., Camper, S. A. and Drouin, J. (2003). Pitx1 and Pitx2 are required for development of hindlimb buds. *Development* **130**, 45-55.

Mariani, F. V. and Martin, G. R. (2003). Deciphering skeletal patterning: clues from the limb. *Nature* **423**, 319-25.

Mark, M., Lufkin, T., Dolle, P., Dierich, A., LeMeur, M. and Chambon, P. (1993). Roles of Hox genes: what we have learnt from gain of function and loss of function mutations in the mouse. *C R Acad Sci III* **316**, 995-1008.

Martin, G. (2001). Making a vertebrate limb: new players enter from the wings. *Bioessays* **23**, 865-8.

Martin, G. R. (1998). The roles of FGFs in the early development of vertebrate limbs. *Genes Dev* **12**, 1571-86.

Martin, P. (1990). Tissue patterning in the developing mouse limb. *Int J Dev Biol* **34**, 323-36.

Matsuoka, T., Ahlberg, P. E., Kessaris, N., Iannarelli, P., Dennehy, U., Richardson, W. D., McMahon, A. P. and Koentges, G. (2005). Neural crest origins of the neck and shoulder. *Nature* **436**, 347-55.

McClintock, J. M., Kheirbek, M. A. and Prince, V. E. (2002). Knockdown of duplicated zebrafish hoxb1 genes reveals distinct roles in hindbrain patterning and a novel mechanism of duplicate gene retention. *Development* **129**, 2339-54.

McGlinn, E. and Tabin, C. J. (2006). Mechanistic insight into how Shh patterns the vertebrate limb. *Curr Opin Genet Dev* **16**, 426-32.

McLeod, M. J. (1980). Differential staining of cartilage and bone in whole mouse fetuses by alcian blue and alizarin red S. *Teratology* **22**, 299-301.

Merabet, S., Kambris, Z., Capovilla, M., Berenger, H., Pradel, J. and Graba, Y. (2003). The hexapeptide and linker regions of the AbdA Hox protein regulate its activating and repressive functions. *Dev Cell* **4**, 761-8.

Mercader, N., Leonardo, E., Azpiazu, N., Serrano, A., Morata, G., Martinez, C. and Torres, M. (1999). Conserved regulation of proximodistal limb axis development by Meis1/Hth. *Nature* **402**, 425-9.

Mercader, N., Leonardo, E., Piedra, M. E., Martinez, A. C., Ros, M. A. and Torres, M. (2000). Opposing RA and FGF signals control proximodistal vertebrate limb development through regulation of Meis genes. *Development* **127**, 3961-70.

Mercader, N., Tanaka, E. M. and Torres, M. (2005). Proximodistal identity during vertebrate limb regeneration is regulated by Meis homeodomain proteins. *Development* **132**, 4131-42.

Merino, R., Macias, D., Ganan, Y., Economides, A. N., Wang, X., Wu, Q., Stahl, N., Sampath, K. T., Varona, P. and Hurle, J. M. (1999). Expression and function of Gdf-5 during digit skeletogenesis in the embryonic chick leg bud. *Dev Biol* **206**, 33-45.

Mic, F. A., Sirbu, I. O. and Duester, G. (2004). Retinoic acid synthesis controlled by Raldh2 is required early for limb bud initiation and then later as a proximodistal signal during apical ectodermal ridge formation. *J Biol Chem* **279**, 26698-706.

Min, H., Danilenko, D. M., Scully, S. A., Bolon, B., Ring, B. D., Tarpley, J. E., DeRose, M. and Simonet, W. S. (1998). Fgf-10 is required for both limb and lung development and exhibits striking functional similarity to Drosophila branchless. *Genes Dev* **12**, 3156-61.

Minguillon, C., Del Buono, J. and Logan, M. P. (2005). Tbx5 and Tbx4 are not sufficient to determine limb-specific morphologies but have common roles in initiating limb outgrowth. *Dev Cell* **8**, 75-84.

Moeller, C., Swindell, E. C., Kispert, A. and Eichele, G. (2003). Carboxypeptidase Z (CPZ) modulates Wnt signaling and regulates the development of skeletal elements in the chicken. *Development* **130**, 5103-11.

Moens, C. B. and Selleri, L. (2006). Hox cofactors in vertebrate development. *Dev Biol* **291**, 193-206.

Molven, A., Wright, C. V., Bremiller, R., De Robertis, E. M. and Kimmel, C. B. (1990). Expression of a homeobox gene product in normal and mutant zebrafish embryos: evolution of the tetrapod body plan. *Development* **109**, 279-88.

Monaghan, A. P., Davidson, D. R., Sime, C., Graham, E., Baldock, R., Bhattacharya, S. S. and Hill, R. E. (1991). The Msh-like homeobox genes define domains in the developing vertebrate eye. *Development* **112**, 1053-61.

Monica, K., Galili, N., Nourse, J., Saltman, D. and Cleary, M. L. (1991). PBX2 and PBX3, new homeobox genes with extensive homology to the human proto-oncogene PBX1. *Mol Cell Biol* **11**, 6149-57.

Moon, A. M., Boulet, A. M. and Capecchi, M. R. (2000). Normal limb development in conditional mutants of Fgf4. *Development* **127**, 989-96.

Moon, A. M. and Capecchi, M. R. (2000). Fgf8 is required for outgrowth and patterning of the limbs. *Nat Genet* **26**, 455-9.

Morata, G. (2001). How Drosophila appendages develop. *Nat Rev Mol Cell Biol* **2**, 89-97.

Morgan, B. A., Izpisua-Belmonte, J. C., Duboule, D. and Tabin, C. J. (1992). Targeted mis-expression of Hox-4.6 in the avian limb bud causes apparent homeotic transformations. *Nature* **358**, 236-9.

Mortlock, D. P., Post, L. C. and Innis, J. W. (1996). The molecular basis of hypodactyly (Hd): a deletion in Hoxa 13 leads to arrest of digital arch formation. *Nat Genet* **13**, 284-9.

Moskow, J. J., Bullrich, F., Huebner, K., Daar, I. O. and Buchberg, A. M. (1995). Meis1, a PBX1-related homeobox gene involved in myeloid leukemia in BXH-2 mice. *Mol Cell Biol* **15**, 5434-43.

Murcia, C. L., Bilovocky, N. A. and Herrup, K. (2004). Dissecting complex genetic interactions that influence the Engrailed-1 limb phenotype. *Mamm Genome* **15**, 352-60.

Nagy, A. (2000). Cre recombinase: the universal reagent for genome tailoring. *Genesis* **26**, 99-109.

Nagy, A. (2003). *Manipulating the Mouse Embryo: A Laboratory Manual*. Cold Spring Harbor Laboratory Press; U.S.A. pp.1-764.

Nakamura, T., Jenkins, N. A. and Copeland, N. G. (1996a). Identification of a new family of Pbx-related homeobox genes. *Oncogene* **13**, 2235-42.

Nakamura, T., Largaespada, D. A., Shaughnessy, J. D., Jr., Jenkins, N. A. and Copeland, N. G. (1996b). Cooperative activation of Hoxa and Pbx1-related genes in murine myeloid leukaemias. *Nat Genet* **12**, 149-53.

Nakashima, K. and de Crombrugghe, B. (2003). Transcriptional mechanisms in osteoblast differentiation and bone formation. *Trends Genet* **19**, 458-66.

Nelson, C. (2004). Selector genes and the genetic control of developmental modules. In Schlosser, G. and Wagner, G.P. (eds.) *Modularity in Development and Evolution.* University of Chicago Press, U.S.A. pp.17-33.

Nelson, C. E., Morgan, B. A., Burke, A. C., Laufer, E., DiMambro, E., Murtaugh, L. C., Gonzales, E., Tessarollo, L., Parada, L. F. and Tabin, C. (1996). Analysis of Hox gene expression in the chick limb bud. *Development* **122**, 1449-66.

Neuteboom, S. T., Peltenburg, L. T., van Dijk, M. A. and Murre, C. (1995). The hexapeptide LFPWMR in Hoxb-8 is required for cooperative DNA binding with Pbx1 and Pbx2 proteins. *Proc Natl Acad Sci U S A* **92**, 9166-70.

Ng, J. K., Kawakami, Y., Buscher, D., Raya, A., Itoh, T., Koth, C. M., Rodriguez Esteban, C., Rodriguez-Leon, J., Garrity, D. M., Fishman, M. C. et al. (2002). The limb identity gene Tbx5 promotes limb initiation by interacting with Wnt2b and Fgf10. *Development* **129**, 5161-70.

Niederreither, K., Subbarayan, V., Dolle, P. and Chambon, P. (1999). Embryonic retinoic acid synthesis is essential for early mouse post-implantation development. *Nat Genet* **21**, 444-8.

Niswander, L. (2003). Pattern formation: old models out on a limb. *Nat Rev Genet* **4**, 133-43.

Niswander, L., Jeffrey, S., Martin, G. R. and Tickle, C. (1994a). A positive feedback loop coordinates growth and patterning in the vertebrate limb. *Nature* **371**, 609-12.

Niswander, L. and Martin, G. R. (1992). Fgf-4 expression during gastrulation, myogenesis, limb and tooth development in the mouse. *Development* **114**, 755-68.

Niswander, L. and Martin, G. R. (1993a). FGF-4 and BMP-2 have opposite effects on limb growth. *Nature* **361**, 68-71.

Niswander, L. and Martin, G. R. (1993b). Mixed signals from the AER: FGF-4 and Bmp-2 have opposite effects on limb growth. *Prog Clin Biol Res* **383B**, 625-33.

Niswander, L., Tickle, C., Vogel, A., Booth, I. and Martin, G. R. (1993). FGF-4 replaces the apical ectodermal ridge and directs outgrowth and patterning of the limb. *Cell* **75**, 579-87.

Niswander, L., Tickle, C., Vogel, A. and Martin, G. (1994b). Function of FGF-4 in limb development. *Mol Reprod Dev* **39**, 83-8.

Nonchev, S., Maconochie, M., Gould, A., Morrison, A. and Krumlauf, R. (1997). Cross-regulatory interactions between Hox genes and the control of segmental expression in the vertebrate central nervous system. *Cold Spring Harb Symp Quant Biol* **62**, 313-23.

Noramly, S., Pisenti, J., Abbott, U. and Morgan, B. (1996). Gene expression in the limbless mutant: polarized gene expression in the absence of Shh and an AER. *Dev Biol* **179**, 339-46.

Nourse, J., Mellentin, J. D., Galili, N., Wilkinson, J., Stanbridge, E., Smith, S. D. and Cleary, M. L. (1990). Chromosomal translocation t(1;19) results in synthesis of a homeobox fusion mRNA that codes for a potential chimeric transcription factor. *Cell* **60**, 535-45.

O'Leary, M. A. (2001). The phylogenetic position of cetaceans: further combined data analyses, comparisons with the stratigraphic record and a discussion of character optimization. *Am Zool* **41**, 487-506.

O'Rourke, M. P., Soo, K., Behringer, R. R., Hui, C. C. and Tam, P. P. (2002). Twist plays an essential role in FGF and SHH signal transduction during mouse limb development. *Dev Biol* **248**, 143-56.

Ohuchi, H., Nakagawa, T., Yamamoto, A., Araga, A., Ohata, T., Ishimaru, Y., Yoshioka, H., Kuwana, T., Nohno, T., Yamasaki, M. et al. (1997). The mesenchymal factor, FGF10, initiates and maintains the outgrowth of the chick limb bud through interaction with FGF8, an apical ectodermal factor. *Development* **124**, 2235-44.

Oliver, G., De Robertis, E. M., Wolpert, L. and Tickle, C. (1990). Expression of a homeobox gene in the chick wing bud following application of retinoic acid and grafts of polarizing region tissue. *Embo J* **9**, 3093-9.

Oliver, G., Wright, C. V., Hardwicke, J. and De Robertis, E. M. (1988a). A gradient of homeodomain protein in developing forelimbs of Xenopus and mouse embryos. *Cell* **55**, 1017-24.

Oliver, G., Wright, C. V., Hardwicke, J. and De Robertis, E. M. (1988b). Differential antero-posterior expression of two proteins encoded by a homeobox gene in Xenopus and mouse embryos. *Embo J* **7**, 3199-209.

Olwin, B. B., Arthur, K., Hannon, K., Hein, P., McFall, A., Riley, B., Szebenyi, G., Zhou, Z., Zuber, M. E., Rapraeger, A. C. et al. (1994). Role of FGFs in skeletal muscle and limb development. *Mol Reprod Dev* **39**, 90-101.

Orlando, V., Strutt, H. and Paro, R. (1997). Analysis of chromatin structure by in vivo formaldehyde cross-linking. *Methods* **11**, 205-14.

Oxnard, C. E. (1967). The functional morphology of the primate shoulder as revealed by comparative anatomical, osteometric, and discriminant function techniques. *Am J Phys Anthropol* **26**, 219-240.

Oxnard, C. E. (1977). Morphometric affinities of the human shoulder. *Am J Phys Anthropol* **46**, 367-74.

Pai, C. Y., Kuo, T. S., Jaw, T. J., Kurant, E., Chen, C. T., Bessarab, D. A., Salzberg, A. and Sun, Y. H. (1998). The Homothorax homeoprotein activates the nuclear localization of another homeoprotein, extradenticle, and suppresses eye development in Drosophila. *Genes Dev* **12**, 435-46.

Papenbrock, T., Visconti, R. P. and Awgulewitsch, A. (2000). Loss of fibula in mice overexpressing Hoxc11. *Mech Dev* **92**, 113-23.

Parr, B. A., Avery, E. J., Cygan, J. A. and McMahon, A. P. (1998). The classical mouse mutant postaxial hemimelia results from a mutation in the Wnt 7a gene. *Dev Biol* **202**, 228-34.

Parr, B. A. and McMahon, A. P. (1995). Dorsalizing signal Wnt-7a required for normal polarity of D-V and A-P axes of mouse limb. *Nature* **374**, 350-3.

Parr, B. A., Shea, M. J., Vassileva, G. and McMahon, A. P. (1993). Mouse Wnt genes exhibit discrete domains of expression in the early embryonic CNS and limb buds. *Development* **119**, 247-61.

Passner, J. M., Ryoo, H. D., Shen, L., Mann, R. S. and Aggarwal, A. K. (1999). Structure of a DNA-bound Ultrabithorax-Extradenticle homeodomain complex. *Nature* **397**, 714-9.

Pautou, M. P. and Kieny, M. (1973). [Ecto-mesodermic interaction in the establishment of dorso-ventral polarity in the chick embryo foot]. *C R Acad Sci Hebd Seances Acad Sci D* **277**, 1225-8.

Pearse, R. V., 2nd and Tabin, C. J. (1998). The molecular ZPA. *J Exp Zool* **282**, 677-90.

Pearson, J. C., Lemons, D. and McGinnis, W. (2005). Modulating Hox gene functions during animal body patterning. *Nat Rev Genet* **6**, 893-904.

Peichel, C. L., Nereng, K. S., Ohgi, K. A., Cole, B. L., Colosimo, P. F., Buerkle, C. A., Schluter, D. and Kingsley, D. M. (2001). The genetic architecture of divergence between threespine stickleback species. *Nature* **414**, 901-5.

Peichel, C. L., Prabhakaran, B. and Vogt, T. F. (1997). The mouse Ulnaless mutation deregulates posterior HoxD gene expression and alters appendicular patterning. *Development* **124**, 3481-92.

Peifer, M. and Wieschaus, E. (1990). Mutations in the Drosophila gene extradenticle affect the way specific homeo domain proteins regulate segmental identity. *Genes Dev* **4**, 1209-23.

Pellegrini, M., Pantano, S., Fumi, M. P., Lucchini, F. and Forabosco, A. (2001). Agenesis of the scapula in Emx2 homozygous mutants. *Dev Biol* **232**, 149-56.

Pendleton, J. W., Nagai, B. K., Murtha, M. T. and Ruddle, F. H. (1993). Expansion of the Hox gene family and the evolution of chordates. *Proc Natl Acad Sci U S A* **90**, 6300-4.

Perry, G. H., Verrelli, B. C. and Stone, A. C. (2006). Molecular evolution of the primate developmental genes MSX1 and PAX9. *Mol Biol Evol* **23**, 644-54.

Peters, H., Neubuser, A., Kratochwil, K. and Balling, R. (1998). Pax9-deficient mice lack pharyngeal pouch derivatives and teeth and exhibit craniofacial and limb abnormalities. *Genes Dev* **12**, 2735-47.

Peters, H., Wilm, B., Sakai, N., Imai, K., Maas, R. and Balling, R. (1999). Pax1 and Pax9 synergistically regulate vertebral column development. *Development* **126**, 5399-408.

Phelan, M. L., Rambaldi, I. and Featherstone, M. S. (1995). Cooperative interactions between HOX and PBX proteins mediated by a conserved peptide motif. *Mol Cell Biol* **15**, 3989-97.

Pinsonneault, J., Florence, B., Vaessin, H. and McGinnis, W. (1997). A model for extradenticle function as a switch that changes HOX proteins from repressors to activators. *Embo J* **16**, 2032-42.

Piper, D. E., Batchelor, A. H., Chang, C. P., Cleary, M. L. and Wolberger, C. (1999). Structure of a HoxB1-Pbx1 heterodimer bound to DNA: role of the hexapeptide and a fourth homeodomain helix in complex formation. *Cell* **96**, 587-597.

Pizette, S., Abate-Shen, C. and Niswander, L. (2001). BMP controls proximodistal outgrowth, via induction of the apical ectodermal ridge, and dorsoventral patterning in the vertebrate limb. *Development* **128**, 4463-74.

Popperl, H., Bienz, M., Studer, M., Chan, S. K., Aparicio, S., Brenner, S., Mann, R. S. and Krumlauf, R. (1995). Segmental expression of Hoxb-1 is controlled by a highly conserved autoregulatory loop dependent upon exd/pbx. *Cell* **81**, 1031-42.

Popperl, H., Rikhof, H., Chang, H., Haffter, P., Kimmel, C. B. and Moens, C. B. (2000). lazarus is a novel pbx gene that globally mediates hox gene function in zebrafish. *Mol Cell* **6**, 255-67.

Post, L. C. and Innis, J. W. (1999). Altered Hox expression and increased cell death distinguish Hypodactyly from Hoxa13 null mice. *Int J Dev Biol* **43**, 287-94.

Prols, F., Ehehalt, F., Rodriguez-Niedenfuhr, M., He, L., Huang, R. and Christ, B. (2004). The role of Emx2 during scapula formation. *Dev Biol* **275**, 315-24.

Pueyo, J. I. and Couso, J. P. (2005). Parallels between the proximal-distal development of vertebrate and arthropod appendages: homology without an ancestor? *Curr Opin Genet Dev* **15**, 439-46.

Raff, R. A. (1996). *The Shape of Life: Genes, Development, and the Evolution of Animal Form*. University of Chicago Press; Chicago. pp.vii-520.

Rallis, C., Bruneau, B. G., Del Buono, J., Seidman, C. E., Seidman, J. G., Nissim, S., Tabin, C. J. and Logan, M. P. (2003). Tbx5 is required for forelimb bud formation and continued outgrowth. *Development* **130**, 2741-51.

Rallis, C., Del Buono, J. and Logan, M. P. (2005). Tbx3 can alter limb position along the rostrocaudal axis of the developing embryo. *Development* **132**, 1961-70.

Ramirez-Solis, R., Zheng, H., Whiting, J., Krumlauf, R. and Bradley, A. (1993). Hoxb-4 (Hox-2.6) mutant mice show homeotic transformation of a cervical vertebra and defects in the closure of the sternal rudiments. *Cell* **73**, 279-94.

Rancourt, D. E., Tsuzuki, T. and Capecchi, M. R. (1995). Genetic interaction between hoxb-5 and hoxb-6 is revealed by nonallelic noncomplementation. *Genes Dev* **9**, 108-22.

Rauskolb, C., Peifer, M. and Wieschaus, E. (1993). extradenticle, a regulator of homeotic gene activity, is a homolog of the homeobox-containing human proto-oncogene pbx1. *Cell* **74**, 1101-12.

Rauskolb, C., Smith, K. M., Peifer, M. and Wieschaus, E. (1995). extradenticle determines segmental identities throughout Drosophila development. *Development* **121**, 3663-73.

Raynaud, A. and Pieau, C. (1985). [Initial stages of the formation of the genital organs in reptiles]. *Arch Anat Microsc Morphol Exp* **74**, 42-9.

Reijntjes, S., Gale, E. and Maden, M. (2003). Expression of the retinoic acid catabolising enzyme CYP26B1 in the chick embryo and its regulation by retinoic acid. *Gene Expr Patterns* **3**, 621-7.

Reno, P. L. and ADD. (2000). Adaptationism and the anthropoid postcranium: selection does not govern the length of the radial neck. *J. Morph.* **246**.

Reno, P. L., Lovejoy, C. O., McCollum, M. A., Hamrick, M. W., Meindl, R. S. and Cohn, M. J. (2001). Ontogenetic data suggest the presence of HOXD targets that act as growth scalars in the hominoid forearm and hand. Poster presented to the American Association of Physical Anthropologists, March 30th, 2001, Kansas City, Missouri.

Reno, P. L., McCollum, M. A., Cohn, M. J., Meindl, R. S., Hamrick, M., White, T. D., Kondo, T. and Lovejoy, C. O. (in press). The evolution of hominoid hands: Growth scaling registers with posterior HOXD expression. *Evol Dev*.

Rhee, J. W., Arata, A., Selleri, L., Jacobs, Y., Arata, S., Onimaru, H. and Cleary, M. L. (2004). Pbx3 deficiency results in central hypoventilation. *Am J Pathol* **165**, 1343-50.

Richardson, M. K., Carl, T. F., Hanken, J., Elinson, R. P., Cope, C. and Bagley, P. (1998). Limb development and evolution: a frog embryo with no apical ectodermal ridge (AER). *J Anat* **192 (Pt 3)**, 379-90.

Richardson, M. K. and Oelschlager, H. H. (2002). Time, pattern, and heterochrony: a study of hyperphalangy in the dolphin embryo flipper. *Evol Dev* **4**, 435-44.

Riddle, R. D., Ensini, M., Nelson, C., Tsuchida, T., Jessell, T. M. and Tabin, C. (1995). Induction of the LIM homeobox gene Lmx1 by WNT7a establishes dorsoventral pattern in the vertebrate limb. *Cell* **83**, 631-40.

Riddle, R. D., Johnson, R. L., Laufer, E. and Tabin, C. (1993). Sonic hedgehog mediates the polarizing activity of the ZPA. *Cell* **75**, 1401-16.

Rieckhof, G. E., Casares, F., Ryoo, H. D., Abu-Shaar, M. and Mann, R. S. (1997). Nuclear translocation of extradenticle requires homothorax, which encodes an extradenticle-related homeodomain protein. *Cell* **91**, 171-83.

Robert, B. and Lallemand, Y. (2006). Anteroposterior patterning in the limb and digit specification: contribution of mouse genetics. *Dev Dyn* **235**, 2337-52.

Roberts, C. W., Shutter, J. R. and Korsmeyer, S. J. (1994). Hox11 controls the genesis of the spleen. *Nature* **368**, 747-9.

Robinson, G. W., Wray, S. and Mahon, K. A. (1991). Spatially restricted expression of a member of a new family of murine Distal-less homeobox genes in the developing forebrain. *New Biol* **3**, 1183-94.

Robledo, R. F., Rajan, L., Li, X. and Lufkin, T. (2002). The Dlx5 and Dlx6 homeobox genes are essential for craniofacial, axial, and appendicular skeletal development. *Genes Dev* **16**, 1089-101.

Rodriguez-Esteban, C., Schwabe, J. W., De La Pena, J., Foys, B., Eshelman, B. and Belmonte, J. C. (1997). Radical fringe positions the apical ectodermal ridge at the dorsoventral boundary of the vertebrate limb. *Nature* **386**, 360-6.

Rodriguez-Esteban, C., Tsukui, T., Yonei, S., Magallon, J., Tamura, K. and Izpisua Belmonte, J. C. (1999). The T-box genes Tbx4 and Tbx5 regulate limb outgrowth and identity. *Nature* **398**, 814-8.

Rodriguez-Niedenfuhr, M., Dathe, V., Jacob, H. J., Prols, F. and Christ, B. (2003). Spatial and temporal pattern of Wnt-6 expression during chick development. *Anat Embryol (Berl)* **206**, 447-51.

Rong, P. M., Teillet, M. A., Ziller, C. and Le Douarin, N. M. (1992). The neural tube/notochord complex is necessary for vertebral but not limb and body wall striated muscle differentiation. *Development* **115**, 657-72.

Ros, M. A., Lopez-Martinez, A., Simandl, B. K., Rodriguez, C., Izpisua Belmonte, J. C., Dahn, R. and Fallon, J. F. (1996). The limb field mesoderm determines initial limb bud anteroposterior asymmetry and budding independent of sonic hedgehog or apical ectodermal gene expressions. *Development* **122**, 2319-30.

Rowe, D. A. and Fallon, J. F. (1982). The proximodistal determination of skeletal parts in the developing chick leg. *J Embryol Exp Morphol* **68**, 1-7.

Ryoo, H. D. and Mann, R. S. (1999). The control of trunk Hox specificity and activity by Extradenticle. *Genes Dev* **13**, 1704-16.

Ryoo, H. D., Marty, T., Casares, F., Affolter, M. and Mann, R. S. (1999). Regulation of Hox target genes by a DNA bound Homothorax/Hox/Extradenticle complex. *Development* **126**, 5137-48.

Sagai, T., Hosoya, M., Mizushina, Y., Tamura, M. and Shiroishi, T. (2005). Elimination of a long-range cis-regulatory module causes complete loss of limb-specific Shh expression and truncation of the mouse limb. *Development* **132**, 797-803.

Sagai, T., Masuya, H., Tamura, M., Shimizu, K., Yada, Y., Wakana, S., Gondo, Y., Noda, T. and Shiroishi, T. (2004). Phylogenetic conservation of a limb-specific, cis-acting regulator of Sonic hedgehog (Shh). *Mamm Genome* **15**, 23-34.

Sagerstrom, C. G. (2004). PbX marks the spot. *Dev Cell* **6**, 737-8.

Saito, D., Yonei-Tamura, S., Takahashi, Y. and Tamura, K. (2006). Level-specific role of paraxial mesoderm in regulation of Tbx5/Tbx4 expression and limb initiation. *Dev Biol* **292**, 79-89.

Saleh, M., Rambaldi, I., Yang, X. J. and Featherstone, M. S. (2000). Cell signaling switches HOX-PBX complexes from repressors to activators of transcription mediated by histone deacetylases and histone acetyltransferases. *Mol Cell Biol* **20**, 8623-33.

Salsi, V. and Zappavigna, V. (2006). Hoxd13 and Hoxa13 directly control the expression of the EphA7 Ephrin tyrosine kinase receptor in developing limbs. *J Biol Chem* **281**, 1992-9.

Samad, O. A., Geisen, M. J., Caronia, G., Varlet, I., Zappavigna, V., Ericson, J., Goridis, C. and Rijli, F. M. (2004). Integration of anteroposterior and dorsoventral regulation of Phox2b transcription in cranial motoneuron progenitors by homeodomain proteins. *Development* **131**, 4071-83.

Sanz-Ezquerro, J. J. and Tickle, C. (2003). Fgf signaling controls the number of phalanges and tip formation in developing digits. *Curr Biol* **13**, 1830-6.

Sarno, J. L., Kliman, H. J. and Taylor, H. S. (2005). HOXA10, Pbx2, and Meis1 protein expression in the human endometrium: formation of multimeric complexes on HOXA10 target genes. *J Clin Endocrinol Metab* **90**, 522-8.

Sassoon, D., Lyons, G., Wright, W. E., Lin, V., Lassar, A., Weintraub, H. and Buckingham, M. (1989). Expression of two myogenic regulatory factors myogenin and MyoD1 during mouse embryogenesis. *Nature* **341**, 303-7.

Saunders, J. W., Jr. (1948). The proximo-distal sequence of origin of the parts of the chick wing and the role of the ectoderm. *J Exp Zool* **282**, 628-668.

Saunders, J. W., Jr. and Gasseling, M. T. (1968). Ectodermal-mesodermal interactions in the origin of limb symmetry. In Fleischmajer, R. and Billingham, R.E. (eds.) *Epithelial-Mesenchymal Interactions*. Williams and Wilkins; Baltimore. pp.78-97.

Saunders, J. W., Jr., Gasseling, M. T. and Gfeller, M. (1958). Interactions of ectoderm and mesoderm in the origin of axial relationships in the wing of the fowl. *J Exp Zool* **137**, 39-74.

Sauvageau, G., Thorsteinsdottir, U., Hough, M. R., Hugo, P., Lawrence, H. J., Largman, C. and Humphries, R. K. (1997). Overexpression of HOXB3 in hematopoietic cells causes defective lymphoid development and progressive myeloproliferation. *Immunity* **6**, 13-22.

Scherz, P. J., Harfe, B. D., McMahon, A. P. and Tabin, C. J. (2004). The limb bud Shh-Fgf feedback loop is terminated by expansion of former ZPA cells. *Science* **305**, 396-9.

Schlosser, G. and Wagner, G. P. (2004). *Modularity in Development and Evolution.* University of Chicago Press; Chicago. pp.x-600.

Schnabel, C. A., Jacobs, Y. and Cleary, M. L. (2000). HoxA9-mediated immortalization of myeloid progenitors requires functional interactions with TALE cofactors Pbx and Meis. *Oncogene* **19**, 608-16.

Schultz, A. (1930). The skeleton of the trunk and limbs of higher primates. *Human Biol.* **2**, 303-438.

Schweitzer, R., Chyung, J. H., Murtaugh, L. C., Brent, A. E., Rosen, V., Olson, E. N., Lassar, A. and Tabin, C. J. (2001). Analysis of the tendon cell fate using Scleraxis, a specific marker for tendons and ligaments. *Development* **128**, 3855-66.

Sears, K. E., Behringer, R. R., Rasweiler, J. J. t. and Niswander, L. A. (2006).

Development of bat flight: morphologic and molecular evolution of bat wing digits. *Proc Natl Acad Sci U S A* **103**, 6581-6.

Sedmera, D., Misek, I. and Klima, M. (1997a). On the development of Cetacean extremities: I. Hind limb rudimentation in the Spotted dolphin (Stenella attenuata). *Eur J Morphol* **35**, 25-30.

Sedmera, D., Misek, I. and Klima, M. (1997b). On the development of Cetacean extremities: II. Morphogenesis and histogenesis of the flippers in the spotted dolphin (Stenella attenuata). *Eur J Morphol* **35**, 117-23.

Sekine, K., Ohuchi, H., Fujiwara, M., Yamasaki, M., Yoshizawa, T., Sato, T., Yagishita, N., Matsui, D., Koga, Y., Itoh, N. et al. (1999). Fgf10 is essential for limb and lung formation. *Nat Genet* **21**, 138-41.

Selleri, L., Depew, M. J., Jacobs, Y., Chanda, S. K., Tsang, K. Y., Cheah, K. S., Rubenstein, J. L., O'Gorman, S. and Cleary, M. L. (2001). Requirement for Pbx1 in skeletal patterning and programming chondrocyte proliferation and differentiation. *Development* **128**, 3543-57.

Selleri, L., DiMartino, J., van Deursen, J., Brendolan, A., Sanyal, M., Boon, E., Capellini, T., Smith, K. S., Rhee, J., Popperl, H. et al. (2004). The TALE homeodomain protein Pbx2 is not essential for development and long-term survival. *Mol Cell Biol* **24**, 5324-31.

Shapiro, M. D., Hanken, J. and Rosenthal, N. (2003). Developmental basis of evolutionary digit loss in the Australian lizard Hemiergis. *J Exp Zoolog B Mol Dev Evol* **297**, 48-56.

Shapiro, M. D., Marks, M. E., Peichel, C. L., Blackman, B. K., Nereng, K. S., Jonsson, B., Schluter, D. and Kingsley, D. M. (2004). Genetic and developmental basis of evolutionary pelvic reduction in threespine sticklebacks. *Nature* **428**, 717-23.

Sharpe, P. T., Miller, J. R., Evans, E. P., Burtenshaw, M. D. and Gaunt, S. J. (1988). Isolation and expression of a new mouse homeobox gene. *Development* **102**, 397-407.

Shen, W. F., Chang, C. P., Rozenfeld, S., Sauvageau, G., Humphries, R. K., Lu, M., Lawrence, H. J., Cleary, M. L. and Largman, C. (1996). Hox homeodomain proteins exhibit selective complex stabilities with Pbx and DNA. *Nucleic Acids Res* **24**, 898-906.

Shen, W. F., Montgomery, J. C., Rozenfeld, S., Moskow, J. J., Lawrence, H. J., Buchberg, A. M. and Largman, C. (1997). AbdB-like Hox proteins stabilize DNA binding by the Meis1 homeodomain proteins. *Mol Cell Biol* **17**, 6448-58.

Sherman, L., Wainwright, D., Ponta, H. and Herrlich, P. (1998). A splice variant of CD44 expressed in the apical ectodermal ridge presents fibroblast growth factors to limb mesenchyme and is required for limb outgrowth. *Genes Dev* **12**, 1058-71.

Shubin, N., Tabin, C. and Carroll, S. (1997). Fossils, genes and the evolution of animal limbs. *Nature* **388**, 639-48.

Silver, L. M. (1995). *Mouse Genetics: Concepts and Applications*. Oxford University Press; U.S.A. pp.1-376.

Simeone, A., Acampora, D., Pannese, M., D'Esposito, M., Stornaiuolo, A., Gulisano, M., Mallamaci, A., Kastury, K., Druck, T., Huebner, K. et al. (1994). Cloning and characterization of two members of the vertebrate Dlx gene family. *Proc Natl Acad Sci U S A* **91**, 2250-4.

Slack, J. M. (1976). Determination of polarity in the amphibian limb. *Nature* **261**, 44-6.

Small, K. M. and Potter, S. S. (1993). Homeotic transformations and limb defects in Hox A11 mutant mice. *Genes Dev* **7**, 2318-28.

Sordino, P., Duboule, D. and Kondo, T. (1996). Zebrafish Hoxa and Evx-2 genes: cloning, developmental expression and implications for the functional evolution of posterior Hox genes. *Mech Dev* **59**, 165-75.

Sordino, P., van der Hoeven, F. and Duboule, D. (1995). Hox gene expression in teleost fins and the origin of vertebrate digits. *Nature* **375**, 678-81.

Soriano, P. (1999). Generalized lacZ expression with the ROSA26 Cre reporter strain. *Nat Genet* **21**, 70-1.

Soshnikova, N., Zechner, D., Huelsken, J., Mishina, Y., Behringer, R. R., Taketo, M. M., Crenshaw, E. B., 3rd and Birchmeier, W. (2003). Genetic interaction between Wnt/beta-catenin and BMP receptor signaling during formation of the AER and the dorsal-ventral axis in the limb. *Genes Dev* **17**, 1963-8.

Spitz, F., Gonzalez, F., Peichel, C., Vogt, T. F., Duboule, D. and Zakany, J. (2001). Large scale transgenic and cluster deletion analysis of the HoxD complex separate an ancestral regulatory module from evolutionary innovations. *Genes Dev* **15**, 2209-14.

Stephens, T. D., Baker, W. C., Cotterell, J. W., Edwards, D. R., Pugmire, D. S., Roberts, S. G., Shaker, M. R., Willis, H. J. and Winger, K. P. (1993a).

Evaluation of the chick wing territory as an equipotential self-differentiating system. *Dev Dyn* **197**, 157-68.

Stephens, T. D., Roberts, S. G., Marchiando, R. J., Degn, L. L., Hackett, D. A., Warnock, M. A., Mason, M. J., Edwards, R., Torres, R. D., Deriemaeker, P. K. et al. (1993b). Axial and paraxial influences on the origin of the chick embryo limb. *Prog Clin Biol Res* **383A**, 317-26.

Stopper, G. F. and Wagner, G. P. (2005). Of chicken wings and frog legs: a smorgasbord of evolutionary variation in mechanisms of tetrapod limb development. *Dev Biol* **288**, 21-39.

Storm, E. E. and Kingsley, D. M. (1999). GDF5 coordinates bone and joint formation during digit development. *Dev Biol* **209**, 11-27.

Stratford, T. H., Kostakopoulou, K. and Maden, M. (1997). Hoxb-8 has a role in establishing early anterior-posterior polarity in chick forelimb but not hindlimb. *Development* **124**, 4225-34.

Studer, M., Gavalas, A., Marshall, H., Ariza-McNaughton, L., Rijli, F. M., Chambon, P. and Krumlauf, R. (1998). Genetic interactions between Hoxa1 and Hoxb1 reveal new roles in regulation of early hindbrain patterning. *Development* **125**, 1025-36.

Studer, M., Lumsden, A., Ariza-McNaughton, L., Bradley, A. and Krumlauf, R. (1996). Altered segmental identity and abnormal migration of motor neurons in mice lacking Hoxb-1. *Nature* **384**, 630-4.

Sturdee, A. and Connock, M. (1975). Embryonic limb bud of the urodele: morphological studies of the apex. *Differentiation* **3**, 43-49.

Suemori, H. and Noguchi, S. (2000). Hox C cluster genes are dispensable for overall body plan of mouse embryonic development. *Dev Biol* **220**, 333-42.

Summerbell, D. (1974). A quantitative analysis of the effect of excision of the AER from the chick limb-bud. *J Embryol Exp Morphol* **32**, 651-60.

Sun, X., Mariani, F. V. and Martin, G. R. (2002). Functions of FGF signalling from the apical ectodermal ridge in limb development. *Nature* **418**, 501-8.

Sun, X., Meyers, E. N., Lewandoski, M. and Martin, G. R. (1999). Targeted disruption of Fgf8 causes failure of cell migration in the gastrulating mouse embryo. *Genes Dev* **13**, 1834-46.

Suzuki, T., Takeuchi, J., Koshiba-Takeuchi, K. and Ogura, T. (2004). Tbx Genes Specify Posterior Digit Identity through Shh and BMP Signaling. *Dev Cell* **6**, 43-53.

Svingen, T. and Tonissen, K. F. (2006). Hox transcription factors and their elusive mammalian gene targets. *Heredity* **97**, 88-96.

Tabata, T. and Takei, Y. (2004). Morphogens, their identification and regulation. *Development* **131**, 703-12.

Tagashira, S., Harada, H., Katsumata, T., Itoh, N. and Nakatsuka, M. (1997). Cloning of mouse FGF10 and up-regulation of its gene expression during wound healing. *Gene* **197**, 399-404.

Takeuchi, J. K., Koshiba-Takeuchi, K., Matsumoto, K., Vogel-Hopker, A., Naitoh-Matsuo, M., Ogura, K., Takahashi, N., Yasuda, K. and Ogura, T. (1999). Tbx5 and Tbx4 genes determine the wing/leg identity of limb buds. *Nature* **398**, 810-4.

Takeuchi, J. K., Koshiba-Takeuchi, K., Suzuki, T., Kamimura, M., Ogura, K. and Ogura, T. (2003). Tbx5 and Tbx4 trigger limb initiation through activation of the Wnt/Fgf signaling cascade. *Development* **130**, 2729-39.

Tanaka, M., Hale, L. A., Amores, A., Yan, Y. L., Cresko, W. A., Suzuki, T. and Postlethwait, J. H. (2005). Developmental genetic basis for the evolution of pelvic fin loss in the pufferfish Takifugu rubripes. *Dev Biol* **281**, 227-39.

Tanaka, M., Munsterberg, A., Anderson, W. G., Prescott, A. R., Hazon, N. and Tickle, C. (2002). Fin development in a cartilaginous fish and the origin of vertebrate limbs. *Nature* **416**, 527-31.

Tank, P. W., Carlson, B. M. and Connelly, T. G. (1977). A scanning electron microscopic comparison of the development of embryonic and regenerating limbs in the axolotl. *J Exp Zool* **201**, 417-29.

Tarchini, B. and Duboule, D. (2006). Control of Hoxd genes' collinearity during early limb development. *Dev Cell* **10**, 93-103.

Tarchini, B., Duboule, D. and Kmita, M. (2006). Regulatory constraints in the evolution of the tetrapod limb anterior-posterior polarity. *Nature* **443**, 985-8.

te Welscher, P., Fernandez-Teran, M., Ros, M. A. and Zeller, R. (2002). Mutual genetic antagonism involving GLI3 and dHAND prepatterns the vertebrate limb bud mesenchyme prior to SHH signaling. *Genes Dev* **16**, 421-6.

Teillet, M. A., Lapointe, F. and Le Douarin, N. M. (1998). The relationships between notochord and floor plate in vertebrate development revisited. *Proc Natl Acad Sci U S A* **95**, 11733-8.

ten Berge, D., Brouwer, A., Korving, J., Martin, J. F. and Meijlink, F. (1998). Prx1 and Prx2 in skeletogenesis: roles in the craniofacial region, inner ear and limbs. *Development* **125**, 3831-42.

Thewissen, J. G., Cohn, M. J., Stevens, L. S., Bajpai, S., Heyning, J. and Horton, W. E., Jr. (2006). Developmental basis for hind-limb loss in dolphins and origin of the cetacean bodyplan. *Proc Natl Acad Sci U S A* **103**, 8414-8.

Thisse, B. and Thisse, C. (2005). Functions and regulations of fibroblast growth factor signaling during embryonic development. *Dev Biol* **287**, 390-402.

Thorsteinsdottir, U., Krosl, J., Kroon, E., Haman, A., Hoang, T. and Sauvageau, G. (1999). The oncoprotein E2A-Pbx1a collaborates with Hoxa9 to acutely transform primary bone marrow cells. *Mol Cell Biol* **19**, 6355-66.

Thorsteinsdottir, U., Sauvageau, G., Hough, M. R., Dragowska, W., Lansdorp, P. M., Lawrence, H. J., Largman, C. and Humphries, R. K. (1997a). Overexpression of HOXA10 in murine hematopoietic cells perturbs both myeloid and lymphoid differentiation and leads to acute myeloid leukemia. *Mol Cell Biol* **17**, 495-505.

Thorsteinsdottir, U., Sauvageau, G. and Humphries, R. K. (1997b). Hox homeobox genes as regulators of normal and leukemic hematopoiesis. *Hematol Oncol Clin North Am* **11**, 1221-37.

Tickle, C. (2003). Patterning systems--from one end of the limb to the other. *Dev Cell* **4**, 449-58.

Tickle, C. (2006). Making digit patterns in the vertebrate limb. *Nat Rev Mol Cell Biol* **7**, 45-53.

Timmons, P. M., Wallin, J., Rigby, P. W. and Balling, R. (1994). Expression and function of Pax 1 during development of the pectoral girdle. *Development* **120**, 2773-85.

Torok, M. A., Gardiner, D. M., Izpisua-Belmonte, J. C. and Bryant, S. V. (1999). Sonic hedgehog (shh) expression in developing and regenerating axolotl limbs. *J Exp Zool* **284**, 197-206.

van den Akker, E., Fromental-Ramain, C., de Graaff, W., Le Mouellic, H., Brulet, P., Chambon, P. and Deschamps, J. (2001). Axial skeletal patterning in mice lacking all paralogous group 8 Hox genes. *Development* **128**, 1911-21.

van der Hoeven, F., Sordino, P., Fraudeau, N., Izpisua-Belmonte, J. C. and Duboule, D. (1996). Teleost HoxD and HoxA genes: comparison with tetrapods and functional evolution of the HOXD complex. *Mech Dev* **54**, 9-21.

Vargesson, N., Clarke, J. D., Vincent, K., Coles, C., Wolpert, L. and Tickle, C. (1997). Cell fate in the chick limb bud and relationship to gene expression. *Development* **124**, 1909-18.

Vaughan, T. A., Ryan, J. M. and Czaplewski, N. J. (2000). *Mammalogy*. Brooks Cole; London. pp.vi-565.

Vidal, A., Capellini, T. D., Yeh, N., Selleri, L., Koff, A. and Bromage, T. G. (2006). Development and cancer: two sides of the same coin. In Bromage, T.G., Vidal, A., Aguirre, E., and Perez-Ochoa, A. (eds) *Integrative Approaches to Human Health and Evolution*. Elsevier; Amsterdam. pp.147-159.

Vogel, A., Rodriguez, C. and Izpisua-Belmonte, J. C. (1996). Involvement of FGF-8 in initiation, outgrowth and patterning of the vertebrate limb. *Development* **122**, 1737-50.

Vogel, A., Rodriguez, C., Warnken, W. and Izpisua Belmonte, J. C. (1995). Dorsal cell fate specified by chick Lmx1 during vertebrate limb development. *Nature* **378**, 716-20.

Von Dassow, G. and Munro, E. (1999). Modularity in animal development and evolution: elements of a conceptual framework for EvoDevo. *J Exp Zool* **285**, 307-325.

Wagner, E. F. and Karsenty, G. (2001). Genetic control of skeletal development. *Curr Opin Genet Dev* **11**, 527-32.

Wagner, G. P., Chiu, C. and Laubichler, M. (2000). Developmental evolution as a mechanistic science: the inference from developmental mecnahisms to evolutionary processes. *Am Zool* **40**, 819-831.

Wagner, K., Mincheva, A., Korn, B., Lichter, P. and Popperl, H. (2001). Pbx4, a new Pbx family member on mouse chromosome 8, is expressed during spermatogenesis. *Mech Dev* **103**, 127-31.

Wahba, G. M., Hostikka, S. L. and Carpenter, E. M. (2001). The paralogous Hox genes Hoxa10 and Hoxd10 interact to pattern the mouse hindlimb peripheral nervous system and skeleton. *Dev Biol* **231**, 87-102.

Wallin, J., Mizutani, Y., Imai, K., Miyashita, N., Moriwaki, K., Taniguchi, M., Koseki, H. and Balling, R. (1993). A new Pax gene, Pax-9, maps to mouse chromosome 12. *Mamm Genome* **4**, 354-8.

Walterhouse, D., Ahmed, M., Slusarski, D., Kalamaras, J., Boucher, D., Holmgren, R. and Iannaccone, P. (1993). gli, a zinc finger transcription factor and oncogene, is expressed during normal mouse development. *Dev Dyn* **196**, 91-102.

Walther, C., Guenet, J. L., Simon, D., Deutsch, U., Jostes, B., Goulding, M. D., Plachov, D., Balling, R. and Gruss, P. (1991). Pax: a murine multigene family of paired box-containing genes. *Genomics* **11**, 424-34.

Wang, B., Fallon, J. F. and Beachy, P. A. (2000). Hedgehog-regulated processing of Gli3 produces an anterior/posterior repressor gradient in the developing vertebrate limb. *Cell* **100**, 423-34.

Wang, B., He, L., Ehehalt, F., Geetha-Loganathan, P., Nimmagadda, S., Christ, B., Scaal, M. and Huang, R. (2005). The formation of the avian scapula blade takes place in the hypaxial domain of the somites and requires somatopleure-derived BMP signals. *Dev Biol* **287**, 11-8.

Waskiewicz, A. J., Rikhof, H. A., Hernandez, R. E. and Moens, C. B. (2001). Zebrafish Meis functions to stabilize Pbx proteins and regulate hindbrain patterning. *Development* **128**, 4139-51.

Waskiewicz, A. J., Rikhof, H. A. and Moens, C. B. (2002). Eliminating zebrafish pbx proteins reveals a hindbrain ground state. *Dev Cell* **3**, 723-33.

Wellik, D. M. and Capecchi, M. R. (2003). Hox10 and Hox11 genes are required to globally pattern the mammalian skeleton. *Science* **301**, 363-7.

Williams, T. M., Williams, M. E. and Innis, J. W. (2005). Range of HOX/TALE superclass associations and protein domain requirements for HOXA13:MEIS interaction. *Dev Biol* **277**, 457-71.

Wilm, B., Dahl, E., Peters, H., Balling, R. and Imai, K. (1998). Targeted disruption of Pax1 defines its null phenotype and proves haploinsufficiency. *Proc Natl Acad Sci U S A* **95**, 8692-7.

Wolf, C., Thisse, C., Stoetzel, C., Thisse, B., Gerlinger, P. and Perrin-Schmitt, F. (1991). The M-twist gene of Mus is expressed in subsets of mesodermal cells and is closely related to the Xenopus X-twi and the Drosophila twist genes. *Dev Biol* **143**, 363-73.

Wolpert, L. (1969). Positional information and the spatial pattern of cellular differentiation. *J Theor Biol* **25**, 1-47.

Wright, E., Hargrave, M. R., Christiansen, J., Cooper, L., Kun, J., Evans, T., Gangadharan, U., Greenfield, A. and Koopman, P. (1995). The Sry-related gene Sox9 is expressed during chondrogenesis in mouse embryos. *Nat Genet* **9**, 15-20.

Wright, S. (1932). The roles of mutation, inbreeding, crossbreeding, and selection in evolution. *Proceedings of the Sixth Annual Congress of Genetics* **1**, 356-366.

Wurst, W., Auerbach, A. B. and Joyner, A. L. (1994). Multiple developmental defects in Engrailed-1 mutant mice: an early mid-hindbrain deletion and patterning defects in forelimbs and sternum. *Development* **120**, 2065-75.

Wysocka, J., Swigut, T., Xiao, H., Milne, T. A., Kwon, S. Y., Landry, J., Kauer, M., Tackett, A. J., Chait, B. T., Badenhorst, P. et al. (2006). A PHD finger of NURF couples histone H3 lysine 4 trimethylation with chromatin remodelling. *Nature* **442**, 86-90.

Xu, X., Weinstein, M., Li, C., Naski, M., Cohen, R. I., Ornitz, D. M., Leder, P. and Deng, C. (1998). Fibroblast growth factor receptor 2 (FGFR2)-mediated reciprocal regulation loop between FGF8 and FGF10 is essential for limb induction. *Development* **125**, 753-65.

Yamamoto, M., Gotoh, Y., Tamura, K., Tanaka, M., Kawakami, A., Ide, H. and Kuroiwa, A. (1998). Coordinated expression of Hoxa-11 and Hoxa-13 during limb muscle patterning. *Development* **125**, 1325-35.

Yamamoto, M. and Kuroiwa, A. (2003). Hoxa-11 and Hoxa-13 are involved in repression of MyoD during limb muscle development. *Dev Growth Differ* **45**, 485-98.

Yaron, Y., McAdara, J. K., Lynch, M., Hughes, E. and Gasson, J. C. (2001). Identification of novel functional regions important for the activity of HOXB7 in mammalian cells. *J Immunol* **166**, 5058-67.

Yashiro, K., Zhao, X., Uehara, M., Yamashita, K., Nishijima, M., Nishino, J., Saijoh, Y., Sakai, Y. and Hamada, H. (2004). Regulation of retinoic acid distribution is required for proximodistal patterning and outgrowth of the developing mouse limb. *Dev Cell* **6**, 411-22.

Yelon, D., Ticho, B., Halpern, M. E., Ruvinsky, I., Ho, R. K., Silver, L. M. and Stainier, D. Y. (2000). The bHLH transcription factor hand2 plays parallel roles in zebrafish heart and pectoral fin development. *Development* **127**, 2573-82.

Young, N. (2004). Modularity and integration in the hominoid scapula. *J Exp Zoolog B Mol Dev Evol* **302**, 226-40.

Young, N. M. (2006). Function, ontogeny and canalization of shape variance in the primate scapula. *J Anat* **209**, 623-36.

Yueh, Y. G., Gardner, D. P. and Kappen, C. (1998). Evidence for regulation of cartilage differentiation by the homeobox gene Hoxc-8. *Proc Natl Acad Sci U S A* **95**, 9956-61.

Zakany, J. and Duboule, D. (1999). Hox genes in digit development and evolution. *Cell Tissue Res* **296**, 19-25.

Zakany, J., Fromental-Ramain, C., Warot, X. and Duboule, D. (1997). Regulation of number and size of digits by posterior Hox genes: a dose-dependent mechanism with potential evolutionary implications. *Proc Natl Acad Sci U S A* **94**, 13695-700.

Zakany, J., Kmita, M. and Duboule, D. (2004). A dual role for Hox genes in limb anterior-posterior asymmetry. *Science* **304**, 1669-72.

Zeller, R. (2004). It takes time to make a pinky: unexpected insights into how SHH patterns vertebrate digits. *Sci STKE* **2004**, pe53.

Zhang, X., Rowan, S., Yue, Y., Heaney, S., Pan, Y., Brendolan, A., Selleri, L. and Maas, R. L. (2006). Pax6 is regulated by Meis and Pbx homeoproteins during pancreatic development. *Dev Biol*.

Zuniga, A. (2005). Globalisation reaches gene regulation: the case for vertebrate limb development. *Curr Opin Genet Dev* **15**, 403-9.

Zuniga, A., Haramis, A. P., McMahon, A. P. and Zeller, R. (1999). Signal relay by BMP antagonism controls the SHH/FGF4 feedback loop in vertebrate limb buds. *Nature* **401**, 598-602.

Zwilling, E. (1955). Ecoderm-mesoderm relationship in the development of the chick limb bud. *J Exp Zool* **128**, 423-441.